

Gene-environment interactions in the causation and prevention of neural tube defects

Sonia Jaishri Sudiwala

UCL Institute of Child Health

Doctor of Philosophy

2018

Declaration of Contribution

I, Sonia Jaishri Sudiwala, confirm that the work presented in this thesis is my own. Where information has been derived from other sources, I confirm that this has been indicated in the thesis, and the largest contributions of others are also declared below.

The collection, preparation and initial microarray analysis on posterior tissue from *curly tail* and *congenic* wild-type embryos was performed by previous lab members.

The quantification of formate in plasma and urine was performed by the lab of Dr John and Margaret Brosnan (Memorial University of Newfoundland, Canada).

Sonia Jaishri Sudiwala

Abstract

The aim of the work described in this thesis is to investigate the mechanisms underlying neural tube defects (NTDs), birth defects of the developing central nervous system. The study makes use of mouse models of NTDs, and particularly focuses on the interaction between nutritional factors and genetic risk factors in determining susceptibility to NTDs. In humans some NTDs are preventable by folic acid supplementation, but this is not fully effective so investigation of alternative strategies was a key focus.

The efficacy of oral nucleotide and/or inositol supplementation was evaluated for prevention of NTDs in the *curly tail* (*Grhl3* hypomorph) mouse, a model for Folic acid-resistant NTDs. Metabolic effects were investigated by mass spectrometry methods for analysis of folate one-carbon metabolism (FOCM) and nucleotide, nucleoside and nucleobase pools.

Genetic factors influencing FOCM in *curly tail* embryos were investigated, focussing on expression of *Mthfd1L*, which encodes an enzyme of mitochondrial FOCM. Effects on downstream metabolites and the potential for rescue by supplementation with one-carbon donors was evaluated, together with mass spectrometry based analysis of the treatment.

The effect of caffeine on neural tube closure was investigated in several mouse strains to test the hypothesis that caffeine may be a risk factor for NTDs. Caffeine did not interfere with neurulation, and was in fact found to prevent spina bifida in *curly tail* mice. This prevention was accompanied by changes in embryonic FOCM, and cellular effects were analysed.

The cellular basis for prevention of NTDs by folic acid was investigated in the *Splotch* (*Pax3* mutant) mouse. Proliferation was investigated in the cranial neuroepithelium of *Splotch* mutant and wild-type embryos, under standard and folic acid supplemented conditions. The molecular basis of NTDs was investigated with a focus on abnormal Sonic Hedgehog signalling and disrupted dorso-ventral patterning as potentially contributing to NTDs in *Splotch* mutants.

Impact Statement

Neural tube defects (NTDs) are common genetic birth defects that affect approximately 1 in 1000 established pregnancies worldwide. While exencephaly is perinatally fatal, survival of the foetus, in the case of spina bifida, results in significant, life-long morbidity and need for care. NTDs therefore have a large emotional and economic burden on individuals, their families and the state.

A major advance in the field has been the finding that folic acid can prevent up to 70 % of human NTD cases. This has resulted in mandatory folic acid fortification of enriched grain products in 86 countries and a decrease in NTD cases in these countries. However, at least 30 % of cases are unresponsive to folic acid, and the long term safety of folic acid supplementation on the human population is unknown. Several studies in mice, which also demonstrate folic acid responsive and unresponsive NTDs, have found transgenerational differences in response to folic acid, and also a worsening of phenotype in some cases. These findings indicate that multiple strategies and therapies may be required for the prevention of NTDs. Furthermore, both animal and epidemiological studies suggest that human NTDs are caused by multiple, heterogeneous factors, and may require different prevention strategies.

The work presented in this thesis furthers understanding of how folic acid may prevent NTDs, the genetic factors which may influence whether NTDs are responsive to folic acid, and furthers research on alternative preventative therapies for folic acid unresponsive NTDs. This project has provided a better understanding of the genetic and metabolic backgrounds of the *ct* and *Splotch* mice by investigating *Mthfd1L* expression, and formate and nucleotide treatments. As human health care moves into the era of personalised medicine, studies such as those presented here may someday assist in determining the course of preventative treatment for individual NTD cases, depending on the genetic and metabolic background of the parents.

Acknowledgments

I would like to thank my supervisor, Nick Greene, for his expertise, guidance, support and incredible patience. You gave me the time and space to truly learn and understand what I was doing, while gently nudge me back on track whenever I got a little carried away! You managed to make some sense of my half-formed ideas, and help clear my confusion on more than one occasion. I am also grateful to Andy Copp, for your critical thoughts that always led to an improvement, and your inspiring presence and interesting experiments in the dissection room.

I am extremely grateful to all members of the Neural Tube Defects group, past and present, who became much more than just colleagues and were always generous with their time and thoughts. In particular, I would like to thank: Sandra C. P. de Castro, who was never too busy and went through very nearly every technique with me for the first time; Kit-Yi Leung, who showed me how to use a mass spectrometer with endless patience; and, Dawn Savery, for making all the mouse work possible.

Last but never least, I would like to thank my family and partner for their unfaltering support and belief in me.

Contents

Declaration of Contribution	III
Abstract.....	IV
Impact Statement	V
Acknowledgments.....	VI
Contents	VII
List of Figures	XVI
List of Tables	XX
Abbreviations.....	XXII
1 General Introduction.....	1
1.1 The use of animal models for the study of human embryonic development	1
1.2 The neural tube and neural tube defects.....	2
1.2.1 Formation of the neural tube.....	2
1.2.1.1 Tissue specification and morphogenesis.....	2
1.2.1.1.1 Gastrulation.....	2
1.2.1.1.2 Specification of the neuroectoderm	3
1.2.1.1.3 Neuromesodermal progenitors and axis extension	4
1.2.1.1.4 Axial rotation	4
1.2.1.2 Neural tube closure	4
1.2.1.2.1 Neural tube closure is a discontinuous process.....	5
1.2.1.2.2 Different modes of closure.....	6
1.2.1.2.2.1 Cranial neurulation.....	6
1.2.1.2.2.2 Spinal neurulation	8
1.2.1.3 Secondary neurulation.....	8
1.2.2 Neural tube defects result from failed neurulation.....	10
1.2.3 Classification of NTDs.....	10
1.2.4 Current understanding of NTDs in humans	11
1.3 Pathways and processes implicated in neural tube closure	12
1.3.1 Shaping of the neuroepithelium	13
1.3.1.1 Planar cell polarity pathway.....	13
1.3.1.2 Mesenchymal expansion.....	14
1.3.1.3 Actin cytoskeleton	14
1.3.2 Proliferation of the neuroepithelium	15
1.3.2.1 Neural progenitor cycling	15
1.3.2.2 Notch Signalling	16
1.3.2.2.1 Pathway overview	16
1.3.2.2.2 Role in proliferation	16
1.3.2.3 Apoptosis	17

1.3.2.4	Interkinetic nuclear migration and other cell movements	18
1.3.2.5	Sonic Hedgehog signalling.....	18
1.3.2.5.1	Pathway overview.....	19
1.3.2.5.2	Role in neuroepithelial bending.....	19
1.3.2.6	BMP signalling.....	20
1.3.2.6.1	Pathway overview.....	20
1.3.2.6.2	Role in neuroepithelial bending.....	21
1.3.2.7	Shh and BMPs in neural tube patterning	22
1.3.3	Fusion of the neuroepithelium.....	24
1.3.3.1	Grainyhead-like genes	25
1.3.4	Caudalising factors	26
1.3.4.1	Retinoic acid signalling	26
1.3.4.2	Fibroblast growth factor signalling.....	27
1.3.4.3	Canonical Wnt signalling	28
1.4	Environmental factors influence rates of NTDs	29
1.4.1	Factors which contribute towards risk of NTDs.....	30
1.4.2	The preventative effect of folic acid supplementation	30
1.4.2.1	The past and present of folic acid supplementation.....	31
1.4.2.2	Folate one-carbon metabolism.....	34
1.4.2.2.1	Main outputs	34
1.4.2.2.2	Folate cofactors.....	34
1.4.2.2.3	Uptake of folates.....	36
1.4.2.2.4	Pathway overview.....	39
1.4.2.2.5	Placental transport	41
1.4.2.3	Association of human NTDs and genetic polymorphisms of FOCM.....	41
1.4.2.4	Mouse models with mutations in FOCM.....	43
1.5	Mouse models for investigating gene-environment influences	44
1.5.1	The <i>curly tail</i> mouse	45
1.5.1.1	Phenotype	46
1.5.1.2	Tissue and cellular defect	46
1.5.1.3	Genetic defect.....	47
1.5.1.4	Sensitivity to environment.....	48
1.5.1.5	Congenic wild-type strain.....	49
1.5.2	The <i>Splotch</i> mouse	49
1.5.2.1	<i>Splotch</i> phenotype	49
1.5.2.2	The role of Pax3 during neural tube closure.....	50
1.5.2.2.1	Interaction with other proteins and pathways	50
1.5.2.2.2	A possible role in neuroepithelial proliferation	51

1.5.2.3 <i>Splotch</i> mice are sensitive to their environment	52
1.6 Overview of thesis	53
2 Materials and Methods.....	54
2.1 Mice	54
2.1.1 Mouse colonies	54
2.1.2 Timed Matings	54
2.1.3 Treatments and interventions	54
2.1.3.1 Intraperitoneal nucleotide and inositol treatments	54
2.1.3.2 Intraperitoneal folic acid treatment	55
2.1.3.3 Oral nucleotide and inositol treatments	55
2.1.3.4 Oral formate treatment	55
2.1.3.5 Oral caffeine treatment.....	55
2.1.3.6 Folate deficient diet.....	55
2.1.3.7 Fenbendazole treatment	56
2.1.4 Sample collection.....	56
2.1.4.1 Embryo collection.....	56
2.1.4.2 Liver collection	56
2.1.4.3 Blood and urine collection	56
2.1.5 Embryo dissection.....	57
2.1.5.1 Assessment of development and growth.....	57
2.1.6 Genotyping and sex-typing	57
2.1.6.1 Genomic DNA extraction for genotyping.....	57
2.1.6.2 Polymerase chain reaction	57
2.1.6.3 Agarose gel electrophoresis	59
2.1.7 Embryo culture.....	59
2.1.7.1 Rat serum	61
2.1.8 Fixation, dehydration and storage of embryos.....	61
2.2 RNA based experiments	61
2.2.1 RNA isolation and cDNA synthesis.....	61
2.2.2 Whole mount <i>in situ</i> hybridisation.....	62
2.2.2.1 Primer and probe design	63
2.2.2.2 Production of insert DNA	63
2.2.2.3 Ligation into vector system.....	64
2.2.2.4 Transformation and cloning	65
2.2.2.5 Plasmid preparation	65
2.2.2.6 Plasmid DNA digestion	65
2.2.2.7 DIG probe transcription	66
2.2.2.8 Hybridisation of probe	66

2.2.2.9	DIG antibody detection	67
2.2.2.10	Colour development	67
2.2.2.11	Vibratome sectioning.....	67
2.2.2.12	Brightfield microscopy	68
2.2.3	Quantitative, real-time polymerase chain reaction	68
2.3	DNA based experiments.....	69
2.3.1	Incorporation of radiolabelled nuclei into DNA.....	69
2.3.1.1	DNA isolation and quantification.....	69
2.3.1.2	Measurement of radiolabelling	70
2.4	Protein based experiments	70
2.4.1	Immunohistochemistry to assess proliferation	70
2.4.1.1	Intraperitoneal 5-bromo-2'-deoxyuridine pulse	70
2.4.1.2	Paraffin wax embedding.....	71
2.4.1.3	Microtome sectioning	71
2.4.1.4	Immunohistochemistry	71
2.4.1.5	Fluorescence microscopy	72
2.4.1.6	Cell counting	72
2.4.2	Western blot analysis.....	72
2.4.2.1	Protein isolation.....	72
2.4.2.2	Bicinchoninic acid protein quantification.....	73
2.4.2.3	Sodium dodecyl sulfate polyacrylamide gel electrophoresis.....	73
2.4.2.4	Western blotting	74
2.4.2.5	Immunoblotting	74
2.4.2.6	Electrochemiluminescence and autoradiography	75
2.4.2.7	Stripping and re-probing.....	76
2.4.2.8	Quantification of bands	76
2.5	Mass spectrometry experiments	76
2.5.1	Quantification of folate cofactors	77
2.5.1.1	Sample preparation	77
2.5.1.2	Bradford assay protein quantification.....	77
2.5.1.3	Mass spectrometry equipment	77
2.5.1.4	Running conditions.....	78
2.5.1.5	Folate quantification	78
2.5.2	Quantification of s-adenosylmethionine and s-adenosylhomocysteine.....	78
2.5.2.1	Sample preparation	78
2.5.2.2	Standard preparation.....	79
2.5.2.3	Running conditions.....	79
2.5.2.4	S-adenosylmethionine and s-adenosylhomocysteine quantification	80

2.5.3	Quantification of formate.....	80
2.5.4	Quantification of nucleotides, nucleosides and nucleobases	80
2.5.4.1	Optimisation of analytical conditions	81
2.5.4.2	Sample preparation	82
2.5.4.3	Protein quantification.....	83
2.5.4.4	Running conditions	83
2.5.4.5	Nucleotide, nucleoside and nucleobase quantification	83
2.6	Statistical analysis	84
2.7	Figures	84
3	Investigating strategies for the optimal prevention of folic acid resistant NTDs...85	
3.1	Introduction.....	85
3.1.1	Inositol	85
3.1.1.1	Protein kinase C pathway.....	86
3.1.1.2	Inositol and neural tube closure in mice	87
3.1.1.3	Inositol and neural tube closure in humans.....	88
3.1.2	Nucleotides	89
3.1.2.1	Generation and regulation of 5-phosphoribosyl-1-pyrophosphate.....	90
3.1.2.2	The <i>de novo</i> synthesis of nucleotides.....	90
3.1.2.2.1	Purines nucleotide synthesis and regulation	90
3.1.2.2.2	Pyrimidine nucleotide synthesis and regulation.....	91
3.1.2.3	The nucleotide salvage pathways and regulation.....	96
3.1.2.4	Nucleotides can prevent folic acid resistant NTDs	96
3.1.3	Aims of this chapter	97
3.2	Results.....	97
3.2.1	mRNA expression of salvage pathway genes	97
3.2.2	Investigating prevention of neural tube defects by nucleotide treatment administered by intra-peritoneal injection	100
3.2.2.1	Novel intra-peritoneal treatments.....	100
3.2.3	Oral nucleotide treatment.....	102
3.2.3.1	Oral nucleotides prevent NTDs.....	102
3.2.3.2	Analysis of size of nucleotide treated embryos.....	103
3.2.4	Quantification of nucleotides, nucleotides and nucleobases in intra-peritoneal and oral nucleotide supplemented embryos	107
3.2.5	Supplementation of oral nucleotides and inositol in <i>curly tail</i> mice.....	113
3.2.5.1	Nucleotides plus inositol treatment prevents neural tube defects	113
3.2.5.2	Analysis of size of nucleotide + inositol treated embryos	113
3.2.6	Do inositol and nucleotide treatments affect folate one-carbon metabolism? ...116	
3.2.6.1	Quantification of folate cofactors	117

3.2.6.2	Effect oral treatments on abundance of SAM and SAH.....	117
3.2.6.3	Effect of inositol on exogenous adenine incorporation	123
3.2.7	Does fenbendazole treatment retard embryonic growth?	125
3.2.8	Can oral nucleotide supplementation prevent NTDs in other mouse models?..	126
3.2.8.1	Glycine decarboxylase (<i>Gldc</i>) null mice	126
3.2.8.2	<i>Splotch</i> (<i>Sp^{2H}</i>)	127
3.3	Discussion.....	130
3.3.1	The prevention of folic acid resistant NTDs.....	130
3.3.2	Supplementation treatments and regimens	130
3.3.2.1	Salvage pathways	130
3.3.2.2	Intra-peritoneal nucleotide treatments	131
3.3.2.3	Efficacy of oral treatments	131
3.3.2.4	Comparison of nucleotide precursor pools	133
3.3.3	Effects of oral treatments on folate one-carbon metabolism	141
3.3.4	Nucleotide treatment in <i>Splotch</i> and <i>Gldc</i>	143
3.3.5	Potential safety considerations	144
4	<i>Curly tail</i> mice show disturbances in FOCM.....	145
4.1	Introduction	145
4.1.1	Flux through the pathway	145
4.1.2	Pathway regulation	147
4.1.3	Formate metabolism	148
4.2	Aims of this chapter.....	150
4.3	Results	150
4.3.1	<i>Curly tail</i> embryos exhibit reduced expression of <i>Mthfd1L</i>	150
4.3.1.1	MTHFD1L protein abundance is reduced in <i>curly tail</i> embryos.....	153
4.3.1.2	<i>Mthfd1L</i> is not a target of <i>Grhl3</i>	155
4.3.2	Formate levels in <i>curly tail</i> mice	156
4.3.2.1	Circulating formate was reduced in the plasma of <i>ct</i> mice.....	156
4.3.2.2	Does pregnancy affect circulating formate levels?.....	156
4.3.2.3	Abnormal formate metabolism in <i>curly tail</i> mice.....	157
4.3.3	Effect of formate supplementation on growth and neurulation	160
4.3.3.1	Formate supplementation reduced the frequency of spina bifida and exencephaly	160
4.3.3.2	Sodium formate supplementation did not affect embryonic growth	162
4.3.3.3	Litter size was increased by formate treatment	163
4.3.4	Effect of formate supplementation on folate one-carbon metabolism.....	164
4.3.4.1	Embryonic folate distribution.....	164
4.3.4.2	Maternal liver folate distribution	164

4.3.4.3	Effect of formate treatment on total folates in liver and embryos	167
4.3.4.4	Measurement of SAM / SAH.....	168
4.3.5	Prevention of spina bifida may be mediated by stimulation of <i>de novo</i> nucleotide synthesis	170
4.3.6	Interaction between disruption of mitochondrial FOCM and reduced <i>Grhl3</i> ? ..	172
4.3.7	<i>Mthfd1L</i> in <i>Splotch</i> mice.....	174
4.3.7.1	Expression of <i>Mthfd1l</i> in <i>Splotch</i> and other mice	174
4.3.7.2	Formate supplementation in <i>Splotch</i> mice.....	175
4.3.8	Sodium formate as a potential prevention strategy	175
4.4	Discussion.....	178
4.4.1	Genetic background influences <i>Mthfd1L</i> expression in mice	178
4.4.2	Does reduced <i>Mthfd1L</i> abundance contribute to neural tube defects in <i>curly tail</i> mice?	179
4.4.3	Formate treatment for prevention of neural tube defects	180
4.4.4	Does reduced <i>Mthfd1L</i> abundance affect folate one-carbon metabolism in <i>curly tail</i> mice?	182
5	The effect of caffeine on neural tube closure.....	185
5.1	Introduction.....	185
5.1.1	Pharmacokinetics of caffeine	185
5.1.2	Animal studies	186
5.1.3	Human studies.....	188
5.1.4	Potential mechanisms.....	189
5.1.5	Aims of this chapter	189
5.2	Results.....	190
5.2.1	Culture of wild-type embryos with caffeine did not cause NTDs.....	190
5.2.2	Caffeine does not exacerbate NTDs in <i>curly tail</i> embryos	195
5.2.3	<i>In vivo</i> supplementation of <i>ct</i> embryos with caffeine	204
5.2.3.1	Maternal treatment of <i>ct</i> mice with caffeine decreases the frequency of spina bifida.....	204
5.2.3.2	Assessment of maternally caffeine treated <i>ct</i> embryos at E10.5.....	208
5.2.4	Does caffeine affect nucleotide synthesis?	211
5.2.4.1	Caffeine did not change the incorporation of exogenous nucleotides in embryo culture	211
5.2.4.2	Caffeine treatment resulted in changes in the folate cycle.....	213
5.2.4.3	Measurement of methionine cycle intermediates.....	213
5.2.5	Assessment of the effects of caffeine by immunoblotting	216
5.2.5.1	Caffeine treatment modestly increased PCNA immunoreactivity	216
5.2.5.2	Caffeine treatment increases total ERK	217

5.2.6	Effect of caffeine on <i>Splotch</i> litters	221
5.3	Discussion.....	225
5.3.1	Importance of investigating caffeine	225
5.3.2	Caffeine administration	225
5.3.3	Developmental and teratogenic NOEL.....	226
5.3.4	Effect of caffeine on neural tube closure.....	227
5.3.5	Known biological effects of caffeine.....	231
5.3.6	Differences in metabolism of caffeine in mice and humans.....	232
6	Investigating the cause and prevention of NTDs in the <i>Pax3</i> mutant mice...	233
6.1	Introduction	233
6.1.1	Excess apoptosis has been proposed as a mechanism	233
6.1.2	Cell cycle exit and premature neurogenesis	234
6.1.2.1	Altered proliferation in Sp^{2H}/Sp^{2H} embryos?	234
6.1.2.2	Folic acid supplementation and <i>Pax3</i> -related NTDs	235
6.1.3	Dorsoventral patterning in Sp^{2H}/Sp^{2H} embryos	235
6.1.3.1	Interaction between Shh and Notch signalling	238
6.2	Aims of this chapter.....	238
6.3	Results	238
6.3.1	Analysis of proliferation in the cranial region.....	238
6.3.1.1	Comparison of $+/+$ and Sp^{2H}/Sp^{2H} embryos	241
6.3.1.2	Effect of folic acid on percentage labelling.....	245
6.3.1.3	Comparison of <i>Cdkn1a</i> expression in $+/+$ and Sp^{2H}/Sp^{2H} embryos	249
6.3.2	Does loss of <i>Pax3</i> alter the effects of sonic hedgehog signalling?	250
6.3.2.1	Analysis of sonic hedgehog signalling in $+/+$ and Sp^{2H}/Sp^{2H} embryos.....	250
6.3.2.1.1	Expression of <i>Pax6</i> , <i>Msx1</i> and <i>Bmp2</i>	253
6.3.2.2	Does Sonic Hedgehog pathway inhibition alter the frequency of exencephaly in Sp^{2H}/Sp^{2H} embryos?	256
6.3.2.2.1	Shh pathway inhibition by cyclopamine in embryo culture	256
6.3.2.2.2	Analysis of cranial neural tube closure in Sp^{2H}/Sp^{2H} embryos.....	261
6.3.2.2.3	Premature closure of PNP in $+/+$ and $Sp^{2H}/+$ embryos.....	262
6.4	Discussion.....	266
6.4.1	Folic acid supplementation and the <i>Splotch</i> mouse	266
6.4.2	Proliferation in the neural tube	266
6.4.3	The Shh pathway in the <i>Splotch</i> mouse.....	267
6.4.3.1	Change in patterning transcription factors.....	269
6.4.4	Increased <i>Bmp2</i> involved in aetiology of NTDs?	271
7	General discussion.....	272
7.1	Summary of key findings	272

7.2	Folate one-carbon metabolism in <i>curly tail</i> and <i>Splotch</i> mice.....	273
7.3	Prevention of neural tube defects in <i>curly tail</i> mice correlate with changes in abundance of folate cofactors	274
7.4	Relevance of the <i>ct</i> and <i>Splotch</i> models to human neural tube defects.....	275
References.....		278
Appendices.....		339

List of Figures

Chapter 1

Figure 1. 1. The discontinuous process of neural tube closure in mouse.....	6
Figure 1. 2. Neural tube closure in the cranial region	7
Figure 1. 3. The three modes of closure in the spinal region.....	9
Figure 1. 4. Sonic Hedgehog and BMP signalling in dorsolateral hinge point formation.....	22
Figure 1. 5. Progenitor cell zones and transcription factors.	24
Figure 1. 6. The structure of folates.	35
Figure 1. 7. Representation of the main synthesis pathways of folate one-carbon metabolism.	37

Chapter 3

Figure 3. 1. Myo-inositol biosynthetic pathway.....	85
Figure 3. 2. Pathways leading to PRPP formation	92
Figure 3. 3. <i>De novo</i> purine nucleotide synthesis.....	93
Figure 3. 4. <i>De novo</i> pyrimidine nucleotide synthesis	94
Figure 3. 5. Nucleotide salvage pathways	95
Figure 3. 6. Expression of salvage enzymes in E8.5 CD1 embryos.....	98
Figure 3. 7. Expression of salvage enzymes in E10 CD1 embryos.....	99
Figure 3. 8. Rates of spina bifida among offspring of <i>curly tail</i> mice treated by intra-peritoneal injection	101
Figure 3. 9. Rates of exencephaly among offspring of <i>curly tail</i> mice treated by intra-peritoneal injection	102
Figure 3. 10. Crown-rump lengths of oral nucleotides treated embryos	106
Figure 3. 11. Abundance of total nucleotides, nucleosides and nucleobases	109
Figure 3. 12. Abundance of nucleoside triphosphates.....	110
Figure 3. 13. Abundance of nucleoside diphosphates	110
Figure 3. 14. Abundance of nucleoside monophosphates	111
Figure 3. 15. Abundance of nucleosides and nucleobases.....	112
Figure 3. 16. The crown-rump lengths of inositol and inositol + nucleotides treated embryos ...	116
Figure 3. 17. Absolute folate levels of embryos on treatments containing inositol and/ or nucleotides.	119
Figure 3. 18. Relative folate levels of embryos on treatments containing inositol and/ or nucleotides.	120
Figure 3. 19. Total folates in inositol and/ or nucleotide treated embryos	121
Figure 3. 20. Quantification of SAM/ SAH in inositol and/ or nucleotide treated embryos	121
Figure 3. 21. Quantification of SAM in inositol and/ or nucleotide treated embryos	122
Figure 3. 22. Quantification of SAH in inositol and/ or nucleotide treated embryos	122
Figure 3. 23. Effect of inositol on [³ H]-adenine and [³ H]-thymidine incorporation into DNA....	124
Figure 3. 24. Fenbendazole treatment did not affect CR length.....	125

Figure 3. 25. Distribution of folate metabolites in E11.5 wild-type and <i>Sp</i> ^{2H} / <i>Sp</i> ^{2H} embryos.....	128
Figure 3. 26. Total folate containing cofactors in E11.5 wild-type and <i>Sp</i> ^{2H} / <i>Sp</i> ^{2H} embryos.....	129
<i>Chapter 4</i>	
Figure 4. 1. Intracellular formate generating pathways.	149
Figure 4. 2. qRT-PCR shows altered expression of <i>Merc</i> , <i>Mthfd1L</i> and <i>Ndufs5</i> in <i>ct</i> embryos.	
.....	153
Figure 4. 3. MTHFD1L protein abundance is reduced in <i>ct</i> embryos.	154
Figure 4. 4. <i>Mthfd1L</i> expression is not dependent on <i>Grhl3</i> expression.....	155
Figure 4. 5. Plasma formate is reduced in <i>ct</i> mice.....	156
Figure 4. 6. Pregnancy increased circulating formate.....	157
Figure 4. 7. Plasma formate concentrations during folate deficient diet and sodium formate supplementation.	158
Figure 4. 8. Formate in plasma under standard and formate treated conditions.	159
Figure 4. 9. Formate in urine under standard and formate treated conditions.	160
Figure 4. 10. Formate reduced the frequency of spina bifida	161
Figure 4. 11. Formate treatment reduced the frequency of exencephaly	162
Figure 4. 12. Formate treatment has no effect on CR length of <i>ct</i> embryos at E12.5.....	163
Figure 4. 13. Formate treatment increased litter size	163
Figure 4. 14. Absolute abundance of folates in control and formate treated embryos.....	165
Figure 4. 15. Relative distribution of folates in control and formate treated embryos.	166
Figure 4. 16. Relative distribution of folates in control and formate treated livers.	167
Figure 4. 17. Total folates in livers and embryos.....	168
Figure 4. 18. Ratio of SAM/ SAH in embryos and livers	169
Figure 4. 19. Concentration of SAM in embryos and livers	169
Figure 4. 20. Concentration of SAH in embryos and livers.....	170
Figure 4. 21. Formate treatment decreases the incorporation of exogenous nucleotides.....	171
Figure 4. 22. PNP lengths of <i>Grhl3</i> / <i>Gldc</i> double heterozygous embryos at E10.5	173
Figure 4. 23. <i>Mthfd1L</i> expression in different strains	174
Figure 4. 24. Appearance of formate-treated embryos at E18.5.....	176
Figure 4. 25. CR lengths of treated and control E18.5 embryos.....	177
Figure 4. 26. Changes in folate profiles of <i>Gldc</i> wild-type embryos.....	183
<i>Chapter 5</i>	
Figure 5. 1. Structure of adenine, guanine and caffeine.....	186
Figure 5. 2. Phenotypes of CD1 embryos cultured with caffeine	193
Figure 5. 3. Frequency of phenotypes in CD1 embryos cultured with caffeine.	194
Figure 5. 4. Images of closed and open PNPs after culture in the presence of caffeine.	198
Figure 5. 5. Culture with caffeine decreased the PNP size of <i>ct</i> embryos without a significant decrease in CR length.....	201

Figure 5. 6. Ratio of CR length to somite number in caffeine-treated embryos.....	202
Figure 5. 7. Scatter plot of CR length against number of somites.....	203
Figure 5. 8. <i>In vivo</i> caffeine treatment decreased the frequency of spina bifida.	205
Figure 5. 9. <i>In vivo</i> caffeine treatment had no effect on exencephaly.....	206
Figure 5. 10. Crown-rump lengths of E12.5 <i>ct</i> embryos maternally treated with caffeine are decreased compared to control embryos.....	207
Figure 5. 11. Posterior neuropore and crown-rump lengths in control and caffeine treated embryos at E10.5	209
Figure 5. 12. Mean number of somites, crown-rump and posterior neuropore lengths.....	210
Figure 5. 13. Caffeine did not affect the incorporation of labelled nucleotides.	212
Figure 5. 14. Absolute folate levels in control and caffeine treated E10.5 embryos.....	214
Figure 5. 15. Relative folate levels in control and caffeine treated E10.5 embryos.....	215
Figure 5. 16. SAM and SAH in control and caffeine treated embryos.....	216
Figure 5. 17. PCNA immunoblotting for control and caffeine treated samples	218
Figure 5. 18. Total ERK is increased by caffeine treatment.....	219
Figure 5. 19. Total ERK is increased in <i>ct</i> samples compared to congenic <i>wt</i>	220
Figure 5. 20. Scatter plot of crown-rump lengths against somite numbers for caffeine-treated embryos generated by intercross of <i>Sp</i> ^{2H} /+ heterozygotes	222
Figure 5. 21. Somite pairs, crown-rump and posterior neuropore lengths of <i>Sp</i> ^{2H} / <i>Sp</i> ^{2H} embryos.....	223
Figure 5. 22. Frequency of exencephaly in <i>Sp</i> ^{2H} / <i>Sp</i> ^{2H} mutants.....	223
Figure 5. 23. Posterior neuropore lengths of wild-types and heterozygous embryos from <i>Sp</i> ^{2H} /+ intercrosses.....	224

Chapter 6

Figure 6. 1. Patterning and cross-repression of ventral transcription factors	237
Figure 6. 2. Analysis of proliferating cells using BrdU and pHH3 staining	240
Figure 6. 3. Pax3 expression in the dorsal midbrain of the cranial neural tube.....	240
Figure 6. 4. Representation of pipeline for BrdU+, pHH+ and double labelled BrdU+ and pHH+ cell counting.	241
Figure 6. 5. Percentage of BrdU positive cells in +/+ and <i>Sp</i> ^{2H} / <i>Sp</i> ^{2H} embryos.....	242
Figure 6. 6. Percentage of pHH3 positive (non-mitotic) cells in +/+ and <i>Sp</i> ^{2H} / <i>Sp</i> ^{2H} embryos....	243
Figure 6. 7. Percentage of pHH3 positive (mitotic) cells in +/+ and <i>Sp</i> ^{2H} / <i>Sp</i> ^{2H} embryos.....	244
Figure 6. 8. Percentage of double labelled BrdU and pHH3 positive cells in +/+ and <i>Sp</i> ^{2H} / <i>Sp</i> ^{2H} embryos.	244
Figure 6. 9. Percentage of BrdU positive cells in folic acid treated +/+ and <i>Sp</i> ^{2H} / <i>Sp</i> ^{2H} embryos.....	246
Figure 6. 10. Percentage of pHH3 (non-mitotic) positive cells in folic acid treated +/+ and <i>Sp</i> ^{2H} / <i>Sp</i> ^{2H} embryos.	246

Figure 6. 11. Percentage of pHH3 (mitotic) positive cells in folic acid treated +/+ and <i>Sp</i> ^{2H} / <i>Sp</i> ^{2H} embryos.....	247
Figure 6. 12. Percentage of doubly labelled BrdU and pHH3 positive cells in folic acid treated +/+ and <i>Sp</i> ^{2H} / <i>Sp</i> ^{2H} embryos.....	248
Figure 6. 13. p21 expression in E9.5 +/+ and <i>Sp</i> ^{2H} / <i>Sp</i> ^{2H} embryos.	249
Figure 6. 14. qRT-PCR analysis of <i>Ptc1</i> and <i>Gli1</i> expression.....	250
Figure 6. 15. Expression of <i>Shh</i> , <i>Ptch1</i> , <i>Gli1</i> and <i>Foxa2</i>	252
Figure 6. 16. Expression of <i>Pax6</i> , <i>Msx1</i> and <i>Bmp2</i>	255
Figure 6. 17. <i>Gli1</i> mRNA expression in CD1 embryos treated with 0 – 50 nM cyclopamine	258
Figure 6. 18. Patterning transcription factors in DAPT and cyclopamine treated whole mount embryos.....	259
Figure 6. 19. Patterning transcription factors in DAPT and cyclopamine treated sections.	260
Figure 6. 20. Cranial phenotype in 4 out of 10 <i>Sp</i> ^{2H} / <i>Sp</i> ^{2H} embryos.	261
Figure 6. 21. Proportion of cyclopamine treated +/+, <i>Sp</i> ^{2H} /+ and <i>Sp</i> ^{2H} / <i>Sp</i> ^{2H} embryos exhibiting premature PNP closure.....	263
Figure 6. 22. CR length and somite stage in cyclopamine treated +/+, <i>Sp</i> ^{2H} /+ and <i>Sp</i> ^{2H} / <i>Sp</i> ^{2H} embryos.....	263
Figure 6. 23. CR and PNP lengths of untreated and treated <i>Sp</i> ^{2H} / <i>Sp</i> ^{2H} embryos	264
Figure 6. 24. CR length of stage matchd treated +/+ and <i>Sp</i> ^{2H} /+embryos.....	265
<i>Appendix</i>	
Figure A1. Comparison of CR lengths of <i>ct</i> embryos with or without NTDs on different treatments.....	339
Figure A2. PNP lengths of +/+ and <i>Sp</i> ^{2H} /+ embryos	340
Figure A3. Comparison of CR lengths of control <i>ct</i> embryos <i>in vivo</i> and cultured.....	341
Figure A 4. Publication of the major findings of Chapter 4.....	342

List of Tables

Chapter 1

Table 1. 1. Environmental factors affecting risk of NTDs	29
--	----

Chapter 2

Table 2. 1. PCR reaction mix for genotyping and sex-typing.	58
--	----

Table 2. 2. Primers used for genotyping and sex-typing.	59
--	----

Table 2. 3. PCR thermal cycling programmes.....	59
---	----

Table 2. 4. Details of novel WMISH probes designed and generated.....	64
---	----

Table 2. 5. Details of probes constructed from plasmids deposited in the plasmid bank.	64
---	----

Table 2. 6. Primers used for qRT-PCR analysis.....	69
--	----

Table 2. 7. Primary antibodies used for western blotting.....	75
---	----

Table 2. 8. ECL developing systems	76
--	----

Table 2. 9. Preparation of SAM standards.....	79
---	----

Table 2. 10. Preparation of SAH standards	79
---	----

Table 2. 11. Optimised analytical conditions for 22 standards.....	82
--	----

Chapter 3

Table 3. 1. Rates of spina bifida in oral nucleotides treated <i>curly tail</i> embryos by dose, stage and before/ after fenbendazole treatment	104
--	-----

Table 3. 2. Rates of exencephaly in oral nucleotides treated <i>curly tail</i> embryos by dose, stage and before/ after fenbendazole treatment	105
---	-----

Table 3. 3. Nucleotides, nucleosides and nucleobases detected by mass spectrometry.	108
--	-----

Table 3. 4. Rates of spina bifida in oral inositol and inositol + nucleotides treated embryos before and after fenbendazole treatment.....	114
---	-----

Table 3. 5. Rates of exencephaly in oral inositol and inositol + nucleotides treated embryos before and after fenbendazole treatment.....	115
--	-----

Table 3. 6. Frequency of NTDs in <i>Gldc^{GT2/GT2}</i> embryos with formate and nucleotide treatment.	127
--	-----

Table 3. 7. Frequency of NTDs in <i>Splotch</i> embryos treated with nucleotides.	129
--	-----

Table 3. 8. Frequency of exencephaly by sex and treatment.....	129
--	-----

Table 3. 9. dNTP, NTP, NDP and NMP pools measured under each treatment.	136
--	-----

Table 3. 10. Published dNTP pools in various cells types.....	138
---	-----

Table 3. 11. Published NTP pools in various cells types.	139
---	-----

Table 3. 12. Published NDP and NMP pools in various cells types.....	140
--	-----

Chapter 4

Table 4. 1. The names and roles of folate and/ or mitochondrial genes identified from the microarray.....	152
--	-----

Table 4. 2. Frequency of NTDs in formate treated <i>Splotch</i> (<i>Sp^{2H}/Sp^{2H}</i>) mutants.	175
--	-----

Table 4. 3. Toxic effects of sodium formate supplementation.	176
---	-----

Chapter 5

Table 5. 1. Growth parameters of E 9.5 CD1 embryos cultured with varying doses of caffeine.	192
Table 5. 2. Cranial NTD rate and growth parameters of <i>ct</i> embryos cultured for different time periods with 750 μ M caffeine.	197
Table 5. 3. Growth and development measurements of cultured, caffeine treated embryos with open or closed PNPs.	199

Chapter 7

Table 7. 1. Similarities and differences in folate one-carbon metabolism between <i>ct</i> and <i>Splotch</i> mice.	274
Table 7. 2. Percentage change in spina bifida and folate cofactors by treatment in <i>ct</i> mice.	275

Abbreviations

°C	degrees Celsius
µ	micro
10-formylTHF	10-formyltetrahydrofolate
5,10-methenylTHF	5,10-methenyltetrahydrofolate
5,10-methyleneTHF	5,10-methylenetetrahydrofolate
5-formylTHF	5-formyltetrahydrofolate
5m-THF	5-methyl-tetrahydrofolate
ADP	adenine diphosphate
ADP	adenosine 5'-diphosphate
AMP	adenosine 5'-monophosphate
ANOVA	analysis of variance
ATP	adenosine triphosphate
ATP	adenosine 5'-triphosphate
AVE	anterior visceral endoderm
AVE	anterior visceral endoderm
BMP	bone morphogenetic protein
bp	base pair
BrdU	5-bromo-2'-deoxyuridine
BSA	bovine serum albumin
Ca2+	calcium ions
cAMP	cyclic adenosine monophosphate
CDP	cytosine 5'-diphosphate
CMP	cytosine 5'-monophosphate
ct	curly tail
CTP	cytosine 5'-triphosphate
dADP	deoxyadenosine 5'-diphosphate
DAG	diacylglycerol
DAPI	4',6-diamidino-2-phenylindole
DAPT	N-[N-(3,5-Difluorophenacetyl)-L-alanyl]-S-phenylglycine t-butyl ester
dATP	deoxyadenosine 5'-triphosphate
dCDP	deoxycytosine 5'-diphosphate
dCTP	deoxycytosine 5'-triphosphate
DEPC	diethylpyrocarbonate
dGDP	deoxyguanosine 5'-diphosphate
dGTP	deoxyguanosine 5'-triphosphate
DHF	7,8-dihydrofolate
DIG	digoxigenin
DLHP	dorsolateral hinge point
DMEM	Dulbecco's Modified Eagle's Medium with high glucose and HEPES formulation
DMSO	dimethyl sulfoxide
DNA	deoxyribonucleic acid
dNDP	deoxynucleoside 5'-diphosphate
dNMP	deoxynucleoside 5'-monophosphate
dNTP	deoxynucleoside 5'-triphosphate
dTDP	deoxythymidine 5'-diphosphate

dTMP	deoxythymidine 5'-monophosphate
dTTP	deoxythymidine 5'-triphosphate
dU	deoxyuridine
dUMP	deoxyuridine 5'-monophosphate
dUTP	deoxyuridine 5'-triphosphate
E	embryonic day
EDTA	ethylenediaminetetraacetic acid
EdU	5-ethynyl-2'-deoxyuridine
ENU	N-Nitroso-N-methylurea
ESI	electrospray ionisation
FBS	foetal bovine serum
FGF	fibroblast growth factor
FOCM	folate one-carbon metabolism
g	grams
GCS	glycine cleavage system
GDP	huanosine 5'-diphosphate
GMP	guanosine 5'-monophosphate
GPCR	G-protein coupled receptors
GTP	huanosine 5'-triphosphate
HCl	hydrochloric acid
IMP	inosine 5'-monophosphate
INM	interkinetic nuclear migration
IP3	Inositol 1,4,5-triphosphate
IQR	Interquartile range
k	kilo
L	litres
M	molar
m	milli
m/z	mass to charge ratio
MAPK	mitogen-activated kinase
MEFs	mouse embryonic fibroblasts
MHP	medial hinge point
min	minutes
MOPS	3-(N-morpholino)propanesulfonic acid
MRM	multiple reaction monitoring
mRNA	messenger ribonucleic acid
Mw	molecular weight
n	number
n mol.	nano moles
NaCl	sodium chloride
NAD+	nicotinamide adenine dinucleotide (oxidised)
NADH	nicotinamide adenine dinucleotide (reduced)
NADP+	nicotinamide adenine dinucleotide phosphate (oxidised)
NADPH	nicotinamide adenine dinucleotide phosphate (reduced)
NCC	neural crest cells
NDP	nucleoside 5'-diphosphate
NICD	Notch intracellular domain
NMP	nucleoside 5'-monophosphate

NTD	neural tube defect
NTP	nucleoside 5'-triphosphate
p	probability (p-value)
p mol.	pico moles
PAGE	polyacrylamide gel electrophoresis
PBS	phosphate buffered saline
PCR	Polymerase chain reaction
PFA	Paraformaldehyde
pHH3	Phospho-histone H3
PNP	posterior neuropore
PRPP	5-phosphoribosyl-1-pyrophosphate
PVDF	polyvinylidene fluoride
qRT-PCR	quantitative real-time polymerase chain reaction
RA	retinoic acid
RIPA	Radio-immunoprecipitation assay
RNA	ribonucleic acid
rpm	revolutions per minute
SAH	s-adenosylhomocysteine
SAM	s-adenosylmethionine
SDS	sodium dodecyl sulfate
sec	seconds
SEM	standard error of the mean
Shh	sonic hedgehog
SNPs	single nucleotide polymorphisms
SSC	saline sodium citrate
TBS	tris-buffered saline
THF	5,6,7,8-tetrahydrofolate
UDP	uridine 5'-diphosphate
UMP	uridine 5'-monophosphate
UPLC	ultraperformance liquid chromatography
UTP	uridine 5'-triphosphate
WMISH	whole mount in situ hybridisation
Wnt	Wingless-related integration site
XMP	xanthosine 5'-monophosphate

1 General Introduction

1.1 The use of animal models for the study of human embryonic development

In mouse, prenatal development occurs over 19 – 20 days, while in humans, gestation proceeds over 9 months. In both mammalian species, basic development proceeds similarly, although at different rates. Early development consists of a series of dynamic morphogenetic processes that take place in order to transition from an initial clump of cells, termed the inner cell mass, which are part of the blastocyst that forms on day 5 – 6 in humans and day 3 in mouse. The inner cell mass gives rise to the epiblast, which will form the embryo proper, and the three germ layers; the ectoderm, the mesoderm and the endoderm, during gastrulation. The germ layers undergo extensive remodelling and growth to form the basic organs of the embryo; the heart, the central nervous system (CNS), the gut etc. Later stages in development are defined by tissue growth.

In addition to comparable development to humans, there are relatively sophisticated tools for the genetic manipulation of mice, an availability of inbred lines, and the occurrence of natural mutations affecting embryonic developmental processes (Peters et al. 2007; Nguyen and Xu 2008). These features have made mice an extremely useful and versatile, and therefore popular, tool to study human development. Importantly, neural tube closure, which is the focus of this thesis, appears to occur in an analogous manner in mice, allowing the investigation of how the neural tube forms and closes, why it fails to close, and how closure can be facilitated. Additionally, the ability to culture mouse embryos *ex vivo* during neural tube closure is a major advantage. The majority of the research discussed, and the experiments conducted for this thesis are in mouse.

Other model organisms; the fruit fly (*Drosophila*), the chick, and amphibians such as frog (*Xenopus*) and newt, have also contributed greatly to the study of embryonic development. *Drosophila*, as a simpler, invertebrate system, has been instrumental to our understanding of conserved signalling pathways and collective cell movements during development. Convergent extension controlled by the planar cell polarity (PCP) pathway, discussed later (**Section 1.3.1.1**), is a key process that precedes mammalian neurulation and was first elucidated in *Drosophila* (Axelrod 2009). Like mice, the genetics of *Drosophila* are mapped and can be manipulated.

Amphibians, as vertebrates, demonstrate many similarities, yet also distinct differences from mammalian development, including differences in neural tube closure. However, due to their robust development outside of a uterus or shell, they have been studied extensively in order to understand early developmental processes such as cleavage, morula and blastocyst formation. Additionally, ease of access to the developing embryo allowed researchers to perform experiments such as tissue grafting, which led to the discovery of the Spemann-Mangold organiser, a cluster of cells that was capable of inducing the development of the CNS from host tissue when transplanted into another

gastrula stage embryo; the result was an embryo with two heads and CNS conjoined at the gut (Elinson and Holowacz 1995; Horder 2001). The discovery of the amphibian organiser was a watershed moment as it introduced the concept of induction to developmental biology. The equivalent structure in amniotes, is generally termed “the node” and “Hensen’s node” in mammals and avians respectively, and was first described by Viktor Hensen in rabbit and guinea pig in 1875 (cited in Leikola 1976; Viebahn 2001).

Lastly, the development of the chick, as a vertebrate and amniote, is similar to mouse and human, but closure of the neural tube proceeds via a different sequence of events. Additionally, chick genetics are currently not as amenable to manipulation as mouse genetics. However, it is one of the first and most extensively studied animal models in developmental biology. Many important concepts and processes relevant to this thesis were first elucidated in chick. These include; the discovery of neural crest cells (reviewed by Stern, 2016), the demonstration of the movements and fates of the neural crest cells (Le Douarin 1980) and the discovery that the notochord induces the floor plate and ventral cell fates of the neural tube (van Straaten et al. 1985; Placzek et al. 1991).

1.2 The neural tube and neural tube defects

1.2.1 Formation of the neural tube

The neural tube is the precursor of the CNS, giving rise to all cells and structures within the brain and spinal cord. It is one of the first structures to begin forming, at around embryonic day (E) 7 in mouse and E17 in humans, in so-called neurula or neurulation-stage embryos.

The neural tube is composed of neural progenitor cells arranged in a pseudostratified epithelium referred to as the neuroepithelium. The neuroepithelium is specified on the dorsal side of an embryo and runs the entire anterior to posterior axis.

1.2.1.1 Tissue specification and morphogenesis

1.2.1.1.1 Gastrulation

After fertilisation, mammalian embryos pass through the cleavage and blastula stages of embryogenesis. At the beginning of gastrulation, from E6.5 in mouse and E15 in humans, a midline structure of thickened linear cells called the primitive streak arises at the caudal and dorsal aspect of the epiblast, thus defining the rostral-caudal and ventral-dorsal embryonic axes. The primitive streak elongates by addition of cells at the caudal end while the rostral end contains a thickened knot of cells; the primitive node. Along the primitive streak a narrow primitive groove develops which becomes the primitive pit in the region of the primitive node. Cells from the epiblast undergo an epithelial-to-mesenchymal transition, migrate towards the primitive streak and ingress at the

primitive groove, becoming committed to a mesendodermal lineage, which will give rise to both the endodermal and mesodermal layers. The initial epiblast layer gives rise to the neural and non-neural (surface) ectoderm.

1.2.1.1.2 Specification of the neuroectoderm

The full events of neural induction are still being elucidated, but appear to involve fibroblast growth factor (FGF) signalling in chick and amphibians, along with inhibition of bone morphogenetic protein (BMP) signalling, which appears essential in chick and amphibians, but essential and sufficient in mouse (Stern 2005; Henrique et al. 2015). In support of this concept, deletion of the mouse BMP receptor, *Bmpr1a*, expression in the epiblast resulted in premature neural differentiation with loss of mesoderm (Di-Gregorio et al. 2007).

The earliest pro-neural markers are *Sox2* and *Otx2*, however, they are generally expressed throughout the mouse epiblast at E6.5, before becoming restricted to the neural plate from E7, which involves the inhibition of BMP signalling. At these early streak stages it is believed that expression of the BMP inhibitors, *Noggin* and *Chordin*, from the primitive node, also called the gastrula organiser, specifies what is known as the anterior neural plate (Davidson and Tam 2000), which goes on to form the forebrain, midbrain and hindbrain structures (Leviton and Cowan 2002; Kondoh, Takada, and Takemoto 2016). As the embryo progresses from early streak (E6.5) to late streak (E7.5) stages the primitive node or gastrula organiser becomes the node.

As well as BMP inhibition within the neural plate, signalling from an extraembryonic region juxtaposed next to the most anterior region of the neural plate, the anterior visceral endoderm (AVE), appears to be a requirement for the generation of forebrain structures (Tam & Steiner 1999). The AVE expresses genes required for forebrain patterning, such as *Otx2*, *Lhx1*, and *Foxa2*, and also the genes *Cer1*, *Lefty1*, and *Dkk1*, which contribute to BMP, Nodal and Wnt inhibition (Andoniadou and Martinez-Barbera 2013). To give rise to more caudal neural plate identities, posteriorising signals from FGFs (**Section 1.3.4.2**), Wnts (**Section 1.3.4.3**), and retinoic acid (RA; **Section 1.3.4.1**) are required. While FGFs and Wnts are secreted from the caudal epiblast, *nodal* is secreted from the node (Zhou et al. 1993; Conlon et al. 1994), and RA is secreted from the presomitic mesoderm and newly formed somites.

From E7, cells which ingress at the primitive pit and subsequently node, give rise to the mesodermal structure termed the notochordal process, which later matures to form the notochord. The notochord is a signalling centre, which has been shown to express the BMP antagonists *Chordin*, *Noggin* and *Follistatin* in chick (Liem, Jessell, and Briscoe 2000) and mouse (McMahon et al. 1998), that stabilise the overlying neural plate in its neuroepithelial identity. Ectodermal tissue lateral to the neural plate where BMP signalling is not inhibited gives rise to the surface ectoderm which will go on to form the epidermis.

The neural plate extends cranially and broadens while the node and primitive streak appear to retreat as the embryo continues to extend until the end of gastrulation; around E8.5 in mouse and E20 in humans.

1.2.1.1.3 Neuromesodermal progenitors and axis extension

After gastrulation is complete, embryos continue to extend via their caudal axis. The details of this process are currently not well understood, but it is currently thought that a single population of neuromesodermal progenitor cells reside in an area close to the node, and where the primitive streak was, called the caudal lateral epiblast and the node streak border. Neuromesodermal progenitors are believed to be important for the continuing formation of the neural tube, the somites and the notochord. They are identified by the co-expression of the neural marker, *Sox2*, and the mesodermal marker *Brachyury* (*Bra*/ *T*; Henrique et al. 2015). Current evidence suggests that in mouse, the neural plate below the level of the eighth somite originates from neuromesodermal progenitors (NMPs); this is considered to be the posterior neural plate (Kondoh, Takada, and Takemoto 2016). As NMPs migrate from the caudal lateral epiblast/ node streak border they encounter Wnt, FGF and RA signalling, which imparts rostrocaudal positional identity (Gouti, Metzis, and Briscoe 2015).

1.2.1.1.4 Axial rotation

The early growth of a mouse embryo is different from similarly staged human and chick embryos in that its overall structure is a “U” shape; concave dorsally and convex ventrally, while human and chick embryos are essentially convex dorsally and concave ventrally. In this “U” topography, the dorsal side of the embryo is on the inside and the ventral side is on the outside. If the embryo continued growing in this orientation, it would find its ectoderm on the inside and endoderm on the outside. Therefore, to correct this situation, at approximately the 12 – 14 somite stage, E9 – 9.5, the mouse embryo undergoes rotation along the longitudinal axis such that the curvature of the embryo is reversed and the dorsal side is convex and the ventral side is concave.

1.2.1.2 Neural tube closure

The neuroepithelium is initially flat and must undergo morphogenetic movements to form a structure with a continuous, hollow lumen and overlying surface ectoderm, thus completing neural tube closure. Briefly, this involves bending and creation of a neural groove and neural folds which are brought into apposition, allowing fusion of the lateral edges of the neuroepithelium. This process is described in more detail in the following sections.

1.2.1.2.1 Neural tube closure is a discontinuous process

Primary neurulation (to be referred to simply as neurulation from this point), or neural tube closure, begins around E8.5 in mouse and E20 in humans. In both mouse (**Figure 1. 1**) and humans, closure is a discontinuous process with the occurrence of discrete closure points.

The first closure, Closure 1, is initiated at the hindbrain – cervical boundary around E8 at the 6 -7 somite stage. Closure propagates bi-directionally from this site to begin forming the cranial neural tube and future brain rostrally, and the spinal neural tube and future spine caudally. Closure 2 occurs at the forebrain – midbrain boundary approximately 12 hours later at the 11 – 13 somite stage, and also moves bi-directionally. Closure 3 occurs a short time after closure 2, at the rostral limit of the neural tube and therefore proceeds in a caudal direction only (Greene and Copp 2009; Copp et al. 2003).

The open regions between closure points are called neuropores. Closure of the cranial region, involving the hindbrain and anterior neuropores, is generally complete by E9.5 at around somite stage 14 - 15. Closure of the spinal region, the posterior neuropore (PNP), is complete by E10.5 and somite stage 28 - 30 (Copp et al. 2003). However, the specific time and developmental stage of closure can vary between strains. In humans, closure is initiated at around E22 – 23; cranial closure is complete by E24 and the PNP closed by E26 – 28 (Greene and Copp 2009).

While the positions of Closure 1 and Closure 3 are invariable in mouse and also occur in humans, the position and occurrence of closure 2 is more polymorphic (Greene and Copp 2009; O’Rahilly and Muller 2002). In mice, the position of Closure 2 appears to be more rostral to the midbrain in some strains, while in others it appears to be more caudally located. Interestingly, a more caudal Closure 2 confers some resistance towards the condition exencephaly (described in **Section 1.2.3**), while the opposite is true for a more rostral Closure 2 (Fleming and Copp 2000). The strain SELH/Bc does not have a Closure 2 event, and approximately 17% of these mice develop exencephaly while the rest develop normally (Macdonald et al. 1989). The existence of Closure 2 in human embryos is contentious; it has been reported in some studies (Van Allen et al. 1993; Golden and Chernoff 1995; Seller 1995; Nakatsu et al. 2000) but not in others (O’Rahilly and Muller 2002). It is possible that Closure 2 may only exist in some groups or may be found very close to Closure 3 making it hard to distinguish (Nakatsu, Uwabe, and Shiota 2000; Greene and Copp 2009).

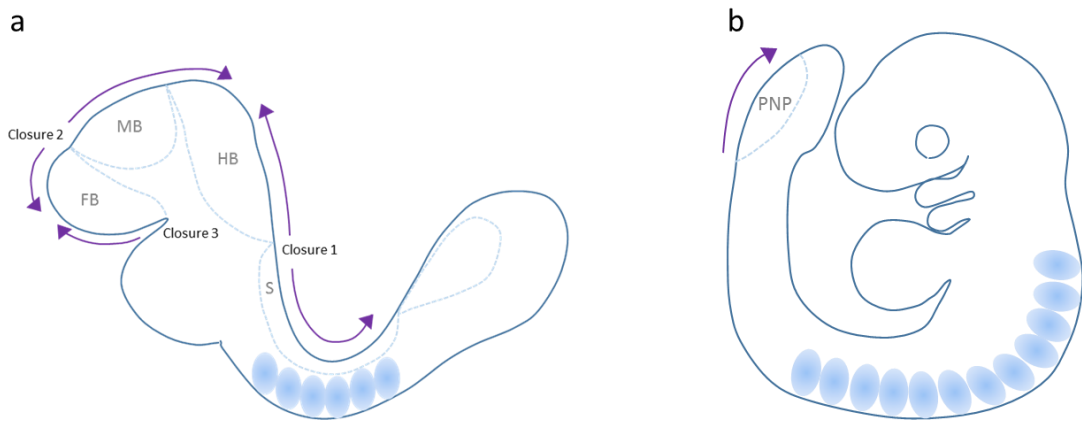


Figure 1.1. The discontinuous process of neural tube closure in mouse.

Neural tube closure begins in the mouse embryo at (a) E8, or the 6 – 7 somite stage, with first Closure 1, at the hindbrain – cervical boundary. Closure 2 occurs soon after, at the midbrain – forebrain boundary, followed by Closure 3 at the rostral limit of the forebrain. Closure 1 and 2 are bi-directional, while Closure 3 is uni-directional. By (b) E9.5, the cranial region has completed neurulation, but spinal neural tube closure, propagated from Closure1, is still proceeding. Spinal neurulation occurs as the embryos extends caudally, and is complete by E10.5. FB = forebrain; MB = midbrain; HB = hindbrain; S = spinal; PNP = posterior neuropore.

1.2.1.2.2 Different modes of closure

Although neurulation essentially involves elevation, apposition and fusion of the neural folds, the overall process requires a complex and precise sequence of events which are still not fully understood. Additionally, different mechanisms are utilised to achieve closure depending on axial level and developmental stage; closure in the cranial region can be distinguished between closure in the upper spinal levels and also from lower spinal levels.

1.2.1.2.2.1 Cranial neurulation

Closure in the cranial region is achieved using midline and dorsolateral bending (**Figure 1.2**). The midbrain region possibly requires the largest movement of the neural plate in order to bring the folds into apposition. In this region, the elevating neural folds initially take on a biconvex orientation with the tips of the folds facing away from each other (**Figure 1.2a**). In the next phase of closure, the folds invert, adopting a biconcave orientation which brings the folds into apposition and allows fusion to occur (Morriss-Kay 1981; **Figure 1.2b**). While the cellular and morphogenetic

cues underlying these events are not properly understood, proliferation and expansion of the mesenchyme (**Section 1.3.1.2**), proliferation of the neuroepithelium (**Section 1.3.2**), contraction of the actin cytoskeleton (**Section 1.3.1.3**), Sonic hedgehog (Shh) (**Section 1.3.2.5**) and BMP signalling (**Section 1.3.2.6**), and emigration of a population of cells termed the neural crest from the dorsal border of the cranial folds, are all thought to play a role in ensuring closure (Copp, Greene, and Murdoch 2003; Copp 2005), and are discussed further in the relevant sections.

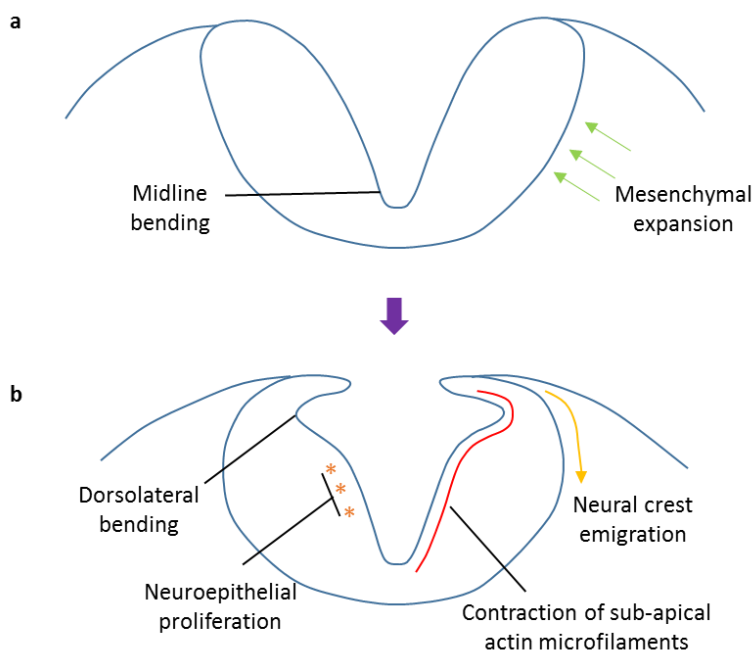


Figure 1.2. Neural tube closure in the cranial region

The elevating cranial neuroepithelium is aided by mesenchymal proliferation and initially adopts a biconvex shape (**a**). Dorsolateral bending subsequently occurs, causing the neural folds to become biconcave to allow fusion at the midline (**b**). Contraction of the actin cytoskeleton, neural crest emigration and neuroepithelial proliferation appear important for dorsolateral bending. Based on diagram from Copp et al. (2003).

1.2.1.2.2.2 Spinal neurulation

Spinal neurulation, unlike cranial neurulation, does not require the surrounding, paraxial mesoderm. Instead, a requirement for the overlying surface ectoderm has been shown (Ybot-Gonzalez et al. 2002)

Along the spinal neural tube, three modes of closure take place. Mode 1 (**Figure 1. 3b**), which occurs at upper spinal levels around E8 – 8.5, and so includes Closure 1, and involves bending solely at the midline in the area overlying the notochord. This bend is called the medial hinge point (MHP). Mode 2 (**Figure 1. 3c**) occurs at intermediate spinal levels at around E9 – 9.5. In Mode 2, a MHP is present and the neural folds additionally bend at dorsolateral regions of the neuroepithelium termed the dorsolateral hinge points (DLHPs). Finally, Mode 3 occurs at the lower spinal levels at around E10 (**Figure 1. 3d**); bending occurs only via DLHPs (Shum and Copp 1996; Ybot-Gonzalez and Copp 1999). Studies to date suggest that DLHP formation is indispensable for completion of spinal neurulation, while MHP formation is dispensable. Two morphogenetic signalling pathways are strongly implicated in DLHP bending; the Shh (**Section 1.3.2.5**) and BMP (**Section 1.3.2.6**) pathways.

1.2.1.3 Secondary neurulation

In mice and humans, the neural tube in the lower sacral region and below is formed by a process known as secondary neurulation. This involves the condensation and canalisation of cells derived from the tail bud to form a tube continuous with the higher spinal levels of the closed neural tube. Cells derived from the tail bud at these later stages give rise to all non-epidermal tissues, including the neural tube, the notochord, the somites and the hindgut (Copp, Stanier, and Greene 2013; Copp and Greene 2013). Less is known about this process and it will not be discussed further as this project focuses on primary neurulation.

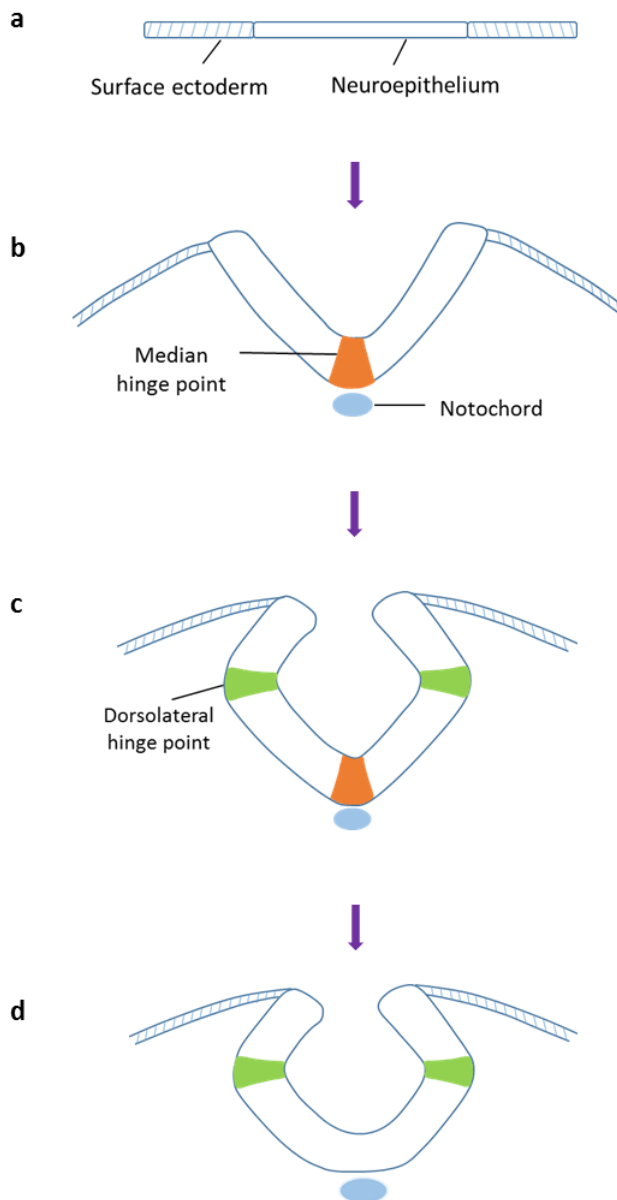


Figure 1. 3. The three modes of closure in the spinal region.

The modes of spinal neural tube closure are dependent on the somite stage and axial region. The neuroepithelium is initially flat (a), it then bends at the median hinge point (MHP) only during Mode 1 closure (b), at both the MHP and dorsolateral hinge points (DLHP) during Mode 2 closure (c), and then by DLHP only during Mode 3 closure (d). Adapted from Copp et al. (2003).

1.2.2 Neural tube defects result from failed neurulation

Open neural tube defects (referred to as simply neural tube defects; NTDs) occur when neural tube closure fails. The type and severity of the defect depends on where closure failed, with similar outcomes in mouse and humans, and will be discussed further in this section.

Closed neural tube defects are thought to result from abnormalities of secondary neurulation and include a heterogeneous group of conditions often referred to as spina bifida occulta or dysraphic disorders. Features include: defects of skeletal development, such as absence of vertebral arches or a midline bony spur; abnormalities of the spinal cord, including widening of the central canal which can cause spinal fluid to accumulate and damage nerves (hydromyelia); a lengthwise duplication (dipomyelia) or splitting (diastematomyelia) of the spine; and spinal cord tethering which can cause stretching and damage of the nerves (Copp and Greene 2013). As with secondary neurulation, closed neural tube defects will not be discussed further.

In current understanding, the conditions encephalocele and meningocele arise when the skull vault or the vertebral column, respectively, do not form correctly to contain the closed neural tube. This can lead to herniation of meningeal tissue and cerebrospinal fluid, and in more severe cases brain tissue or the spinal cord can also herniate (Copp and Greene 2013). These and associated conditions are not strictly NTDs as their occurrence is believed to be a failure in mesoderm not neural tube development, and as such they will not be considered further.

1.2.3 Classification of NTDs

NTDs occur when the neural folds fail to fuse together, leaving open regions which subsequently inhibit both mesoderm and epidermis from forming around the open defect. For the most part, the neuroepithelium appears to develop, proliferate, pattern and differentiate as normal, but the continued exposure of neural tissue to the amniotic environment results in neural degeneration. It is this degeneration of neural tissue which defines the symptoms of NTDs.

The largest lesion occurs with a failure to initiate Closure 1, which results in craniorachischisis. In this condition the neural tube is open from the midbrain, as Closure 2 and 3 usually occur normally, to the sacral spinal level, and is invariably incompatible with survival. Approximately 10 % of human NTDs cases comprise craniorachischisis (Copp and Greene 2013).

When the neural tube fails to close in the cranial region, the condition is referred to as exencephaly, which subsequently becomes anencephaly as brain tissue is lost due to degeneration. In mice, exencephaly predominantly affects either the midbrain, the hindbrain or both, depending on where closure arrests and whether Closure 2 occurred. A failure of Closure 3 gives rise to a forebrain exencephaly with a characteristic “split face” phenotype in mice. In humans, exencephaly affecting

the rostral brain is termed meroacrania while those affecting the posterior brain is termed haloacrania. All anencephalic phenotypes demonstrate perinatal lethality in mouse and humans.

Spina bifida aperta (to be referred to simply as spina bifida), occurs when propagation of Closure 1 down the spinal region is interrupted. Spina bifida is usually compatible with survival but the larger the open region, the more severe the complications. The spinal cord can be completely exposed in myeloschisis, or covered by the meninges in myelomeningocele. In humans, lumbosacral spina bifida is most common, with lower limb paralysis, bladder incontinence, urinary tract infections and bowel dysfunction are common symptoms.

1.2.4 Current understanding of NTDs in humans

In humans, NTDs are the second most common birth defect world-wide, affecting on average 0.5 – 2 per established pregnancies (Mitchell 2005). Of interest, the actual frequency of affected pregnancies is known to vary widely with ethnicity and geographic region. These findings suggest a genetic component to susceptibility to NTDs, as does the increased risk for siblings of index cases (2 – 5 %) compared to the general population (~ 0.1 %), and the risk associated with having an affected pregnancy increasing to 10 % if two previous pregnancies were affected. Other strong evidence for a genetic component includes the higher prevalence in same sex twins, assumed to be monozygotic, compared to different sex twins (Copp, Stanier, and Greene 2013; Kleijer et al. 2006). However, studies of migrants and their descendants also suggest a locality influence, or environmental factors, which impact NTD rates (Leck 1974). One such environmental factor identified in the 1960s was socioeconomic status.

Most NTD cases are found to be sporadic and non-syndromic. The high prevalence but sporadic appearance has given rise to the multifactorial threshold hypothesis, whereby susceptibility to NTDs is conferred in a polygenic or oligogenic pattern with an important role for environmental factors (Carter 1974). Overall, it is estimated that genetic factors are responsible for approximately 70 % of the risk associated with an affected pregnancy (Leck 1974).

Generally, anencephaly and spina bifida tend to occur equally in human NTD cases, with a much smaller occurrence of craniorachischisis. Another feature is the greater preponderance of females affected by anencephaly (Carter 1974). While the reason behind this phenomenon is unknown, it suggests that the X chromosome in some way may affect cranial neurulation.

To date, no single gene or pathway has stood out as being implicated in a significant proportion of human NTDs, with the exception of the PCP pathway in craniorachischisis (**Section 1.3.1.1**). Analysis has mainly been confined to looking for associations between single nucleotide polymorphisms (SNPs) in candidate pathways, such as folate one-carbon metabolism (**Section 1.4.2.2**) and the PCP pathway, in relatively small case-control studies. Associations between SNPs

in the genes of these pathways and NTD cases have been found in certain populations and will be detailed in the relevant sections. Additionally, other studies have looked at copy number variants (Xiaoli Chen et al. 2013) and changes in gene methylation status (Shangguan et al. 2015) in association with NTDs with some positive results, but these have yet to be tested in other populations.

1.3 Pathways and processes implicated in neural tube closure

The study of neural tube closure in mice has provided a wealth of information and insights into this process. Mouse mutants have helped to elucidate the importance of various molecular pathways and biological processes for achieving neural tube closure, as has the ability to pharmacologically interfere with specific pathways and processes during neurulation. Currently, there are over 200 genes, which when disrupted in mice result in NTDs (Harris and Juriloff 2007, 2010). This list is expected to continue growing for the near future and confirms the complexity of the morphogenetic processes which are required for neural tube closure.

Of the 200 plus mouse mutants which exhibit NTDs, most are single gene mutants, including genes which have spontaneously mutated and those which have been disrupted using: N-Nitroso-N-methylurea (ENU) mutagenesis screens; targeted null, conditional or hypomorphic alleles; hypermorphic alleles and misexpression. Also present are digenic and trigenic mutants and combinations of heterozygotes.

Of interest, there are mutants which also demonstrate an increased prevalence of exencephaly in females. Examination of mouse embryos revealed that females are delayed in development at the time of neural tube closure compared to males (Seller and Perkins-Cole 1987b), raising suggestions this could be causal, but the rate of development through neurulation was shown to be equal in both sexes, and so unlikely to account for the female excess (Brook, Estibeiro, and Copp 1994). More recently, Chen et al. (2008) concluded that increased risk is due to the presence of two X chromosomes, not gonadal sex or protection by the Y chromosome. It is not understood exactly how this increased risk is conferred, but the increased requirement of methyl groups in females for the inactivation of one X chromosome in each somatic cell has been proposed (Juriloff and Harris 2000; Juriloff and Harris 2012). Interestingly, the methyltransferase *Dnmt3b* is expressed specifically in the closing cranial neural folds, and knockout of *Dnmt3b* results in cranial NTDs and an impairment in *de novo* DNA methylation in mice (Okano et al. 1999).

Approximately 20% of the mutants present with 100 % penetrance of an NTD. While it is unlikely that these mutations are representative of the human condition, they assist in discerning the essential processes which allow closure. Additionally, while many of the homozygous null mutants demonstrate multiple developmental defects (syndromic), the presence of NTDs alone can result when expression is hypomorphic, in combinations of heterozygous mutations, or is bred onto other

backgrounds. Generally, phenotypes can vary markedly depending on the genetic background, demonstrating the importance of modifier genes (Greene et al. 2009).

Another consideration when extrapolating from NTD mouse models to human NTDs is that approximately 65 % of the mutants reported exhibit exencephaly only, 5 % exhibit spina bifida only, and nearly 20 % display exencephaly and/ or spina bifida (Harris and Juriloff 2007, 2010). The reason behind the higher proportion of exencephaly in mice compared to the proportion in humans NTD cases (~45 %) is not understood. It has been suggested that cranial neurulation may be a more sensitive process in mice, because they have proportionally larger heads at this stage compared to humans (Copp 2005). The data from mice suggests that while there does appear to be some regulatory overlap between cranial and lower spinal neurulation, cranial closure in mice is a more demanding process compared to spinal neural tube closure.

Overall, the study of neural tube closure in mice and genetic mouse models of NTDs have made a major contribution to our knowledge of the molecular and cellular requirements for neural tube closure. Some of the main pathways and processes which have been implicated in neural tube closure are detailed below.

1.3.1 Shaping of the neuroepithelium

1.3.1.1 Planar cell polarity pathway

The PCP pathway, a non-canonical Wnt signalling pathway, establishes polarity and coordination within the plane of epithelial tissues. It is responsible for driving convergent-extension of the neural plate, whereby neuroepithelial cells intercalate at the midline (Keller, Shook, and Skoglund 2008). Failure of this process results in a broad and short, instead of a narrow and elongated, neural plate, which is unable to achieve Closure 1 on account of the neural folds being too far apart to appose (Ybot-Gonzalez et al. 2007). Therefore, mice with defects in this pathway mainly present with highly penetrant craniorachischisis. The first PCP mouse mutant described was the *Loop-tail* mouse found to be homozygous null for *Vangl2* (Kibar et al. 2001; Murdoch et al. 2001). Since then, numerous PCP mutants have been created which also result in craniorachischisis and also other NTD types when heterozygous in digenic and trigenic combinations (Harris and Juriloff 2007, 2010).

The striking correlation between disruption of PCP signalling and craniorachischisis led to the search for SNPs in PCP genes which associate with human craniorachischisis cases, with many reports of associated missense variants which have not yet been studied for a causal role (De Marco et al. 2012, 2013; Shi et al. 2014). NTD-associated variants in *VANGL1* (Kibar et al. 2007), *VANGL2* (Lei et al. 2010), *CELSR1* and *SCRIB* (Robinson et al. 2012) and *DACT1* (Shi et al. 2012) have been shown to have defects in protein function, such as protein-protein interaction and translocation

to the plasma membrane. To date, none of these variants have been introduced into mice to assess whether they cause NTDs.

1.3.1.2 Mesenchymal expansion

During the two-phase closure of the cranial neural tube, expansion of the cranial mesenchyme, by proliferation and a substantial increase of the extracellular space, appears to play an essential role during the first phase when the neural folds elevate to form a biconvex shape (Morriis and Solursh 1978). This is evidenced by the two mouse mutant knockouts for *Twist* and *Cart1*, which fail to expand their cranial mesenchyme and close their cranial neural tubes (Chen and Behringer 1995; Q. Zhao, Behringer, and de Crombrugghe 1996). Importantly, *Cart1* is expressed in the cranial mesenchyme and not the neuroepithelium, while chimera analysis suggested that *Twist* was required in the cranial mesenchyme and not the neuroepithelium.

1.3.1.3 Actin cytoskeleton

The second phase of cranial neural tube closure, where the neural folds appose by inverting to a biconcave orientation (**Figure 1. 2**), requires the actin cytoskeleton. Actin microfilaments are located circumferentially at the apical border of all neuroepithelial cells (Sadler et al. 1982), and have been postulated to contract the apical surface of the cells to assist in bending and closure of the neural tube. This theory was initially probed using cytochalasin D, which inhibits polymerisation of actin microfilaments, and was found to cause exencephaly in rodents (Wiley 1980; Austin, Wind, and Brown 1982; Morriis-Kay and Tuckett 1985). This finding is corroborated by numerous mouse mutants, which when made null for cytoskeletal proteins such as palladin (Luo et al. 2005), vinculin (Baribault, and Adamson 1998) or cofilin 1 (Gurniak, Perlas, and Witke 2005) and MARCKS (Stumpo et al. 1995), or double and triple null mutants for actin regulatory proteins such as MENA, VASP or EVL (Menzies et al. 2004; Furman et al. 2007), also exhibit exencephaly.

A longstanding issue has been the presence of apical actin microfilaments in spinal neuroepithelial cells but an apparent lack of requirement for the actin cytoskeleton; spinal neurulation is resistant to cytochalasin D and only the null mouse mutants for *Shroom3* and *Marcks1* exhibit spina bifida as well as exencephaly, but at a much lower frequency in respect to exencephaly (Wu et al. 1996; Hildebrand and Soriano 1999). More recently, Escuin et al. (2015) demonstrated that, unlike cranial neurulation, actin polymerisation and ATP dependant actomyosin contraction are dispensable for spinal neurulation, while F-actin turnover and disassembly of actomyosin complexes are required for spinal neurulation.

1.3.2 Proliferation of the neuroepithelium

1.3.2.1 Neural progenitor cycling

The neuroepithelium is a pseudostratified epithelium that is entirely proliferative before neural tube closure occurs, with differentiation into neurons proceeding only after neural fold fusion. As neuroepithelial cells traverse the cell-cycle, they exhibit interkinetic nuclear migration (INM); the nucleus of these cells moves between apical and basal locations of the neuroepithelia in period with the cell-cycle.

During G₁-phase of the cell-cycle, nuclei undertake an apical-to-basal migration, and S-phase occurs at basal positions. During G₂-phase, the migration is reversed by a basal-to-apical movement, so mitosis occurs at the apical surface. It has been shown that while INM can be uncoupled or halted, and is not required for cell-cycle progression (Murciano et al. 2002; Schenk et al. 2009), blocking or delaying progression of the cell-cycle results in either arrest or decreased migration (Baye and Link 2007).

While this movement was first described in detail by FC Sauer in 1935, the reason behind it has remained elusive. One proposal was that this movement allowed the maximal number of mitoses on the apical surface at any given time, leading to efficient progenitor expansion. More recently, data suggests that INM is necessary for cell fate decisions, with perturbation of migration impacting neurogenesis and causing premature depletion of neuronal precursors and imbalanced neuronal cell fates (Murciano et al. 2002; Schenk et al. 2009).

This is of interest because the balance between neural progenitor cell proliferation and differentiation appears key for neural tube closure. Genetic ablation of both positive and negative cell cycle regulators in mice can result in exencephaly. This includes the positive regulator *Nup50* (Smitherman et al. 2000), which inhibits the negative cell-cycle regulator p27^{Kip1} (CDKN1B), and negative regulators including *Jarid2* (formerly known as *jumonji*; Takeuchi et al. 1995) and *Nap1l2* (Rogner et al. 2000). While the exencephalic phenotype of *Jarid2* null embryos appears to originate from cranial neural folds which fail to become biconcave, defects in *Nap1l2* null embryos correlate with an increase in neuronal progenitor cells. These studies suggest that both insufficient and excess neuroepithelial cells can prevent closure of the cranial neural tube.

Another feature known for the spinal neuroepithelium is a ventral-low and dorsal-high proliferation gradient, which involves increased expression of *cyclin D1* and *cyclin D2* in the dorsal neural tube (*cyclin A1* and *cyclin B3* are expressed equally throughout), was first shown in the closed neural tube (Megason and McMahon 2002). Later, McShane et al. (2015) found that cdk4 and cyclin D1 protein were more highly expressed in the dorsolateral regions of the elevated neural folds, and surgical removal of the surface ectoderm resulted in a loss of cyclin D1 immunoreactivity. While

this gradient has yet to be demonstrated in the cranial neuroepithelium, mice null for *Phactr4*, a protein expressed in the ventral neural tube before closure that acts as a negative regulator of cell cycle progression, display exencephaly, aberrant ventral proliferation and decreased neurogenesis (Kim et al. 2007).

1.3.2.2 Notch Signalling

Notch was initially discovered as a gene in whose mutation resulted in a serrated wing margin phenotype in *Drosophila melanogaster* (Dexter 1914), and then in whose loss-of-function resulted in hypertrophy of the neural ectoderm at the expense of surface ectoderm (Poulson 1940). The Notch pathway is now understood to be important at multiple points during development of the nervous system, functioning as a molecular switch driving binary fate choices. An overview of the pathway and our current understanding of the role of Notch signalling in proliferation of the neuroepithelium is detailed below.

1.3.2.2.1 Pathway overview

Notch is a conserved signalling pathway that requires cell-cell contact via single-pass, transmembrane ligands, either Delta-like (Dll1,3,4) or Jagged (Jag1,2), and single-pass, heterodimeric, transmembrane Notch receptors (Notch1 - 4 in mammals) on neighbouring cells for pathway activation (Kopan and Ilagan 2009). Ligand-receptor binding triggers endocytosis of the ligand-receptor complex, a process requiring ubiquitination of the ligand by E3 ligases Mindbomb (Mib1,2), and of the receptor by E3 ligase Deltex (Dx; Fortini & Bilder 2009). Crucially, upon activation, the Notch receptor intracellular domain (NICD) is cleaved by Presenilin proteases (Psen1/2) of a γ -secretase complex (Selkoe and Kopan 2003).

The NICD then translocates to the nucleus (Struhl and Adachi 1998; Schroeter, Kisslinger, and Kopan 1998), where it acts as an activation and recruitment element, binding the Notch effectors RBP-J κ /CBF1 and Mastermind-like 1 (Maml1), which assemble transcriptional complexes to drive target gene expression (Pierfelice, Alberi, and Gaiano 2011). While the full complement of Notch responsive genes is still unknown, in the embryonic nervous system the basic helix-loop-helix (bHLH) Notch targets, Hes and Hey, have a relatively well characterised role. Hes and Hey proteins form homo- and heterodimers with family members and interact with transcriptional core-repressors of the Gro/TLE family which have histone deacetylate activity (Iso, Kedes, and Hamamori 2003; Kageyama, Ohtsuka, and Kobayashi 2008).

1.3.2.2.2 Role in proliferation

Notch pathway activation and expression of the transcriptional repressors Hes and Hey has been shown to inhibit neurogenesis and maintain neuroepithelial cells in the neural progenitor state. Neural progenitor cells in mice and in culture failed to differentiate into neurons when transfected

with a *Hes1* expression construct (Ishibashi et al. 1994). Conversely, mutation of *Notch1* and *RBP-Jκ* in mice resulted in premature expression of the neural transcription factors (**Section 1.3.2.7**) *Math4*, *neuroD* and *NSCL-1*, which are required for neuronal differentiation (de la Pompa et al. 1997). The proneural gene *Mash1* is also upregulated when *Hes1* is ablated (Ishibashi et al. 1995), and is likely a direct negative target of *Hes1* (Chen et al. 1997).

Mouse mutants of the Notch pathway demonstrate that Notch signalling and neuroepithelial proliferation has a substantial role in neural tube closure. Null mutants of *RBP-Jκ* and *Hes1* exhibit decreased neural progenitor proliferation with concomitant premature neuronal differentiation and incomplete cranial closure (Ishibashi et al. 1995; Oka et al. 1995) Additionally, mice null for *Numb*, which encodes a membrane-associated protein found in neural progenitor cells that segregates asymmetrically with progenitor cell daughters, also exhibited premature neurogenesis and fully penetrant exencephaly (Zhong et al. 2000).

Conversely, overexpression of *Notch3* increases the numbers of nestin (a neural stem cell marker)-positive progenitor cells found in open cranial neuroepithelia (Lardelli et al. 1996). Significantly, these findings are in agreement with the genetic studies of cell cycle regulator above; both over and under proliferation can interfere with cranial neural tube closure.

1.3.2.3 Apoptosis

Concurrently, there are a number of mouse mutants which exhibit increased apoptosis in the neural tube, of which a proportion do not complete neurulation. These include mice null for the anti-apoptotic factors *Bcl10* (Ruland et al. 2001) and *Mdm4* (Migliorini et al. 2002), and also mice null for genes not involved in apoptosis, but found to undergo increased apoptosis in the neural tube, such as *ApoB* (Homanics et al. 1995) and *Tulp3* (Ikeda et al. 2001). It is supposed that excess apoptosis, like decreased proliferation, could result in insufficient cell numbers.

Similarly, as mice with excessive proliferation can present with exencephaly, so can mice deficient in apoptosis. Mice null for the proapoptotic mediator *Casp3* (Kuida et al. 1996) and its upstream activators *Casp9* (Kuida et al. 1998) and *Apaf1* (Cecconi et al. 1998; Yoshida et al. 1998) demonstrate a failure in cranial neurulation, as do mice deficient for the tumour suppressor p53 (Sah et al. 1995). These mutants demonstrated increased neural progenitor cells and neural hyperplasia (Kuida et al. 1998; Honarpour et al. 2000; Pompeiano et al. 2000).

To date, genetic studies in mice suggest that cell number is crucial for cranial neural tube closure, but irrelevant for spinal neurulation. However, Ybot-Gonzalez et al. (2002) found that the surface ectoderm was necessary for DLHP formation and Mode 3 spinal neural tube closure (**Section 0**). This may suggest a link between surface ectoderm induced cyclin D1, proliferation, DLHP formation and spinal neural tube closure.

It is not known how either over or under proliferation (or insufficient/ excess apoptosis) of the neuroepithelium inhibits neural tube closure, but it is conceivable that both scenarios would change the density and stiffness of the tissue, which could imbalance the biomechanical forces acting to close the neural folds.

Whether apoptosis is required during the remodelling stages of neural tube closure has also been investigated. Culture of neurulation stage mouse embryos with z-VAD-fmk, or the p53 inhibitor pifithrin- α , did not prevent neurulation in the cranial or spinal regions when added several hours prior to each closure event. Post-fusion remodelling of the neuroepithelia and surface ectoderm was indistinguishable from control embryos (Massa et al. 2009). Bending of the neuroepithelium

1.3.2.4 Interkinetic nuclear migration and other cell movements

INM is involved in MHP formation; in both chick (Schoenwolf and Franks 1984) and mouse (McShane et al. 2015) respectively, 70 % and 60 % of nuclei of the MHP are basally located. This occurs because nuclei spend longer in S-phase, resulting in these cells adopting a ‘wedge’ shape that is broad basally and narrow apically, which possibly assists with bending. In comparison, nuclei positioned in lateral, non-bending neuroepithelium were basally located approximately 35 % in both chick and mouse, implying no single cell shape dominates in this region.

However, DLHP bending in mice does not appear to rely on the same mechanism. McShane et al. (2015) found that the number of cells forming the dorsolateral region (the neuroepithelia dorsal of a horizontal line drawn where the neuroepithelia meets paraxial mesoderm and surface ectoderm) increases from Modes 1 to 2, and 2 to 3. Proliferation alone could not account for the cell numbers in the dorsolateral region; this was greater than expected, while in the more ventral regions, the number of cells was less than expected. The authors demonstrated that ventrally located DiI labelled cells migrated dorsally within the neural folds as closure proceeded. A requirement for sufficient cell number, and of a possible ‘buckling’ mechanism, in the formation of DLHPs was proposed (McShane et al. 2015).

1.3.2.5 Sonic Hedgehog signalling

Shh is a member of the hedgehog family of secreted signalling molecules which was first described in *Drosophila*, and most of our basic knowledge of Shh signalling derives from *Drosophila*. The family also includes Indian Hedgehog and Desert Hedgehog in mammals (Hammerschmidt, Brook, and McMahon 1997). Shh, together with BMPs (Section 1.3.2.6), function to regulate neuroepithelia morphogenesis and patterning (Section 1.3.2.7). The hedgehog signalling pathway is highly regulated and complicated; only the core elements are briefly described below.

1.3.2.5.1 Pathway overview

Shh, after undergoing autocatalysis and addition of a cholesterol and palmitoyl group, is released from the synthesising cell in a process mediated by Dispatched (Dsp; Burke et al. 1999). Signal transduction occurs when secreted Shh binds to the transmembrane receptor Patched (Ptch1,2; of which Ptch1 is believed to predominantly act in the neural tube) relieving the inhibitory effect of Ptch on the G-protein-like receptor Smoothened (Smo; Murone et al. 1999). Activated Smo is internalised and translocates to the primary cilium, which is essential for downstream signalling events. This means that molecules required for cilia function, such as intraflagellar transport proteins, can also regulate the pathway and general cilia health can impact on Shh signalling (Sasai and Briscoe 2012).

Translocation of Smo stimulates the movement of Gli (Gli2,3) transcription factors from the cytoplasm to cilia tips. In the absence of activated Smo, Gli2 and Gli3 proteins interact with pathway repressor Sufu. Additionally, Gli3, in particular, is thought to undergo proteolytic cleavage and function as a transcriptional repressor (Gli3^{REP}), a potent Shh pathway antagonist, in the off state (B. Wang, Fallon, and Beachy 2000; Jacob and Briscoe 2003). Alternatively, Gli proteins can be ubiquitinated and targeted for proteasome degradation. On activation of the pathway and translocation to cilia, the Gli proteins lose interaction with Sufu, and Gli2, in particular, undergoes phosphorylation and becomes a transcriptional activator (Gli2^{ACT} ; Ingham *et al.*, 2001; Ulloa and Marti, 2010). Downstream targets of Shh signalling include Gli1, which is thought to act as a transcriptional activator, and the negative regulator Ptch1 (Lee *et al.* 1997; Litingtung and Chiang 2000b). The expression of Gli3 is repressed by Shh signalling (Marigo *et al.* 1996).

1.3.2.5.2 Role in neuroepithelial bending

Shh is a morphogen implicated in both the formation of MHPs and inhibition of DLHPs during spinal neurulation. *Shh* is initially expressed by the notochord and then by the overlying floorplate (**Section 1.3.2.7 & Figure 1. 5**; Echelard *et al.* 1993; Marti *et al.* 1995). The strength of this expression is found to correlate with the appearance of MHPs, and inversely correlate with that of DLHPs: at upper spinal levels where the neural tube bends solely by MHPs *Shh* expression is at its highest; at the mid-spinal level where both MHP and DLHPs are found, *Shh* expression is moderate; while at the lower spinal levels *Shh* expression is at its lowest and only DLHPs occur (Ybot-Gonzalez *et al.* 2002). Furthermore, unilateral implantation of Shh soaked beads prevented DLHP formation during culture *ex vivo*. This is supported by the observation that *Shh*-null mutants present with DLHPs throughout the whole rostro-caudal spinal axis (Ybot-Gonzalez *et al.* 2002).

Of interest, loss of *Shh* (Ybot-Gonzalez *et al.* 2002) or repression of the pathway (Ding *et al.* 1998; Matise *et al.* 1998; Park *et al.* 2000) does not prevent neural tube closure despite loss of the MHP in some embryos. Conversely, *Shh* overexpression (Echelard *et al.* 1993), or over-activation of this

pathway through the mutation of negative regulators such as: *Ptch1*; *Rab23*; *Tulp3*; (Johnson 1967; Goodrich et al. 1997; Patterson et al. 2009; Huang, Roelink, and McKnight 2002), does impair closure in the cranial and lower spinal regions where dorsolateral bending and DLHPs usually occur. Furthermore, *Tulp3^{hhkr}* mutants have been histologically examined and found to display reduced dorsolateral bending (Patterson et al. 2009).

It has, however, been noted that closure occurs in the region where dorsoventral patterning (a measure of Shh pathway activation; **Section 1.3.2.7**) is most severely affected in both *Tulp3* and *Rab23* mutants, but fails at a point more caudally (Murdoch and Copp 2010). Overall, it is not known whether dorsolateral bending is compromised in all cases where failure of neurulation does occur, and whether other processes required for neural tube closure may be jeopardised by Shh pathway over-activation.

It remains to be demonstrated whether medial and dorsolateral bending in the cranial region are under the same regulation as MHPs and DLHPs in the spinal region. Of the mutant/ transgenic mice with over-activation of the Shh pathway studied, a varying percentage of all fail to complete cranial neurulation, and a varying percentage of approximately half fail to close both their cranial and spinal region (Harris and Juriloff 2007, 2010; Murdoch and Copp 2010), indicating some overlap and some differences in regulation.

1.3.2.6 BMP signalling

BMPs are part of the transforming growth factor- β (TGF β) superfamily of secreted molecules that were first discovered by their ability to induce ectopic bone development. There are over 15 known BMPs which signal via a heterotetrameric complex of type I and type II serine/ threonine kinase receptors, of which 3 of each types are known to interact with BMPs (Wang et al. 2014). To date, four BMPs, BMP2, BMP4, BMP5 and BMP7, have been shown to be expressed by the surface ectoderm adjacent to the neuroepithelia, depending on embryonic stage and axial location (Solloway and Robertson 1999; Danesh et al. 2009; Jessell 2000).

1.3.2.6.1 Pathway overview

Depending on which type, BMPs bind to either type I or type II receptors which are typically both present at the cell surface as dimers. Ligand binding triggers recruitment of the opposite type receptors and upon formation of the heterotetrameric complex, the constitutively active type II receptor transphosphorylates the type I receptor. This activation step then recruits and results in phosphorylation of receptor-regulated Smads (Smad1,5,8). Receptor-regulated Smads then associate with co-mediator Smad (Smad4) and translocate to the nucleus where they interact with both coactivators and corepressors to modulate target gene transcription. Pathway activation

induces the expression of inhibitory Smads (Smad6,7), and also, directly or indirectly, secreted negative pathway regulators such as *Noggin* and *Chordin* (Wang et al. 2014).

1.3.2.6.2 Role in neuroepithelial bending

There is evidence that *Bmp2* expressed from the surface ectoderm of the elevating neural folds also antagonises DLHP formation. Unilateral implantation of a *Bmp2* soaked bead next to one side of the elevating neural folds was sufficient to suppress DLHP formation on the proximal neural fold (Ybot-Gonzalez et al. 2007). The authors also determined that the expression of *Noggin* at the dorsal tips of the neuroepithelium varied along the rostro-caudal axis, increasing at mid-low spinal levels (Mode 2 and 3), so as to allow DLHPs to form. Furthermore, they demonstrated that *Noggin* expression was induced by *Bmp2* and suppressed by *Shh*.

Together with previous data (Ybot-Gonzalez et al. 2002), the authors set out a model which accounts for the existence of DLHPs in Mode 2 and 3, where *Shh* expression decreases and *Noggin* expression is high, but not in Mode 1, where *Shh* expression is high (Figure 1.4; Ybot-Gonzalez et al. 2007). The authors also found that the *Kumba* mouse, a mutant null for the transcription factor *Zic2*, fails to express *Noggin* and therefore fails to form DLHPs (Ybot-Gonzalez et al. 2007). Additionally, the *Kumba* mouse suggests that dorsolateral bending in the cranial region and DLHP formation in the spinal region are differentially regulated to some extent, as *Kumba* mice exhibit fully penetrant spina bifida but exencephaly at only 10% frequency (Nagai et al. 2000).

A proportion of *Bmp2* heterozygous and hypomorphic mice are found to exhibit exencephaly (Singh et al. 2008; Castranio and Mishina 2009), as do mice null for *Smad5* (Chang et al. 1999). Double knockout mice for *Bmp5* and *Bmp7* also present with fully penetrant exencephaly (Solloway and Robertson 1999). Together with the requirement of the overlying surface ectoderm for spinal neurulation, this suggests there may be a need for a precise threshold of BMP signalling in the neural tube, which is self-regulated via feedback expression of *Noggin*. In agreement, mice null for *Noggin* also develop exencephaly and spina bifida (McMahon et al. 1998; Stottmann et al. 2006). Of interest, while the frequency of exencephaly was dependant on genetic background, the frequency of spina bifida was not (Stottmann et al. 2006).

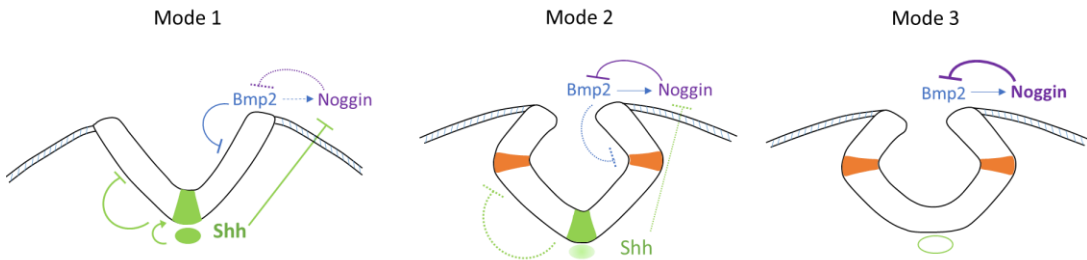


Figure 1. 4. Sonic Hedgehog and BMP signalling in dorsolateral hinge point formation.

Representation of the current understanding of the signalling pathways involved in DLHP (orange filled) formation in the spinal neural tube. In **Mode 1**, Shh from the notochord and floorplate (both green filled) is high; Noggin is repressed by Shh so it cannot repress Bmp2 from the surface ectoderm; both Shh and Bmp2 inhibit DLHP formation. In **Mode 2**, there is decreased Shh expression from the notochord and floorplate; Noggin is less strongly repressed, and offers some repression over Bmp2. This allows DLHP formation. In **Mode 3**, Shh expression is lost from the notochord and floorplate, therefore Noggin is completely derepressed and strongly inhibits Bmp2; the neural tube bends only from DLHPs. Based on diagram from Ybot-Gonzalez et al. (2007).

1.3.2.7 Shh and BMPs in neural tube patterning

As the precursor of the brain and spinal cord, the neural tube must give rise to the large number of cell types contained within the CNS. To achieve this, neuroepithelial cells differentiate into different populations of neurons (followed by other cell types) depending on their location within the neuroepithelia. Patterning by transcription factors along the dorsoventral and rostro-caudal axis imparts three-dimensional positioning information, which establishes the regional specialisations. Dorsoventral patterning is linked to neural tube closure, at least in part, because Shh and BMP signalling are involved in progenitor cell patterning.

Initial patterning begins before elevation of the neural folds along the mediolateral axis of the neuroepithelium. The underlying notochord and the lateral ectoderm are sources of *Shh* and BMPs respectively (Liem et al. 1995; Liem, Tremml, and Jessell 1997). Due to proximity, *Shh* has the greatest effect on medial, overlying neuroepithelial cells, which becomes the floorplate and ventral neuroepithelia when the lateral edges elevate to neural folds. By the same account, BMPs have the greatest influence on the lateral and then dorsal neuroepithelia. At our current understanding of neural tube patterning, the three BMPs can be considered to fulfil the same function and will be referred to collectively as BMPs.

In the simplest model, the opposing gradients of Shh and BMP signalling divide the dorsoventral axis of the spinal neural tube into eleven progenitor domains; five ventrally (pMN and p0 – 3) and

six dorsally (dP1 – 6), which from around E10 onwards give rise to eleven domains of post-mitotic neurons. Progenitor domains occupy more apical positions in the neural tube, referred to as the ventricular zone, while post-mitotic neurons come to occupy the basal positions, referred to as the mantle layer (**Figure 1. 5**). Broadly, the five ventral domains give rise to neurons which regulate motor output, while the six dorsal domains produce neurons which mediate and integrate sensory input. Each progenitor cell domain expresses a characteristic set of homeodomain and bHLH proneural transcription factors that relate to their dorsoventral position and are required for differentiation into distinct neuronal classes (Jessell 2000; Caspary & Anderson 2003).

Shh and BMP signalling are mutually antagonistic and this antagonism results in the correct expression of ventral and dorsal transcription factors. In chick neural tube explants, *Shh* inhibits the expression of dorsal transcription factors (Liem et al. 1995), and electroporation of a construct which blocks *Shh* signalling (a *Shh*-insensitive Patched1 protein) caused cell-autonomous ventral-to-dorsal changes in progenitor cell fate (Briscoe et al. 2001). Over activation of the *Shh* pathway in mice results in an expansion of the ventral domains, with loss of dorsal cell fates and a failure in neurulation (Goodrich et al. 1997; Zhang, Ramalho-Santos, and McMahon 2001; Eggenschwiler et al. 2006; Patterson et al. 2009), while loss of *Shh* signalling results in dorsalisation of the neural tube with loss of most ventral progenitor cell fates (Chiang et al. 1996; Park et al. 2000). Conversely, BMPs can inhibit the formation of *Shh* induced ventral cell fates in both mouse and chick (Basler et al. 1993; Arkell and Beddington 1997).

In addition to its requirement in neurulation, ablation of *Noggin* results in loss of some ventral cell fates from the level of the forelimb, with the severity of the phenotype increasing caudally. Also, *Bmp4* was found to be ectopically expressed from the notochord and floor plate near the tail region (McMahon et al. 1998). Thus, notochord derived inhibition of BMP signalling is required for *Shh* expression to correctly pattern the ventral spinal cord, also demonstrated by Liem et al. (2000) in chick. These studies demonstrate that the network of *Shh*, *Noggin* and *BMP* cross inhibition is required for correct patterning of the neural tube and for neural tube closure.

Dorsoventral patterning has been mostly studied in the upper spinal neural tube, and the diagram shown in **Figure 1. 5** is of progenitor cell patterning in the spinal region. There are known to be transcription factors that are not expressed uniformly throughout the rostrocaudal axis. This is particularly prominent in the cranial neural tube, which develops into the different centres of the brain, and patterning is often varied between forebrain-midbrain-hindbrain boundaries. For example, at E9.5 *Pax3* is not expressed in a region of the midbrain – hindbrain boundary (Zhao et al. 2014) and *Pax6* is not expressed in a region of the midbrain (Mastick et al. 1997). Additionally, *Cdx2* is expressed in the caudal spinal tube only. While *Cdx2* is required for caudal body axis elongation, it is unknown whether it has a role in spinal progenitor domain patterning (Zhao et al. 2014). Therefore, our picture of neural tube patterning is currently incomplete, especially in the cranial and lower spinal regions.

Lastly, although *Shh* and *BMPs* are grossly responsible for the formation of the progenitor domains, Notch signalling, as well as its role in neural progenitor cell proliferation, also functions in dorsoventral patterning and will be discussed later (Section 6.1.3.1). Additionally, RA signalling (Section 1.3.4.1) and Wnt signalling (Section 1.3.4.3) play a role.

1.3.3 Fusion of the neuroepithelium

Assuming fold elevation, bending and apposition proceeds correctly, there are several events which must occur to allow fusion: A) the surface ectoderm and neuroepithelia must delaminate from one another; B) cells extend projections for initial contact and intercalation; C) the neural folds come into full contact and adhere; and D) the neuroepithelial and ectodermal layers undergo remodelling at the dorsal midline. Grainyhead-like transcription factors are expressed by the surface ectoderm during neural tube closure and loss of either in mice results in NTDs.

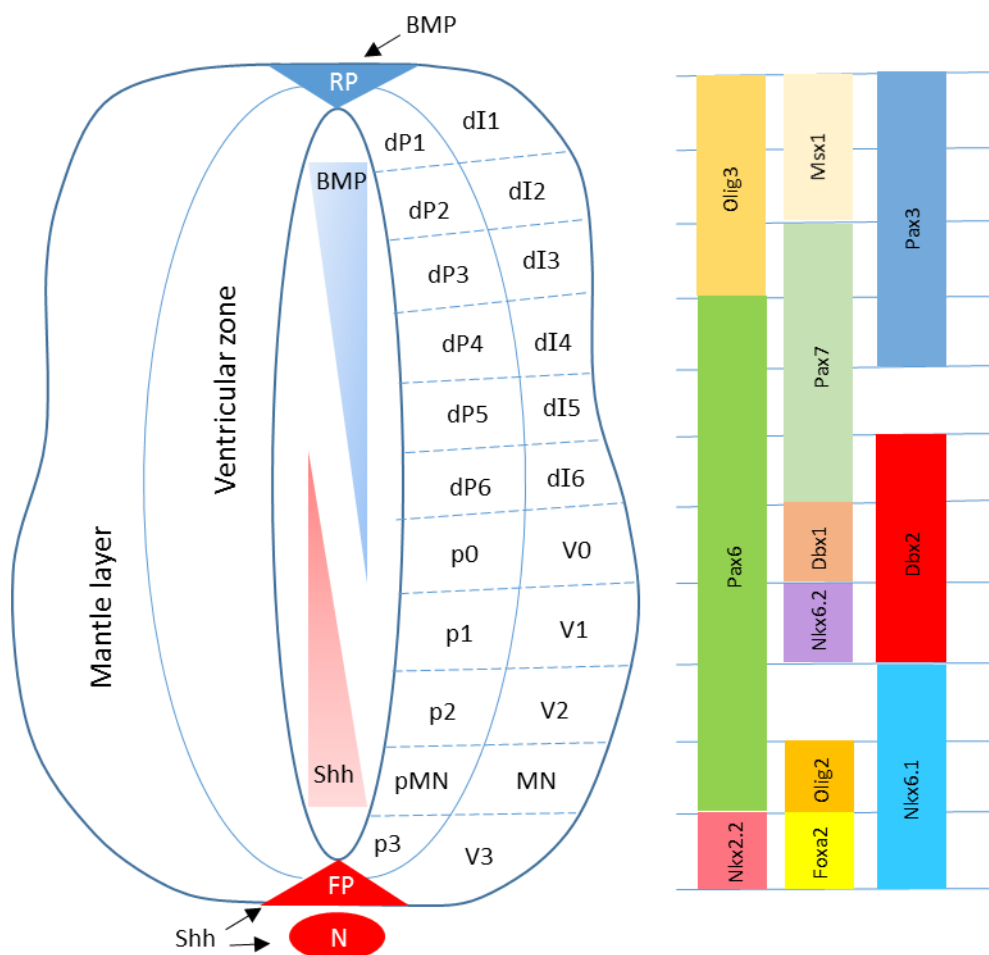


Figure 1. 5. Progenitor cell zones and transcription factors.

Figure 1. 5. Progenitor cell zones and transcription factors.

The neural tube is divided into eleven progenitor cell and eleven post-mitotic domains, which express a unique combination of patterning transcription factors grossly coordinated by ventral Shh, and dorsal BMP expression. The transcription factors shown to the left of the diagram are expressed by progenitor cells along the dorsoventral axis in the domains indicated. This is not a complete list by any means. Additionally, although a closed neural tube is depicted, progenitor cell patterning transcription factors begin to be expressed from ~ E8.5 i.e. before neural tube closure.

1.3.3.1 Grainyhead-like genes

As well as being expressed by the surface ectoderm, *Grainyhead-like 2,3* (*Grhl2,3*) are also expressed by the endoderm of the developing hindgut. Additionally, *Grhl3* is expressed in the forebrain and dynamically in the closing neural tube but extinguished after closure is achieved (Gustavsson et al. 2007).

Of interest, the null and overexpressing mouse mutants of both genes exhibit NTDs, demonstrating that dose of these transcription factors is crucial for neural tube closure. *Grhl3* knockout and overexpression results in fully penetrant thoraco-lumbosacral spina bifida and a low frequency of exencephaly (Yu et al. 2006; Ting et al. 2005; de Castro 2011). Knockout of *Grhl2* results in fully penetrant exencephaly with split face, and 88 – 100 % spina bifida, depending on the background (Rifat et al. 2010; Werth et al. 2010; Brouns et al. 2011), while *Grhl2* overexpression results in fully penetrant spina bifida only (Brouns et al. 2011). Additionally, *curly tail* (*ct*) mice harbouring two hypomorphic alleles of *Grhl3* present with 15-20 % lumbosacral spina bifida and ~ 5 % exencephaly (Gustavsson et al. 2007). However, the aetiology of NTDs in the *ct* mouse is likely to differ from that in either the *Grhl3* knockout or overexpression mutants, and is described in greater detail in **Section 1.5.1**.

The genetic studies demonstrate that neither of these transcription factors are required for Closure 1, while only *Grhl2* is required for closure 3. *Grhl3* is required in the thoracic region of the neural tube, while both transcription factors mediate PNP closure in the lumbosacral region (Rifat et al. 2010). Genetic complementation studies appear to suggest that at least in PNP closure, the overexpression of *Grhl2* or *Grhl3* can compensate for the under-expression of the other Grhl gene (N. Greene; personal communication).

The Grhl family of transcription factors are known to be important regulators of epidermal development and influence epidermal barrier formation and wound healing, but their role in mammalian neural tube closure has remained elusive. Recently, *Grhl2* was reported to be required for the promotion of epithelial character and suppression of epithelial-to-mesenchymal transition. Loss of *Grhl2* resulted in loss of surface ectoderm integrity and increased cell movements *in vivo*,

and led to the appearance of mesenchymal morphology and behaviour in IMCD-3 cells *in vitro* (Ray and Niswander 2016). *Grhl3* was reported to be a downstream effector of Wnt signalling driving uncommitted progenitor cells into surface ectoderm fates at the surface ectoderm-neuroepithelial border (Kimura-Yoshida et al. 2015). The NTDs displayed by the mouse mutants are severe, with the neural folds appearing not to appose properly. Live imaging of cranial neurulation in *Grhl2* null mouse mutants demonstrate a lack of movement of the whole neuroepithelium when compared to wild-types (Ray and Niswander 2016). How the single celled surface ectoderm mediates these tissue dynamics, and how loss of surface ectoderm cell number or character can stall these movements is to be elucidated.

1.3.4 Caudalising factors

The neural plate appears to have anterior forebrain character as a default, with RA, Wnt and FGF, which are known as caudalising factors, required for formation of the: caudal forebrain, midbrain and anterior hindbrain (Wnts); posterior hindbrain and cervical spinal cord (RA); and posterior spinal cord (FGF). Mice null for some components of these signalling pathways are found to exhibit NTDs; the open regions coinciding with areas of pathway activation and influence.

1.3.4.1 Retinoic acid signalling

In neurulation stage mouse embryos, RA is synthesised by RALDH2 in the presomitic mesoderm of the hindbrain and the newly forming somites (Maden 2006). RA is a small lipophilic molecule able to diffuse across cell membranes. Signalling is initiated when RA binds heterodimers of RA receptors (RARs) and retinoid X receptors (RXRs), which then binds to RA response elements (RAREs) and recruit co-activators to drive target gene transcription. In absence of RA, RAR/RXR recruit co-repressors. Both deficiency and excess of RA is associated with developmental malformations, and *in vivo*, RA levels are controlled by tissue specific degradation via the cytochrome P450 family of metabolising enzymes (Rhinn & Dolle 2012).

RA from the paraxial mesoderm is required for correct specification of the posterior hindbrain and cervical spinal cord (Diez del Corral and Storey 2004; Rhinn and Dolle 2012). Studies from chick and mouse have demonstrated that *Pax6* and *Dbx1/2* are downstream targets of RA (Pierani et al. 1999; Molotkova et al. 2005). Both *Pax6* and *Dbx1/2* are patterning transcription factors whose expression is inhibited by both high Shh and BMP signalling (Pierani et al. 1999; Timmer, Wang, and Niswander 2002; Novitch et al. 2003), which positions them in the intermediate region between the floorplate and roofplate.

RA signalling and Shh signalling are found to integrate at multiple levels. In *Raldh2* null mice, RA was found to be required for robust expression of Shh protein in the floorplate (*Shh* mRNA was not changed; Ribes et al. 2009). RA signalling also integrates with Shh signalling through modulation

of Gli expression; *Gli1* expression is reduced in *Raldh2* null mice while *Gli2* expression is increased (Ribes et al. 2009). Additionally, both RA and Shh signalling regulate early *Ngn2* expression via RAREs and a Gli binding site (Ribes et al. 2008). The *Raldh2* null mice display reduced *Ngn2* and reduced spinal neuron differentiation (Ribes et al. 2009). RA is believed to be required for induction of neurogenesis throughout the whole spinal cord.

Mouse mutants demonstrate that both excessive and insufficient RA signalling can interfere with neural tube closure, and suggest the importance of sufficient RA signalling in the rostral embryo, but reduced signalling in the caudal embryo. Mice null for *Raldh2* fail to turn, present with extreme truncation from the cervical region and an open neural tube from the hindbrain to spinal levels at E10.5, along with other defects (Niederreither et al. 1999). Additionally, double knockouts for the RA receptors, *Rara* and *Rarg*, exhibit hindbrain exencephaly (Lohnes et al. 1994). Meanwhile, mice null for the RA degrading enzyme *Cyp26a1* displayed varying phenotypes of caudal truncation from the hind limb, nearly always present with spina bifida. A few females also exhibited exencephaly (Abu-Abed et al. 2001).

1.3.4.2 Fibroblast growth factor signalling

The requirement for FGF signalling during neural tube formation has been studied most in chick, and particularly in respect to *Fgf8* expression. In both chick and mouse, *Fgf8* is expressed in a relatively small domain at the hindbrain-midbrain boundary, where it appears to have organiser function for midbrain structures (Liu and Joyner 2001). It is also expressed in a relatively large domain called the caudal stem zone where the primitive streak is regressing and NMPs are believed to reside, as well as the surrounding unsegmented mesoderm (Lee et al. 1997; Diez del Corral and Storey 2004). There is growing evidence that FGF signalling is required to sustain the stem zone, by maintaining its integrity and inhibiting differentiation (Mathis, Kulesa, and Fraser 2001).

FGF signalling and RA signalling are found to be mutually repressive (Ribes et al. 2009; Diez del Corral et al. 2003), and as RA acts as an instigator of neural patterning and differentiation, FGFs act to maintain the proliferative, unpatterned and undifferentiated state of the neuroepithelium. FGFs appear to also inhibit the Shh signalling pathway (Morales et al. 2016; Novitch et al. 2003). But as the presomitic mesoderm undergoes somitogenesis and begins to express RA, *Fgf8* expression is inhibited, and the adjacent neural tube comes under the influence of RA signalling (Diez del Corral, Breitkreuz, and Storey 2002).

The importance of FGF signalling in caudal neural tube closure is highlighted by the development of fully penetrant spina bifida in mice genetically ablated for FGF receptor 1 α (*Fgfr1a*; Xu et al. 1999). Of note, no somites were visible caudal to the forelimb bud and the distal spinal cord was truncated and malformed. These mice, along with the mutants of RA signalling may suggest that correct posterior mesoderm development is required for closure of the PNP.

1.3.4.3 Canonical Wnt signalling

Canonical Wnt signalling involves the binding of Wnt ligands to Frizzled (Fz) receptors and Lrp5/6 co-receptors with downstream activation of disheveled (Dvl). Activated Dvl prevents degradation of β -catenin via a multiprotein complex including APC, Axin, GSK3 and CK1. This allows β -catenin to accumulate, and results in its translocation to the nucleus and activation of the TCF/LEF family of transcription factors and target gene expression, one of which is *Axin* for negative feedback regulation. Of note, both the Fz and Lrp6 receptors function in PCP signalling also (Gray et al. 2013).

In the midbrain-hindbrain boundary, *Wnt1* and *Fgf8* are part of a positive regulatory loop which reinforces and maintains their overlapping expression; loss of either factor results in loss of midbrain structures (Raible and Brand 2004). In the caudal stem zone area, *Wnt3a* is expressed in a domain largely overlapping with that of *Fgf8*, and together with *Wnt8a*, appears to be upstream of *Fgf8* and required for *Fgf8* expression and hence, NMP maintenance (Cunningham et al. 2015).

Additionally, *Wnt1* and *Wnt3a* are expressed throughout most of the dorsal neural tube where they are mitogenic (Megason and McMahon 2002) and implicated in dorsoventral patterning. In both mouse and chick, it appears that dorsal β -catenin signalling induces expression of *Gli3^{REP}*, and therefore antagonises Shh signalling in the dorsal half of the neural tube (Alvarez-Medina et al. 2008; Yu et al. 2008). Also, the secreted Wnt pathway inhibitor protein *sFRP2* is expressed in the ventral neural tube and blocks canonical Wnt signalling mediated by *Tcf4*. This action was shown to set the dorsal boundary of the p3 domain patterning transcription factor *Nkx2.2* (Figure 1.5; Lei et al. 2006). Furthermore, mice expressing a stabilised version of β -catenin in mosaic fashion in the ventral neural tube saw the expression of dorsal patterning transcription factors, such as *Pax7* and *Msx1/2*, expressed in the ventral neural tube, while *Dbx1* expression in the intermediate region was reduced. *Gli3* was found to be partially responsible for repression of ventral fates in response to β -catenin, and loss of β -catenin signalling promoted the ventral most fates (Yu et al. 2008).

Deregulation of canonical Wnt signalling can result in NTDs, but which events of neural tube closure are sensitive to Wnt signalling is not clear. Mice with null mutations in negative regulators of the pathway present with varying loss of anterior forebrain structures and in some, infrequent NTDs. Mice genetically ablated for the negative regulator *Ctnnbip1* (*ICAT*), display exencephaly and split face with 15 % penetrance (Satoh et al. 2004). Additionally, a mutation resulting in expression of a dominant negative protein of *Axin1* also resulted in exencephaly and spina bifida, in 10 % and 30 % of mutants respectively (Theiler and Gluecksohn-Waelsch 1956; Zeng et al. 1997).

Lastly, insufficiency of canonical Wnt signal can also result in a failure of spinal neurulation. Loss of β -catenin in the dorsal neural tube resulted in reduced *Pax3* and *Cdx2* expression (Zhao et al.

2014). *Pax3* expression is required for neural tube closure and the conditional mouse mutants present with fully penetrant spina bifida. The *Pax3* null mouse, *Splotch*, is described in **Section 1.5.2**. *Wnt3a* null mice often fail to achieve spinal neural tube closure (Takada et al. 1994), as do *Lef1*; *Tcf1* double null mutants (Galceran et al. 1999). However, this failure is accompanied by extreme morphological mispatterning of the mesoderm caudal to the forelimb bud, with ectopic neural tissue forming instead of somites (Yoshikawa et al. 1997). Therefore, as with the severe disruptions seen in RA and FGF signalling mouse mutants, failure of closure could be more of a secondary consequence.

1.4 Environmental factors influence rates of NTDs

To date, a range of environmental factors have been associated with an increased risk of having a NTD affected pregnancy, while periconceptional folic acid supplementation is currently the only proven factor which decreases risk (**Table 1. 1**). Factors that contribute towards the risk of having an NTD affected pregnancy will be briefly discussed first, followed by the prevention via folic acid supplementation, together with folate deficiency.

Environmental factor	Influence	Proposed mechanism
<i>Maternal nutrition</i>		
Folic acid supplementation	Decreased	Increased folate one-carbon metabolism
Folate insufficiency	Increased	Disturbed folate one-carbon metabolism
Cobalamin insufficiency	Increased	Disturbed folate one-carbon metabolism
<i>Maternal health</i>		
Maternal hyperthermia	Increased	Unknown
Maternal diabetes	Increased	Increased reactive oxygen species, apoptosis, epigenetic changes & unknown
Maternal obesity	Increased	Unknown
<i>Maternal medication</i>		
Carbamazepine (epilepsy drug)	Increased	Inhibition of cellular folate uptake
Trimethoprim (antibiotic)	Increased	Disturbed folate one- carbon metabolism
Valproic acid (epilepsy drug)	Increased	Inhibition of histone deacetylase activity
<i>Others</i>		
Fumonisin (fungus)	Increased	Disturbed sphingolipid synthesis

Table 1. 1. Environmental factors affecting risk of NTDs

1.4.1 Factors which contribute towards risk of NTDs

The increase in risk associated with cobalamin (vitamin B₁₂) insufficiency is possibly explained by its requirements by the FOCM enzyme MTR (**Figure 1. 7**; Ray and Blom, 2003; Ray *et al.*, 2007), however, just as the precise mechanism of folic acid prevention and folate insufficiency is unknown (**Section 1.4.2.1**), exactly how cobalamin deficiency increases risk of NTDs remains to be better understood.

Both the anti-convulsion drug carbamazepine and the antibiotic trimethoprim are folate antagonists and their use during pregnancy is found to increase the risk of having an NTD affected foetus (Hernandez-Diaz *et al.* 2001). Valproic acid, another anti-convulsion drug, is found to be a potent histone deacetylase inhibitor which is reported to increase the risk of having an affected pregnancy by more than 10-fold (Lammer, Sever, and Oakley 1987; Gurvich *et al.* 2005), possibly due to misregulation of gene expression. Another histone deacetylase inhibitor, Trichostatin A, can induce NTDs in chick (Murko *et al.* 2013).

Fumonisin is a mycotoxin produced by a common contaminant of maize that inhibit ceramide synthase, causing the accumulation of intermediates, and depletion of glycosphingolipid end products (Marasas *et al.* 2004). Of interest, this depletion of sphingolipids was found to impair trafficking and membrane localisation of the glycosylphosphatidylinositol (GPI)- anchored folate receptor, and can induce exencephaly in mice. Furthermore, folate supplementation was found to reduce the incidence of fumonisin induced NTDs by nearly half, while supplementation with gangliosides (molecule composed of ceramide, oligosaccharide and sialic acids) reduced the incidence by approximately 95 % (Gelineau-van Waes *et al.* 2005). There is evidence that fumonisin may also via G-protein coupled receptors (GPCRs) which have sphingolipid ligands act to induce NTDs (Gelineau-van Waes *et al.* 2012).

Maternal diabetes predisposes to multiple birth defects including NTDs, and may involve a range of mechanisms such as increased oxidative stress, hypoxia, apoptosis and epigenetic changes (Ornoy *et al.* 2015). Maternal obesity is also a risk factor (McMahon *et al.* 2013), and may act via glycaemic dysregulation, while reports also suggest that maternal hyperthermia, such as from fever or sauna usage, also increases risk (Suarez, Felkner, and Hendricks 2004).

1.4.2 The preventative effect of folic acid supplementation

Folic acid is a synthetic folate (vitamin B₉) that is converted into its bioactive form in cells. How maternal nutrition became recognised as centrally important to both foetal development and long term adult health is summarised to date in brief with respect to NTDs.

1.4.2.1 The past and present of folic acid supplementation

Mammalian maternal nutrition as an important factor in the development of birth defects was first conclusively reported between 1933 and 1937 by Fred Hale, who mated female pigs maintained on a vitamin A deficient diet to males maintained on a normal diet. Defects described in the offspring include: anophthalmia; microphthalmia; harelip; cleft palate; accessory ears; otocleisis; malformed hind legs; unascended kidneys; ectopic ovaries; cryptorchidism and subcutaneous cysts; never all in the same animal. Supplementation of female pigs on the vitamin A deficient diet with cod liver oil, a good source of vitamin A, resulted in all normal offspring (Hale 1933, 1935, 1937). Subsequently, insufficiencies of riboflavin, pantothenic acid, vitamin E and folates, via dietary restriction, sometimes together with antagonists, were all demonstrated to produce developmental defects in mammals (reviewed in Kalter & Warkany 1959).

The Dutch famine of 1944, which began in November 1944 and lasted until May 1945, gave one of the first indications that maternal nutrition may also be an important factor in the development of human foetuses. As was found in animal studies, the effects of undernutrition depended upon the gestational stage under exposure; only foetuses subjected to undernutrition during early development showed an increase in the prevalence of NTDs. Also, NTDs were more commonly associated with socioeconomically disadvantaged families, but other factors apart from undernutrition could factor into this.

In 1964, Hibbard presented a study following a cohort of pregnant women in Liverpool, where the link between folate deficiency, megaloblastic anaemia, abruptio placentae, spontaneous abortion and foetal malformations was investigated. The study found that the incidence of foetal malformations in patients with excessive formiminoglutamic acid (FIGLU) excretion, a sensitive test where excess excretion indicates folate deficiency, were twice that of patients with normal FIGLU excretion, although the results were not significant (B. M. Hibbard 1964). The following year, the same group reported that 69 % of mothers with a pregnancy affected by CNS malformations had excessive FIGLU excretion, while 17 % of mothers with normal pregnancies exhibited excess FIGLU excretion. Both groups were matched for age, parity and time of conception (Hibbard and Smithells 1965).

During the 1970s, Smithells and colleagues studied maternal nutrition during pregnancy according to social classes and in mothers of foetuses affected by CNS malformations. As well as finding higher levels of red blood cell folate, vitamin C, riboflavin and vitamin A in mothers from the top social classes compared to all other groups, they also found mothers affected by CNS malformation pregnancies to have significantly lower red blood cell folate compared to the control group (Smithells, Sheppard, and Schorah 1976). Subsequently, Smithells and colleagues conducted a preliminary, multicentre, intervention trial recruiting women who had already had an NTD affected pregnancy and were planning another in the UK. The women were given a mixture of vitamins,

including folic acid, to take periconceptionally. Significantly, only 1 out of 178 (0.6 %) supplemented mothers had an affected pregnancy while 13 out of 260 (5.0 %) unsupplemented mothers had an NTD affected pregnancy (Smithells et al. 1980). This trial was later expanded to include ‘partially supplemented’ women and some more unsupplemented controls, but the overall results and conclusion were not changed (Smithells et al. 1981). A second intervention trial recruiting women who had already had at least one NTD affected pregnancy was conducted with a similar outcome; recurrence rates were 0.9 % for 234 fully supplemented pregnancies compared with 5.1 % for 215 unsupplemented pregnancies (Smithells et al. 1983).

This work lay the foundation for an international, multicentre, double-blind, randomised trial conducted by the Medical Research Council, UK (MRC), involving 1817 women. Importantly, this trial had a separate folic acid supplementation (4 mg) group and multivitamin (vitamins: A; B₁; B₂; B₆; C and D) group, as well as the unsupplemented control groups. The trial was launched in July 1983 and was prematurely halted by April 1991 because the protective effect of folic acid supplementation (72 %) was significant, while the multivitamin supplement which excluded folic acid showed no protection (Wald et al. 1991). Shortly after, in December 1992, Czeizel & Dudas (1992) published their randomised clinical trial which looked at the first occurrence of NTDs. Women planning pregnancy were randomly assigned to either take a multivitamin supplement, which contained 0.8 mg of folic acid together with 12 other vitamins, or a supplement containing trace elements. Of the 2104 pregnant women who received the vitamin supplement, none presented with NTDs, while of the 2052 pregnant women who received the trace-elements supplement, there were 6 cases of NTDs.

These studies were conclusive evidence that periconceptional folic acid supplement prevented NTDs. In 1995, Daly et al. reported a dose-response relationship between erythrocyte folate and risk of an NTD affected pregnancy, with concentrations over 906 ng/ mL providing significant protection, which has since been corroborated by another study (Crider et al. 2014). This led to the recommendation that women planning pregnancy should receive 0.4 mg of folic acid daily; women who had already had an affected pregnancy were advised to take 4 mg of folic acid daily. While the governments of the United Kingdom and United States and other countries began recommending that all women of childbearing age receive 0.4 mg of folic acid per day, compliance was universally low, and in the case of unplanned pregnancies, unachievable. In 1998, the United States became the first country to introduce mandatory fortification of enriched cereal grain products with folic acid. Canada (1998), Costa Rica (1998) and Chile (2000) swiftly introduced mandatory fortification programs of their own; to date, 86 countries operate mandatory fortification of some type of grain product (The Food Fortification Initiative 2016).

As expected, there have been many studies which have assessed the rates of NTD affected pregnancies before and after fortification in various different countries. In the United States, serum folate levels were found to increase 136 %, while erythrocyte folate concentrations increased 57 %,

in all sex and age groups (Dietrich, Brown, and Block 2005), while rates of NTD cases reduced by approximately 27 % (Williams et al. 2005). Of interest, there was a greater preventative effect against spina bifida (31 %) compared to anencephaly (23 %). Additionally, the extent of prevention was found to vary by race/ ethnicity, with Hispanic women experiencing the greatest prevention (36 %), followed by non-Hispanic white women (34 %) and then non-Hispanic black women (15 %; borderline significance; Williams et al. 2005). Of particular interest, the level of prevention correlated with the rate of NTDs pre-fortification within the race/ ethnic groups i.e. Hispanic women had the highest rates of NTD cases before fortification and saw the highest prevention after.

In general, this correlation between highest rates and greatest prevention has also been noted in regional variances pre and post fortification in Canada (Eichholzer, Tonz, and Zimmermann 2006), South America (Rosenthal et al. 2014) and South Africa (Sayed et al. 2008). Globally, it has been estimated that folic acid fortification has decreased the rates of NTDs by 46 % (Blencowe et al. 2010), and a recent systematic review and meta-analysis found countries with a mandatory fortification program experienced 33 % lower rates of spina bifida compared to unfortified countries (Atta et al. 2016). However, it has become clear that folic acid supplementation, through pills or fortification, cannot prevent all NTD cases; there appears to be a floor, which at its lowest is around 4 affected pregnancies per 10,000 pregnancies, which folic acid supplementation does not decrease further (Heseker et al. 2009). Additionally, evidence suggests that increased folic acid supplementation above the levels reached by current fortification will not confer more protection against NTDs in the United States (Mosley et al. 2009). It appears that while the majority of NTD cases are sensitive to folic acid supplementation, especially in populations with high prevalence, there is a significant minority that are folic acid resistant.

Exactly how folic acid prevents NTDs has not been fully explained. The question of whether it is a simple case of correcting existing folate deficiency has been raised, and while studies continue to find an association between low folate status and risk of an NTD affected pregnancy (Kirke et al. 1993; Steegers-Theunissen et al. 1994; Mills et al. 1995; B. Christensen et al. 1999; Candito et al. 2008), most women with affected pregnancies present with a folate status that is within the normal range (Scott 1999; Kirke et al. 1993). This suggests that while low folate status is a risk factor, it is unlikely to be causative by itself; not all women with folate deficiency will have an NTD affected pregnancy and a normal folate status doesn't ensure against an affected pregnancy.

It is, however, highly likely that prevention via folic acid, a synthetic folate, is mediated through modulation of folate one-carbon metabolism (FOCM) and the products of this pathway, which is described below.

1.4.2.2 Folate one-carbon metabolism

FOCM is found in virtually every cell and organism and comprises a large network of enzymes which mediate transfer of a one-carbon moiety from one cofactor to another, in a chain of reactions which eventually sees the one-carbon unit transferred to form a terminal product. The cofactors required for FOCM are called folates. While FOCM appears almost ubiquitous, not all components are expressed in every tissue and expression can change during development. An overview of FOCM is given below.

1.4.2.2.1 Main outputs

FOCM takes one-carbon units from amino acids, and their derivatives, for *de novo* nucleotide biosynthesis, methyl group biosynthesis, polyamine biosynthesis and also produces redox equivalents and cysteine for glutathione synthesis (**Figure 1. 7**). This pathway is therefore vital for many cellular processes, such as proliferation, genome maintenance, epigenetic stability, protein and lipid synthesis, amino acid metabolism and redox homeostasis.

Aberrant proliferation has been implicated in the aetiology of NTDs by genetic mouse mutants as outlined in **Section 1.3.2** and also in the *ct* strain (**Section 1.5.1**). Additionally, the anti-mitotic agent, hydroxyurea, is found to induce exencephaly in ~30 % of *wild-type* mouse embryos (Guan et al. 2015). Meanwhile, the requirement for methyl group biosynthesis is implicated by NTDs in the *Dnmt3b* null mouse (Okano et al. 1999), and the finding that cobalamin insufficiency is associated with an increased risk of an NTD affected pregnancy in folic acid supplemented populations (Ray et al. 2007). Aberrant methylation could affect protein function and gene expression.

1.4.2.2.2 Folate cofactors

Folates cannot be synthesised by animals and so must be obtained from diet or supplements. Good dietary sources for humans include beans and lentils, and green vegetables including spinach, from where folate was first isolated, asparagus and broccoli. Chemically, a folate is composed of a 2-amino-4-oxo-6-methylpteridine ring, a ρ -aminobenzoic acid moiety and a polyglutamate tail (**Figure 1. 6**).

The major dietary form of folate is 5-methyltetrahydrofolate (5-methylTHF; Zhao et al. 2009). This is also the major form in which folates are transported around the mammalian body via the blood circulation. 5-methylTHF is a so-called activated or reduced folate which is ‘charged’ with a one-carbon unit. Folates can carry one-carbon units on positions N⁵ and/ or N¹⁰; the other major ‘charged’ folates being: 5-formylTHF; 10-formylTHF; 5,10-methenylTHF and 5,10-methyleneTHF. The form which acts as the first one-carbon acceptor is 5,6,7,8-THF (THF), while

the non-activated or oxidised synthetic folate, folic acid, is converted to the endogenous non-activated folate, 7,8-dihydrofolate (DHF), *in vivo*. DHF must be converted to THF in order to accept one-carbon units. 5-formylTHF is believed to act as a cellular storage of folates and not partake in biosynthesis (Field, Szebenyi, and Stover 2006). Folic acid is a synthetic folate used in supplements which has greater stability than any of the naturally occurring folates. The structure and main forms of folates are shown in **Figure 1. 6**.

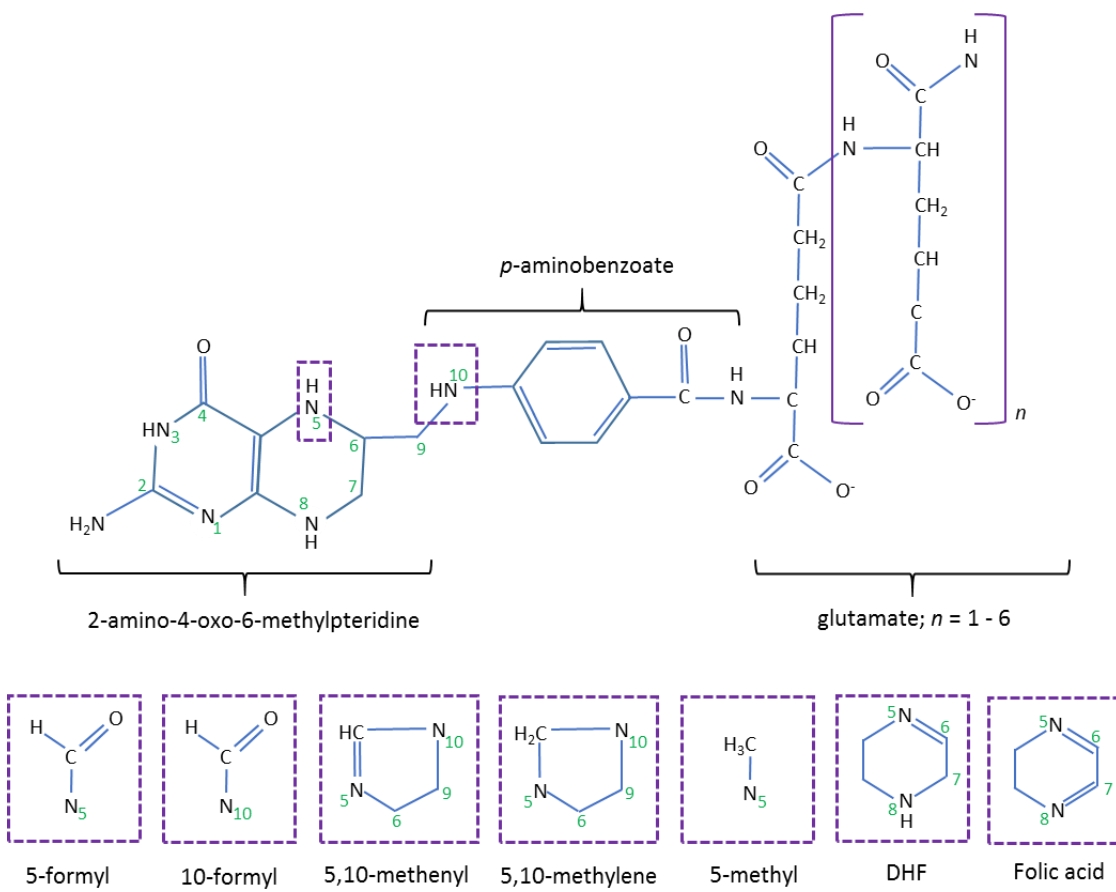


Figure 1. 6. The structure of folates.

The structure of THF is shown in full. One-carbon units can be carried on N^5 and N^{10} of the molecule, as indicated by the broken purple boxes. The changes in molecular structure which occur once THF picks up a one-carbon unit are shown for the naturally occurring folates (5-formyl, 10-formyl, 5,10-methenyl, 5,10-methylene and 5-methyl), along with the naturally occurring deactivated folate, DHF, and the synthetic folate, folic acid. Folates carry between 1 – 7 glutamate residues linked via γ linkage. Based on diagrams from: Blom et al. (2006) and Tibbetts & Appling (2010).

1.4.2.2.3 Uptake of folates

Dietary and cellular forms of folates contain chains of poly- γ -glutamate residues, the addition of which is catalysed by the enzyme folypolyglutamate synthetase (FPGS). The polyglutamate tails prevent folates from being transported across membranes, therefore folates (largely 5-methylTHF) must be hydrolysed, by glutamate carboxypeptidase II (GCPII) in humans and γ -glutamyl hydrolase (γ -GH) in rodents (Shafizadeh and Halsted 2007), and converted into their monoglutamated form in the intestinal lumen so they can be taken up by intestinal enterocytes, primarily via proton-coupled folate transporters (PCFR; Qiu et al. 2006). Folic acid does not contain a polyglutamate tail and is taken up without the need for hydrolysis, but it must be converted into 5-methylTHF, via DHF, for release into the circulation. In general, after intestinal absorption, folates are transported to the liver via the hepatic portal system. Folates which enter the liver can either be taken up and stored, secreted into bile which returns them back to the intestine, or enter systemic circulation via the hepatic portal vein (Zhao, Matherly, and Goldman 2009).

5-methylTHF in the systemic circulation enters cells via the ubiquitously expressed, organic anion antiporter, the reduced folate carrier (RFC; SLC19A1) and also via endocytosis mediated by high-affinity folate receptors (FR) α and β , which show tissue specific expression. FR α (FOLR1 in mice) tends to be expressed at epithelial surfaces, while FR β (FOLR2 in mice) in haematopoietic tissues (Zhao et al. 2011). In mouse, it has been shown that FOLR1 is expressed by the closing neuroepithelium and along with LRP2, is required for complete neural tube closure (Saitsu et al. 2003; Kur et al. 2014). Intracellular folates are then re-polyglutamated by FPGS to ensure retention. Polyglutamate tails can contain between 1 – 7 glutamate residues depending on the cell type and subcellular location, however penta- and heptaglutamate are the major forms in eukaryotic cells, and these forms confer maximum efficiency to the folate-dependant enzymes (Tibbetts and Appling 2010).

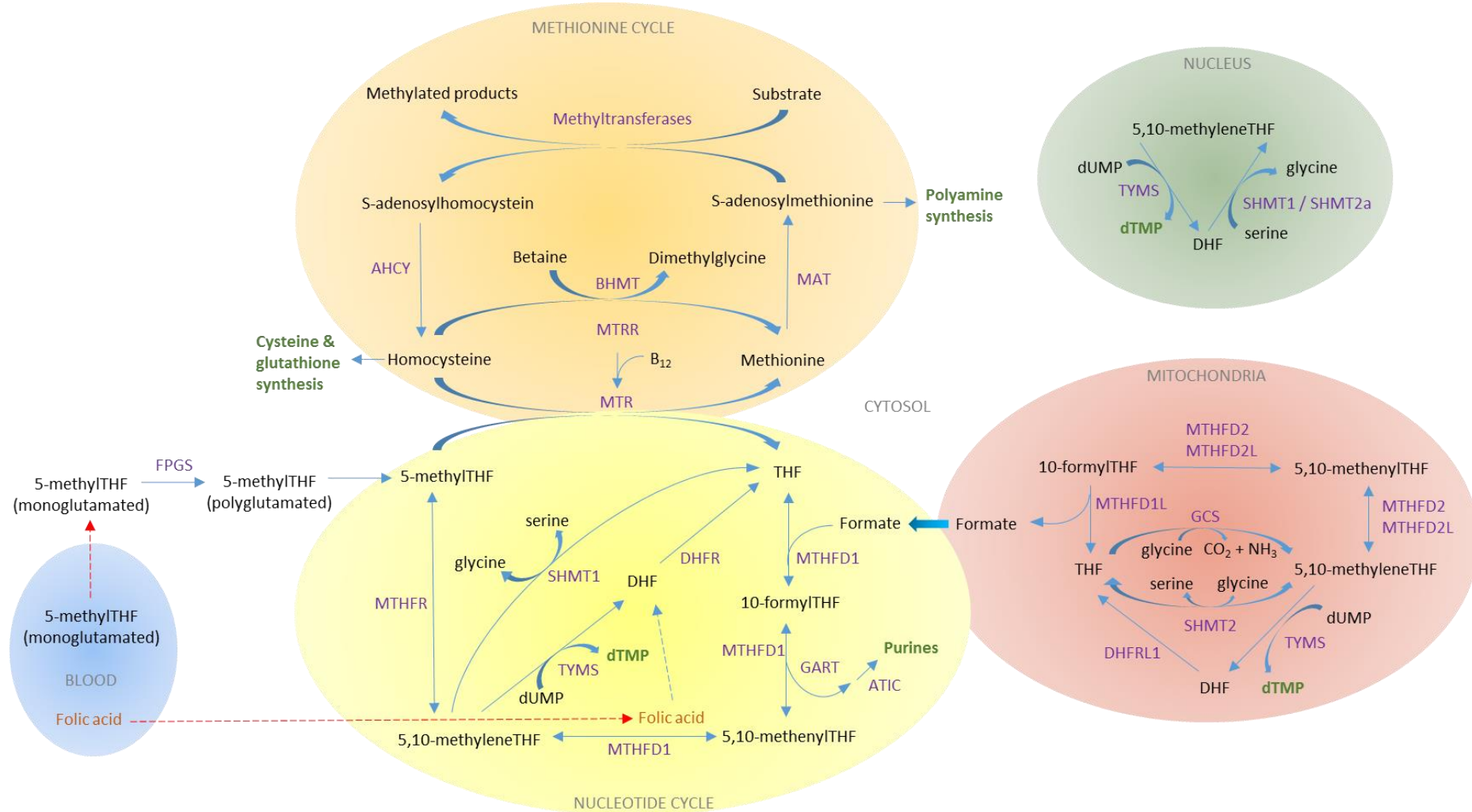


Figure 1. 7. Representation of the main synthesis pathways of folate one-carbon metabolism.

Figure 1. 7. Representation of the main synthesis pathways of folate one-carbon metabolism.

Folates, in the form of 5-methylTHF or folic acid, are transported through the blood (blue shading). Once 5-methylTHF enters cells, it is polyglutamated to allow retention. All folates which take part in FOCM (yellow, red and green shading) are polyglutamated. As a synthetic folate, folic acid is not polyglutamated, but enters FOCM via conversion to DHF. In the mitochondria (red shading), one-carbon units are obtained for the production of formate, which then leaves mitochondria and enters the cytosol and the *de novo* nucleotide cycle (yellow shading). One-carbon units are also used to produce thymidylate (dTMP; green writing denotes major outputs of FOCM) in mitochondria, presumably for mitochondrial DNA synthesis. In the cytosol, the one-carbon unit of formate, and from serine, can be used for purine and thymidylate synthesis. 2 moles of 10-formylTHF are required to produce each purine nucleotide, via the enzymes GART and ATIC. One-carbon units not used for *de novo* nucleotide synthesis enter the methionine cycle (orange shading) via 5-methylTHF. Vitamin B₁₂ is required for conversion of homocysteine to methionine. The methionine cycle provides for polyamine synthesis and for the methylation of nearly all macromolecules such as proteins, lipids, DNA and RNA, and allows methionine to be converted to cysteine and glutathione. The enzymes for thymidylate synthesis translocate to the nucleus (green shading) during S-phase of the cell cycle, most likely to prevent uracil misincorporation. Adapted from: Copp et al. (2013) and Field et al. (2006).

1.4.2.2.4 Pathway overview

FOCM is composed of two interconnected, cyclic pathways; the folate cycle and the methionine cycle (**Figure 1. 7**). While the components of the methionine cycle are entirely cytosolic, the folate cycle has components in the mitochondria and nucleus, as well as the cytosol. The folate cycle has seven main points of input for one-carbon units: four in the mitochondria, via serine hydroxymethyltransferase (SHMT) 2, the glycine cleavage system (GCS), dimethylglycine dehydrogenase and sarcosine dehydrogenase; and three in the cytosol via SHMT1, formimidoyltransferase-cyclodeaminase (FTCD) and methylenetetrahydrofolate dehydrogenase (MTHFD) 1 (Ducker and Rabinowitz 2017). While an input for one-carbon units via betaine homocysteine S-methyltransferase (BHMT) in the methionine cycle has been depicted (**Figure 1. 7**), its expression in mammals is restricted to the liver and kidneys (Sunden et al. 1997).

It is noteworthy that while SHMT1 is considered cytosolic and SHMT2 mitochondrial, the *SHMT2* gene produces two transcripts, one which targets the protein to mitochondria, and an alternative transcript with no targeting sequence which leads to cytosolic expression. Cytosolic SHMT undergoes sumoylation and nuclear import during S-phase of the cell cycle (Anderson and Stover 2009). Both SHMT1 and SHMT2 catalyse the same reversible reaction, the transfer of C³ from serine to THF to produce 5, 10-methyleneTHF and glycine. The SHMT enzymes also catalyse the irreversible conversion of 5,10-methyleneTHF to 5-formylTHF (reaction not depicted in **Figure 1. 7**), which is believed to function as a store of folates (Field, Szebenyi, and Stover 2006).

The mitochondria and cytosol also both catalyse the reversible reactions interconverting: 5,10-methyleneTHF and 5,10-methenylTHF, and 5,10-methenylTHF and 10-formylTHF. However, the cytosolic and mitochondrial enzymes which catalyse these reactions are encoded by different genes, which, because of their location, utilise different redox cofactors in the cytosol and mitochondria; nicotinamide adenine dinucleotide (NAD) and nicotinamide adenine dinucleotide phosphate (NADP) respectively. The ratio of high reduced to oxidised NAD (NADPH/ NAD⁺) maintained in the cytosol favours reductive processes, while the high ratio of oxidised to reduced NADP (NADP+/ NADPH) and adenine diphosphate to adenine triphosphate (ADP/ ATP), favours oxidative processes (Pelletier and MacKenzie 1995). Mitochondrial FOCM, therefore, obtains one-carbon units from one-carbon donors, primarily serine and glycine, via SHMT2 and the GCS respectively, and converts THF to 5,10-methyleneTHF. 5,10-methyleneTHF is converted to 5,10-methenylTHF, which is then converted to 10-formylTHF. The enzymes which catalyses these two conversions during development is the bifunctional MTHFD2; in adult tissue, it is catalysed by the bifunctional parologue MTHFD 2-like (MTHFD2L). Both enzymes possess methyleneTHF dehydrogenase and methenylTHF cyclohydrolase capabilities. Lastly, the one-carbon unit is either cleaved from 10-formylTHF by MTHFD 1-like (MTHFD1L) and released as formate, or it is cleaved by 10-

formylTHF dehydrogenase (FDH; also known as ALDH1L2) and released as carbon dioxide (CO₂; reaction not depicted in **Figure 1. 7**). THF is regenerated by both reactions to begin the cycle again. In another fate, the one-carbon unit from 5,10-methyleneTHF can be transferred to deoxyuridine monophosphate (dUMP) to generate deoxythymidine monophosphate (dTMP; also known as thymidylate), a reaction catalysed by mitochondrial thymidylate synthase (mTYMS). The folate produced from this transfer, DHF, is converted to THF by DHF reductase-like 1 (DHFRL1).

While CO₂ is a terminal end product of one-carbon group oxidation, formate is quickly transported from the mitochondria to the cytosol where it can act as a one-carbon donor for cytosolic FOCM. Formate is combined with THF to form 10-formylTHF by the 10-formylTHF synthetase activity of the trifunctional enzyme MTHFD1. Cytosolic 10-formylTHF is used for *de novo* purine synthesis, with 2 one-carbon moieties required per purine nucleotide. Alternatively, 10-formylTHF can be converted to THF and CO₂ by ALDH1L1 (reaction not depicted in **Figure 1. 7**), or can be converted to 5,10-methenylTHF, which is converted to 5,10-methyleneTHF. These conversions are catalysed by the methyleneTHF dehydrogenase and methenylTHF cyclohydrolase activities of MTHFD1. 5,10-methyleneTHF represents an important branch point in FOCM; it can pass its one-carbon unit to dUMP for thymidylate synthesis via cytosolic TYMS (cTYMS), or to glycine for serine synthesis via SHMT1. This scenario is the opposite of that outlined in mitochondrial FOCM and constitutes the reductive pathway. Alternatively, 5,10-methyleneTHF can be irreversibly converted to 5-methylTHF by methyleneTHF reductase (MTHFR), an enzyme only present in the cytosol. The only fate of 5-methylTHF is transfer of the one-carbon unit to the methionine cycle, which begins with methylation of homocysteine for synthesis of methionine, and is catalysed by the cobalamin (vitamin B12) dependant enzyme methionine synthase (MTR).

Having entered the methionine cycle with conversion of homocysteine to methionine, the enzyme methionine adenosyltransferase (MAT) catalyses the addition of a S-adenosyl moiety to methionine with synthesis of S-adenosylmethionine (SAM). SAM is a universal methyl group donor and is used for the methylation of proteins, RNA, DNA and lipids. Transfer of the methyl group by methyltransferases converts SAM to S-adenosylhomocysteine (SAH), which is converted to homocysteine by adenosylhomocysteinase. Homocysteine can either enter the trans-sulphuration pathway which synthesises cysteine and glutathione, or can be remethylated by 5-methylTHF. Alternatively, SAM can be used for polyamine synthesis.

It is worth noting that as 5-methylTHF is the major species in circulation, after entering a cell, it transfers its one-carbon unit to the methionine cycle to generate THF which can then accept new one-carbon units and take part in the other FOCM processes. However, this does not appear to be a major route of entry for one-carbon units into the cycle; serine and glycine catabolism in the

mitochondria are the most significant one-carbon donors (Davis et al. 2004; Kikuchi et al. 2008; Tibbetts and Appling 2010).

As all the FOCM enzymes are nuclear encoded, the presence of folates in the mitochondria requires the existence of folate transporters. The transporter, called the mitochondrial folate transporter (MFT; SLC25A32), was first isolated in the human genome (Titus & Moran 2000). It is believed to be the only mitochondrial transporter for folates in mammals, but to date, a study of this transporter's tissue distribution or developmental expression has not been reported, and the exact species which are transported *in vivo* is an unresolved question. Evidence to date suggests reduced, monoglutamated forms cross the mitochondrial inner membrane via carrier-mediated transport, and are then polyglutamated by the mitochondrial splice variant of FPGS (Chen et al. 1996). Studies also suggest that there is limited flux between the cytoplasmic and mitochondrial compartments with protection of mitochondrial pools (Horne et al. 1989; Trent et al. 1991). There is also transport of the one-carbon donors into and out of the mitochondria, through as yet undefined transporter systems. Formate, in particular, is toxic to mitochondria and exported to the cytosolic efficiently (Lamarre et al. 2012).

1.4.2.2.5 Placental transport

Embryos must obtain folates, namely 5-methylTHF, from the maternal circulation, necessitating placental folate transport. It is known that FR α , FR β , PCFR and RFC are all highly expressed on the maternal side of the placenta to facilitate transport to the embryonic circulation in humans and rodents (Zhao et al. 2009 and references therein; Yasuda et al. 2008). Assessment of folate transport using the trophoblastic cell line BeWo grown in a monolayer has shown that there is vectorial transport driven by a pH gradient, with a high level of low-pH transport activity and a lower level of activity at neutral pH (Yasuda et al. 2008).

A family of folate-unspecific (low affinity, high capacity) transporters, termed ATP-binding cassette (ABC) transporters are expressed in many tissues. Some members of ABC transporters were found to mediate resistance against many drugs and antibiotics and have thus been named multidrug resistance-associated proteins (MRPs; Slot et al. 2011). While MRP1-3 and ABCG2 were found to be expressed at apical (maternal) membrane and oppose transport of folates to the embryo (St-Pierre et al. 2000), there is evidence that MRP1 is also expressed at the basal surface to oppose folate transport from the embryonic circulation (Nagashige et al. 2003).

1.4.2.3 Association of human NTDs and genetic polymorphisms of FOCM

The protective effect of folic acid supplementation has led researchers to question whether SNPs in FOCM genes may contribute to the risk of an NTD affected pregnancy in the human population.

Mice engineered with mutations in FOCM genes (below; **Section 1.4.2.4**) have also informed the search for candidate genes.

To date, the most significant finding is the MTHFR 677C>T (A222V) polymorphism that is associated with an increased risk of NTDs in the Dutch and Irish populations (van der Put et al. 1995; Shields et al. 1999). Although it was not found to increase risk in the German and Caucasian American populations (Stegmann et al. 1999; Boyles et al. 2006), and has even shown a protective effect in Italian and British populations (De Marco et al. 2002; Doudney et al. 2009). However, recent meta-analyses have found a significant association between the homozygous TT polymorphism in mothers and increased risk of an affected pregnancy (Yadav et al. 2015), or between the TT polymorphism in mothers or cases, and increased risk of an affected pregnancy in Asian and Caucasian populations (Yang et al. 2015). In the Irish population, the homozygous TT variant in offspring was found to approximately double the risk of having an NTD affected pregnancy, while the heterozygous CT variant was also found to increase risk (Shields et al. 1999; Kirke et al. 2004). Together, the CT and TT genotypes were estimated to account for 26 % of the NTDs in Ireland (Kirke et al. 2004). The homozygous TT variant encodes a thermolabile protein which has reduced activity, and is associated with decreased plasma folate and elevated plasma homocysteine (van der Put et al. 1995).

The number of studies which have looked for genetic polymorphisms in other FOCM related genes in association with NTDs is large, and many provide contradictory or insignificant results. While most of these case-control studies have looked for polymorphisms in a single, or couple of genes, the study by Pangilinan et al. (2012) is notable as common polymorphisms in 82 candidate genes were evaluated in an Irish population but no associations were found after correcting for multiple testing and, like many other studies, they may be limited by their sample size. Therefore, only the results of recent meta-analyses are detailed below.

Two recent meta-analyses have found a significant association between the MTHFD1 G1958>A polymorphism in Caucasian mothers and risk of an NTD affected pregnancy (Jiang et al. 2014; Zheng et al. 2015), and with maternal MTRR A66>G polymorphism in Asian and Caucasian populations (Yadav et al. 2015). In contrast, no associations were found between the MS A2756>G polymorphism (Yang et al. 2013), CBS T833>C polymorphism (Ouyang et al. 2014) or the RFC A80>G polymorphism (Wang et al. 2012) in mothers, fathers or offspring of mainly Caucasian or Chinese origin, or in the MTRR A66>G polymorphism in Caucasian cases (Ouyang et al. 2013), and increased risk of an affected pregnancy.

Additionally, a collaborative study comprising cohorts from Japan, the UK and Sweden looked at the involvement of the GCS in human NTDs. They found two unique non-synonymous changes in the *AMT* gene, and a splice acceptor site mutation together with five non-synonymous changes in

the *GLDC* gene (Narisawa et al. 2012). Of interest, the variants in *GLDC* were found to significantly reduce enzymatic activity. This is particularly noteworthy as mice null for *Amt* or *Gldc* exhibit NTDs (Narisawa et al. 2012; Pai et al. 2015; **Section 1.4.2.4**).

Lastly, Dunlevy et al. (2007) found impairments of FOCM in a subset of MEFs derived from NTD patients which did not correlate with 7 known variants in *MTHFR*, *MTHFD1*, *DHFR*, *GCPII*, *MTR*, *MTRR* or *RCFI*. This suggests that there may be more genetic variants to be discovered. Larger studies and whole genome sequencing may aid the search in the future.

1.4.2.4 Mouse models with mutations in FOCM

Inducing severe folate deficiency in wild-type mice does not cause NTDs in offspring, supporting the notion that NTDs in humans are not simply a consequence of vitamin deficiency, and are likely to involve an interplay between genetic and environmental factors. The importance of folic acid status as a risk factor for NTDs has, however, spurred the creation of mice with targeted mutations in genes encoding components of FOCM, with varying results, as some, but not all exhibit NTDs.

Of note, *Mthfr* null mice do not present with NTDs, despite exhibiting 10-fold higher plasma homocysteine levels and 25-fold lower liver 5-methylTHF (Chen et al. 2001). The mutant mice demonstrate increased alterations in homocysteine and folate metabolism than those seen in human individuals homozygous for the 677C>T variant, which display approximately 1.4-fold higher homocysteine and 1.3-fold lower plasma folate (De Bree et al. 2003). They also exhibited DNA hypomethylation (Chen et al. 2001). This may reflect a species difference in respect to neural tube closure, as both human patients with very low or undetectable MTHFR activity and the *Mthfr* null mice exhibit early postnatal death or severe neurological problems (Goyette et al. 1996; Chen et al. 2001).

Mice null for *Mthfd2*, and hypomorphic for *Mtrr*, also do not exhibit NTDs (Di Pietro et al. 2002; Elmore et al. 2007), with *Mtrr* hypomorphs exhibiting changes in homocysteine metabolism and global DNA hypomethylation (Elmore et al. 2007; Jadavji et al. 2014). 22 % of mice null for *Rcf1* survived to E18.5 with high dose maternal folic acid supplementation, but no NTDs were present (Gelineau-van Waes et al. 2008). Mice null for *MS* and *Mthfs* are early lethal, precluding assessment of neural tube closure (Swanson et al. 2001; Field, Anderson, and Stover 2011). Dietary supplementation of dams with 5-formylTHF, purines and thymidine, and other one-carbon donors could not rescue the lethality of *MS* null embryos (Swanson et al. 2001), while MEFs derived from heterozygous *Mthfs* embryos demonstrated a deficit in *de novo* purine synthesis, but *Mthfs* null embryos could not be rescued by hypoxanthine (Field, Anderson, and Stover 2011). *Mthfd1* null mice are embryonic lethal, however, at what stage the embryos die and any phenotype was not mentioned (MacFarlane et al. 2009). The heterozygotes demonstrated decreased hepatic SAM

levels and decreased uracil misincorporation compared to *wild-type*. Mice homozygous for a gene-trapped allele inactivating just the 10-formylTHF synthetase activity are lethal at E10.5 and developmentally delayed by 2 to 3 days and have not turned, precluding assessment of neural tube closure. Heterozygous mice had reduced 10-formylTHF in plasma and liver, and MEFs demonstrated impaired *de novo* purine synthesis (Christensen et al. 2013).

Conversely, genetic ablation of *Mthfd1L*, *Amt* and *Gldc* results in partially penetrant exencephaly and a low frequency of craniorachischisis in *Amt* and *Mthfd1L* mice. *Gldc* mice homozygous for a gene-trapped allele (*Gldc*^{GT1}) showed glycine accumulation and a depletion in one-carbon carrying folates. Maternal formate supplementation was found to fully rescue the NTD phenotype (Pai et al. 2015). Mice homozygous for a second gene-trapped allele of *Gldc* (*Gldc*^{GT2}) are briefly described in **Section 3.2.8.1**. *Mthfd1L* null embryos were partially rescued by formate (Momb et al. 2013), while *Amt* null embryos were partially rescued by methionine and methionine plus TMP supplementation (Narisawa et al. 2012). Additionally, 1 out of 13 mice null for the folate receptor, *Folbp1*, exhibited exencephaly when dams were supplemented with dietary folic acid to prevent lethality shortly after implantation (Piedrahita et al. 1999).

Of interest, *Shmt1* null mice are viable and do not present with NTDs on a standard chow diet (MacFarlane et al. 2008). It was hypothesised that this could be due to the expression of some cytosolic *Shmt2* (Anderson and Stover 2009). However, NTDs can be induced in *Shmt1* heterozygous embryos in response to folate and choline deficiency (Beaudin et al. 2011), and in *Shmt1* null embryos in response to a folate deficient diet (Beaudin et al. 2012). Additionally, NTDs in folate deficient *Shmt1* null embryos was exacerbated by maternal uridine supplementation, but partially rescued by deoxyuridine supplementation (Martinova et al. 2015).

It is notable that to date, mice which present with a clear NTD phenotype are all mutants of mitochondrial FOCM. That variants of these genes are also implicated in human NTDs is a significant finding. Both *Amt* and *Gldc* encode proteins of the GCS which obtain one-carbon units from glycine, leading to its catabolism, while MTHFD1L is the liberator of formate, a cytosolic one-carbon donor. These NTD mouse models provide agreement on the substantial contribution (~75 %) of mitochondria-derived one-carbon units for cytoplasmic FOCM outputs in embryonic cells (Pike et al. 2010).

1.5 Mouse models for investigating gene-environment influences

Genetic mouse models of NTDs provide an opportunity to investigate how environmental factors may interact with genetic factors which predispose towards NTDs. Questions that need addressing include: how does folic acid prevent NTDs; can the efficacy of folic acid treatment be predicted for

individuals; are there alternative prevention strategies for folic acid resistant NTDs, and; are there other environmental factors which are deleterious for neural tube closure?

Of the 300 plus mouse mutants which exhibit NTDs, only a handful have been tested for a rescue effect with folic acid or another folate derivative, typically 5-formylTHF, which is also known as folinic acid (Harris and Juriloff 2007, 2010). Those which do respond to folic acid include mice null for *Cart1* (Zhao, Behringer, and de Crombrugghe 1996), *Cited2* (Barbera et al. 2002), and *Splotch* mice (both *Sp*^{2H} and *Sp*; Fleming and Copp 1998; Wlodarczyk et al. 2006). Mice in which NTDs do not respond to folic acid include mice null for: *Grhl3* (Ting et al. 2003), *Nog* (Stottmann et al. 2006) and the *ct* mouse (Seller 1994).

The *Splotch* mouse (*Sp*^{2H}) and the *curly tail* (*ct*) mouse are described further in this section.

1.5.1 The *curly tail* mouse

The *ct/ct* mouse has been one of the most extensively studied models for NTDs, at least in part because of its similarity with human NTDs, and their amenability to environmental factors, as described below.

The *ct* mouse was first described by Grüneberg (1954). The strain arose in the Glaxo Laboratories in 1950, after a spontaneous mutation in a litter of inbred GFF mice, which manifested tail deformities such as kinks and curls. The *ct* stock is derived from the offspring of a phenotypically mutant female mated to a CBA/Gr male, and has been maintained as a closed, randomly-bred colony (*ct/ct* x *ct/ct*) ever since (van Straaten and Copp 2001).

Early studies found that the penetrance of NTDs in offspring varied depending on the tail phenotype of the parents (Grüneberg 1954; Embury et al. 1979), but from the 1980s onwards, the phenotype of the parents no longer influenced the penetrance on NTDs (van Straaten and Copp 2001). This occurred after closed breeding for many years, and re-derivation of the *ct* stock from a few mice on a number of occasions, so that the *ct* mice were considered to be genetically homogenous. In agreement, *ct* mice at the Jackson Laboratories were found to be homozygous at 22 loci that are used for genetic quality control (Neumann et al. 1994). The exception to this homogeneity was seen in mice treated with exogenous agents such as retinoic acid (Seller, Perkins, and Adinolfi 1983; Chen, Morriss-Kay, and Copp 1994, 1995) or L-methionine (van Straaten et al. 1995), where penetrance of NTDs was found to depend on parental phenotype. The reason behind this is not understood.

1.5.1.1 Phenotype

Closed *ct* matings result in offspring in which approximately 50 % present with an NTD and the rest are apparently normal. The most severe NTD seen is midbrain exencephaly, in approximately 0 to 5 % of mice, while lumbosacral spina bifida with a tail flexion defect is found in 10 to 20 % of mice, and the remaining 30 to 40 % present with a tail flexion defect alone. As *ct* mice are considered genetically identical, the *ct* phenotype shows incomplete penetrance and variable expressivity. Of note, the frequency of each phenotype can vary quite significantly, and the frequency of exencephaly and spina bifida usually demonstrate an inverse relationship, presumably under the influence of environmental factors (van Straaten and Copp 2001).

The tail defect can range from either a slight curl or kink at the middle or distal end, to a tight curl at the proximal end leaving the tail significantly shortened. A tight curl at the base of the tail is often associated with a small sacral spina bifida. While mice with exencephaly and a large lumbosacral spina bifida die at or shortly after birth, mice with a small sacral opening survive, with the spina bifida covered by new-grown skin during the first few days, and appear to have no further problems. Similar to humans, exencephaly predominates in female *ct* mice (Copp and Brook 1989; Embury et al. 1979), while there is a slight male excess for spina bifida (Copp and Brook 1989).

1.5.1.2 Tissue and cellular defect

While the mechanism underlying the exencephaly is not understood, spinal NTDs result from a delay in PNP closure. Detailed study of *ct* and wild-type mice revealed that PNP closure is achieved by the 30 somite-stage in wild-type mice, whereas approximately 50 % of *ct* mice had an open PNP at 30 to 34 somite-stages, and approximately 20 % of *ct* mice had open PNPs beyond the 34 somite-stage. These frequencies correspond to that of spinal NTDs (spina bifida + curly tails) and spina bifida, respectively. (Copp, Seller, and Polani 1982). Therefore, when PNP closure is delayed but achieved by the 34 somite-stage, only a tail flexion defect occurs, while if closure is delayed beyond the 34 somite-stage, closure cannot be achieved and spina bifida plus a tail flexion defect results (Copp 1985).

PNP closure is delayed during the transition from Mode 2 to Mode 3 of closure (Shum and Copp 1996). The delay is due to increased ventral curvature of the posterior of affected *ct* embryos, which mechanically interferes with dorsolateral bending and PNP closure. The cause of the increased curvature was identified as a proliferation imbalance between ventral and dorsal tissues, with decreased proliferation in the hindgut endoderm and notochord underlying the closing PNP, but normal proliferation in the neuroepithelia itself, in 27 to 29 somite stage embryos (Copp et al. 1988). The molecular mechanism underlying reduced proliferation in the hindgut endoderm and notochord is not understood. However, the reduced proliferation does correlate with reduced RAR β expression

in the hindgut of affected mice (Chen, Morriss-Kay, and Copp 1995). Additionally, RAR γ is reduced in the tail bud at the same somite stage (Chen, Morriss-Kay, and Copp 1995), and a reduction in *Wnt5a* in the ventral tail bud was found to precede the changes in RAR γ expression in 20 to 22 somite stage embryos (Gofflot, Hall, and Morriss-Kay 1998).

1.5.1.3 Genetic defect

While the tissue and cellular defects underlying spinal NTDs was being elucidated, the genes involved in the *ct* mutation remained unknown. Grüneberg performed outcrosses with *ct* mice and pure CBA/Gr mice, and several intercrosses and backcrosses with the F₁ mice, to conclude that the *ct* mutation was likely recessive and influenced by modifier genes that vary with genetic background (Grüneberg 1954), a finding which was supported by Embury et al. (1979). However, subsequent studies have observed the *ct* phenotype in heterozygotes (*ct* +/−), indicating that the *ct* mutation can be dominant in the presence of particular modifier genes (van Straaten and Copp 2001).

A better understanding of the genetic defect(s) was provided by Neumann et al. (1994), who used linkage analysis to map the main *ct* mutation to distal Chromosome 4. It was considered the main *ct* mutation because the relative frequency of NTDs in backcrosses of (C57BL/6 x *ct/ct*) F₁ females to affected *ct* males suggested variation at a single major locus. The authors also performed backcrosses which allowed them to estimate that at least 3 modifier loci influenced the frequency of NTDs in the backcrosses; one mapping to Chromosome 3 and another to Chromosome 5 (Neumann et al. 1994). Independently, Beier et al. (1995) also mapped the *ct* defect to distal Chromosome 4, and Letts et al. (1995) identified a third modifier locus on Chromosome 17.

In 2003, Ting et al. published a report providing evidence to suggest that *Grhl3*, located on distal Chromosome 4, could be the gene affected in *ct* mice (Ting et al. 2003). The *ct* mutation was subsequently confirmed as a hypomorphic allele of *Grhl3*, with overexpression of *Grhl3* from a bacterial artificial chromosome (BAC) able to eliminate the *ct* phenotype in transgenic mice (Gustavsson et al. 2007). The expression of *Grhl3* during PNP closure was found in the ventral neural tube, the notochord and in the hindgut endoderm (Gustavsson et al. 2007), correlating with the regions of reduced proliferation previously identified.

Lastly, *ct* mice were found to harbour a polymorphic variant of lamin B1, which is missing one of a series of nine glutamic acid residues. The hindgut endoderm of *ct* mice expressing variant lamin B1 demonstrated decreased labelling of the thymidine analogue, 5-ethynyl-2'-deoxyuridine (EdU), during S-phase of the cell cycle, compared to the hindgut of *ct* mice with wild-type lamin B1 bred onto them. Furthermore, the frequency of spina bifida was reduced 3-fold in *ct* mice expressing wild-type lamin B1 (de Castro et al. 2012). The authors concluded that lamin B1 is required for

normal cell cycle progression and is a modifier gene on the *ct* background. Additionally, while congenic wild-type mice (below; **Section 1.5.1.5**) with the lamin B1 variant did not present with spina bifida, approximately 2.5 % did exhibit exencephaly (de Castro et al. 2012). This study demonstrated that both hypomorphic *Grhl3* expression and variant lamin B1 contribute towards the aetiology of exencephaly

1.5.1.4 Sensitivity to environment

A variety of exogenous agents affect the penetrance of NTDs in *ct* mice. Anti-mitogens, such as hydroxyurea, 5-fluorouracil, mitomycin C and cytosine arabinoside reduce the frequency of spinal NTDs when administered at E9.5, but increase the penetrance of exencephaly when given at E8.5 (Seller 1983; Seller and Perkins 1983, 1986). Additionally, hyperthermia at E8 increased the frequency of exencephaly to 20 % (Seller and Perkins-Cole 1987a), while at E10, spina bifida was partially prevented (Copp et al. 1988). Maternal food deprivation for 48 hours prior to PNP closure almost completely prevented spina bifida in *ct* mice (Copp et al. 1988).

These agents and treatments have a growth retarding effect on developing embryos that is hypothesised to affect the more rapidly dividing cells to a greater extent than the more slowly dividing cells. The use of [³H]thymidine labelling in *ct* embryos subjected to hyperthermia demonstrated that hindgut proliferation was preferentially reduced, in effect correcting the proliferation imbalance between ventral and caudal tissues and ameliorating a proportion of spinal NTDs (Copp et al. 1988). On the other hand, some of these growth retarding treatments are able to induce exencephaly in wild-type mice, as well as increasing rates in the predisposed *ct* mice, highlighting the importance of tissue growth in cranial neurulation.

Vitamin A, and its active metabolite, retinoic acid, are well known teratogens which can induce NTDs and other defects during embryogenesis. When administered at E8.5, retinoic acid increased the frequency of exencephaly without affecting the rates of spinal NTDs. However, when given at E9.5, retinoic acid reduced the frequency of spina NTDs (Seller et al. 1979; Seller 1983; Seller and Perkins 1982; Chen, Morriss-Kay, and Copp 1994). Furthermore, both RAR β and RAR γ were upregulated in the caudal region 2 hours after administration (Chen, Morriss-Kay, and Copp 1995).

Inositol and nucleotide precursors (thymidine + adenine or thymidine + GMP) are able to prevent a proportion of NTDs in *ct* mice (Seller 1994; Greene and Copp 1997; Leung et al. 2013). Inositol deficiency, conversely, increases and induces exencephaly in *ct* and wild-type mice respectively (Cockcroft, Brook, and Copp 1992). Of interest, inositol is the only nutrient/ vitamin which appears to be required specifically for neural tube closure. The topic of inositol and nucleotide precursors for the prevention of NTDs is expanded in **Chapter 3**.

Lastly, NTDs in the *ct* mice are resistant to folic acid supplementation, and the dU suppression test (Killmann 1964), a sensitive assessment of the ability of FOCM to biosynthesise dTMP, found no impairments in this process (Fleming and Copp 1998). However, the frequency of exencephaly is increased by the imposition of a folate deficient diet (Burren et al. 2010).

1.5.1.5 Congenic wild-type strain

As the original strain in which the *ct* mutation originally arose no longer existed, and the lack of a co-isogenic, wild-type, control strain limited investigations, a congenic wild-type strain was bred. This involved backcrossing the wild-type *Grhl3* allele derived from the SWR strain onto the *ct* background for four generations. The partially congenic strain, (+^{ct}), was found to share more than 90 % of its genetic background with *ct* mice (van Straaten and Copp 2001).

1.5.2 The *Splotch* mouse

Splotch mice harbour mutations in *Pax3*, which encodes a highly conserved transcription factor that is expressed in approximately the dorsal third of the neural tube from around E8 onwards. In the neural tube, *Pax3* is expressed along the entire rostrocaudal axis, apart from within the midbrain-hindbrain boundary region. *Pax3* is also expressed in developing somites, where it is required for development of the dermomyotome, and subsequently for axial muscle formation. *Pax3* is also expressed by the neural crest, a multipotent, migratory cell population which is induced at the dorsal most limit of the neural tube (Goulding et al. 1991).

Numerous *Splotch* alleles have either arisen spontaneously (5), been radiation induced (4) or generated by gene targeting (at least 3). Most studies on the role of *Pax3* in neural tube closure have been carried out using mice homozygous for the *Sp* or *Sp*^{2H} alleles; both are predicted to be null alleles (Greene et al. 2009). Mice harbouring the *Sp*^{2H} allele have been used in this project. For clarity, *Sp/Sp* and *Sp*^{2H}/*Sp*^{2H} will be used to highlight research carried out using mice harbouring the corresponding alleles, while *Splotch* or *Pax3* mutant is used generally.

1.5.2.1 *Splotch* phenotype

All *Sp*^{2H}/*sp*^{2H} mice exhibit an NTD; 85 to 100 % exhibit lumbosacral spina bifida and approximately 60 % exhibit midbrain exencephaly (Greene et al. 2009). *Sp/Sp* mice also present with spina bifida in 85 to 100 % of mutants but the reported rate of exencephaly is lower, varying from 8 to 18 % (Greene et al. 2009). The position of Closure 2 appears to affect the rate of exencephaly in *Splotch*; a more rostral position increases the frequency and a more caudal position decreases it (Fleming and Copp 2000). Additionally, exencephaly affects more females than males (Burren et al. 2008).

Splotch mutants die between E12.5 and 13.5, most likely due to cardiac neural crest defects (Li et al. 1999). *Splotch* heterozygotes are viable and indistinguishable from *wild-types* apart from the appearance of a white belly spot due to neural crest derived pigmentation defects.

1.5.2.2 The role of Pax3 during neural tube closure

Both chimera and transgenic rescue experiments suggest that *Pax3* is required cell-autonomously in the dorsal neural folds for closure to be achieved, while lack of expression in the somites does not affect neural tube closure (Li et al. 1999; Mansouri et al. 2001). However, the role of *Pax3* in neural tube closure is not understood.

As a transcription factor, the loss of *Pax3* may result in the mis-regulation of key gene(s) involved in closure. Conversely, members of the family of Pax transcription factors are known to regulate the decision between progenitor cell renewal and differentiation (Blake and Ziman 2014). Therefore, loss of *Pax3* may affect neuroepithelial cell proliferation in the dorsal neural tube, and a precise rate of proliferation appears important for neural tube closure, particularly in the cranial region (**Section 1.3.2**).

What is currently known about the interaction of *Pax3* with other proteins expressed in the neural tube, and their cross-regulation, is briefly summarised first, followed by a discussion on the possible role of *Pax3* in regulating proliferation. Of note, it is possible that different factors underlie the failure of neural tube closure in the cranial and spinal regions.

1.5.2.2.1 Interaction with other proteins and pathways

Recently, canonical Wnt signalling was demonstrated to positively regulate the expression of *Pax3* in the dorsal neural tube. The authors used *Pax3*^{Cre} mice to conditionally knockout β -catenin expression from the dorsal neural tube, which resulted in a significant down-regulation of *Pax3* expression and fully penetrant spina bifida (Zhao et al. 2014). Putative Tcf/Lef1 binding sites were found in the *Pax3* promoter and chromatin immunoprecipitation assays demonstrated β -catenin-Tcf binding. Additionally, the expression of *Msx1*, another dorsally expressed transcription factor which is a known downstream target of canonical Wnt signalling, was also reduced (Zhao et al. 2014). There is evidence that *Msx1* regulates *Pax3* expression in *Xenopus* (Monsoro-Burq, Wang, and Harland 2005), but this has not been shown in mouse.

Pax3 appears to directly regulate *Wnt1* expression. *Wnt1* expression is reduced in the dorsal neural tube of *Sp/Sp* embryos (Conway et al. 2000), and *Pax3* was found to regulate a *Wnt1* 5' proximal promoter sequence in a dose dependant manner *in vitro*, and bind the *Wnt1* promoter *in vivo* (Fenby, Fotaki, and Mason 2008). Therefore, there appears to exist a positive regulatory loop between canonical Wnt signalling and *Pax3* expression. *Pax3* also binds the TGF β 2 promoter and positively

regulates its expression (Mayanil et al. 2006), while N-cadherin expression was found to be significantly reduced in *Sp/Sp* embryos (Bennett et al. 1998). However, it is not clear how a reduction in the expression of these genes may lead to NTDs in *Splotch* mice, and mice null for Wnt1 (McMahon and Bradley 1990), TGF β 2 (Sanford et al. 1997) or N-cadherin (Radice et al. 1997) do not present with NTDs.

Loss of *Pax3* was found to upregulate the expression of *Msx2* in the hindbrain. However, while loss of *Msx2* appeared to rescue the cardiac neural crest defect, neural tube closure was still impaired (Kwang et al. 2002).

1.5.2.2.2 A possible role in neuroepithelial proliferation

While less is known about the role of *Pax3* in neuroepithelial cells, its various roles in neural crest derivatives are better defined. It is apparent that *Pax3* expression in cardiac neural crest is required for correct specification and subsequent proliferation; while cardiac neural crest migrate to the outflow region of the heart, their premigratory expansion is insufficient (Conway et al. 2000; Olaopa et al. 2011). Kioussi et al. (1995) saw an inverse correlation between *Pax3* expression and myelin basic protein in neural crest derived Schwann cells. Myelin basic protein is expressed when Schwann cells make axonal contact and exit the cell cycle; the researchers found evidence that *Pax3* represses expression of myelin basic protein, thus maintaining a proliferative and immature phenotype until external cues dictate otherwise. In melanoblasts derived from the neural crest, *Pax3* induces *Mitf* expression, which can be thought of as a master regulator of the melanocytic program and is necessary for the survival and proliferation of melanoblasts. However, the continuing expression of *Pax3*, until such a time that signals from the target skin are encountered, prevents *Mitf* from executing melanocyte differentiation (Opdecamp et al. 1997; Lang et al. 2005).

Reeves et al. (1998) reported that when cells of the neuronal cell line ND7 were induced to differentiate, the DNA binding activity of *Pax3* protein was downregulated within 1 hour, along with *Pax3* mRNA 2 hours post induction. Conversely, the same group showed that anti-sense knockdown of *Pax3* resulted in rapid cell cycle exit and morphological differentiation of ND7 cells, leading to the proposition that *Pax3* is required to maintain the undifferentiated phenotype of ND7 cells (Reeves et al. 1999). Of interest, *Pax3* knockdown failed to result in cell cycle exit and neuron differentiation in the presence of epidermal growth factor (EGF), suggesting that mitogenic signals can compensate for loss of *Pax3*.

Lastly, Nakazaki et al. (2008) found increased expression of the sensory neurogenesis marker *Brn3a* in neural crest explants from the caudal neural tube of E10.5 *Sp/Sp* embryos, implying premature neurogenesis in the absence of *Pax3*. This coincided with decreased expression of *Hes1*, which is involved in the maintenance of neural stem cells, and *Ngn2*, which is important for neuronal specification, reflecting the control Pax genes have between progenitor renewal and differentiation.

Of interest, mice null for the Notch effectors *Hes1*, *Hes1;Hes5* and *Numb* exhibit premature neurogenesis and exencephaly (**Section 1.3.2.2.2**).

1.5.2.3 *Splotch* mice are sensitive to their environment

In contrast to *ct* mice, both cranial and spinal NTDs in *Splotch* mice can be partially prevented by folic acid supplementation. In *Sp^{2H}/Sp^{2H}* mice, Fleming and Copp (1998) demonstrated that approximately 50 % of NTDs could be prevented *in vitro*, while approximately 30 % were prevented *in vivo*. Additionally, thymidine was found to prevent 40 – 50 % of exencephaly cases (Fleming and Copp 1998). In *Sp/Sp* mice on a CXL background, folic acid, and to a lesser extent, 5-methylTHF was found to prevent NTDs (Wlodarczyk et al. 2006). In keeping with these findings, *Splotch* embryos have demonstrated an impairment in thymidylate biosynthesis using the dU suppression test, suggesting that supplementation with folic acid (and other FOCM intermediates) is correcting an existing deficiency in FOCM (Fleming and Copp 1998). It was further shown that purine biosynthesis is reduced in homozygous mutants, which also demonstrated decreased TYMS and increased SHMT1 protein (no changes found in mRNA abundance), demonstrating compensatory mechanisms for thymidylate synthesis (Beaudin et al. 2011).

Maternal folate deficiency, imposed via a folic acid deficient diet, also exacerbates the frequency and severity of cranial NTD. Exencephaly increased from approximately 60 % to 90 % in *Sp^{2H}/Sp^{2H}* mice, and induced exencephaly in approximately 10 % of *Sp^{2H}/+* mice (Burren et al. 2008). Of interest, while folic acid supplementation reduced the incidence of exencephaly in folate deficient *Splotch*, thymidine did not, although the severity of exencephaly may have been reduced. Also of interest, while folate deficiency increased exencephaly similarly in both sexes, folic acid supplementation only prevented exencephaly in males *Splotch* embryos, not females. Overall, a complex gene-environment interaction was observed.

1.6 Overview of thesis

The aim of this thesis is to investigate the gene-environment interaction of NTDs, focusing on two relatively well studied mouse models of NTDs: the *ct* and *Splotch* mice.

The *ct* mouse is considered a good model for human NTDs: there is a female bias in exencephaly; there are multiple modifier genes which affect the expressivity and penetrance of NTDs, and; environmental factors interact with the *ct* genetic background to affect the frequency of NTDs. The *ct* mouse is also a model of folate resistant NTDs, which can be used to develop alternative preventative therapies.

The *Splotch* mice are a model for folic acid responding NTDs, in which the underlying, cellular cause of NTDs are not known. *Splotch* mice can be used to help elucidate the mechanism by which folic acid prevents NTDs. Likewise, a better understanding of how loss of *Pax3* results in NTDs could inform on why some NTDs are preventable by folic acid.

Chapter 3 furthers investigations into the preventative effects of nucleotides and inositol on NTDs in the *ct* mice, and briefly *Gldc* and *Splotch* mice.

Chapter 4 investigates reduced expression of *Mthfd1L* in *ct* mice. The effect of formate treatment on the rate of NTDs in both *ct* and *Splotch* mice is assessed.

Chapter 5 investigates the potential association between caffeine and NTDs in wild-type, *ct*, and briefly, *Splotch* mice.

Chapter 6 investigates the aetiology of NTDs in *Splotch* mice, with a focus on exencephaly. Proliferation in the cranial region is assessed, and the possibility of over activation of the Shh pathway is investigated.

2 Materials and Methods

2.1 Mice

Animal studies were carried out under regulations of the Animals (Scientific Procedures) Act 1986 of the UK Government, and in accordance with the guidance issued by the Medical Research Council, UK in Responsibility in the Use of Animals for Medical Research (July 1993).

2.1.1 Mouse colonies

The *ct*, *Splotch*, *Gldc*^{GT2} and *Grhl3* colonies were maintained by Dawn Savery at the UCL Institute of Child Health animal facility. The CD1 wild-type colony was maintained by facility staff. The *Splotch*, *Gldc*^{GT2} and *Grhl3* mice were maintained as a heterozygous colony, and the *ct* mice a homozygous colony. Each strain was maintained as a closed, random-bred colony. From 6 – 8 weeks, males were individually housed, while similar aged females were kept in communal cages. Animal rooms were kept at 22°C, with relative humidity 52 %, and on a controlled diurnal cycle of 12-hour light/ 12-hour dark (08:00 to 20:00 and vice versa). Food and water, both standard and supplemented/ modified, was available *ad libitum* at all times.

2.1.2 Timed Matings

Timed matings between males (1 per cage) and females (1 – 3 per cage) were either set up in the morning, around 10:00, or the afternoon, around 16:00. Females with copulation plugs were separated, and for those set up at 10:00, midnight of the same day was designated E0.5, while for mice set up at 16:00, noon on the day a copulation plug was found was designated E0.5.

2.1.3 Treatments and interventions

2.1.3.1 Intraperitoneal nucleotide and inositol treatments

Stock solutions of 6 mg/ mL adenine (\geq 99 % purity; Sigma-Aldrich), 6 mg/ mL thymidine (\geq 99 % purity; Sigma-Aldrich) and 6 mg/ mL guanosine 5'-monophosphate disodium salt hydrate (GMP; \geq 99 % purity; Sigma-Aldrich) and 100 mg/ mL myo-inositol (\geq 99 % purity; Sigma-Aldrich) were made in ultrapure MilliQ water. For injections, each of the nucleotides/ nucleotides/ nucleobases were present at a final concentration of 2 mg/ mL, and injected at a dose of 20 mg/ kg body weight. Myo-inositol was present at a final concentration of 50 mg/ mL and injected at a dose of 500 mg/ kg body weight. Doses were myo-inositol only, adenine + GMP or adenine + thymidine + GMP and adenine + GMP + myo-inositol. Doses for myo-inositol (N. D. Greene and Copp 1997) and nucleotides (K. Y. Leung et al. 2013) were based on previous studies for the treatment of NTDs.

For all treatments, injections were administered first, at 7 days and 15 hours post copulation, and then on E8.5, E9.5 and E10.5.

2.1.3.2 Intraperitoneal folic acid treatment

Folic acid ($\geq 97\%$ purity; Sigma-Aldrich) was dissolved in MilliQ water at a concentration of 2 mg/ mL. Mice were injected with 20 mg/ kg body weight at 7 days and 15 hours post copulation, and then on E8.5, E9.5 and E10.5.

2.1.3.3 Oral nucleotide and inositol treatments

Adenosine 5'-monophosphate monohydrate (AMP; $\geq 99\%$ purity; Sigma-Aldrich), inosine 5'-monophosphate disodium salt hydrate (IMP; $\geq 99\%$ purity; Sigma-Aldrich), thymidine, GMP, and myo-inositol were dissolved in tap water to a final concentration of 0.5 mg/ mL of each constituent (AMP + IMP + GMP + thymidine) or 5 mg/ mL of each constituent of the following treatments: myo-inositol only, AMP + IMP + GMP + thymidine and AMP + IMP + GMP + thymidine + myo-inositol. When mice were administered oral nucleotide treatment (AMP + IMP + GMP + thymidine) from E7.5 until collection, fresh treatment was given on E7.5, E8.5 and E9.5. When mice were administered oral nucleotide, nucleotide + myo-inositol or myo-inositol only treatment from E0.5 until collection, fresh treatment was given every 2 – 3 days, but always on E7.5 and E9.5.

2.1.3.4 Oral formate treatment

Sodium formate ($\geq 97\%$ purity; Sigma-Aldrich) was dissolved in tap water to a final concentration of either 20 mg/ mL or 30 mg/ mL. Mice were administered formate treatment from E0.5 until litters were collected.

2.1.3.5 Oral caffeine treatment

Caffeine ($\geq 99\%$ purity; Sigma-Aldrich) was dissolved in tap water to a final concentration of 2 mg/ mL. Mice were administered caffeine treatment from E7.5 until litters were collected, with fresh treatment given daily from E7.5 – E10.5.

2.1.3.6 Folate deficient diet

Mice were placed on a folate deficient diet (Harlan Teklad; TD.01432) at least 3 weeks prior to mating and maintained on the diet during plugging and until collection of litters. This diet contained no folic acid and 1 % succinylsulfathiazole (10 g/ kg).

2.1.3.7 Fenbendazole treatment

Mice were placed on sterilisable chow containing 18 % fenbendazole (8 mg/ kg; Harlan Teklad; TD0.2490) over a three-month period to treat pinworm infection. Litters collected after this diet are indicated.

2.1.4 Sample collection

2.1.4.1 Embryo collection

Pregnant mice were sacrificed by cervical dislocation and the uterus removed. For embryos younger than E11.5, uteri were placed in a bijou tube containing Dulbecco's Modified Eagle's Medium with high glucose and HEPES formulation (DMEM; Invitrogen; 42430) and 10 % foetal bovine serum (heat inactivated at 58°C; FBS; Invitrogen). For embryos of E11.5 and older, uteri were placed in sterile phosphate buffered saline (PBS; Sigma-Aldrich; tablets dissolved in MilliQ water and autoclaved) which was treated with diethyl pyrocarbonate (DEPC; Sigma-Aldrich). Embryos were dissected from the uterus as described below (**Section 2.1.5**).

2.1.4.2 Liver collection

Maternal livers were collected from pregnant mice only, along with the uterus. After removal of the uterus, the liver, typically the right, left and caudate lobes, were removed, while the median lobe was not. The lobes from each mouse were transferred into a bijou tube and placed immediately on dry ice. The bijou tubes were then stored at -80°C.

2.1.4.3 Blood and urine collection

Blood from adult mice was collected via cardiac puncture under anaesthetic, which was performed by either Dawn Savery or staff from the animal facility. Lithium heparin collection tubes (BD Microtainer) were used to prevent blood from clotting. Plasma was obtained by centrifuging tubes twice at 3500 rmp for 5 min. The top, plasma layer was transferred to 1.5 mL tubes and placed immediately on dry ice, and then stored at -80°C.

Urine was collected from mice placed for 1 hour in individual cages without bedding at around 10:00 each day until enough urine (~200 µl) was collected from all mice. The urine was centrifuged briefly to remove any debris, placed on dry ice and then stored at -80°C.

2.1.5 Embryo dissection

From stages E8.5 – E10.5, litters were dissected using watchmaker’s forceps (number 5, Dumont) from uteri in DMEM plus 10 % FBS, pre-warmed to 37°C, under a stereomicroscope (Zeiss SV6 or SV11). The exception to this was for 5-bromo-2’-deoxyuridine (BrdU) injected *Splotch* litters, which were dissected in ice-cold DMEM only (**Section 2.4.1**). For stages E11.5 – E18.5, litters were dissected in ice-cold PBS. Any resorptions were noted. First deciduas were removed from uteri using forceps, then the deciduas were opened to reveal the conceptus contained within the trophoblast. The trophoblast tissue and Reichert’s membrane were then removed to expose the yolk sac covered embryo. For the purposes of embryo culture, conceptuses were dissected to their yolk sac, carefully ensuring the ectoplacental cone was left intact. For all other purposes, once the yolk sac was reached, it together with the chorion, was opened to reveal the embryo. The amnion, allantois/ umbilical cord and blood vessels connecting the embryo and yolk sac were separated. The yolk sacs were kept for genotyping in the case of litters from heterozygous *Splotch* and *Gldc^{GT2}* intercrosses, and heterozygous *Gldc^{GT2/+}* X *Grhl3^{+/+}* intercrosses. Embryos were washed briefly in DEPC treated PBS (DEPC-PBS) and processed for storage accordingly (**Section 2.1.8**).

2.1.5.1 Assessment of development and growth

To stage embryonic development before E11.5, the number of somite pairs were counted after embryos were dissected from their yolk sacs. If the embryo had undergone axial turning, the crown-rump length (CR length) was measured using an eyepiece graticule to assess growth. The extent of neural tube closure in the cranial region was also noted, and if the embryo had turned, the length of the PNP, the region of neural tube still open in the spinal region, was also measured.

2.1.6 Genotyping and sex-typing

2.1.6.1 Genomic DNA extraction for genotyping

Yolk sacs of embryos were collected during dissections and frozen at -20°C. To obtain genomic DNA, DNA lysis buffer (Invitrogen) was mixed together with proteinase K (10 mg/ mL) in a 49: 1 ratio. 50 µl of DNA lysis buffer plus proteinase K was added to each yolk sac in a 0.2 mL tube. The tubes were then placed in a TC-512 thermal cycler (TECHNE) which incubated the samples at 55 °C for 3 hr, and then at 85 °C for 45 min, before holding at 10 °C.

2.1.6.2 Polymerase chain reaction

The reaction mix for polymerase chain reaction (PCR) genotyping or sex-typing is shown in **Table 2. 1**, and the primers which were used are shown in **Table 2. 2**. The primers for *Splotch* (*Sp^{2H}*)

genotyping span the 32 bp deletion of the mutant allele and therefore the wild-type allele produces a band size which is 32 bp longer than the mutant allele (**Table 2. 1**). PCR cycling condition 1 was used to genotype the *Splotch* strain (**Table 2. 3**).

The *Gldc*^{GT2} mutant allele was produced by a gene-trap insertion between exons 19 and 20 which produces a truncated Gldc protein with an EGFP reporter. The wild-type primers bind to a region of intron 19-20 which is only present in the wild-type allele, while the mutant primers bind the EGFP reporter sequence which is only present in the mutant allele (Pai 2015). Therefore, both wild-type and mutant primer sets must be used to genotype the *Gldc*^{GT2} strain (**Table 2. 2**), using PCR condition 2 (**Table 2. 3**).

To genotype mice from the *Gldc*^{GT2/+} x *Grhl3*^{+/+} intercross, the primers for *Gldc*^{GT2} genotyping, as described above, were used together with primers to genotype the *Grhl3* alleles. The *Grhl3* mutant allele has a deletion from exon 4 to exon 7, which is *Cre* excised (Z. Yu et al. 2006). Therefore, primers detecting the presence of the engineered LoxP sites and primers which amplify exons 3 – 8 (**Table 2. 2**) were used with PCR condition 1 (**Table 2. 3**).

Sex-typing was accomplished using primers binding to the *smcX* (*Kdm5c*) and *smxY* (*Kdm5d*) genes which are located on the X and Y chromosomes respectively, and produce different fragment sizes (**Table 2. 2**). PCR cycling condition 1 was used to sex-type mice (**Table 2. 3**).

PCR Reagent	Volume per reaction (μl)
10 x PCR buffer	5
Deoxynucleoside triphosphate mix (2 mM)	5
Magnesium chloride (50 nM)	1.5
Forward primer (40 μM)	0.3
Reverse primer (40 μM)	0.3
<i>Taq</i> DNA polymerase (5 U/ μl)	0.25
Distilled, deionised water	35.65
DNA	2
Total	50

Table 2. 1. PCR reaction mix for genotyping and sex-typing.

Allele	Primer	Sequence (5'-3')	Band size (bp)
<i>Pax3</i> (<i>Splotch</i>)	F	CCTCGGTAAGCTCGCCCTCTG	Wild type: 122 Mutant: 90
	R	CAGCGCAGGAGCAGAACACCTTC	
<i>Gldc</i> ^{GT2} wild type	F	TCTGCCGCCCTGGGGACTTT	658
	R	GCTGTCTGCCCTTCCAACTA	
<i>Gldc</i> ^{GT2} mutant	F	GCGAGGAGCTGTTCACCGGG	325
	R	ACCTCGGCGCGGGTCTGTGA	
<i>Grhl3</i> floxed	F	TGCAGGCTGTTAGTGTCTGG	Wild type: 352 Floxed: 404
	R	CACAGCCCTGAAAATGACCT	
<i>Grhl3</i> deletion	F	GAATTACAAGTCTGTGCCACCA	Wild type: 204 Mutant: 0
	R	ATTTGCTGACCTTTCTGAGC	
<i>SmcX</i> & <i>SmcY</i>	SMCX	CCGCTGCCAAATTCTTGG	X Chr: 350 Y Chr: 300
	SMCY	TGAAGCTTTGGCTTGAG	

Table 2. 2. Primers used for genotyping and sex-typing.

PCR step	PCR conditions 1	PCR conditions 2	No. of cycles
Initial denaturation	94°C for 2 min	94°C for 2 min	1
Denaturation	94°C for 30 sec	94°C for 1 min	
Annealing	60°C for 30 sec	58°C for 1 min	32
Extension	72°C for 45 sec	72°C for 1 min	
Final extension	72°C for 5 min	72°C for 5 min	1

Table 2. 3. PCR thermal cycling programmes

2.1.6.3 Agarose gel electrophoresis

After PCR reactions were complete, DNA bands were separated by agarose gel electrophoresis with ethidium bromide, and visualised by ultraviolet light from a Gel Doc™ XR1 visualiser (BIO-RAD). For *Splotch* and *sex* genotyping, PCR products were separated on 2-3 % agarose gel, while all others were separated on a 1 % agarose gel.

2.1.7 Embryo culture

Litters between E8.5 and E9.5 were dissected to their yolk sacs with the ectoplacental cone still attached. Embryos in their yolk sac were cultured in 100 % rat serum. Round bottom, 50 mL tubes were greased around the opening so that an airtight seal was formed when the tube was closed. Heat inactivated rat serum (**Section 2.1.7.1**) was defrosted, pooled and then filtered through a 0.45 µm

pore membrane. The rat serum was then divided between the culture tubes and gassed with air that contained either: (a) 5 % O₂; 5 % CO₂ and 90 % N₂ for E8.5 embryos, or (b) 20 % O₂; 5 % CO₂ and 75 % N₂ for E9.0 – E9.5 embryos. It is normal for embryos to vary in growth and developmental stage, even from the same litter, so embryos were divided equally between experimental groups by size, and then carefully placed into tubes containing filtered and gassed rat serum. Generally, around 4 E8.5 embryos were added per mL of serum, or 2 – 3 E9.0 – E9.5 embryos per mL serum. The serum containing embryos was then gassed again according to embryo stage, the lid sealed tightly and the tubes placed in a Galaxy® 170 S incubator (Eppendorf) at 37 °C with constant, low speed, rotation.

For culture with caffeine only (concentrations below) or cyclopamine-KAAD (Calbiochem, Merck; concentrations below), embryos were cultured for at least 1 hour in 100 % rat serum before either compounds (or PBS control) were added, to allow acclimatisation. For culture with radiolabelled adenine (³H-adenine; MP Biomedical), thymidine (³H-thymidine; Perkin Elmer) or cytosine triphosphate (³H-CTP; Perkin Elmer), the radiolabelled compound was added to pooled rat serum after filtration. The rat serum was then left on rotation for at least 10 min to ensure the radiolabel was distributed evenly. The radiolabelled serum was then distributed equally between the control and experimental tubes. Before addition of embryos, caffeine, sodium formate or myo-inositol (concentrations below) was added to the experimental tube while PBS was added to the control tube. The rat serum was then gassed before and after embryos were added and placed in the incubator.

Caffeine was dissolved in sterile PBS to make a stock concentration of 100 mM. A range of 500 – 3000 µM in rat serum was used. Similarly, sodium formate and myo-inositol were dissolved in PBS to make stock solutions of 50 mM and 250 mM respectively, with 50 µM and 250 µM added in culture. Cyclopamine-KAAD was dissolved in dimethyl sulfoxide (DMSO) to obtain a 5 mM solution. This was further diluted in sterile PBS to obtain a 5 µM stock which was added to rat serum for a final concentration of 50 – 0.1 nM.

When litters were dissected in the afternoon, the rat serum was gassed with the appropriate concentration of O₂ before and after the embryos were placed in the tubes. Then the serum was gassed between 08:00 and 09:00 the next morning. For embryos which were around E8.5 when dissected, gas mix (a) was used. These embryos were gassed again around 13:00 with gas mix (b), and again with gas mix (b) around 18:00 if the culture was to continue overnight. When litters were dissected in the morning, at E9.0, the rat serum was gassed before and after addition of embryos with gas mix (b), and again, around 18:00. The next morning, gas mixture (c); 40 % O₂; 5 % CO₂ and 55 % N₂, was used. These cultures were then gassed with (c) again between 12:00 – 13:00 and then stopped in the late afternoon. Cultures from E9.5 – 10.5 would be gassed first with mix (b), and then subsequently with mix (c). Embryos were cultured for between 24 – 42 hours. Cultures

were stopped by dissecting embryos from their yolk sac in DEPC-PBS. They were assessed for growth and development (**Section 2.1.5.1**). In addition, the extent of yolk sac circulation and strength of embryo heartbeat were scored as follows: (0) not at all; (1) present but not extensive or strong, and; (2) present and extensive or strong. Embryos were stored as detailed below (**Section 2.1.8**).

2.1.7.1 Rat serum

Male Sprague Dawley rats at the end of their breeding life were terminally anaesthetised and bled from abdominal blood vessels. The blood was centrifuged 4000 rpm for 5 min at 4 °C and allowed to clot. This procedure was carried out by staff from UCL Animal Central Services. Lab members, including myself, then took over the process. The fibrin clots were squeezed, and the samples centrifuged at 4000 rpm for 5 min at 4 °C. The top serum layer was transferred to fresh 50 mL tubes and centrifuged again at 4000 rpm for 5 min at 4 °C to pellet any blood cells. The serum was transferred to fresh 50 mL tubes and placed in a water bath at 56 °C for 30 min to heat inactivate immune factors. Once cooled to room temperature, the serum was aliquoted and stored at -20 °C.

2.1.8 Fixation, dehydration and storage of embryos.

For the purposes of RNA or protein extraction and mass spectrometry analysis, embryos were placed in 1.5 mL tubes, the excess liquid removed, and placed on dry ice immediately, followed by storage at -80°C.

Embryos were fixed overnight at 4°C, with 4 % paraformaldehyde (PFA) made with DEPC-treated PBS, for use in whole mount *in situ* hybridisation (WMISH), or with 4 % PFA for use in immunohistochemistry. To store fixed embryos for WMISH, embryos were washed twice in DEPC-PBS for 15 min, then dehydrated in a series of washes in methanol and DEPC-PBS: 25 %, 50 %, 75 % and 100 %. The length of washes depended on the stage of embryos: 15 min for E8.5; 20 min for E9.5 and 45 min for E10.5. They were then stored in 100 % methanol at -20 °C. Embryos for use in immunohistochemistry were washed twice in PBS, then dehydrated in a series of washes in ethanol and PBS: 25 %, 50 %, and 70 %. The length of washes depended on the stage of embryos as described above. They were then stored in 70 % ethanol at 4 °C.

2.2 RNA based experiments

2.2.1 RNA isolation and cDNA synthesis

RNA isolation began by addition of 500 µL of TRIzol® Reagent (Ambion® RNA) to the still frozen tissue, and homogenized by pipetting in Trizol several times. The tubes were incubated at room

temperature for 5 min, then 100 μ L of chloroform (BDH, UK) added and the tubes vigorously shaken for 10 sec. A 3 min incubation at room temperature followed, then the tubes were centrifuged at 12,000 g for 15 min at 4 °C. The upper, aqueous phase was transferred to new 1.5 mL tubes, 250 μ L of isopropyl alcohol added, and incubated on ice for 10 min. The tubes were then centrifuged at 18,800 g for 10 min at 4 °C, and the supernatant decanted. The RNA pellet washed with 500 μ L of 75% ethanol, vortexed briefly and centrifuged again at 18,800 g for 5 min at 4 °C. The pellet was air dried for 5 to 10 min and re-suspended in 20 μ L of DEPC-treated MilliQ water.

The RNA samples were treated with DNase to remove DNA contamination using DNA-free™ DNase Treatment and Removal kit (Ambion® RNA). 0.5 μ L of RNase Inhibitor (Roche), 2.5 μ L of 10X DNase 1 buffer, and 0.5 μ L rDNase-1 enzyme were added to RNA samples. The mix was incubated at 37 °C for 30 min, after which, 2.5 μ L of DNase Inactivation Reagent was added, and further incubated for 2 min. The samples were centrifuged at 9,600 g for 2 min and the RNA containing supernatant transferred to fresh tubes.

The purity of the RNA sample was assessed by its absorbance ratio at 260/280 nm and 260/230 nm using the Nanodrop Spectrophotometer ND-1000 (Thermo Scientific). The ideal 260/280 ratio is within the range 2.0 – 2.2; ratios appreciably lower may indicate the presence of protein, phenol or DNA contamination. As it is possible that the same nucleic acid sample can vary \pm 0.4 on two spectrophotometers, a range of \pm 0.5 the ideal range was used. Samples outside the range 1.5 – 2.7 were discarded. The 260/230 ratio is a secondary purity measure which could indicate the presence of contaminants such as ethylenediaminetetraacetic acid (EDTA), carbohydrates and phenol. A range of 1.5 – 2.7 was accepted. The RNA concentration of the samples (ng/ μ L) were also ascertained.

The SuperScript® VILO™ cDNA Synthesis Kit (Invitrogen) was used to generate cDNA from RNA samples. 4 μ L of 5X VILO™ Reaction Mix and 2 μ L of 10X SuperScript® Enzyme Mix were added to 2 μ g of RNA and the volume made to 20 μ L using molecular biology grade water (Sigma-Aldrich). The reactants were placed in a thermocycler, where it was incubated at 25 °C for 10 min, then 42 °C for 1 hour, and then 85 °C for 5 min. The resultant cDNA was diluted 1:5 to a concentration of 400 ng/ μ L and stored at -20 °C for use in whole mount *in situ* hybridisation (WMISH) RNA probe construction (**Section 2.2.2**) and quantitative, real-time, reverse-transcriptase PCR (qRT-PCR; **Section 2.2.3**)

2.2.2 Whole mount *in situ* hybridisation

The spatial and temporal expression pattern of target mRNAs can be visualised using whole mount *in situ* hybridisation (WMISH). Probes for *Aprt*, *Hprt*, *TK1* and *TK2* were designed and constructed for this project (**Table 2. 4**). All other probes used in this project were constructed from plasmids

taken from the lab's plasmid bank (**Table 2. 5**), and continued the protocol below from the stage of transformation and cloning (**Section 2.2.2.4**).

2.2.2.1 Primer and probe design

RNA probes and cDNA primers were constructed for the genes *Aprt* (ENSMUSG00000006589), *Hprt* (ENSMUST00000026723), *TK1* (ENSMUSG00000025574) and *TK2* (ENSMUSG00000035824). The Ensembl website (www.ensembl.org) was used to download the mouse cDNA FASTA sequence for the genes, and the Primer-BLAST tool at the NCBI website (www.ncbi.nlm.nih.gov) used to design the probe and obtain primers. The probe or PCR product size was designed to be between 250 and 650 bp and to span exon-intron junctions (will not bind genomic DNA) when possible. Primers were purchased from Sigma-Aldrich (**Table 2. 4**).

2.2.2.2 Production of insert DNA

Primers and cDNA were mixed with PCR synthesis reagents as shown in **Table 2. 1**, and using PCR conditions 2 (**Table 2. 3**). The efficiency of reaction and size of the PCR product were checked using 1 % agarose gel electrophoresis as described previously (**Section 2.1.6.3**).

The PCR product DNA was then purified using QIAquick PCR Purification Kit (Qiagen). 5 volumes of Buffer PB was added to 1 volume of PCR sample and mixed. The sample was applied to the QIAquick column and centrifuged for 1 min and the flow-through discarded. 750 μ L of Buffer PE was then applied to the column and the column centrifuged for 1 min to wash the DNA, and the flow-through discarded. 30 μ L of molecular biology grade water was then added to the column, incubated for 1 min, and then centrifuged for 1 min. This process was repeated once again, with the 30 μ L flow-through to obtain a maximum yield of DNA. RNA concentration was measured by Nanodrop spectrophotometer.

Allele	Primer	Sequence (5'-3')	Band size (bp)	Restriction enzyme for antisense probe	Start site
<i>Aprt</i>	F	CTCCTTCCGAGCTTCCATCC	639	Nde I	T7
	R	CTATGCTCCAGGGTGTGTGG			
<i>Hprt</i>	F	CCATCACATTGTGGCCCTCT	564	Sac II	SP6
	R	GGCCACAGGACTAGAACACC			
<i>TK1</i>	F	AAGTCTTCAGCCCAGACTGC	469	Nde I	T7
	R	GGCATAAAATGGGGAGCTGT			
<i>TK2</i>	F	GGTGATTGAGGCTGACCACA	466	Sac II	SP6
	R	ACAATGCTCTGGCTTGACGA			

Table 2. 4. Details of novel WMISH probes designed and generated.

Allele	Band size (bp)	Restriction enzyme for antisense probe	Start site	Gift from
<i>Shh</i>	640	Hind III	T3	Andy McMahon
<i>Ptch1</i>	841	BamH I	T3	Matt Scott
<i>Gli1</i>	1700	Not I	T3	Alexandra Joyner
<i>Foxa2</i>	1500	BamH I	T3	Brigid Hogan
<i>Pax6</i>	260	EcoR I	T3	Peter Gruss
<i>Msx1</i>	700	Bgl II	SP6	Paul Sharp
<i>Bmp2</i>	1200	XbaI	T3	Not recorded

Table 2. 5. Details of probes constructed from plasmids deposited in the plasmid bank.

2.2.2.3 Ligation into vector system

The purified PCR product i.e. the probe sequence, was ligated into pGEM®-T Easy Vector System (Promega) which contains T7 and Sp6 polymerase recognition sites. A ligation mixture containing 5 µL of 2X Rapid Ligation Buffer, 1 µL of pGEM-T Easy Vector, 1 µL of T4 Ligase, and a variable volume of PCR product DNA were incubated for an hour at room temperature. The amount of PCR product added to the mix was calculated for optimal ligation efficiency with a 3:1 product/insert to vector ratio as followed:

ng vector × kb size of insert

kb size vector × insert: vector molar ratio (3:1) = ng PCR product

2.2.2.4 Transformation and cloning

After ligation, 50 μ L of DH5 α TM competent cells were added to 2 μ L of ligation reaction. The tube was flicked gently to mix, then incubated on ice for 20 min. The cells were heat-shocked for 45–50 sec at 42 °C, and incubated on ice for a further 2 min. 950 μ L of Luria Bertani (LB) broth was added to the tube and the mix incubated at 37 °C with shaking, for 90 min. 50 μ L and 100 μ L of the transformation mix was plated onto LB plates (32 g of LB-agar per L, containing 100 μ g/mL of Ampicillin (Amp), pre-spread with 10 μ mol. of isopropyl β -D-1-thiogalactopyranoside (IPTG; Sigma-Aldrich), and ~5 μ mol. of X-gal (Sigma-Aldrich; prepared in dimethyl formamide)), and incubated overnight (16–18 hrs) at 37 °C. White colonies (carrying the vector insert) were picked and inoculated into 10 mL of LB-Amp broth and incubated at 37 °C overnight on a shaker.

2.2.2.5 Plasmid preparation

The following morning, the LB-Amp was taken from the shaker and assessed for cloudiness. Plasmid DNA was isolated using the QIAprep Spin Miniprep Kit (Qiagen). First, the broth was centrifuged at 4,600 rpm for 15 min at room temperature. The supernatant was discarded and the pelleted cells resuspended in 250 μ L of chilled Buffer P1 (Resuspension Buffer). 250 μ L of Buffer P2 (Lysis Buffer) was added and mixed, followed by addition of 350 μ L of Buffer N3 (Neutralization Buffer). This solution was then centrifuged for 10 min at 13,000 rpm and the supernatant added to the QIAprep spin column. The spin column was centrifuged for 1 min at 13,000 rpm and the flow-through discarded. The column was centrifuged for an additional min to remove residual wash buffer. 50 μ L of molecular biology grade water was added to the column, incubated for 1 min, and centrifuged for 1 min at 13,000 rpm to elute DNA from the column. The concentration of DNA was determined using the Nanodrop spectrophotometer.

2.2.2.6 Plasmid DNA digestion

Test digests of the plasmids were carried out using 200 ng of plasmid DNA and 5 U of an appropriate restriction enzyme which does not cut the insert DNA (**Table 2.4 & Table 2.5**), which for the novel probes was identified using the webcutter tool (rna.lundberg.gu.se/cutter2). A digest was also carried out using EcoRI, which has restriction sites on either side of the inserted DNA. The plasmid DNA and Promega reagents (2 μ L 10X restriction enzyme buffer, 0.5 μ L restriction enzyme and 0.2 μ L bovine serum albumin (BSA) made to 20 μ L using molecular biology grade water) were incubated for 2 hours at 37 °C, after which a sample was run on agarose gel to confirm the presence of the DNA insert itself and the single, linearized plasmid DNA band at approximately 4 kb. With the presence of the DNA insert confirmed, the plasmid DNA was sent for sequencing (Source BioScience, Cambridge, UK) which revealed the 5'-3' direction of the insert DNA. The

plasmid DNA could then be used for large scale digest (below), or further amplified by repeating the transformation with 50–100 ng of plasmid DNA and the plasmid isolation steps.

Large-scale digest (linearization only) was carried out using 3–5 µg of plasmid DNA and 20–50 U of restriction enzyme. The efficiency of the digest was checked by agarose gel again and incubation time increased if needed. After digestion was complete, the linearized DNA was purified using the QIAquick PCR Purification Kit (Qiagen) protocol as described in **Section 2.2.2.2**. The concentration of linearised DNA was measured by Nanodrop.

2.2.2.7 DIG probe transcription

To make the digoxigenin(DIG)-labelled, single-stranded RNA probes, 2 µg of linearised plasmid DNA, 2 µL of DIG RNA labelling mix (Roche), 2 µL of transcription buffer (Roche), 0.5 µL of RNase Inhibitor (Roche), and 2 µL of the appropriate RNA polymerases (**Table 2. 4 & Table 2. 5**), were added in a 1.5 mL tube and made to a final volume of 20 µL with molecular biology grade water. For the novel probes, both sense and anti-sense probes were constructed. The reagents were incubated for 2 hrs at 37 °C, and 1 µL of this mix run on an agarose gel to assess transcription efficiency.

The DIG-labelled probes were purified using CHROMA SPIN-1000 DEPC-H2O Columns (CloneTech). The columns were prepared by re-suspension by vigorous shaking and centrifuged at 700 g for 5 min at 4 °C to dry the columns. The probes were then applied to the centre of the column and centrifuged at 700 g for 5 min at 4 °C into a clean, RNase-free tube. 1 µL of RNase Inhibitor (Roche) was added to the purified probes, which were stored at -20 °C.

2.2.2.8 Hybridisation of probe

The embryos were rehydrated from storage in 100 % methanol with a series of methanol washes (100%, 75%, 50%, 25%) in DEPC-PBS containing 0.1% Tween-20 (DEPC-PBT), followed by DEPC-PBT washes. All wash steps were conducted with shaking. Embryo were then bleached with 6% hydrogen peroxide in DEPC-PBT for 1 hour with shaking, washed, then treated with 5 µg/ mL proteinase K in DEPC-PBT at room temperature for either 1 min (for E8.5 embryos), 4 min (for E9.5 embryos) or 9 min (for E10.5 embryos), and briefly incubated in 2 mg/mL of glycine in DEPC-PBT for 5 min at room temperature. The embryos were then re-fixed in 0.2% glutaraldehyde prepared in 4% DEPC-PFA for 20 min at room temperature with shaking. After fixation, the embryos were washed in DEPC-PBT, transferred to 1 mL of pre-warmed pre-hybridisation buffer (50% formamide, 5X saline sodium citrate (SSC; 3 M sodium chloride (NaCl), 300 mM trisodium citrate, pH 4.5 with hydrochloric acid (HCl)), 50 µg/mL yeast RNA, 1% sodium dodecyl sulfate (SDS), and 50 µg/mL heparin in DEPC-treated water) and incubated at 70 °C for at least 3 hours.

10 µL of anti-sense (and sense for novel probes) RNA probe was added per 1 mL of pre-hybridisation buffer and left to incubate overnight at 70 °C.

2.2.2.9 DIG antibody detection

After hybridisation, the embryos were washed in pre-warmed formamide solutions: 3 times in Solution 1 (50% formamide, 5X SSC, and 1% SDS in DEPC-treated water) for 30 min each at 70 °C, and then twice in Solution 2 (50% formamide, 2X SSC, and 1% SDS in DEPC-treated water) for 30 min each at 65 °C. Embryos were washed in tris-buffered saline (TBS; 50 mM of Tris-Cl at pH 7.6 and 150 mM of NaCl) with 1% Tween-20 (TBST) and blocked with 10% heat-inactivated sheep serum (Invitrogen) in TBST for 90 min at room temperature. The blocking solution was replaced with anti-DIG-AP antibody (Roche; 11 093 274 910) at 1:2,000 dilution prepared in TBST containing 1% sheep serum. The embryos were incubated 4°C overnight with shaking.

The following day, embryos underwent five 1 hour washes in TBST and left washing in TBST overnight at 4°C with shaking.

2.2.2.10 Colour development

Embryos were washed in 3 changes of NTMT buffer (100 mM NaCl, 100 mM Tris at pH 9.5, 50 mM magnesium chloride, 1% Tween-20, and approximately 25 mg/ 50 mL NTMT solution of tetramisole hydrochloride, in MilliQ water). For colour development, 4.5 µL/ mL of 4-nitroblue tetrazolium chloride (Roche) and 3.5 µL/ mL of 5-bromo-4-chloro-3-indoylphosphate (Roche) were added to NTMT buffer, mixed and then incubated with embryos in the dark. Signal development was stopped after sufficient staining was achieved by washing in PBT overnight. Embryos were also washed in 70 % ethanol to dissolve any crystals which formed and also increase the intensity of staining. Embryos were then re-fixed in 4% PFA overnight at 4°C, washed in PSB, and then photographed using a Leica DFC490 camera mounted on top of a stereomicroscope and Adobe Photoshop (version 6.0) software, with the help of clear agar plates to position embryos.

2.2.2.11 Vibratome sectioning

Embryos were embedded in a gelatine/albumin mix (0.45% gelatine, 27% albumin, and 18% sucrose in PBS) for vibratome (Leica VT1000 S) sectioning, which allows 40 µm sections (or thicker) to be obtained. Embryos were incubated in 1 mL of the gelatine/albumin embedding medium overnight at 4°C. Approximately 200 µL of embedding medium was pipetted into plastic embedding moulds. 20 µL of glutaraldehyde (0.2%) was added to the medium and mixed quickly. The embryos were transferred into the moulds and orientated before the medium began to set. The blocks were left to set for 30 – 60 min, then cut out of the mould and placed in PBS for at least 1 hr

at 4°C. Embedded embryos were orientated, and then sectioned at a thickness of 40 µm for each sample. The sections were mounted in glycerol: water (1:1) and coverslips sealed with clear nail varnish.

2.2.2.12 Brightfield microscopy

Images of WMISH sample sections were taken on a Axiophot 2 microscope (Zeiss) with a Leica DC500 camera and AxioVision 4.8 (Zeiss) software.

2.2.3 Quantitative, real-time polymerase chain reaction

Before new primers (**Table 2. 6**) were used for quantification of sample mRNA, they were tested for linearity to input cDNA, efficiency and specificity. Six serial 10-fold dilutions of the starting amount of 25 ng RNA were made. The CFX Manager software was used to assess the melt curve, which should be a single peak with no shouldering. The standard curve plot was used to assess efficiency and the range of cDNA over which the application was linear. Lastly, the PCR product was run on an agarose gel alongside a DNA ladder to check that the size of the amplified product was equal to the expected size given during primer design.

The abundance of target mRNAs can be quantified in relation to mRNA of a stably expressed housekeeping gene, such as *Gapdh*, as used here. Quantitative, real-time polymerase chain reaction (qRT-PCR) was performed on a CFX96 Touch™ Real-Time PCR Detection System (BIO-RAD) and Hard-Shell™ 96-well PCR plates. A master mix (10 µl iTaq™ universal SYBR® Green supermix (2x), 1 µl forward primer (10 µM), 1 reverse primer (10 µM) and 7 µl MilliQ water per well) was made for each gene to be assessed, along with *Gapdh* (**Table 2. 6**). Biological samples were assessed in triplicate; 1 µl of cDNA (**Section 2.2.1**) was pipetted onto the side of each well, followed by 19 µl of the master mix. The plates were sealed with adhesive PCR plate sealing film and centrifuged briefly to collect contents to the bottom before placing in the machine.

Gene expression analysis was conducted using the CFX Manager software (BIO-RAD). The software calculated the standard deviation between triplicate samples, and where the standard deviation was greater than 0.2, one of the three samples (the outlier) was excluded so that the standard deviation was less than 0.2. The melt curves were assessed, and finally a sample well from each biological sample and each gene, along with any samples showing different dissociation curves, were ran on an agarose gel and the expected band size confirmed.

Gene	F/R	Sequence (5' – 3')	Size (bp)	New?
<i>Gapdh</i>	F	ATGACATCAAGAAGGTGGT	200	No
	R	CATACCAGGAAATGAHCTT		
<i>Gli1</i>	F	CCAAGCCAACCTTCTGTCAGGG	80	No
	R	AGCCCGCTTCTTGTTAATTGA		
<i>Grhl3</i>	F	CCAGACTCCAGTAACAATG	218	No
	R	AAGGGTGAGCAGGTCGCTT		
<i>Gsr</i>	F	GAUTGCCTTACCCGATGT	98	Yes
	R	TGCCAACACCCTTCCCTCT		
<i>Hspala</i>	F	ATTGACCCGAGTTCAAGGATGG	114	Yes
	R	TCTTGCATGGTGGTTGCACT		
<i>Lcmt2</i>	F	TATTTTCGTCTGAAAGCGG	148	Yes
	R	CCGAGTCCCCGATCTTGAAA		
<i>Mecr</i>	F	TCGTCCAGCTGAAGAACCTG	129	Yes
	R	GCTTGGGAAGGAGGCCATA		
<i>Mthfd1dL</i>	F	TCATGGCCGTGCTGGCCTTG	216	Yes
	R	TGGCAAAGGGACCAGCGTG		
<i>Ndufs5</i>	F	ACAAAACGATGAGGCGAAT	150	Yes
	R	GAAAACAGAGCATGACAGC		

Table 2. 6. Primers used for qRT-PCR analysis.

2.3 DNA based experiments

2.3.1 Incorporation of radiolabelled nuclei into DNA

After the culture of embryos with 3 H-adenine, 3 H-thymidine or 3 H-CTP (**Section 2.1.7**), embryos were frozen and stored at -80 °C until DNA isolation could be performed.

2.3.1.1 DNA isolation and quantification

To isolate DNA, 400 μ L of DNA extraction buffer (100 mM Tris-HCl pH 8.5, 5 mM EDTA pH 8.0, 200 mM NaCl, 0.2 % SDS and 0.5 mg/ mL freshly added proteinase K) was added to embryos in 1.5 mL tubes, which were incubated overnight at 56 °C. The following day, the tubes were vortexed, 64 μ L of 6M sodium acetate added, then incubated on ice for 1 hour, before centrifugation at 13,200 rpm, for 30 min, at 4 °C. The supernatant was transferred to fresh tubes, 480 μ L of ice-cold 100 % ethanol was added and the tubes vortexed. The samples were centrifuged at 13,200 rpm,

for 30 min, at 4 °C, the supernatant decanted and 400 µL of 70 % ethanol added, before centrifuging at 13,200 rpm, for 5 min. The supernatant was decanted and the remaining ethanol pipetted out. The DNA was left to air dry for 10 min before being resuspended in 50 µL of MilliQ water.

DNA concentration was measured by Qubit® Fluorometric Quantitation Model 2.0 (Thermo Fisher Scientific), together with the Qubit® dsDNA Assay Kit (Thermo Fisher Scientific). The working solution was made by diluting the Qubit® dsDNA reagent 1: 200 with the Qubit® dsDNA buffer. Two dsDNA standards are provided with the kit; 10 µL of each standard and 1 µL of isolated DNA + 9 µL of MilliQ water, was mixed with 190 µL of the working solution. The reactants were vortexed briefly, incubated for 2 min at room temperature and then read on the Qubit® fluorometer, which allowed total DNA (µg/ µL) to be calculated.

2.3.1.2 Measurement of radiolabelling

To quantify radiolabelled nuclei incorporated into genomic DNA under the control and treated experimental groups, 45 µL of resuspended DNA from biological samples, as well as a control water sample, were pipetted into a 24-well clear microplate (Perkin Elmer). 800 µL of Ultima Gold™ scintillation fluid (Perkin Elmer) was added to the DNA/ water samples, and the plate left to equilibrate overnight, in the dark, at room temperature. The following day, the plate was read by the 1450 MicroBeta® TriLux microplate scintillation counter, which measured the counts per minute (CPM) for each well.

The final data is presented as CPM/ DNA per 45 µL.

2.4 Protein based experiments

2.4.1 Immunohistochemistry to assess proliferation

Litters from *Splotch* heterozygous intercrosses were dissected to obtain 14 – 15 somite stage (E9.0 – E9.5) +/+ and *Sp*^{2H}/*Sp*^{2H} embryos. Litters were from females maintained on standard diet, and females maintained on standard diet plus intra-peritoneal folic acid supplementation (**Section 2.1.3.2**). All mice were treated with BrdU (below).

2.4.1.1 Intraperitoneal 5-bromo-2'-deoxyuridine pulse

Plugged mice were injected with 10 mg/ mL BrdU (Invitrogen) at 50 mg/ kg body weight at E9.5. Mice were returned to their cages for 15 min before being sacrificed by cervical dislocation. Litters were dissected in ice-cold DMEM (**Section 2.1.5**) and immediately fixed, then dehydrated (**Section 2.1.8**).

2.4.1.2 Paraffin wax embedding

Embryos stored in 70 % ethanol were dehydrated to 100 % ethanol in a series of washes (85 %, 95 %, 100 %) at room temperature, and for 30 min in 100 % ethanol to ensure complete dehydration. Glass moulds were used for the following steps. Embryos were cleared in two changes of histoclear (Agar Scientific) for 20 min each at room temperature. Embryos were then placed in two changes of histoclear for 20 min each at 60 °C. Then for 20 min at 60 °C at a 1:1 ratio in histoclear: paraffin wax. Embryos were then incubated in 4 changes of paraffin wax for 30 min each at 60 °C. After the final change, embryos were embedded in the centre of the moulds with the aid of a stereomicroscope (Leica) for orientation.

2.4.1.3 Microtome sectioning

The wax was left overnight to set completely before being taken out from the glass moulds. The wax was cut down in size to fit onto wooden blocks approximately 1 inch square, and melted wax used to adhere the embedded embryos to the wooden blocks. These were left to set, before being positioned on a microtome (Leica). Coronal sections at 4 µm were obtained, placed on glass slides with prewarmed (~30 °C) water to straighten out the sections. After approximately 1 hr on the slides, the water was wiped away and the slides left overnight at 37 °C for the sections to adhere.

2.4.1.4 Immunohistochemistry

For immunohistochemistry, all steps were performed at room temperature unless stated otherwise and all washes were 10 min with shaking. Sections were deparaffinised in two 15 min washes of histoclear. Sections were then rehydrated in a series of washes in ethanol and MilliQ water (100 %, 75 %, 50 %, 25 % and then running tap water) for 5 min each. Antigen retrieval for phospho-histone H3 (pHH3) was performed by boiling sections in 0.01 M citric acid (0.96 g in 500 mL MilliQ water; Sigma Aldrich; pH 6.0) with use of a steamer for 40 min. Once the slides had cooled to room temperature, they were washed twice in PBST (PBS with 0.1 % Triton-X100; Sigma Aldrich). Slides were incubated in blocking solution (5 % sheep serum, 0.15 % glycine and 2 % BSA in PBST) for 30 min in a humidity chamber. Blocking solution was then replaced with anti-pHH3 (ser-10) primary antibody raised in rabbit (06-570; Merck Millipore), diluted in PBST (1:300) and incubated overnight at 4 °C.

The following day, slides were washed three times in PBST, then incubated with a fluorescent conjugated goat, anti-rabbit secondary antibody (Alexa Fluor 568; A11077; Life Technologies) diluted in blocking solution (1:500) for 1 hr. Slides were washed twice in PBST, then once in PBS, before incubation with the nuclear stain, 4',6-diamidino-2-phenylindole (DAPI), diluted in PBS (1:10,000) for 5 min. Slides were then washed three times in PBST, and then fixed in 4 % PFA for 50

min. Slides were washed in twice in PBST, and then incubated in 1 M HCl for 10 min at 4 °C. This was followed by incubation in 2 M HCl for 10 min at room temperature, then in 2 M HCl for 10 min at 37 °C. These HCl incubations were to denature DNA and expose the BrdU antigen. Slides were then washed in 0.1 M sodium borate (pH8.5) to neutralise the acid, followed by one wash in PBST. The slides were incubated with blocking solution (10 % sheep serum in PBST) for 1 hr, followed by incubation with anti-BrdU primary antibody raised in mouse (347583; BD Bioscience), diluted in blocking solution (1:100) overnight at 4 °C.

The following day, slides were washed three times in PBST, then incubated with a fluorescent conjugated rabbit, anti-mouse secondary antibody (Alexa Fluor 488; A11070; Life Technologies) diluted in blocking solution (1:500) for 1 hr. Slides were washed three times in PBST, before being mounted in Mowiol® 4-88 (Sigma-Aldrich) mounting medium (pH 6.8, 12% Mowiol, 0.2 M Tris Base, 0.2 M Tris HCl, and 30% glycerol) with coverslips secured with nail varnish.

2.4.1.5 Fluorescence microscopy

Fluorescent images were taken on an inverted microscope (Leica DMI8) with camera (Leica DFC9000 GT), and Leica Application Suite X (LAS X) software. This set-up was used to acquire single plane images and z-stacks. Deconvolution was performed on all images using the LAS X software. Images were taken at 40x and 10x magnification for each section to be analysed.

2.4.1.6 Cell counting

Cell counting was performed on 40x images in ImageJ with Fiji. Sequential images were stitched together with the Stitching (Grid/ Collection Stitching) plugin and then made into a composite image. The Cell Counter plugin was used, together with Channel Tools, to count pHH3 positive, BrdU positive and double labelled pHH3 + BrdU positive nuclei. This plugin keeps track of cell counting and marked cells which have been counted.

2.4.2 Western blot analysis

Western blotting was used to semi-quantitatively compare protein expression of MTHFD1L, PCNA, phosphor-ERK and total ERK. GAPDH was used as a housekeeping protein.

2.4.2.1 Protein isolation

Radio-immunoprecipitation assay (RIPA) buffer (150 mM NaCl, 1 % Nonidet P-40, 0.5 % sodium deoxycholate, 0.1 % SDS, 50 mM Tris-HCl pH7.4, 1x protease inhibitor cocktail II, 1x protease inhibitor cocktail III and 1x cOmplete™ Protease Inhibitors in MilliQ water) was added to tissue while the tissue was still frozen. For E10.5 cranial regions, 150 µL of RIPA buffer was used, while

for E10.5 whole embryos, 300 μ L was added. The samples were homogenised on ice by sonication (High Intensity Ultrasonic Processor, SONICS VIBRA CELL) at 40 % amplitude, using 1 sec pulses and ensuring no frothing occurred, until no large tissue pieces were visible. Samples were centrifuged at 11,000 rmp for 15 min at 4 °C to pellet debris, and the solubilised proteins transferred to clean 1.5 mL tubes. 10 μ L of this solution was taken for protein quantification.

2.4.2.2 Bicinchoninic acid protein quantification

A bicinchoninic acid (BCA) based assay (Pierce™ BCA Protein Assay Kit, Thermo Fisher Scientific) was used to quantify protein concentration. A calibration curve from 0.0 – 10.0 μ g protein in 50 μ L was set up using 0.2 mg/ mL BSA (provided with the kit at 2 mg/ mL) and MilliQ water. 1 – 2 μ L of experimental RIPA-protein solution was added to clean 1.5 mL tubes in duplicate and made to 50 μ L using MilliQ water. Working reagent was made by mixing 50 parts BCA Reagent A with 1 part BCA Reagent B. 950 μ L was then added to each 50 μ L of standard and experimental sample, and tubes incubated for 30 min at 56 °C. Samples were cooled on ice, transferred to cuvettes and absorbance measured at 562 nm on a UV Mini spectrophotometer (Shimadzu). The calibration curve was read first, followed by experimental samples to give protein concentration (μ g/ mL) in 1 mL. This was used to calculate the concentration in 1 – 2 μ L of RIPA-protein solution.

2.4.2.3 Sodium dodecyl sulfate polyacrylamide gel electrophoresis

Samples to be run by SDS polyacrylamide gel electrophoresis (PAGE) were defrosted on ice. Clean 1.2 mL tubes were placed on ice, and 0.5 μ L β -mercaptoethanol (Sigma-Aldrich), 5 μ L 4x Laemmli loading buffer (BIO-RAD) and 5 – 10 μ g protein was added to the tubes. The volume was made to 20 or 25 μ L with RIPA buffer (made without protease inhibitors). Samples were denatured for 3 min at 100 °C, centrifuged briefly to collect contents and placed on ice.

NuPAGE® Novex® 4 – 12 % Bis-Tris gels (10 wells, 1.0 mm) were used. Gels were removed from their packaging and rinsed with MilliQ water. The electrode contact tape was removed from the bottom of cassettes, as well as the lane combs. The cassettes, if running two, were labelled, as well as the lanes. Gel cassettes were assembled in a NuPAGE® XCell SureLock™ (Invitrogen) electrophoresis tank, using a dam (empty cassette) if running one gel. 500 mL of 3-(N-morpholino)propanesulfonic acid (MOPS) running buffer was prepared from 20x NuPAGE™ MOPS SDS Running Buffer (Invitrogen; 1x composition: 2.5 mM MOPS, 2.5 mM Tris base, 0.005 % SDS, 0.05 mM EDTA, pH 7.7) by dilution in MilliQ water. The running buffer was then poured between the cassettes first to ensure they would not leak. Then the remaining buffer was poured around the cassettes into the outer reservoir. Protein samples were loaded into each well, along with 8 μ L Precision Plus dual colour protein standards (BIO-RAD) into the first well. The lid of the tank

was attached, making sure the electrodes sat properly, and connected to a PowerEase® 500 power supply (Invitrogen). Electrophoresis was carried out at 200 V for 50 min.

2.4.2.4 Western blotting

Semi-wet transfer onto a 0.45 μ m polyvinylidene fluoride (PVDF) membrane (Immobilon-P, Millipore) was carried out using a XCell™ blot module (Invitrogen) and the XCell SureLock™ tank.

Blotting paper (3MM Chr, Whatman) and the PVDF membrane were cut to size (9 x 9 cm) ensuring the membrane was only touched by clean nitrile gloves and forceps. 1x transfer buffer was prepared from 20x NuPAGE™ Transfer Buffer (Invitrogen; 1 x contain 1.25 mM bicine, 1.25 mM Bis-Tris, 0.05 mM EDTA, 0.0025 mM chlorobutanol and 10/ 20 % methanol in MilliQ water, pH 7.2) by diluting in 10 % methanol (for one gel) or 20 % methanol (for two gels) in MilliQ water. The PVDF membrane was first wet in 100 % methanol, then transferred into transfer buffer. Blotting pads and blotting paper were also soaked in transfer buffer. The outer plastic gel cassette was carefully opened and the gels trimmed down. The transfer apparatus was assembled so that from the cathode pole there was 2 blotting pads, followed by blotting paper, gel 1, PVDF membrane, blotting paper (gel 2, PVDF membrane, blotting paper, if 2 gels), and lastly 2 blotting pads. It was ensured the gel and membrane did not dry and a roller was used to eliminate any air bubbles. The cell was closed and secured in the tank, transfer buffer poured into the cell to cover the blotting pads, and MilliQ water poured into the surrounding reservoir. Protein was transferred for 1 hr at 30 V for a single gel, but for 2 hr at 30 V for two gels. In the case of 2 hr transfer, the tank was placed on ice to prevent overheating.

2.4.2.5 Immunoblotting

Once transfer was complete, the PVDF membrane was allowed to air dry, before re-wetting in 100 % methanol, and then placed in blocking solution (TBS containing 5 % BSA and 0.1 Tween-20) for 1 hr. Blocking solution was then replaced with primary antibody diluted in blocking solution as described (**Table 2. 7**), and incubated overnight at 4 °C with shaking.

Name	Supplier	Species	Primary dilution	Developing reagent
GAPDH (MAB374)	Merck Millipore	Mouse	1:1000	Promega
MTHFD1L (PA5-31360)	Thermo Fisher Scientific	Rabbit	1:200	GE Healthcare
PCNA (ab426)	Abcam	Rabbit	1:200	GE Healthcare
pERK/ p38 MAPK (#4511)	Cell Signalling	Rabbit	1:500	Promega
tERK/ p38 MAPK (#9212)	Cell Signalling	Rabbit	1:500	Promega

Table 2. 7. Primary antibodies used for western blotting

The following day, the primary antibody was removed from blots, and blots washed 3 x 10 min with TBS with 0.1 % Tween-20 (TBST). After washing, blots were incubated with horseradish peroxidase conjugated secondary antibodies (Dako) raised against the species of the primary antibody, diluted in blocking solution (1: 10,000), for 1 hr at room temperature. At this point the X-ray cassette was left open. The secondary antibody was removed and the blots washed 5 x 3 min with TBST.

2.4.2.6 Electrochemiluminescence and autoradiography

During these washes, the developing reagent (**Table 2. 7** and **Table 2. 8**) was made and cling film laid out. The blot was laid on top of the cling film, ensuring it was completely flat, and excess liquid blotted off. The membrane was incubated with developing solution (1 mL per blot; **Table 2. 8**), before the membrane was blotted, wrapped in fresh cling film, placed in the X-ray cassette as fast as possible, and taken to a dark room, along with autoradiography film (Amersham Hyperfilm ECL; GE Healthcare Life Sciences). A corner of the film was cut for orientation, and the film taped to the opposite side of the cassette so that it would be positioned over the membrane when closed. The cassette was closed for a timed interval, to obtain unsaturated signal bands, and the films were developed by machine (PROTEC).

Name	Supplier	Working solution	Incubation
ECL Western Blotting Substrate	Promega	1:1 Luminol Enhancer Solution to Peroxide Solution	5 min
ECL Prime Western Blotting System	GE Healthcare Life Sciences	1:1 Luminol Solution to Peroxide Solution	1 min

Table 2. 8. ECL developing systems

2.4.2.7 Stripping and re-probing

Membranes were stripped after probing with phospho-ERK in order to probe with total ERK. After autoradiography, membranes were washed 2 x 6 min in MilliQ water, then washed in 0.2 M sodium hydroxide for 20 min at 37 °C with rocking (HB-1000 Hybridizer oven). The sodium hydroxide solution was then discarded and the membrane washed 2 x 10 min in TBST at room temperature. The membrane was re-blocked and re-probing carried out as described above (**Sections 2.4.2.5** and **2.4.2.6**).

2.4.2.8 Quantification of bands

Films were scanned using a GS-800 Imaging Densitometer® (BIO-RAD) and band volumes analysed using Quantity One® software (BIO-RAD). The background optical density was subtracted from band optical densities from the same blot. In Microsoft Excel, the optical density of proteins of interest were divided by that of the housekeeping protein, GAPDH, in the same sample, to obtain a ratio for each of the samples. The ratios for each protein of interest were then compared between biological samples.

2.5 Mass spectrometry experiments

Mass spectrometry can be used for the detection of different types of molecules with high sensitivity. The quantification of folate cofactors and s-adenosylmethionine (SAM) and s-adenosylhomocysteine (SAH) are established methods in the lab (Cabreiro et al. 2013; Burren et al. 2006). A method to detect nucleotides, nucleosides and nucleobases was set up during this project by myself, Dr Kit-Yi Leung and Leonor Quintaneiro, and was based on a published method (Laourdakis et al. 2014). The quantification of formate was performed by the Brosnan lab (Memorial University of Newfoundland, Canada).

2.5.1 Quantification of folate cofactors

2.5.1.1 Sample preparation

E10.5 embryos and liver samples (~50 mg) were taken from -80 °C and placed on ice. 200 – 300 µL of folate buffer (20 mM ammonium acetate, 0.1 % ascorbic acid, 0.1 % citric acid and 15 mg/ mL 1,4-dithiothreitol in MilliQ water, pH to 7.0 using ammonia) with the internal standard, methotrexate (final concentration 0.2 µM), was added to tissue while it was still frozen. Samples were sonicated at 40 % amplitude and 1 sec pulses on ice until homogenised. The samples were centrifuged at 11,000 rpm for 3 min to remove debris, and a 10 µL sample removed for protein quantification based on the Bradford assay (below, **Section 2.5.1.2**). 2x volume of acetonitrile (400 – 600 µL) was added and the samples mixed by hand for 2 min to deproteinate the samples. Samples were then centrifuged at 14,200 rpm for 15 min at 4 °C. The supernatants were transferred to fresh 1.5 mL tubes, lyophilised (Savant SPD1010; Thermo Fisher Scientific), and stored at -80 °C. On the day the samples were run, they were resuspended in 30 – 50 µL of MilliQ water, centrifuged at 11,000 rpm for 5 min at 4 °C, and the supernatants transferred to glass autosampler vials (Thermo Fisher Scientific).

2.5.1.2 Bradford assay protein quantification

The BCA protein assay (**Section 2.4.2.2**) is a more sensitive method for the quantification of proteins, however, it is incompatible with the folate buffer. Therefore, a method based on the Bradford assay (Bradford Protein Assay, BIO-RAD) was used. The dye reagent was diluted in MilliQ water (1: 10) and filtered. BSA (0.2 mg/ mL) was used to make standards containing 0 – 10 µg protein, made to 10 µL volume with MilliQ water. 1 µL of folate buffer was added to each standard. Duplicates of 1 µL of experimental sample plus 9 µL MilliQ water were added to fresh 1.5 mL tubes and 1 mL of colour reagent added to each standard and experimental sample, incubated at room temperature for 10 min, then transferred to cuvettes to read absorbance at 595 nm. The standard curve was used to calculate the concentration of protein in 1 µL of sample.

2.5.1.3 Mass spectrometry equipment

Mass spectrometry analysis was carried out by ultraperformance liquid chromatography, electrospray ionisation tandem mass spectrometry (UPLC-ESI-MS/MS). Autosampler vials were loaded onto an autosampler connected to a Waters ACQUITY H-class UPLC™ liquid chromatography system (Waters USA) in tandem with a Xevo TQ-S™ mass spectrometer (Waters, USA), controlled through the Mass-Lynx Intellistart software (Version 4.1, Waters, USA). The parameters: capillary 2.5 kV, source temperature 150 °C, desolvation temperature 600 °C, cone gas flow rate 150 L h⁻¹, and desolvation gas flow rate 1,200 L h⁻¹, were optimised for this equipment.

2.5.1.4 Running conditions

Reverse-phase UPLC (ACQUITY UPLC BEH C18 column, Waters Corporation, UK) was used to resolve folates, along with a gradient mobile phase consisting of Buffer A (line A2): 5% methanol, 95% Milli-Q water and 5mM dimethylhexylamine at pH 8.0; and Buffer B (line B2): 100% methanol, 5mM dimethylhexylamine. The column was equilibrated with 95% Buffer A: 5% Buffer B. The UPLC protocol consisted of 95% Buffer A: 5% Buffer B for 1 min, followed by a gradient of 5 – 60% Buffer B over 9 min and then 100% Buffer B for 6 min before re-equilibration for 4 min. The metabolites were eluted at a flow rate of 500 nL min⁻¹ and the wash step with 100% Buffer B was at flow rate of 600 nL min⁻¹. 25 µL of sample was injected and folates were measured by multiple reaction monitoring (MRM) with cone voltage and collision energy for precursor and product ions optimised previously. 5 µL of a mix of folate standards, DHF, THF, 5,10-methenylTHF, 5,10-methyleneTHF, formylTHF (1 – 6 glutamated) and folic acid (1, 3 – 7 glutamated; Schircks Laboratories, Switzerland) was run first to ensure conditions were optimal.

2.5.1.5 Folate quantification

6 folate cofactors, and their 2 – 7 glutamated versions, were quantified. Folates were quantified from the chromatograms using the Mass Lynx software, and using the folate standards as reference. The area of each peak relating to a folate cofactor (and different glutamated versions) was calculated by the software. The peak areas of the 6 different cofactors which were quantified as a total of their glutamated versions, and the peak area for each cofactor divided by the total peak area of all folates combined, to obtain a relative percentage distribution of folates. Additionally, the methotrexate internal standard and protein quantification was used to quantify each folate cofactor (as a total of their glutamated versions) in pmoles per µg protein.

2.5.2 Quantification of s-adenosylmethionine and s-adenosylhomocysteine

2.5.2.1 Sample preparation

200 µL of Buffer A (4 mM ammonium acetate, 0.1 % formic acid and 0.1 % heptafluorobutyric acid in MilliQ water) containing 1 µM deuterium labelled SAM (SAM-D3) was added to E10.5 embryos while still frozen. Samples were sonicated on ice at 40 % amplitude and then centrifuged at 11,000 rpm for 3 min to remove debris, and a 10 µl sample removed for protein quantification based on the BCA assay (**Section 2.4.2.2**). Samples were heated at 80 °C for 5 min to precipitate endogenous proteins and then cooled on ice for 2 min, before being centrifuged for 11,000 rpm for 15 min. 2 µL of the supernatant was transferred to fresh 1.5 mL tubes and 198 µL of Buffer A added (1: 100 dilution; SAM-D3 now at 10 nM). The 200 µL sample was transferred to autosampler vials.

2.5.2.2 Standard preparation

For quantification of SAM and SAH, a standard curve was constructed, ranging from 0 – 5.0 nM for SAM (**Table 2. 9**) and 0 – 0.5 nM for SAH (**Table 2. 10**). The stock concentration of SAH (Sigma-Aldrich) was 1 μ M, while for SAH (Sigma-Aldrich) it was 0.1 μ M. After the first dilution of SAM or SAH in the required amount of Buffer A, 2 μ L was taken and diluted 1: 100 again with Buffer A and transferred to autosampler vials. The final concentrations which were analysed are given in the right-most column of the tables and highlighted in bold.

SAM (nM)	Vol. of SAM* (μ L)	Vol. of SAM-D3 (μ L)	Buffer A (μ L)
0	0	4	196
10	2	4	194
50	10	4	186
100	20	4	176
250	50	4	146
500	100	4	96

Table 2. 9. Preparation of SAM standards

* Concentration of SAM stock at 1 μ M

SAH (nM)	Vol. of SAH* (μ L)	Vol. of SAM-D3 (μ L)	Buffer A (μ L)
0	0	4	196
1	2	4	194
5	10	4	186
10	20	4	176
25	50	4	146
50	100	4	96

Table 2. 10. Preparation of SAH standards

* Concentration of SAH stock at 0.1 μ M

2.5.2.3 Running conditions

The mass spectrometry equipment was as described above (**Section 2.5.1.3**), but operating in positive-ion mode.

Reverse-phase UPLC (Xselect HSS PFP column, Waters Corporation, UK) was used to resolve SAM and SAH, along with a gradient mobile phase consisting of Buffer A (line A2) as described

above (Section 2.5.2.1), and Buffer B (line B2): 100% methanol. The column was equilibrated with 60 % Buffer A: 40 % Buffer B. The UPLC protocol consisted of 60 % Buffer A: 40 % Buffer B for 2 min, followed by a gradient of 40 – 100% Buffer B over a 2 min, then 100% Buffer B for 4 min before re-equilibration for 7 min. The metabolites were eluted at a flow rate of 500 nL min⁻¹ and the wash step with 100% Buffer B was at flow rate of 600 nL min⁻¹. 10 µL of sample or standard was injected and folates were measured by MRM with cone voltage and collision energy for precursor and product ions optimised previously.

2.5.2.4 S-adenosylmethionine and s-adenosylhomocysteine quantification

The peak area of each of the standards was obtained, and divided by the peak area of SAM-D3 in each standard, and used to construct a standard curve for SAM and SAH. The peak area of SAM and SAH in each of the experimental samples was obtained, divided by the peak area of SAM-D3 in each sample, and the concentrations of SAM and SAH calculated from the standard curve. Using protein quantification, final results were expressed as pmol. per µg protein.

2.5.3 Quantification of formate

Plasma and urine samples were sent to the Memorial University of Newfoundland, Canada on dry ice. Samples were still frozen when they arrived. 25 µL samples were vortexed and incubated with 65 µL of 100 mM pentafluorobenzyl bromide in acetone for 15 min at 60 °C. Tubes were cooled to room temperature, and 165 µL of n-hexane added, vortexed and the top organic phase (100 µL) extracted. The organic phase samples were loaded on to a AS3000 Autosampler, and 1 µL was injected through an Agilent DB-225 J&W GC column on a Thermo Fisher TRACE ULTRA Gas Chromatograph, which was coupled to an ISQ mass selective detector in electron-impact ionisation mode. Formate was quantified with reference to a standard curve (Lamarre et al. 2014). Formate levels were analysed by Theerawat (Oody) Pongnopparat (Memorial University of Newfoundland, Canada).

2.5.4 Quantification of nucleotides, nucleosides and nucleobases

The method implemented is based on a published method (Laourdakis et al. 2014), which was developed using the same UPLC-MS/MS instruments used in this project. The method provided analytical conditions and retention times for 35 purine and pyrimidine nucleobases, nucleoside and nucleotides. Their ion transitions, cone voltage and collision energy used for ESI-MS/MS were determined using the Mass-Lynx Intellistart software (Waters, USA).

However, the conditions for analysis can be quite specific to individual equipment, so where standards were available, optimum analytical conditions were obtained for this instrument.

Additionally, the desolvation gas temperature and rate were changed from 450 °C and 600 L/ h in the published method, to 600 °C and 1,200 L/ h, which are the normal working conditions for this spectrometer.

2.5.4.1 Optimisation of analytical conditions

In total, 22 standards were available (Sigma-Aldrich). Each standard was made as a 1 mM solution in MilliQ water. The standards were mixed with water and methanol in a ratio of 1:1:2 (standard: water: methanol), so the final concentration of each standard was 0.25 mM and this was infused into the mass spectrometer. Generally, the ions of nucleotides were present in negative ion-mode, and therefore had a mass corresponding to approximately their Mw minus one. The ions of nucleobases and nucleosides, with the notable exception of thymidine, were present in the positive ion-mode, and had an ion mass of approximately Mw plus one. Once the parent ion was detected, the cone voltage was adjusted to give the maximum relative ion count possible. A spectrum was recorded and the mass of the parent ion peak was obtained. The parent ion mass was then used to specify the precursor ion which would be fragmented by collision induced decay. A collision energy which fragmented approximately 90 % of the precursor ion and gave a suitable fragmented ion peak was selected, and a spectrum obtained. A suitable daughter ion was selected based on it having a sufficiently large ion count and it being ideally over 100 Da.

Having determined the parameters needed for MS/MS detection, the standards were run through the HPLC system followed by MS/MS detection. The list of the 22 nucleotides, nucleoside and nucleobases, their corresponding Mw, ion-mode, parent ion and daughter ion mass (m/z; mass to charge ratio), cone voltage, collision energy and retention times are shown (**Table 2. 11**). Each of the 22 standards were spiked in to determine any matrix effects.

In addition, the analytical conditions for 13 more nucleotides/ nucleosides/ nucleobases (inosine, dADP, dATP, CDP, dCDP, dCTP, dGDP, GDP, GTP, dGTP, dTDP, UDP and XMP), for which standards were not obtained, were taken from Laourdakis et al. (2014) and incorporated into the method.

Compound	Mw	Ion-mode	m/z*	Cone voltage (V)	Collision energy (eV)	Retention time (s)
Adenine	135.13	+	135.94 > 118.86	28	20	1.70
ADP	427.2	-	425.94 > 134.03	20	27	5.53
AMP	347.2	-	345.94 > 78.94	25	25	4.08
ATP	507.18	-	506.15 > 158.91	20	30	7.27
CMP	323.2	-	322.05 > 78.91	20	22	1.23
CTP	483.15	-	482.11 > 158.92	10	20	5.97
Cytidine	243.22	+	242.01 > 109.06	30	20	0.67
Cytosine	111.1	+	111.97 > 95.12	10	22	0.62
dTMP	320.19	-	320.98 > 78.92	15	20	4.40
dTTP	482.17	-	480.86 > 158.88	10	25	7.26
dUMP	308.2	-	306.98 > 194.16	10	22	1.36
dUTP	468.14	-	466.88 > 159.21	20	25	6.75
GMP	363.2	-	362.01 > 78.97	20	22	1.55
Guanine	151.13	+	149.96 > 132.95	20	22	1.02
Guanosine	283.24	+	282.04 > 150.04	30	20	3.17 + 3.74
Hypoxanthine	136.11	+	135.02 > 92.00	20	25	1.17
IMP	348.2	-	346.97 > 78.93	20	22	1.74
Orotate	156.99	-	154.96 > 110.99	20	12	1.23
Thymidine	242.23	-	241.08 > 42.08	22	20	4.24
UMP	324.18	-	323.00 > 78.80	20	22	1.24
Uridine	244.2	+	243.02 > 110.00	30	20	1.66
UTP	484.14	-	482.90 > 158.63	20	22	6.44

Table 2. 11. Optimised analytical conditions for 22 standards

* mass to charge ratio

2.5.4.2 Sample preparation

100 – 200 μ l of 0.5 M perchloric acid, with 100 μ M 5-fluorodeoxyuridine triphosphate (5-dUTP) and 40 μ M 5-fluorocytosine as internal standards, was added to E10.5 embryos while still frozen. Samples were homogenised by sonication at 40 % amplitude using 1 sec pulses, and then incubated on ice for 20 min. Samples were centrifuged at 11,000 rpm for 5 min at 4 °C, and the aqueous portion transferred to fresh tubes. The pellets were kept for protein quantification (below; **Section 2.5.4.3**). Aqueous extracts were neutralised by addition of 5 M potassium hydroxide at 10: 1 (perchloric acid: potassium hydroxide), vortexed and incubated on ice for 20 min. Samples were

centrifuged for 10 min at 10,000 rpm at 4 °C, and supernatants transferred to Amicon® Ultra (0.5 mL) centrifugal filters and centrifuged for 30 min at 13,000 rpm at 4 °C. 100 µL of the filtrate was transferred to autosampler vials.

2.5.4.3 Protein quantification

Protein concentrations were measured by Qubit® Fluorometric Quantitation Model 2.0 (Thermo Fisher Scientific), together with the Qubit® Protein Assay Kit (Thermo Fisher Scientific). The working solution was made by diluting the Qubit® Protein Reagent 1: 200 with the Qubit® Protein buffer. Three protein standards are provided with the kit; 10 µL of each standard and 2 µL of isolated protein + 8 µL of MilliQ water, was mixed with 190 µL of the working solution. The reactants were vortexed briefly, incubated for 15 min at room temperature and then read on the Qubit® fluorometer, which allowed total protein (µg/ µL) to be calculated.

2.5.4.4 Running conditions

The mass spectrometry equipment was as described above (**Section 2.5.1.3**). Both negative-ion mode and positive-ion mode was used.

Reverse-phase UPLC (ACQUITY HSS T3 column, Waters Corporation, UK) was used to resolve nucleotides, nucleoside and nucleobases, along with a gradient mobile phase consisting of Buffer A (line A2): 10 mM ammonium formate and 1.25 mM dibutylammonium acetate in MilliQ water, pH 5.2 using 1 % formic acid, and Buffer B (line B2): 10 mM ammonium formate and 1.25 mM dibutylammonium acetate in 1: 9 MilliQ water and acetonitrile. The column was equilibrated with 100 % Buffer A. The UPLC protocol consisted of a gradient of 0 – 11 % Buffer B over 10 min, 67 % Buffer A and 33 % Buffer B for 1 min, followed by 100 % Buffer B for 4 min and re-equilibration for 5 min in 100 % Buffer A. The metabolites were eluted at a flow rate of 300 µL min⁻¹ and the wash step with 100% Buffer B was at flow rate of 600 µL min⁻¹. 5 µL of nucleotide standard mix (22 standards; **Table 2. 11**) was analysed first to ensure conditions were optimal before 20 µL of sample was injected and nucleotides, nucleoside and nucleobase were measured by MRM.

2.5.4.5 Nucleotide, nucleoside and nucleobase quantification

The peak area of each nucleotide, nucleoside and nucleobase was obtained. The peak area of the internal standards and the known concentrations, together with protein concentration, was used to calculate the concentration of each nucleotide, nucleoside or nucleobase in nmol. per µg protein. Pairs of nucleotides (ATP and dGTP; CTP and UTP; ADP and dGDP; CDP and UDP; GMP and XMP; AMP and IMP, and; CMP and UMP) were found to have indistinguishable MRMs, however, their retention times varied enough to be distinguished.

2.6 Statistical analysis

Statistical probabilities were calculated, and graphical representations constructed, using GraphPad Prism 6 software. Microsoft Excel 2010/ 2016 was used to collate data and perform simple calculations. Results are shown as mean \pm standard error of the mean (SEM), unless found to be non-parametric, whereby median and the interquartile range (IQR) is presented.

For single group analysis, t-tests were used when comparing two means, while 1way ANOVA was used when comparing more than two means. If significance was found using ANOVA, multiple comparisons (t-tests) were made using either Dunnett's correction when only one mean (i.e. control) was compared with all other means, or with Tukey's correction when all means were compared with each other. For analysis of two groups of variables, 2way ANOVA was performed, and followed by Sidak's multiple comparison test if significance was found. Fishers exact test was used to analyse contingency tables of categorical outcomes.

2.7 Figures

Figures were constructed using: ImageJ for scale bars, and processes such as cropping and rotation; Adobe Photoshop CC 2017 for background correction of WMISH images, and; Microsoft PowerPoint 2016 for representations.

3 Investigating strategies for the optimal prevention of folic acid resistant NTDs

3.1 Introduction

The *ct* mouse is a model for folate resistant NTDs. The treatments which are known to prevent spina bifida in the *ct* mouse are outlined in **Section 1.5.1.4**. Of those mentioned, only inositol and nucleotide supplementation have the potential to be suitable preventative therapies for humans, as the other treatments appear to inhibit cellular proliferation. What is known about inositol and nucleotides, in relation to neurulation, is described below.

3.1.1 Inositol

Inositol is a sugar-alcohol molecule which has nine stereoisomers. In nature, *myo*-inositol is the predominant form, and can be obtained from diet or biosynthesised from glucose-6-phosphate in mammals via a highly conserved pathway (Frej, Otto, and Williams 2017; **Figure 3. 1**). From this point, *myo*-inositol will be referred to as inositol.

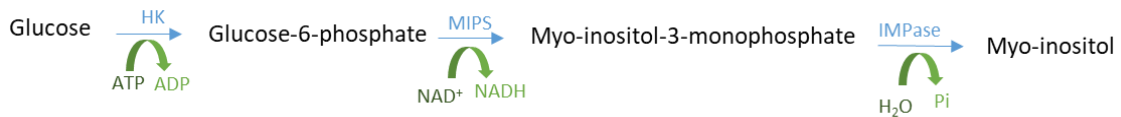


Figure 3. 1. Myo-inositol biosynthetic pathway.

Glucose can be converted to myo-inositol via a highly conserved, two-step pathway. HK = hexokinase; MIPS = Inositol-3-phosphate synthase; IMPase = Inositol monophosphatase. Modified from Voet and Voet (2004).

Inositol is a constituent of cell membranes as phosphatidylinositol and other inositol phospholipids (phosphoinositides). The importance of these phospholipids, which typically represent less than 10 % of the total phospholipids in eukaryotic cells, was first reported in the 1950s when Hokin and Hokin first observed changes in the turnover of phospholipids after stimulation of exocrine tissues, which was later attributed to phosphatidylinositol and its phosphorylated derivatives (Di Paolo and De Camilli 2006).

Phosphatidylinositol can be reversibly phosphorylated on carbons 3,4 and 5 of the inositol ring, which can result in seven different phosphoinositide species in total, that together typically represents approximately 1 % of all phospholipids (Di Paolo and De Camilli 2006). Inositol phospholipids are phosphorylated by numerous specific kinases and, conversely, dephosphorylated by numerous phosphatases, which either add or subtract a single phosphate group, the position of which depends on their class (Zhang and Majerus 1998; Di Paolo and De Camilli 2006). It is now understood that in addition to the cell membrane, phosphoinositides are present in the membranes of possibly all organelles, including the nucleus. Furthermore, the seven phosphoinositide species have distinct subcellular locations which help define and distinguish compartments and the signalling events and processes that take place (Di Paolo and De Camilli 2006; Barlow, Laishram, and Anderson 2010).

Phosphoinositides are implicated in nearly all areas of cell physiology, through classical signal transduction pathways, and also through regulation of membrane traffic, the cytoskeleton, and nuclear events such as import, pre-mRNA processing and DNA repair (Di Paolo and De Camilli 2006; Mellman and Anderson 2009). They are involved in regulation of proliferation, differentiation, apoptosis, stress responses and gene expression (Di Paolo and De Camilli 2006; Barlow, Laishram, and Anderson 2010).

In *ct* mice, the preventative mechanism against NTDs has been shown to depend on inositol phosphate (e.g. IP₃) recycling and require the activation of protein kinase C (PKC; Greene & Copp 1997); the activation of this pathway is described below.

3.1.1.1 Protein kinase C pathway

Inositol phospholipids are found on the inner surface of the plasma membrane which allows them to take part in intracellular signal transduction. The pathway is typically activated upon growth factor ligand binding to GPCRs or membrane receptor tyrosine kinases, which recruit and activate PLC β and γ respectively, at the plasma membrane (Rhee and Choi 1992). PLC cleaves phosphatidylinositol-4,5-bisphosphate, to generate the second messenger IP₃ and diacylglycerol (DAG) (Zhang and Majerus 1998). IP₃ diffuses freely in the cytosol to bind IP₃ receptors located on the sarcoplasmic reticulum. The sarcoplasmic reticulum acts as an intracellular store of calcium ions (Ca²⁺) and binding of IP₃ to its receptors results in a local release. The spatiotemporal increase in both DAG and Ca²⁺ allosterically activates conventional PKCs (Liu and Heckman 1998), which translocate from the cytosol to the plasma membrane, and initiates downstream signalling cascades, one of which is activation of the pro-proliferative MAPK pathway. However, PKCs are known to be promiscuous kinases with a wide range of substrates and effects which are tissue and context dependent (Cooke et al. 2017).

Ten PKC isozymes have been well characterised to date, and these are classified by the nature of their activation: conventional PKCs are activated by both DAG and Ca^{2+} ; novel PKCs by DAG only; and atypical PKCs by neither DAG nor Ca^{2+} , but by other lipid metabolite second messengers (Wu-Zhang and Newton 2013). Cogram et al. (2004) investigated which PKC isoforms mediated the preventative response in *ct* mice by the use of isoform specific inhibitors in embryo culture. This revealed that the conventional PKCs, $\text{PKC}\beta\text{I}$ and $\text{PCK}\gamma$, were required for this response.

3.1.1.2 Inositol and neural tube closure in mice

In the *ct* mouse, NTD prevention via myo-inositol treatment and PKC activation was associated with upregulation of $\text{RAR}\beta$ in the hindgut (N. D. Greene and Copp 1997), which was subsequently shown to undergo increased proliferation (Cogram et al. 2004). It is not yet known whether the protective effect is mediated by changes in gene expression or whether $\text{RAR}\beta$ up-regulation is a secondary marker of normalised proliferation in the hindgut. However, *ct* mice do not appear to be inositol deficient, nor do affected embryos demonstrate impaired uptake or incorporation of [^3H]inositol into phosphatidylinositol compared to unaffected embryos (Greene and Copp 1997).

The importance of inositol for neural tube closure in mice and rats has been demonstrated (Cockcroft 1991; Cockcroft, Brook, and Copp 1992). In these experiments, rat serum was dialysed to remove small metabolites/ vitamins, glucose and amino acids and these were then added back to the medium in a series of cultures in which each vitamin was selectively omitted. In both species, selective omission of inositol led to a specific impairment of cranial neural tube closure, but embryos otherwise appeared morphologically normal. In rats, 90 % of embryos presented with incomplete closure of the cranial neural tube (Cockcroft 1991), while in mice, 26 % of embryos from the wild-type PO stain were affected. However, embryos of the *ct* strain and wild-type CBA strain embryos, exhibited cranial NTDs at rates of 70 % and 60 % respectively (Cockcroft, Brook, and Copp 1992).

Hyperglycaemia is a risk factor for NTDs in humans (Section 1.4.1), and the induction of hyperglycaemia in rats and mice results in decreased levels of embryonic inositol and an increased risk of NTDs in offspring (Hashimoto et al. 1990; Hod et al. 1990; Akashi et al. 1991). Conversely, inositol supplementation was found to increase embryonic inositol content and decrease risk of NTDs (Hashimoto et al. 1990; Hod et al. 1990; Akashi et al. 1991; Reece et al. 1997; Khandelwal et al. 1998).

Further evidence of the importance of inositol in neural tube closure comes from the presence of cranial NTDs in mouse embryos carrying mutations in genes encoding the inositol metabolising enzymes Pip5k1c , Inpp5e , or Itpk1 (Y. Wang et al. 2007; Jacoby et al. 2009; M. P. Wilson et al. 2009). These mice have revealed the role of inositol phosphate metabolism in primary cilia stability

and function, and cell-cell contact through focal adhesions, a requirement for which is implicated in neural tube closure.

Phosphoinositides are also regulators of proliferation and the cytoskeleton, which are known to be important for cranial neural tube closure. For example, the actin interacting protein, MARCKS, binds phosphatidylinositol-4,5-bisphosphate and is a substrate of PKC (Wang et al. 2001; Hartwig et al. 1992), and mice lacking MARCKS present with exencephaly at a frequency of 25 % (Stumpo et al. 1995). Therefore, exactly how inositol deficiency causes NTDs in mice is currently not well understood, and may involve multiple pathways and mechanisms.

3.1.1.3 Inositol and neural tube closure in humans

Evidence from pilot studies in humans suggests that inositol supplementation may prevent folic acid resistant NTDs. The first report came from Italy and involved the case of two mothers who had each had two previous pregnancies affected by spina bifida despite periconceptional daily use of 4 mg folic acid, indicating that these were likely folic acid resistant NTDs. The chance of another affected pregnancy was estimated to be around 1 in 9. In advance of a third pregnancy, the mothers took a combined treatment of 500 mg inositol and 2.5 mg folic acid per day, starting three months before conception and continuing three months after; both mothers delivered unaffected infants (Cavalli and Copp 2002).

A following study reported five unaffected births from three women who had also had at least two previously affected pregnancies and taken folic acid supplementation in at least one pregnancy (Cavalli, Tedoldi, and Riboli 2008). The same group went on to report a similar result in fifteen pregnancies from twelve mothers (Cavalli et al. 2011).

A recent pilot study examined the preventative effects of periconceptional inositol (1 g) plus folic acid (5 mg), compared to 5 mg folic acid alone, for the treatment of NTDs in women who had already had an affected pregnancy and were planning to conceive again. Of 69 women taking part, 33 established pregnancies received randomised treatment (double-blind), while 24 pregnancies did not receive randomised treatment. In total, 3 out of 22 pregnancies which received only folic acid were affected by an NTD, while 0 out of 35 pregnancies receiving inositol plus folic acid were affected by an NTD (Greene et al. 2016). The authors concluded that inositol should be investigated further for the prevention of NTDs.

While inositol deficiency has not been reported with regards to NTDs, a case-control study in the Netherlands found that both mothers of infants with spina bifida and the infants themselves had 5 % and 7 % lower serum inositol concentrations compared to controls, and low serum inositol increased the risk of spina bifida 2.6 fold (Groenen et al. 2003).

Furthermore, Guan et al. (2014) reported four maternal SNPs in the inositol metabolism gene *ITPK1*, which significantly associated with spina bifida cases, and in particular, the rs3783903 SNP was found to decrease expression of the gene by approximately one third. The maternal plasma concentrations of the cellular signal transduction second messenger, inositol-1,2,3,4,5,6-phosphate (IP₆), was found to be significantly (7 %) lower in mothers with spina bifida affected pregnancies compared to controls, and also significantly reduced by homozygosity for variant genotype. It is noteworthy that this is the same gene which when hypomorphic in mice can result in exencephaly (Wilson et al. 2009).

3.1.2 Nucleotides

Nucleotides are the building blocks of nucleic acids, a store of chemical energy, coenzymes for numerous enzymes, carriers of activated metabolites for biosynthetic processes, and metabolic regulators. Therefore, nucleotides are essential for nearly every aspect of cell physiology and are constantly being synthesised. These synthesis processes are greatly enhanced during DNA synthesis and cellular proliferation.

The availability of both purines and pyrimidines appears to modulate the rate and progression through the cell cycle (Sigoillot et al. 2003; Quemeneur et al. 2003), just as mitogenic regulators and progression through the cell cycle are known to modulate the rate of *de novo* nucleotide synthesis (Huang, Roelink, and McKnight 2002; Sigoillot et al. 2003; Lane and Fan 2015). The transcription factors MYC and RB/ E2F, in particular, have been found to regulate the expression of enzymes involved in the biosynthesis pathways of precursors required for all nucleotides (Liu et al. 2008; Mannava et al. 2008), as well as co-ordinate the regulation of RNA and protein biosynthesis (Cunningham et al. 2014).

All nucleotides contain a ribose sugar moiety attached to a nucleobase via a β —N₁-glycosidic bond and between 1 – 3 phosphate groups attached to ribose via a 5' ester bond. The ribose sugar is 2'-deoxyribose in the case of DNA, and ribose, in the case of RNA and other nucleotide requiring processes. Nucleobases are either purines (adenine, guanine and hypoxanthine) or pyrimidines (uracil, cytosine and thymine).

There are two routes for the generation of nucleotides: the *de novo* synthesis pathways and the salvage pathways. While non-proliferative, terminally differentiated cells are thought to be able to rely on salvage pathways (Pedley and Benkovic 2017), which are less energy requiring and less metabolically demanding, proliferation stimulates the *de novo* pathways, the rate of which can be increased around 20-fold (Yamaoka et al. 1997).

The precursor of the ribose/ deoxyribose moiety of nucleotides and nucleosides is 5-phosphoribosyl-1-pyrophosphate (PRPP). PRPP is synthesised via the pentose phosphate pathway

and is also salvaged. The pathways for PRPP synthesis and *de novo* nucleotide synthesis are briefly outlined below, following by the salvage pathways.

3.1.2.1 Generation and regulation of 5-phosphoribosyl-1-pyrophosphate

PRPP can be generated via an oxidative branch of the pentose phosphate pathway, which generates NADPH, or a non-oxidative branch, as well as salvage and direct phosphorylation of ribokinase to produce ribose-5-phosphate ((Tozzi et al. 2006; Lane & Fan 2015; **Figure 3. 2**).

Two isoforms of mammalian PRPS (PRPS1 and PRPS2) generate PRPP from ribose-5-phosphate, encoded by highly conserved genes which, in humans, share very similar coding sequences but only 42 % similarity of promoter sequences, suggesting they are differentially regulated (Fox and Kelley 1971). While both genes appear to be highly expressed in proliferating cells, there are substantial differences in expression in differentiated tissues. Both isoforms are allosterically activated by inorganic phosphate (Pi), which arises as nucleoside triphosphates, such as ATP, are broken down. Conversely, PRPS are allosterically inhibited by dinucleotides (Switzer and Sogin 1973).

3.1.2.2 The *de novo* synthesis of nucleotides

The synthesis of purines is more complex than the synthesis of pyrimidines as the structure of the base is more complex. As outlined in **Section 1.4.2.2.1**, FOCM is required for the synthesis of purines (AMP and GMP) and thymidylate, but not for synthesis of cytosine monophosphate (CMP).

Purine and pyrimidine synthesis differ, in that the purine ring is constructed using PRPP from the beginning, while for pyrimidine synthesis, the pyridine ring is constructed freely and later combined with PRPP. Additionally, a single step of pyrimidine nucleotide synthesis requiring orotate dehydrogenase occurs in the mitochondria, while purine nucleotide synthesis is entirely cytosolic (Lane and Fan 2015). The synthesis of purine nucleotides is outlined first, followed by that of pyrimidine nucleotide synthesis.

3.1.2.2.1 Purines nucleotide synthesis and regulation

While AMP and GMP are the two functional purine nucleotides, IMP is the precursor of both molecules. The synthesis of 1 mole of IMP requires 5 moles of ATP, 2 moles of glutamine, 1 mole of glycine, 1 mole of CO₂, 1 mole of aspartate and 2 moles of 10-formylTHF (Lane and Fan 2015). A representation of the IMP synthesis pathway is shown in **Figure 3. 3**. While glycine and aspartate donate their whole carbon-backbones, glutamine is used for the donation of amine groups, and 10-formylTHF donates the formyl group.

The first enzyme reaction of purine biosynthesis catalysed by PPAT is believed to be rate limiting (Lane and Fan 2015; Pedley and Benkovic 2017). PPAT is allosterically inhibited by the downstream products AMP and GMP, and also adenosine and guanosine di- and trinucleotides, while it is stimulated by PRPP. Additionally, the branch point at IMP, for either AMP or GMP synthesis, is feedback regulated by the inhibiting action of AMP and GMP on ADSL and GMPS, which respectively catalyse the first step of their synthesis (Lane and Fan 2015).

3.1.2.2.2 Pyrimidine nucleotide synthesis and regulation

Synthesis of the nucleotide base uridine monophosphate (UMP) is the common first step in pyrimidine synthesis. The synthesis of 1 mole of UMP requires 1 mole of glutamine, 1 mole of aspartate and 2 moles of ATP, with production of 1 mole each of CO_2 and H_2O (Lane and Fan 2015). As with purine synthesis, aspartate donates its carbon backbone for UMP synthesis (

Figure 3. 4). While both *de novo* cytidine and thymidine nucleotides are synthesised from UMP, the pathway does not branch as seen in formation of AMP and GMP from IMP. Instead, sequential steps can convert one to the other, as outlined below.

The rate limiting steps of pyrimidine biosynthesis are thought to be the first enzyme reaction (carbamoyl phosphate synthase II; CPSII) catalysed by the trifunctional CAD protein and the fourth step catalysed by the mitochondrial dihydroorotate dehydrogenase (DHODH; Lane & Fan 2015). Additionally, CPSII is allosterically inhibited by UTP and activated by PRPP (Evans and Guy 2004; Lane and Fan 2015).

The *Cad* gene is regulated at both the transcriptional and the posttranscriptional level. Its expression is known to be upregulated at the G_1/S boundary of the cell-cycle in response to MAPK signalling and MYC binding of an upstream promoter element. Of interest, CAD is subjected to an activating phosphorylation event by PKC in response to MAPK signalling (Sigoillot et al. 2007), while cyclic-AMP (cAMP) activated protein kinase A (PKA) phosphorylates and antagonises CAD activation on exit of S-phase (Kotsis et al. 2007). Additionally, CAD was reported to be phosphorylated and activated by S6 kinase I in response to mechanistic target of rapamycin complex I (mTORC1) signalling, a pathway with nutrient sensing capabilities which regulates anabolic growth and proliferation (Ben-Sahra et al. 2013; Robitaille et al. 2013). Lastly, CTP synthase is inhibited by CTP and activated by GTP. Both this, and the activation of CPSII by PRPP are mechanisms which coordinate pyrimidine and purine synthesis (Evans and Guy 2004).

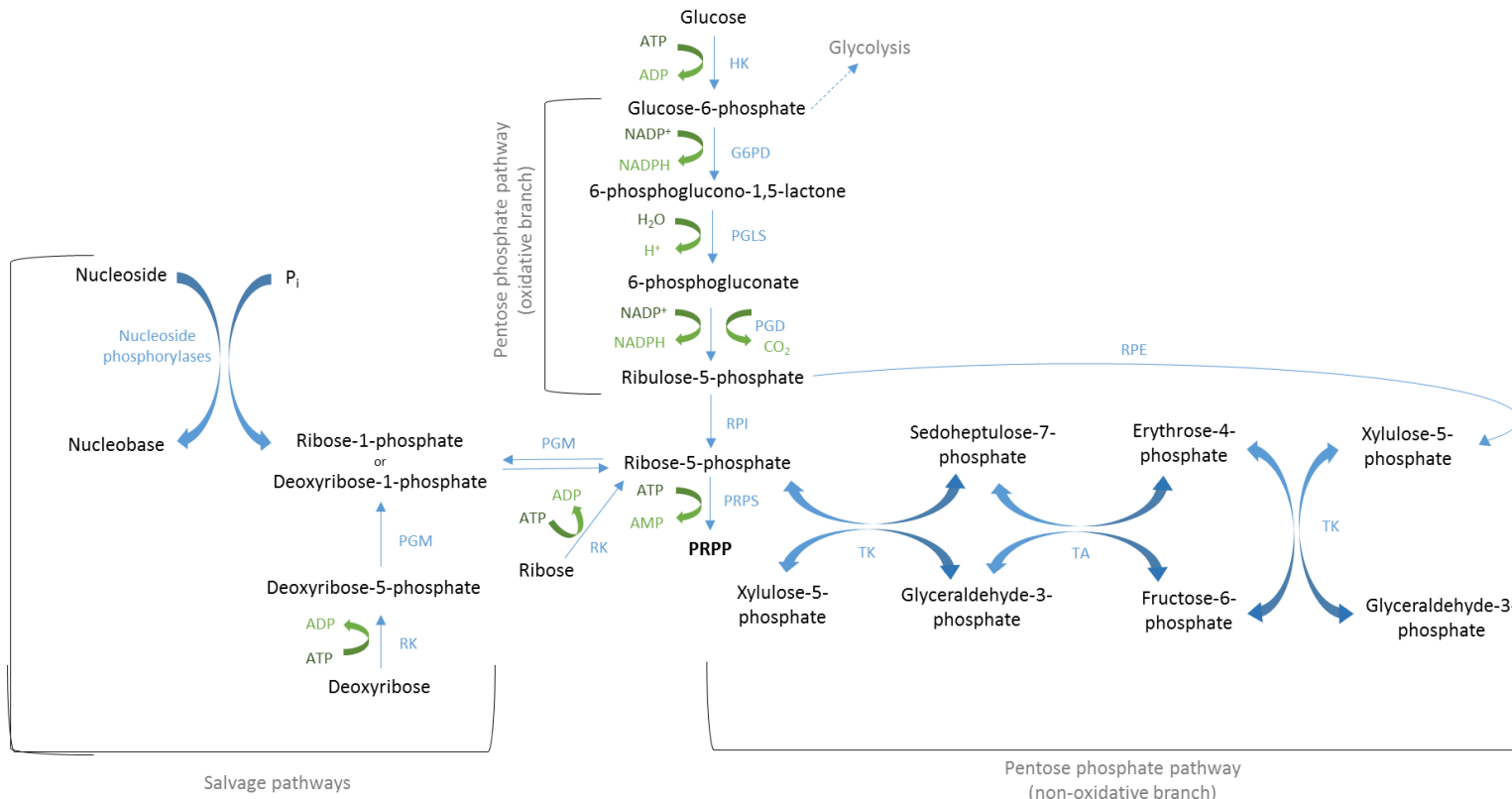


Figure 3. 2. Pathways leading to PRPP formation

The various pathways producing PRPP. G6PD = glucose-6-phosphate dehydrogenase; HK = hexokinase; PGD: 6-phosphogluconate dehydrogenase; PGLS = 6-phosphogluconolactonase; PGM = phosphoglucomutase; PRPS = ribose-phosphate pyrophosphokinase; RK = ribokinase; RPE = PGLS 3-epimerase; RPI = ribulose-5-phosphate isomerase; TK = transketolase; TA= transaldolase. Nucleoside phosphorylases are thymidine, uridine and purine nucleoside phosphorylases. Pathway constructed using (Voet and Voet 2004; Lane and Fan 2015; Tozzi et al. 2006; KEGG Pathway 2016a).



Figure 3. 3. *De novo* purine nucleotide synthesis

The sequential pathway for IMP synthesis, the common precursor and branching point for ATP, dATP, GTP and dGTP synthesis. The “d” before nucleotide abbreviations denotes deoxynucleoside versions. NDK = nucleoside diphosphate kinase; RNR = ribonucleotide reductase. Pathway constructed using (Voet and Voet 2004; Lane and Fan 2015; Tozzi et al. 2006; KEGG Pathway 2016a).

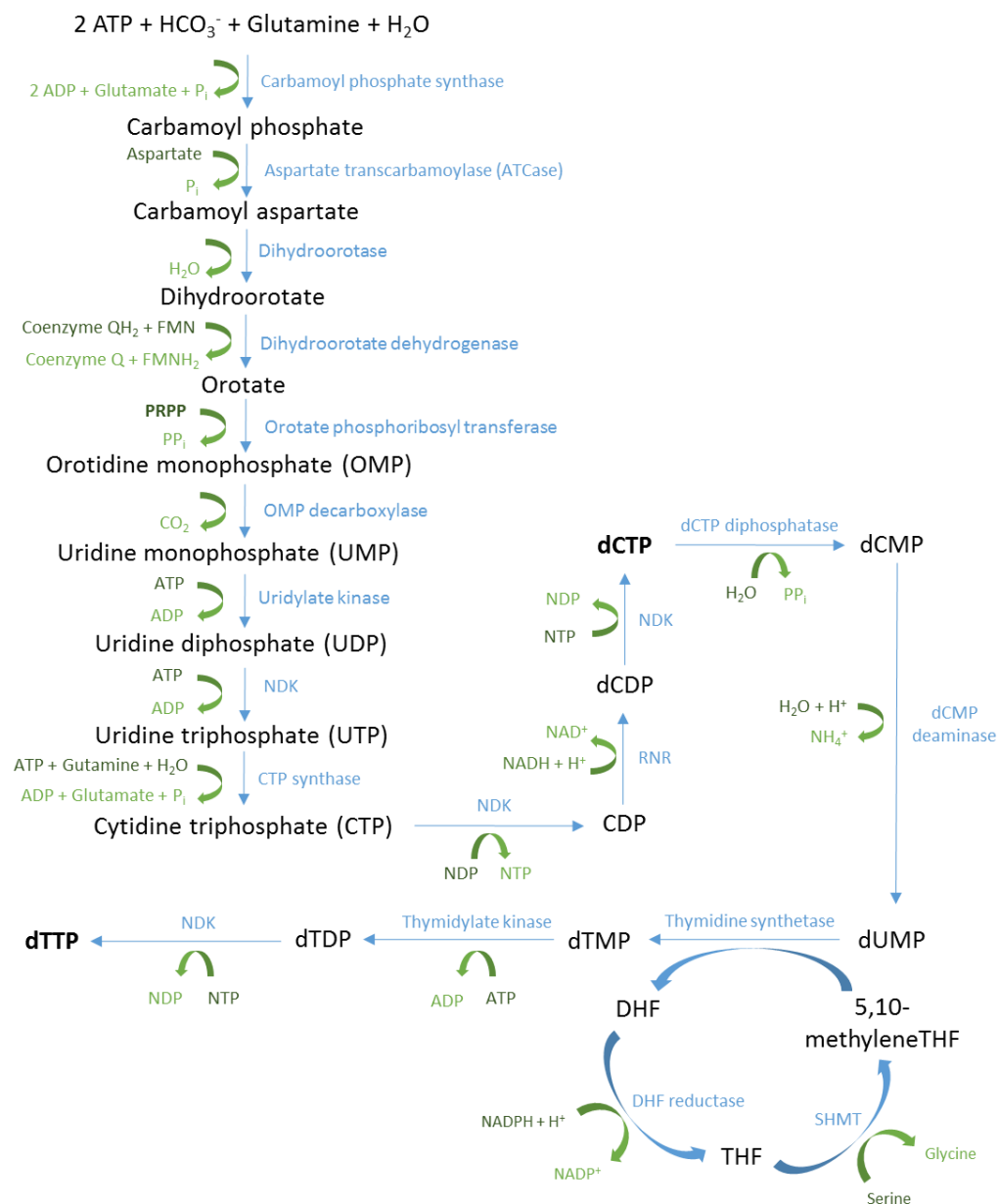


Figure 3. 4. *De novo* pyrimidine nucleotide synthesis

The sequential pathway for pyrimidine and deoxy-pyrimidine nucleotide synthesis. The “d” before nucleotide abbreviations denotes deoxynucleoside versions. NDK = nucleoside diphosphate kinase; RNR = ribonucleotide reductase; THF = tetrahydrofolate; DHF = dihydrofolate; dTMP = thymidine monophosphate; dTDP = thymidine diphosphate, and dTTP = thymidine triphosphate. Pathway constructed using (Voet and Voet 2004; Lane and Fan 2015; KEGG Pathway 2016b).

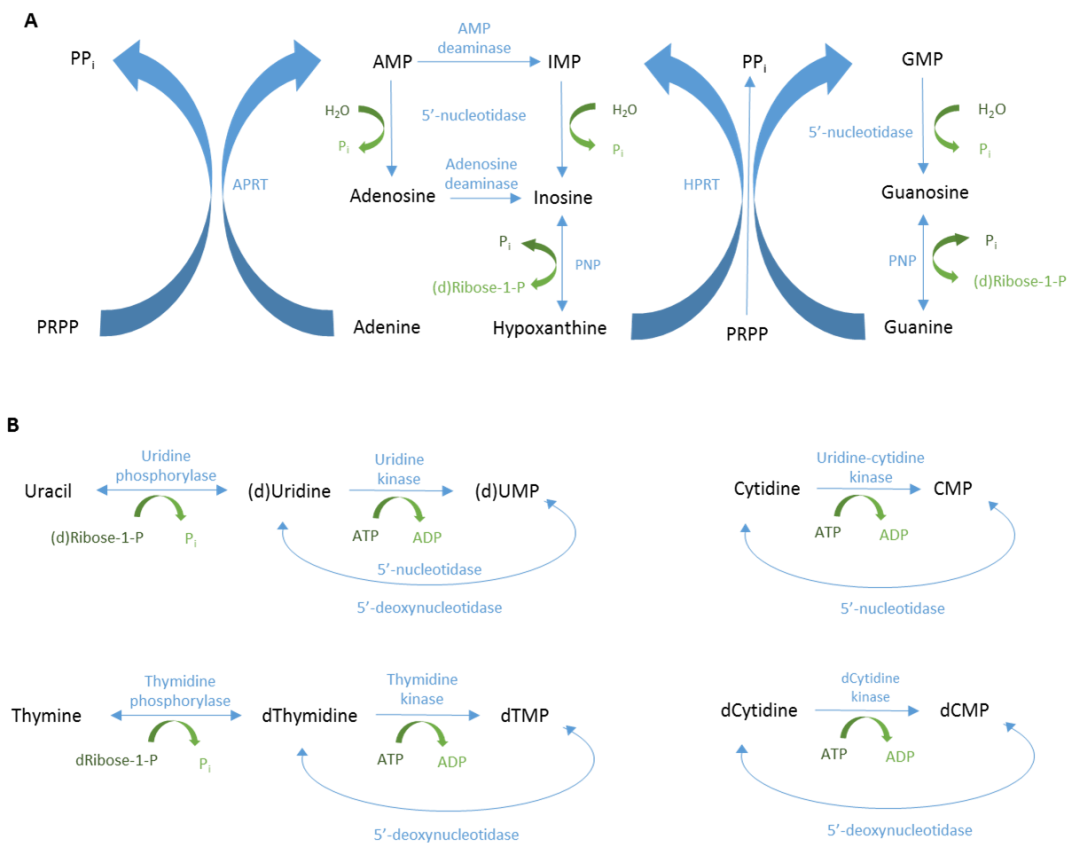


Figure 3.5. Nucleotide salvage pathways

The purine salvage pathways (A) and pyrimidine salvage pathways (B). The enzyme uridine-cytidine kinase can also catalyse conversion of uridine to UMP, but not that of deoxyuridine to dUMP. The “d” before nucleosides names and nucleotide abbreviations denotes deoxynucleoside versions. PNP = purine nucleotide phosphorylase; AMP = adenosine monophosphate; IMP = inosine monophosphate; GMP = guanosine monophosphate; UMP = uridine monophosphate; dTMP = thymidine monophosphate; CMP = cytidine monophosphate. Pathway constructed using (Voet and Voet 2004; Lane and Fan 2015; KEGG Pathway 2016a, 2016b).

3.1.2.3 The nucleotide salvage pathways and regulation

Purine and pyrimidine nucleosides and deoxynucleoside triphosphates (NTPs and dNTPs) and diphosphates (NDPs and dNDPs) can be converted to their monophosphates (NMPs and dNMPs) by various phosphatases which have nucleoside triphosphatase, nucleoside diphosphatase and nucleotide diphosphatase activities. The NMPs/ dNMPs are then hydrolysed to their respective nucleosides by 5'-nucleotidase, and nucleosides can be hydrolysed to their respective nucleobases by their respective phosphorylases mentioned previously (**Section 3.1.2.1**). While only purine nucleobases are salvaged for nucleotide synthesis, pyrimidine nucleosides and nucleobases can both be salvaged (**Figure 3. 5**).

Both APRT and HPRT appear to be ubiquitously expressed in adult somatic tissue and have been considered housekeeping genes, although there is known to be significantly higher HPRT expression in the CNS (Stout and Caskey 1985; Bollee et al. 2012). An inverse correlation between expression of *de novo* purine metabolism genes and those of the purine salvage pathway has been noted (Stout and Caskey 1985). Overall, there are not many reports describing the regulation of these genes or their protein products.

More is known about the regulation of TK, of which there are two isoforms encoded by different genes. TK1 is regulated with the cell cycle (Bello 1974), peaking during G₁/S-phase and declining during G₂/M-phase due to ubiquitin-mediated proteasomal degradation. TK1 also phosphorylates deoxyuridine as well as thymidine, and is inhibited by dTTP. TK2 is expressed at constant low levels and is imported into the mitochondria where it is important for mitochondrial DNA integrity (Berk and Clayton 1973; L. Wang 2016).

3.1.2.4 Nucleotides can prevent folic acid resistant NTDs

Given the central importance of nucleotides and their precursors for proliferation, and the finding that *ct* mice exhibit a defect of proliferation in the hindgut, it can be envisaged that supplementation of these mice with nucleotide precursors may stimulate proliferation and prevent spina bifida. This theory was tested by Leung et al. (2013), who found that intraperitoneal injections of adenine + thymidine, or GMP + thymidine (each at 20 mg/ kg) prevented a significant proportion of spina bifida, while there was also a trend for reduced rates of exencephaly. The treatments were found to significantly increase the mitotic index in the developing hindgut and neuroepithelium. The authors also confirmed the activity of the salvage enzymes HPRT, APRT and TK as ³H-labelling was detected in genomic DNA after culture of embryos with ³H-thymidine, ³H-adenine or ³H-hypoxanthine.

3.1.3 Aims of this chapter

The aim of this chapter was to investigate whether inositol and nucleotide treatments, in *ct* mice, are still effective and/or have greater efficacy when combined, compared to either treatment alone. Additionally, the ability of inositol and nucleotides to prevent NTDs when administered orally, was investigated. Lastly, the efficacy of oral nucleotides treatment in preventing NTDs in the *Splotch* and *Gldc* mouse models was investigated.

3.2 Results

3.2.1 mRNA expression of salvage pathway genes

The expression pattern of the salvage enzymes *Aprt*, *Hprt* and *Tk*, to our knowledge, have not been described in neurulation stage embryos. Therefore, digoxigenin-labelled RNA probes were designed and WMISH conducted in CD1 embryos.

There are two genes and proteins for the salvage of thymidine, *Tk1* and *Tk2*, which were originally referred to as foetal and adult *Tk* respectively, because *Tk1* is highly expressed in foetal tissue and *Tk2* was more abundant in adults. Further investigation found that while *Tk1* is present in proliferating cells, *Tk2* is expressed ubiquitously at low levels in mitochondria (Munch-Peterson et. al. 2010). Analysis of *Tk1* and *Tk2* expression in E8.5 CD1 embryos corroborated these findings. While staining is comparable between E8.5 embryos incubated with *Tk1* and *Tk2* probes, staining was developed for 8 hours in *Tk1* embryos and 24 hours in *Tk2* embryos (**Figure 3. 6**). Both genes were found to be expressed ubiquitously throughout the embryos, however, there is a slight increase in intensity of staining in the neural tube compared to the surrounding mesenchyme. The purine salvage enzymes, *Aprt* and *Hprt*, were also shown to be expressed ubiquitously throughout E8.5 embryos (**Figure 3. 6**). Again, there appears to be slightly increased intensity of staining in the neuroepithelium compared to the surrounding mesenchyme.

Analysis of E10 CD1 embryos, found varied expression of each of the savage enzymes at this stage (**Figure 3. 7**). While *Aprt* is more ubiquitously expressed throughout the neural tube at this stage (**a - c**), *Hprt* expression appears reduced in the cranial and mid-spinal levels (**d & e** respectively), regions of the neural tube which have closed, but increased in the recently closed and still open caudal neural tube (**f & g**). *Tk1* appears to be strongly expressed in the neural tube (**h - k**), although it appears to be excluded from the dorsal tips of the recently closed and still open caudal neural tube (**j & k**). Lastly, *Tk2* expression appears to be much reduced compared to *Tk1* even after the increased colour development time (**l - o**). Of interest, there is perhaps increased intensity of staining in the caudal neuroepithelium (**n & o**) compared to that of the cranial and mid-spinal (**l & m**).

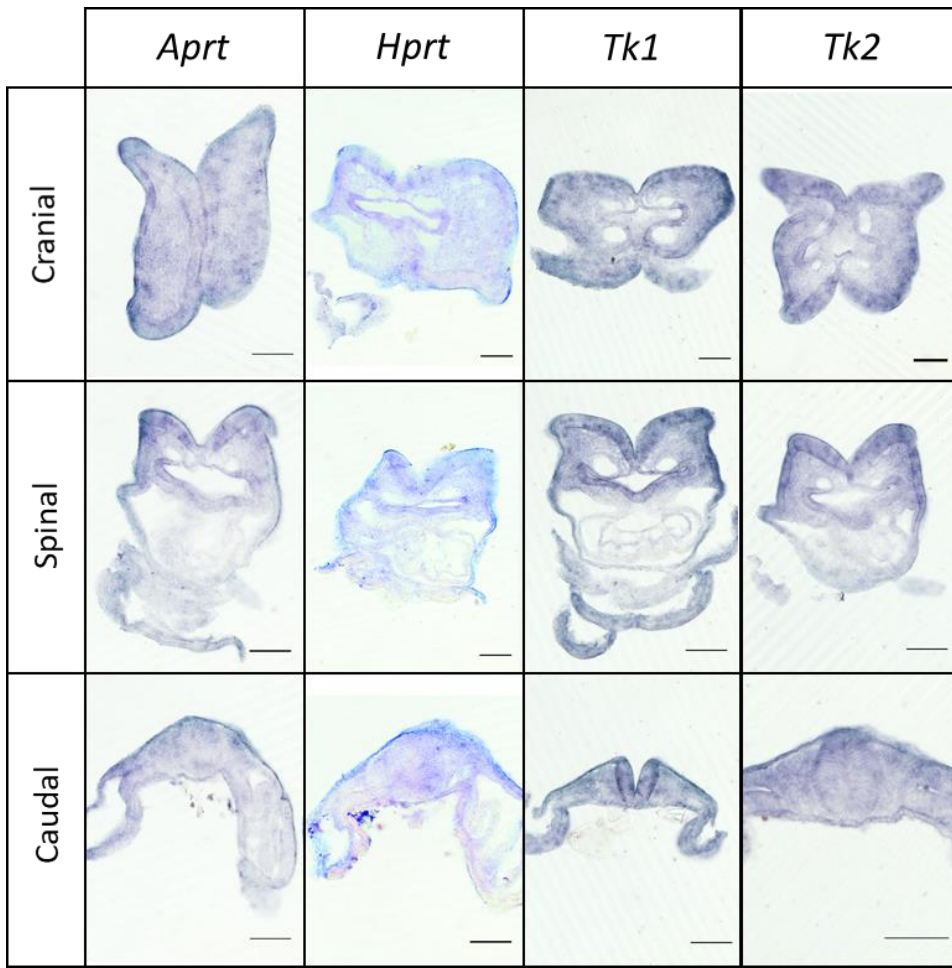


Figure 3. 6. Expression of salvage enzymes in E8.5 CD1 embryos.

Transverse sections through E8.5 CD1 embryos after WMISH using probes to *Aprt* (a – c), *Hprt* (d – f), *Tk1* (g – i) and *Tk2* (j – l). For *Aprt*, *Hprt* and *Tk1* probes, staining was developed for 8 hours, while for the *Tk2* probe, staining was developed for 24 hours. Scale bars represent 100 µm.

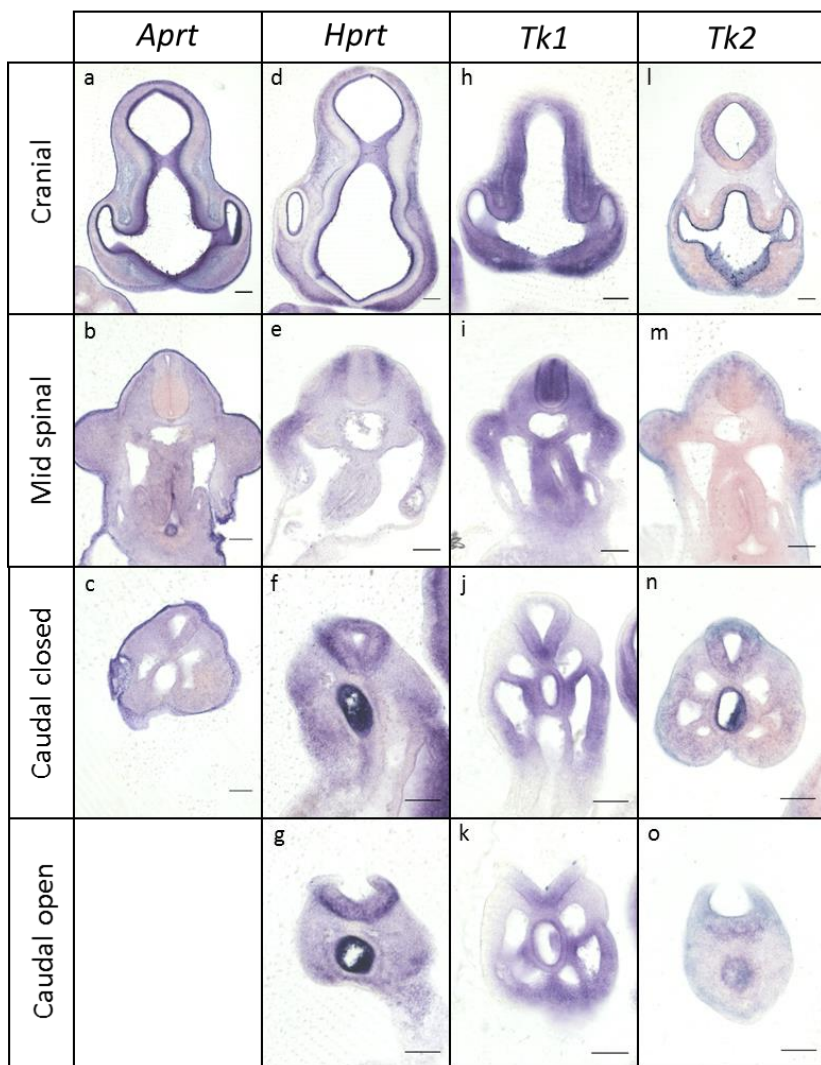


Figure 3.7. Expression of salvage enzymes in E10 CD1 embryos.

Coronal sections through the cranial region and transverse sections through the spinal region of E10 CD1 embryos after WMISH using probes to *Aprt* (a – c), *Hprt* (d – g), *Tk1* (h – k) and *Tk2* (l – o). For *Aprt*, *Hprt* and *Tk1* probes, staining was developed for 8 hours, while for the *Tk2* probe, staining was developed for 24 hours. Scale bars represent 100 μ m.

3.2.2 Investigating prevention of neural tube defects by nucleotide treatment administered by intra-peritoneal injection

Neither the inositol or nucleotide treatments described previously (Greene and Copp 1997; Leung et al. 2013) achieved full prevention of spina bifida; intra-peritoneal injections of inositol reduced the frequency by approximately 50 %, and nucleotide precursors by 80 – 90 %. Whether inositol and nucleotide treatments can be combined without any detriment, and whether combining these treatments can increase prevention, was investigated.

In previous studies the most effective treatment was nucleotide precursors (adenine + thymidine or GMP + thymidine), so this was the starting point for further treatments. Two modifications were made; combination of the three nucleotides into a single treatment (thymidine + adenine + GMP), and addition of inositol to thymidine + adenine. The results of these treatments on rates of spina bifida and exencephaly are described in the following chapter.

3.2.2.1 Novel intra-peritoneal treatments

Each of the two treatments were delivered as a single intra-peritoneal injection daily, from E7 until E10. The first treatment was delivered at approximately 7 days and 15 hours' post-conception, while the following three were delivered at E8.5, 9.5 and 10.5. Nucleobases/ nucleotides were at a dose of 20 mg/ kg, while inositol was at 50 mg/ kg.

To assess efficacy of the new treatments, plugged *ct* mice were also treated with thymidine + adenine only, and inositol only. Lastly, the frequency of spina bifida in all treatment groups can be compared to control *ct* litters collected over the same period (**Figure 3. 8**). Although adenine + thymidine treatment did not cause a statistically significant decrease in rates of spina bifida in this experiment ($p = 0.07$), it became apparent that neither the triple nucleotide precursor mix nor adenine + thymidine + inositol was more efficacious than adenine + thymidine treatment.

No significant differences were found in the rates of exencephaly in any of the treatment groups (**Figure 3. 9**), with the low frequency of exencephaly in control embryos hindering assessment of trends towards a reduced frequency of exencephaly. Although there appears to be a trend towards higher frequency of exencephaly in the inositol only treatment group, the sample size was too small to draw definitive conclusions.

It was surprising that the treatment with inositol alone did not provide an increased level of prevention compared with control *ct* mice (8.1% vs 11.5 % spina bifida). This equates to 30 % prevention, while at least 50 % prevention has been seen previously via intraperitoneal injection, sub-cutaneous pump and oral gavage (Greene and Copp 1997; Cogram et al. 2002). A possible

explanation for this difference could possibly be the timing of injections. In Greene & Copp (1997), a single injection on day 9 post-conception at 17:00 – 18:00 was found to be more efficacious than a single injection between 09:00 – 10:00.

Instead of testing differing regimens for intraperitoneal treatments, the effect of inositol (5 mg/ mL) in maternal drinking water was investigated alone and together in combination with oral nucleotides/ nucleobases. The results of these experiments are described in **Section 3.2.3**.

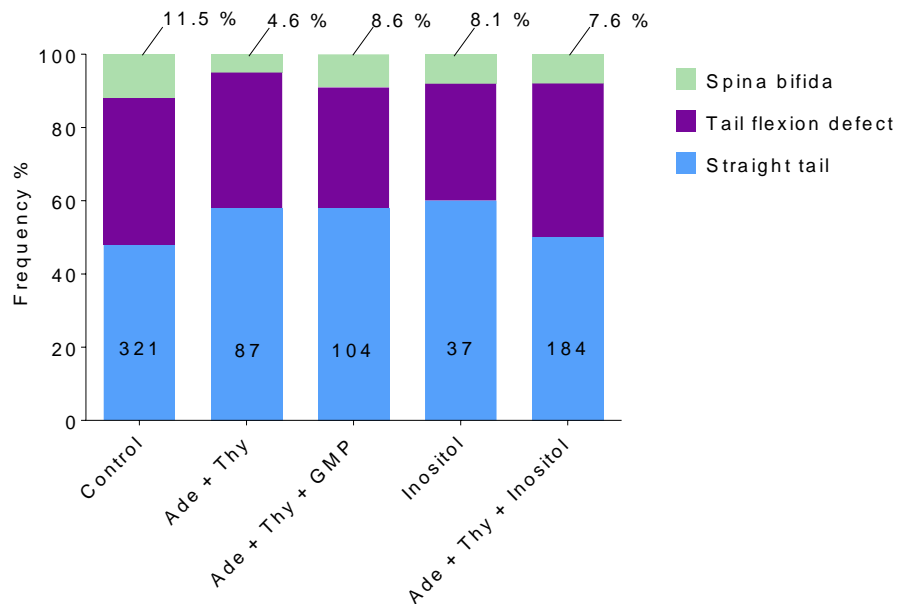


Figure 3. 8. Rates of spina bifida among offspring of *curly tail* mice treated by intraperitoneal injection

No significant differences between the frequency of spina bifida were found between groups. Ade = adenine; Thy = thymidine. Numbers in bars show the number of embryos per group.

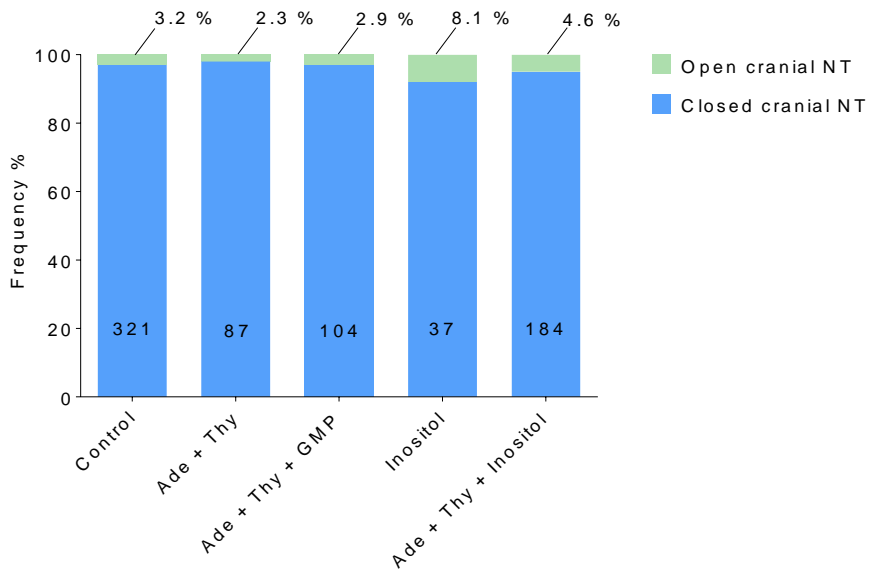


Figure 3. 9. Rates of exencephaly among offspring of *curly tail* mice treated by intra-peritoneal injection

No significant changes in the frequency of exencephaly were found between treatment groups. Ade = adenine; Thy = thymidine. Numbers in bars show the number of embryos per group.

3.2.3 Oral nucleotide treatment

3.2.3.1 Oral nucleotides prevent NTDs

While it has been shown that intra-peritoneal administration of nucleotide precursors can prevent NTDs in the *ct* mice (K. Y. Leung et al. 2013), an important question was whether a similar prevention could be achieved from orally administered precursors, which must be absorbed through the intestinal tract before being released into the systemic circulation to cross the placenta.

To this end, the ability of the nucleotides, AMP, IMP and GMP, and the nucleoside thymidine, to prevent NTDs when administered *ad lib* in maternal drinking water was investigated. For brevity, the combined supplement of AMP, IMP, GMP and thymidine will be referred to collectively as “nucleotide treatment”. Initially, each nucleotide/ nucleoside was present in maternal drinking water at 0.5 mg/ mL, predicted to deliver a total of 100 mg/ kg/ day. Plugged *ct* mice were given supplemented drinking water from E7.5 until collection between E11.5 and E14.5. The dose was then increased to 5 mg/ mL of each nucleotide/ nucleoside (predicted to deliver 1000 mg/ kg/ day), with the same period of treatment E7.5 until collection. Lastly, using the 5 mg/ mL, an extended period of treatment, from E0.5 until collection, was tested. However, among the litters which received treatment from E0.5, a proportion received the supplemented water having previously been maintained for 4 months on chow supplemented with the anthelmintic fenbendazole. The mice were

back on ordinary chow when the supplementation took place. The number of litters under each regimen are shown (**Table 3. 1**).

None of the individual treatments yielded a significant reduction in the rate of spina bifida compared to untreated controls (**Table 3. 1**). The baseline rate of NTDs appeared to change among offspring of mice that had been maintained on fenbendazole. Therefore, the pre-fenbendazole mice were considered separately. Comparing the combined effect of all nucleotide treatments before fenbendazole treatment, the frequency of spina bifida was significantly reduced by approximately 50 % compared to control embryos ($p = 0.01$). It was noted that after fenbendazole treatment, the rate of spina bifida in control embryos decreased from ~ 12 % to ~ 7 %, and nucleotide supplementation appeared to have no effect or could even have been detrimental (**Table 3. 1**).

Similarly, oral nucleotide treatment was found to significantly reduce the frequency of exencephaly by approximately 35 % ($p = 0.03$) when treatments pre-fenbendazole were combined (**Table 3. 2**). Again, it appears that oral nucleotide supplementation became ineffective at preventing exencephaly after fenbendazole treatment.

3.2.3.2 Analysis of size of nucleotide treated embryos

The supplementation of embryos with nucleotides via intra-peritoneal injections was shown to increase proliferation in the hindgut and neural tube but did not result in a significant increase in embryonic growth, as measured by crown-rump (CR) length at E13.5 (K. Y. Leung et al. 2013). Similarly, the CR length of E12.5 control and treated embryos were assessed according to dose (0.5 and 5 mg/ mL) for embryos treated from E7.5 – E12.5 (**Figure 3. 10**). This assessment found that embryos treated with 0.5 mg/ mL had increased CR lengths compared to both control embryos ($p = 0.0001$) and those treated with 5 mg/ mL oral nucleotides ($p < 0.0001$).

		Frequency % (n)			
Oral nucleotide treatment	No. of litters	Straight tail	Flexion defect	Spina bifida	TOTAL
Control	25	40.64 (76)	44.92 (84)	14.39 (27)	187
0.5 mg/ mL (E7.5 – 12.5)	11	54.44 (49)	38.89 (35)	6.67 (6)	90
Control	26	48.19 (93)	39.90 (77)	11.92 (23)	193
5 mg/ mL (E7.5 – 12.5)	16	51.89 (55)	40.57 (43)	7.55 (8)	106
Control	13	51.52 (51)	37.37 (37)	11.11 (11)	99
5 mg/ mL (From E0.5)	4	57.58 (19)	39.39 (13)	3.03 (1)	33
Total control before fen.	64	45.93 (220)	41.34 (198)	12.73 (61)	479
Total treated before fen.	30	53.71 (123)	39.30 (90)	6.55 (15)*	229
Total control after fen.	23	51.20 (85)	41.57 (69)	7.23 (12)	166
Total treated after fen. (5 mg/ mL from E0.5)	14	50.94 (54)	38.68 (41)	9.43 (10)	106

Table 3. 1. Rates of spina bifida in oral nucleotides treated *curly tail* embryos by dose, stage and before/ after fenbendazole treatment

*p = 0.01; Fisher's exact test, Total treated before fen. compared to Total control before fen. Fen. = fenbendazole

Oral nucleotide treatment	No. of litters	Frequency % (n)		TOTAL
		Cranial closure	Exencephaly	
Control	25	92.51 (173)	7.49 (14)	187
0.5 mg/ mL (E7.5 – 12.5)	11	97.78 (88)	2.22 (2)	90
Control	26	97.93 (189)	2.07 (4)	193
5 mg/ mL (E7.5 – 12.5)	16	98.11 (104)	1.89 (2)	106
Control	13	93.94 (93)	6.06 (6)	99
5 mg/ mL (From E0.5)	4	100.00 (33)	0 (0)	33
Total control before fen.	64	94.99 (455)	5.01 (24)	479
Total treated before fen.	30	98.25 (225)	1.75 (4)*	229
Total control after fen.	23	95.78 (159)	4.22 (7)	166
Total treated after fen. (5 mg/ mL from E0.5)	14	96.33 (102)	3.77 (4)	106

Table 3. 2. Rates of exencephaly in oral nucleotides treated *curly tail* embryos by dose, stage and before/ after fenbendazole treatment

* $p = 0.03$; Fisher's exact test. Total treated before fen. compared with Total control before fen. Fen. = fenbendazole

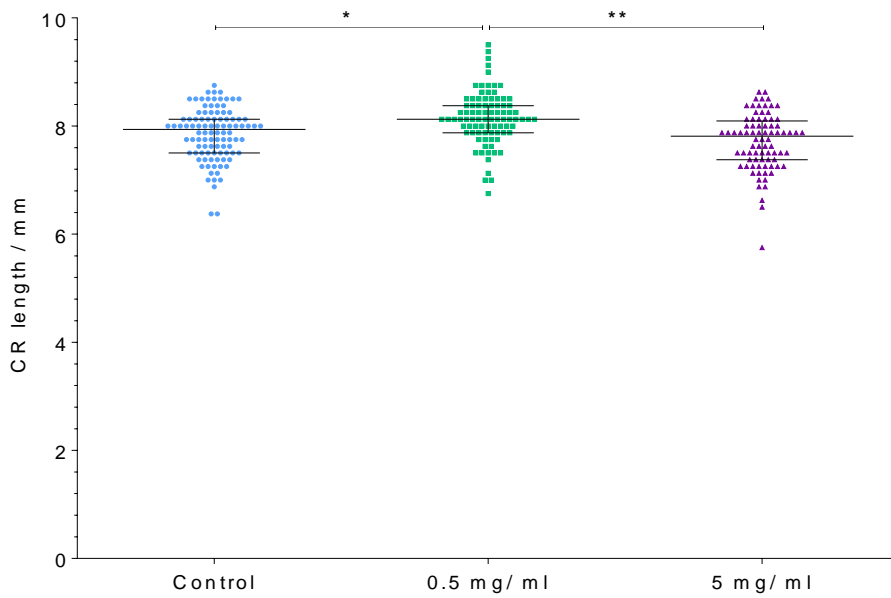


Figure 3. 10. Crown-rump lengths of oral nucleotides treated embryos

Embryos treated with 0.5 mg/ mL oral nucleotides (8.15 ± 0.005 mm) had increased CR lengths compared to control embryos (7.85 ± 0.05 mm; $*p = 0.0001$) and embryos treated with 5 mg/ mL oral nucleotides (7.70 ± 0.05 mm; $**p < 0.0001$). Assess by ANOVA with Tukey's multiple comparison test. For control, $n = 100$; for 0.5 mg/ mL, $n = 88$; and for 5 mg/ mL, $n = 80$.

3.2.4 Quantification of nucleotides, nucleosides and nucleobases in intra-peritoneal and oral nucleotide supplemented embryos

To assess whether the abundance of nucleotides and nucleosides is changed in embryos supplemented by oral and intra-peritoneal nucleotides as compared to control embryos, a published method which utilised the same mass spectrometer and liquid chromatography equipment as that available for this project (Laourdakis et al. 2014), was adapted and implemented. The method was used to quantify 25 nucleotides, 5 nucleosides, 4 nucleobases and orotic acid, a precursor for pyrimidine synthesis (**Table 3. 3**) in whole, E10.5 embryos, with results presented as pmol. per μ g protein. Oral nucleotide treated embryos received a predicted dose of 1000 mg/ kg/day AMP + IMP + GMP + thymidine from E0.5 to E10.5, while intraperitoneal injected nucleotide treated embryos received adenine + thymidine at 20 mg/ kg/ day from E7.5 to E10.5. The nucleotides, nucleosides and nucleobases which were detected in samples are highlighted in **Table 3. 3**.

This assessment revealed that embryos supplemented with oral nucleotides had increased levels of total dNMPs/ NMPs ($p = 0.01$), total nucleosides ($p = 0.04$) and total nucleobases ($p = 0.004$) compared to control embryos. In addition, oral nucleotide treated embryos had increased total monophosphate nucleotides ($p = 0.03$) and total nucleobases ($p = 0.02$) compared with intra-peritoneal treated embryos (**Figure 3. 11**). Total dNTP/ NTPs and dDNP/DNPs per μ g of protein were not found to vary with treatment.

Closer analysis of individual NTPs/ dNTPs and NDPs/ dNDPs found no significant changes in individual nucleotides (**Figure 3. 12 & Figure 3. 13**). On the other hand, it can be seen that the difference found in total NMPs/ dNMPs is primarily due to the increased abundance of AMP in oral treated embryos in comparison to control (~ 10 times; $p = 0.009$) and intra-peritoneal treated embryos (~4 times; $p = 0.02$). Increases in GMP in comparison to control (~14 time; $p = 0.02$) and intra-peritoneal treated (~5 times; $p = 0.04$), UMP in comparison to control (~4 times; $p = 0.02$), and to a lesser extent, dTMP in comparison to control ($p = 0.003$) and intra-peritoneal treated (~ 18 times; $p = 0.004$), also contribute (**Figure 3. 14**). Of interest. AMP and GMP were constituents of the oral nucleotide treatment while UMP and dTMP were not.

The main contribution to the increase in total nucleoside levels in orally treated compared to control samples is from cytidine (~ 18 times; $p = 0.01$), and to a lesser extent guanosine (~ 4 times; $p = 0.0008$; **Figure 3. 15**). Guanosine is approximately 3 times increased in intra-peritoneal treated embryos in comparison to control ($p = 0.004$). Additionally, uridine was increased by oral treatment compared to control (~ 9 times; $p = 0.005$) and intra-peritoneal treated (~ 6 times; $p = 0.007$). Of interest, thymidine was present in both oral and intra-peritoneal nucleotide treatment but it was not detected in embryo samples, however dTMP is increased in orally treated samples.

Closer examination of individual nucleobases (**Figure 3. 15**) reveals that the abundance of hypoxanthine was increased in oral treated embryos in comparison to control (~7 times; $p = 0.004$) and intra-peritoneal treated (~3 times: $p = 0.01$) embryos, while adenine (~2 times; $p = 0.02$) and guanine (~4 times; $p = 0.006$) levels were increased in oral treated embryos in comparison to control embryos.

In summary, while no differences were found in the abundance of NTPs/ dNTPs or NDPs/ dNDPs, oral nucleotide treatment increased the abundance of NMPs/ dNMPs, nucleosides and nucleobases, in comparison to control samples, but to a lesser extent compared to intra-peritoneal treated samples. While intra-peritoneal treated embryos only demonstrated increased guanosine in comparison to control embryos, they were not significantly different in the majority of nucleosides and nucleobases compared to orally treated embryos.

Nucleotides		Nucleosides	Nucleobases & precursors
AMP	GTP	Adenosine	Adenine
ADP	dGTP	Cytosine	Cytidine
dADP	IMP	Guanosine	Guanine
ATP	dTMP	Thymidine	Hypoxanthine
dATP	dTDP	Uridine	Orotic acid
CMP	dTTP		
CDP	UMP		
dCDP	dUMP		
CTP	UDP		
dCTP	UTP		
GMP	dUTP		
GDP	XMP		
dGDP			

Table 3. 3. Nucleotides, nucleosides and nucleobases detected by mass spectrometry.

The nucleotides, nucleosides and nucleobases which were present above the level of detection in samples are highlighted in red script.

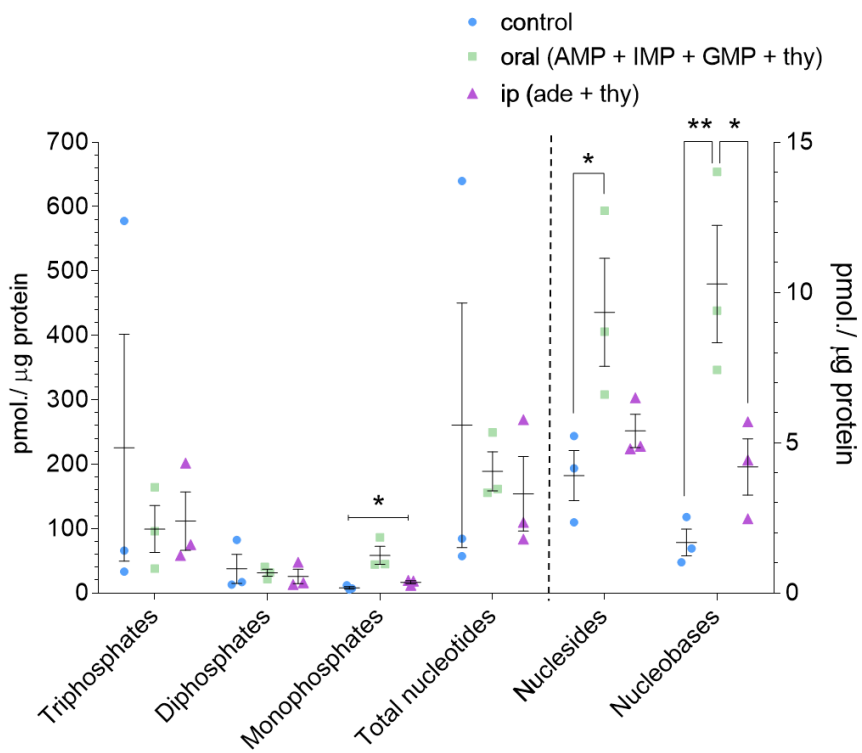


Figure 3.11. Abundance of total nucleotides, nucleosides and nucleobases

Embryos treated with oral nucleotides (58.36 ± 13.95 pmol/ µg protein) have increased total **nucleoside monophosphates** in comparison to control (8.13 ± 1.99 pmol/ µg protein; $*p = 0.01$) and intraperitoneal (16.80 ± 2.32 pmol/ µg protein; $*p = 0.02$) treated embryos. Oral treatment also increased the abundance of total **nucleosides** (9.34 ± 1.80 pmol/ µg protein) in comparison to control embryos (3.91 ± 0.84 pmol/ µg protein; $*p = 0.04$), and **nucleobases** (4.08 ± 0.44 pmol/ µg protein) in comparison to control (1.33 ± 0.24 pmol/ µg protein; $**p = 0.004$) and intraperitoneal treated embryos (2.03 ± 0.37 pmol/ µg protein; $*p = 0.02$). Black dotted line separates data plotted on left and right axis. $N = 3$ for each group. All statistics calculated by ANOVA followed by Tukey's multiple comparison test.

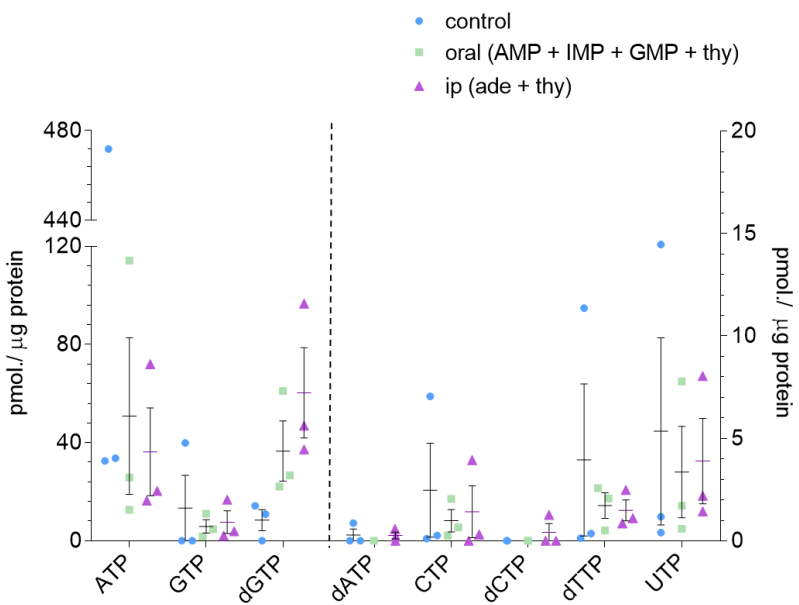


Figure 3.12. Abundance of nucleoside triphosphates

No changes in individual nucleoside triphosphates were found. Black dotted line separates data plotted on left and right axis. $N = 3$ for each. Only nucleotides which were above the level of detection are plotted.

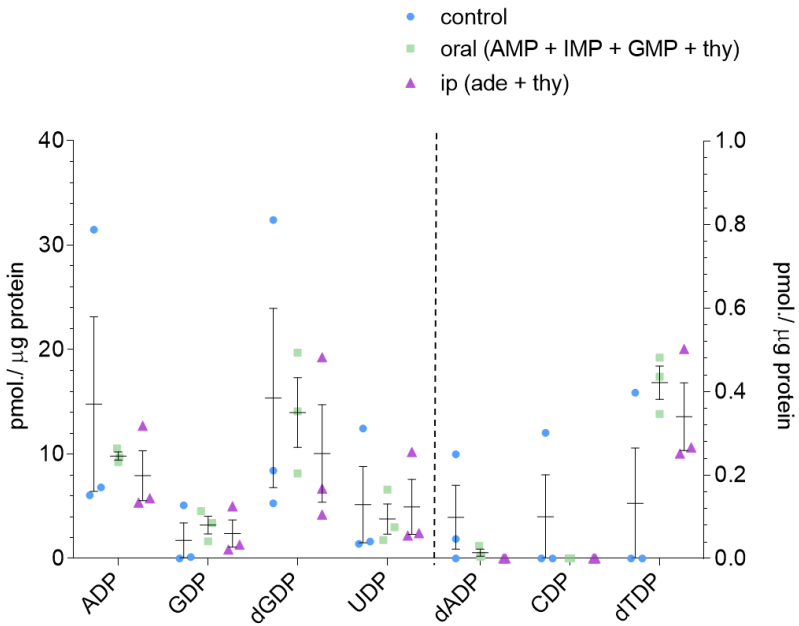


Figure 3.13. Abundance of nucleoside diphosphates

No changes in individual nucleoside diphosphates were found. Black dotted line separates data plotted on left and right axis. $N = 3$ for each. Only nucleotides which were above the level of detection are plotted.

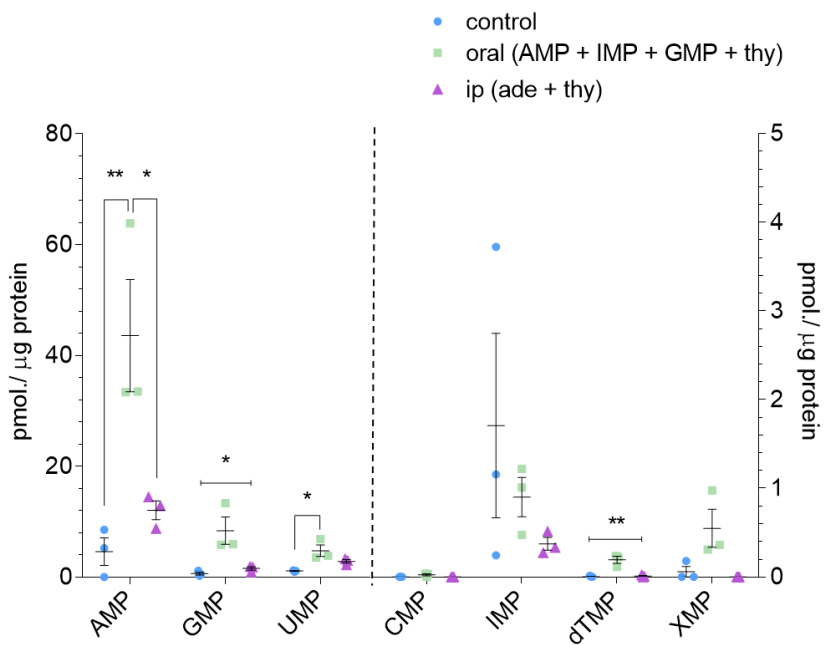


Figure 3.14. Abundance of nucleoside monophosphates

Oral treated embryos had increased: **AMP** (43.58 ± 10.13 pmol/ μ g protein) in comparison to control (4.73 ± 2.61 pmol/ μ g protein; $**p = 0.009$) and intraperitoneal treated embryos (12.03 ± 1.70 pmol/ μ g protein; $*p = 0.03$); **GMP** (8.36 ± 2.47 pmol/ μ g protein) in comparison to control (0.60 ± 0.21 pmol/ μ g protein; $*p = 0.02$) and intraperitoneal treated embryos (1.56 ± 0.32 pmol/ μ g protein; $*p = 0.04$); **dTMP** (0.19 ± 0.040 pmol/ μ g protein) in comparison to control (0.0 ± 0.0 pmol/ μ g protein; $*p = 0.003$) and intraperitoneal treated embryos (0.01 ± 0.007 pmol/ μ g protein; $*p = 0.003$); **UMP** (4.75 ± 1.05 pmol/ μ g protein) in comparison to control (1.07 ± 0.07 pmol/ μ g protein; $*p = 0.02$) embryos. Black dotted line separates data plotted on left and right axis. $N = 3$ for each. All statistics calculated by ANOVA followed by Tukey's multiple comparison test. Only nucleotides which were above the level of detection are plotted.

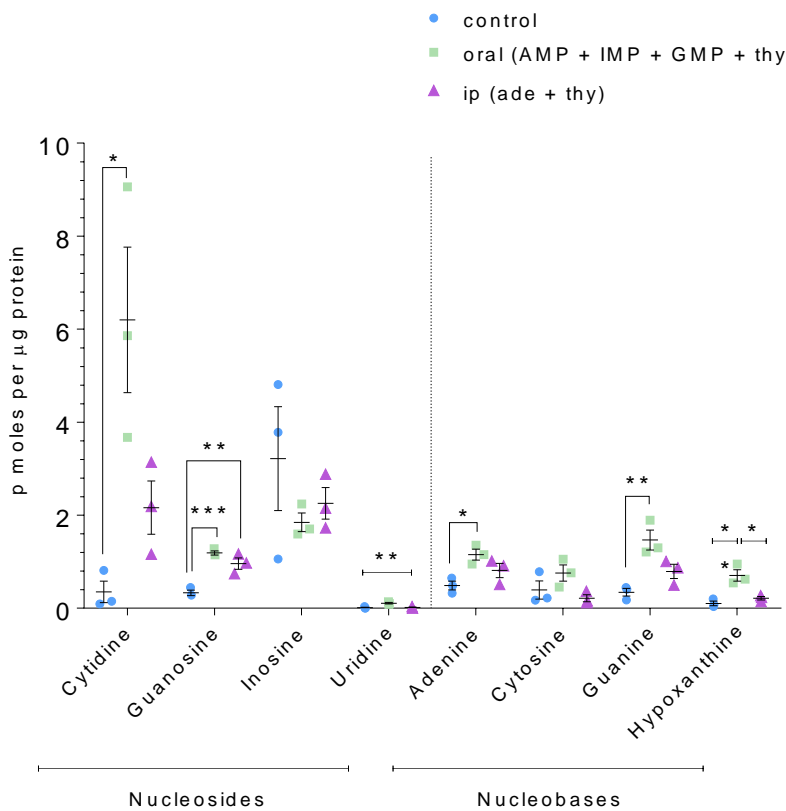


Figure 3.15. Abundance of nucleosides and nucleobases

Oral treated embryos had increased: **cytidine** (6.20 ± 1.56 pmol/ μ g protein) in comparison to control embryos (0.35 ± 0.23 pmol/ μ g protein; $*p = 0.01$); **guanosine** (1.19 ± 0.05 pmol/ μ g protein) in comparison to control embryos (0.33 ± 0.06 pmol/ μ g protein; $***p = 0.0008$); **uridine** (0.11 ± 0.02 pmol/ μ g protein) in comparison to control (0.01 ± 0.01 pmol/ μ g protein; $**p = 0.005$) and intraperitoneal treated embryos (0.02 ± 0.01 pmol/ μ g protein; $**p = 0.07$); **adenine** (1.15 ± 0.12 pmol/ μ g protein) in comparison to control embryos (0.49 ± 0.09 pmol/ μ g protein; $*p = 0.02$); **guanine** (1.47 ± 0.21 pmol/ μ g protein) in comparison to control embryos (0.34 ± 0.08 pmol/ μ g protein; $**p = 0.004$), and; **hypoxanthine** (0.71 ± 0.17 pmol/ μ g protein) in comparison to control (0.10 ± 0.05 pmol/ μ g protein; $**p = 0.004$) and intraperitoneal treated embryos (0.22 ± 0.04 pmol/ μ g protein; $*p = 0.01$). Additionally, **guanosine** was increased in embryos treated with intraperitoneal nucleotide precursors (0.96 ± 0.12 pmol/ μ g protein) in comparison to control (0.33 ± 0.06 pmol/ μ g protein; $**p = 0.004$). $N = 3$ for each. All statistics calculated by ANOVA followed by Tukey's multiple comparison test. Only nucleosides/ nucleobases which were above the level of detection are plotted.

3.2.5 Supplementation of oral nucleotides and inositol in *curly tail* mice

Pregnant mice were supplemented with inositol (5 mg/ mL) in drinking water, to test whether this is protective as found for intra-peritoneal, sub-cutaneous or gavage treatment (Greene and Copp 1997; Cogram et al. 2002, 2004). Treatment began at E0.5 and continued until collection at E12.5. Administered orally, inositol treatment tended to reduce the frequency of spina bifida by ~50 % (**Table 3. 4**) demonstrating a comparable preventative effect to that measured previously. The next step was to assess whether a combined treatment of oral nucleotides + inositol is effective and to check that these approaches do not interfere with each other.

3.2.5.1 Nucleotides plus inositol treatment prevents neural tube defects

Each of the nucleotides/ nucleosides specified above and inositol (referred to as nucleotides + inositol treatment) was added to maternal drinking water at 5 mg/ mL starting from E0.5. This treatment was found to significantly reduce the frequency of spina bifida ($p = 0.01$; **Table 3. 4**) and exencephaly ($p = 0.0007$; **Table 3. 5**). Both inositol alone and nucleotide + inositol treatments were also continued after the completion of 4 months of fenbendazole treatment. Once again, fenbendazole treatment appeared to make each of these treatments less efficacious or, in the case of nucleotides + inositol, even detrimental to the rate of spina bifida in *ct* mice (**Table 3. 4**). In contrast, the treatment of nucleotides + inositol still appeared to offer some protection against exencephaly after fenbendazole treatment (**Table 3. 5**). The control embryo data in these tables was also used for comparison with embryos treated with 5 mg/ mL oral nucleotide treatment from E0.5, as these experiments were conducted over the same period. Likewise, the results from 5 mg/ mL oral nucleotide treatment from E0.5 are included for a comparison.

3.2.5.2 Analysis of size of nucleotide + inositol treated embryos

Neither inositol alone nor nucleotide + inositol treatment affected the CR length of embryos at E12.5, as compared to control embryos (**Figure 3. 16**).

Time period	Treatment	Frequency % (n)			TOTAL
		Straight tail	Flexion defect	Spina bifida	
Before fenbendazole	Control	51.52 (51)	37.37 (37)	11.11 (11)	99
	Nucleotides (5 mg/ mL from E0.5)	57.58 (19)	39.39 (13)	3.03 (1)	33
	Inositol	48.28 (28)	46.55 (27)	5.17 (3)	58
	Nucleotides + inositol	56.57 (56)	41.41 (41)	2.02 (2)*	99
After fenbendazole	Control	51.20 (85)	41.57 (69)	7.23 (12)	166
	Nucleotides (5 mg/ mL from E0.5)	50.94 (54)	38.68 (41)	9.43 (10)	106
	Inositol	52.05 (38)	41.10 (30)	6.85 (5)	73
	Nucleotides + inositol	68.67 (57)	20.48 (17)	10.84 (9)	83

Table 3. 4. Rates of spina bifida in oral inositol and inositol + nucleotides treated embryos before and after fenbendazole treatment.

* $p = 0.01$; Fisher's exact test. Frequency of spina bifida in Nucleotides + inositol treated group compared to Control (before fenbendazole).

Time period	Treatment	Frequency % (n)		TOTAL
		Normal cranial closure	Exencephaly	
Before fenbendazole	Control	93.94 (93)	6.06 (6)	99
	Nucleotides (5 mg/ mL from E0.5)	100.00 (33)	0 (0)	33
	Inositol	100.00 (58)	0 (0)	58
	Nucleotides + inositol	100.00 (99)	0 (0)*	99
After fenbendazole	Control	95.78 (159)	4.22 (7)	166
	Nucleotides (5 mg/ mL from E0.5)	96.33 (102)	3.77 (4)	106
	Inositol	95.89 (70)	4.11 (3)	73
	Nucleotides + inositol	98.80 (82)	1.20 (1)	83

Table 3. 5. Rates of exencephaly in oral inositol and inositol + nucleotides treated embryos before and after fenbendazole treatment.

* $p = 0.0007$; Fisher's exact test. Frequency of exencephaly in Nucleotides + inositol treated group compared to Control (before fenbendazole).

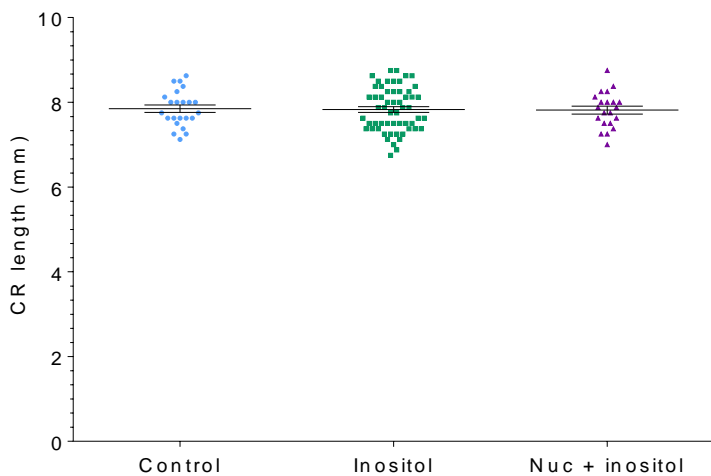


Figure 3. 16. The crown-rump lengths of inositol and inositol + nucleotides treated embryos

There were no differences in CR length of E12.5 embryos. For control, $n = 23$; for inositol, $n = 57$ and for inositol + nucleotides, $n = 21$.

3.2.6 Do inositol and nucleotide treatments affect folate one-carbon metabolism?

There are several lines of evidence that led to the hypothesis that inositol could influence FOCM. Inositol is a molecule which has been shown to affect proliferation via a PKC-dependent mechanism, proposed to be downstream of membrane phosphatidylinositol signalling (Greene and Copp 1997). The cell-cycle is known to be coupled to expression and nuclear localisation of the FOCM enzymes MTHFD1, TYMS and SHMT1 in mammalian cells (Lane and Fan 2015; Anderson et al. 2012; Field et al. 2014). Although not well characterised, this is at least partly mediated through the action of transcription factors which are activated by proliferative stimuli, such as MYC and RB/ E2F. *Dhfr* and *Gart* are also known to be regulated by pro-proliferative transcription factors (Lane and Fan 2015).

Another potential link between inositol and FOCM is the fact that inositol can be used for *de novo* nucleotide synthesis via conversion to glucose 6-phosphate, which can be used to synthesise serine, glutamine or PRPP, which are all substrates for nucleotide biosynthesis (Section 3.1.2). Additionally, increases in PRPP are known to stimulate nucleotide biosynthesis (Lane and Fan 2015). Lastly, work conducted by the lab found that while folate deficiency led to an expected reduction in the ratio of s-adenosylmethionine (SAM) to s-adenosylhomocysteine (SAH; more detail below; Section 3.2.6.2), in congenic wild-type mice on a *ct* background ($+^{ct}/+^{ct}$), inositol

treatment not only normalised the SAM / SAH ratio but increased it (De Castro et al. 2010). It was, therefore, possible that treatments containing inositol could affect the relative distribution of folates.

3.2.6.1 Quantification of folate cofactors

To investigate possible effects of inositol or nucleotide treatment on FOCM, six folates (DHF, THF, 5,10-methenylTHF, 5,10-methyleneTHF, 5-methylTHF and formylTHF) were quantified using HPLC-MS/MS (Garrett and Santi 1979; Cabreiro et al. 2013; Pai et al. 2015). This method quantifies the mono-glutamated and 2 – 7 glutamated forms of each folate. For completeness, E10.5 embryos from each of the oral treatment groups (beginning from E0.5) were assessed. This is the earliest stage at which the level of detection of the assay allows quantification of folates from individual embryos and corresponded to the end of spinal neurulation.

The absolute levels (normalised to total protein) and relative levels (percentage of total folates), for control, oral nucleotide treated, inositol treated, and nucleotide + inositol treated embryos, for each folate cofactor, are shown as the sum of all glutamated forms. The absolute levels of folate cofactors finds a decrease in the abundance of 5-methylTHF by 34 % in inositol, and by 49 %, in nuc + inositol treated embryos ($p = 0.003$ and $p < 0.0001$ respectively; **Figure 3. 17**). The relative levels of folate cofactors demonstrate that as 5-methylTHF levels decrease, the relative abundance of THF and formylTHF tend to increase. Inositol and nuc + inositol treatments were found to significantly reduce the relative proportion of 5-methylTHF by approximately 20 % and 30 % respectively ($p = 0.02$ and $p > 0.0001$ respectively; **Figure 3. 18**). While there was a tendency for inositol treatment to increase the relative abundance of THF ($p = 0.06$), in nuc + inositol treated embryos the increase in relative THF reached significance ($p = 0.01$; **Figure 3. 18**). Summation of the absolute levels of each folate cofactor did not find any changes (**Figure 3. 19**).

3.2.6.2 Effect oral treatments on abundance of SAM and SAH

The relative decrease in 5-methylTHF and increase in THF observed in inositol and nuc + inositol treated embryos could either suggest an increased flux of one-carbon units passing into the methionine cycle, or a decreased synthesis of 5-methylTHF, with one-carbon units instead being retained within the pool of folates supplying *de novo* nucleotide synthesis (**Figure 1. 7**). In the second scenario, THF is regenerated by either SHMT1, or the combination of TYMS and DHF.

The methionine cycle can be assessed by quantification of SAM and SAH. After methionine is generated by the addition of a one-carbon unit donated by 5-methylTHF to homocysteine, methionine is converted to SAM by s-adenosylmethionine synthetase and the addition of ATP. SAM is the methyl donor for the numerous cellular methyltransferases (and is also used in polyamine synthesis). Transfer of the one-carbon unit from SAM to a substrate generates SAH, which is converted to homocysteine by adenosylhomocysteinase, completing the cycle (**Figure 1.**

7). If more one-carbon units are transferred to the methionine cycle, it could be expected that the capacity for SAM production would increase. A shortage of one-carbon units would be expected to increase SAH and decrease SAM.

To gain further insight into the status of the methionine cycle and potentially also the folate cycle, SAM and SAH were measured by HPLC-MS/ MS in E10.5 *ct* embryos under each of the different treatment conditions. The SAM / SAH ratio was found to be significantly increased by nucleotide treatment ($p = 0.001$; **Figure 3. 20**), despite 5-methylTHF (and THF) being unchanged (**Figure 3. 17 & Figure 3. 18**). Conversely, both inositol only and nucleotide + inositol treatments decreased the SAM / SAH ratio ($p = 0.02$ for both; **Figure 3. 20**). Nucleotide treatment showed a strong tendency towards reducing SAM ($p = 0.06$; **Figure 3. 21**), while both inositol only and nucleotide + inositol treatment had no significant effect (**Figure 3. 21**). SAH measurements were found to be significantly reduced by nucleotide treatment ($p = 0.02$; **Figure 3. 22**), while nucleotide + inositol treatment increased the levels of SAH ($p = 0.0002$; **Figure 3. 22**).

In summary, while nucleotide-only treatment appears to have increased the methylating potential of embryos by leading to a substantial reduction in SAH levels, inositol-only and nucleotide + inositol treatments had the opposite effect of increasing SAH levels. This suggests a decrease in methylating potential which would be consistent with observed reduction in the relative abundance of 5-methyl THF. Hence, these treatments may increase the amount of one-carbon units being retained within the folate cycle for *de novo* nucleotide synthesis. This is also suggested by the tendency of these treatments to increase formylTHF.

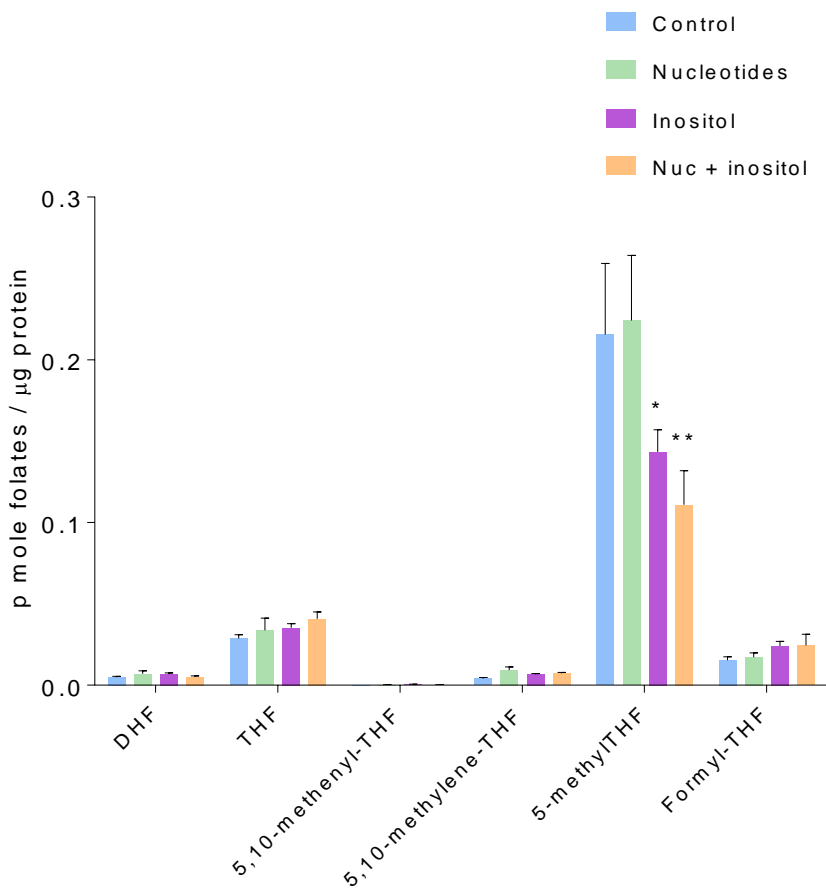


Figure 3. 17. Absolute folate levels of embryos on treatments containing inositol and/ or nucleotides.

Absolute folate profiles of control, nucleotide only treated (nucleotides), inositol only treated (inositol) and nucleotides + inositol (nuc + inositol) treated E10.5 embryos. Nucleotide treatment had no significant effect on the abundance of folates. Inositol treatment (0.143 ± 0.014 pmol./ μ g protein; $*p = 0.003$) and nucleotides + inositol treatment (0.111 ± 0.021 pmol./ μ g protein; $**p < 0.0001$) decreased the abundance of 5-methylTHF compared to control (0.216 ± 0.043 pmol./ μ g protein). For all treatments, $n = 4$ embryos each. Analysed by 2way ANOVA with Sidak's test.

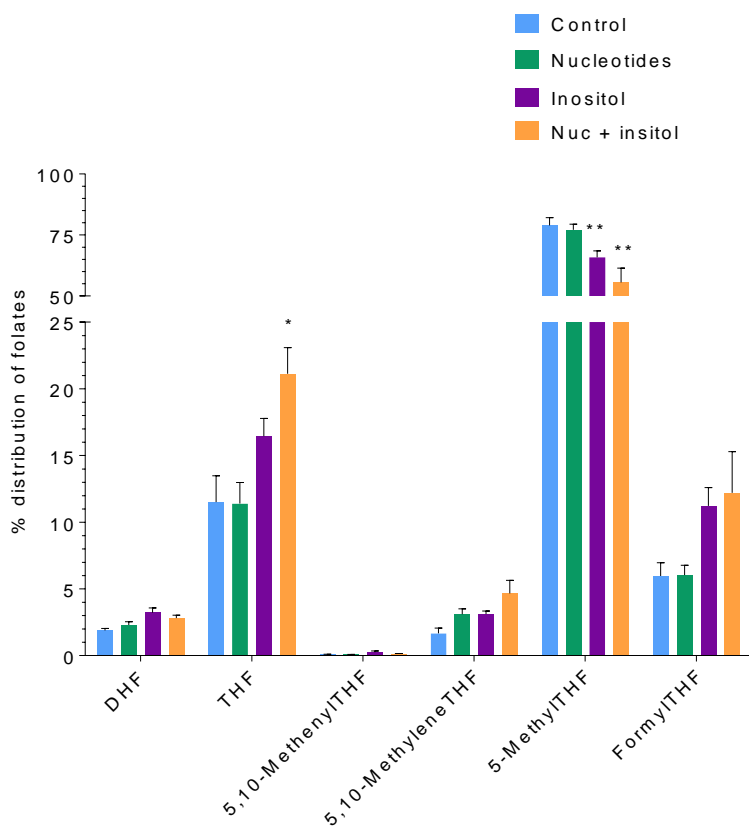


Figure 3. 18. Relative folate levels of embryos on treatments containing inositol and/ or nucleotides.

Relative folate profiles of control, nucleotide only treated (nucleotides), inositol only treated (inositol) and nucleotides + inositol (nuc + inositol) treated E10.5 embryos. Nucleotide treatment had no significant effect on the abundance of folates. Inositol treatment ($65.77 \pm 2.75\%$) and nucleotides + inositol treatment ($55.54 \pm 5.92\%$) decreased the relative abundance of 5-methylTHF compared to control ($78.90 \pm 3.23\%$; $**p < 0.0001$ for both). Nucleotide + inositol treatment ($21.13 \pm 1.96\%$) also increased the relative abundance of THF compared to control ($11.50 \pm 1.97\%$; $*p = 0.01$) embryos. For all treatments, $n = 4$ embryos each. Analysed by 2way ANOVA with Sidak's test.

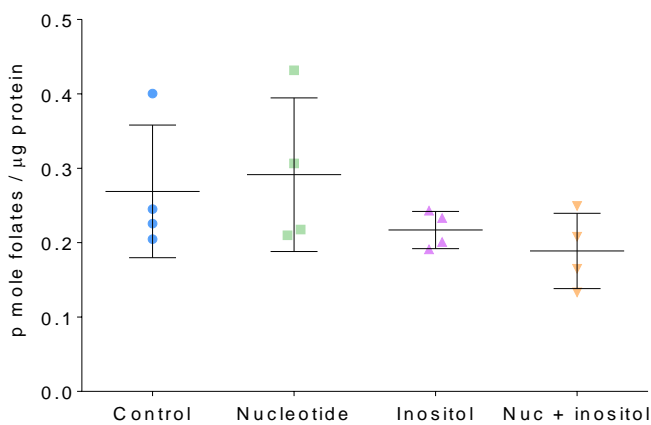


Figure 3. 19. Total folates in inositol and/ or nucleotide treated embryos

No significant differences found in total folate pools. $N = 4$ for each group.

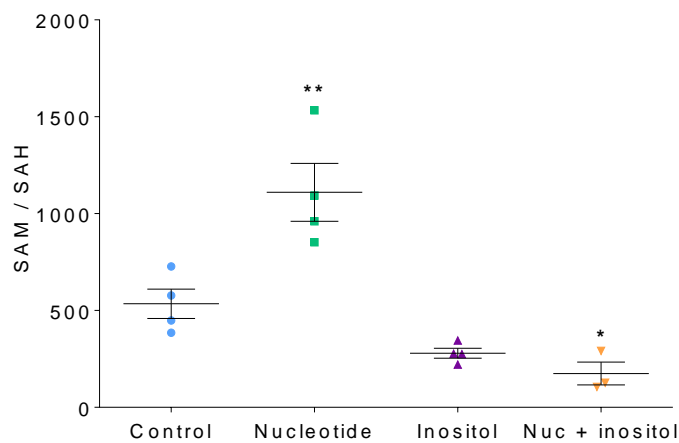


Figure 3. 22. Quantification of SAH in inositol and/ or nucleotide treated embryos

SAH/SAH ratios were increased in nucleotide treated embryos (1110 ± 149.5 ; $**p = 0.001$), while nucleotide + inositol (nuc + inositol) treatment (174.6 ± 58.8 ; $*p = 0.02$) decreased ratios, compared to control samples (534.6 ± 75.8). Data analysed by ANOVA followed by Fisher's least significant difference. For each group; $n = 4$, except for nuc + in group where $n = 3$.

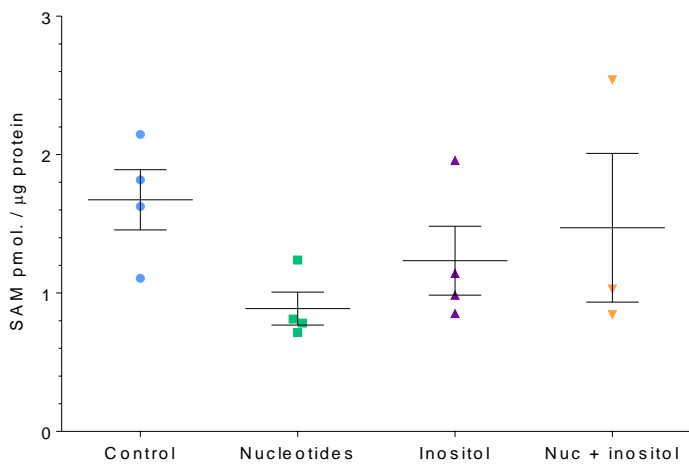


Figure 3. 21. Quantification of SAM in inositol and/ or nucleotide treated embryos

No significant changes found between treatment groups. For each group; $n = 4$, expect for nuc + in group where $n = 3$.

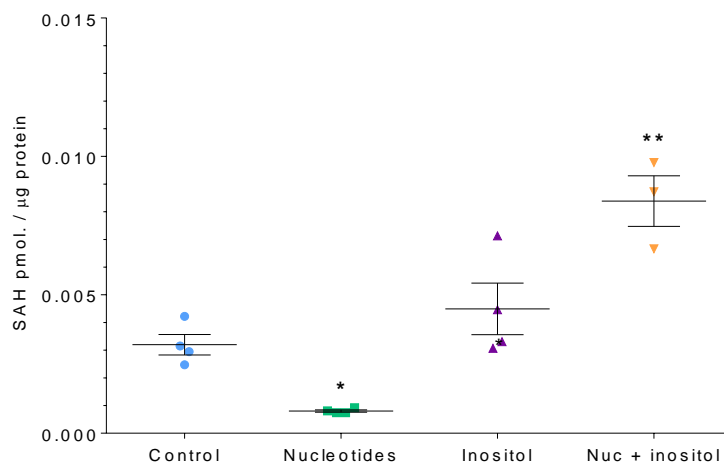


Figure 3. 22. Quantification of SAH in inositol and/ or nucleotide treated embryos

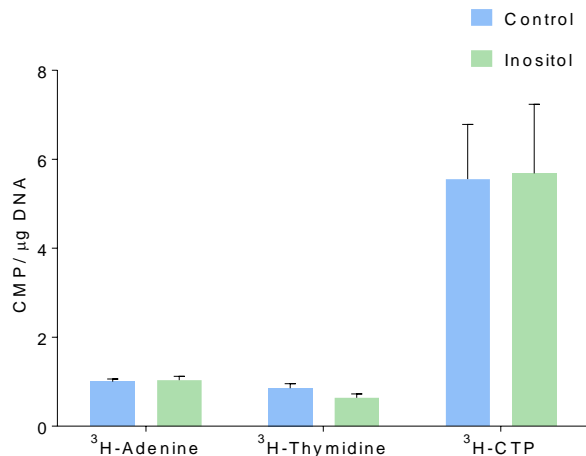
While nucleotides only treatment decreased levels of measured SAH (0.0008 ± 0.00004 pmol./ μ g; $*p = 0.02$), nucleotides + inositol (nuc + in) treatment increased levels (0.0084 ± 0.0009 pmol./ μ g; $**p = 0.0002$) relative to control samples (0.0032 ± 0.0004 pmol./ μ g). Data analysed by ANOVA followed by Fisher's least significant difference. For each group; $n = 4$, expect for nuc + in group where $n = 3$.

3.2.6.3 Effect of inositol on exogenous adenine incorporation

To further investigate the possibility that supplemental inositol stimulates *de novo* nucleotide synthesis, the incorporation of labelled adenine (^3H -adenine), thymidine (^3H -thymidine) and CTP (^3H -CTP) into DNA was assessed. Incorporation of the labelled nucleotide precursors is mediated by the salvage pathway, and changes in label incorporation imply a change in the relative contribution of nucleotides from *de novo* and salvage pathways. The salvage enzymes *Appt* and *TK* are required for salvage of adenine and thymidine respectively. Both these enzymes were found to be expressed ubiquitously in neurulation stage embryos, including in the neuroepithelia (**Section 3.2.1**). ^3H -CTP does not require the action of a salvage enzyme before it can be incorporated into DNA, nor are cytosine containing nucleotides synthesised *de novo* via FOCM. In this way, incorporation of ^3H -CTP can suggest whether any changes found in ^3H -adenine and ^3H -thymidine incorporation specifically implicates FOCM.

Curly tail embryos at E9 were explanted from the uterus within their yolk sacs and cultured in [^3H]-adenine, [^3H]-thymidine or [^3H]-CTP, either with or without 250 μM inositol. The addition of inositol to the cultures did not affect incorporation of the radiolabelled nucleotide precursors (**Figure 3. 23A**). The DNA content per embryo was unchanged between treatment groups (**Figure 3. 23B**).

(A)



(B)

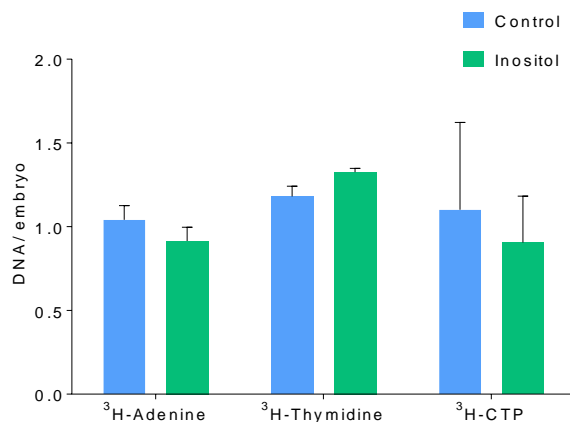


Figure 3. 23. Effect of inositol on $[{}^3\text{H}]\text{-adenine}$ and $[{}^3\text{H}]\text{-thymidine}$ incorporation into DNA

(A) Inositol (250 μM) added to culture had no significant effect on incorporation of radiolabelled nucleotide precursors. (B) No differences in DNA content per embryo were found.

Results from four separate experiments shown. Results within each experiment normalised to an arbitrarily chosen control sample. For $[{}^3\text{H}]\text{-adenine}$; $n = 8$ each, and for $[{}^3\text{H}]\text{-thymidine}$; $n = 9$ each, and for $[{}^3\text{H}]\text{-CTP}$; $n = 4$ each.

3.2.7 Does fenbendazole treatment retard embryonic growth?

Fenbendazole, like similar benzimidazoles, is believed to bind parasitic tubulin, disrupting microtubule networks that are required for mitosis and intracellular trafficking and secretion. It is believed to affect helminthic but not mammalian cells because of differences in the microtubule structures (McKellar and Scott 1990).

In an effort to understand the apparent protective effect of fenbendazole treatment on NTDs in the *ct* mouse, particularly spina bifida, the growth of control E10.5 embryos collected before and after fenbendazole treatment was assessed. A reduction in CR length would suggest that embryos are growth retarded, which has been found to prevent spina bifida in *ct* mice in the context of experimental settings such as hyperthermia (Copp et al. 1988; Seller 1983). To assess growth in relation to development, CR length was divided by somite number for each embryo (Figure 3.24). No differences were found between the two groups. This is in keeping with the lack of increase in exencephaly which usually accompanies growth retardation (Seller and Perkins 1983, 1986; Seller and Perkins-Cole 1987a). It is not known how fenbendazole may have modulated the rate of NTDs in *ct* mice.

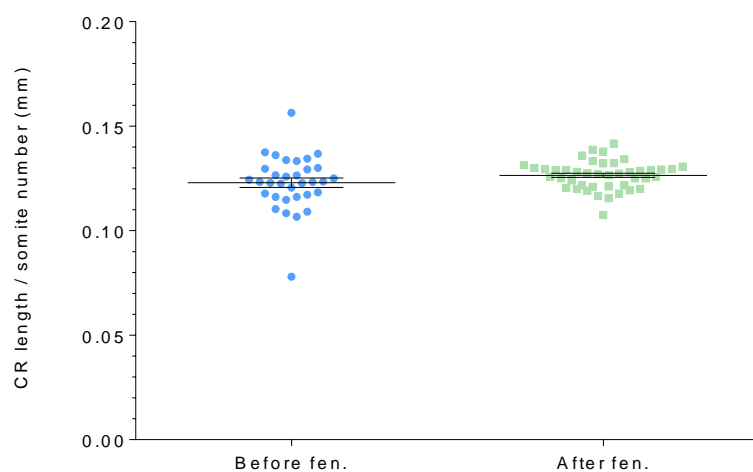


Figure 3.24. Fenbendazole treatment did not affect CR length

Fenbendazole (fen.) had no effect on the ratio of CR length to somite number. $n = 33$ for before fen. group and $n = 43$ for after fen. group.

3.2.8 Can oral nucleotide supplementation prevent NTDs in other mouse models?

In addition to the *ct* mouse, both the *Splotch* and *Gldc* NTD mouse models potentially involve reduced proliferation as part of their aetiology. Therefore, *Splotch* and *Gldc* litters from heterozygous intercrosses were treated with 5 mg/ mL oral nucleotide treatment from E0.5 until E11.5, when litters were explanted and embryos examined for NTDs.

3.2.8.1 Glycine decarboxylase (*Gldc*) null mice

Gldc encodes a protein (GLDC or P-protein) that is highly expressed in the neuroepithelia of neurulation stage embryos (Pai et al. 2015). GLDC is one of four proteins constituting the multienzyme, mitochondrial GCS, which catabolises glycine. The products of this catabolism are CO₂, ammonia, NADH and a one-carbon unit, which is transferred to THF to produce 5, 10-methyleneTHF. Unless utilised by mitochondrial TYMS, this one-carbon unit can either be released as formate and take part in cytosolic FOCM processes, or can be catabolised to CO₂ by 10-formylTHF dehydrogenase (**Figure 1.7**).

Genetic ablation of *Gldc* via gene-trapping results in loss of glycine cleavage capacity, and approximately a 20 % (hypomorphic expression) or 60 % (null expression) frequency of midbrain-hindbrain exencephaly in homozygous null mutants, depending on the gene trap model. Additionally, exencephaly in this model does not show any sex bias (Pai 2015). The *Gldc*^{GT1} allele contains a conditional gene-trap construct inserted into intron 2-3 of the *Gldc* gene, and around 20 % of null *Gldc*^{GT1/GT1} mice present with exencephaly. The *Gldc*^{GT2} allele contains a gene-trap construct inserted into intron 19-20 of the *Gldc* gene, and approximately 60 % of *Gldc*^{GT2/GT2} mice present with exencephaly. The decreased frequency of exencephaly in *Gldc*^{GT1/GT1} mice appears to be due to a residual ~10 % expression of *Gldc*, which overall confers a lower risk of NTDs (Pai 2015).

Gldc^{GT1/GT1} embryos have been well characterised, and demonstrate alterations in their folate profile; increased THF and DHF (folates which do not carry a one-carbon unit) and decreased 5-methylTHF. Mutant embryos also exhibit decreased mitotic index in the rostral hindbrain at E9.5 (Pai et al. 2015). Formate supplementation significantly reduced the frequency of exencephaly from 22 % to 2% of mutants, and also normalised their folate profile and mitotic index (Pai et al. 2015).

Proliferation and formate rescue studies have not been carried out in *Gldc*^{GT2/GT2} embryos, however, their folate profiles show the same disturbances as those seen in *Gldc*^{GT1/GT1} embryos (N Greene, personal communication). Additionally, *Gldc*^{GT2} and *Mthfr* heterozygous mice were crossed to generate double heterozygous offspring (*Gldc*^{GT1/+}; *Mthfr*^{+/+}), which were subsequently crossed and the litters examined for NTDs. This study found that loss of *Mthfr* on a *Gldc*^{GT2} null background

decreased rates of exencephaly (Unpublished data), implying that retention of one-carbon units for nucleotide synthesis prevents exencephaly.

The increase in THF and DHF, together with the decrease in abundance of 5-methylTHF, suggests a depletion of one-carbon units owing to loss of GCS capability. The rescue effect of formate supplementation, which does not correct for accumulating glycine (Pai et al. 2015), suggests that reduced availability of one-carbon units for cytosolic FOCM output, *de novo* nucleotide synthesis in particular, may be involved in the causation of NTDs. Therefore, supplemental nucleotides may also provide a preventative effect.

Due to the higher proportion of mutants affected by NTDs using the *Gldc*^{GT2} allele, which would increase the likelihood of detecting an ameliorating effect, nucleotide treatment was undertaken in the *Gldc*^{GT2} strain. However, there was the possibility that because the genetic defect was more severe in the *Gldc*^{GT2} strain, they would be resistant to rescue. Therefore, plugged *Gldc*^{GT2/+} mice were supplemented with 30 mg/ mL sodium formate, which was found to significantly prevent NTDs in *Gldc*^{GT2/GT2} embryos ($p = 0.008$; **Table 3. 6**), demonstrating NTDs in this strain were amenable to rescue. However, oral nucleotide treatment was not found to have any effect on the frequency of exencephaly in *Gldc*^{GT2/GT2} mice (**Table 3. 6**).

	Frequency of exencephaly in <i>Gldc</i> ^{GT2/GT2} embryos % (n)
Control	66.67 (4/6)
Formate treatment	0 (0/10)*
Control	61.54 (16/26)
Nucleotide treatment	66.67 (22/33)

Table 3. 6. Frequency of NTDs in *Gldc*^{GT2/GT2} embryos with formate and nucleotide treatment.

Sodium formate supplementation into maternal drinking water significantly decreased the proportion of *Gldc*^{GT2/GT2} embryos with cranial NTDs (* $p = 0.008$; Fisher's exact test).

3.2.8.2 *Splotch* (*Sp*^{2H})

While the cellular and tissue level defect which leads to NTDs in *Splotch* is currently not well understood, reduced proliferation is a potential cause (investigated and discussed further for the cranial region in **Chapter 6**). Two lines of evidence support a theory that NTDs in *Splotch* mutants would be amenable to nucleotide treatment; *Splotch* mice displayed deficits in *de novo* purine and thymidylate synthesis (Fleming & Copp 1998; Beaudin et al. 2011) and, folic acid and thymidine

supplementation have ameliorating effects. Additionally, loss of *Mthfr* in *Sp/Sp* embryos did not exacerbate NTDs (D. Li et al. 2006), suggesting that the problem was not related to depletion of one-carbon units entering the methionine cycle. Therefore, oral nucleotide treatment was considered to be a potential strategy to prevent NTDs in *Splotch* mutants. Of interest, homozygous loss of *Pax3* does not affect the distribution of folate cofactors. In particular, 5,10-methyleneTHF, which provides the one-carbon unit for dTMP synthesis, is not reduced in *Sp^{2H}/Sp^{2H}* embryos (**Figure 3. 25**). Additionally, total pools of folate cofactors were not affected by loss of *Pax3* (**Figure 3. 26**).

Nucleotide treatment did not influence the frequency of spina bifida or exencephaly in *Splotch* mutants (**Table 3. 7**). Due to the sex bias in exencephaly, the effect of nucleotide treatment was assessed separately in males and females (**Table 3. 8**). While no statistically significant changes in the frequency were found for either sexes, it is perhaps of interest that while 100 % of control females present with exencephaly, nucleotide treatment tended to reduce the frequency to 60 %.

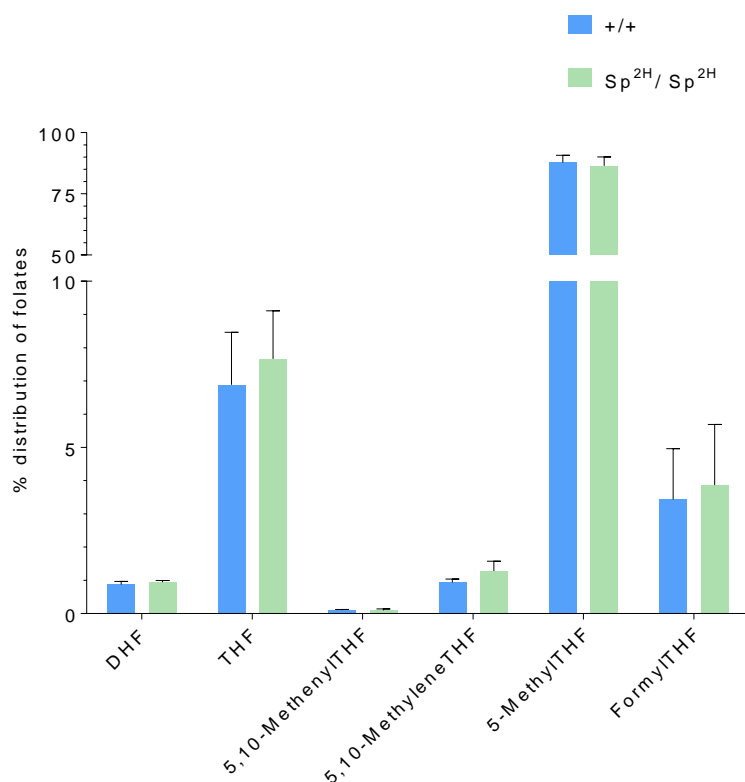


Figure 3. 25. Distribution of folate metabolites in E11.5 wild-type and *Sp^{2H}/Sp^{2H}* embryos

No differences are found in the distribution of folate cofactors between wild-type (+ / +) and *Splotch* (*Sp^{2H}/Sp^{2H}*) embryos.

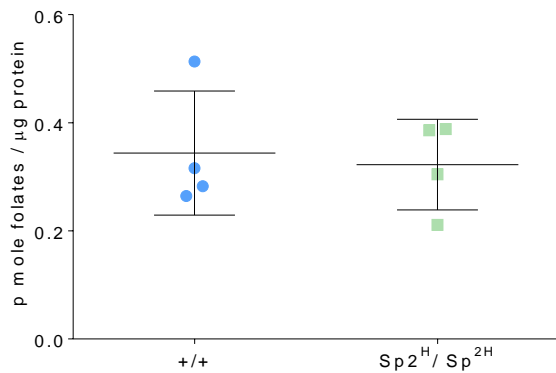


Figure 3. 26. Total folate containing cofactors in E11.5 wild-type and *Sp*^{2H}/*Sp*^{2H} embryos

Total pools of folate cofactors are not different between wild-type (+ / +) and *Splotch* (*Sp*^{2H}/*Sp*^{2H}) embryos.

	Frequency of NTDs % (n)	
	Spina bifida	Exencephaly
Control	94.59 (35/37)	67.57 (25/37)
Nucleotides treated	100.00 (15/15)	60.00 (9/15)

Table 3. 7. Frequency of NTDs in *Splotch* embryos treated with nucleotides.

Nucleotide treatment did not affect the frequency of either spina bifida or exencephaly in *Sp*^{2H}/*Sp*^{2H} embryos.

	Frequency of Exencephaly % (n)	
	Females	Male
Control	100.00 (7/7)	36.36 (4/11)
Nucleotide treated	60.00 (3/5)	60.00 (3/5)

Table 3. 8. Frequency of exencephaly by sex and treatment.

Nucleotide treatment did not significantly affect the frequency of exencephaly in either male or female *Sp*^{2H}/*Sp*^{2H} embryos.

3.3 Discussion

3.3.1 The prevention of folic acid resistant NTDs

Studies suggest that up to 70 % of NTD cases are responsive to folic acid supplementation (Wald et al. 1991; Heseker et al. 2009; Mosley et al. 2009). The investigations in this chapter were aimed at investigating alternative treatments for folic acid-resistant NTDs.

NTDs in the *ct* mouse are folic acid resistant, and its multiple, predisposing genetics and sensitivity to the environment make this a suitable model to test potential treatments, as has been done since the 1980s. This study builds on the previous findings that inositol and nucleotide supplementation have individually been found to increase proliferation in the hindgut and caudal neural tube, preventing a significant proportion of spina bifida cases in *ct* mice (Leung et al. 2013; Greene and Copp 1997; Seller 1994).

3.3.2 Supplementation treatments and regimens

3.3.2.1 Salvage pathways

Both intraperitoneal and oral treatments are believed to be taken up by embryonic tissue in their nucleoside or nucleobase form. While nucleotides given orally are hydrolysed by luminal alkaline phosphatase in the small intestine, nucleotides intraperitoneal administered are hydrolysed to their nucleosides by other extracellular 5'-nucleotidases (Wachstein and Sigismondi 1958). Circulating nucleosides and nucleobases cross the cell membrane via a process of facilitated diffusion and, in the case of purine nucleosides, are converted to their free nucleobases in order to be converted to NTPs by the purine salvage enzymes APRT and HPRT. In contrast, pyrimidine NTPs are formed via phosphorylation of pyrimidine nucleosides by TK1/2 and uridine kinase (**Section 3.1.2.3**). Therefore, the salvage enzymes APRT, HPRT and TK1 are required to utilise the nucleotides and nucleotide precursors present in oral and intra-peritoneal treatments for DNA synthesis

While Leung et al. (2013) demonstrated that whole embryos are able to incorporate exogenous nucleosides and nucleotides, it remained to be shown which tissues express nucleotide salvage enzymes. *In situ* hybridisation using labelled RNA probes for detection of mRNAs has demonstrated that each of the salvage enzymes are expressed in the hindgut and neural epithelium at neurulation stage, therefore allowing exogenous nucleotide precursors to be used by these key tissues.

3.3.2.2 Intra-peritoneal nucleotide treatments

Intra-peritoneal nucleotide treatments of thymidine + adenine or thymidine + GMP was previously shown to prevent up to 80 – 90 % of spina bifida in *ct* mice (K. Y. Leung et al. 2013). Of interest, the use of thymidine or adenine treatment alone did not significantly reduce the frequency of spina bifida. This finding prompted the investigation of whether a combination of three nucleotides, namely thymidine + adenine + GMP, could increase the efficacy of nucleotide treatments compared to the combination of two nucleotides. Additionally, the treatment of thymidine + adenine + inositol was investigated to understand whether the preventative effects of nucleotides and inositol could be additive.

While there was a substantial trend towards a reduced proportion of spina bifida and increased proportion of straight tails under thymidine + adenine treatment, it did not reach the levels previously reported (K. Y. Leung et al. 2013). This apparent difference in efficacy is not overly surprising; the NTD rates in *ct* mice can vary quite substantially over years and this could have some effect on their amenability to treatments (van Straaten and Copp 2001). Despite the lack of significance, it was clear that in the current study the addition of GMP or inositol to thymidine + adenine treatment did not increase efficacy of treatment using intra-peritoneal injection. However, an important finding was that inositol and nucleotides did not mutually inhibit each other's protective effect suggesting that a combination treatment could be investigated further in other models.

3.3.2.3 Efficacy of oral treatments

An important part of this study was to understand whether nucleotide treatments could effectively prevent NTDs when given orally. This is significant because a successful prevention strategy requires compliance from the public, which is more likely if the action necessary is easy and familiar, such as taking oral vitamins in this case.

The oral route of administration requires that nucleotide precursors are taken up by enterocytes of the intestine and released into systemic circulation so that they can reach the placenta and embryonic circulation. Intra-peritoneal injections by their nature bypass the need for intestinal absorption. A study which delivered the same amount of radiolabelled adenine to rats, intravenously or orally, report that a larger proportion of intravenously delivered adenine was incorporated into body tissues (Savaiano et al. 1980). This difference is presumed to be due to the amount of adenine that passes through the gut, and is the reason why in this study, the dose of nucleotide precursors for intra-peritoneal injections was 20 mg/ kg, while the (predicted) doses for oral treatments were 100 and 1000 mg/ kg.

The oral ingestion of nucleotides, nucleoside and nucleobases is not novel, as mammalian milk contains a complex mixture of these molecules, as does many foods, particularly rich sources being meat and legumes (Hess and Greenberg 2012). Additionally, enterocytes of the small intestine in humans and rodents do not have the capacity for *de novo* purine synthesis (Savaiano and Clifford 1981) and so actively take up dietary nucleosides, as well as relying on circulating nucleosides, for their own purine salvage requirements. Studies suggest that nucleosides are the preferred means of uptake by enterocytes, with nucleotides hydrolysed by alkaline phosphatase in the intestinal lumen, while nucleobases are also absorbed (Wilson and Wilson 1958; Wilson and Wilson 1962; Hess and Greenberg 2012). Therefore, AMP, IMP and GMP are expected to be hydrolysed to adenosine, inosine and guanosine respectively. Studies investigating the transport of nucleosides/ nucleobases across the epithelial membrane are not comprehensive. Data available on purine nucleobases suggest that the transport of adenine (12 %) across the intestinal wall of rats is highest (Savaiano et al. 1980), and is also the most extensively incorporated purine into body tissue (Ho et al. 1979). Some studies suggest that guanine is extensively and rapidly metabolised to xanthine and uric acid in the lumen and not appreciably taken up by enterocytes (Savaiano et al. 1980; Parsons and Shaw 1983). In addition, thymidine was reported to be transported across the rat small intestine, however, while 26 % was recovered intact, 24 % was metabolised to thymine after 60 minutes (50 % had not crossed the epithelium; Novotny et al. 1984).

As the percentage of oral AMP, IMP, GMP and thymidine which was likely to be absorbed and released into systemic circulation was not known, two doses were tested; 0.5 mg/ mL and 5 mg/ mL of each component. Overall, results demonstrate that a combination of AMP + IMP + GMP + thymidine prevented a significant proportion of spina bifida (50 %) and exencephaly (35 %) in *ct* mice. As outlined, these results are the summation of three different regimens of oral nucleotide treatment. Importantly, there is evidence that the regimen of 0.5 mg/ mL nucleotide treatment from E7.5 to E10.5 may be more effective at preventing spina bifida than the 5 mg/ mL nucleotide treatment over the same stages (55 % and 47 %). Although the difference in efficacy measured is small, the increase in CR length seen with 0.5 mg/ mL treatment suggests it may in fact be more efficacious than the current sample indicates. A larger sample group would be required to determine whether this is a real effect. Given the small sample of embryos treated with the regimen of 5 mg/ mL oral nucleotides from E0.5 to E10.5, it is not possible to assess its efficacy against the other regimens.

Both nucleotide precursor and inositol treatments have been shown to increase proliferation individually. It is expected that nucleotide precursors directly stimulate proliferation by the increased availability of nucleoside triphosphates for DNA synthesis. On the other hand, increased proliferation after inositol supplementation has been shown to be dependent on PKC pathway activity (Greene and Copp 1997). Given the different mechanisms likely to be involved, it was

possible that together, nucleotide + inositol treatment could provide greater prevention of NTDs compared to either treatment alone.

The addition of inositol to nucleotide treatment was assessed and although a tentative observation at this point (due to the small sample size), it appears that nucleotide + inositol treatment may provide increased prevention of spina bifida (82 %) and exencephaly (100 %), when compared to nucleotide (5 mg/ mL from E0.5) or inositol treatment alone.

3.3.2.4 Comparison of nucleotide precursor pools

In this investigation, both intra-peritoneal (20 mg/ kg/ day adenine + thymidine, E7.5 – 10.5) and oral treatment (1000 mg/ kg/ day AMP + IMP + GMP + thymidine, E0.5) of nucleotide precursors tended to prevent the frequency of spina bifida by ~ 50 %. Their effectiveness at preventing exencephaly cannot be compared, given the comparatively smaller sample size and low exencephaly rate during intra-peritoneal treatment.

In order to compare the two regimens' effects on total nucleotide/ nucleoside/ nucleobase pool, an ion-pairing-reverse phase-HPLC-MS/MS (IP-RP-HPLC-MS/MS) method (Laourdakis et al. 2014) was adapted and implemented to measure 35 such molecules in control and treated embryos at E10.5. Use of MS/MS is both sensitive and efficient in terms of sample material and processing time compared to the DNA polymerase assay and HPLC coupled to UV detection which have been used previously. Orally treated embryos were found to have greater NMPs/ dNMPs and nucleobase pools, as well as individual nucleosides, compared to both control and intraperitoneal treated embryos. This is perhaps not too surprising given the that oral dose is expected to deliver 50 times the dose received by intra-peritoneal injection. However, given the reports of the very active conversion of purines to uric acid in the gut (Savaiano et al. 1980; Parsons and Shaw 1983; Salati et al. 1984), this result was not a foregone conclusion.

The interesting results to note from these data are that while adenine was present in the intra-peritoneal treatment and AMP in the oral treatment, the levels of adenine are not significantly different in embryos from these two treatments. On the other hand, the levels of AMP are approximately 3.5 times higher in orally treated samples compared to controls. Guanine containing purines were present in oral treatment but not in the intra-peritoneal treatment, and while guanine shows a strong trend towards being increased in oral treated samples compared to intra-peritoneal treated samples ($p = 0.054$), the levels of guanosine are not different, while GMP is approximately 5 times greater in oral treated samples. As it is presumed that AMP and GMP in the oral treatment are hydrolysed and enter embryonic cells as adenosine and guanosine, it appears that they are converted back to AMP and GMP and increase their respective pools by approximately 10 times the level of control embryos. Conversely, thymidine, which was present in both treatments, was not detectable in any samples, while dTMP was found to be increased in orally treated samples only.

Additionally, other pyrimidines, such as cytidine, uridine and UMP were increased by oral treatment although cytosine or uracil containing precursors were not a constituent. There is not a known pathway which can convert thymidine to either uridine, UMP or cytidine (KEGG Pathways). A possible theory is that the increase in dGTP stimulates an increase in production of UMP which is used to produce dCTP. Stimulation of UMP and CTP synthesis in amounts greater than required could result in conversion of these nucleotides to uridine and cytidine respectively. While an increase in dCTP was not measured, it is possible that cytidine and thymidine nucleotides are not detected well by this method. This is, however, purely conjecture at this point. It would be of interest to treat embryos with each of the nucleotides/ nucleosides separately and assess what changes are found in nucleotide/ nucleoside/ nucleobase pools.

There were no significant changes in NTP/ dNTP or NDP/ dNDP pools, although it must be noted that there is more variability in these results. Additionally, there was a tendency for both routes of nucleotide treatment to increase dGTP pools in comparison to control samples, which was nearly significant for intraperitoneal treated compared to control samples ($p = 0.06$; **Table 3. 9**).

dNTPs are the building blocks for DNA, and their pools directly affect DNA synthesis. The addition of exogenous nucleotides (dATP, dCTP, dTTP and dUTP) to HeLa cells in culture was found to double early S-phase replication (Malinsky et al. 2001). In addition, in budding yeast, upregulation of RNR, the single enzyme which reduces all four NDPs to dNDPs in prokaryotic and eukaryotic cells, resulted in increased elongation, indicating that dNTP pools were limiting for DNA synthesis (Poli et al. 2012). RNR is a large enzyme which utilises a single catalytic site to reduce all four NDPs. Allosteric binding of ATP, dATP, dGTP and dTTP offers complex control via alteration of the catalytic site specificity so that different NDPs (or none) are favoured (Thelander and Reichard 1979). dNTP pools are known to be small compared to NTP pools (1 – 10 %), which varies with the cell cycle, peaking during S and G₂ phases (Reichard 1988; Mark Meuth 1984). It is also reported that while pyrimidine dNTP pools are usually the largest, dGTP pools are the smallest (Reichard 1988). This is in contrast to the results reported here, where dGTP pools were found to be largest, followed by dTTP and then by similar, low levels of dATP and dCTP (**Table 3. 9**). Additionally, thymidine, which is present in both the nucleotide treatments, is expected to increase the pool of dTTP, as it has been reported widely to do so when supplemented in cell culture (Bjursell and Reichard 1973; Leyva, Appel, and Pinedo 1982). Again, in contrast, the mean dTTP levels in control samples was found to be higher than that following either of the nucleotide treatments. However, it is noted that one of the three control samples tended to give higher values for dNTPs, NTPs, dNDPs and NDPs. If this sample is omitted, oral treatment and intraperitoneal treatment are found to increase dTTP pools 7 times and 6 times respectively. Of interest, dTTP allosterically inhibits and stimulates reduction of CDP and GDP respectively, by RNR (Reichard 1988; Thelander and Reichard 1979). Therefore, an increase in dTTP could result in decreased dCTP and increased dGTP pools, as is found for dGTP pools presently.

As proposed above, it is possible that the method employed does not detect all nucleotides equally, in the case of dNTPs, dCTP and dATP are not well represented. To assess whether this could be the case, the literature was searched for measurements of dNTP and also NTPs, and a range of reported concentrations compiled, to which the present results could be compared with (**Table 3. 10**). Most studies have used cultured cells and reported their results in pmol/ 10^6 cells. However, three results were given as pmol/ μg DNA. To convert to pmol/ 10^6 cells, the value of 10^6 cells = 5.1 μg DNA was used, which was reported by Bray & Brent (1972) for post mitotic, non-S-phase HeLa cells. The lower and upper values reported from all cell types, was then used to construct limits for each of the dNTPs. In order to compare reported results with those presented here, an estimation of the protein content of 10^6 cells was required. It is estimated that adult mouse cells contain 40 – 500 pg protein per cell (Wisniewski et al. 2014), while HeLa cells contain \sim 150 pg per cell (Volpe and Eremenko-Volpe 1970). Therefore, as a much simplified estimate, given the range of different cell types reported, the value of 200 μg protein per 10^6 cells was used. The upper and lower limits from published data are presented at the bottom of **Table 3. 10**. This comparison demonstrates that the levels of dGTP and dTTP are approximately a factor of 10 higher than the reported upper values. The reason behind this apparent discrepancy is not known, but it is possible that the results are accurate for mouse embryos proliferating *in vivo*. As to whether this method is able to detect dCTP and dATP properly, it is difficult to assess, because the levels which were detected are in the range of reported values. However, because dCTP was measured in only one out of nine samples, and dATP measured in six out of nine samples, it appears possible that other metabolites present in the samples may interfere with detection of these dNTPs. Alternatively, the use of perchloric acid may not adequately and reproducibly allow the low levels of these dNTPs to be extracted from tissue. Perchloric acid extracts nucleotides (and other small metabolites) by precipitating proteins and inhibiting nucleotidase. A study comparing methods for the extraction of ATP from tissue reported that extraction of ATP from tissue, which has a higher protein content than cells in culture, was better accomplished by a phenol based method, due to some ATP being precipitated along with proteins during perchloric acid extraction and possibly also during neutralisation (Werner 1993; Chida et al. 2012). Lastly, it has been reported that the use of strong acids such as perchloric and trichloroacetic can degrade dNTP/NTPs (Braasch, Villacres, and Butler 2015), and in particular, reduced pyrimidine nucleotides (Werner 1993).

A search for literature values was also done for NTPs, NDPs and NMPs (**Table 3. 11 & Table 3. 12**). Overall, the results are in keeping with those reported, except for the control samples' mean for ATP, and to a lesser extent, ADP and AMP. Once again, one control sample has a particularly high ATP value (472 pmol/ μg protein; **Figure 3. 12**), exclusion of this sample brings the mean of ATP in control samples to 4.36 pmol/ μg protein, which is within the reported range and more in keeping with the rest of the data.

dNTPs	Concentration pmol./ μ g protein			
	Control	Control_1*	Intra-peritoneal	Oral
dATP	0.29 \pm 0.29	0.00	0.0 \pm 0.0	0.27 \pm 0.17
dCTP	0.0 \pm 0.0	0.00	0.0 \pm 0.0	0.42 \pm 0.42
dGTP	8.38 \pm 4.31	8.81 \pm 1.44	36.56 \pm 12.31	60.33 \pm 18.39
dTTP	3.95 \pm 3.71	0.24 \pm 0.11	1.72 \pm 0.62	1.48 \pm 0.51
NTPs				
ATP	160.19 \pm 155.85	4.36 \pm 4.36	36.24 \pm 17.91	50.84 \pm 31.91
CTP	2.47 \pm 2.29	0.18 \pm 0.074	1.42 \pm 1.27	0.98 \pm 0.54
GTP	13.30 \pm 13.30	0.00	7.57 \pm 4.61	5.83 \pm 2.72
TTP	0.00	0.00	0.00	0.00
NDPs				
ADP	14.793 \pm 8.35	6.44 \pm 0.38	9.82 \pm 0.38	7.94 \pm 2.39
CDP	0.10 \pm 0.10	0.00	0.00	0.00
GDP	1.75 \pm 1.68	0.07 \pm 0.07	3.21 \pm 0.84	2.40 \pm 1.31
TDP	0.00	0.00	0.00	0.00
NMPs				
AMP	4.59 \pm 2.49	2.62 \pm 2.62	12.03 \pm 1.70	43.58 \pm 10.14
CMP	0.00	0.00	0.00	0.024 \pm 0.012
GMP	0.64 \pm 0.26	0.39 \pm 0.13	1.56 \pm 0.32	8.36 \pm 2.48
TMP	0.00	0.00	0.00	0.00

Table 3. 9. dNTP, NTP, NDP and NMP pools measured under each treatment.

Data from graphs in Figure 3.11. to Figure 3.13. * Excluding one control embryo sample

Cell type	pmol./ 10 ⁶ cells				Detection method	Reference
	dATP	dCTP	dGTP	dTTP		
MEF cell line C3H10T1/2	0.17	0.57	0.28	1.07	PCA, DNA polymerase assay	(McCormick et al. 1983)
Mouse fibroblast cell line L292	15.00	17.00	17.00	20.00	TCA, DNA polymerase assay	(Adams, Berryman, and Thomson 1971)
Mouse fibroblast cell line 3T6	18.36	25.50	9.18	15.30	MeOH, DNA polymerase assay	(M Meuth, Aufreiter, and Reichard 1976)
Mouse fibroblast cell line 3T6	26.00	110.00	24.00	80.00	MeOH, DNA polymerase assay	(Spyrou and Holmgren 1996)
Mouse fibroblast cell line 3T3	54.00	-	80.00	61.00	TCA, IP-HPLC & UV detection	(D. Huang, Zhang, and Chen 2003)
Mouse leukaemia cell line L1210	6.52	5.25	2.78	9.06	MeOH, IP-HPLC-MS/MS	(Cohen et al. 2009)
Mouse leukaemia cell line L1210	16.90	26.80	7.00	57.70	TCA, IE-HPLC & UV detection	(Leyva, Appel, and Pinedo 1982)
Mouse lymphoma S-49	42.00	34.00	20.00	81.00	PCA, IE-HPLC & UV detection	(Albert and Gudas 1985)
Mouse lymphoma S-49	65.20	67.90	24.00	74.20	PCA, IE-HPLC & UV detection	(Garrett and Santi 1979)
Rat primary spleen cells	2.20	61.60	3.90	22.30	TCA, IP-HPLC & UV detection	(Cross, Miller, and James 1993)
Chinese hamster epithelial cell line CHO	15.30	81.60	1.28	10.20	MeOH, DNA polymerase assay	(Bjursell and Reichard 1973)
CHO	17.34	53.04	3.88	15.81	MeOH, DNA polymerase assay	(Skoog and Bjursell 1974)
CHO	26.00	40.00	10.00	50.00	TCA, DNA polymerase assay	(Mun and Mathews 1991)
CHO	27.00	76.00	10.00	104.00	PCA, DNA polymerase assay	(Walters, Tobey, and Ratliff 1973)

(Continued on next page)

Cell type	pmol./ 10 ⁶ cells				Detection method	Reference
	dATP	dCTP	dGTP	dTTP		
Human primary fibroblasts	25.00	20.00	8.00	50.00	TCA, DNA polymerase assay	(Martomo and Mathews 2002)
Human hepatocellular cell line HepG2	4.24	4.20	7.40	18.35	TCA, IP-HPLC-MS/MS	(W. Zhang et al. 2011)
Human cervical cancer cell line HeLa	7.00	19.00	7.00	24.00	PCA, DNA polymerase assay	(Bray and Brent 1972)
Human primary lymphocytes	11.36	10.36	7.42	6.05	PCA, IP- HPCL & UV detection	(Di Pierro et al. 1995)
Human lung cancer cell line H23	12.75	9.12	7.07	68.32	TCA, IP-HPLC-MS/MS	(W. Zhang et al. 2011)
Human colon cancer cell line WiDr	14.00	14.60	8.00	30.00	TCA, IP- HPCL & UV detection	(Decosterd et al. 1999)
Human lymphocyte cell line H9	16.57	7.96	7.60	62.12	TCA, IP-HPLC-MS/MS	(W. Zhang et al. 2011)
Human Novikoff hepatoma cell line	17.16	21.78	17.49	41.25	TCA, IE- HPCL & UV detection	(Arezzo 1987)
Human pancreatic cell line PANC1	28.50	18.54	15.77	91.64	TCA, IP-HPLC-MS/MS	(W. Zhang et al. 2011)
Human leukaemia cell line MOLT-4	29.62	-	7.59	13.97	PCA, IE- HPCL & UV detection	(Shewach 1992)
Lower limit (all cell types)	0.17	0.57	0.28	1.07		
Upper limit (all cell types)	65.20	110.00	80.00	104.00		

Table 3. 10. Published dNTP pools in various cells types.

*Detection methods: extraction method is stated first, followed by separation and detection method. MEF = mouse embryonic fibroblast; PCA = perchloric acid; MeOH = 60 % methanol; TCA = trichloroacetic acid. IP-HPLC = ion pairing high performance liquid chromatography; IE-HPLC = ion exchange-HPLC; MS/MS = tandem mass spectrometry

Cell type	pmol./ 10 ⁶ cells				Detection method	Reference
	ATP	CTP	GTP	TTP		
MEF cell line C3H10T1/2	5620	-	350	700	PCA, IE-HPLC & UV detection	(McCormick et al. 1983)
Mouse fibroblast cell line 3T3	948	264	335	446	TCA, IP-HPLC & UV detection	(Huang et al. 2003)
Mouse leukaemia cell line L1210	3798	152	391	509	MeOH, IP-HPLC-MS/MS	(Cohen et al. 2009)
Rat primary spleen cells	403	187	117	133	TCA, IP-HPLC & UV detection	(Cross et al. 1993)
CHO	890	50	80	130	MeOH, IP-HPLC-MS/MS	(Cordell et al. 2008)
CHO	15000	1500	2500	5000	PCA, IP-HPLC & UV detection	(Kochanowski et al. 2006)
Human Novikoff hepatoma cell line	142	10	111	31	TCA, IE- HPCL & UV detection	(Arezzo 1987)
Primary human lymphocytes	916	77	235	88	PCA, IP- HPCL & UV detection	(Di Pierro et al. 1995)
Human lung cancer cell line H23	4609	3180	3608	4544	TCA, IP-HPLC-MS/MS	(Zhang et al. 2011)
Human hepatocellular cell line HepG2	4959	669	1956	3093	TCA, IP-HPLC-MS/MS	(Zhang et al. 2011)
Human pancreatic cell line PANC1	6190	3221	2464	3890	TCA, IP-HPLC-MS/MS	(W. Zhang et al. 2011)
Human lymphocyte cell line H9	7316	2731	3544	5480	TCA, IP-HPLC-MS/MS	(W. Zhang et al. 2011)
Lower limit (all cell types)	142	10	111	31		
Upper limit (all cell types)	15000	3221	3608	5480		

Table 3. 11. Published NTP pools in various cells types.

*Detection methods: extraction method is stated first, followed by separation and detection method. MEF = mouse embryonic fibroblast; PCA = perchloric acid; MeOH = 60 % methanol; TCA = trichloroacetic acid. IP-HPLC = ion pairing high performance liquid chromatography; IE-HPLC = ion exchange-HPLC; MS/MS = tandem mass spectrometry.

Cell type	pmol./ 10 ⁶ cells				Detection method	Reference
	ADP	CDP	GDP	TDP		
CHO	349	112	152	166	MeOH, IP-HPLC-MS/MS	(Cordell et al. 2008)
Human lung cancer cell line H23	316	89	176	197	TCA, IP-HPLC-MS/MS	(W. Zhang et al. 2011)
Human hepatocellular cell line HepG2	1161	89	324	484	TCA, IP-HPLC-MS/MS	(W. Zhang et al. 2011)
Human pancreatic cell line PANC1	348	102	165	121	TCA, IP-HPLC-MS/MS	(W. Zhang et al. 2011)
Human lymphocyte cell line H9	349	112	152	166	TCA, IP-HPLC-MS/MS	(W. Zhang et al. 2011)
Lower limit (all cell types)	316	0	10	10		
Upper limit (all cell types)	1161	112	324	484		
Cell type	Detection method				Reference	
	AMP	CMP	GMP	TMP		
CHO	132	340	25	54	MeOH, IP-HPLC-MS/MS	(Cordell et al. 2008)
Human lung cancer cell line H23	120	422	22	86	TCA, IP-HPLC-MS/MS	(W. Zhang et al. 2011)
Human hepatocellular cell line HepG2	557	402	197	407	TCA, IP-HPLC-MS/MS	(W. Zhang et al. 2011)
Human pancreatic cell line PANC1	87	532	19	42	TCA, IP-HPLC-MS/MS	(W. Zhang et al. 2011)
Human lymphocyte cell line H9	132	340	25	54	TCA, IP-HPLC-MS/MS	(W. Zhang et al. 2011)
Lower limit (all cell types)	20	30	0	30		
Upper limit (all cell types)	557	532	197	407		

Table 3. 12. Published NDP and NMP pools in various cells types.

*Detection methods: extraction method is stated first, followed by separation and detection method. PCA = perchloric acid; MeOH = 60 % methanol; IP-HPLC = ion pairing high performance liquid chromatography; MS/MS = tandem mass spectrometry.

In summary, IP-RP-HPLC-MS/MS analysis of nucleotide precursor pools has provided some interesting insights into changes in nucleotide precursor pools in embryos that have undergone oral and intraperitoneal nucleotide supplementation. It is clear that oral supplementation (1000 mg/ kg/ day from E0.5) results in substantial increases in NMPs and nucleosides. However, it appears possible that this method cannot accurately detect cytidine containing nucleotides and perhaps others. Given the variability of dNTP levels depending on cell type and very likely culture conditions, and as there are no reports on the quantification of dNTPs from tissue, similar to E10.5 mouse embryos or otherwise, it has not been possible to make a full assessment of the method. It was noted during the literature search that two other studies were not able to report a value for dCTP (Shewach 1992; Huang, Zhang, and Chen 2003). Both studies implied that dCTP levels were below the limit of detection. To help evaluate whether dCTP levels are in fact very low, and to have a comparison to this method, another extraction method should be tried. In consideration of the current literature, a good starting point would be comparison with ice-cold 60 % methanol and 70 % methanol: chloroform; while the methanol degrades cell membranes and precipitates proteins, chloroform solubilises lipids which could interfere with detection (Di Pierro et al. 1995; Braasch, Villacres, and Butler 2015).

3.3.3 Effects of oral treatments on folate one-carbon metabolism

Six folate cofactors were quantified in oral inositol, nucleotide and nucleotide + inositol treated E10.5 *ct* embryos. Embryos supplemented with nucleotides only did not demonstrate any changes in folate profile when compared to the profile from control embryos. However, nucleotide treatment did increase the SAM/ SAH ratio owing to a significant decrease in the level of SAH present in embryos treated with nucleotides alone. This finding is intuitive; an increase in exogenous nucleotide precursors stimulates nucleotide salvage processes and to some extent may spare *de novo* nucleotide synthesis, allowing more one-carbon units to be transferred to the methionine cycle. What was less expected was the decrease in SAM levels also. This may be a function of the cycle; if SAH levels are so low, there may be less requirement to maintain high SAM levels as the cycle is working more efficiently.

On the other hand, inositol only and nucleotide + inositol treatment was found to elicit changes in embryo folate profiles. Of interest, while inositol treatment decreased levels of 5-methylTHF by 17 %, the addition of nucleotides + inositol decreased 5-methylTHF by 30 % and increased THF by 84 %. As nucleotides only treatment had no effect on either 5-methylTHF or THF, this suggests some level of synergy between nucleotide and inositol treatments when combined. Together with data of SAM and SAH levels, the results suggest that inositol only and nucleotide + inositol treatments promote the use of one-carbon units for *de novo* nucleotide synthesis.

Investigation of the incorporation of exogenous [³H]-adenine, [³H]-thymidine and [³H]-CTP into E9 embryos found 250 μ M inositol added to culture had no significant effect. However, there is a possibility that inositol may have a small effect of decreasing [³H]-thymidine incorporation. [³H]-thymidine incorporation was measured in two separate experiments; the first found a 23 % decrease in [³H]-thymidine incorporation which did reach significance ($p = 0.006$), while the second found an 18 % decrease which did not reach significance. As there were no differences in the DNA content per embryo between control and inositol treated embryos, this could suggest a small stimulation in *de novo* thymidylate synthesis which suppresses incorporation of exogenous [³H]-thymidine. There are two theories which could possibly account for a reduction in [³H]-thymidine incorporation with inositol treatment, without affecting [³H]-adenine incorporation. The first is that inositol, via conversion to glucose, can be converted to PRPP. PRPP is used for the *de novo* synthesis and salvage of purine nucleotides, and therefore inositol, through PRPP production, could stimulate both pathways without changing the ratio of *de novo* synthesis of AMP to salvage of adenine. On the other hand, PRPP is only used for *de novo* thymidylate synthesis, and not salvage. A stimulation in *de novo* thymidylate and AMP synthesis would be consistent with the tendency towards increased abundance of methylene-THF and formyl-THF upon inositol (and nucleotide + inositol) treatment. Lastly, inositol could specifically affect the incorporation of exogenous [³H]-thymidine via activation of PCK and its target, the pyrimidine specific enzyme CAD. Further studies are needed to first confirm this effect on [³H]-thymidine incorporation, and then investigate how inositol could be acting.

To better understand to what extent the changes in FOCM associated with inositol treatment are dependent on inositol signalling, neurulation stage *ct* embryos could be cultured in inositol with, and without, lithium chloride or a more specific inhibitor of inositol monophosphate cycling e.g. L690330. Lithium is an inhibitor of inositol phosphate recycling (Berridge, Downes, and Hanley 1989), consequently, if changes in folate prolife are lost with lithium treatment, it can be concluded that active inositol phosphate signalling and recycling is required. Additionally, lithium inhibition of inositol phosphate recycling was found to abolish the protective effect of inositol on reducing PNP lengths in culture (Greene and Copp 1997). Therefore, if the changes in FOCM were abolished by lithium chloride, it would also suggest that these changes in FOCM are involved in the prevention of spina bifida in *ct* mouse. Additionally, it would be interesting to assess the phosphorylation of the CAD enzyme at the PKC phosphorylation site (Thr456; Sigoillot et al. 2007). To confirm the presumed increase in *de novo* nucleotide synthesis, nucleotide precursor pools could be assessed by IP-HPLC-MS/MS once an extraction method is fully validated. Lastly, to better understand how the addition of nucleotides to inositol treatment could lead to synergistic effects, RNA-seq could be employed to assess genome wide transcriptional changes associated with the different treatments.

3.3.4 Nucleotide treatment in *Splotch* and *Gldc*

Given the apparent success of oral nucleotide treatment in *ct* mice, two further mouse models of NTDs were supplemented with oral nucleotides and embryos collected at E11.5 for assessment. To some surprise, this treatment failed to prevent NTDs in either of these models in which decreased proliferation has been measured, previously in the case of *Gldc* mice (Pai et al. 2015), and during this project in the cranial region of *Splotch* mice (**Chapter 6**) and by Alexandra Palmer in the caudal region (Palmer 2014). For both of these models, it is possible that while there is reduced proliferation in the neural tube, this is a secondary effect of the genetic defect, and increasing proliferation alone does not address the primary, or equally important defect affecting neural tube closure. Efforts were made in this project to study other mechanisms potentially contributing to exencephaly in *Splotch* mice, with the Shh pathway investigated (**Section 6.3.2**). Work is also ongoing in the lab to better understand the full biological implications of loss of *Gldc*, such as loss of mitochondrial integrity, as mitochondrial FOCM is linked to the respiration chain and redox balance (Fan et al. 2014; Ducker and Rabinowitz 2017).

Alternatively, it is possible that oral nucleotides did not each reach the embryos in adequate amounts. Once again, analysis of nucleotide precursor pools in treated and control, E10.5 *Splotch* and *Gldc* embryos would help evaluate this possibility. The finding that *Splotch* mice do not demonstrate any changes in folate cofactor pools but demonstrate reduced capacity for *de novo* thymidylate and purine synthesis (Fleming & Copp 1998; Beaudin et al. 2011) may suggest that the defect is upstream, in providing precursors for *de novo* nucleotide synthesis via FOCM. It would be interesting to compare the effect of thymidine only and thymidine + adenine intraperitoneal injections on NTD rates and nucleotide precursor pools. The effect of intraperitoneal injections of nucleotides should be tested on *Gldc* mice also as an alternative route of administration.

Lastly, mice homozygous null for *Amt*, which also encodes a protein of the GCS, but not exclusive to the GCS, also present with exencephaly (87 %). While intraperitoneal supplementation of embryos with folic acid or TMP (30 mg/ kg from E7.5 – 10.5) had no effect on frequency, the use of methionine (70 mg/ kg from E7.5 – 10.5) or methionine + TMP produced a significant reduction in the frequency to approximately 60 % (Narisawa et al. 2012). Knockout of *Mthfr* on a *Gldc* null background (Pai 2015) and supplementation of *Gldc* null mice with methionine (N. Greene, personal communication) was found to be protective against exencephaly. Overall, these results suggest that while direct supplementation with nucleotide precursors perhaps cannot prevent NTDs in *Gldc* null mice, increasing or sparing one-carbon units for *de novo* nucleotide synthesis can.

3.3.5 Potential safety considerations

Studies have shown that dNTP pools are not maintained equally and that changes in the balance of physiological dNTP pools can have deleterious consequences. Supplementation of thymidine at over 1 mM increases dTTP pools in a variety of mammalian cell lines and also inhibits the rate of DNA synthesis (Adams, Berryman, and Thomson 1971; Bjursell and Reichard 1973; Leyva, Appel, and Pinedo 1982). This occurs through allosteric inhibition of dCDP synthesis via RNR by the increasing dTTP pool, with addition of dCTP relieving the inhibition (Bjursell and Reichard 1973). Additionally, increasing dGTP, which is generally maintained as the smallest dNTP pool is found to increase rates of DNA synthesis but decrease proofreading efficiency with a concomitant increase in mismatch mutation rates (Meuth 1984; Bebenek, Roberts, and Kunkel 1992; Martomo and Mathews 2002).

The predicted dose of thymidine in oral treatments was 100 mg/ kg/ day (0.5 mg/ mL) or 1000 mg/ kg/ day (5 mg/ mL), although it is not known what the circulating concentration was. In considering of these findings, it may be that the amount of thymidine given in relation to the purine precursors should be reviewed and a range of doses tested. As, supplementation with adenine or GMP + thymidine was more successful at preventing NTDs than a purine precursor alone, it appears that a pyrimidine precursor should be included, however, uridine could also be tested, which may lead to a more physiological balance between the dTTP and dCTP pools. In relation to the finding that increases in dGTP could be mutagenic, this aspect should be assessed thoroughly in conjunction with finding a dose that offers the best prevention of NTDs. The possibility that lower doses may offer the same level of prevention, or even greater, should be explored.

Lastly, this information provides a potential logic and mechanism as to why embryos treated with 0.5 mg/ mL of oral nucleotides had increased CR lengths compared to those treated with 5 mg/ mL.

4 *Curly tail* mice show disturbances in FOCM

4.1 Introduction

Previous studies have found that NTDs in the *ct* mice are sensitive to maternal folate deficiency (Burren et al. 2010) and can be prevented by nucleotide supplementation (K. Y. Leung et al. 2013). Additionally, *ct* mice were found to have a decreased SAM/ SAH ratio compared to congenic wild-type (+^{ct}/+^{ct}) mice (De Castro et al. 2010). These studies suggest the possibility of disturbed FOCM in *ct* mice.

FOCM has a central role in cellular metabolism and is vital for cell physiology. It is, therefore, necessary that FOCM can be adapted for the demands of the cell and organism, which are stage, organ and context specific. While much of the regulation of FOCM is still unknown, investigations into pathway flux and specific regulation of FOCM enzymes, which may be of relevance to embryonic studies, are detailed below.

4.1.1 Flux through the pathway

Whole body flux experiments in human adults indicate that mitochondrial one-carbon production is 20 times that required for methylation of homocysteine (Lamers et al. 2009), and approximately 41 % of catabolised glycine is utilised for serine synthesis by SHMT2 (Lamers et al. 2007). This suggests one-carbon units are not a limiting factor for cytosolic FOCM outputs in healthy adults.

These studies do not, by their nature, take into account possible differences between organs. For example, the bone marrow in adults, as the site of haematopoiesis, is highly proliferative compared with other tissue, and folate (or vitamin B12) deficiency usually manifests first with the condition megaloblastic anaemia. The liver and kidneys, additionally, because of their role in homeostasis, have been found to exhibit differences in FOCM compared to other tissues such as muscle. It has been estimated that the liver carries out 80 % of total body methylation reactions (Stead et al. 2006). The liver also produces methionine for other organs and expresses BHMT, allowing betaine derived from choline to donate one-carbon units for methylation of homocysteine. Of interest, MTHFR null mice die soon after birth and exhibit abnormalities of brain structure. Maternal supplementation with betaine prevents both brain defects and death (Schwahn et al. 2004), suggesting liver BHMT can provide methionine for the whole body. FOCM also directly controls the levels of serine and glycine, and indirectly, cysteine through the transsulphuration pathway. Studies have demonstrated that in the fasted state, the liver is a net consumer of methionine and glycine, which is produced by muscle (Felig 1975), while the kidney is a net producer of serine from: glucose; protein catabolism

or from glycine via SHMT (Brosnan 1987; Ducker and Rabinowitz 2017), which is utilised by many peripheral organs (Felig 1975).

It is anticipated, however, that the requirements of FOCM during embryogenesis are likely to differ from those of an adult. Embryonic development is characterised by a high rate of cellular proliferation. Concurrently, there is a high demand for FOCM outputs, particularly *de novo* nucleotide synthesis and methyl groups for chromatin and DNA methylation, and mitochondrial derived formate appears to be crucial. Metabolic tracer experiments using deuterated serine and radiolabel monitoring after incubation with [3-¹⁴C] serine or [¹⁴C] formate have revealed that between 75 – 90% of the one-carbon units which contribute to purine synthesis (Fu, Rife, and Schirch 2001; Patel, Di Pietro, and MacKenzie 2003), thymidylate synthesis (Fu, Rife, and Schirch 2001; Herbig et al. 2002; Anguera et al. 2006) and methionine synthesis (Herbig et al. 2002; Anguera et al. 2006; Pike et al. 2010) are derived from formate in proliferative MCF-7 (breast cancer cell line), neuroblastoma and immortalised mouse embryonic fibroblast (MEF) cell lines.

Metabolic tracing studies which utilised [²H]-labelling of NAD(P)H and cytoplasmic or mitochondrial reporters also found that mitochondrial FOCM proceeded in the oxidative direction, producing NAD(P)H, while cytosolic FOCM was largely reductive (transfer of H⁻ from NAD(P)H to form serine), in non-small-cell lung cancer cell lines (Lewis et al. 2014). In support of the requirement for mitochondrial formate, both *Mthfd1l* and *Mthfd2* null mice are embryonic lethal (Di Pietro et al. 2002; Momb et al. 2013). Additionally, while cytosolic catabolism of serine via SHMT1 was found to increase 9-fold in *Mthfd2* null MEFs (Pike et al. 2010), *Mthfd2* null mice are growth retarded and embryonic lethal by E13.5 (Di Pietro et al. 2002), demonstrating the requirement of formate as a cytosolic one-carbon donor during embryogenesis. In contrast to whole embryos, cell lines appear to be able to survive the loss of mitochondrial formate. *Mthfd2* null immortalised MEFs showed no deficit in growth compared to *wild-type* control MEFs, although addition of hypoxanthine to the media stimulated proliferation of null but not *wild-type* MEFs (Patel, Di Pietro, and MacKenzie 2003). HEK293T cells with CRISPR/ Cas9 mediated deletions in mitochondrial FOCM enzymes (MTHFD2, MTHFD1L and SHMT1), demonstrated cell doubling times which were also largely unaffected, although SMHT2 and ALDH1L2 deletion resulted in modest increases (Ducker et al. 2016). Metabolic tracing in these cells found that upon disruption of mitochondrial FOCM and depletion of 10-formylTHF, the cytosolic pathway adapted by becoming oxidising, using SHMT1 to catabolise serine and generate one-carbon units. However, this reversal of SHMT1 rendered cells serine and glycine auxotrophs; while serine was required for one-carbon units, glycine was required for glutathione (γ -glutamyl-cysteinyl-glycine) synthesis (Ducker et al. 2016). Furthermore, Fan et al. (2014) reported that in the HEK 293T (human embryonic kidney) cell line, both mitochondrial and cytosolic SHMT enzymes catalysed the oxidative reaction of serine to glycine with transfer of the C³ unit to generate 5, 10-methyleneTHF.

Mitochondrial FOCM appeared to fully oxidise one-carbon units to CO₂, while cytosolic FOCM contributed one-carbon units for purine and dTMP synthesis.

Thus, studies suggest that FOCM is an adaptable pathway, with cytosolic FOCM capable of carrying out oxidative reactions. While this appears to be sufficient to sustain the growth of cells in culture, it does not appear to sustain embryonic development.

4.1.2 Pathway regulation

As outlined in **Section 3.1.2**, nucleotide synthesis pathways are known to be influenced by cellular signalling cascades, such as MAPK, but understanding of the integration of intracellular and/ or extracellular signals for the modulation of FOCM outputs is just beginning.

Studies suggest that the reaction catalysed by SHMT1 is readily reversible *in vivo*. SHMT1 has been found to prioritise one-carbon units (5,10-methyleneTHF) for thymidylate synthesis via TYMS in MCF-7 cells, with increased expression of SHMT1 increasing the proportion of one-carbon units used for thymidylate synthesis at the expense of methionine synthesis (Herbig et al. 2002) and vice versa (MacFarlane et al. 2008). It was subsequently shown that small ubiquitin-like modifier (SUMO) modification of the components required for thymidylate synthesis: SHMT1 (and cytosolic SHMT2); TYMS; and DHFR, occurs. This results in translocation of these enzymes to the nucleus during S-phase of the cell cycle, and formation of a multienzyme complex that associates with the nuclear lamina (Woeller et al. 2007; Anderson, Woeller, and Stover 2007; MacFarlane et al. 2011; Anderson et al. 2012). MTHFD1 was also found to translocate to the nucleus in response to cell cycle progression and during folate deficiency. The resulting model is that SHMT acts primarily as a scaffolding protein, to bring the multienzyme complex into association with the nuclear lamina, while MTHFD1 catalyses the transfer of a one-carbon unit from 5, 10-methyleneTHF to dUMP (Field et al. 2014). Multienzyme complexes are predicted to help stabilise intermediates and allow substrate shuttling, increasing flux through a pathway. Additionally, shuttling of one-carbon units for efficient thymidylate synthesis prevented misincorporation of uracil into DNA.

The enzymes catalysing *de novo* purine synthesis (**Section 3.1.2.2.1**), including GART and ATIC, which utilise 10-formylTHF, have been found to cluster in a multi-enzyme complex called the purinosome. It was demonstrated in HeLa cells that purine-depleted media induced clustering of the enzymes, while their expression was diffuse when cultured in purine-rich media (An et al. 2008). The purinosomes were also shown to also be dynamically regulated by protein kinase casein kinase 2 and GPCRs (An, Kyoung, et al. 2010; Verrier et al. 2011), and their assembly shows some dependence on Hsp70/ Hsp90 chaperone machinery (French et al. 2013) and microtubules (An et al. 2010). Additionally, purinosome assembly was found to be cell-cycle dependant, with a five-

fold increase in number during mid G₁-phase to S-phase. The concentration of the nucleotide precursor PRPP molecule (**Section 3.1.2**) was also found to increase three-fold which is predicted to increase flux (Chan et al. 2015). Of interest, French et al. (2016) reported on the association of purinosomes with mitochondria. This is predicted to increase availability of ATP and 10-formylTHF. Additionally, mTORC1 signalling, which has already been noted as activating pyrimidine synthesis (**Section 3.1.2.2.2**), was found to be required for the colocalisation of purinosomes with mitochondria (French et al. 2016). Furthermore, mTORC1 is found to regulate expression of mitochondrial *Mthfd2* via the transcription factor ATF4 (Ben-Sahra et al. 2016). Therefore, mTORC1 signalling can synchronise and regulate *de novo* nucleotide synthesis at multiple points in multiple pathways. Lastly, it has been hypothesised that enzymes of mitochondrial FOCM form a multiprotein complex; SHMT2, GCS, DMGDH, MTHFD2L and MTHFD1L have all been shown to partly or wholly associate with the inside of the inner mitochondrial membrane (Tibbetts and Appling 2010).

4.1.3 Formate metabolism

Formate is found to be a key metabolite for embryonic development as a cytosolic one-carbon donor. The majority of formate is believed to be produced from oxidative FOCM in mitochondria, via MTHFD1L, which catalyses the overall reaction:



However, other pathways also produce formate (**Figure 4. 1**). In brief, formate is can be produced by the catabolism of: the amino acid tryptophan; branched chained fatty acids, such as dietary phytanic acid, and 2-hydroxylated straight chain fatty acids, through α -oxidation; and during the synthesis of cholesterol from lanosterol, via the CYP450 lanosterol 14-demethylase enzyme (Lamarre et al. 2013). Additionally, methanol, which is present in plasma at low levels, at least in part due to gut bacteria fermentation, is also catabolised to formate (Lamarre et al. 2013). The contribution of formate derived from these folate-independent pathways to cytosolic FOCM are currently unknown.

Formate itself, when not utilised for FOCM outputs, is catabolised to CO₂, by either mitochondrial or cytosolic 10-formylTHF dehydrogenase, and oxidation by catalase, which requires hydrogen peroxide (Lamarre et al. 2013).

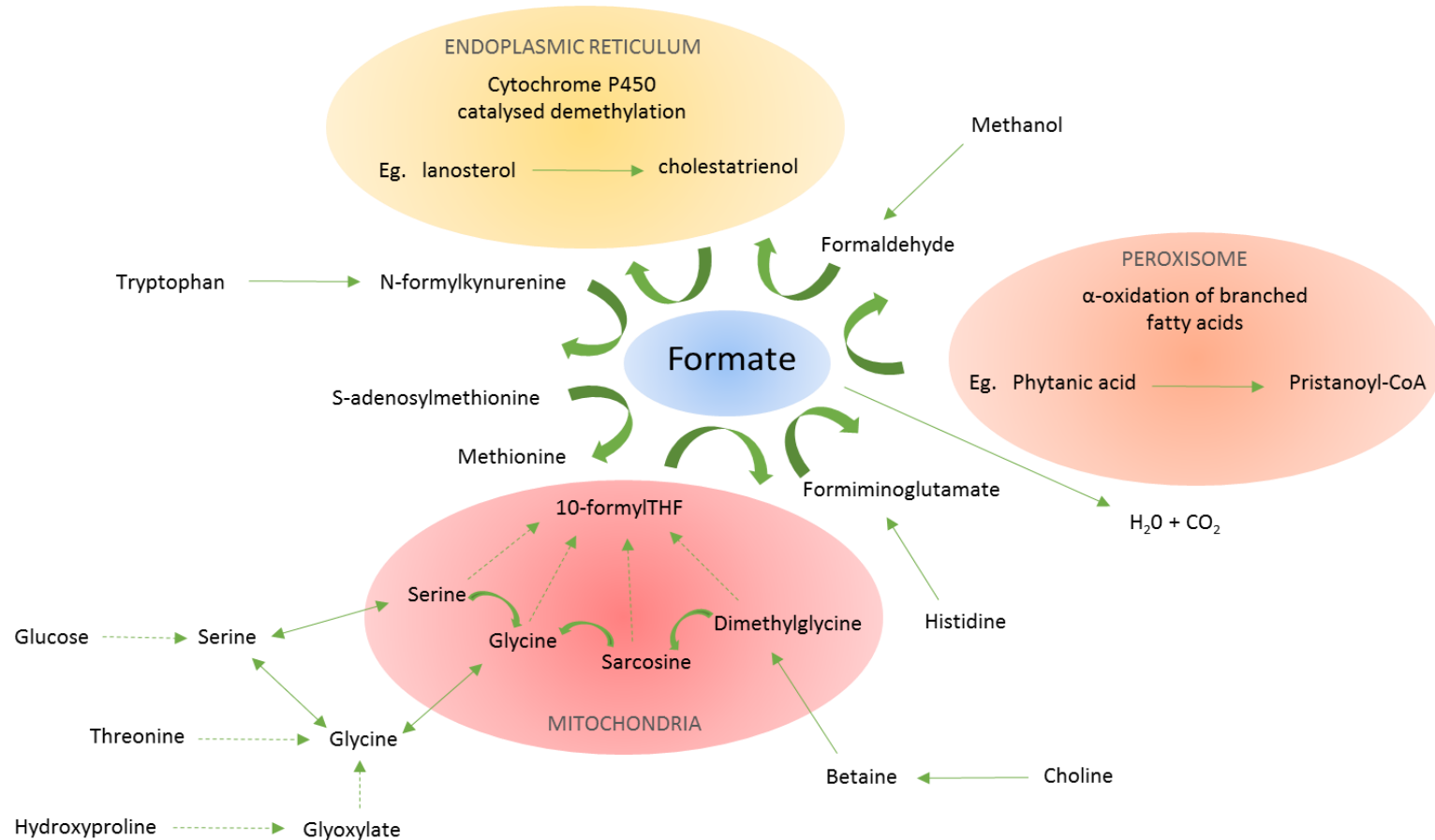


Figure 4. 1. Intracellular formate generating pathways.

Intracellular formate synthesis occurs in mitochondria, endoplasmic reticulum, peroxisomes, as well as the cytosol. Formate production via serine, glycine, sarcosine, dimethylglycine and histidine all require THF. Other formate producing reactions are THF-independent (based on diagram from Brosnan et al. 2015).

4.2 Aims of this chapter

The aim of this chapter is to investigate the functional significance of altered expression of FOCM-related genes, such as *Mthfd1L*, in *ct* mice. The effects of formate supplementation were investigated in the *ct* mouse, and then briefly, in the *Splotch* mouse. The major findings from the *ct* mouse have been published (Sudiwala et al. 2016; **Appendix, Figure A 4**).

4.3 Results

4.3.1 *Curly tail* embryos exhibit reduced expression of *Mthfd1L*

The caudal tissue of *ct* / *ct* embryos and $+^{ct}$ / $+^{ct}$ embryos with 28 -29 somites was isolated at the level of somites 22 – 23 and RNA was extracted. Microarray analysis (Affymetrix) was conducted and a list of differentially expressed genes between *ct/ct* and $+^{ct}$ / $+^{ct}$ samples was obtained. After applying filters of a corrected *p* value of 0.05, expression fold-change of greater than 1.5, and excluding genes that were absent in some samples, 154 differentially expressed genes were identified. Among these genes, 87 were up-regulated and 67 were down-regulated in *ct* / *ct* compared to $+^{ct}$ / $+^{ct}$ (unpublished data; microarray performed previously by the lab).

Due to the importance of mitochondria for folate metabolism and *de novo* purine metabolism, and the presence of NTDs in mice carrying mutations in genes encoding components of mitochondrial FOCM (Pai et al. 2015; Narisawa et al. 2012), the list of 154 differentially expressed genes were interrogated for genes related to mitochondrial and folate metabolism. This was done by first uploading protein IDs onto the IntAct website (<http://www.ebi.ac.uk/intact/>) and downloading the graphical results of reported protein – protein interactions. Cytoscape and the plugin BinGO 2.44 was used to enrich for Gene Ontology (GO) terms and generate Functional Annotation Clustering networks. The clusters enriched for mitochondria-related terms contained 13 genes.

To enquire about folate-related genes, the *ct* gene list was cross referenced with a published list of 64 genes (Mehrmohamadi et al. 2014). The authors constructed this list to include enzymes of three KEGG (Kyoto Encyclopedia of Genes and Genomes) defined pathways: folate biosynthesis; glycine-serine and threonine metabolism and cysteine and methionine metabolism. This analysis highlighted 2 genes.

Altogether, 15 genes were found to be either mitochondrial or folate related. These 15 genes were followed up individually for potential involvement in the *ct* phenotype, and resulted in This resulted in 5 mitochondria-related genes of interest (*Gsr*, *Hspa1a*, *Lcmt2*, *Mecr* and *Ndufs5*), and in particular, 2 genes of interest which were both mitochondrial and on the published list of folate-

related genes (*Mthfd1L* and *Alas2*). As *Alas2* is an erythroid-specific gene (Cox et al. 2004), it was not assessed further. A brief summary of the remaining 6 enzymes of interest encoded by these genes is found in **Table 4. 1**.

Primers were designed for each of the 6 genes and qRT-PCR was carried out to validate the microarray results using cDNA obtained from the caudal end of 28 – 29 somite stage embryos, as per samples for microarray analysis. qRT-PCR results replicated microarray findings for 3 out of the 6 genes: *Mecr* (reduced in *ct*; $p < 0.0001$); *Mthfd1L* (reduced in *ct*; $p = 0.004$) and *Ndufs5* (increased in *ct*; $p = 0.001$; **Figure 4. 2**). Notably, *Mthfd1L* encodes the mono-functional enzyme methylenetetrahydrofolate dehydrogenase 1-like, which catalyses the last step in mitochondrial FOCM; the release of one-carbon units as formate from 10-formylTHF for use in cytosolic FOCM. *Mthfd1L* is expressed in the forebrain, midbrain and spinal neural tube of mice at E9.5 (Pike et al. 2010). Deletion of *Mthfd1L* in mice caused exencephaly in nearly 60 % of mutants, and an aberrant, wavy spinal neural tube and growth retardation in all mutants (Momb et al. 2013). The potential involvement of reduced expression of *Mthfd1L* in NTDs in the *ct* strain was further investigated in this chapter.

Gene	Chromosome	Enzyme	Up or Down*	Function
<i>Gsr</i>	8	Glutathione reductase	Up	Reduces the disulphide bond of glutathione, so it can act as an antioxidant and reducing agent .
<i>Hspal1a</i>	17	Heat shock protein 1A	Up	Member of the heat shock protein 70, a chaperone of newly translated and misfolded proteins. Function in metabolic homeostasis and can protect against apoptosis
<i>Lcmt2</i>	2	Leucine carboxyl methyltransferase 2	Down	S-adenosyl-L-methionine-dependent methyltransferase that acts as a component of the wybutosine biosynthesis pathway.
<i>Mecr</i>	4	Mitochondrial trans-2- enoyl-CoA reductase	Down	Enzyme of mitochondrial fatty acid synthesis (mt FAS II). Important for synthesis of lipoic acid
<i>Mthfd1l</i>	10	Methylenetetrahydrofolate dehydrogenase 1-like	Down	Enzyme of mitochondrial FOCM. Produces formate from 10-formyTHF
<i>Ndufs5</i>	4	NADH dehydrogenase (ubiquinone) Fe-S protein 5	Up	Subunit of the Complex I of the electron transport chain

Table 4. 1. The names and roles of folate and/ or mitochondrial genes identified from the microarray.

*in *ct / ct* embryos compared to *+^{ct} / +^{ct}*

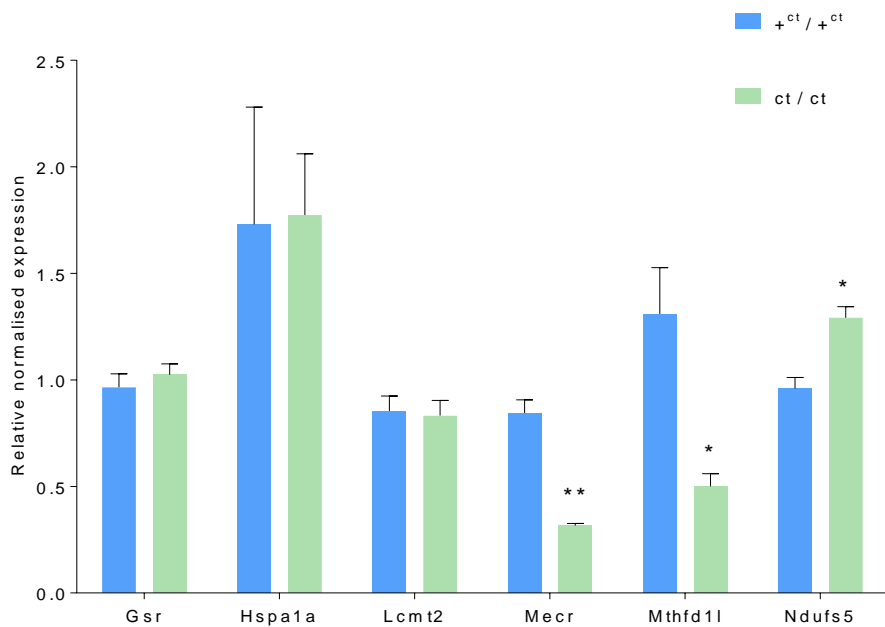


Figure 4. 2. qRT-PCR shows altered expression of *Merc*, *Mthfd1L* and *Ndufs5* in *ct* embryos.

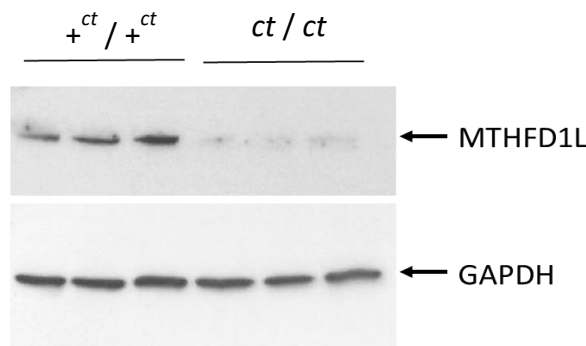
3 out of 6 genes were validated by qRT-PCR. *Merc* ($p < 0.0001$, $n = 6$ each) and *Mthfd1L* ($p = 0.004$, $n = 3$ for $+^{ct} / +^{ct}$ and $n = 5$ for *ct* / *ct*) were reduced in *ct* / *ct* compared to $+^{ct} / +^{ct}$. *Ndufs5* was increased in *ct* / *ct* ($p = 0.001$, $n = 6$ each). Assessed by individual t-tests.

4.3.1.1 MTHFD1L protein abundance is reduced in *curly tail* embryos

Multiple regulatory processes occur that impact upon protein abundance, such as post-transcriptional and post-translational regulation and mRNA/ protein destruction, so that mRNA and protein levels do not always correlate. Therefore, after validating reduced expression of *Mthfd1L* mRNA in *ct* embryos, protein levels were assessed.

Protein was obtained from the cranial region of 28 – 29 somite stage $+^{ct} / +^{ct}$ and *ct* / *ct* embryos. The cranial region was assessed because *Mthfd1L* is reduced in this region to the same extent as the caudal region (Sudiwala et al. 2016) and given it is larger, more protein could be obtained. Western blots were probed for MTHFD1L and GAPDH as loading control. This revealed that while *Mthfd1L* mRNA was reduced by approximately 60 %, the reduction in protein was approximately 90 % ($p = 0.002$; **Figure 4. 3**).

(A)



(B)

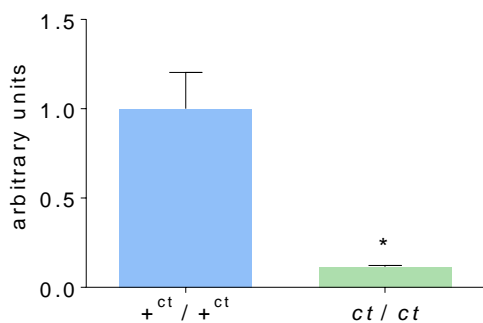


Figure 4. 3. MTHFD1L protein abundance is reduced in *ct* embryos.

(A) Representative western blot showing immunoreactivity against MTHFD1L protein at 106 kDa and GAPDH, as loading control, at 37 kDa. Protein from 28 – 29 somite stage cranial region of embryos. (B) Densitometry values for MTHFD1L were normalised to GAPDH. The mean value for +^{ct} / +^{ct} was 0.43 ± 0.09 , while average value of ct / ct was 0.05 ± 0.01 . (* $p = 0.002$; $n = 6$ for both groups; t-test). These values were adjusted so the value of +^{ct} / +^{ct} was equal to 1.0 (plotted on graph).

4.3.1.2 *Mthfd1L* is not a target of *Grhl3*

The major genetic factor in *ct* NTDs has been found to correspond to a hypomorphic allele of *Grhl3*. Therefore, to assess whether *Mthfd1L* could be either a direct or indirect transcriptional target of *Grhl3*, *Mthfd1L* expression was assessed in *Grhl3* null and wild-type embryos. *Mthfd1L* expression was not changed between these genotypes (**Figure 4. 4**).

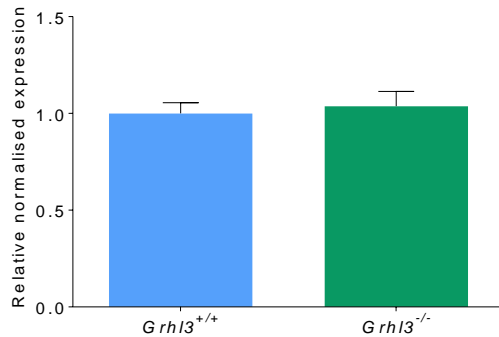


Figure 4. 4. *Mthfd1L* expression is not dependent on *Grhl3* expression.

Mthfd1L expression was unchanged between *Grhl3*^{+/+} ($n = 6$) and *Grhl3*^{-/-} ($n = 7$) embryos.

4.3.2 Formate levels in *curly tail* mice

4.3.2.1 Circulating formate was reduced in the plasma of *ct* mice

To understand whether there is a physiological effect of reduced Mthfd1L abundance in adult mice, blood was collected from non-pregnant, female, *ct* mice. At this time, $^{+ct} / +^{ct}$ mice were no longer available for live experiments. Non-pregnant female wild-type mice from the *Splotch* (Sp^{2H}) strain were used as a wild-type (*wt*) reference due to both these strains sharing parts of the CBA background. Blood collected via cardiac puncture was centrifuged, and the plasma used for quantification of formate by gas-phase chromatography mass spectrometry (performed by the Brosnan lab, Memorial University of Newfoundland, Canada). Circulating formate levels were significantly lower in *ct* mice compared with the *wt* reference levels ($p = 0.03$; **Figure 4. 5**).

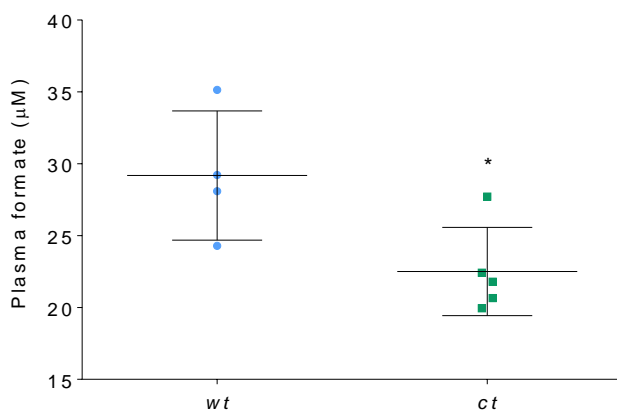


Figure 4. 5. Plasma formate in reduced in *ct* mice.

Plasma formate concentrations from female, non-pregnant *ct* mice ($22.50 \pm 1.37 \mu\text{M}$; $n = 5$) were reduced compared to *wt* ($29.19 \pm 2.25 \mu\text{M}$; $n = 4$; $*p = 0.03$; t-test).

4.3.2.2 Does pregnancy affect circulating formate levels?

To ascertain whether pregnancy affects plasma formate, blood was collected from pregnant (E12.5) and non-pregnant *ct* and *wt* mice and analysed by the Brosnan lab. The results demonstrated that

plasma formate concentration increases during pregnancy in both *ct* and *wt* mice (**Figure 4. 6**). However, formate concentrations from pregnant *wt* mice were higher than those in pregnant *ct* mice ($p = 0.003$), and the increase seen in *ct* mice between non-pregnant and pregnant mice (65 %; $p = 0.02$) was, in general, reduced compared to the increase seen in *wt* mice between non-pregnant and pregnant (85 %; $p = 0.0004$).

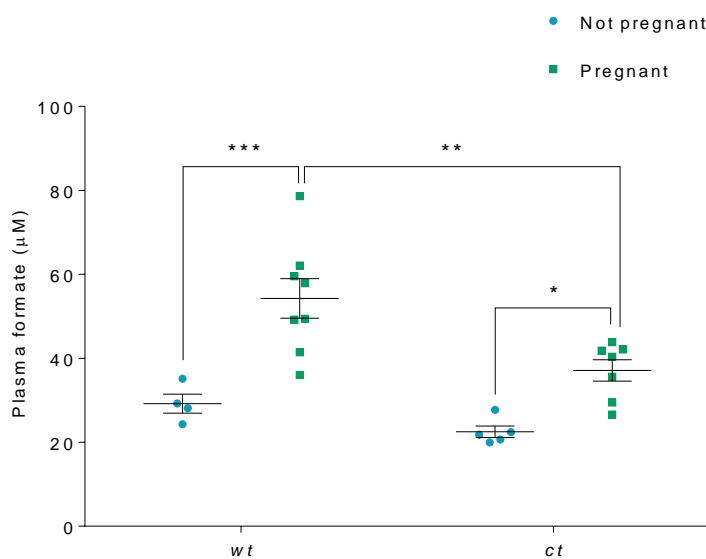


Figure 4. 6. Pregnancy increased circulating formate

Overall, strain ($p = 0.005$; 2way ANOVA) and pregnancy ($p < 0.0001$; 2way ANOVA) were a source of variation. Pregnancy increased plasma formate in *ct* mice ($22.50 \pm 1.37 \mu\text{M}$ vs. $37.12 \pm 2.55 \mu\text{M}$; $*p = 0.02$) and *wt* mice ($(29.19 \pm 2.25 \mu\text{M}$ vs. $54.28 \pm 4.71 \mu\text{M}$; $***p = 0.0004$). Pregnant wild-type mice (54.28 ± 4.71) had increased formate compared to pregnant *ct* mice (37.12 ± 2.55 ; $**p = 0.003$). Individual comparisons carried out using Sidak's multiple comparison test. For *wt* not pregnant, $n = 4$; for *wt* pregnant, $n = 8$; for *ct* not pregnant, $n = 5$; and for *ct* pregnant, $n = 7$.

4.3.2.3 Abnormal formate metabolism in *curly tail* mice

Blood was collected from (non-pregnant) *ct* mice maintained on a folate-deficient diet for 3 weeks prior, and *ct* mice supplemented with 30 mg/mL sodium formate for 12 days (described in more detail in **Section 4.3.3**). Both treatments are expected to increase the concentration of plasma formate: sodium formate, through simply being consumed (Pai et al. 2015); and folate deficiency,

through depletion of THF which incorporates formate to form 10-formylTHF in the cytosol (Pai et al. 2015; Lamarre et al. 2012). Plasma formate concentrations in *ct* mice were unchanged by folate deficiency and only marginally increased by 12 days of sodium formate supplementation as compared to control levels (**Figure 4. 7**). These findings are quite unlike the 1.8 times increase and 15 times increase seen in heterozygous mice from the *Gldc* strain in response to folate deficiency and 12 days of sodium formate supplementation respectively (Pai et al. 2015). Rats on a folate deficient diet for 4 weeks demonstrated an increase in plasma formate levels of 5.6 times (Lamarre et al. 2012).

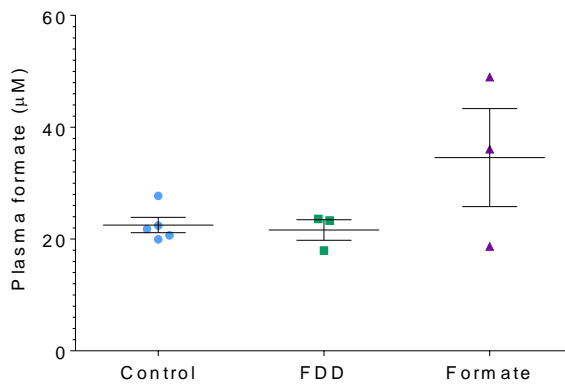


Figure 4. 7. Plasma formate concentrations during folate deficient diet and sodium formate supplementation.

No changes in plasma formate levels in control *ct* mice ($22.50 \pm 1.37 \mu\text{M}$; $n = 5$) and those maintained on a folate deficient diet (FDD) for 3 weeks ($21.62 \pm 1.84 \mu\text{M}$; $n = 3$), nor to mice treated with sodium formate for 12 days ($34.57 \pm 8.77 \mu\text{M}$; $n = 3$).

To test the possibility that *ct* mice excrete increased levels of formate, blood and urine were collected under control and formate treated conditions, from *ct* and *wt* mice. The same mice were used for both urine and blood collection. For formate-treated mice, urine was collected after mice had been supplemented for 12 days; mice were then maintained on sodium formate supplementation and blood was collected, which was 6 weeks after supplementation began. Formate concentration in urine was normalised to creatinine.

Of interest, after 6 weeks on formate supplementation, both *wt* and *ct* mice have a range of plasma formate levels, with each having a single sample which has a much higher value than the mean of the others; ~ 3.5 times for the *wt* sample and ~ 2 times for the *ct* sample (**Figure 4. 8**). With the small datasets collected here, it is unknown whether this is a representative finding. Analysis by ANOVA finds that only the increase in plasma formate in *wt* mice is significant ($p = 0.02$) However, using individual t-tests, the increase in plasma formate levels in both *wt* mice ($p = 0.04$; not shown)

and *ct* mice ($p = 0.008$; not shown) after formate treatment was significant. These findings demonstrate that both *wt* and *ct* mice accumulate formate in plasma over time. They also suggest that *wt* mice tend to accumulate more formate compared to *ct* mice; 25 times the control mean in *wt* and 16 times the control mean in *ct*.

Formate levels in urine again show a wide range in values for formate treated *wt* mice (**Figure 4.9**). When assessed by ANOVA, a significant difference was found ($p = 0.04$), however, multiple comparisons followed by Sidak's correction did not find any significant differences between means. When individual t-tests were used, formate levels in *ct* urine was significantly reduced compared to *wt* urine under control conditions ($p = 0.0005$; not shown), as was the increase in formate levels in treated *ct* mice compared to control *ct* mice ($p = 0.05$; not shown).

Overall, formate supplementation was found to increase the concentration of formate in urine and plasma of *ct* mice, but this effect is not greater than that seen in *wt* mice, and under standard conditions, *ct* mice excrete significantly less formate. In conclusion, there is no evidence from this experiment that *ct* mice excrete more formate compared to *wt* mice.

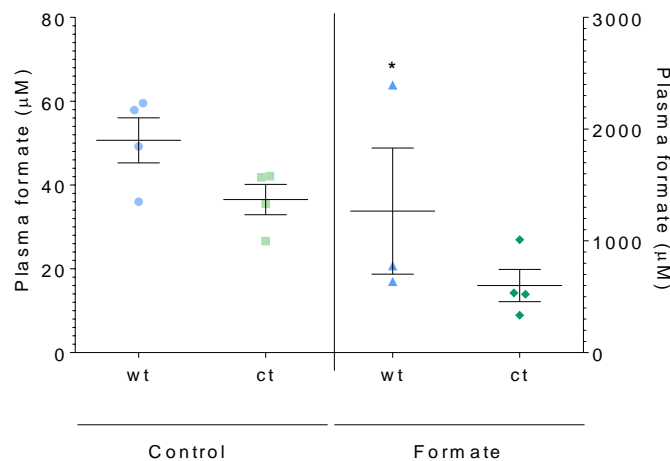


Figure 4.8. Formate in plasma under standard and formate treated conditions.

Plasma formate in *wt* and *ct* mice, under control (left y axis) and formate treated (right y axis) conditions. Formate treatment significantly increased the concentration of formate in *wt* plasma ($1266.97 \pm 564.0 \mu\text{M}$) from control ($50.66 \pm 5.4 \mu\text{M}$; $*p = 0.02$; ANOVA with Holm-Sidak's test). For control *wt* and *ct* samples, $n = 4$ each; for formate treated samples, $n = 3$ and 4 respectively.

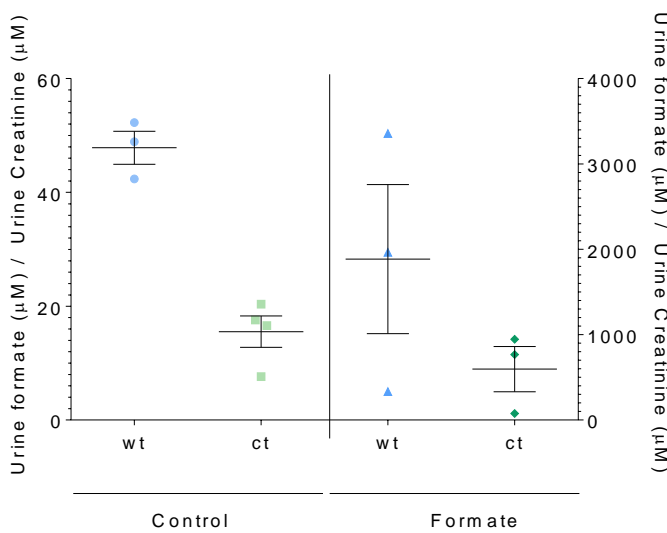


Figure 4.9. Formate in urine under standard and formate treated conditions.

Urine formate in *wt* and *ct* mice, under control (left y axis) and formate treated (right y axis) conditions. Formate concentration was normalised to creatinine concentration within the same sample. A significant difference was found by ANOVA ($p = 0.04$), however, multiple comparisons followed by Sidak's correction did not find any significant differences between means. For control *wt* and *ct* samples, $n = 3$ and 4 respectively; for formate treated samples, $n = 3$ each.

4.3.3 Effect of formate supplementation on growth and neurulation

4.3.3.1 Formate supplementation reduced the frequency of spina bifida and exencephaly

Next, the effect of supplemental formate on the rate of NTDs in *ct* mice was investigated. Formate supplementation is expected to increase the provision of one-carbon units for cytosolic FOCM outputs, including *de novo* nucleotide synthesis, and so could stimulate proliferation and prevent NTDs.

Pregnant dams were supplemented with sodium formate in drinking water from E0.5 until collection of litters at E12.5. The doses used were based on Momb et al. (2013), who used an initial dose of 20 mg/ mL and then increased this to 30 mg/ mL of sodium formate. These doses are intended to deliver approximately 5,000 or 7,500 mg per kg per day respectively.

At the dose of 20 mg/ mL sodium formate, there was a strong trend of reduced frequency of spina bifida in formate treated *ct* embryos compared to contemporaneous control embryos (Control¹; $p = 0.07$; **Figure 4.10**). Increasing the dose to 30 mg/ mL led to a significant prevention in spina bifida compared to the contemporaneous cohort of control embryos (Control²; $p = 0.04$; **Figure 4.10**)

A trend of decreased frequency of exencephaly was also observed in formate-treated embryos compared to control embryos (**Figure 4. 11**). At each dose, the comparisons are not significant, but combining data for all formate treated embryos and all control embryos yields a result of a significant reduction in exencephaly with sodium formate supplementation ($p = 0.02$).

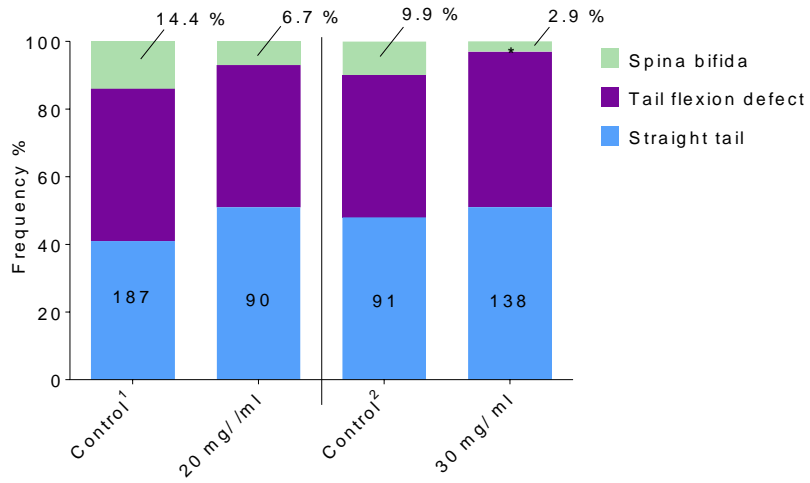


Figure 4. 10. Formate reduced the frequency of spina bifida

Embryos treated with 20 mg/ mL sodium formate showed a tendency towards a reduced frequency of spina bifida compared to Control¹ embryos ($p = 0.07$; Fisher's exact test), which became significant when treated with 30 mg/ mL, compared to Control² embryos (* $p = 0.04$; Fisher's exact test). Number of embryos in each group shown on bars.

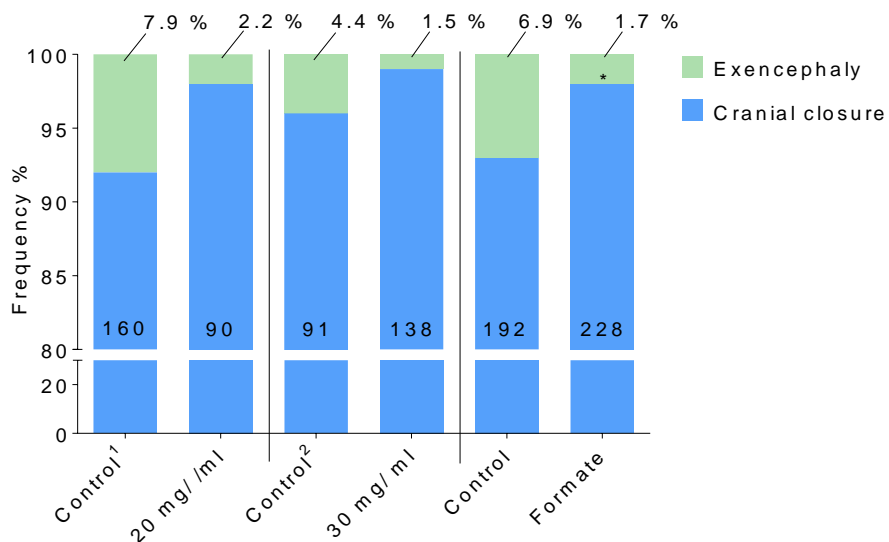


Figure 4. 11. Formate treatment reduced the frequency of exencephaly

Individually, the frequency of exencephaly was not significantly different between embryos treated at each of the doses and their respective control cohorts. Grouping all formate treated embryos (Formate) and all control embryos (Control), there is a significant difference between these groups (* $p = 0.02$; Fisher's exact test). Number of embryos in each group shown on bars.

4.3.3.2 Sodium formate supplementation did not affect embryonic growth

Measurements of CR length, as a measure of growth, were taken from embryos at E12.5 (Figure 4. 12). Neither dose of formate was found to affect the size of embryos, implying that formate treatment is unlikely to prevent spina bifida by growth retardation, as found for treatments such as high temperature (Seller and Perkins-Cole 1987a).

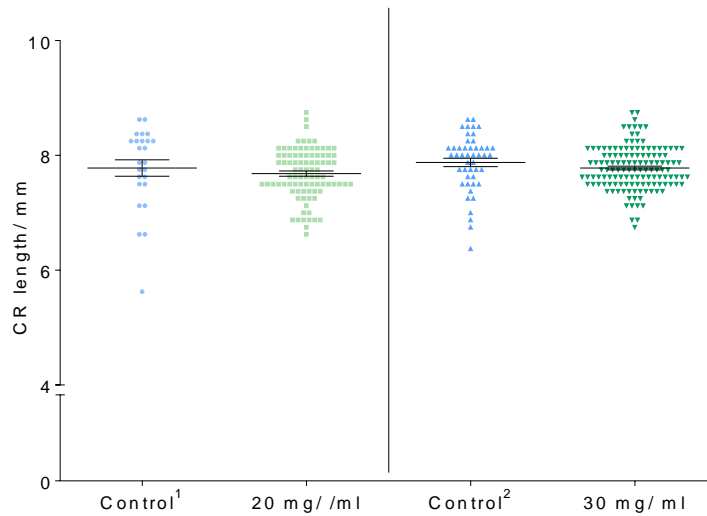


Figure 4. 12. Formate treatment has no effect on CR length of *ct* embryos at E12.5.

No differences in CR length found.

4.3.3.3 Litter size was increased by formate treatment

Maternal sodium formate supplementation was found to increase the average litter size of pregnant dams in a dose dependant manner (**Figure 4. 13**). Dams receiving 20 mg/ mL of sodium formate had on average 9.0 ± 0.9 embryos compared with 6.9 ± 0.5 embryos from control dam (Control¹. $p = 0.04$), while those given 30 mg/ mL had on average 9.57 ± 0.4 embryos compared with 7.0 ± 0.6 embryos from control dams (Control². $p = 0.001$). No differences were found in the number of resorptions between all groups.

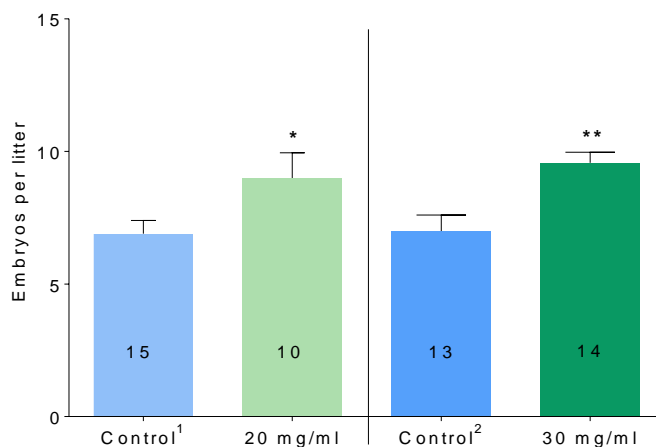


Figure 4. 13. Formate treatment increased litter size

Figure 4. 13. Formate treatment increased litter size

Litters were bigger in dams receiving 20 mg/ mL of sodium formate (9.0 ± 0.9 embryos) compared with control litters (Control¹; 6.9 ± 0.5 embryos; $*p = 0.04$; t-test). Those on 30 mg/ mL showed a greater increase in litter size (9.57 ± 0.4 embryos) compared with their contemporaneous control litters (Control²; 7.0 ± 0.6 embryos; $**p = 0.001$; t-test). The number of litters collected for each group are indicated on the graph.

4.3.4 Effect of formate supplementation on folate one-carbon metabolism

As a metabolite of FOCM, it was hypothesised that formate supplementation could have a direct effect on the relative abundance of other components of FOCM. To investigate the consequences of sodium formate supplementation on FOCM, the abundance of folate cofactors, as well as SAM and SAH, was measured in control and formate treated E10.5 embryos and maternal liver. The analysis of both embryonic and maternal liver tissue may provide some insight into the relative importance of FOCM intermediates in both mother and foetus.

4.3.4.1 Embryonic folate distribution

The folate profile of formate-treated and control embryos was analysed by LC-MS/MS. The sum of all glutamated forms of each of the six folate cofactors in control and sodium formate treated (30 mg/ mL) E10.5 embryos are shown. Absolute levels of folate cofactors showed a 33 % decrease in 5-methylTHF ($p = 0.003$; **Figure 4. 14**). The relative folate abundance profile found that as 5-methylTHF was decreased by formate treatment (20 %; $p < 0.0001$), a significant increase was found in the relative abundance of THF (2.4 times; $p < 0.0001$) and formylTHF (10 times; $p = 0.01$) in formate-treated embryos compared to control embryos (**Figure 4. 15**).

These changes in the folate profile of embryos treated with formate are reminiscent of the changes seen with nucleotides + inositol treatment (**Section 3.2.6.1**). Again, both increased flux through the methionine cycle or partitioning of one-carbon units away from the methionine cycle could possibly increase the relative abundance of THF while decreasing 5-methylTHF (**Figure 1. 7**). The substantial increase in relative formylTHF suggests partitioning away from the methionine cycle.

4.3.4.2 Maternal liver folate distribution

The liver contains the majority of folates, together with the most complete complement of folate-dependant enzymes and is important for homeostasis. Therefore, livers were collected from pregnant, control and formate-treated mice at the same time as collection of litters at E12.5; hence

12 days of sodium formate supplementation for treated livers. For each sample, 50 mg of liver was processed for folate analysis. The results are shown as the relative distribution of folates.

Significant changes were seen in the distribution of folates in control and supplemented maternal liver (**Figure 4. 16**); 5-methylTHF was increased by formate treatment ($p = 0.005$), and THF was decreased ($p = 0.02$). These results are conspicuous in showing an opposite trend compared to embryonic folates under the same treatment.

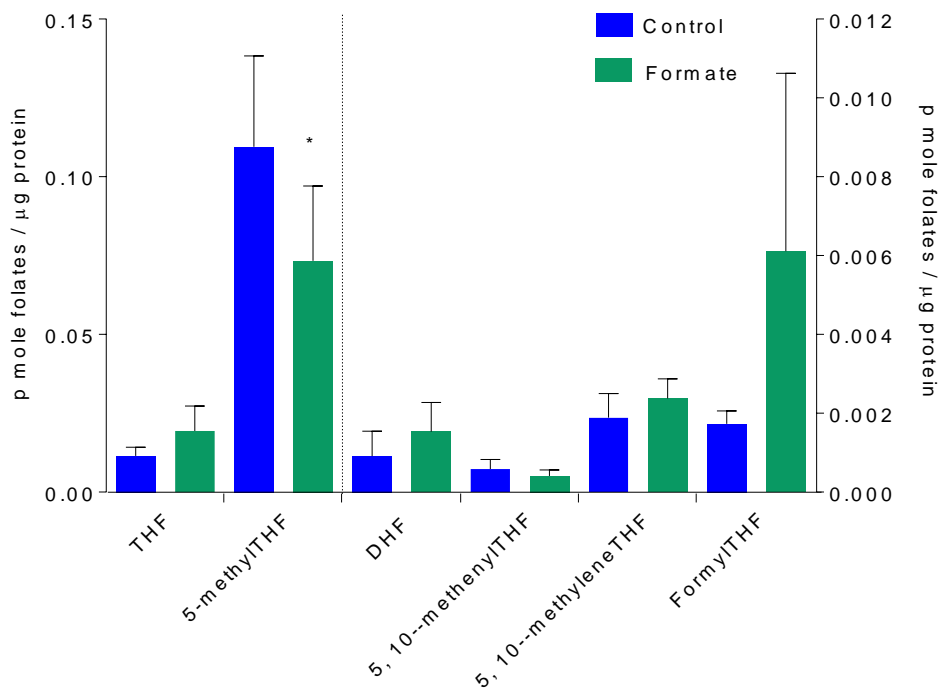


Figure 4. 14. Absolute abundance of folates in control and formate treated embryos.

The absolute level of 5-methylTHF was decreased by formate treatment (0.073 ± 0.012 pmol./ μ g protein) when compared to control (0.109 ± 0.014 pmol./ μ g protein, $*p = 0.003$; 2way ANOVA with Sidak's test). For control and formate treated, $n = 4$ each. Bars left of the dotted line are plotted on the left axis, while bars right of the dotted line are plotted on the right axis.

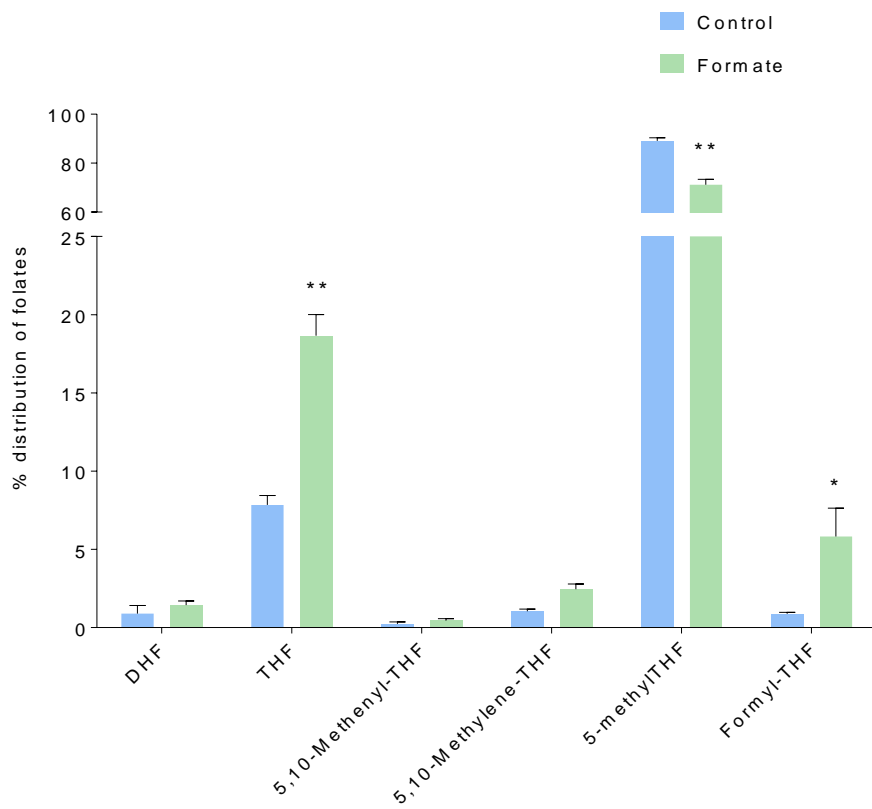


Figure 4. 15. Relative distribution of folates in control and formate treated embryos.

Relative folate profiles of control and formate treated E10.5 embryos. THF and Formyl-THF ($18.66 \pm 1.35\%$ and $5.82 \pm 1.82\%$ respectively) were increased in formate treated embryos compared to control embryos ($7.84 \pm 0.61\%$ and $0.88 \pm 0.10\%$; $**p < 0.0001$ and $*p = 0.01$ respectively). 5-methylTHF was decreased by formate treatment ($89.08 \pm 1.28\%$) compared to control ($17.17 \pm 2.22\%$, $**p < 0.0001$) Assessed by 2way ANOVA with Sidak's test. For control and formate treated, $n = 4$ each.

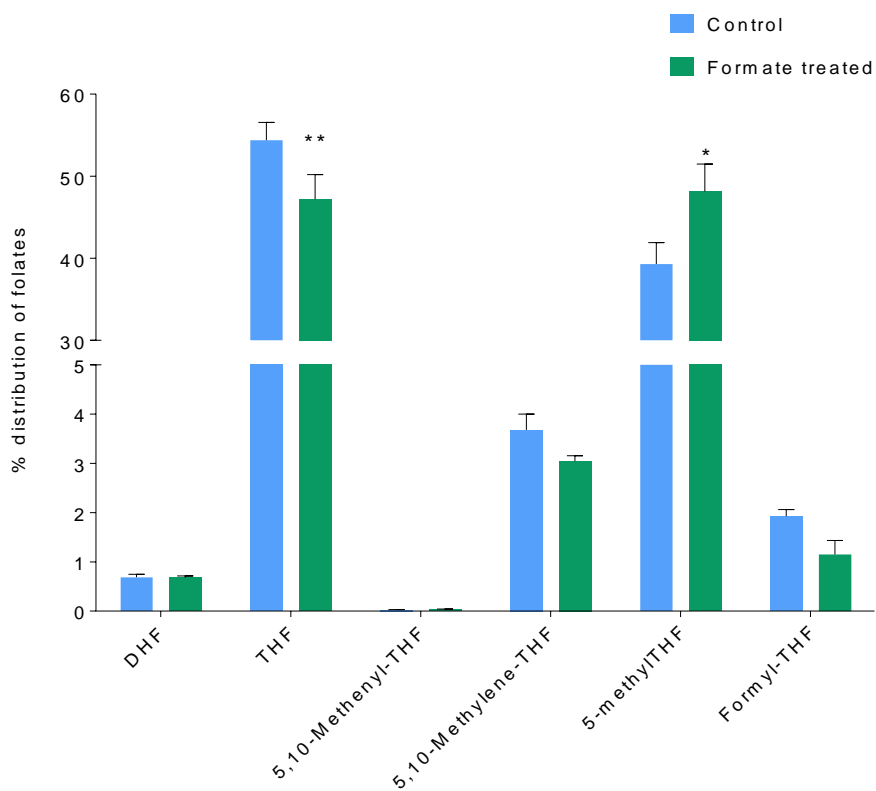


Figure 4. 16. Relative distribution of folates in control and formate treated livers.

Sodium formate supplementation increased the relative abundance of 5-methylTHF ($48.13 \pm 3.36\%$) compared to control ($39.30 \pm 2.61\%$; $**p = 0.005$; 2way ANOVA with Sidak's test), and decreased the relative abundance of THF ($47.17 \pm 3.03\%$) was compared to control ($54.38 \pm 2.18\%$; $*p = 0.02$; 2way ANOVA with Sidak's test). For control and formate treated, $n = 3$.

4.3.4.3 Effect of formate treatment on total folates in liver and embryos

As a direct metabolite of FOCM, it is possible that formate supplementation could influence the absolute pool of folates. To investigate this possibility, the collective peak area of each of the folates was normalised to the peak area of the internal standard, methotrexate, in which the number of moles present in each sample were known; this gave the number of moles of folates in the sample. The total moles of folate were then normalised to the total protein in the sample.

Overall, there were no significant changes associated with formate treatment in livers or embryos (**Figure 4. 17**). It was noted that livers contain more folates per μg protein compared to embryos ($0.85 \pm 0.15\text{ pmol/ }\mu\text{g}$ and $0.12 \pm 0.13\text{ pmol/ }\mu\text{g}$ respectively; $p < 0.0001$; t-test), and that formate treated samples show more variation in total folates compared to their control counterparts.

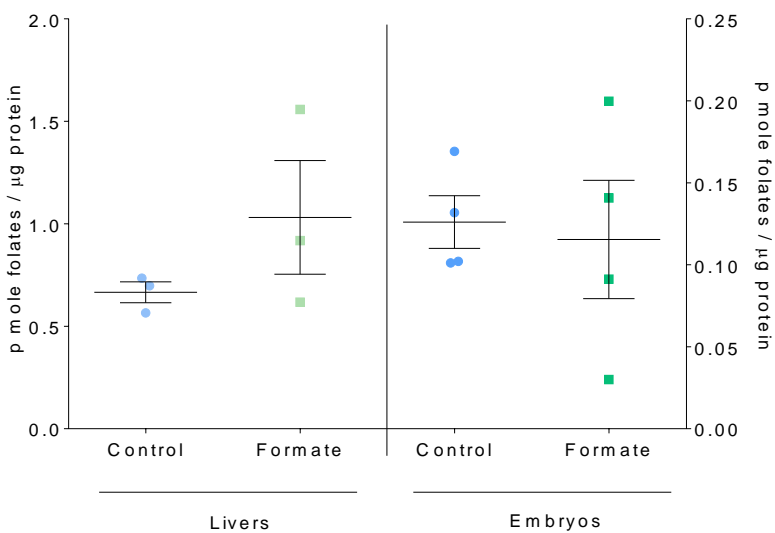


Figure 4.17. Total folates in livers and embryos.

There were no significant differences in total folates between formate treated livers (left y axis) or embryos (right y axis) and controls. For livers, $n = 3$ each, and for embryos, $n = 4$ each.

4.3.4.4 Measurement of SAM / SAH

As highlighted in **Section 3.2.6.2**, changes in SAM and SAH can provide an indication as to whether flux of one-carbon units into the methionine cycle is increased. Both SAM and SAH were measured in control and formate treated adult liver and E10.5 embryos.

The SAM / SAH ratio of formate treated embryos was significantly decreased ($p = 0.005$) compared to control embryos, while those of maternal liver samples showed perhaps a small tendency towards an increased value with formate treatment (**Figure 4.18**). SAM levels did not vary significantly with treatment in either liver or embryo samples, although there may have been a tendency towards decreased SAM levels in formate-treated embryos (**Figure 4.19**). SAH was significantly increased by formate treatment in embryos ($p = 0.01$) and showed a strong tendency towards being decreased in liver samples ($p = 0.06$; **Figure 4.20**). It is noteworthy that in general, liver and embryo samples appear to contain broadly the same amount of SAM per μg protein, while liver samples contain approximately one thousand times more SAH per μg protein, compared to embryo samples. These results support a scenario where formate treatment in embryos is driving one-carbon units away from the methionine cycle to be kept for *de novo* nucleotide synthesis. In contrast, formate treatment appears to increase the flux of one-carbon units into the methionine cycle in maternal liver.

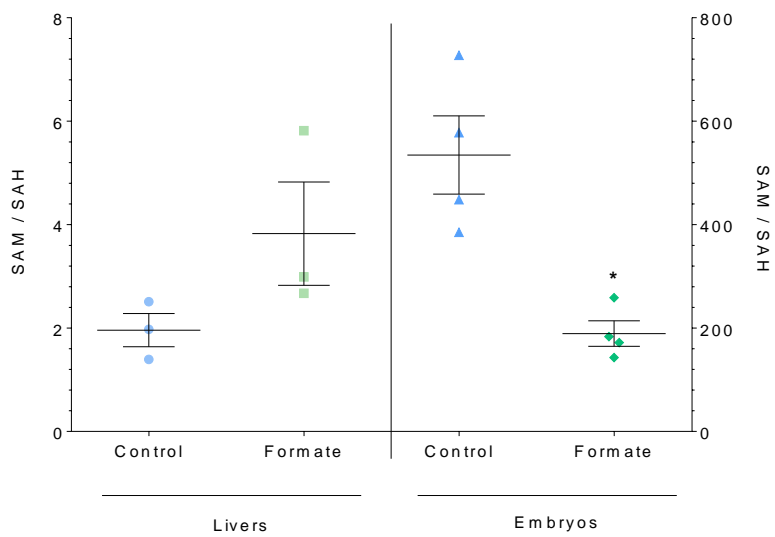


Figure 4. 18. Ratio of SAM/ SAH in embryos and livers

The SAM/SAH ratios of liver samples were not significantly changed by formate treatment, while formate treatment (189.3 ± 24.6) reduced the SAM/SAH of formate treated embryos compared to control embryos (534.6 ± 75.8 ; $*p = 0.005$; t-test). For livers, $n = 3$ each, and for embryos, $n = 4$ each.

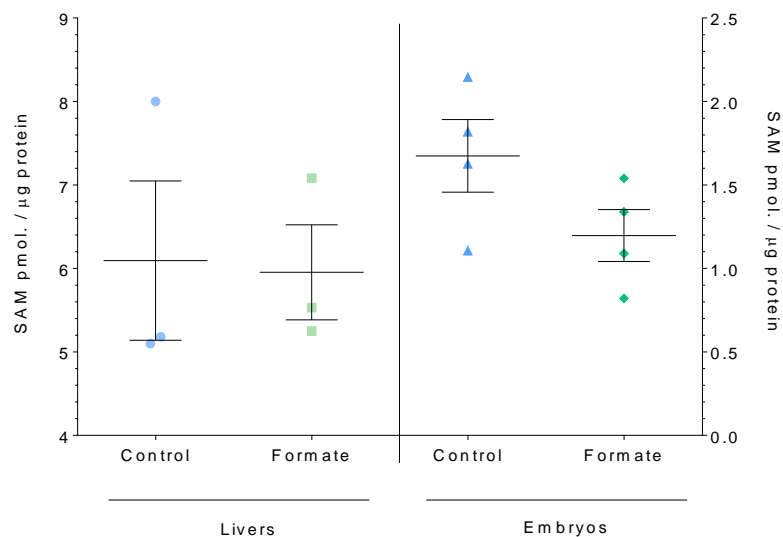


Figure 4. 19. Concentration of SAM in embryos and livers

SAM levels in liver samples and embryo samples were unchanged by formate treatment. For livers, $n = 3$ each, and for embryos, $n = 4$ each.

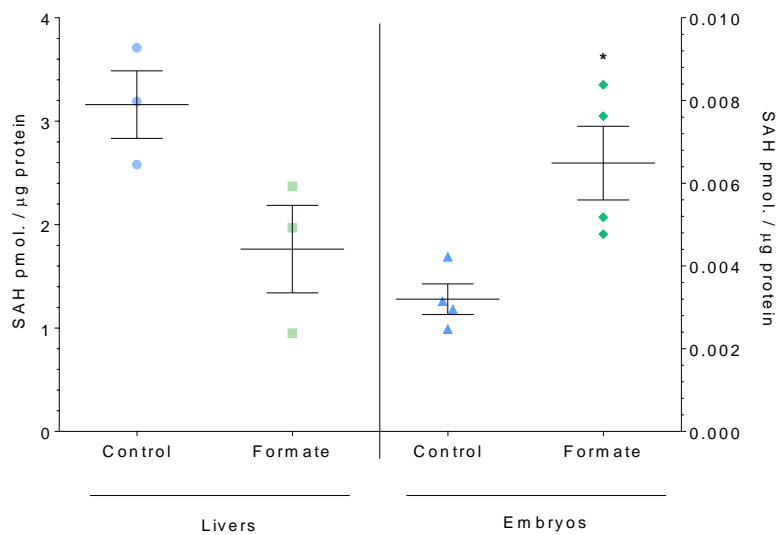


Figure 4. 20. Concentration of SAH in embryos and livers

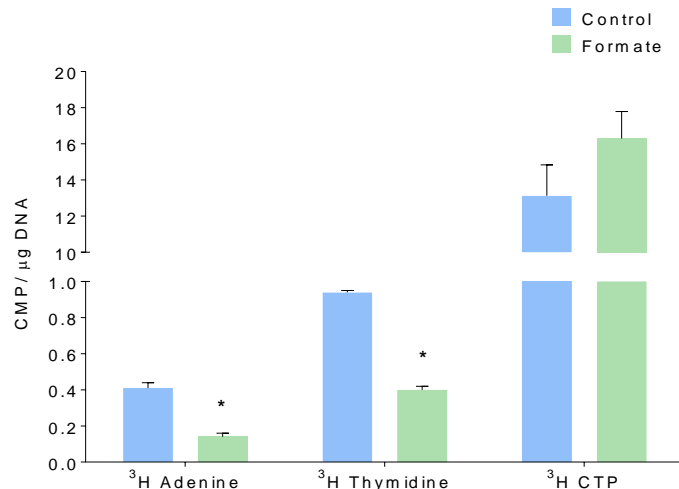
SAH in liver samples demonstrated a strong tendency towards decreased levels with formate treatment (1.76 ± 0.42 pmol./ μ g) in comparison to control livers (3.16 ± 0.33 pmol./ μ g; $p = 0.06$), while formate treatment (0.0065 ± 0.0009 pmol./ μ g increased the SAH levels compared to control embryos (0.0032 ± 0.0004 pmol./ μ g; $*p = 0.01$). For livers, $n = 3$ each, and for embryos, $n = 4$ each.; significance calculated by t-tests.

4.3.5 Prevention of spina bifida may be mediated by stimulation of *de novo* nucleotide synthesis

To assess more directly whether formate treatment stimulates *de novo* nucleotide synthesis in neurulation stage embryos, *ct* embryos were explanted at E9 and cultured with either 3 H-adenine, 3 H-thymidine or 3 H-CTP, with and without 5 mM sodium formate. DNA was isolated from individual embryos and the counts per minute (CPM) from labelled nucleotides were normalised to total DNA.

This experiment demonstrated that formate treatment decreased the amount of exogenous 3 H-adenine and 3 H-thymidine found in DNA ($p < 0.0001$ for both; **Figure 4. 21**), which strongly suggests that formate increases the rate of *de novo* purine and thymidylate synthesis such that uptake of exogenous nucleotides (for salvage pathways of nucleotide synthesis) is diminished. The effect appears to be specific to FOCM as incorporation of 3 H-CTP (which does not rely on 1C donors from FOCM) was not affected (**Figure 4. 21A**) and DNA content per embryo was not a significant factor (**Figure 4. 21B**).

(A)



(B)

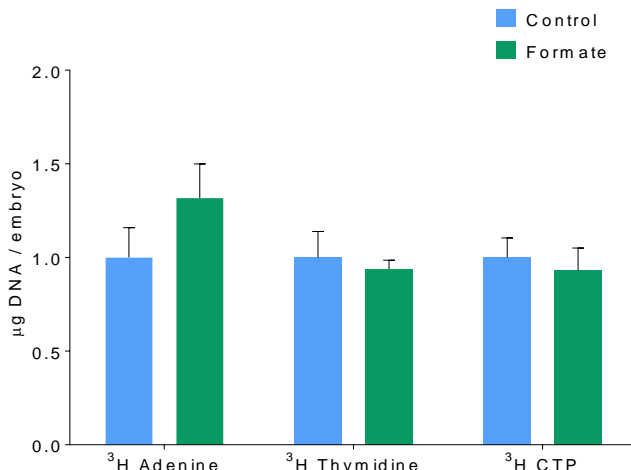


Figure 4. 21. Formate treatment decreases the incorporation of exogenous nucleotides.

(A) Formate treatment in culture decreased the incorporation of ³H-adenine from 0.41 ± 0.02 CMP/µg DNA in control embryos to 0.14 ± 0.02 CMP/µg DNA ($*p < 0.0001$; t-test), and decreased ³H-thymidine incorporation from 0.94 ± 0.01 CMP/µg DNA to 0.40 ± 0.02 CMP/µg DNA ($*p < 0.0001$; t-test). ³H-CTP incorporation was unchanged. (B) Sodium formate treatment had no significant effect on the DNA content per embryo. Results from three separate experiments shown. Results within each experiment normalised to an arbitrarily chosen control sample.

For ³H-adenine experiment, $n = 6$ each; for ³H-thymidine experiment, $n = 3$ control and 4 treated, and; for ³H-CTP, $n = 3$ each.

4.3.6 Interaction between disruption of mitochondrial FOCM and reduced *Grhl3*?

Although formate supplementation is able to prevent NTDs in the *ct* mouse, it is unknown whether reduced expression of *Mthfd1L* could have a role, alongside the known role of reduced *Grhl3* expression, in the causation of NTDs in this model. Although this question was not addressed directly, for example, by assessment of *Grhl3*^{+/−}; *Mthfd1L*^{+/−} embryos, an effort was made to try and understand whether disruption of mitochondrial FOCM and reduced *Grhl3* can interact to affect neural tube closure,

Embryos heterozygous for *Grhl3* and *Gldc* expression (*Grhl3*^{+/−}; *Gldc*^{GT2/+}) were obtained by mating mice heterozygous for *Grhl3* with mice heterozygous for *Gldc*^{GT2}. In addition, these litters also contained single heterozygous littermates, which act as controls for this experiment, and wild-type embryos. Litters were examined at E10 – 10.5, and the number of somites and PNP lengths were assessed, and any cranial NTDs noted. In total, 14 double heterozygous embryos were examined, alongside 30 *Grhl3* heterozygous mutants (*Grhl3*^{+/−}; *Gldc*^{+/+}), 8 *Gldc* heterozygous mutants (*Grhl3*^{+/+}; *Gldc*^{GT2/+}) and 18 wild-type (*Grhl3*^{+/+}; *Gldc*^{+/+}) embryos. The number of double heterozygous embryos (14) is not different from the predicted number based on Mendelian inheritance of 17.5.

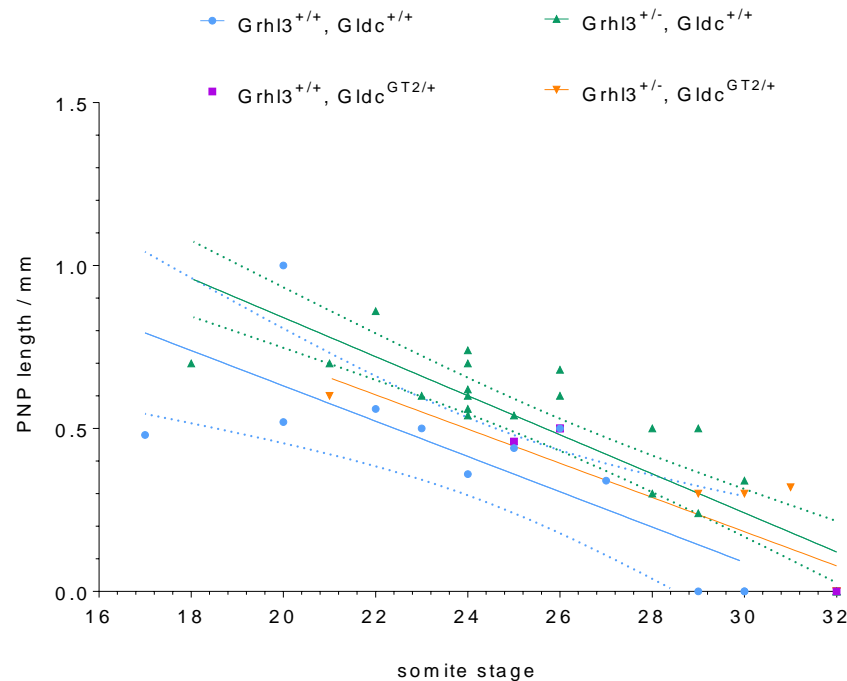
Among all the embryos examined, 1 *Grhl3*^{+/+}; *Gldc*^{GT2/+} presented with split face. Cranial NTDs have been noted as occurring in approximately 5 % of *Gldc*^{GT2} heterozygotes (unpublished data, Yun Jin Pai). Therefore, heterozygosity for null alleles of *Grhl3* and *Gldc* does not indicate a genetic interaction that affects cranial neural tube closure.

A scatter plot of PNP length against somite number for all embryos with up to 32 somites is shown in **Figure 4. 22A**. In keeping with unpublished data from the lab, *Grhl3* heterozygous embryos (*Grhl3*^{+/−}; *Gldc*^{+/+}) displayed delayed PNP closure compared to wild-type mice ($p = 0.005$; linear regression analysis), however all *Grhl3*^{+/−}; *Gldc*^{+/+} embryos with more than 32 somites (7/ 7) did achieve PNP closure.

Although only 4 *Grhl3*^{+/−}; *Gldc*^{GT2/+} embryos had open PNPs to measure, it is evident that they display the same delay in PNP closure as their *Grhl3*^{+/−}; *Gldc*^{+/+} control littermates. Inverting the axes to suppose somite stage is the dependant variable, **Figure 4. 22B** illustrates that embryos of both genotypes are predicted to achieve PNP closure at the same somite stage. All *Grhl3*^{+/−}; *Gldc*^{GT2/+} embryos with more than 32 somites (10/ 10) had achieved PNP closure.

From this experiment, the conclusion is that *Grhl3* and *Gldc* do not appear to interact to affect either cranial or spinal neural tube closure.

(A)



(B)

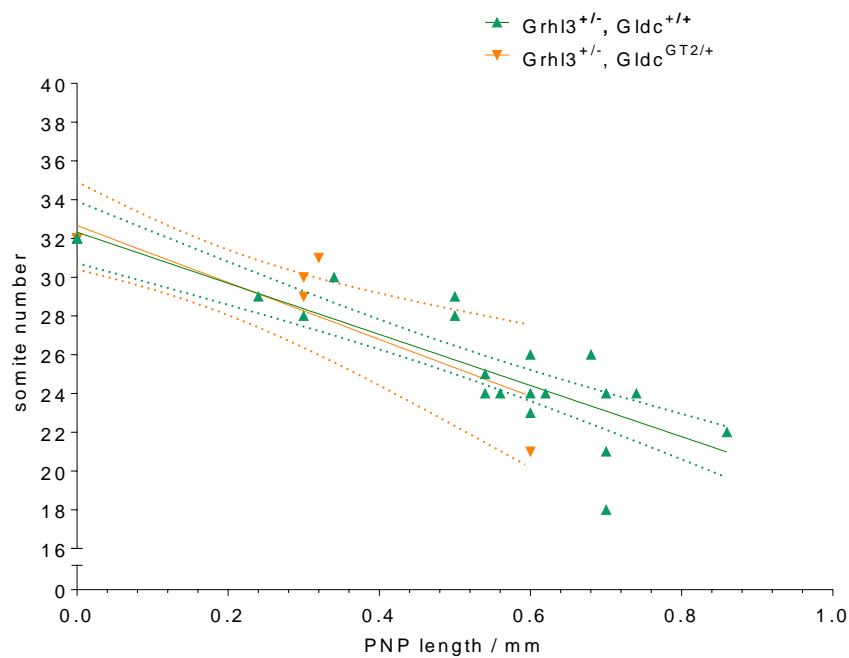


Figure 4. 22. PNP lengths of *Grhl3/Gldc* double heterozygous embryos at E10.5

Figure 4. 22. PNP lengths of *Grhl3*/*Gldc* double heterozygous embryos at E10.5

(A) Scatter plot with PNP size and somite stage of all embryos 32 somites and under. Linear regression lines are plotted for *Grhl3*^{+/+}, *Gldc*^{+/+}, *Grhl3*⁺⁻, *Gldc*^{+/+} and *Grhl3*⁺⁻, *Gldc*⁺⁻ ($r^2 = 0.63$, 0.79 and 0.77 respectively). Linear regression analysis found significant difference in intercept ($p = 0.005$). For the different genotypes, $n = 12$ for *Grhl3*^{+/+}, *Gldc*^{+/+}; $n = 25$ for *Grhl3*⁺⁻, *Gldc*^{+/+}; $n = 4$ for *Grhl3*^{+/+}, *Gldc*^{GT2/+} and $n = 8$ for *Grhl3*⁺⁻, *Gldc*^{GT2/+}. (B) Graph of *Grhl3*⁺⁻, *Gldc*^{+/+} and *Grhl3*⁺⁻, *Gldc*^{GT2/+} data only. Axes have been reversed, as if PNP length was the independent variable and somite stage the dependant variable. For *Grhl3*⁺⁻, *Gldc*^{+/+} $n = 25$ and for *Grhl3*⁺⁻, *Gldc*^{GT2/+} $n = 8$. $R^2 = 0.79$ and 0.77 respectively.

4.3.7 *Mthfd1L* in *Splotch* mice

4.3.7.1 Expression of *Mthfd1l* in *Splotch* and other mice

Splotch mice are known to share part of their CBA background with *ct* mice. *Mthfd1l* expression was assessed in *Splotch* wild-type mice (*Sp2H*^{+/+}), along wild-type mice on a C57BL/6 background (Figure 4. 23). Somewhat surprisingly, *Mthfd1l* was found to be expressed at similar levels to *ct/ct* mice in *Splotch* wild-type mice. Their expression levels were reduced in respect to congenic wild-type mice ($+^{ct}/+^{ct}$; $p = 0.002$ and $p = 0.02$ respectively). Wild-type mice on a C57BL/6 background were found to have comparable expression to congenic wild-type mice; *ct/ct* had reduced expression in relation to C57BL/6 ($p = 0.03$).

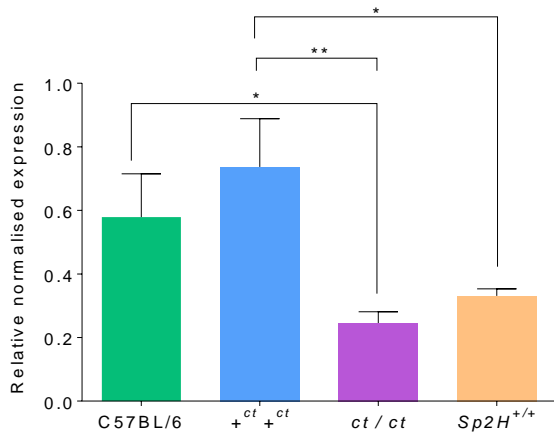


Figure 4. 23. *Mthfd1L* expression in different strains

ct/ct mice (0.25 ± 0.04 ; $n = 5$) had reduced *Mthfd1l* expression compared to wild-type mice on a C57BL/6 background (0.58 ± 0.14 ; $n = 3$; $*p = 0.03$) and congenic wild-type ($+^{ct}/+^{ct}$) mice (0.74 ± 0.15 ; $n = 3$; $**p = 0.002$). *Sp2H*^{+/+} mice (0.33 ± 0.02 ; $n = 3$) had reduced *Mthfd1L* expression compared to $+^{ct}/+^{ct}$ mice (0.74 ± 0.15 ; $n = 3$; $*p = 0.02$ respectively). Assessed via ANOVA with Tukey's multiple comparison test.

4.3.7.2 Formate supplementation in *Splotch* mice

As *Splotch* (*Sp*^{2H}) mice expressed *Mthfd1L* at a similar level to *ct* mice, formate supplementation (30 mg/ mL) was given to pregnant *Sp*^{2H/+} mice (after mating with *Sp*^{2H/+} males) mice and litters examined at E11.5. This treatment had no effect on the frequency of NTDs.

	Frequency % (n)	
	Spina bifida	Exencephaly
Control	94.59 (35/37)	67.57 (25/37)
Formate treated	100.00 (5/5)	60.00 (3/5)

Table 4. 2. Frequency of NTDs in formate treated *Splotch* (*Sp*^{2H}/*Sp*^{2H}) mutants.

No changes were observed in the frequency of formate-treated compared with control embryos.

4.3.8 Sodium formate as a potential prevention strategy

An ambition for this PhD project has been to find an optimum prevention strategy for the prevention of folic acid resistant NTDs, and sodium formate treatment was effective at preventing approximately 70 % of spina bifida and exencephaly in the *ct* mouse. Any strategy must be safe for mothers and their foetus in the long term, as it would need to act periconceptionally. To better understand the consequences of long-term exposure of dams and embryos to sodium formate supplementation, pregnant, wild-type mice (C57BL/6 genetic background) were supplemented with 30 mg/ mL sodium formate from E0.5 for 18 days, after which the embryos were explanted, examined grossly and the CR length measured.

After 18 days, both formate-supplemented and control dams appeared identical, showing the same nesting behaviour; the dams were not studied further. Out of 8 copulation plugs found for control dams, 7 were full term pregnancies; out of 24 copulation plugs found for sodium formate-supplemented dams, 17 were full term pregnancies (no statistical difference).

Abnormal growth and development were seen in 51 % of treated embryos, compared to 2% in control embryos ($p < 0.0001$; **Table 4. 3**). The abnormal phenotype consisted of haemorrhage: if alone, in patches commonly around the face and eyes; or throughout most of the face and trunk when together with whole body oedema. Formate treated embryos could be grouped as either unaffected, moderately affected or extremely affected. Representative images of embryos in each of these groups are shown in **Figure 4. 24**.

The CR length was found to be significantly reduced in formate-treated embryos compared to control ($p = 0.0002$; **Figure 4. 25A**). However, it was noted that there appeared to be more variation in CR length in the formate treated group, and perhaps two distinct groups within this dataset. Therefore, CR lengths of formate treated embryos were further grouped and divided by haemorrhage/ oedema phenotype (unaffected, moderately affected or extremely affected; **Figure 4. 25B**). Unsurprisingly, this analysis found CR length to reduce in relation to severity of phenotype.

	No. of litters examined	Litter size Mean \pm SEM	No. of haemorrhage & oedema
Control	7	8.4 ± 0.8	1.7 % (1 / 58)
Formate treated	13	7.2 ± 0.6	51.1 % (48 / 94)*

Table 4. 3. Toxic effects of sodium formate supplementation.

* $p < 0.0001$; Fisher's exact test. No. of haemorrhage & oedema in formate treated group compared to control group.

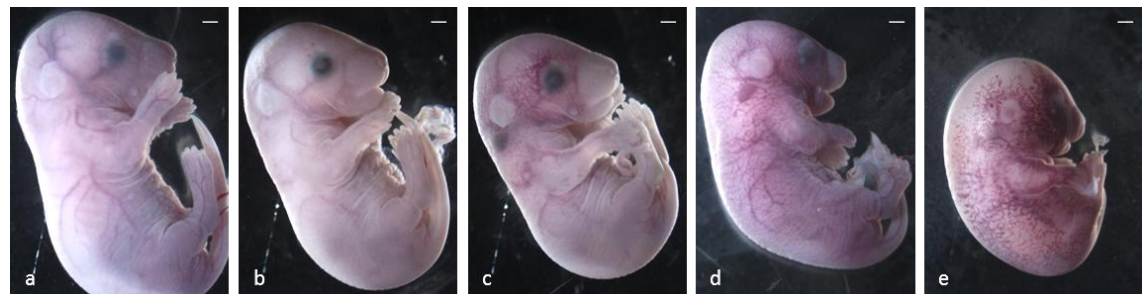
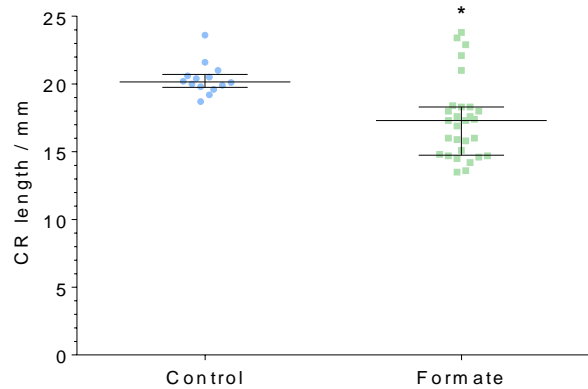


Figure 4. 24. Appearance of formate-treated embryos at E18.5.

In comparison to (a) control, a range of phenotypes were seen with formate treatment: unaffected (b); moderately affected (c) and (d); and extremely affected (e). Scale bar represents 1 mm.

(A)



(B)

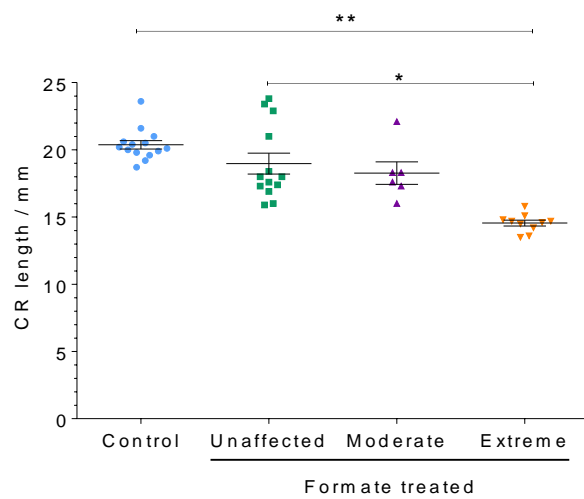


Figure 4. 25. CR lengths of treated and control E18.5 embryos

(A) Median CR lengths of sodium formate treated embryos (median = 20.37; IQR = 14.75 – 18.30 mm; $n = 29$) were reduced compared to control embryos (median = 17.30; IQR = 19.74 – 20.15 mm; $n = 14$; $*p = 0.0002$; Mann-Whitney test). **(B)** Embryos extremely affected by sodium formate treatment (Extreme; 14.55 ± 0.21 mm), had significantly reduced CR lengths compared to control embryos (Control; 20.37 ± 0.31 mm; $**p < 0.0001$; Kruskal-Wallis test) and compared to unaffected embryos treated with sodium formate (Unaffected; 18.97 ± 0.78 ; $*p = 0.003$). Moderate refers to embryos moderately affected by sodium formate treatment. For Control, $n = 14$; for Unaffected $n = 13$; for Moderate, $n = 6$, and for Extreme, $n = 10$.

4.4 Discussion

4.4.1 Genetic background influences *Mthfd1L* expression in mice

It has been somewhat of a puzzle to observe that the aetiology of spina bifida in *ct* mice involves reduced proliferation, and that treatment of embryos with molecules which increase proliferation, such as retinoic acid and nucleotide precursors (Chen, Morriss-Kay, and Copp 1995; Leung et al. 2013), prevents a significant proportion of NTDs. However, folic acid supplementation, which is assumed to increase provision for *de novo* nucleotide synthesis, and has been shown to increase proliferation *in vitro* (H Liu et al. 2010), is not an effective treatment in this model (Seller 1994). The finding that *Mthfd1L* abundance is significantly reduced in *ct* mice compared with congenic wild-type mice which share approximately 95 % of the genetic background, offers a potential reason behind this fact; if one-carbon units are limiting, increasing the abundance of folates, in particular the non-activated folate DHF, will not lead to an increase in nucleotide output.

What causes reduced expression of *Mthfd1L* is currently unknown; the main *ct* mutation relates to hypomorphic expression of *Grhl3*, however, qRT-PCR experiments in this project found *Mthfd1L* mRNA expression was not dependent on *Grhl3* expression. Additionally, microsatellite markers and SNPs in the DNA flanking and encompassing the *Mthfd1L* gene in the $+^{ct}$ strain was found to be identical to the *ct* strain, but not the SWR strain, which was used to breed wild-type *Grhl3* onto the *ct* strain (Sudiwala et al. 2016). The entire coding region of *Mthfd1L* was also sequenced and found to be identical in *ct* and $+^{ct}$ strains (Sudiwala et al. 2016). Possibly, the differential expression between *ct* and $+^{ct}$ strains arises from differences in the genetic sequence of a distal promoter region which strongly affects this gene's expression. The finding that *Mthfd1L* expression in *Splotch* and *Grhl3* strains is at a similar level to *ct* mice presents the possibility that this may be a common variant and could be part of the shared CBA background in *ct* and *Splotch*. It would be interesting to test this hypothesis by comparing *Mthfd1L* expression in wild-type embryos on a pure CBA and C57BL/6 background.

In contrast, the two other genes found to differ between *ct* and $+^{ct}$ embryos, *Mecr* and *Ndufs5*, are located on Chromosome 4, in a region close to where *Grhl3* is located (67.76 cM, 64.52 cM and 57.42 cM for *Grhl3*, *Mecr* and *Ndufs5* respectively). Previous work from the lab suggests that the region encompassing *Mecr* and *Ndufs5* were bred from the SWR strain onto the *ct* background along with *Grhl3* (Nick, Greene, personal communication).

The protein encoded by *Mecr* is potentially of interest in the context of the *ct* phenotype. It is the last enzyme in the mitochondrial fatty acid synthesis (mtFASII) pathway. Eukaryotes synthesise most cellular fatty acids in the cytosol, and the function of the mtFASII pathway is still being elucidated; it does not appear to contribute greatly to the composition of mitochondrial phospholipid membranes (Clay et al. 2016). However, two products of this pathway are 3-hydroxymyristoyl-

ACP and lipoic acid. 3-hydroxymyristoyl-ACP becomes a component of respiratory Complex 1, and loss of mtFAS II results in a respiratory deficient phenotype (Hiltunen et al. 2010). Lipoic acid is a component of keto acid dehydrogenases, which in mammals includes; pyruvate dehydrogenase; α -ketoglutarate dehydrogenase and the H-protein of the GCS. The lipoic acid prosthetic group binds the methylamine moiety after decarboxylation of glycine; therefore, it is integral to the functioning of the GCS (Fujiwara, Okamura-Ikeda, and Motokawa 1991). In addition, a study found that upregulating mtFAS II by overexpressing *Mecr* resulted in increased intermediates of the pentose phosphate pathway for PRPP synthesis (Clay et al. 2016). Reduced *Mecr* expression, therefore, has the potential to negatively affect mitochondrial function and FOCM.

4.4.2 Does reduced *Mthfd1L* abundance contribute to neural tube defects in *curly tail* mice?

The lack of NTD or delayed PNP closure phenotype in *Grhl3*^{+/−}; *Gldc*^{GT2/+} embryos (greater than that seen in *Grhl3*^{+/−}; *Gldc*^{+/+} embryos) is possibly a small suggestion that hypomorphic *Mthfd1L* does not contribute towards NTD risk in the *ct* strain. However, there is evidence to suggest otherwise, which is consistent with the fact that *Mthfd1L* deletion results in exencephaly in 35 % of mutant embryos (Momb et al. 2013). Both *Mthfd1L* and *Grhl3* are expressed in the cranial and caudal region of the embryo during neurulation (Sudiwala et al. 2016; Gustavsson et al. 2007). Transgenic expression of *Grhl3* in the *ct* strain via a bacterial artificial chromosome (BAC; *ct/ct*^{TgGrhl3/0}), results in complete abrogation of spinal defects, but these embryos still exhibit reduced *Mthfd1L* expression and exencephaly (approximately 8 %; n = 140; Sudiwala et al. 2016); very similar to the rates recorded in non-transgenic *ct* embryos. On the other hand, *+ct/+ct* mice, which have increased *Grhl3* and *Mthfd1L* expression, compared with *ct/ct* embryos, do not display any NTDs (Burren et al. 2010). Hence, *Mthfd1L* appears unlikely to be a direct target of *Grhl3* and may represent an independent modifier gene. Overall, this suggests that cranial NTDs in the *ct/ct* strain are dependent on genetic factors additional to hypomorphic *Grhl3*.

In the *Mthfd1L* knockout mouse model, spinal NTDs were reported in 3 % of embryos (Momb et al. 2013). While *+ct/+ct* mice do not exhibit spina bifida, there is a possibility that hypomorphic *Mthfd1L*, together with hypomorphic *Grhl3*, could contribute towards spina bifida in *ct* mouse. To fully understand if and how *Mthfd1L* is a modifier locus on the *ct* background in respect to both cranial and spinal NTDs, wild-type *Mthfd1L* would need to be bred onto the *ct* strain. Since the region of DNA which leads to reduced *Mthfd1L* expression has not been identified, it has not been possible to conduct this experiment.

In humans, a common variant of MTHFD1L in the Irish population was found to strongly associate with NTD risk. Using a cohort of 277 complete NTD triad families and 340 controls, the authors identified two separate 5' and 3' regions of the MTHFD1L gene which appear to independently associate with NTD cases (Parle-McDermott et al. 2009). In the 5' region, an intronic splicing variant which was predicted to produce more functional MTHFD1L protein was found to associate

with NTD cases (Parle-McDermott et al. 2009), while in the 3' region, a SNP located in the 3'-UTR was associated with NTD cases and was predicted to decrease MTHFD1L expression due to increased microRNA (miR-197) binding (Minguzzi et al. 2014). Although these studies did not prove the variants were disease causing, the findings are of interest and should be investigated in other populations.

4.4.3 Formate treatment for prevention of neural tube defects

Formate treatment prevents NTDs in *ct* mice and gene-trap models for *Mthfd1L* and *Gldc*, both genes which contribute to mitochondrial formate synthesis (Momb et al. 2013; Pai et al. 2015). Of interest, NTDs in *Splotch* mice, which express *Mthfd1L* at very similar levels as *ct* mice, were not responsive to formate treatment. This finding in *Splotch* is discussed elsewhere (Section 7.2).

Folate profiles, SAM/SAH data, and the incorporation of exogenous ^3H -adenine and ^3H -thymidine in neurulation stage embryos, suggest that formate supplementation prevents NTDs in *ct* embryos by directing one-carbon units towards *de novo* nucleotide synthesis. It is interesting to note that formate treatment does not appear to affect the absolute levels of folates, but rather results in the redistribution of individual folate cofactors. Additionally, formate treatment may result in less one-carbon units being transferred to the methionine cycle, although this effect appears to be modest, with a 28.5 % decrease in SAM levels. On the other hand, SAH levels were found to increase 100 %, which may suggest increased maternally derived methionine (or SAM) in the embryo. Additionally, investigations from our lab find that inhibition of the methionine cycle cause NTDs (N. Greene, personal communication), so it is unlikely that the methionine cycle is compromised by formate treatment. Nevertheless, it is surprising to find decreased SAM; with the influx of one-carbon units occurring with formate treatment, one could expect that all cytosolic FOCM outputs would be stimulated, not diverted from the methionine cycle to *de novo* nucleotide synthesis. It is possible that this occurs partly because folates become limiting. It would be of interest to test supplementation of formate and folic acid together in *ct* mice, and in *Splotch* mice, whose NTDs are sensitive to folic acid, to assess whether this provides greater prevention than either treatment alone.

The comparison of embryonic and maternal liver tissues suggests that while nucleotide synthesis is prioritised in embryos, SAM production is prioritised in liver. This is not surprising given that the liver is the site for an estimated 80 % of all methylation reactions (Stead et al. 2006). It is assumed that diversion of one-carbon units towards particular outputs is mediated by changes to the expression levels of folate binding enzymes. It would be interesting to quantify the relative abundance of each of the folate binding enzymes in embryos and liver, and under control and formate treated conditions. This would aid in knowledge of embryonic regulation of FOCM.

Formate treatment was also found to increase litter size in a dose dependent manner, an effect which was not seen in supplemented *Gldc* litters. As treatment was started approximately 12 hours after finding of a copulation plug, and there were no differences in rates of resorptions, it can be speculated that formate treatment increases the number of successful implantations or increases the survival of post-implantation embryos. Implantation requires the rapid, new growth of blood vessels, and folate deficiency has been found to decrease the number of implantations and increase the resorption rate in *ct* mice (Burren et al. 2010). It is possible that formate treatment supports increased proliferation and angiogenesis. Another study reported that folate deficiency impaired decidual angiogenesis and observed abnormalities in vascular density, concomitant with elevated homocysteine levels (Li et al. 2015). Elevated levels of homocysteine is reported to adversely affect blood vessel health and integrity (Topal et al. 2004; Goveia, Stapor, and Carmeliet 2014). Although not measured in plasma, it is possible that formate treatment decreases maternal, circulating homocysteine as formate decreased levels of SAH in the liver. Additionally, there may also be a link between FOCM status and pregnancy success in humans; a Danish prospective cohort study found that folic acid supplementation increased fecundity in their sample (Cueto et al. 2015).

Sodium formate treatment, at approximately 6000 mg/ kg/ day, does not appear to be safe for long-term use in mice. Half of wild-type C57BL/6 embryos, at E17.5 and E18.5, displayed varying amounts of oedema and or/ haemorrhage. Of interest though, out of four *ct* litters assessed at E18.5, no embryos were found to be similarly affected. This could be because *ct* mice appear to maintain lower circulating levels of formate. Excess formate (formic acid) production is thought to underlie a large part of the toxicity of methanol in humans (Lamarre et al. 2013), and may also inhibit the mitochondrial respiration chain (Nicholls 1976). Formate concentrations of less than 8 mM do not typically result in any clinical symptoms in non-pregnant humans (McMartin, Jacobsen, and Hovda 2016). Mice cultured in 5 mM formate in this study did not show any signs of toxicity, but toxicity has been reported at concentrations exceeding 20 mM (Andrews et al. 1995; Hansen, Contreras, and Harris 2005). Formate treated (30 mg/ mL) *ct* and *Gldc* mice reached a maximum plasma formate concentration of 0.60 ± 0.14 mM after four weeks, and 0.43 ± 0.25 mM after twelve days, respectively. However, rodents have a greater capacity to oxidise and remove formate and so may be able to tolerate higher formate concentrations (Lamarre et al. 2013). The ingestion of 3900 mg (a dose of 78 mg/ kg/ day for a 50 kg person) of calcium formate in female adults resulted in a peak plasma concentration of 0.5 ± 0.04 mM from a baseline of 0.024 ± 0.008 mM, at 60 minutes' post-dose. Formate concentrations returned to baseline after 225 minutes and the authors considered that this dose was safe and did not lead to formate accumulation, even if taken up to 3 times a day (Hanzlik, Fowler, and Eells 2005). However, the safety for pregnant women and their baby is unknown at this point and needs further research. Another consideration is that perhaps the sodium component could also have some toxic effects. Sodium ions (Na^+) help regulate the electrolyte and osmotic balance between the fluid in blood and lymph vessels and extracellular fluid. Increased Na^+

carried in the blood could conceivably cause swelling and leaking of blood and lymph vessels resulting in the oedema and haemorrhage observed in embryos.

4.4.4 Does reduced *Mthfd1L* abundance affect folate one-carbon metabolism in *curly tail* mice?

This study has found that *ct* mice have reduced circulating formate, both during pregnancy and outside of pregnancy, which does not appear to be caused by excess excretion. While this tends to suggest that intracellular formate would be similarly reduced, this is not known for sure. Ideally, the formate levels in maternal liver and E10.5 embryos should have been assessed, however, the assay which measured formate in plasma is not suitable for tissue.

As a comparison, *ct* mice also have reduced circulating formate when compared to *Gldc*^{GT1/GT1} mutant mice (27.9 μ M), which do not exhibit reduced circulating formate in comparison to wild-type control mice (*Gldc*^{+/+}) (Pai et al. 2015). Although *Gldc*-deficient mice can generate formate from mitochondrial FOCM through SHMT2 (Section 4.1.3), they demonstrate a decreased abundance of one-carbon carrying folates, reduced CR length and diminished mitotic index (Pai et al. 2015), as well as exencephaly, suggesting that 1C supply from glycine is needed for outputs of cytosolic FOCM. Formate treatment of *Gldc*^{GT1/GT1} embryos results in an increase in the relative abundance of one-carbon carrying folates, concomitant with a relative decrease in non-carbon carrying DHF and THF. *In silico* modelling of hepatic FOCM (Nijhout et al. 2006) also predicts that loss of the GCS would result in approximately 50 % less formate leaving the mitochondria (Narisawa et al. 2012). On the other hand, *ct* mice display reduced plasma formate in comparison to *Gldc*^{+/+} mice, but in response to formate treatment, the change in folate profile of *ct* embryos is similar to that of *Gldc*^{+/+} embryos (Figure 4. 26). This finding may suggest that hypomorphic expression of *Mthfd1L* in *ct* mice does not cause significant derailments in FOCM. It is possible that *ct* mice have evolved compensatory mechanism to cope with reduced formate production, which could be suggested by the fact that while *Mthfd1L* protein is reduced by nearly 90 %, plasma formate is reduced by about 23 %. As pure speculation, it is possible that *ct* embryos have adapted by sequestering more formate from the maternal circulation, or that cells sequester more formate intracellularly rather than releasing it into the extracellular environment. This kind of scenario could explain why folate deficiency did not convincingly increase circulating formate concentrations as it has been shown to in *Gldc* mice and sheep (Pai et al. 2015; Washburn et al. 2015), and why formate does not accumulate during formate treatment to the same extent in *ct* mice as *Splotch* and *Gldc* mice. Cellular metabolism is known to change significantly as cells differentiate, which may decrease embryonic formate production and require a maternal source of formate to sustain rapid growth and development. In sheep, albeit in the third trimester of gestation, Washburn et al. (2015) reported that formate levels were nearly 6 times higher in foetal plasma compared with maternal, suggesting that either foetuses are producing increased amounts of

formate compared to the mothers, or are able to sequester formate in the foetal circulation, perhaps through the placenta. To date, a mammalian formate transporter has not been identified.

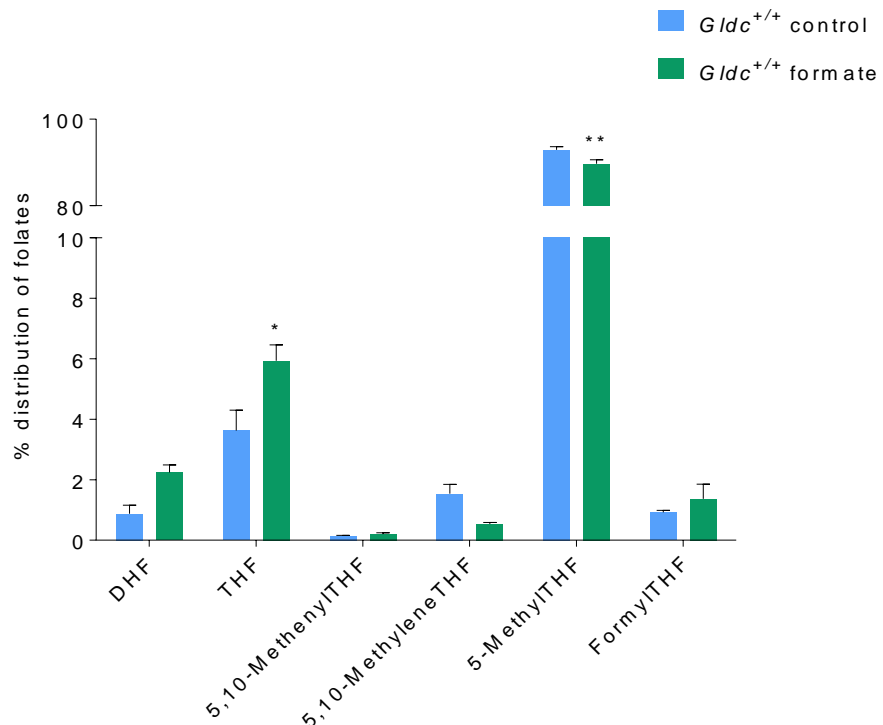


Figure 4. 26. Changes in folate profiles of *Gldc* wild-type embryos.

THF is increased by formate treatment (* $p = 0.004$). while 5-methylTHF is decreased by formate treatment (** $p < 0.0001$). For control, $n = 8$ and formate treated $n = 9$. These are the same major changes exhibited by formate treated *ct* embryos. Data courtesy of Dr Kit-Yi Leung.

The *ct* mouse does not demonstrate a deficit in thymidylate synthesis as measured by the dU suppression test (Fleming & Copp 1998). However, *de novo* purine synthesis has not been investigated. If a suitable congenic wild-type strain were available, ¹⁴C-formate (used for *de novo* synthesis) and ³H-hypoxanthine (used for salvage) could be added during embryo culture and the ratio of ¹⁴C/³H incorporated into DNA assessed as a purine synthesis assay. Cytosolic formate is first incorporated to form 10-formylTHF, the one-carbon donor for *de novo* purine biosynthesis. As a consequence this may give purine biosynthesis priority over thymidylate biosynthesis (Pike et al. 2010) in use of formate from mitochondrial FOCM and potentially greater sensitivity to diminished supply of formate. On the other hand, while remethylation of homocysteine and thymidylate synthesis are “highly sensitive to network disruptions”, while within cytosolic FOCM purine

biosynthesis appears to be more protected (Field, Szebenyi, and Stover 2006). This may be because serine, via SHMT1, can act as a provider of one-carbon units in the cytosol. Increased formation of 5,10-methenylTHF, could then supply thymidylate biosynthesis preferentially over purine biosynthesis. Of interest, when *Mthfd1L* was deleted in MEFs, serine, via SHMT1, became the source of one-carbon units (Pike et al. 2010). Furthermore, in HEK293T cells with *Mthfd2* deletion, Ducker et al. (2016) found that removal of exogenous formate resulted in a 10-fold drop in 10-formylTHF within 5 minutes, and a rapid increase in cytosolic serine oxidation over the first 30 minutes. The large decrease in 10-formylTHF switched the thermodynamically favoured direction of MTHFD1 from 10-formylTHF reduction to 5,10-methyleneTHF oxidation and 10-formylTHF production. Additionally, AICAR expression was demonstrated to be inversely proportional to cytosolic formate levels.

Metabolic flux experiments using isotopically labelled precursors coupled to mass spectrometry analysis of metabolites is significantly increasing knowledge on how FOCM is regulated and responds to genetic insults (Pike et al. 2010; Fan et al. 2014; Ducker et al. 2016; K.-Y. Leung et al. 2017). Application of these approaches to *ct* embryos could be insightful. Culture of embryos in labelled [2,3,3-²H]-serine and detection of labelled outputs such as dTMP/dTTP and methionine would allow the ratio of one-carbon units derived from serine in the mitochondria and cytosol to be estimated (Gregory et al. 2000; Herbig et al. 2002).

5 The effect of caffeine on neural tube closure

5.1 Introduction

The association between maternal caffeine consumption and risk of an NTD affected pregnancy has been investigated in animal models, primarily chick and rats, and in case-control studies in humans. While animal studies lend support to the consideration of caffeine as an agent that may interfere with neural tube closure, human studies have been largely inconclusive. The results of these studies is outlined below, after a brief summary of the pharmacokinetic properties of caffeine.

5.1.1 Pharmacokinetics of caffeine

Caffeine, also known as 1,3,7-trimethylxanthine, is a purine that is chemically related to adenine and guanine (**Figure 5. 1**). Caffeine is found in the seeds and leaves of numerous plant species, where it acts as a natural pesticide. The main sources of caffeine in the human diet are coffee, teas, caffeinated soft drinks, chocolate, and some medicines. Caffeine is a central nervous system stimulant which is believed to act, by virtue of its analogous structure, as a competitive inhibitor of adenosine at G-protein coupled adenosine (A₁ and A_{2A}) receptors in the brain and other peripheral organs such as the heart, gastrointestinal tract and blood vessels (Fredholm et al. 1999).

Studies in humans and animals such as rats, mice and rabbits have highlighted many similarities between, such as: peak plasma levels between 30 and 120 min post consumption; increased absorption rates with increased dosage; and rapid distribution and equilibration between blood and tissues, including in embryos or foetus (Bonati et al. 1984; Fredholm et al. 1999; Brent, Christian, and Diener 2011).

Elimination of caffeine is rapid after biotransformation, although human studies have demonstrated that caffeine retention is increased during pregnancy, from 2 to 6 hours in adult non-smokers to between 10 to 20 hours in pregnant women. While caffeine is broken down by several members of the Cytochrome P450 (CYP) superfamily of metabolising enzymes, CYP1A2 is the primary enzyme responsible for the first and rate limiting reaction by which caffeine is catabolised in humans and mice (Butler et al. 1992; Buters et al. 1996; Kot and Daniel 2008). CYP2C8/9 and CYP3A4 have also been found to have a role in humans (Kot and Daniel 2008), and several polymorphisms have been described (Zanger et al. 2008). Following metabolism by cytochrome P450 enzymes, the action of N-acetyltransferase 2 (NAT2) allows the excretion of caffeine metabolites in urine (Grant, Tang, and Kalow 1984).

While there are many studies investigating the pharmacokinetics of caffeine, average plasma caffeine concentrations in the human population have not been well reported. A study of 600 medical outpatients reported a mean plasma caffeine concentration of 2.12 mg/L (10.9 µM; Smith,

Pearson and Marks, 1982). While in the US, the average dose of caffeine intake was found to be 3 mg/ kg/ day (Barone and Roberts 1996), a dose which was found to result in a median plasma caffeine concentration of 1.11 mg/L in smokers (n = 21) and 2.88 mg/L in non-smokers (n = 48) in a small pilot study (de Leon et al. 2003).

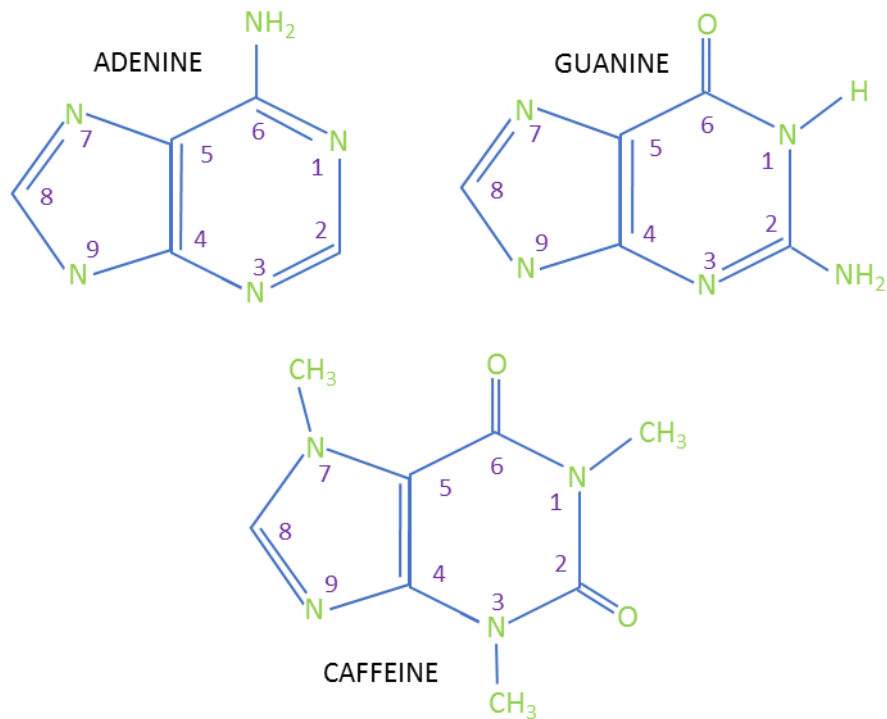


Figure 5. 1. Structure of adenine, guanine and caffeine

Caffeine (1,3,7-trimethylxanthine) is structurally related to the purine bases adenine and guanine.

5.1.2 Animal studies

Nishimura & Nakai (1960) are thought to be the first to report caffeine-induced malformations in animals, in this case mice. Caffeine was administered as a single intraperitoneal injection of 0.25 mg per g body weight to the mother. Defects of the skeletal system such as cleft palate were found but no NTDs were reported. However, later studies have found caffeine to induce NTDs. NTDs have been reported in chick, rat and mice embryos, following culture with caffeine or maternal administration (mammals only). As caffeine is rapidly metabolised in both animals and humans (Bonati et al. 1984), culturing embryos allows for the direct effects of caffeine itself to be examined, while effects from *in vivo* supplementation can be due to caffeine and/ or its metabolites. Although *in vivo* analysis would be expected to more accurately mimic the effects that may occur in human pregnancy, these results can be influenced by other maternal metabolic conditions and disturbances

which could lead to secondary effects. Therefore, both approaches are informative and studies involving both methods are outlined below.

Chick embryos cultured for 19 – 22 hours in 200 to 300 $\mu\text{g}/\text{mL}$ (1.03 – 1.54 mM) of caffeine were found to have a significantly increased incidence of neural tube defects, usually in the cranial region, while concentrations of 500 $\mu\text{g}/\text{mL}$ (2.57 mM) or higher inhibited the morphogenesis of nearly all organ primordia. Furthermore, using both transmission electron microscopy and scanning electron microscopy, the authors found that caffeine treatment resulted in decreased and thinner apical microfilaments in the cranial neuroepithelium (Lee, Nagele, and Pietrolungo 1982). The authors also reported the abnormal appearance of somites next to regions where neural folds had failed to fuse. Gilani et al. (1983) also reported a high incidence of exencephaly in chick embryos cultured with 400 μg of caffeine per egg for 48 hours. Microphthalmia, reduced body size and everted viscera were also seen. More recently, doses of caffeine between 10 and 25 μmol per egg over 9 days was found to result in neural tube defects in a maximum of 40 % of cultured chick embryos, however the region affected was not given. The authors also found that the caffeine content in the brains of treated chicks increased with increasing dose, and appeared not to be metabolised (Li et al. 2012). Ma et al. (2012) also reported that caffeine at doses of 0.5 to 1.5 mg/ mL (2.57 – 7.72 mM) over 36 hours resulted in a failure of cranial neural tube closure in cultured chicks. While closure occurred at spinal levels, the neuroepithelium was visibly thickened, and in both the cranial and spinal regions, the mesenchyme appeared expanded and denser compared to untreated chicks.

Jacombs et al. (1999) and Wilkinson and Pollard (1994) found that maternally administered caffeine at 15 – 30 mg/ kg and 25 mg/ kg respectively, resulted in developmental delay and growth retardation of rat embryos. Jacombs et al. (1999) reported a significant reduction in neural tube closure (axial level not stated) of treated embryos, and at the higher dose, they found caffeine treated embryos had an enlarged forebrain cavity and irregularly aligned neuroepithelium. Caffeine (30 – 60 mg/ kg) had no effect on preimplantation embryos. Wilkinson and Pollard (1994) explanted rat embryos approximately one day before the expected completion of neurulation. They found that 25 mg/ kg of caffeine administered maternally resulted in 91 % of treated embryos demonstrated open neural folds, usually the PNP, compared to 14 % in untreated embryos. Of interest, caffeine treated rats were also allowed to carry to term, at which time no NTDs were found. The authors concluded that caffeine treatment delayed embryonic development but did not specifically affect neural tube closure.

The culture of rat embryos in 1 mmol./ mL of caffeine in rat serum was found to prevent anterior neuropore closure and PNP closure in 33.3 % and 58.3 % of embryos respectively Fadel and Persaud 1992). Lastly, 10 % of NMRI mouse embryos exposed to 105 or 310 μM caffeine in culture failed in cranial neural tube closure (Marret et al. 1997). Other abnormalities were noted, such as

thickening and premature invagination of the neuroepithelium. Overall, in the published literature, there is evidence that high doses of caffeine may impair neural tube closure.

5.1.3 Human studies

Investigation of a possible association between maternal consumption of caffeine and NTDs in humans have given variable findings, with approximately equal numbers reporting an association, as reporting no association.

Rosenberg et al. (1982) concluded that caffeine is not a major human teratogen after finding no correlation between maternal caffeine consumption and 6 different defects in their case-control study involving 2030 infants with malformations, including 101 infants with neural tube defects. Yazdy et al. (2012) looked specifically at tea consumption and risk of spina bifida in 518 mothers with affected pregnancies and 6424 mothers with unaffected pregnancies. They found no association. This conclusion was reflected by Benedum et al. (2013), whose case-control study involved mothers of 776 cases of spina bifida and mothers of 8756 control cases. They also reported no association between caffeine consumption and spina bifida, a conclusion which also held when only women who ingested less than the recommended daily amount of folic acid (400 µg) were analysed.

On the other hand, in a case-control study involving 133 case mothers in Italy, found that high caffeine intake, which was classed as more than 3 cups of a caffeinated beverage per day, increased the risk of having a spina bifida affected pregnancy (De Marco et al. (2011)).

A group which examined data from the National Birth Defects Prevention Study register in the US, which included 768 cases of NTDs, have taken a more nuanced approach. First, the authors distinguished between caffeine from coffee, tea or soda, and also considered maternal race/ ethnicity, and looked for a correlation with cases of spina bifida, anencephaly or encephalocele. This study found an association between caffeinated coffee consumption with increased risk of spina bifida, however, caffeinated tea consumption was associated with a decreased risk of spina bifida (Schmidt et al. 2009). There was a slightly elevated risk of spina bifida associated with caffeinated soda consumption. For spina bifida, associations between total caffeine consumption and increased risk were primarily observed, or were stronger, in racial/ ethnic groups other than non-Hispanic white. An association between caffeine consumption and increased risk of anencephaly was found with non-Hispanic whites, but a decreased risk was associated with other races/ ethnicities, so that no increase in risk was found overall (Schmidt et al. 2009).

In a follow-up study, Schmidt et al. (2010) analysed the same National Birth Defects Prevention Study data with consideration of genetic polymorphisms in caffeine-related genes. They reported associations between caffeine consumption and increased risk of NTDs depending on CYP1A2 and

NAT2 polymorphisms in mother and infant, which conferred either fast or slow metabolism. NTDs were associated with caffeine consumption for mothers who had fast *CYP1A2* status. Maternal slow *NAT2* status and caffeine consumption was also associated with increased risk. When stratified for maternal *CYP1A2* and *NAT2* status, the association between caffeine consumption and risk of NTDs was most elevated for infants whose mothers had fast *CYP1A2* status and slow *NAT2* status. In infants, slow *CYP1A2* status increased risk of NTDs with maternal caffeine consumption. NTDs were also independently associated with infant slow *NAT2* status and with maternal fast *CYP1A2* status.

In finding significant associations between caffeine consumption and individual NTD types dependant on race, and association between NTDs and caffeine consumption dependant on the genetic caffeine metabolism status, Schmidt et al. offers a potential explanation for the conflicted data available to date in humans.

5.1.4 Potential mechanisms

Two mechanisms have been proposed, which could in theory account for a specific effect of caffeine on neural tube closure:

- 1) As a purine analogue, caffeine may inhibit the adenine salvage enzyme APRT (**Section 3.1.2.3**), which may interfere with the supply of dATP for DNA synthesis and therefore, proliferation.
- 2) Caffeine has been demonstrated to block inositol-1,4,5-triphosphate (IP₃) regulated calcium (Ca²⁺) channels in various tissues (Bezprozvanny et al. 1994; Hume et al. 2009). IP₃ is an important signalling metabolite and blockade of IP₃ channels could potentially mimic inositol deficiency, which can induce NTDs in wild-type mice (**Section 3.1.1.1**).

It is interesting to note that if either of these mechanisms did result from caffeine treatment, both would be predicted to preferentially interfere with cranial neural tube closure, which is the main defect found in animal studies.

5.1.5 Aims of this chapter

The aim of this chapter is to better understand whether caffeine is a teratogen which can affect neural tube closure in mice. This chapter begins by examining the effects of caffeine on the neurulation of wild-type, CD1 embryos, followed by its effects on neurulating *ct* embryos, a model genetically predisposed towards NTDs. As a preventive effect of caffeine was observed in the *ct* mouse, possible mechanisms underlying this effect were investigated. Lastly, the effect of caffeine on *Splotch* heterozygous litters was briefly investigated.

5.2 Results

5.2.1 Culture of wild-type embryos with caffeine did not cause NTDs

CD1 embryos, with yolk sacs intact, were explanted from the uterus at E 8.5 and cultured in rat serum with varying concentrations of caffeine (500, 750, 1000, 2000, 2500 or 3000 μ M) or vehicle control (0 μ M). After 24 hours, the cultures were stopped by removing the embryos from rat serum and into PBS, where they could be examined. Embryos were scored for yolk sac circulation, whether they had completed turning and cranial neural tube closure, and the number of pairs of somites were counted. If embryos had completed turning, the crown-rump (CR) length and posterior neuropore (PNP) length were also measured. Any changes in gross morphology were noted. After culture, normal development was considered to be completion of turning by the 15 somite stage and completion of cranial neural tube closure by the 18 somite stage. These parameters were based on prior examination of non-cultured CD1 embryos.

The most apparent difference observed between caffeine-treated embryos and control embryos was an increase in heartbeat frequency, and particularly, in heartbeat strength at all doses tested. At higher doses, this translated to movement of the embryos across the examination dish by their beating hearts. Most likely as a consequence, caffeine treated embryos tended to have higher circulation scores (2.7) compared to control embryos (2.4).

Growth and development measurements were compared between treatment groups (**Table 5. 1**). Mean somite pair numbers of all embryos treated with 2500 μ M caffeine were found to be reduced compared to all control embryos ($p = 0.03$). However, when only embryos which have turned were included for analysis, the mean somite pair number of caffeine-treated embryos from any of the doses used were not different from control embryos. Signs of general toxicity began to be evident at doses of 2000 μ M and higher. These were observed as small, blister-like lesions (2/18 embryos) and enlarged hearts (5/ 18 embryos; **Figure 5. 2A**). Therefore, experiments with incrementally higher doses of caffeine were discontinued after 3000 μ M.

In terms of morphological development, broadly four categories were observed: (1) embryos which were normal for their somite stage i.e. turned by the 15 somite stage and completed cranial neural tube closure by the 18 somite stage; (2) embryos which had failed to turn by the 15 somite stage but had completed cranial neural tube closure by the 18 somite stage; (3) embryos which had failed to turn by the 15 somite stage and failed to complete cranial neural tube closure by the 18 somite stage; and, (4) those which had turned by the 15 somite stage but failed to complete cranial neural tube closure by the 18 somite stage (**Figure 5. 2B**).

The frequency of embryos falling into the four categories at each dose of caffeine was plotted for all cultured embryos irrespective of somite stage (**Figure 5. 3A**), and for cultured embryos which

reached the 18 somite stage or more by the end of culture (**Figure 5. 3B**). As a conclusion on cranial neural tube closure cannot be made for embryos below the 18 somite stage, **Figure 5. 3B** allows for assessment of the effects of caffeine on cranial neural tube closure. A specific effect on cranial neural tube closure would be indicated if an embryo completed turning but failed to close their cranial neural tube i.e. the fourth category. Overall, 1 cranial NTD was observed among 26 caffeine cultured embryos (18+ somite stage; 4.00 %), which was not significantly different from the rate in control embryos (3.33 %; Fisher's exact test). These findings suggest that caffeine does not affect cranial neural tube closure in CD1 embryos.

Comparing the two graphs, it is evident that at caffeine doses greater than 2000 μM , 50 % of caffeine treated embryos show an increased frequency of failing to turn. This was quantified by grouping all embryos cultured with 2000 to 3000 μM caffeine ($n = 18$), and the control embryos ($n = 20$), and comparing the frequency of embryos which failed to turn. This analysis revealed that the increased frequency of failure to turn in high dose caffeine treated embryos was statistically significant ($p = 0.01$; Fisher's exact test).

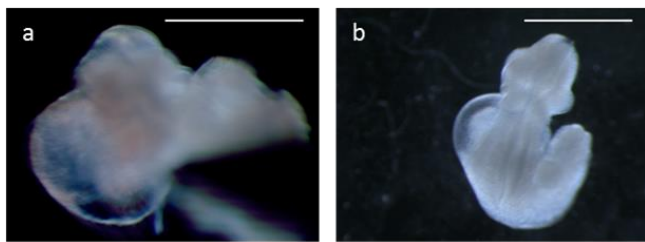
These results suggest that while caffeine does not interfere with neural tube closure over the doses tested, it does affect embryonic development and the ability of CD1 embryos to turn at doses greater than 2000 μM .

Caffeine/ μ M	All embryos		Parameters in embryos which had completed turning			
	Somites Mean \pm SEM (n)	Number (n)	Somites Mean \pm SEM	CR length (mm) Mean \pm SEM	PNP length (mm) Mean \pm SEM	
0	20.58 \pm 0.37 (33)	30	21.07 \pm 0.28	2.21 \pm 0.06	0.24 \pm 0.01	
500	19.60 \pm 0.75 (5)	5	19.60 \pm 0.75	2.20 \pm 0.11	0.28 \pm 0.04	
750	19.75 \pm 1.25 (4)	4	19.75 \pm 1.25	2.26 \pm 0.07	0.31 \pm 0.04	
1000	20.83 \pm 0.48 (6)	6	20.83 \pm 0.48	2.17 \pm 0.06	0.31 \pm 0.05	
2000	19.00 \pm 0.58 (4)	3	19.33 \pm 0.67	2.12 \pm 0.04	0.21 \pm 0.01	
2500	17.67 \pm 1.65 (6)*	3	21.00 \pm 0.58	2.13 \pm 0.04	0.26 \pm 0.02	
3000	19.00 \pm 1.02 (8)	4	21.00 \pm 0.71	2.25 \pm 0.04	0.30 \pm 0.02	

Table 5. 1. Growth parameters of E 9.5 CD1 embryos cultured with varying doses of caffeine.

* p = 0.03; ANOVA followed by Dunnett's test. Mean somite pair number in 2500 μ M caffeine group differed from 0 μ M caffeine group.

(A)



(B)

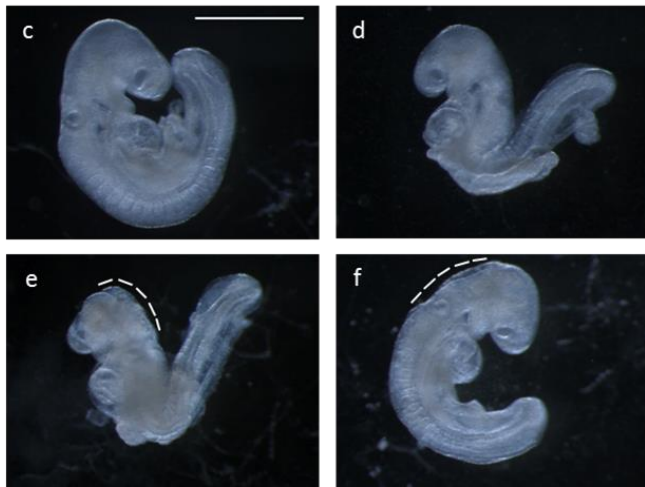
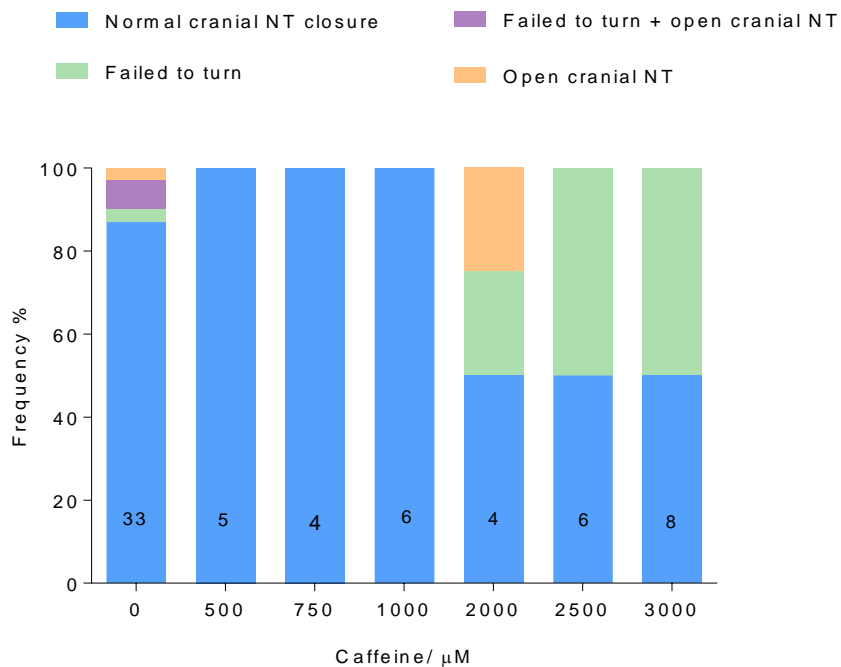


Figure 5. 2. Phenotypes of CD1 embryos cultured with caffeine

(A) At caffeine doses of 2000 μ M and above, there were signs of general embryo toxicity, mainly the appearance of blister-like lesions (a) and enlargement of the developing heart (b). **(B)** The main 4 phenotypes seen during culture: normal development (c); a failure to turn (d); a failure to turn and open cranial neural tube (e) and an open cranial neural tube only (f). Dashed white line highlights area of open cranial neural tube in c & d. Scale bars represent 1000 μ m. Images in (B) have the same magnification.

(A)



(B)

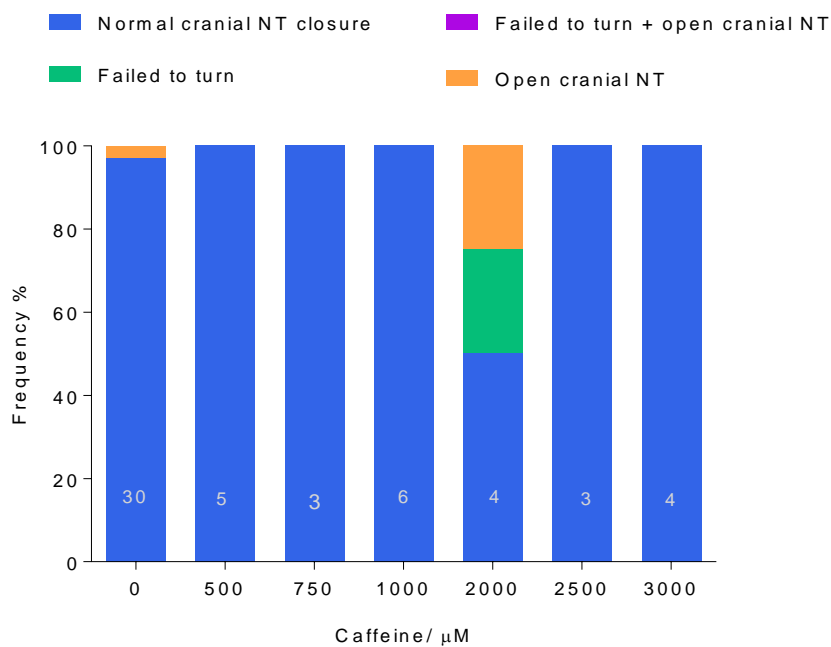


Figure 5. 3. Frequency of phenotypes in CD1 embryos cultured with caffeine.

The frequency of each phenotype at each dose of caffeine. (A) All embryos irrespective of somite stage included. (B) Only embryos of 18 somite stage and above included. Normal cranial NT closure = turned and completed cranial neural tube closure; Failed to turn = failed to turn but had completed cranial neural tube closure; Failed to turn + open cranial NT = failed to turn and failed to complete cranial neural tube closure; and, Open cranial NT = turned but failed to close cranial neural tube. NT = neural tube. Total number of embryos examined indicated on bars.

5.2.2 Caffeine does not exacerbate NTDs in *curly tail* embryos

After finding no specific effect of caffeine on neurulation in wild-type embryos, the effect of caffeine on embryos which have a genetic predisposition towards the development of NTDs was investigated. The *ct* mouse model used in this experiment are genetically identical (effectively inbred), with NTDs that are sensitive to various environmental factors including folate deficiency and inositol deficiency (Cockcroft, Brook, and Copp 1992; Burren et al. 2010). A dose of 750 μ M caffeine was used in all experiments, which is below the concentration at which embryo toxicity was observed in CD1 embryos (Section 1.2.1), but still had an effect, as judged by increased heartbeat strength and frequency.

Initially, embryos were explanted at E8.5 and cultured for 24 hours with 750 μ M caffeine or vehicle (control group). However, *ct* embryos were found to be at an earlier stage of development compared to CD1 embryos explanted and cultured at similar times post copulation. Additionally, the event of turning appeared to occur later in *ct* embryos; the data suggesting that this was finished by around the 17 somite stage. The average somite stage of control and caffeine-treated embryos cultured during this period was 15.00 ± 1.19 and 16.50 ± 1.11 respectively (Table 5.2), and therefore cranial neural tube closure could not be assessed reliably.

Embryos were then cultured for a 24-hour period starting slightly later in development; from approximately E8.75 to E9.75 post copulation such that the culture period would encompass cranial closure. However, based on the average number of somites at the end of culture, 27.29 ± 0.63 and 25.62 ± 0.69 for control and caffeine treated embryos respectively, and assuming a rate of addition of somites of around 1 per 2 hours, it can be concluded that embryos were approximately 13 – 15 somites when the culture was started. At this stage, cranial neural tube closure is between halfway and complete; too late for an effect on cranial neurulation to be assessed. So, although 3/ 21 control and 2/26 caffeine treated embryos displayed cranial NTDs (14 – 8 % in cultured embryos in comparison to ~ 5 % in non-cultured embryos), this could have been influenced by the process of being explanted during cranial closure.

During this period of culture, it was observed in the caffeine treated group that 10/ 37 (27 %) embryos appeared to have completed PNP closure, while 0/44 control embryos completed closure. These embryos had a mean somite stage of 24.13 ± 0.91 , which is an earlier stage than PNP closure would be expected to be completed in this strain (Copp 1985). The other 73% of caffeine treated embryos had on average 26.29 ± 0.93 somites and a mean PNP length of 0.66 ± 0.04 mm. Caffeine treated embryos which had not completed PNP closure were closer in somite stage and PNP length to their control counterparts in both these measurements (27.29 ± 0.63 and 0.65 ± 0.03 mm; Table 5.2).

To allow full evaluation of the effect of caffeine on cranial neural tube closure, embryos were cultured from E8.5 for a period of 48 hours, to allow embryos to develop to a stage at which closure should be complete. Overall, caffeine had no effect on the ability to complete cranial neural tube closure (**Table 5. 2**). However, there was a significant reduction in the PNP length of caffeine treated embryos at the end of culture compared to control embryos ($p = 0.005$). The difference in PNP lengths is, again, due to the presence of embryos with closed PNPs in the caffeine treated group (2/ 10; 20 %; **Table 5. 2**). There were also 3 embryos with closed PNPs which had failed to turn. In this culture period, embryos from all categories (control, caffeine treated embryos with open PNPs and caffeine treated embryos with closed PNPs) all had a very similar number of somites at the end of culture (24.43 ± 0.76 , 24.75 ± 0.85 and 25.00 ± 1.41 respectively). However, the PNP lengths of caffeine treated embryos with open PNPs tended to be smaller (0.48 ± 0.04 mm) compared to the control embryos PNP lengths (0.67 ± 0.06 mm; **Table 5. 2**). The data for control embryos from differing culture periods (**Table 5. 2**) were combined and the caffeine-treated embryo data were separated on the basis of whether embryos had open or closed PNPs (**Table 5. 3**). Embryos which had not completed turning were excluded from this analysis. Comparison of mean CR lengths found caffeine treated embryos with closed PNPs to have a reduced size compared to control embryos ($p = 0.04$), but not caffeine treated embryos with open PNPs. Analysis of mean somite stage found that although caffeine treated embryos with closed PNPs tended to have a reduced number of somite pairs compared to both control and caffeine treated embryos with open PNPs, the difference was not significant.

In summary, caffeine was not found to interfere with cranial neural tube closure in either CD1 or *ct* embryos in culture at the doses stated. However, as mean CR lengths were smaller in caffeine treated *ct* embryos with closed PNPs, caffeine may retard the growth of a proportion of *ct* embryos. This effect appears distinct from the effect of high dose caffeine (2000 – 3000 μ M) on the development and ability of CD1 embryos to turn.

		Growth parameters among embryos that had completed turning					
		Somites Mean \pm SEM (n)	Number	Somites Mean \pm SEM	CR length/ mm Mean \pm SEM	PNP length/ mm Mean \pm SEM	Cranial NT open % (n)
Treatment	Control	15.00 \pm 1.19 (10)	3	20.00 \pm 1.53	2.95 \pm 0.05	0.66 \pm 0.24	0
	Caffeine	16.50 \pm 1.11 (12)	4	20.25 \pm 0.63	2.40 \pm 0.16	0.48 \pm 0.03	0
E8.5 (24 hrs)	Control	23.74 \pm 0.77 (23)	20	24.43 \pm 0.76	2.98 \pm 0.16	0.67 \pm 0.06	8.69 (2)
	Caffeine	24.20 \pm 1.01 (10)	7	25.80 \pm 0.58	2.87 \pm 0.11	0.29 \pm 0.12*	0
E 8.75 (24 hrs)	Control	27.29 \pm 0.63 (21)	21	27.29 \pm 0.63	3.27 \pm 0.10	0.65 \pm 0.03	14.29 (3)
	Caffeine	25.62 \pm 0.69 (26)	26	25.62 \pm 0.69	2.94 \pm 0.15	0.45 \pm 0.06	7.69 (2)

Table 5. 2. Cranial NTD rate and growth parameters of *ct* embryos cultured for different time periods with 750 μ M caffeine.

* p = 0.005; t-test. PNP length of caffeine treated embryos compared to control embryos in culture from E8.5 for 48 hrs.

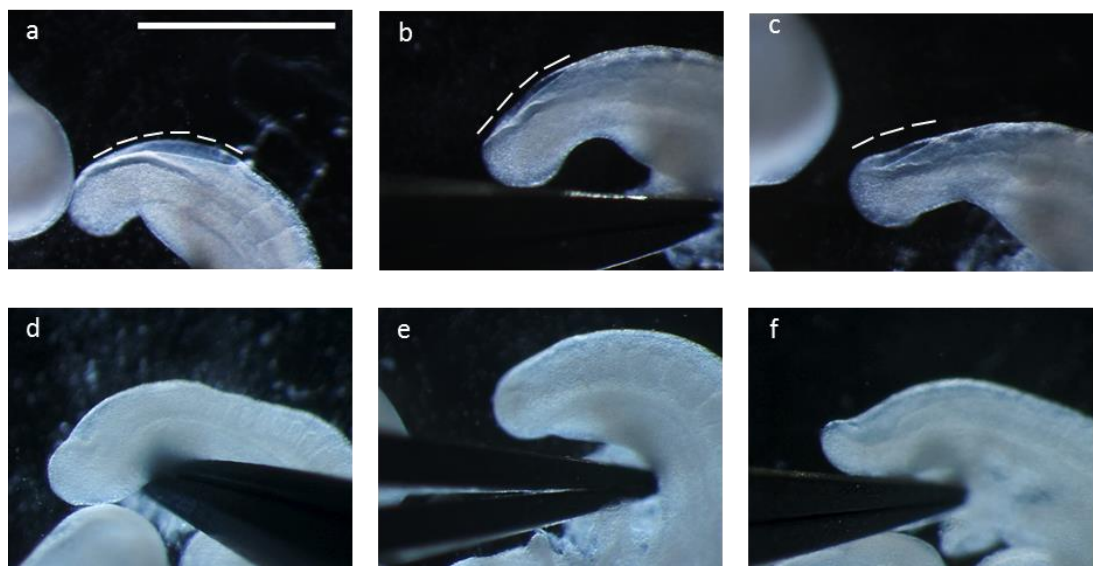


Figure 5.4. Images of closed and open PNPs after culture in the presence of caffeine.

Open PNPs (a, b, c) can be distinguished from closed PNPs (d, e, f). Dashed white line highlights area of open PNP. Scale bar represents 1000 μm ; all images have the same magnification.

Group	Number	Somites	CR length (mm)	PNP length (mm)
		Mean ± SEM	Mean ± SEM	Mean ± SEM
Control	44	26.14 ± 0.54	3.09 ± 0.09	0.64 ± 0.03
Caffeine treated PNP open	27	25.20 ± 0.78	2.94 ± 0.15	0.60 ± 0.03
Caffeine treated PNP closed	10	24.46 ± 0.76	2.52 ± 0.18*	0**
Caffeine treated total	37	24.95 ± 0.57	2.82 ± 0.12	0.40 ± 0.05

Table 5. 3. Growth and development measurements of cultured, caffeine treated embryos with open or closed PNPs.

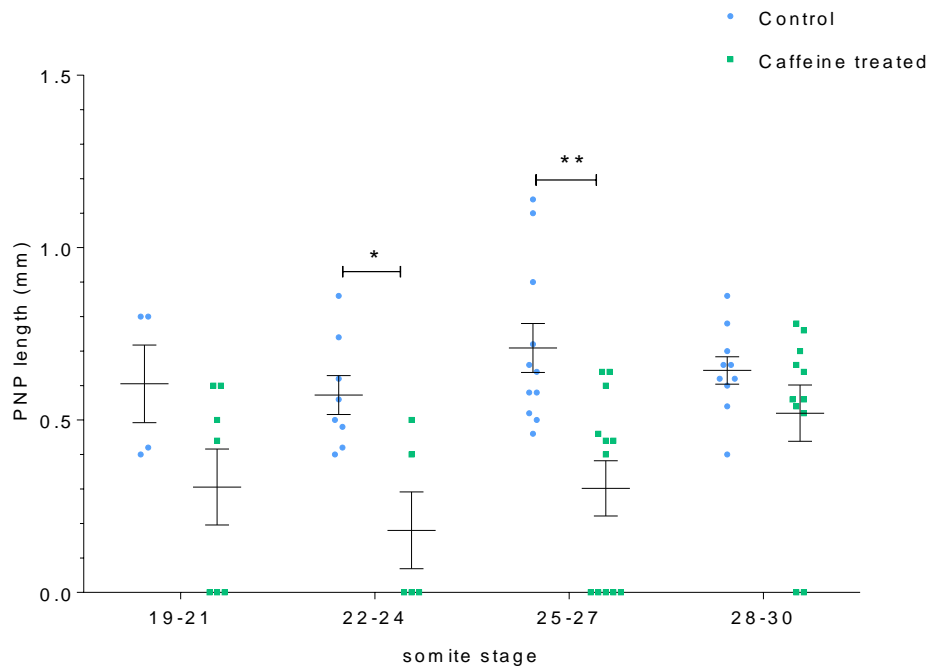
* $p = 0.04$; ANOVA & Holm-Sidak test. CR length of caffeine treated embryos with closed PNPs (caffeine treated PNPs closed) with control embryos.

** $p < 0.0001$; ANOVA & Holm-Sidak test. PNP length of caffeine treated embryos with closed PNPs compared to both control and caffeine treated embryos with PNPs open (caffeine treated PNP open).

To understand more precisely at which stages the PNP lengths of control and caffeine treated embryos diverged, embryos were grouped by somite stage and their PNP lengths plotted (**Figure 5. 5A**). Treatment was found to be a significant source of variation ($p = 0.005$), and post-hoc analysis revealed that PNP lengths at the 22 – 24 and 25 – 27 somite stages were reduced in caffeine treated embryos ($p = 0.02$ and $p = 0.0005$ respectively). Previous studies in the *ct* strain have shown that an increase or decrease in cellular proliferation in the hindgut can result in prevention of spina bifida (Copp et al. 1988). The decreased mean CR length of caffeine-treated embryos with closed PNPs (**Table 5. 3**) suggests that caffeine may inhibit growth and in this way may affect PNP closure. However, although not significant, caffeine treated embryos with closed PNPs had on average less somites compared with control embryos; this could mean that they had a smaller CR length because they were at an earlier developmental stage.

Following these observations, the caffeine treated embryo group was split into caffeine treated embryos with open PNPs (caffeine treated PNP open) and caffeine treated embryos with closed PNPs (caffeine treated PNP closed), and their CR lengths plotted by somite group (**Figure 5. 5B**). From this analysis, it was clear that most of the embryos which were smaller in the 22 – 24 somite group were caffeine treated embryos with closed PNPs. However, this does not hold true at the other somite stages and treatment was not found to be a source of variation in the data. It is possible that with the relatively small number of PNP length values in the caffeine treated closed PNP group (10), there is not sufficient power to detect a significant difference in grouped analysis. As an alternative means of comparing growth and development, the average CR length, a ratio of CR length / somite number was obtained for each embryo in the 3 groups (**Figure 5. 6**). Therefore, higher values indicate embryos which are bigger for their somite stage, and the opposite is true for smaller values. This analysis demonstrates that embryos in the caffeine treated PNP closed group had smaller CR lengths for their somite stage compared to both control ($p < 0.006$) and caffeine treated embryos with open PNPs ($p < 0.03$).

(A)



(B)

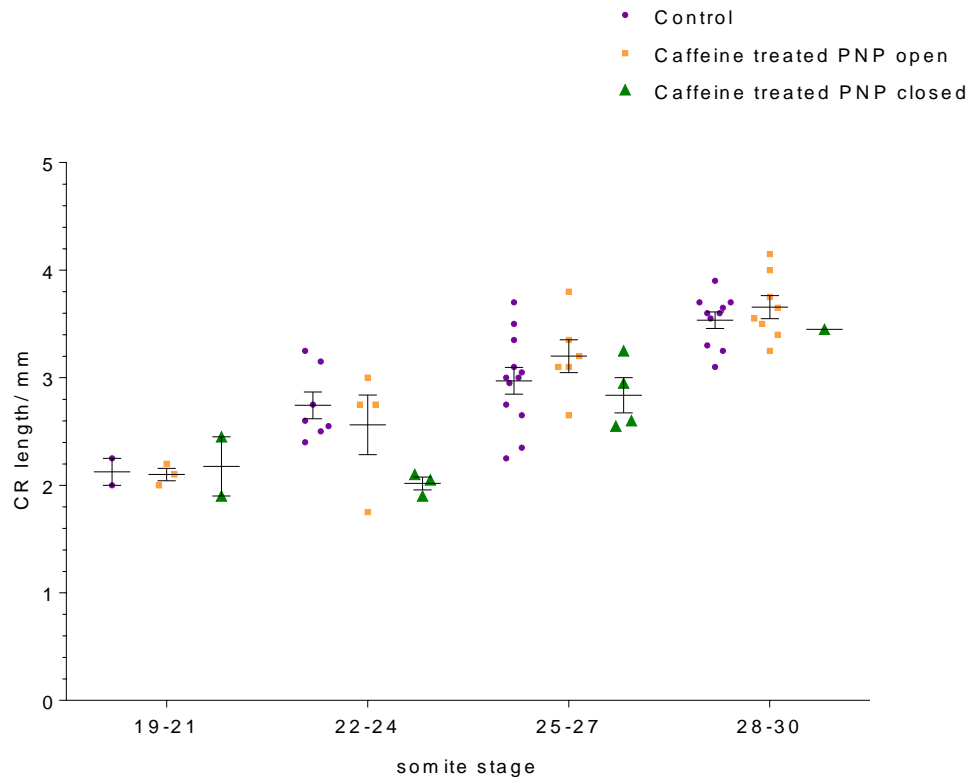


Figure 5.5. Culture with caffeine decreased the PNP size of *ct* embryos without a significant decrease in CR length.

Figure 5. 5. Culture with caffeine decreased the PNP size of *ct* embryos without a significant decrease in CR length.

(A) Grouped analysis of PNP lengths by somite stage. 2way ANOVA found a significant difference by somite stage ($p = 0.03$) and treatment ($p = 0.005$). PNP lengths in the 22 – 24 somite group (0.18 ± 0.11 mm; $n = 5$, vs. 0.57 ± 0.06 mm; $n = 8$; $*p = 0.02$) and in the 25 – 27 somite group (0.31 ± 0.11 mm; $n = 12$, vs. 0.71 ± 0.07 mm, $n = 11$; $**p = 0.0005$) were reduced in caffeine treated embryos compared to control embryos (t-test and Sidak's multiple comparison correction). (B) Grouped analysis of CR lengths by somite stage. Only somite stage was found to account for a significant amount of the variation ($p < 0.0001$; 2way ANOVA)

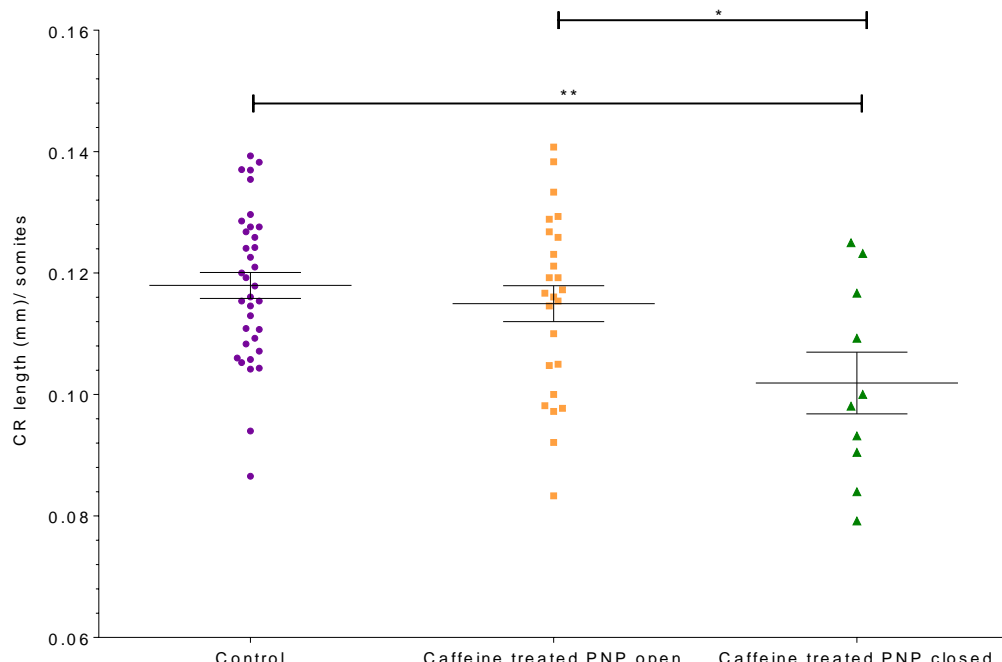


Figure 5. 6. Ratio of CR length to somite number in caffeine-treated embryos.

Caffeine treated embryos with closed PNPs (caffeine treated PNP closed) had smaller ratios (0.102 ± 0.005 ; $n = 10$) than both control (0.118 ± 0.002 ; $*p < 0.006$; $n = 44$) and caffeine treated embryos with open PNPs (caffeine treated PNP open; 0.115 ± 0.003 ; $*p < 0.03$; $n = 25$) Analysed by ANOVA and Holm-Sidak test.

Another way to evaluate this data is to plot the CR length and somite number individually for each embryo creating a scatter plot (Figure 5. 7). This plot demonstrates that there is essentially no difference in the relationship between somite number and CR length between control embryos and

caffeine treated embryos whose PNPs are still open. Linear regression analysis revealed that while the gradients of the lines of best fit are not different for control (and caffeine treated embryos with open PNPs) and caffeine treated embryos with closed PNPs, the y intercepts differ ($p = 0.02$). Hence for any given somite stage, the CR lengths of caffeine treated embryos with closed PNPs are smaller than their control counterparts by a constant value.

There are two scenarios which could explain this kind of relationship. Caffeine could have retarded the growth of these embryos at a single time point during the culture, after which the embryos continued to grow at the same rate in relation to somite development as control embryos. Alternatively, these embryos, in which caffeine was elicited early PNP closure, were already smaller in CR length compared to other embryos at the beginning of culture, and caffeine did not affect their overall growth at all. A scenario where caffeine continues to impede growth at the same rate throughout culture does not fit this model.

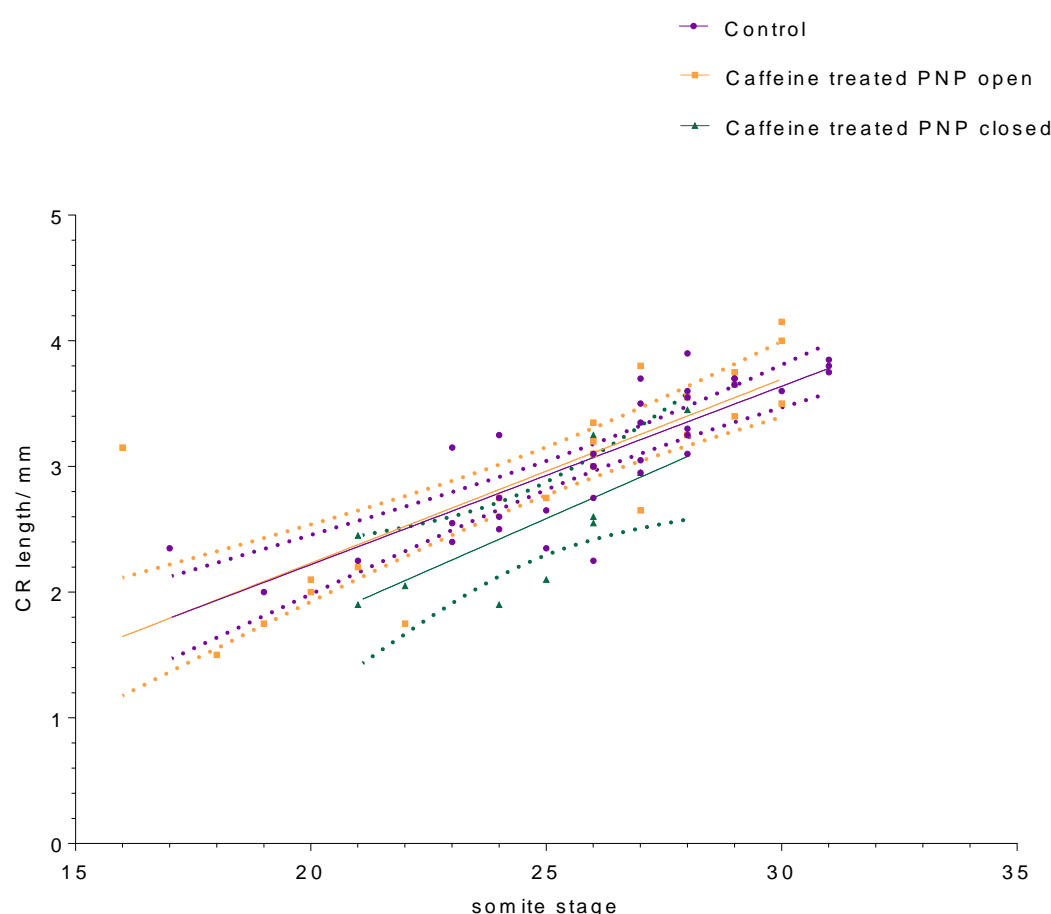


Figure 5. 7. Scatter plot of CR length against number of somites

Figure 5. 7. Scatter plot of CR length against number of somites

Scatter plot of somite stage and PNP length for each embryo grouped as control, caffeine treated with open PNPs (caffeine treated PNP open) or caffeine treated with closed PNPs (caffeine treated PNP closed). Lines of best-fit and 95 % confidence intervals are also plotted. Linear regression analysis finds no difference between the best-fit lines of control embryos ($n = 35$) and caffeine treated embryos with open PNPs ($n = 24$). Control/ caffeine treated embryos with open PNPs and caffeine treated embryos with their PNPs closed ($n = 10$) differ by their y intercept values ($p = 0.02$) but not by their slopes. The r^2 value for control = 0.68; r^2 for caffeine treated PNP open = 0.65 and r^2 for caffeine treated PNP close = 0.55.

5.2.3 *In vivo* supplementation of *ct* embryos with caffeine

Following the results of the culture experiments, the effect of caffeine on embryonic development of *ct* embryos *in vivo* was investigated. It was possible that we would not see the same effect as in culture. Caffeine is rapidly metabolised by the liver in humans and mice (Christian and Brent 2001; Brent, Christian, and Diener 2011; Bonati et al. 1984), while in culture, protected from light, caffeine is expected to be stable over the durations used (Sigma-Aldrich data sheet).

The way in which caffeine is administered in animals is known to significantly affect the peak plasma concentration achieved. A bolus dose, either orally or by injection has been reported to achieve 10 times the plasma concentration as the equivalent dose sipped through drinking water (Brent, Christian, and Diener 2011). Bonati et al. (1984) state the half-life of caffeine in mice and rats is estimated to be approximate 0.7 – 1.2 hours for doses less than 10 mg/ kg, which is in agreement with the half-life of caffeine found to be 40 – 60 min in mice given an oral dose of 18 mg/ kg, (Hartmann M). In contrast, Buters et al. (1996) gave intraperitoneal injections of caffeine at 2 mg/ kg and found the half-life to be 25 min.

In this study, caffeine was administered ad libitum in the drinking water of *ct* dams at 2 mg/ mL, a high dose which has been used by previous studies (Li et al. 2008; Li et al. 2011). On the estimate that a 20 – 25 g mouse would drink 4 – 5 mL of water per day, the dose of ingested caffeine is predicted to be approximately 400 mg/ kg/ day. Mice were supplemented from E7.5 until E10.5.

5.2.3.1 Maternal treatment of *ct* mice with caffeine decreases the frequency of spina bifida

Litters were explanted from the uterus from E11.5 – 12.5 and scored for the presence of NTDs. In conjunction, litters from control dams (normal drinking water only) were also collected and scored for NTDs.

In total, 204 embryos were collected from control dams and 147 from caffeine treated dam. Analysis of the frequency of spina bifida in both groups by Fisher's exact test found a significantly reduced frequency of spina bifida in caffeine treated embryos ($p = 0.03$; **Figure 5. 8**). However, caffeine treatment did not change the proportion of embryos with straight tails (i.e. prevent tail flexion defects). As in embryo culture the frequency of exencephaly, was not affected by *in vivo* caffeine supplementation (**Figure 5. 9**).

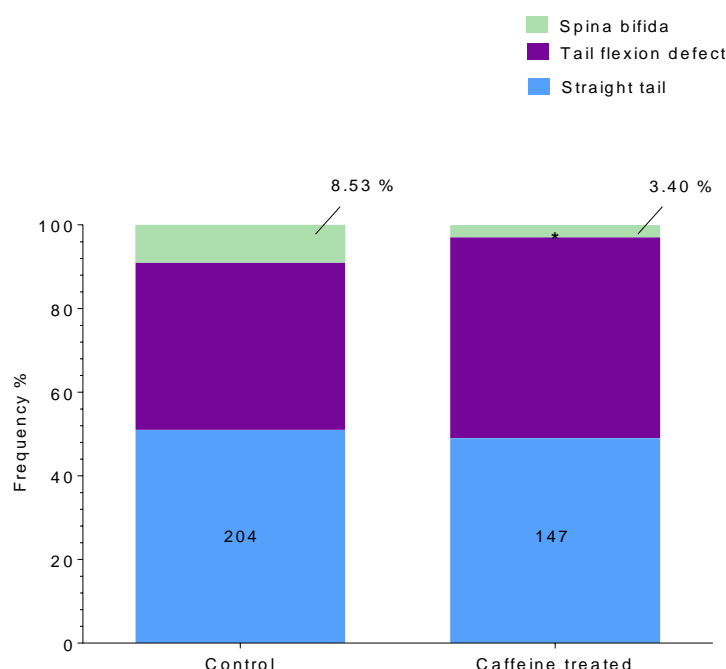


Figure 5. 8. *In vivo* caffeine treatment decreased the frequency of spina bifida.

ct embryos maternally supplemented with caffeine had a lower frequency of spina bifida (3.40 %; $n = 147$) compared to control embryos (8.53 %; $n = 204$) using Fisher's exact test (* $p = 0.03$).

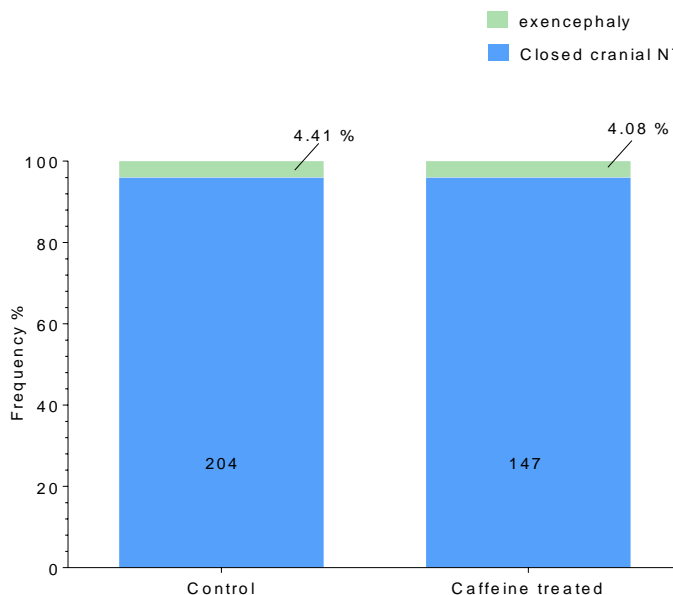


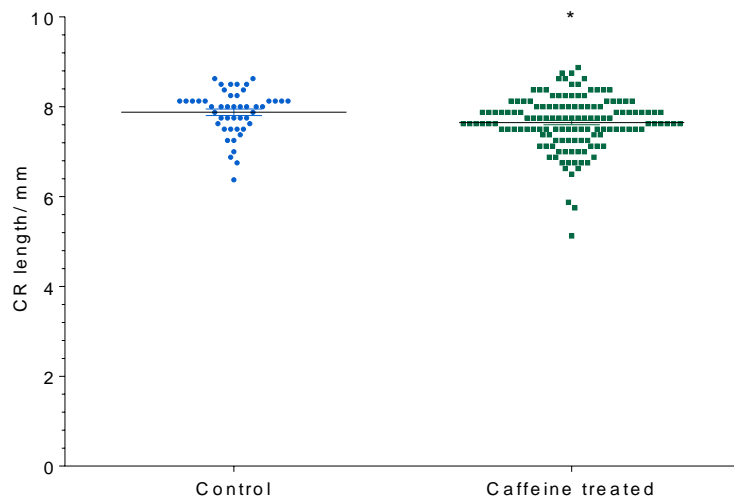
Figure 5. 9. In vivo caffeine treatment had no effect on exencephaly.

The frequency of exencephaly was unchanged between control (4.41 %; $n = 204$) and caffeine treated (4.08 %; $n = 147$. $p = 1.0$; Fisher's exact test) embryos.

Embryo size was analysed on the basis of CR length at E12.5 (**Figure 5. 10A**). The mean CR length of caffeine treated embryos was significantly reduced compared to control embryos ($p = 0.02$). The difference in the means was small (0.23 mm), and the potential biological significance of this value is unknown. For example, the CR length of caffeine treated embryos (7.65 ± 0.05 mm) is very similar to the mean CR length of *ct* embryos supplemented with 20 mg/mL formate (7.68 ± 0.05 mm; **Section 4.3.3.1**). Both the mean CR lengths of caffeine treated and formate treated embryos are not significantly different from the mean CR lengths of control embryos during that period (7.78 ± 0.14 mm). As the evidence suggests that formate stimulates proliferation (**Section 4.3.5**), conclusions from the comparison of CR lengths of control and caffeine treated embryos are not clear.

It was noted from this and other experiments that control and caffeine-treated embryos *ct* embryos with exencephaly were smaller, on the basis of CR length, than their non-exencephalic counterparts, while the presence of spina bifida only had no significant effect (**Appendix; Figure A1A & Figure A1C**). This relationship was also true for formate treated embryos (**Appendix; Figure A1B**). As caffeine appears to have no influence on the rate of exencephaly (**Figure 5. 9**), but the CR lengths of exencephalic embryos could skew the data, CR lengths were assessed again with data from exencephalic embryos in both groups excluded (**Figure 5. 10B**). However, CR lengths of caffeine treated embryos were still found to be smaller than control embryos ($p = 0.007$).

(A)



(B)

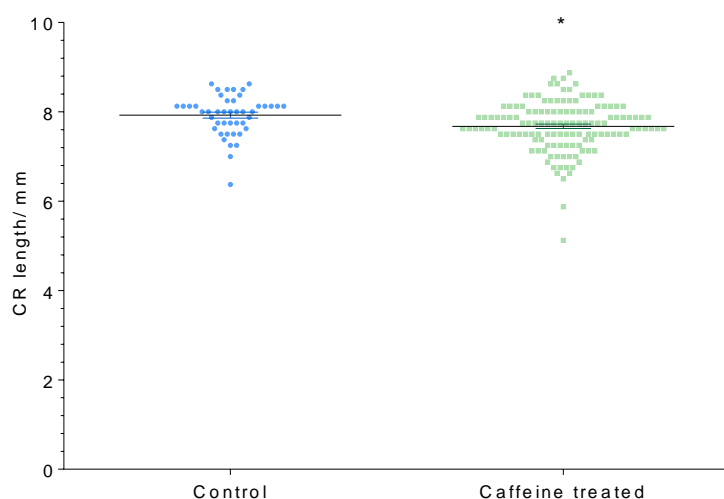


Figure 5. 10. Crown-rump lengths of E12.5 *ct* embryos maternally treated with caffeine are decreased compared to control embryos.

(A) CR lengths of control embryos (7.89 ± 0.07 mm; $n = 47$) were increased compared to caffeine treated embryos (7.65 ± 0.05 mm; $n = 139$; $*p = 0.02$). **(B)** Analysis of CR lengths with exencephalic embryos excluded from both groups. CR lengths of control embryos (7.93 ± 0.07 mm; $n = 45$) were increased compared to caffeine treated embryos (7.68 ± 0.05 mm; $n = 133$; $*p = 0.007$). Both results assessed by Student's t-test.

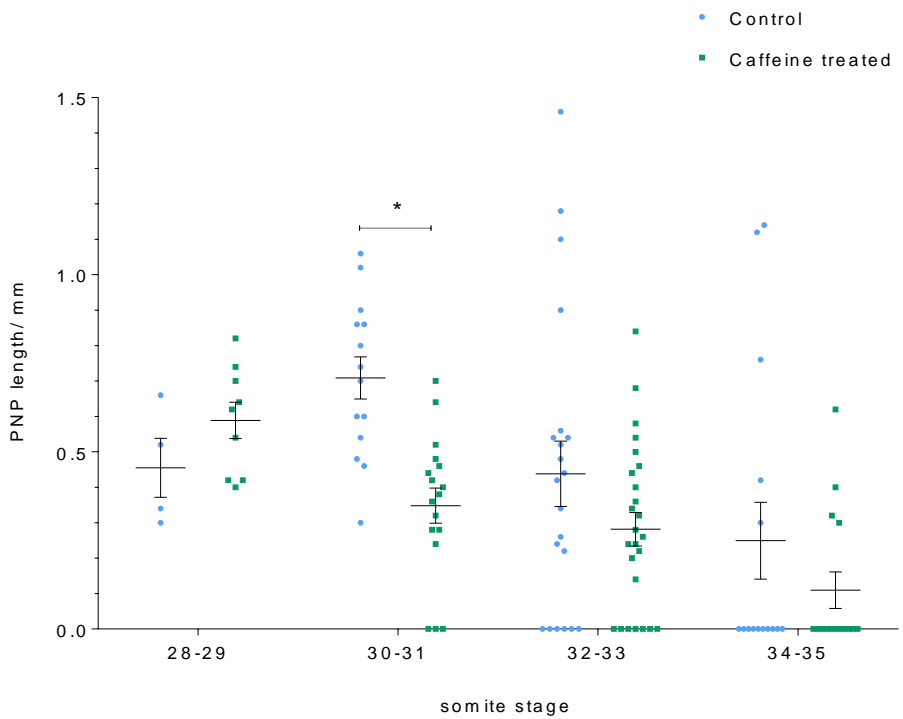
5.2.3.2 Assessment of maternally caffeine treated *ct* embryos at E10.5

To further investigate whether caffeine affects growth and/or PNP closure, *ct* embryos were explanted from the uterus at E10.5. PNP length was analysed with respect to somite stage in control and caffeine treated embryos (**Figure 5. 11A**). Treatment and somite stage were found to be a significant source of variation ($p = 0.04$ and $p < 0.0001$ respectively). This was also found to be the case when CR length was analysed with respect to somite stage; treatment ($p = 0.04$) and somite stage ($p < 0.001$) were significant sources of variation (**Figure 5. 11B**). Additionally, when multiple comparisons were performed, PNP length ($p = 0.004$) and CR length ($p = 0.004$) were significantly different at the 30 – 31 somite stage. While studying the graphs for grouped analysis in **Figure 5. 11**, an inverse pattern was observed: PNP lengths tended to be larger in caffeine treated embryos while CR lengths were smaller compared to control embryos at 28 – 29 somite stage; then from 30 – 31 somite stages, PNPs of caffeine treated embryos are found to be smaller while the CR lengths are bigger than control embryos. This is interesting because the 28 – 29 somite stage is when PNP closure becomes impeded in *ct* embryos.

Lastly, data for all control and caffeine-treated embryos at E10.5 was grouped together for analysis. As no significant differences were found in mean somite pair numbers (**Figure 5.12A**) or CR length (**Figure 5.12B**), the mean PNP length was then compared with caffeine treated embryos demonstrating significantly decreased PNP lengths ($p = 0.01$; **Figure 5.12C**).

Overall, *in vivo* results at E10.5 were consistent with the finding of reduced frequency of spina bifida at E12.5, and with embryo culture experiments which indicated earlier PNP closure in a proportion of embryos. In contrast, the apparent effect of caffeine on growth observed at E12.5 was not observed E10.5.

(A)



(B)

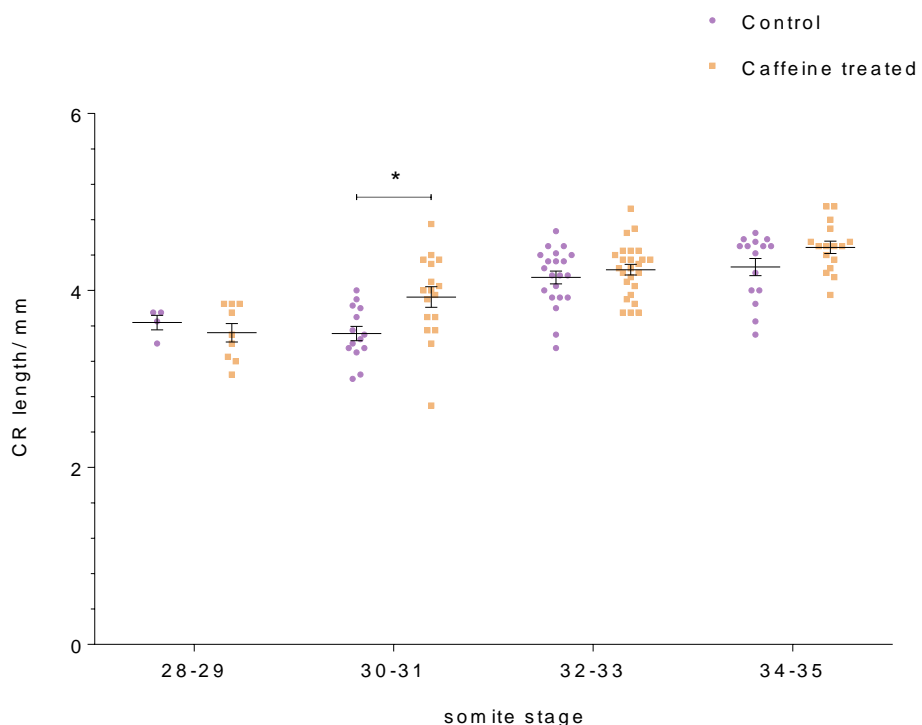


Figure 5. 11. Posterior neuropore and crown-rump lengths in control and caffeine treated embryos at E10.5

Figure 5. 11. Posterior neuropore and crown-rump lengths in control and caffeine treated embryos at E10.5

(A) Analysis of PNP length with respect to somite stage found treatment ($p = 0.04$) and somite stage a significant source of variation ($p < 0.0001$) between control and caffeine-treated embryo. PNP lengths were different at the 30 – 31 somite stage group (0.71 ± 0.06 mm for control and 0.35 ± 0.05 mm for caffeine treated; $n = 14$ and 17 respectively; $*p = 0.004$; Sidak's multiple comparison test). (B) Analysis of CR length with respect to somite stage found treatment ($p = 0.04$) and somite stage a significant source of variation ($p < 0.0001$) between control and caffeine-treated embryo. CR lengths were different at the 30 – 31 somite stage group (3.51 ± 0.08 mm for control and 3.93 ± 0.12 mm for caffeine treated; $n = 14$ and 17 respectively; $*p = 0.004$; Sidak's multiple comparison test).

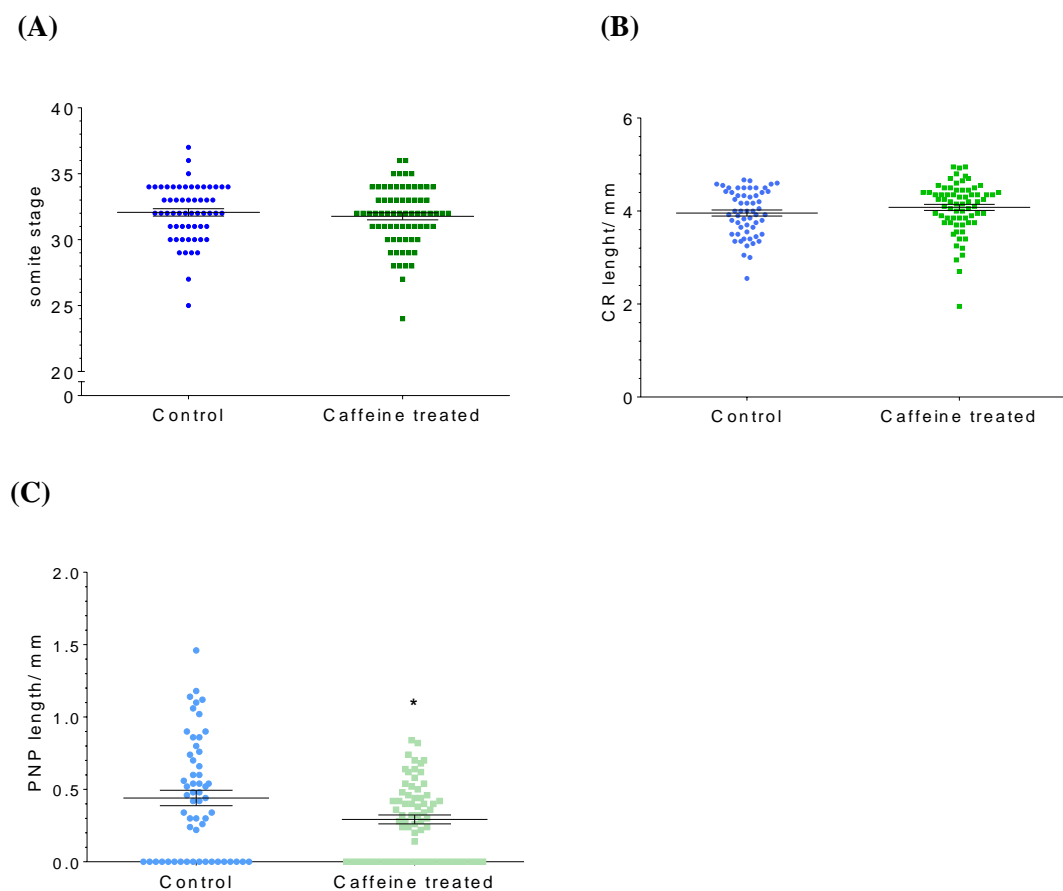


Figure 5. 12. Mean number of somites, crown-rump and posterior neuropore lengths

No difference found between mean somite stage (A) and Mean CR length (B). Mean PNP length (C) is reduced in caffeine treated embryos (0.29 ± 0.03 mm; $n = 68$) compared to control embryos (0.44 ± 0.05 mm; $n = 58$; $p = 0.01$; t-test)

5.2.4 Does caffeine affect nucleotide synthesis?

The aetiology of spina bifida in the *ct* mouse suggests that caffeine treatment could affect proliferation. As a purine analogue, it is possible that caffeine could inhibit the purine salvage pathway, and there is some evidence to suggest this; Wu & Melton (1993) found a small decrease in the incorporation of ^3H -adenine into DNA of mouse embryonic stem cells in the presence of caffeine. On the other hand, an earlier report by Goth & Cleaver (1976) described the metabolism of ^3H -caffeine and incorporation of caffeine's methyl groups into purines via *de novo* synthesis of nucleotides in human and mouse cell lines and human primary fibroblasts.

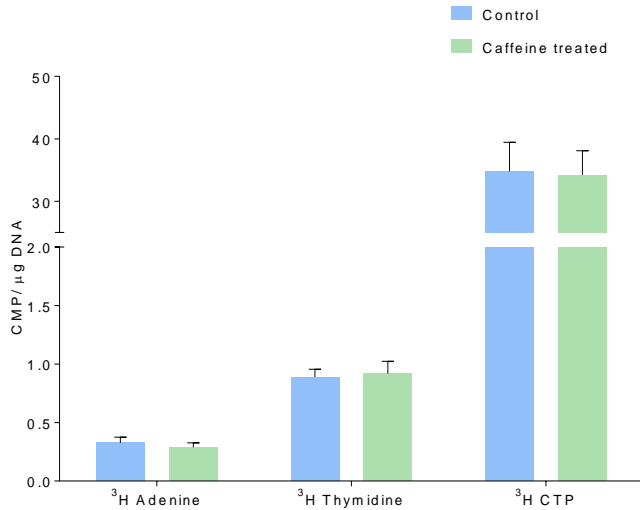
To further understand how caffeine may influence PNP closure, the ability of caffeine to affect incorporation of exogenous, radiolabelled nucleotides into DNA was assessed.

5.2.4.1 Caffeine did not change the incorporation of exogenous nucleotides in embryo culture

Curly tail embryos were explanted at E9 and cultured with and without 750 μM caffeine in the presence of each of the labelled nucleotides/ nucleotide precursors. After isolation of DNA, the counts per minute (cpm) from incorporated tritium nuclei were normalised to total μg DNA.

Overall, caffeine at this dose had no discernible effect on the incorporation of exogenous nucleotides quantified as cpm/ DNA (**Figure 5. 13A**), or the average counts per embryo, without normalisation to DNA (**Figure 5. 13B**), which demonstrates that there were no overt differences in embryonic DNA content between treatment groups.

(A)



(B)

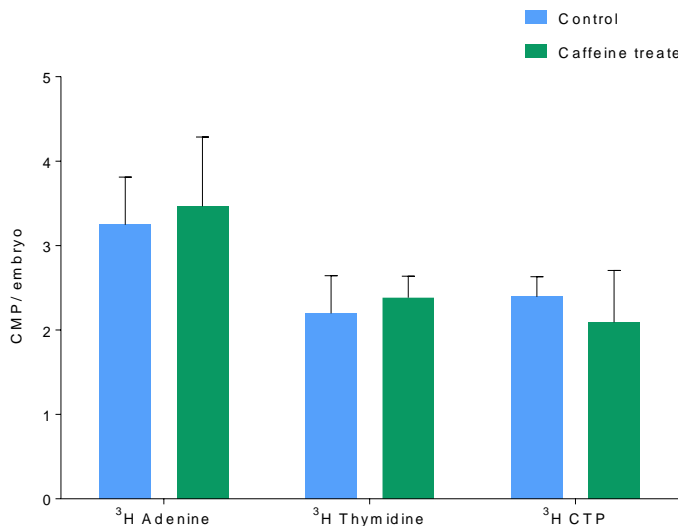


Figure 5. 13. Caffeine did not affect the incorporation of labelled nucleotides.

(A) Incorporation of ^3H -adenine, ^3H -thymidine and ^3H -CTP, normalised to DNA, were unchanged in control and caffeine treated embryos. For ^3H -adenine: $n = 18$ for control and $n = 21$ for caffeine treated, for both ^3H -thymidine and ^3H -CTP; $n = 4$ for control and $n = 5$ for caffeine treated. (B) Incorporation of ^3H -adenine, ^3H -thymidine and ^3H -CTP, without normalisation, were unchanged in control and caffeine treated embryos. Numbers in each group are as above in (A).

5.2.4.2 Caffeine treatment resulted in changes in the folate cycle

It is possible that caffeine could affect proliferation via the *de novo* nucleotide synthesis pathways without altering the ratio of contribution from salvage and *de novo* pathways. Therefore, the folate profiles of control and caffeine-treated embryos at E10.5 were assessed. The sum of all glutamated forms for each of the folates are shown. Of interest, although no significant changes were found in the absolute levels of folates (**Figure 5. 14**), the tendency for 5-methylTHF to decrease, and THF and formylTHF to increase closely resemble changes in the relative abundance of folates between control and caffeine treated embryos (**Figure 5. 15**). Caffeine treatment decreased the abundance of 5-methylTHF by 20 % ($p = 0.003$), and increased the relative abundance of THF by approximately 2 times ($p = 0.02$), compared to control embryos. Once again, the relative decrease in 5-methylTHF and increase in THF could either suggest that there is increased flux of one-carbon units passing into the methionine cycle, or retention within the pool of folates supplying *de novo* nucleotide synthesis. The trend of increased formylTHF in caffeine treated embryos (12.10 ± 1.42 %) compared to control embryos (5.59 ± 0.82 %) supports the second scenario.

5.2.4.3 Measurement of methionine cycle intermediates

To gain further insight into the status of the methionine cycle, SAM and SAH in E10.5 embryos were quantified by HPLC-MS/ MS.

The SAM/ SAH ratio for caffeine treated embryos appeared reduced compared to control samples but this did not reach significance (**Figure 5. 16A**). Similarly, measurements of SAM showed a strong tendency towards reduction by caffeine treatment ($p = 0.055$; **Figure 5. 16B**). Lastly, measurements of SAH showed some variability in caffeine treated samples but were not changed from control samples (**Figure 5. 16C**).

Overall, the results suggest that caffeine treatment tended to reduce the levels of SAM, and this in turn tended to reduce the SAM/ SAH of caffeine treated embryos.

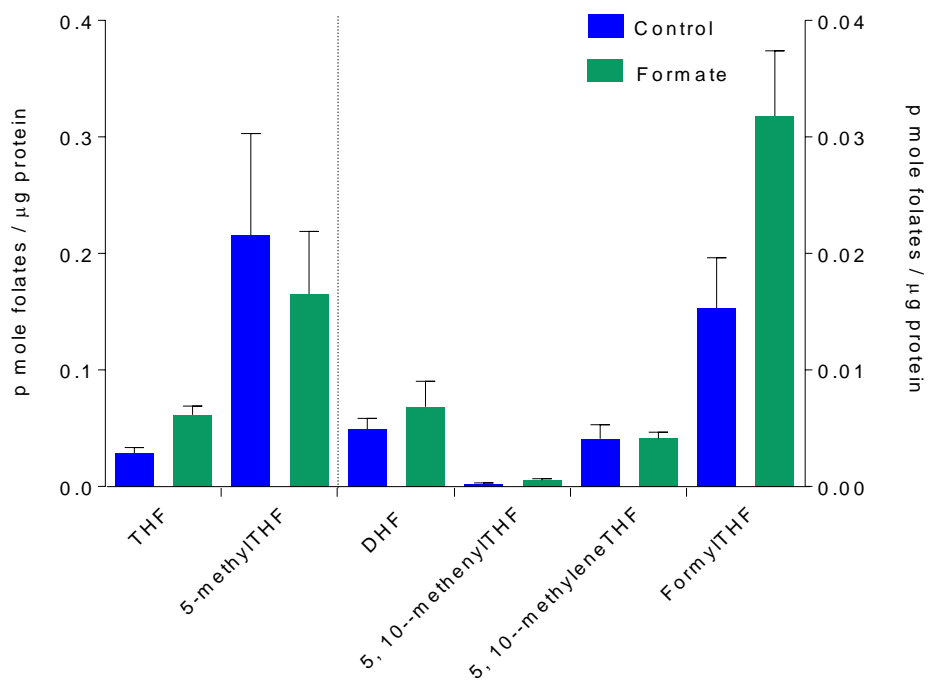


Figure 5. 14. Absolute folate levels in control and caffeine treated E10.5 embryos.

No significant changes in folate cofactors; $n = 4$ for both treatment groups. Bars left of the dotted line are plotted on the left axis, while bars on the right of the dotted line are plotted on the right axis.

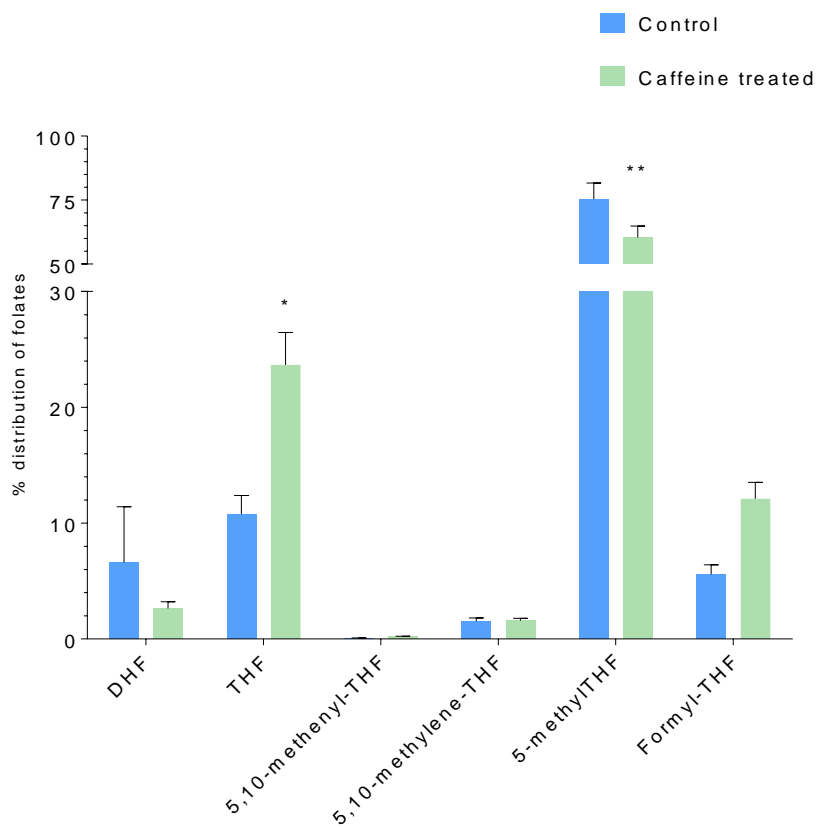


Figure 5. 15. Relative folate levels in control and caffeine treated E10.5 embryos.

Caffeine treatment reduced relative abundance of 5-methyl-THF ($60.42 \pm 1.42\%$) in caffeine treated embryos compared to control embryos (75.43% ; $**p = 0.003$), while it increased the relative abundance of THF embryos ($23.67 \pm 2.79\%$) compared to control embryos ($10.77 \pm 1.61\%$; $*p = 0.02$). Assessed by 2way ANOVA with Sidak's test. $N = 4$ for both treatment groups.

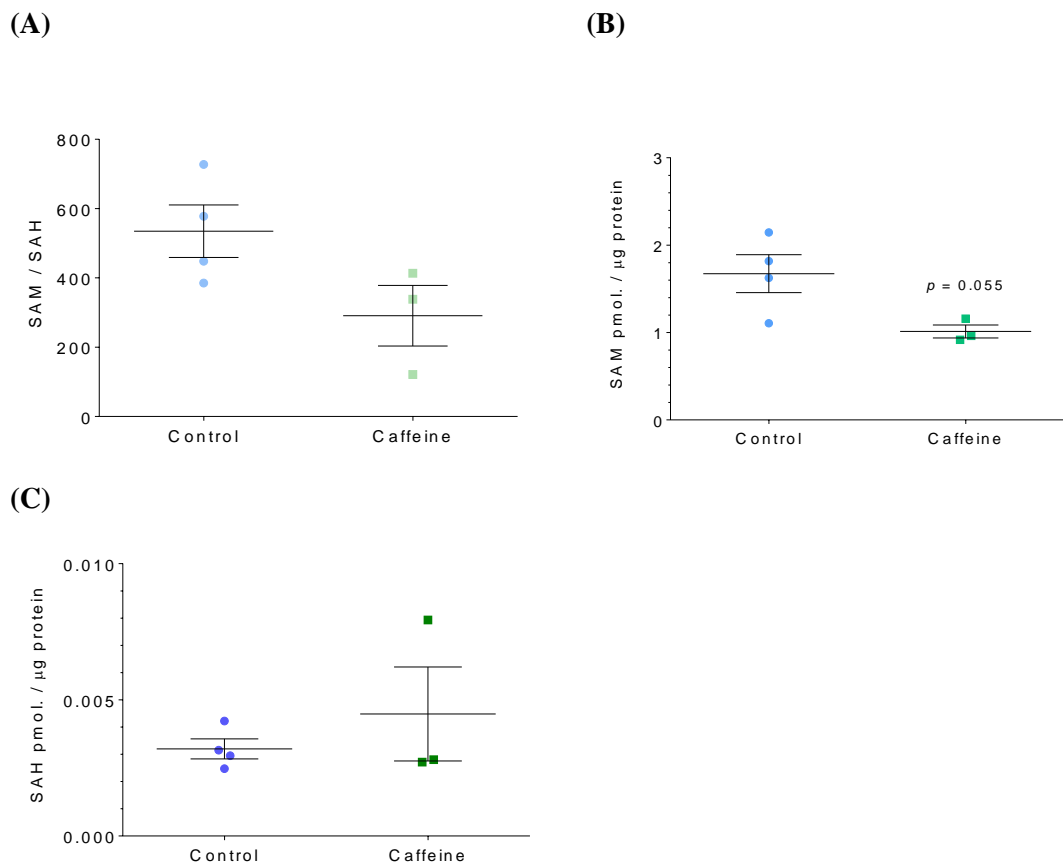


Figure 5.16. SAM and SAH in control and caffeine treated embryos.

Shown is the ratio of SAM/ SAH (A), and the amount of SAM (B) and SAH (B), normalised to protein. No significant differences found in SAM or SAH between control and caffeine treated embryos at E10.5. For Control, n = 4; and for Caffeine, n = 3.

5.2.5 Assessment of the effects of caffeine by immunoblotting

Western blotting was used to assess the relative abundance of PCNA and activation of ERK1/2 (p44/42 MAPK) in protein lysates from whole E10.5 control and caffeine-treated *ct* embryos.

5.2.5.1 Caffeine treatment modestly increased PCNA immunoreactivity

PCNA is a protein which is expressed in the nuclei of proliferating cells only. It binds DNA and acts as a scaffold to recruit other proteins involved in DNA replication, including DNA polymerase delta; it is therefore expressed during S-phase of the cell-cycle (Moldovan, Pfander, and Jentsch 2007). PCNA begins to be expressed in late G₁ phase, peaks during S phase and declines during G₂ – M phase. It is very weakly expressed in G₀ cells (Kurki et al. 1986). PCNA expression is often

assessed by immunohistochemistry, however, studies have demonstrated that differences in the proportion of PCNA positive cells are also reflected by PCNA western blotting (Yadav 2010; Lin 2015; Li 2016). GAPDH immunoreactivity was used as a loading control, with the assumption that cellular GAPDH expression is uniform.

Quantification of immunoblots using densitometry found a small increase in PCNA/GAPDH immunoreactivity in caffeine treated samples ($p = 0.02$; **Figure 5. 17A & B**), suggesting an overall increase in cellular proliferation.

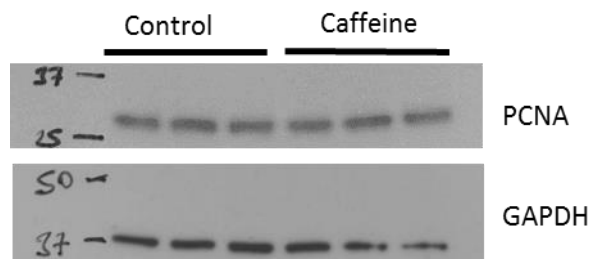
5.2.5.2 Caffeine treatment increases total ERK

To further investigate the potential effects of caffeine treatment on neurulating embryos, the ERK1/2 pathway was assessed by immunoblotting for phosphorylated forms of the proteins (the active forms). Caffeine has been found to modulate ERK1/2 signalling in the brain of adult rodents (Acquas et al. 2010; Zeitlin et al. 2011) and in numerous cell lines (Okano et al. 2008; Liu and Chang 2010; Wang et al. 2014).

Quantification of phospho-ERK1/2 in relation to total ERK (pERK/ERK; **Figure 5. 18A & B**) and a house-keeping protein (pERK/GAPDH; **Figure 5. 18A & C**) did not show significant differences between treatment groups, while analysis of total ERK/GAPDH (**Figure 5. 18A & D**) found that total ERK was significantly increased (~ 70 %) by caffeine treatment ($p = 0.004$). Total ERK and pERK were also assessed in congenic wild-type (*wt*) samples and *ct* (control) samples. Of interest, ERK/GAPDH was also found to be increased (~ 30 %) in *ct* samples compared to *wt* ($p = 0.04$; **Figure 5. 19A & D**), while pERK/ERK (**Figure 5. 19A & B**) and pERK/GAPDH (**Figure 5. 19A & C**) showed trends towards being reduced in *ct* samples.

Overall, control *ct* samples exhibited increased abundance of total ERK in comparison to *wt* samples, and this was increased further by caffeine treatment. However, while control *ct* samples demonstrated a tendency towards reduced pERK in comparison to *wt*, caffeine treatment tended to increase pERK.

(A)



(B)

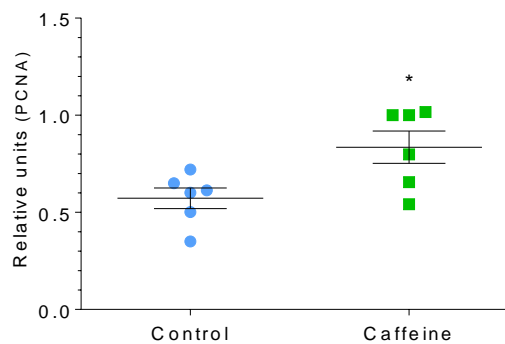


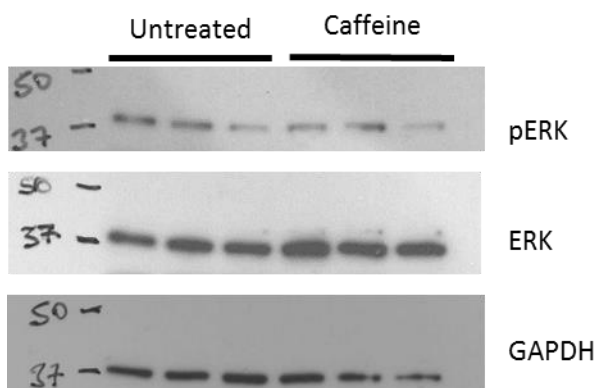
Figure 5. 17. PCNA immunoblotting for control and caffeine treated samples

(A) Representative blots for PCNA and GAPDH. (B) PCNA immunoreactivity was increased for

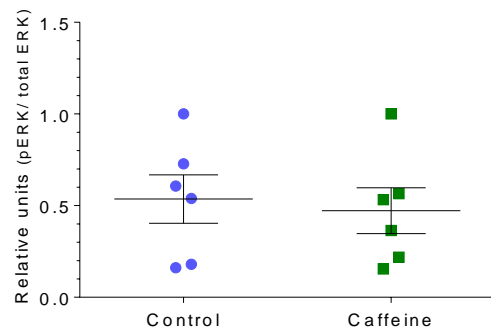
caffeine treated embryo samples (0.84 ± 0.08) compared to control (0.57 ± 0.05 ; $*p = 0.02$; t-test).

$N = 6$ for each group.

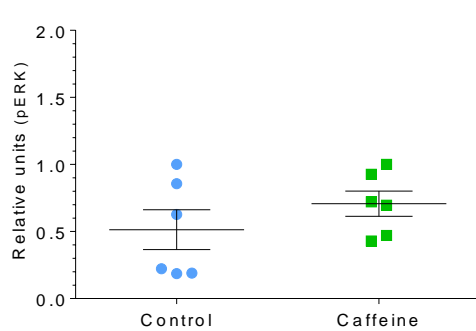
(A)



(B)



(C)



(D)

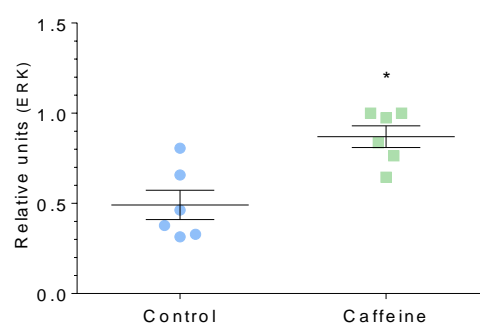
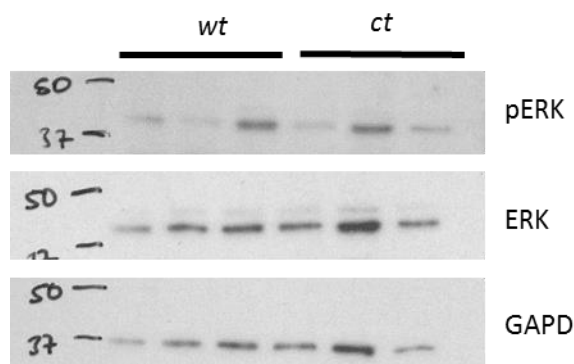


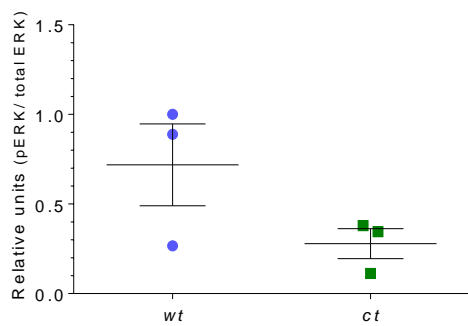
Figure 5. 18. Total ERK is increased by caffeine treatment.

(A) Immunoblots of pERK, total ERK (ERK) and GAPDH. While no significant differences were found in **(B)** pERK/ERK or **(C)** pERK/GAPDH, immunoreactivity against **(D)** total ERK/ GAPDH was increased by caffeine treatment (0.87 ± 0.06) compared to control (0.49 ± 0.08 ; $*p = 0.004$; t-test). $N = 6$ for each group.

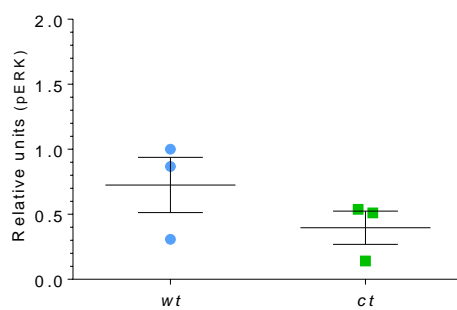
(A)



(B)



(C)



(D)

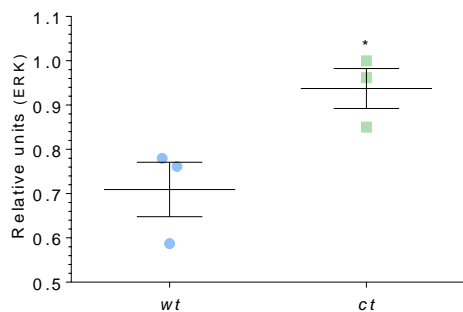


Figure 5. 19. Total ERK is increased in *ct* samples compared to congenic *wt*

(A) Immunoblots of pERK, total ERK (ERK) and GAPDH. While no significant differences were found in (B) pERK/ERK or (C) pERK/GAPDH, immunoreactivity against (D) total ERK/ GAPDH was increased in *ct* samples (0.94 ± 0.05) in comparison to congenic wild-type (*wt*) (0.71 ± 0.06 ; $*p = 0.04$; t-test). $N = 3$ for each group.

5.2.6 Effect of caffeine on *Splotch* litters

Embryos of the *Splotch* strain have also demonstrated variability in phenotype in response to environmental factors (Burren et al. 2008; Fleming & Copp 1998). To understand better whether the decrease in frequency of spina bifida was a specific effect of caffeine treatment on *ct* embryos, the effect of caffeine on litters from heterozygous *Splotch* matings was assessed.

Heterozygous *Splotch* females were treated with 2 mg/ mL caffeine in drinking water from days 7.5 – 10.5 after finding of a copulation plug. Litters were explanted on E10.5. In total, 79 embryos from 12 control litters, and 64 embryos from 9 caffeine treated litters were examined. Due to the small sample size of data for wild-type or heterozygous embryos in both conditions, CR and PNP lengths were compared between wild-type and heterozygotes in both conditions and were found not to vary significantly (**Appendix; Figure A2A & B**). Therefore, data for wild-type and heterozygous embryos were pooled, depending on somite stage and treatment.

A comparison of CR lengths and somite numbers for control and caffeine-treated wild-type and heterozygous embryos demonstrates that caffeine had no effect on embryonic growth over the period treated (**Figure 5. 20**). The same conclusion was found for control and caffeine treated *Splotch* mutant embryos (**Figure 5. 20**). To better understand the effect of caffeine treatment on *Splotch* mutants, an analysis of their mean somite pair numbers was performed, which found that the treatment groups did not significantly differ (**Figure 5. 21A**). Therefore, the mean CR lengths and mean PNP lengths of the two groups were compared and no significant differences were found between control and caffeine treated mutant embryos (**Figure 5. 21B & C**, respectively). Additionally, caffeine treatment did not significantly affect the frequency of exencephaly in either female or male embryos (**Figure 5. 22**). However, there may be a trend towards lower rates of exencephaly in caffeine-treated females. Overall, a larger sample size is required to reach a conclusion for both male and female mutant embryos.

Lastly, while considering the data, there appeared to be a higher proportion of caffeine treated wild-type and heterozygous *Splotch* embryos which completed PNP closure at earlier somite stages compared to their control counterparts. PNP lengths were assessed between the 28 – 34+ somite stages (**Figure 5. 23**). A significant interaction was found ($p = 0.02$), indicating that while PNP lengths vary significantly with somite group ($p = 0.0002$) as expected, the effect is treatment dependant. However, what is interesting is that caffeine treated embryos averaged larger PNP lengths in the 28 – 29 somite group, but by the 30 - 31 somite group, they averaged smaller PNP lengths. This pattern is similar to what was found for control and caffeine treated *ct* mice. While intriguing, the sample sizes, especially for *Splotch* wild-type and heterozygote embryos, are too small to confirm a real, shared effect.

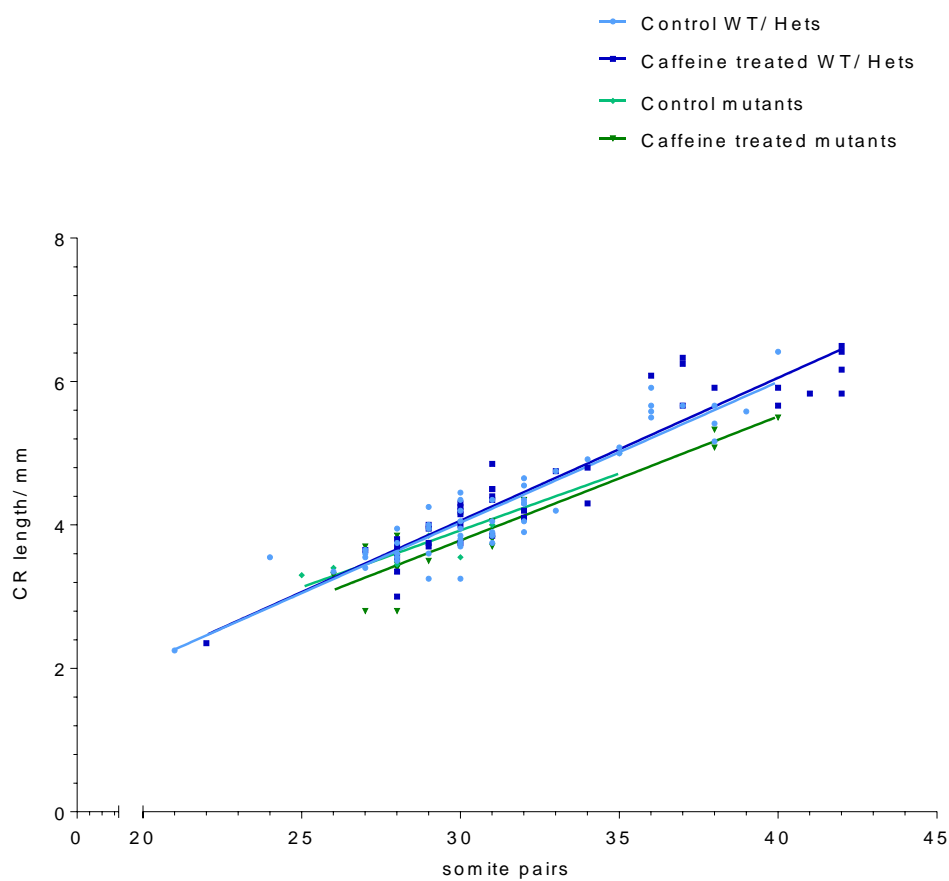


Figure 5. 20. Scatter plot of crown-rump lengths against somite numbers for caffeine-treated embryos generated by intercross of *Sp*^{2H}/+ heterozygotes

Scatter plot of somite stage and CR lengths of all control and caffeine treated embryos. Wild-type and heterozygous embryos (WT/ Hets) were grouped together by treatment and mutants grouped together by treatment. Linear regression analysis found no differences between control and caffeine-treated wild-type and heterozygous embryos or between control and caffeine-treated mutant embryos. For control WT/ Hets, $r^2 = 0.86$; for caffeine treated WT/ Hets, $r^2 = 0.89$; for control mutants, $r^2 = 0.81$; and for caffeine treated mutants, $r^2 = 0.87$.

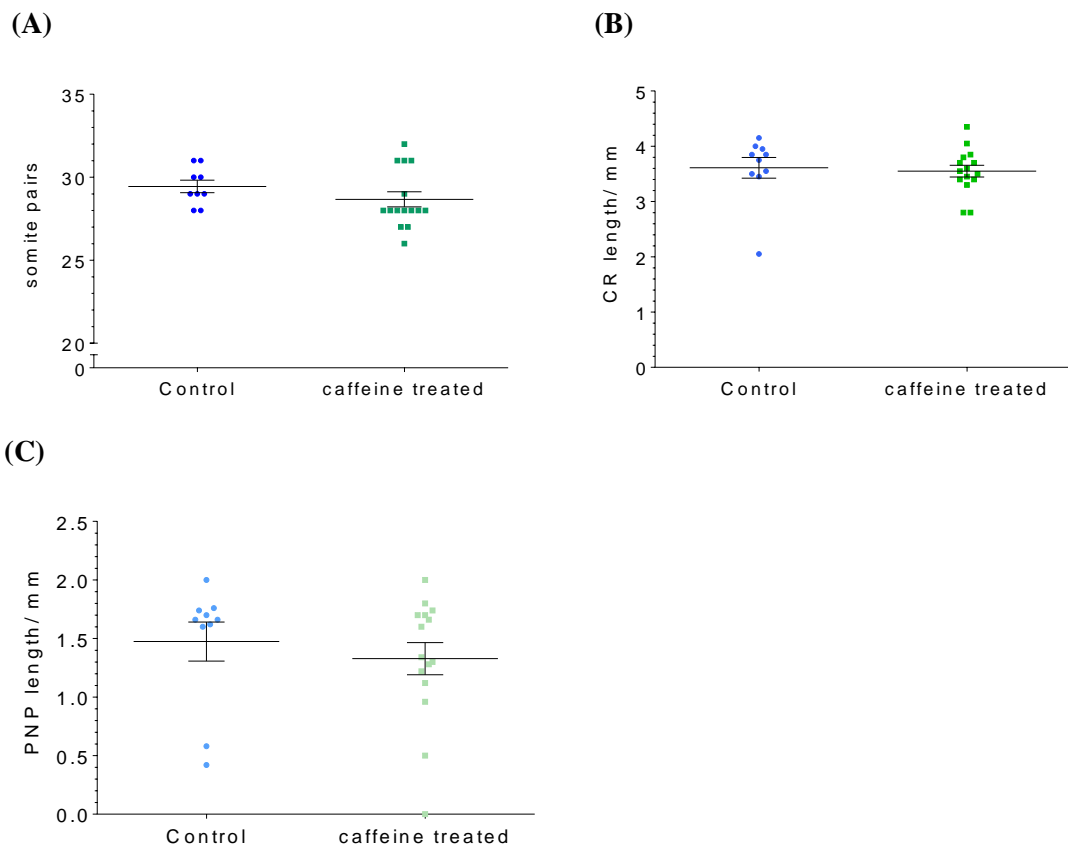


Figure 5. 21. Somite pairs, crown-rump and posterior neuropore lengths of Sp^{2H}/Sp^{2H} embryos
 No differences were found in mean somite stage, CR length or PNP length of control ($n = 10$) and caffeine treated ($n = 15$) *Splotch* embryos.

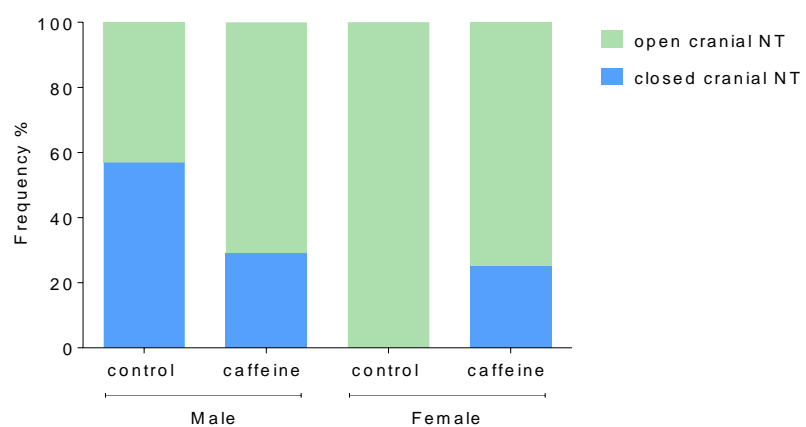


Figure 5. 22. Frequency of exencephaly in Sp^{2H}/Sp^{2H} mutants

Caffeine treatment did not affect the rate of exencephaly, in either male (control, $n = 7$; caffeine treated, $n = 5$) or female (control, $n = 7$; caffeine treated, $n = 11$) *Splotch* embryos.

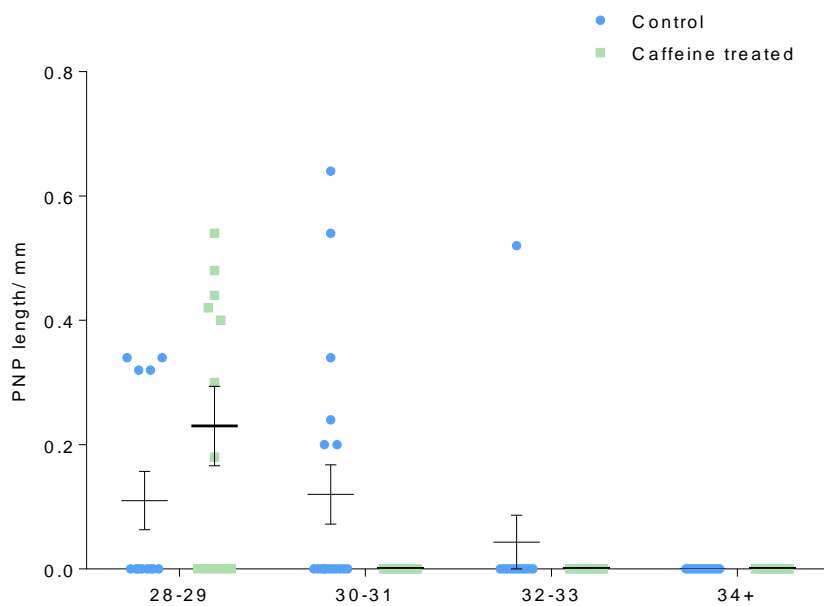


Figure 5. 23. Posterior neuropore lengths of wild-types and heterozygous embryos from *Sp2H/+* intercrosses.

Analysis by 2way ANOVA found somite stage a significant source of variation ($p = 0.0002$), and also found a significant interaction between somite stage and treatment ($p = 0.02$).

5.3 Discussion

5.3.1 Importance of investigating caffeine

Caffeine is accepted to be the most widely and regularly used psychostimulant in the adult population worldwide, the majority of caffeine being consumed from either tea or coffee. However, consumption can vary greatly between countries. Data suggests that the average person in the UK and US consumes approximately 300 mg of caffeine per day (Fredholm et al. 1994; Somogyi 2010), relating to around 3 – 4 cups of caffeinated beverage per day (Fredholm et al. 1994; Christian and Brent 2001; Mandel 2002).

Although the effects of caffeine on reproductive and pregnancy outcomes are not clear (Christian and Brent 2001; Brent, Christian, and Diener 2011), the National Health Service (NHS) in the UK and pregnancy advisory websites in the UK and US recommend that pregnant women drink no more than 200 mg of caffeine per day (NHS Choices; Babycentre; American Pregnancy Association). It has been reported that pregnant women tend to consume slightly less caffeine than the average person, which may be due to taste aversion during pregnancy (Christian and Brent 2001). However, the period for neural tube closure occurs before confirmation of pregnancy or the usual onset of pregnancy associated changes. Additionally, it is estimated that approximately 16 % and 45 % of pregnancies in the UK and US, respectively, are unplanned (Wellcome Trust; Guttmacher Institute). Together, this indicates that a significant proportion of pregnant women are likely to consume more than the recommended daily amount of caffeine during neural tube closure.

As the literature on both epidemiological and experimental investigations into the effects of caffeine on neural tube closure are conflicting and inconclusive, research was undertaken in this project to attempt to clarify any possible effect on neural tube closure in wild-type CD1 embryos and genetically predisposed *ct* embryos.

5.3.2 Caffeine administration

The direct effects of caffeine on neurulation was assessed by embryo culture, while the *in vivo* effects of caffeine, to which the metabolites of caffeine may contribute, were assessed by providing 2 mg/ mL of caffeine in drinking water. This method of delivery, rather than intra-peritoneal injection or gavage, was chosen for several reasons: a) it is the least intrusive, and therefore, assumed to be the least stressful for the mice, and b) it was more desirable for the mice to consume caffeine over the day rather than as a bolus dose. The gradual consumption of caffeine over the day, together with the increased half-life which is expected in pregnant mice (Christian and Brent 2001), is assumed to provide the simplest means of attaining as steady a plasma caffeine concentration as possible without use of a subcutaneous pump or similar. The down-side of this methodology is there

is no certainty over how much caffeine each mouse consumes daily or at what times. The timing of caffeine ingestion may be a factor when collecting embryos for folate, SAM and SAH measurements. Additionally, caffeine itself is bitter, and some mice may have a greater aversion to the taste than others.

The relationship between caffeine dose and peak plasma caffeine concentrations has been quite thoroughly investigated in humans, with similar results reported between studies. Fredholm et al. (1994) reports that from a single cup of caffeinated beverage containing 100 mg (1.67 mg/ kg for a 60 kg person), peak plasma caffeine levels are about 2 – 15 μ M. Stavric (1988) reported that human consumption of a single intake of 1 – 2 mg/ kg caffeine results in a plasma caffeine concentration of 5 - 10 μ M, while a 3 – 5 mg/ kg dose results in a plasma concentration of approximately 26 μ M. The peak plasma concentrations achieved from the single high dose (3 – 5 mg/ kg) are broadly in keeping with another study which found a single dose of 4 mg/ kg caffeine in a capsule resulted in plasma caffeine concentrations of 38 μ M (Benowitz et al. 1995). Of interest, when a similar dose of caffeine, 4.2 mg/ kg, was consumed over a 12-hour period, the peak caffeine plasma concentration was 15 μ M (Denaro et al. 1990), highlighting the difference in plasma concentration gained from a bolus or gradual dose. At the extreme end of human consumption, patients admitted to hospital with acute caffeine poisoning have demonstrated plasma caffeine levels of around 300 μ M (Fredholm et al. 1994), and the mean plasma caffeine concentration of 51 cases of caffeine related deaths was 964 μ M (Jones 2017).

The doses of caffeine used in this study, 750 – 3000 μ M in culture, and approximately 400 mg/ kg/ day *in vivo*, are extremely high doses which cannot be reached by consumption in humans without acute toxicity and death. These high doses were chosen purposely to investigate whether there is any possibility at all of caffeine causing NTDs (without other detrimental toxicity effects).

5.3.3 Developmental and teratogenic NOEL

The toxicity of substances can be compared by stating the maximum dose above which an effect is observed (no-observable-effect level; NOEL). Of interest, the developmental NOEL cited in literature for caffeine is approximately 30 mg/ kg/ day while the teratogenic NOEL is approximately 80 – 100 mg/ kg/ day in rodents (Christian and Brent 2001). The predicted dose (400 mg/ kg/ day), or even half the predicted dose used for *in vivo* assessment in this study far exceed the stated developmental and teratogenic NOEL. However, no developmental or teratological effects were observed in litters derived from heterozygous *Splotch* matings treated with 2 mg/ mL caffeine. In litters from *ct* mice treated with caffeine, there was no evidence to suggest any teratogenic effects, while the evidence for a developmental effect (reduced CR length at E12.5) could be anomalous as it is not supported by other data (see discussion below).

A possible reason for these differences is that the NOELs cited from literature are based on bolus doses, with NOELs when caffeine is administered through food or drinking water said to be much higher (Brent, Christian, and Diener 2011). Other variabilities could include the gestational period looked at and the length of caffeine treatment.

The teratogenic plasma NOEL measured from animal studies is 60 µg/ mL (Brent 2011), or 60 mg/ L, which is equivalent to approximately 310 µM. As caffeine concentrations in rat serum are analogous to plasma caffeine concentrations, culture experiments with CD1 embryos found a detrimental effect on embryo development (namely ability to turn), and a teratogenic effect (enlarged heart phenotype), from doses of 2000 µM and above only. This is much larger than the dose of 60 mg/ L (310 µM) cited.

5.3.4 Effect of caffeine on neural tube closure

In contrast to most of the published studies which have reported on the effect of caffeine on neural tube closure in chick, rats and mice, this study did not find caffeine to interfere with neural tube closure in CD1, *ct* or *Splotch* mice. Taking the volume of a chicken egg to be 50 mL (Paganelli, Olszowka, and Ar 1974), the doses of caffeine used in this study are in excess of those used previously, except for the 0.5 – 1.5 mg/ mL (2.5 – 7.7 M) used with leghorn chicks (Ma et al. 2012), and 1 mmol./ mL (1 M) used in culture with rat embryos (Fadel and Persaud 1992). In most of the studies which observed NTDs at equivalent or lower doses of caffeine, from 40 µM to 1500 µM (Lee, Nagele, and Pietrolungo 1982; Gilani, Giovinazzo, and Persaud 1983; Li et al. 2012) and 15 mg/ kg to 30 mg/ kg (Jacombs et al. 1999), it is possible that species differences may play a part. In chick especially, neural tube closure propagates bi-directionally from only one closure site, similar to Closure 1 in mice. On the other hand, Marret et al. (1997) found that wild-type, NMRI mice cultured in 105 or 310 µM caffeine demonstrated an increased incidence of cranial NTDs. However, the scale of this study, which appears to be a single experiment, is small, with only 7 control embryos for control and 1 out of 9 embryos at 105 and 310 µM caffeine displaying NTDs. Additionally, 0 out of 5 cases of NTDs were found at the highest dose of 620 µM. Considering these factors, more studies of the effect of caffeine on neural tube closure in NMRI mice are required to confirm this effect.

The lack of a specific effect of caffeine on cranial neurulation suggests that even at the high doses used in this study, caffeine does not significantly interfere with inositol metabolism/ signalling, as abrogation of inositol metabolism by either removal of inositol from culture medium or genetic ablation of key pathway genes does cause cranial NTDs in mice (Cockcroft et al. 1992; Wang et al. 2007; Jacoby et al. 2009; Wilson et al. 2009; **Section 3.1.1.2**). Of interest, IP₃ receptors are expressed throughout the neural tube of neurulation stage mouse embryos (Rosemblit et al. 1999), and the concentration of caffeine required to directly affect IP₃ receptors (for instance 50 %

inhibition) is in the range of about 2 mM, while maximal inhibition requires approximately 10 mM caffeine (Fredholm 1995). In reported studies, 10 mM caffeine was used to inhibit IP₃ receptors in smooth muscle cells Hume et al. (2009), while a caffeine concentration of at least 1 mM caffeine is required to inhibit IP₃ receptors of the cerebellum (Bezprozvanny et al. 1994). While these levels are not attainable through regular caffeine consumption in humans and concentrations of over 300 µM are toxic, the doses of 1000 – 3000 µM caffeine used in the current study could potentially have some inhibitory effect on IP₃ receptors. However, because caffeine also blocks adenosine receptors and inhibits phosphodiesterases over the full range of caffeine concentrations used in culture (Fredholm 1995: see below), the overall outcome of each of these processes is a complex matter. For example, while caffeine non-competitively inhibits the frequency of IP₃ receptor opening, increasing IP₃ concentrations can overcome the effects of caffeine (Ehrlich et al. 1994). At the same time, blockade of adenosine A₁ receptors by caffeine can activate some phospholipase C subtypes which can increase the production of IP₃ (Fredholm 1995), and potentially counteract the effects of caffeine on IP₃ receptor opening.

Caffeine was found to facilitate PNP closure in cultured *ct* embryos and *in vivo* treated *ct* embryos analysed at E10.5. At E12.5, this stimulation of PNP closure translated to a significant decrease in the rate of spina bifida in *ct* embryos. An attempt was made to understand the mechanism behind caffeine facilitated PNP closure and the decreased frequency of spina bifida associated with treatment of 400 mg/ kg/ day caffeine. A possible explanation was that caffeine retarded the growth (measured by CR length) of *ct* embryos, a mechanism which has been shown to prevent spina bifida previously (Seller 1983; Copp, Crolla, and Brook 1988). While initial consideration of the culture and E12.5 data appeared to support this mechanism, further analysis does not provide strong support. Firstly, the plot of CR against somite pair number suggests that *ct* embryos with closed PNPs by the end of culture are either: a) smaller than average at the initiation of culture, or that; b) caffeine impeded the growth of these embryos at a single point in time, after which they continued to grow at the same rate as all other embryos. It is believed that the first scenario (a) is the most likely, because embryos from the same litter can often be at different developmental or growth stages, whereas it is hard to understand how caffeine could retard the growth of just a proportion of treated embryos at a single time point.

Similarly, at E12.5, while comparison of control and caffeine treated embryos finds CR lengths to be reduced in the caffeine treated group, the mean CR lengths of caffeine treated embryos were very close to the mean CR lengths of formate treated embryos (0.06 mm difference), collected in parallel experiments. These embryos are unlikely to be growth inhibited as formate appears to stimulate *de novo* nucleotide synthesis (**Section 4.3.5**). Furthermore, the mean CR lengths of caffeine treated embryos are not reduced compared to the mean CR length of control embryos collected as controls for formate treatment. Similarly immunoblots using PCNA and pHH3 antibodies, showed increased PCNA immunoreactivity in caffeine treated samples. In addition,

growth retardation in *ct* mice has been shown to reduce spina bifida but also to promote exencephaly (Seller and Perkins-Cole 1987a), an effect not observed with caffeine treatment. Lastly, CR lengths of CD1 mice or mice from *Splotch* heterozygous litters were not reduced in response to caffeine treatment.

If a growth retarding effect of caffeine on *ct* embryos can be ruled out, an alternative mechanism could be that increased proliferation mediates the prevention of spina bifida as found for inositol or nucleotides (Cogram 2004, Leung 2013). In support of this hypothesis, the folate profiles of E10.5 caffeine-treated and formate-treated *ct* embryos were similar, with evidence to suggest that formate treatment stimulates *de novo* nucleotide synthesis. Caffeine treatment increased the relative abundance of THF, decreased the relative abundance of 5-methylTHF, and tended to increase formyl THF. As 10-FormylTHF provides one-carbon units for purine synthesis, this could suggest that caffeine treatment increases the proportion of one-carbon units available for *de novo* nucleotide synthesis. However, unlike formate treatment, there was no evidence to suggest that caffeine affects the ratio of nucleotides in DNA which are derived from *de novo* pathways and those derived from the salvage pathways. This suggests that it is unlikely that caffeine directly contributes to the pool of nucleotide precursors and thereby stimulates proliferation. To test for a specific pro-proliferative effect, the mitotic index of the hindgut and neural tube should be assessed in 28 – 29 somite-stage control and caffeine treated *ct* embryos.

Biological effects of caffeine are thought to be mediated through the blockade of adenosine receptors (Fredholm et al. 1999; Mandel 2002). Among four known adenosine receptors, A₃ receptors have been shown to be poorly affected by caffeine, and A_{2B} receptors only respond to higher concentrations of adenosine than those found in resting tissue, and so are unlikely to mediate most effects of caffeine. On the other hand, both A₁ and A_{2A} receptors are activated at basal levels of adenosine and are inhibited by physiological concentrations of caffeine (Fredholm 1995). Both the A₁ and A_{2A} receptors are coupled to G-proteins, however, A₁ receptors couple to G_i and G_o proteins which can inhibit adenylyl cyclase, while A_{2A} receptors couple to G_s proteins which can activate adenylyl cyclase. A₁ receptors may also inhibit certain types of voltage gated Ca²⁺ channels (N- and Q-channels) but activate some K⁺-channels, PLC and phospholipase D. Meanwhile, A_{2A} receptors may also activate certain types of voltage gated Ca²⁺ channels, especially L-channels. Thus, blockade of A₁ and A_{2A} receptors can have complex and opposing actions. Additionally, in adult tissue such as the CNS, both receptors can be co-expressed in the same cell, adding to the complexity (Fredholm 1995).

Adenylyl cyclase produces the second messenger cAMP, which activates the cAMP-dependant kinase or protein kinase A (PKA) as well as Epac1/2 (Godinho, Duarte, and Pacini 2015). The opposing functions of the adenosine receptors means that A₁ receptors will tend to inhibit PKA and Epac while A_{2A} receptors will tend to activate them. Additionally, as mentioned above,

phosphodiesterases which break down cyclic nucleotides including cAMP, could possibly be directly inhibited over the range of caffeine concentrations used in culture and *in vivo* treatment. Therefore, the overall likely cellular outcome would depend on the relative expression of these receptors and overall abundance of cAMP. Adenosine A₁ receptor mRNA expression has been examined in rats on E8, E11 and E14. While expression was detected in the heart from E8 (Rivkees 1995), no expression was detected in neural structures until E14 (Rivkees 1995; Weaver 1996). A_{2A} receptor mRNA expression has been examined from E12 in rat embryos, with no expression found in neural structures until E14 (Weaver 1993). No mRNA or protein expression data could be found for the A₁ receptor in embryonic mouse (Massee 2012; MGI), but A_{2A} receptor mRNA is present in the future spinal cord and cranial neural tissue at E11.5. To further understand the potential effects of caffeine on PNP closure, it would be of interest to determine the mRNA expression of A₁ and/or A_{2A} receptors in neurulation stage mouse embryos, as well as quantification of cAMP and PKA activity in control and caffeine treated embryos.

Epac activation has been shown to activate PLC- ϵ with concomitant IP₃ production and Ca²⁺ release (Schmidt et al. 2001). This pathway is known to activate H-Ras and ERK (Keiper et al. 2004), which could result in increased proliferation. Active PKA signalling is involved in the regulation of the actin cytoskeleton, including activation of Rac which is demonstrated to be important for PNP closure (Rolo et al. 2016). Additionally, active PKA is involved in the inhibition of Shh signalling by promoting the repressor forms of the Gli proteins (Tuson, He, and Anderson 2011). The ability of PKA to inhibit the Shh pathway is particularly intriguing; the finding that caffeine treatment resulted in a proportion of wild-type and heterozygous *Splotch* embryos completing PNP closure at earlier somite stages was also found during culture of heterozygous *Splotch* litters with the Shh pathway inhibitor cyclopamine-KAAD (**Section 6.3.2.2**). Lastly, active PKA has been shown to phosphorylate the protein carbamoyl phosphate synthase (CAD), which catalyses the rate limiting reaction of pyrimidine biosynthesis. Phosphorylation by PKA antagonises CAD activation (Kotsis et al. 2007; **Section 3.1.2.2.2**), providing an example of how loss of PKA activity could result in increased proliferation and prevention of spina bifida. Therefore, if adenosine receptors are expressed in neurulation stage embryos, and cAMP and PKA activity measured, these avenues of further study can be followed.

ERK activation after *in vivo* caffeine treatment was assessed but the conclusions are not clear. While caffeine treatment tended to increase pERK, on average by about 40 % compared to control *ct* samples, caffeine treatment also significantly increased total ERK, resulting in no difference in pERK/ERK between treatments. It is unknown whether the tendency towards increased pERK/GAPDH in caffeine treated samples could suggest increased cAMP/ Epac/ PKA. However, increased cAMP/ PKA has been found to have different effects on ERK activation depending on the cell type and context (Dumaz and Marais 2005; Stork and Schmitt 2002). Additionally,

increased cAMP/ PKA activity has been shown to have pro-proliferative effects in some cells and anti-proliferative effects in others (Naviglio et al. 2009).

5.3.5 Known biological effects of caffeine

The cellular effects of caffeine have mostly been studied in terminally differentiated tissue with respect to: cancer/ cell survival; the protective effects against neurodegenerative diseases, brain injury and liver disease, and; psychostimulatory effects.

Of interest, caffeine at concentrations between 0.25 – 5 mM has been demonstrated to arrest cell-cycle progression at G₁ phase, in a process which seems be independent of p53 function. Caffeine has been found to induce G₁ arrest by different mechanisms which may be cell-type and dose specific: in human lung carcinoma cell line, 5 mM caffeine inhibited Cdk2 activity (Qi, Qiao, and Martinez 2002), but at 1 – 2 mM, inhibited the cyclin D1/ Cdk4,6 complex and PI3 kinase/ Akt/ GSK-3 β pathway in the JB6 epidermal cell line (Hashimoto et al. 2004) and in Chinese hamster ovary cells (Foukas et al. 2002). Additionally, many studies report that caffeine inhibits G₂/M phase arrest and DNA repair, therefore promoting apoptosis in response to DNA damage inducing agents (Bode and Dong 2007). In contrast, caffeine was found to stimulate proliferation in human lung adenocarcinoma and small airway epithelial cells via activation of PKA and ERK1/2 (Al-Wadei, Takahashi, and Schuller 2006).

The psychostimulatory and neuroprotective effects of caffeine appear to be mediated to a large part via blockade of A_{2A} receptors and/or decreased oxidative stress (Madeira et al. 2017; Chen et al. 2007; Fisone, Borgkvist, and Usiello 2004). Studies have reported the moderate activation of ERK by caffeine in certain regions of the brain including the cortex and hippocampus (Valjent et al. 2004; Acquas et al. 2010), and also increased activation of PKA in the hippocampus (Arendash et al. 2009). On the other hand, in the striatum caffeine appears to inhibit cAMP/ PKA and does not affect ERK phosphorylation (Sahin et al. 2007). The protective effect of caffeine in the liver is also reported to be through decreased cAMP/ PKA/ pERK via blockade of A_{2A} receptors (Wang et al. 2014; Wang et al. 2015).

Overall these findings suggest that caffeine could have multiple cell-signalling outcomes due to A_{2A} receptor blockade. While there is compelling evidence to suggest that caffeine has multiple protective effects in humans and animal models of disease involving inflammation, it also appears to have largely anti-proliferative and pro-apoptotic effects. At this point, further investigation is required to understand whether these cell signalling pathways contribute to the possible pro-proliferative effects found in *ct* mice.

5.3.6 Differences in metabolism of caffeine in mice and humans

A question that should be considered is the validity of using mice to model the interaction between caffeine and human NTDs. While early studies established that absorption, tissue distribution and primary metabolism of caffeine via CYP1A2 was similar in humans and other animals including mice (Bonati et al. 1984; Arnaud 1987), there are differences in human and mouse pharmacokinetics. The reported half-life of caffeine is shorter in mice and rats (0.7 – 1.2 hour; Bonati et al. 1984) compared to humans (2.5 – 4.5 hours; Arnaud 1987). Murine and human CYP1A2 demonstrate an approximate amino acid sequence homology of about 70 % and this enzyme is responsible for more than 90 % of caffeine clearance in humans and 87 % clearance in mice (Labedzki et al. 2002; Buters et al. 1996). However, 65 – 80 % of caffeine is metabolised to paraxanthine and 16 – 30 % to theobromine and theophylline via CYP1A2 in humans (Gu et al. 1992; Lelo et al. 1986), while in mice and rats, slightly more theophylline than paraxanthine is produced (Ferrero and Neims 1983; Berthou et al. 1988). While paraxanthine has been found to have similar effects to caffeine in humans, theophylline is said to be 3 – 5 times more potent an inhibitor of A₁ and A_{2A} receptors compared to caffeine (Benowitz et al. 1995; Fredholm et al. 1999). Thus, it appears that species differences probably exist and care must be taken when trying to extrapolate mice or rat data to humans.

These considerations should not be a concern for the culture of embryos in caffeine, as caffeine is expected to be stable over these periods, but they do apply to *in vivo* treatments. Increased theophylline production in mice is likely to potentiate the effects of caffeine, possibly resulting in an over-estimation of the effects. As no detrimental effects in relation to neural tube closure were found in mice, differences in metabolism is not a major consideration for this study. However, protective effects due to differences in metabolism in mice cannot be ruled out. Additionally, due to the decreased half-life of caffeine in rodents, it is generally assumed that 10 mg/ kg in rodents represents 3.5 mg/ kg in humans (considered to be an average weight of 70 kg), which would correspond to 2 – 3 cups of coffee (Fredholm et al. 1999). Therefore, our anticipated dose of 400 mg/ kg / day in mice is approximately equivalent to 128 mg/ kg/ day and 12 – 18 cups of coffee in humans. Despite the very high doses used in this study, neither caffeine nor its metabolites appear to be detrimental to neural tube closure in mice.

As the effects of caffeine on other stages of embryonic development have not been studied here, these results cannot suggest that high levels of caffeine consumption are safe during pregnancy. It would be prudent for pregnant mothers to follow the current recommended daily limit on caffeine consumption until the effects of caffeine on all stages of development have been thoroughly investigated.

6 Investigating the cause and prevention of NTDs in the *Pax3* mutant mice

The mechanism(s) underlying partially penetrant exencephaly in *Pax3* mutants are not well understood, nor is the full role of *Pax3* in the neuroepithelium. *Pax3* mutant mice are a model for folic acid sensitive NTDs (Fleming & Copp 1998), and understanding how folic acid prevents NTDs in *Pax3* mutants could further knowledge of how folic acid prevents NTDs in humans. It is likely that an understanding of the mechanism(s) underlying NTDs in *Pax3* mutants will increase understanding of how folic acid can prevent them. The possible mechanism(s) involved in *Pax3* mutant NTDs are discussed first. This chapter focuses on the cranial neuroepithelium, although the spinal region is also discussed.

6.1 Introduction

6.1.1 Excess apoptosis has been proposed as a mechanism

To date, the only proposed mechanism for the cause of NTDs in *Pax3* mutants is apoptosis. Pani et al. (2002) reported that loss of p53 function, by genetic means and using the p53 inhibitor pifithrin- α , resulted in prevention of NTDs (spina bifida and exencephaly were not distinguished apart) in *Sp/Sp* embryos. *Pax3* protein was reported to down regulate p53 protein, and loss of *Pax3* led to increased apoptosis at E10.5, which loss of *p53* reverted. It was hypothesised that the function of *Pax3* was to prevent death of neuroepithelial cells until neural tube closure is complete and that excess apoptosis in *Sp* mutants was the cause of NTDs. An increase in apoptosis due to *Pax3* knockdown was also previously reported in the alveolar rhabdomyosarcoma cell line Rh30 (Bernasconi et al. 1996). However, while the finding that loss of *Pax3* increases *p53* is in corroboration with Kochilas et al. (1999), who found expanded *p53* expression in the myocardium of *Sp* mutants at E10.5 – 11.5, the authors found enhanced expression of *p53* to coincide with premature differentiation of cardiomyocytes, and did not mention apoptosis. In addition, Borycki et al. (1999) used TUNEL assay to look at apoptosis in E9.5 – 11.5 *Sp/Sp* embryos. They reported increased apoptosis in the presomitic mesoderm, somites and limbs of *Sp/Sp* mutants but not in the neural tube.

Unpublished studies from our lab have found no prevention of NTDs when *Sp^{2H}/Sp^{2H}* embryos were made null for *p53*, while treatment of *Sp^{2H}/Sp^{2H}* embryos with pifithrin- α reduced the frequency of exencephaly by approximately 50 %. Additionally, whole mount TUNEL staining was conducted on E8.5 – 9.5 embryos which found no difference in the number of apoptotic cells in the cranial region, and culture with the pan-caspase inhibitor ZVAD-FMK actually increased the frequency of exencephaly in mutants and resulted in cases of exencephaly in *Sp^{2H}* heterozygotes (personal communication, N Greene). Together these findings suggest that while other processes

regulated by p53, such as cell cycle exit, may be implicated in exencephaly of *Pax3* mutants, apoptosis is unlikely to be the main causal mechanism.

6.1.2 Cell cycle exit and premature neurogenesis

Premature cell cycle exit and neuronal differentiation are processes which correspond with the understanding that a key role of Pax transcription factors in the specification and maintenance of progenitor cell populations (Blake and Ziman 2014). Evidence that *Pax3* also function in this capacity in various progenitor cell types (**Section 1.5.2.2**) prompted research in this lab to investigate whether *Sp^{2H}/Sp^{2H}* embryos display increased neurogenesis before or during cranial neural tube closure compared to wild-type littermates. This was judged by class III beta-tubulin (Tuj1) immunostaining on coronal sections through the forebrain to hindbrain. Tuj1 is one of the earliest neuron specific markers to be expressed and can be used to identify immature neurons during this stage of development (Menezes and Luskin 1994). Significantly, in the dorsal neural folds of the forebrain-midbrain boundary, it was found that *Sp^{2H}/Sp^{2H}* embryos showed a two-fold increase in Tuj1 staining at the 14 somite stage, and a three-fold increase at the 15 somite stage. Remarkably, pifithrin- α treatment, which prevented exencephaly, reduced Tuj1 staining in *Sp^{2H}* mutants to approximately wild-type levels (personal communication, N Greene).

6.1.2.1 Altered proliferation in *Sp^{2H}/Sp^{2H}* embryos?

While no differences between the *Sp^{2H}* genotypes is found in developmental stage or size within litters, premature neurogenesis implies a disturbance in proliferation. It is possible that a reduced rate of cell proliferation may accompany increased neurogenesis, with progenitor cells exiting the cell cycle to give rise to immature neurons. However, increased Tuj1 staining in *Sp^{2H}/Sp^{2H}* embryos is not definitive proof of decreased proliferation, as Tuj1 has been shown to be expressed in cells still undergoing mitosis (Memberg and Hall 1995).

The pro-proliferative potential of *Pax3* is suggested by its strong expression in embryonal rhabdomyosarcomas, while normal adult skeletal muscle shows very weak *Pax3* expression (Frascella, Toffolatti, and Rosolen 1998). Additionally, the chromosomal translocation t(2;13)(q35;q14), generates a gene fusion of *Pax3* and *FOXO1*, which is specifically associated with alveolar rhabdomyosarcoma. This fusion protein is a potent transcriptional activator, displaying 100-fold greater activation of *Pax3* target genes (Reeves et al. 1998; Bennicelli, Edwards, and Barr 1996).

Given that proliferation and/ or cell number in the neuroepithelium appears to be an important factor in cranial neural tube closure (**Section 1.3.2**), and the link between folic acid supplementation and

increased proliferation (below), the assessment of proliferation/ the cell cycle in Sp^{2H}/Sp^{2H} embryos is of interest.

6.1.2.2 Folic acid supplementation and Pax3-related NTDs

A proportion (30 – 50 %) of cranial and spinal NTDs in the Sp^{2H}/Sp^{2H} mouse can be prevented by supplementation with folic acid (Fleming & Copp 1998). As outlined in **Section 1.4.2.2.1**, two major outputs of FOCM are nucleotides and methyl groups. Folic acid is converted to non-carbon carrying DHF *in vivo*, after conversion to THF, it can pick up a one-carbon unit as either formate or a methyl group donated from serine, and potentially support *de novo* nucleotide synthesis or the methionine cycle. However, loss of *Mthfr*, which generates 5-methylTHF for the methionine cycle, did not exacerbate NTDs in *Sp/Sp* mice (D. Li et al. 2006), suggesting that modulation of the methionine cycle was unlikely to modify risk of NTDs in *Pax3* mutants. On the other hand, Ichi et al. (2012) generated neurospheres from neural crest derived cells of the lower lumbar region of E10.5 *Sp/Sp* and wild-type littermates. They found that cells from mutant embryos were significantly less likely to proliferate and form neurospheres compared to cells from wild-type embryos; a situation which supplemental folic acid was able to correct.

Overall, the results from our lab and current literature suggest that Pax3 may be implicated in the regulation of proliferation and differentiation in neural progenitor cells, and folic acid supplementation may increase the proliferative capacity of *Pax3* null neuroepithelial cells.

6.1.3 Dorsalventral patterning in Sp^{2H}/Sp^{2H} embryos

While Shh signalling is important for ventral neural tube patterning, cross-repressive action between pairs of adjacently expressed transcription factors is also essential for overall patterning and discrete boundary formation. It is known that loss of a particular transcription factor can change the expression domain of other dorsoventral patterning transcription factors: for example, *Pax3* has a repressive action against *Pax7* expression (Borycki et al. 1999), while *Pax3* and *Pax7* both repress *Dbx1* expression (Gard et al. 2017). Other examples known include the mutually repressive actions of *Pax6* and *Nkx2.2* (Ericson et al. 1997; J Briscoe et al. 1999), and *Nkx6.1* and *Dbx2*, and also others (Briscoe & Small 2015; **Figure 6. 1**). BMP signalling has, likewise, been shown to orchestrate the patterning of the dorsal spinal neural tube, having the ability to regulate dorsal *Pax6* expression, to repress *Dbx1/2* expression and induce *Msx1/2* expression; again cross-repression of adjacent transcription factors is evident with *Msx1* mediating the repression of *Dbx2* (Timmer, Wang, and Niswander 2002). These observations have been gleaned from studies of the spinal cord around the forelimb bud level. To date, studies have not investigated the loss of *Pax3* on multiple patterning transcription factors along the dorsoventral axis, and have not looked at the cranial region.

It is currently unknown whether correct dorsoventral patterning is required for cranial neural tube closure. Mutant mouse models have demonstrated that over-activation of the Shh and BMP pathways can cause exencephaly (Echelard et al. 1993; J. A. McMahon et al. 1998). In mutants with excess Shh signalling it has been noted that there is a correlation between the extent of dorsoventral mispatterning and the frequency of exencephaly (Murdoch and Copp 2010). The cause of exencephaly in these mutants is unknown. It is possible that excess Shh and BMP signalling interfere with bending of the cranial neuroepithelium, similar to how both factors appear to inhibit DLHP formation in the spinal neural tube (Ybot-Gonzalez et al. 2002; Ybot-Gonzalez et al. 2007). However, it is also possible that transcription factor misregulation and mispatterning also contributes towards the cause of exencephaly.

Pax3 expression is known to be responsive to Shh; loss of *Shh* results in the ventral expansion of the *Pax3* expression domain (Rash and Grove 2007; Martinelli and Fan 2007), while notochord grafting experiments in the chick demonstrated that ectopic *Shh* expression next to the dorsal neural tube represses *Pax3* expression (Goulding, Lumsden, and Gruss 1993). The Shh repression of *Pax3* has also been demonstrated in mouse and is mediated by Gli activator function (Goodrich et al. 1997; Litingtung and Chiang 2000). However, the effect of loss of *Pax3* on Shh signalling and/ or dorsoventral patterning is largely unknown. It is possible that *Pax3* expression acts to inhibit the expression of one or more ventral transcription factors, and thus defines their dorsal border. This could lead to an apparent ventralisation of the neural tube when *Pax3* expression is lost. Additionally, it is unknown whether changes in the cellular transcriptional network could affect changes in interpretation of Shh signalling, or have potential effects on the Shh gradient itself, through modulation of positive and negative regulators. A study investigating loss of *Pax6* in mutant rat embryos found a shift in dorsoventral progenitor domain boundaries, and small changes in expression of Shh signalling components such as *Ptch1*, *Gli1* and *Gli2*, without any change in Shh protein itself (Takahashi and Osumi 2002). These studies suggest the possibility that loss of *Pax3* results in changes in Shh pathway activation and/ or dorsoventral patterning which affect neural tube closure.

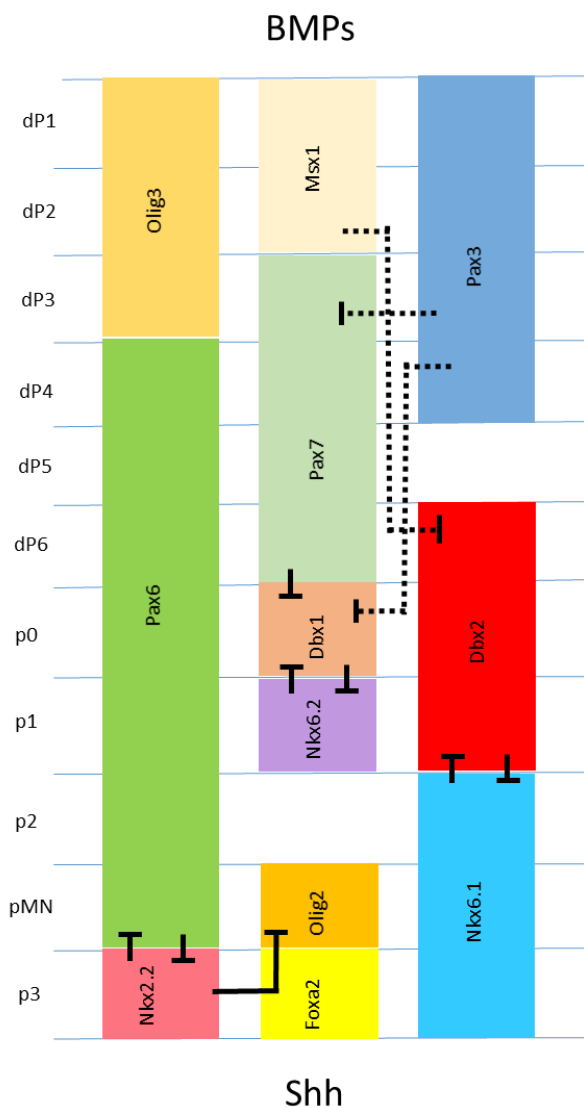


Figure 6. 1. Patterning and cross-repression of ventral transcription factors

Representation of the some of the progenitor cell patterning transcription factors, showing the domains in which they are expressed and the repressive actions which have been elucidated to date. Solid lines indicate direct effects while broken lines indicate indirect effects.

6.1.3.1 Interaction between Shh and Notch signalling

Along with its role in regulation of progenitor cell cycling, recent studies have found that Notch signalling modulates the response of neuroepithelial cells to Shh in the ventral neural tube, with Notch1 activation leading to a cell-autonomous increase in Shh pathway activation (Kong et al. 2015; Stasiulewicz et al. 2015). This was found to be independent of Shh but also additive upon the presence of Shh ligand: Notch signalling alone caused elongation and translocation of Smo to primary cilia, in effect priming the cells for response to Shh ligand, with addition of Shh further increased cilia length and Smo accumulation (Kong et al. 2015; Stasiulewicz et al. 2015).

Preliminary results from our lab found that treatment of *Sp^{2H}* litters in culture with the γ -secretase inhibitor N-[N-(3,5-Difluorophenacetyl)-L-alanyl]-S-phenylglycine t-butyl (DAPT), which inhibits Notch1 receptor cleavage by presenilin (PS), prevented exencephaly *Sp^{2H}/Sp^{2H}* embryos by approximately 90%. DAPT treatment was found to reduce *Notch1*, *Hes1* and *Hes5* expression, as confirmed by qRT-PCR, while *Dll1* expression was upregulated, as would be expected from Notch inhibition (personal communication, N Greene). However, the mRNA expression of *Notch1*, *Hes1*, *Hes5* or *Dll1* was not changed between mutants and wild-type littermates.

6.2 Aims of this chapter

This chapter aims to investigate the cellular defect which causes NTDs when *Pax3* expression is lost. It begins by assessing changes in proliferation, as a potential defect causing, and mechanism by which folic acid prevents exencephaly, in the cranial neural tube of E9.5 *Sp^{2H}/Sp^{2H}* and *+/+* embryos. The chapter then investigates the possibility that loss of *Pax3* results in a ventralising effects and/ or increase in apparent Shh signalling, in which the cranial and spinal region are both assessed. Lastly, the effect of cyclopamine, an inhibitor of Shh signalling, on rates of exencephaly in *Sp^{2H}/Sp^{2H}* embryos was determined.

6.3 Results

6.3.1 Analysis of proliferation in the cranial region

While mitotic index was studied previously in *Splotch* mutants, the objective was to conduct a more in-depth analysis of cell-cycle dynamics at the forebrain/ midbrain boundary region of 14 -15 somite stage *+/+* and *Sp^{2H}/Sp^{2H}* embryos. This is the stage immediately preceding cranial closure and the stage when a significant difference in Tuj1 staining was found in homozygous mutant embryos. Embryos were pulse labelled with the synthetic thymidine analogue 5-bromo-2'-deoxyuridine (BrdU) for 15 minutes *in vivo* before collection, fixed in 4 % PFA and paraffin wax embedded. Immunohistochemistry using anti-BrdU and anti-phosphohistone H3 (pHH3) antibodies was

performed on coronal sections through the forebrain – midbrain region. Sections were also counter-stained with 4', 6-diamidino-2-phenylindole (DAPI) to visualise nuclei.

BrdU is incorporated into DNA during S-phase of the cell cycle, therefore BrdU positive labelling records the proportion of cells which experienced S-phase during the 15-minute pulse labelling. pH3 is a marker encompassing early G₂ to M-phases of the cell cycle and is a snapshot in time at the point of fixation. Therefore, nuclei may be labelled positive for both markers if they were in late S-phase during the BrdU pulse and moved in to G₂ before the tissue was fixed. Furthermore, both BrdU and pH3 labelling vary with respect to the cell-cycle (Hendzel et al. 1997; Takahashi, Nowakowski, and Caviness 1992). Overall, four types of labelled nuclei can be easily distinguished: BrdU positive; pH3 positive (not mitotic); pH3 positive (mitotic); and, doubled labelled BrdU and pH3 positive (**Figure 6. 2**).

In the cranial neural tube, *Pax3* is expressed highly in the dorsal midbrain and in a small region of the dorsal forebrain, while it is excluded from the ventral neural tube (**Figure 6. 3**). After staining, the cranial neural tube was divided in three equal areas to encompass the dorsal midbrain (dorsal 1/3), the dorsal forebrain (ventral 1/3) and the ventral neural tube (middle 1/3; **Figure 6. 4**). It can be seen that the dorsal 1/3 encompasses the *Pax3* expression domain of the dorsal midbrain, while there is no *Pax3* expression in the ventral 1/3, which corresponds to the dorsal forebrain (**Figure 6. 3**). The three regions were assessed for the number of each of the four types of nuclei as shown in **Figure 6. 2**. The number of nuclei demonstrating each pattern of labelling was then calculated as a percentage of total cells in each region.

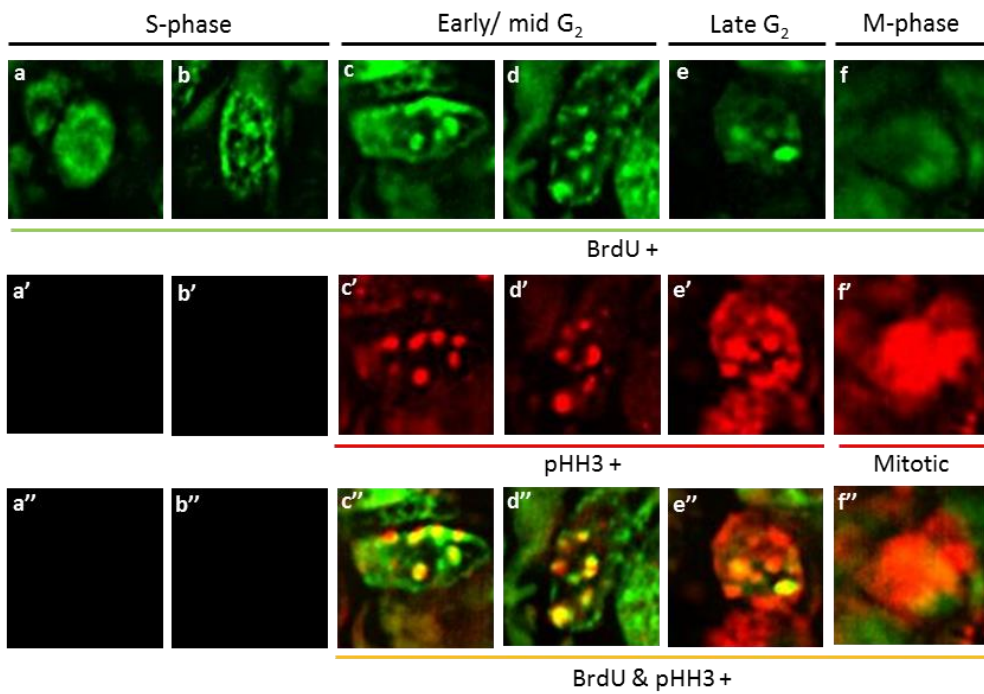


Figure 6.2. Analysis of proliferating cells using BrdU and pHH3 staining

(a – f) BrdU staining is most uniform during S-phase and generally becomes more punctate as the cycle moves towards M-phase. Cells can be only BrdU positive (BrdU+) as in a and b. (a' – f') pHH3 staining is visible as large puncta from early G₂ and becomes more uniform as the cycle approaches M-phase. During mid/ late M-phase, pHH3 staining is at its most homogenous and intense. Cells can be only pHH3 positive (pHH3+ & mitotic), or doubly labelled for BrdU and pHH3 (a'' – f''; BrdU & pHH3 +).

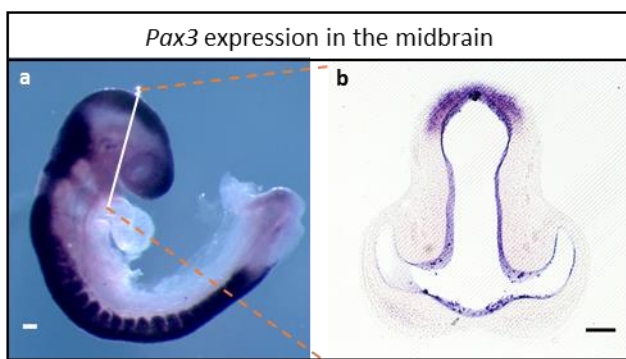


Figure 6.3. Pax3 expression in the dorsal midbrain of the cranial neural tube

(a) *Pax3* expression as assessed by WMISH, and in (b) coronal sections, demonstrating expression in the dorsal midbrain region only, in the cranial regions investigated. Scale bars represent 100 µm.

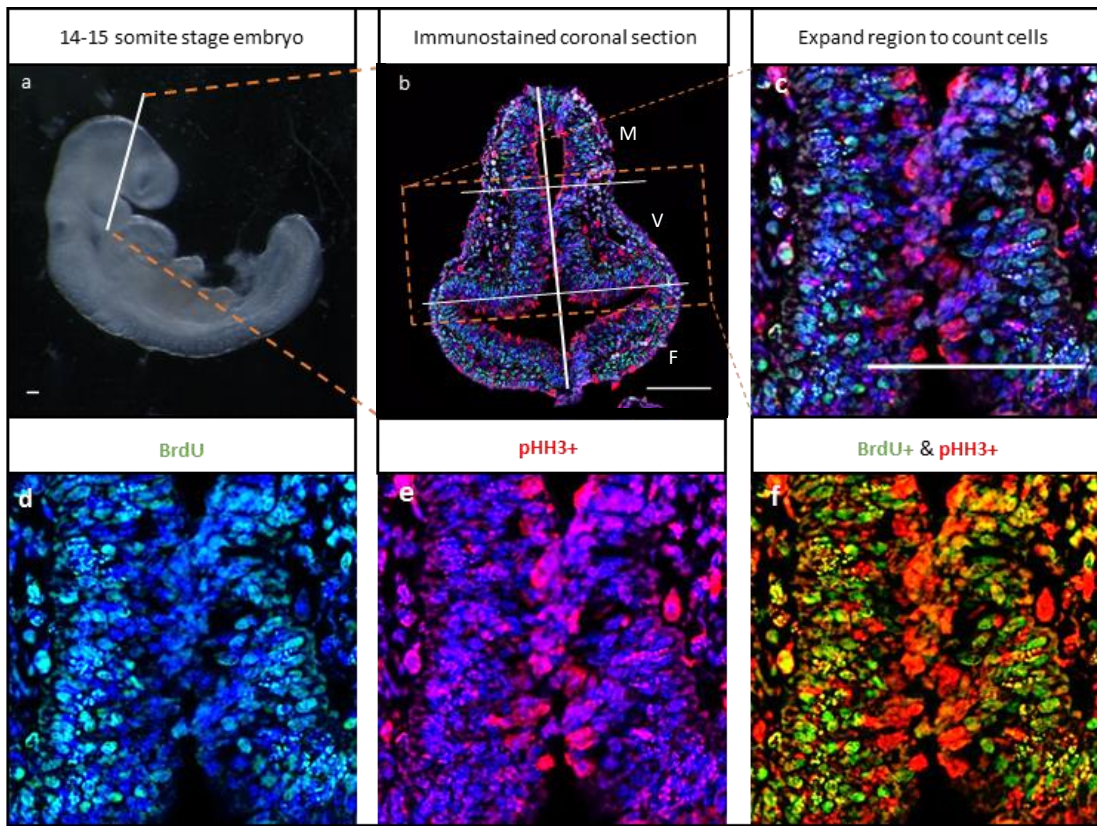


Figure 6.4. Representation of pipeline for BrdU+, pHH+ and double labelled BrdU+ and pHH+ cell counting.

(a) 14 – 15 state $+/+$ and Sp^{2H}/Sp^{2H} embryos were fixed, serially sectioned (3 sections per serial; 4 μm) and fluorescently stained using anti-BrdU and anti-pHH3 antibodies. Sectioned were imaged (b), and the neuroepithelium divided into equal thirds. In (b), M = dorsal midbrain; V = ventral, and; F = dorsal forebrain. Sections for cell counting were taken at 40x magnification (c - f), and visualised with DAPI (blue channel) to count positively labelled (d) BrdU+ (e) mitotic and pHH3+ and (f) double labelled BrdU+ and pHH3+ cells. Scale bar represents 100 μm .

6.3.1.1 Comparison of $+/+$ and Sp^{2H}/Sp^{2H} embryos

The percentage of positively labelled cells was assessed in two serial sections per embryo to obtain an average from three embryos per genotype. A comparison of the percentage of BrdU positive cells found that 50 % more cells are BrdU labelled in the dorsal, *Pax3* expressing midbrain region compared to the ventral region in $+/+$ embryos ($p = 0.002$; **Figure 6.5**). This is in contrast to Sp^{2H}/Sp^{2H} embryos, which have the same proportion of BrdU positive cells in the ventral and dorsal midbrain region, resulting in the percentage of BrdU positive cells in the dorsal midbrain being significantly less in Sp^{2H}/Sp^{2H} embryos in comparison to $+/+$ embryos ($p = 0.02$).

The percentage of pHH3 positive cells is similarly found to be increased in the dorsal midbrain region in comparison to the ventral region in $+/+$ embryos ($p = 0.003$), but not in Sp^{2H}/Sp^{2H} embryos (**Figure 6. 6**). A comparison of $+/+$ and Sp^{2H}/Sp^{2H} embryos finds that the percentage of pHH3 positive cells is approximately 20 % less in the dorsal midbrain neuroepithelia ($p = 0.01$) of Sp^{2H}/Sp^{2H} embryos, while it is greater in the dorsal forebrain neuroepithelia ($p = 0.009$) and the ventral neuroepithelia ($p = 0.01$). Lastly, the percentage of non-mitotic pHH3 positive cells is found to be greater in the dorsal forebrain region of Sp^{2H}/Sp^{2H} embryos in comparison to the dorsal midbrain region ($p = 0.0008$); the opposite tendency is true for $+/+$ embryos.

No significant differences were found in the percentage of pHH3 positive mitotic cells (**Figure 6. 7**) or in the percentage of doubly labelled cells (**Figure 6. 8**).

In summary, a smaller proportion of cells were found to have been in S-phase (during the 15-minute pulse), and in G₂/ M-phase when fixed, in the dorsal midbrain region of Sp^{2H}/Sp^{2H} embryos, suggesting that loss of *Pax3* affects the cell cycle. Additionally, the data suggests that loss of *Pax3* may eliminate the ventral-low, dorsal-high proliferation gradient found in the cranial neural tube of $+/+$ embryos.

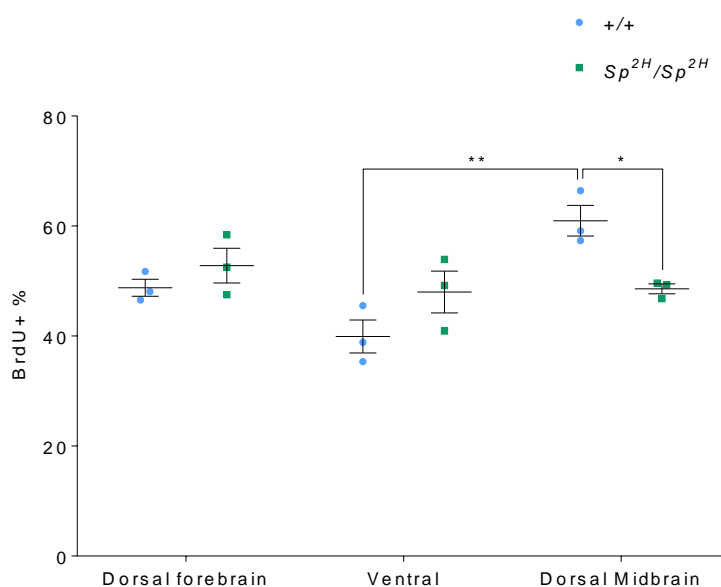


Figure 6. 5. Percentage of BrdU positive cells in $+/+$ and Sp^{2H}/Sp^{2H} embryos.

The percentage of BrdU+ cells was significantly greater in the dorsal midbrain regions of $+/+$ embryos (60.96 ± 2.78 %) compared to the ventral region (39.92 ± 2.98 %; $**p = 0.002$). There were less BrdU+ cells in the dorsal midbrain of Sp^{2H}/Sp^{2H} (48.59 ± 0.89 %) compared to $+/+$ (60.96 ± 2.78 %; $*p = 0.02$) embryos. Results assessed by 2way ANOVA with Sidak's test. $N = 3$ per genotype.

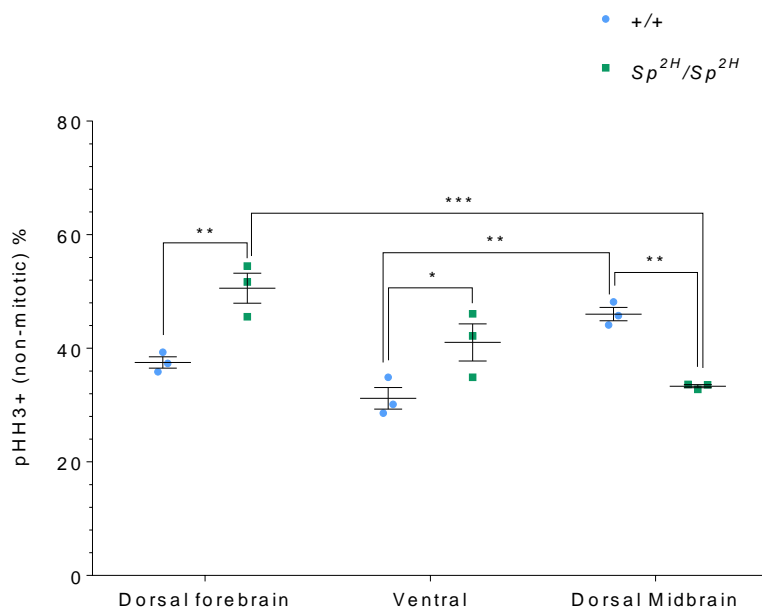


Figure 6. 6. Percentage of pHH3 positive (non-mitotic) cells in +/+ and *Sp*^{2H}/*Sp*^{2H} embryos.

The percentage of pHH3+ cells was significantly less in the dorsal midbrain of *Sp*^{2H}/*Sp*^{2H} embryos ($33.33 \pm 0.28\%$) compared to +/+ ($46.02 \pm 1.18\%$; $**p = 0.002$). Conversely, the proportion of pHH3+ labelled cells was greater in the dorsal forebrain ($50.57 \pm 2.64\%$) and ventral region ($41.04 \pm 31.20\%$) compared to +/+ embryos ($37.50 \pm 1.0\%$ and $31.20 \pm 2.0\%$; $**p = 0.002$ and $*p = 0.002$ respectively). There were an increased proportion of labelled cells in the dorsal forebrain of *Sp*^{2H}/*Sp*^{2H} embryos compared to the dorsal midbrain ($***p = 0.008$), while in +/+ embryos, the proportion of positive cells is greater in the dorsal midbrain compared to the ventral region ($**p = 0.003$). Results assessed by 2way ANOVA with Sidak's test. $N = 3$ per genotype.

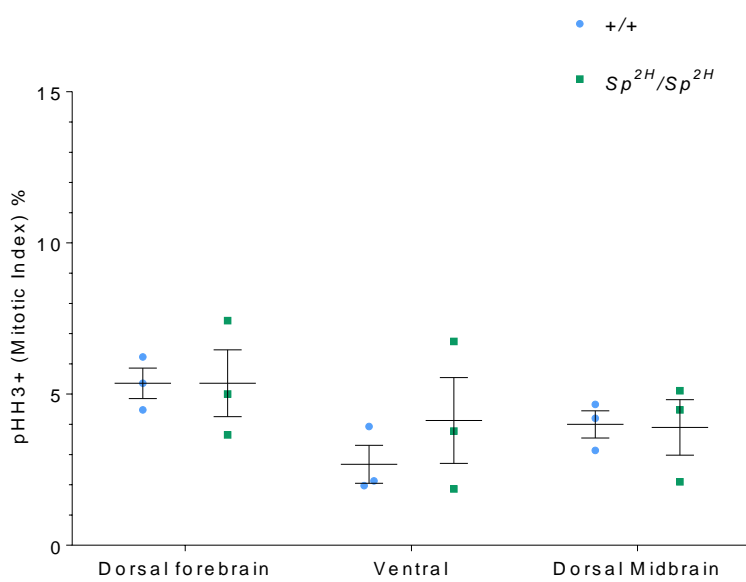


Figure 6. 7. Percentage of pHH3 positive (mitotic) cells in +/+ and *Sp*^{2H}/*Sp*^{2H} embryos.

No significant differences found. $N = 3$ per genotype.

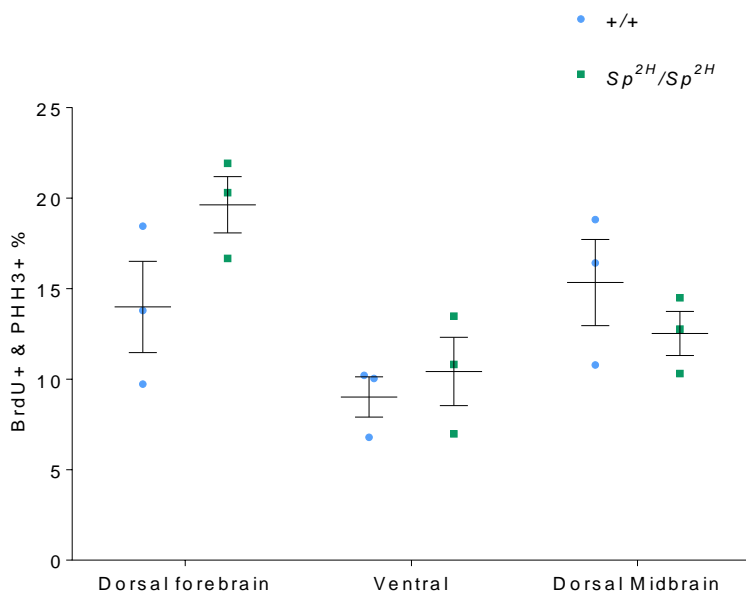


Figure 6. 8. Percentage of double labelled BrdU and pHH3 positive cells in +/+ and *Sp*^{2H}/*Sp*^{2H} embryos.

No significant differences found. $N = 3$ per genotype.

6.3.1.2 Effect of folic acid on percentage labelling

To understand whether supplemental folic acid has any effect on BrdU and pHH3 labelling, pregnant *Sp^{2H}*/+ dams were given intraperitoneal injections of 20 mg per kg folic acid on E7.5, E8.5 and E9.5. This dose and treatment regime have previously been shown to reduce the rate of cranial NTDs (Fleming and Copp 2000). Folic acid on E9.5 was given 2 hours before BrdU injection. While the results for *Sp^{2H}*/*Sp^{2H}* and +/+ which were shown in **Figures 6.5 – 6.8** are repeated in **Figures 6.9 – 6.12** to compare with their corresponding folic acid treated counterparts, significant results reported between *Sp^{2H}*/*Sp^{2H}* and +/+ are not shown again.

Folic acid status had little effect on numbers of BrdU positive cells, although there may be a small and somewhat varied tendency for folic acid treatment to increase the percentage of BrdU positive cells in the dorsal midbrain region of *Sp^{2H}*/*Sp^{2H}* embryos (**Figure 6.9**).

Folic acid treatment had significant effects on the percentage of pHH3 (non-mitotic) positive cells (**Figure 6.10**). Crucially, folic acid treatment significantly increased the percentage of non-mitotic pHH3 positive cells in the dorsal midbrain region of *Sp^{2H}*/*Sp^{2H}* embryos ($p < 0.0001$). This resulted in the percentage of labelled cells in folic acid treated *Sp^{2H}*/*Sp^{2H}* embryos surpassing that of control +/+ embryos in the dorsal midbrain region ($p = 0.002$), and also resulted in increased percentage labelling in the dorsal midbrain region in comparison to the ventral region in folic acid treated *Sp^{2H}*/*Sp^{2H}* embryos ($p < 0.0001$). This ventral-low, dorsal-high proliferation gradient was evident in control +/+ embryos but absent in *Sp^{2H}*/*Sp^{2H}* embryos (**Figure 6.6**). On the other hand, no differences were observed in the percentage of mitotic cells (**Figure 6.11**).

Of interest, folic acid supplementation also increased the percentage of doubly labelled BrdU and pHH3 positive cells in the dorsal midbrain region of *Sp^{2H}*/*Sp^{2H}* embryos ($p = 0.007$), and also in the ventral region of +/+ embryos ($p = 0.009$; **Figure 6.12**).

These results suggest that folic acid supplementation of *Sp^{2H}*/*Sp^{2H}* embryos increases the rate of DNA synthesis (the increased percentage of pHH3 positive and doubly labelled BrdU and pHH3 positive cells), without significantly increasing the proportion of cells in S-phase at a given time (no change in percentage of BrdU positive cells), in the dorsal midbrain region. This may indicate that folic acid supplementation increases the rate of proliferation in this region and therefore re-establishes the ventral-low, dorsal-high proliferation gradient that appears to be lost with loss of *Pax3* expression.

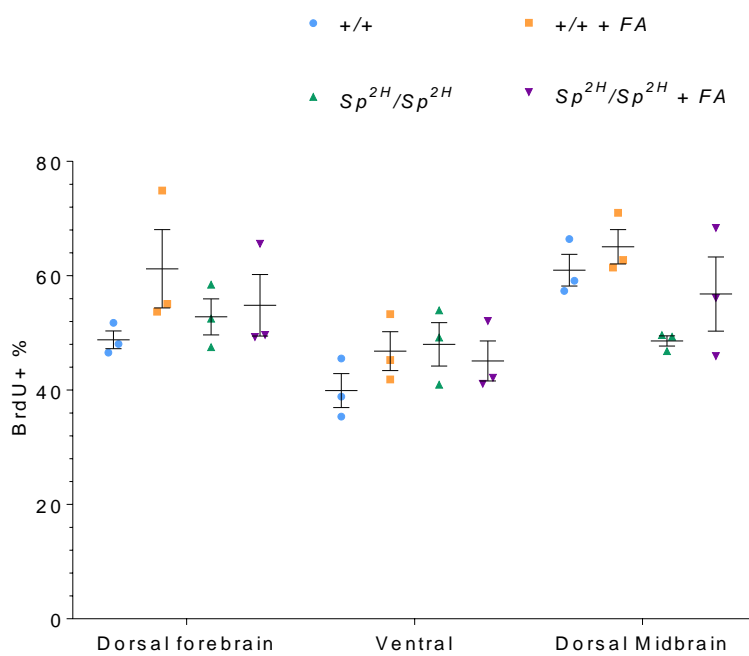


Figure 6. 9. Percentage of BrdU positive cells in folic acid treated +/+ and *Sp*^{2H}/*Sp*^{2H} embryos.

No significant changes found. $N = 3$ per genotype and treatment.

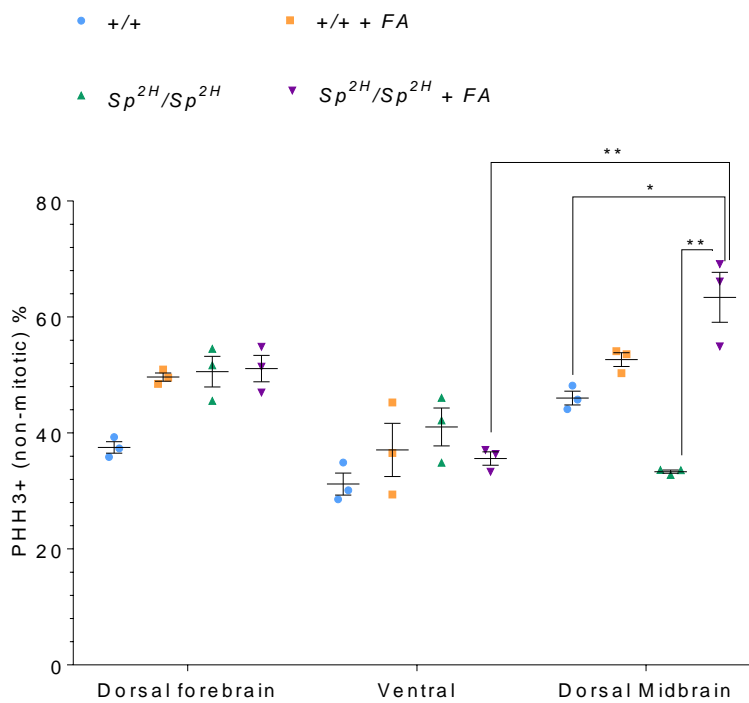


Figure 6. 10. Percentage of pHH3 (non-mitotic) positive cells in folic acid treated +/+ and *Sp*^{2H}/*Sp*^{2H} embryos.

Figure 6. 10. Percentage of pHH3 (non-mitotic) positive cells in folic acid treated +/+ and *Sp*^{2H}/*Sp*^{2H} embryos.

The percentage of pHH3 (non-mitotic) positive cells was increased by folic acid treatment in the dorsal midbrain region of *Sp*^{2H}/*Sp*^{2H} embryos ($33.3 \pm 0.28\%$ vs. $63.39 \pm 4.31\%$; $^{**}p < 0.0001$). This led to the percentage of positive cells being higher in the dorsal midbrain region ($63.39 \pm 4.31\%$) compared to the ventral region ($35.60 \pm 1.15\%$; $^{**}p < 0.0001$) of folic acid treated *Sp*^{2H}/*Sp*^{2H} embryos. In the dorsal midbrain region, the percentage of labelled cells was also higher in folic acid treated *Sp*^{2H}/*Sp*^{2H} embryos compared to control +/+ embryos ($46.02 \pm 1.18\%$; $^{*}p = 0.002$). Results assessed by 2way ANOVA with Sidak's test. $N = 3$ per genotype and treatment.

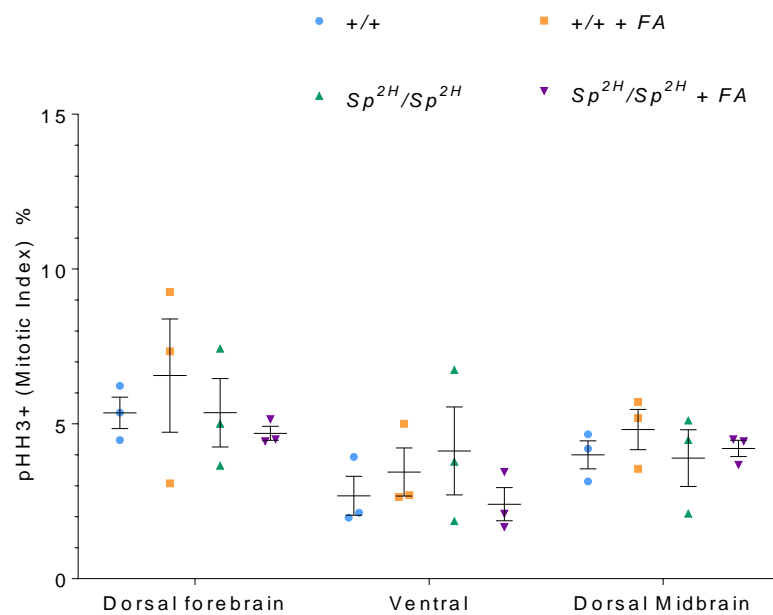


Figure 6. 11. Percentage of pHH3 (mitotic) positive cells in folic acid treated +/+ and *Sp*^{2H}/*Sp*^{2H} embryos.

No significant changes found. $N = 3$ per genotype and treatment.

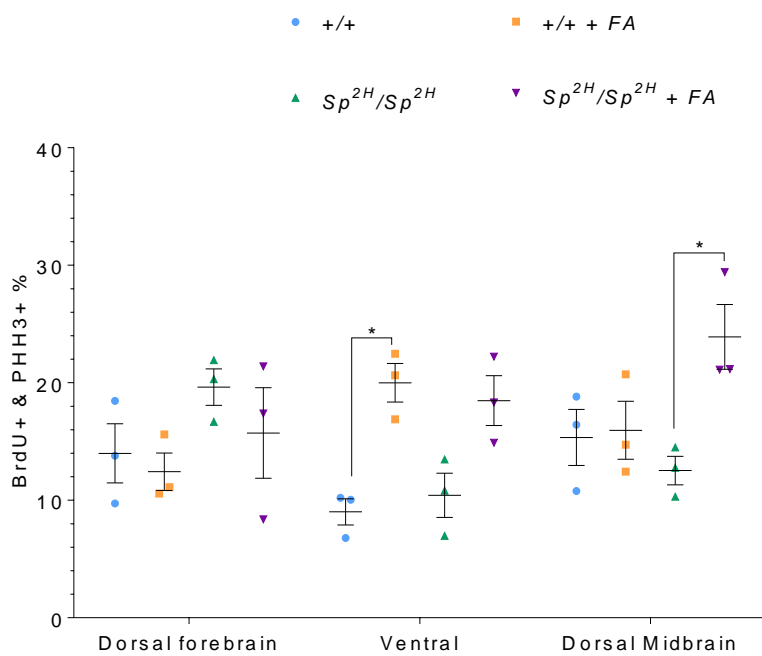


Figure 6.12. Percentage of doubly labelled BrdU and pHH3 positive cells in folic acid treated +/+ and *Sp*^{2H}/*Sp*^{2H} embryos.

Folic acid treatment significantly increased the percentage of doubly labelled cells in the dorsal midbrain of *Sp*^{2H}/*Sp*^{2H} embryos ($12.53 \pm 1.21\%$ vs. $23.90 \pm 2.76\%$; $*p = 0.007$). Folic acid treatment also increased the percentage of doubly labelled cells in the ventral region of +/+ embryos ($9.01 \pm 2.52\%$ vs. $20.00 \pm 1.64\%$; $*p = 0.009$). Results assessed by 2way ANOVA with Sidak's test. $N = 3$ per genotype and treatment.

6.3.1.3 Comparison of *Cdkn1a* expression in *+/+* and *Sp^{2H}/Sp^{2H}* embryos.

Previous results found that Tuj1 immunostaining was increased in *Sp^{2H}/Sp^{2H}* embryos compared to *+/+* embryos in the dorsal midbrain. This may suggest premature exit of neuroepithelial cells from the cell cycle. p21, the protein expressed from *Cdkn1a*, is a cell cycle inhibitor of the CIP/ KIP family, which cause cell cycle arrest in G₁ when overexpressed. p21 is induced by the tumour suppressor gene p57 as part of the DNA damage response. However, p21 is also expressed independently of p57 during embryogenesis and cellular differentiation (Macleod et al. 1995; Parker et al. 1995), which requires exit from the cell cycle.

The expression of *Cdkn1a* was investigated in the dorsal midbrain of *Sp^{2H}/Sp^{2H}* and *+/+* embryos at the 14 – 15 somite stage (**Figure 6. 13**). There was perhaps an increase in *Cdkn1a* expression at the very tips of the dorsal neural tube, but this more likely correlates with *Cdkn1a* expression in neural crest cells, rather than neuroepithelial cells. Overall, there was not judged to be a significant difference in *Cdkn1a* expression in relation to the *Pax3* expression domain in the two genotypes.

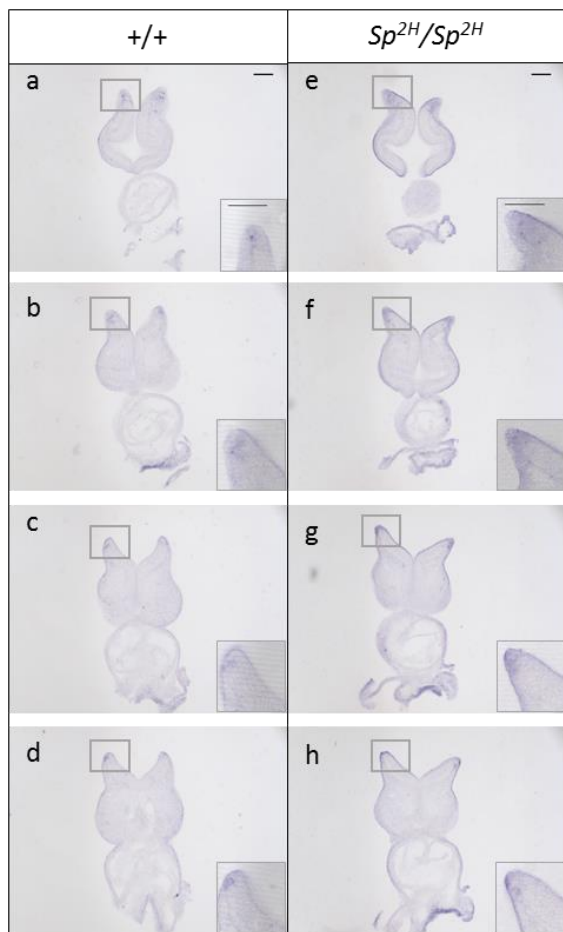


Figure 6. 13. p21 expression in E9.5 *+/+* and *Sp^{2H}/Sp^{2H}* embryos.

p21 mRNA expression in *+/+* (**a – d**) and *Sp^{2H}* (**e – h**) embryos. Magnification of the dorsal tips of the midbrain neuroepithelium is shown inset. Scale bars represent 100 μ m. Two embryos per genotype assessed.

6.3.2 Does loss of *Pax3* alter the effects of sonic hedgehog signalling?

The results of DAPT culture experiments and recent data implicating Notch signalling in the amplification of Shh signalling (Kong et al. 2015; Stasiulewicz et al. 2015) prompted the question; does loss of *Pax3* increase the level of Shh signalling experienced within the neural tube? Furthermore, because increased Shh signalling is demonstrated to interfere with cranial neural tube closure (Milenkovic et al. 1999; Eggenschwiler, Espinoza, and Anderson 2001; Bulgakov et al. 2004; Cooper et al. 2005), it was hypothesised that increased Shh signalling could be involved in the aetiology of exencephaly in *Sp*^{2H}/ *Sp*^{2H} embryos

6.3.2.1 Analysis of sonic hedgehog signalling in +/+ and *Sp*^{2H}/ *Sp*^{2H} embryos

To investigate outcomes of the Shh pathway in *Sp*^{2H}/ *Sp*^{2H} embryos, the relative mRNA expression of the direct, positive, targets of Shh signalling, *Ptch1* and *Gli1* (Goodrich et al. 1996; Bai et al. 2002), were assessed in the anterior and posterior regions of 14 – 15 somite stage +/+ and *Sp*^{2H}/ *Sp*^{2H} embryos. Anterior and caudal tissues were separated between the ninth and tenth somite junction and RNA isolated. This analysis found no significant changes in *Ptch1* or *Gli1* expression in either of the regions (**Figure 6. 14**).

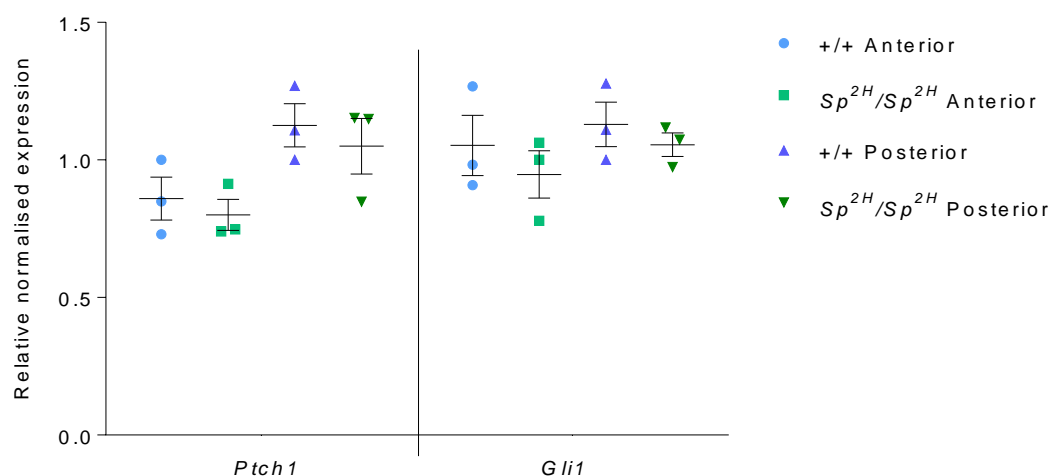


Figure 6. 14. qRT-PCR analysis of *Ptch1* and *Gli1* expression

No differences were found in either anterior tissues or posterior tissues. Expression was normalised to *Gapdh* and an arbitrarily chosen anterior +/+ sample set as a relative expression of 1.0. $N = 3$ per genotype.

While the qPCR results did not indicate changes in global *Ptch1* and *Gli1* expression, it remained possible that if there were changes in the neural tube only, this might not be detected as both genes are expressed in surrounding tissues, or that there could be changes in the range and/ or dorsal extent of their expressions, without a large change in the overall expression levels. Therefore, WMISH was conducted to visualise the tissue expression of *Ptch1*, *Gli1*, *Foxa2* and *Shh* mRNA in 14 – 16 somite stage +/+ and *Sp*^{2H}/*Sp*^{2H} embryos. *Foxa2* is a positive target of *Shh* signalling which is expressed in the floorplate (Goodrich et al. 1996). Unlike qPCR, WMISH is not a quantitative method. However, when embryos undergo parallel treatment under the same protocol and same experiment, including the same colour development time, some tentative comparisons can be made.

Coronal sections through the cranial neural tube, and transverse sections through the spinal neural tube at multiple regions along the rostrocaudal axis, were analysed (Figure 6. 15). There appeared to be a small increase in the intensity of *Shh* expression in the ventral neural tube of the midbrain region of *Sp*^{2H}/*Sp*^{2H} embryos (arrows in **b** – **d** compared with arrows in **h** – **j**), and also in the lower spinal region (**e** & **k**) and in the caudal most region of the neural tube (**f** & **l**). Of interest, it can be seen that *Shh* expression is also increased in the hindgut, although *Pax3* is not normally expressed in this tissue (Goulding et al. 1991). On the other hand, there does not appear to be any changes in the cranial expression of *Ptch1* (**m** – **p** & **s** – **v**), *Gli1* (**y** – **ab** & **ae** – **ah**) or *Foxa2* (**ak** – **an** & **aq** – **at**), while the intensity and/or area of staining corresponding to *Ptch1* (difference in intensity only in **q** & **w**; difference in area and intensity in **r** & **x**), *Gli1* (difference in area, 14 % and 24 %, and intensity in **ac** & **ai** respectively; difference in area and intensity in **ad** & **aj**) and *Foxa2* (difference in intensity in **ao** & **au**; difference in area, 21 % and 30 % in **ap** & **av** respectively) expression in the spinal regions, as well as the surrounding mesoderm, do appear to be increased in *Sp*^{2H}/*Sp*^{2H} embryos.

As there are no changes in staining for *Ptch1*, *Gli1* and *Foxa2* in relation to genotype in the cranial neuroepithelium, this region acts as an internal control for these experiments, and suggests that the changes seen in the spinal region between genotypes are real. The increases in intensity and/or area of *Ptch1*, *Gli1* and *Foxa2* staining suggest that the increase in *Shh* staining could be real.

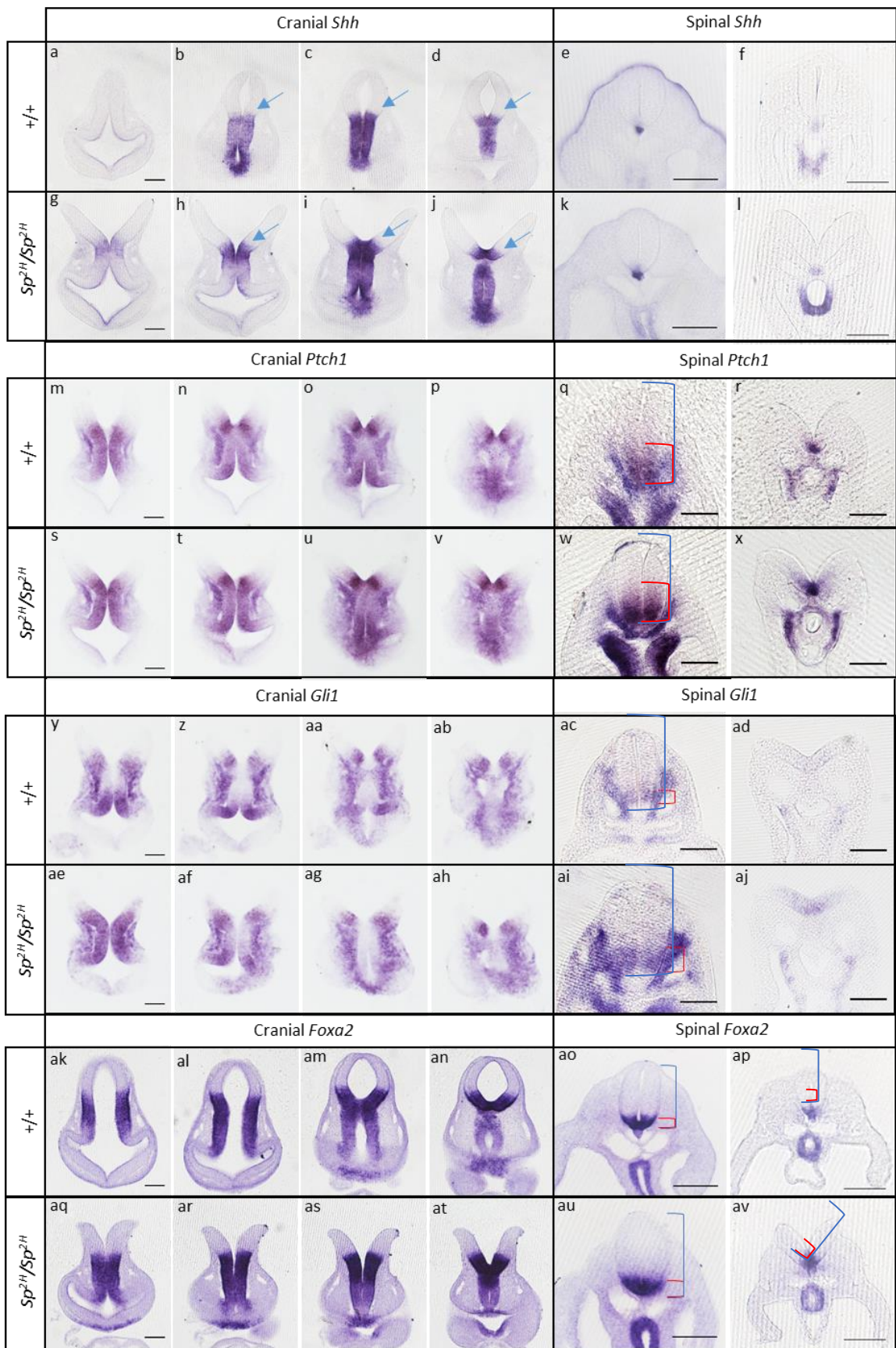


Figure 6. 15. Expression of *Shh*, *Ptch1*, *Gli1* and *Foxa2*.

Figure 6. 15. Expression of Shh, Ptch1, Gli1 and Foxa2.

Shh expression: coronal sections through the cranial region of $+/+$ (**a** - **d**) and Sp^{2H}/Sp^{2H} (**g** - **j**) embryos. Areas of increased intensity indicated by blue arrows. Transverse sections through the mid-spinal and most caudal regions of the neural tube in $+/+$ (**e** & **f**, respectively) and Sp^{2H}/Sp^{2H} (**k** & **l**, respectively) embryos. *Ptch1* expression: coronal sections through the cranial region of $+/+$ (**m** - **p**) and Sp^{2H}/Sp^{2H} (**s** - **v**) embryos. Transverse sections through the upper spinal and most caudal regions of the neural tube in $+/+$ (**q** & **r**, respectively) and Sp^{2H}/Sp^{2H} (**w** & **x**, respectively) embryos. *Gli1* expression: coronal sections through the cranial region of $+/+$ (**v** - **ab**) and Sp^{2H}/Sp^{2H} (**ae** - **ah**) embryos. Transverse sections through the upper spinal and most caudal regions of the neural tube in $+/+$ (**ac** & **ad**, respectively) and Sp^{2H}/Sp^{2H} (**ai** & **aj**, respectively) embryos. Red brackets indicate the peak *Gli1* expression domain. *Foxa2* expression: coronal sections through the cranial region of $+/+$ (**ak** - **an**) and Sp^{2H}/Sp^{2H} (**aq** - **at**) embryos. Transverse sections through the mid-spinal and most caudal regions of the neural tube in $+/+$ (**ao** & **ap**, respectively) and Sp^{2H}/Sp^{2H} (**au** & **av**, respectively) embryos. The *Foxa2* expression domain (red brackets) in relation to the ventrodorsal length of the neural tube (blue brackets) is indicated (**ao**, **au**, **ap** & **av**). At least two embryos for each probe per genotype assessed. Scale bars represent 100 μ m.

6.3.2.1.1 Expression of *Pax6*, *Msx1* and *Bmp2*

After finding that *Shh* expression appeared to be modestly increased in Sp^{2H}/Sp^{2H} embryos, the expression of the intermediate neural tube patterning transcription factor *Pax6*, and the dorsal patterning transcription factor *Msx1*, were assessed (Figure 6. 16). While no changes in *Pax6* expression in the cranial region could be detected (**a** - **b** & **f** - **i**), there was a dorsal shift in the dorsal boundary of *Pax6* expression, leading to an increase in the *Pax6* expression domain, in the intermediate neural tube of Sp^{2H}/Sp^{2H} embryos (ventral domain of no *Pax6* expression = 30 % in $+/+$ and 32 % in Sp^{2H}/Sp^{2H} ; *Pax6* expression domain = 41 % in $+/+$ and 48 % in Sp^{2H}/Sp^{2H} ; dorsal domain of no *Pax6* expression = 28 % in $+/+$ and 21 % in Sp^{2H}/Sp^{2H}) as highlighted by the red and blue brackets (**e** & **k**). *Msx2* expression has been found to increase with loss of *Pax3* in Sp/Sp embryos (Kwang et al. 2002), and here, *Msx1* expression is also found to be increased in Sp^{2H}/Sp^{2H} embryos. It is interesting to note that while *Msx1* expression is substantially increased in what is assumed to be the cranial neural crest and cranial neural crest derived mesenchyme (blue arrows in **s** & **w** - **y**), this does not appear to be the case in the neural tube. In the cranial region, this may be due to the failure of neural tube closure, as decreased *Msx1* expression has been noted in the case of *Cited2* homozygous mutants with open cranial regions but not in mutants with closed cranial regions (Barbera et al. 2002). However, while *Msx1* expression may be slightly increased in the

upper spinal region of the neural tube in Sp^{2H}/Sp^{2H} embryos, it appears to become decreased in the neural tube in comparison to $+/+$ embryos moving along the rostrocaudal axis (**p – r** & **w – y**). Of interest, the mesodermal expression of *Msx1* remains increased in Sp^{2H}/Sp^{2H} embryos.

As *Msx1/2* are positively regulated by BMPs (Timmer, Wang, and Niswander 2002; Esteves et al. 2014) it was predicted that the expression of one or more BMPs expressed in the overlying surface ectoderm could be increased in Sp^{2H}/Sp^{2H} embryos. The expression of *Bmp2* was investigated because it has been shown to be involved in the regulation of DLHP formation and, therefore, in Mode 2 and 3 closure of the PNP (Section 0). *Bmp2* expression was found to be increased in the roof plate region of the dorsal neural tube in the midbrain region, and possibly in the overlying surface ectoderm (**z – ac** & **ag – aj**). Additionally, the difference between the dorsal-high, ventral-low expression gradient was reduced in Sp^{2H}/Sp^{2H} embryos such that the ventral region appeared to have higher *Bmp2* expression compared to $+/+$ embryos. *Bmp2* expression was also substantially increased in the hindbrain region (**ad** & **ak**), the mid-spinal region (**ae** & **al**) and the most caudal region (**af** & **am**), as well as in the surrounding mesenchyme. Lastly, surface ectoderm expression of *Bmp2* appeared decreased in Sp^{2H}/Sp^{2H} embryos at the hindbrain level.

In conclusion, the loss of *Pax3* does not appear to cause a major shift in the boundaries of *Pax6* or in the cranial region. There appears to be a shift in the *Pax6* boundary in the spinal region but this needs to be confirmed. Of possible interest, *Bmp2* expression appears expanded in Sp^{2H}/Sp^{2H} embryos.

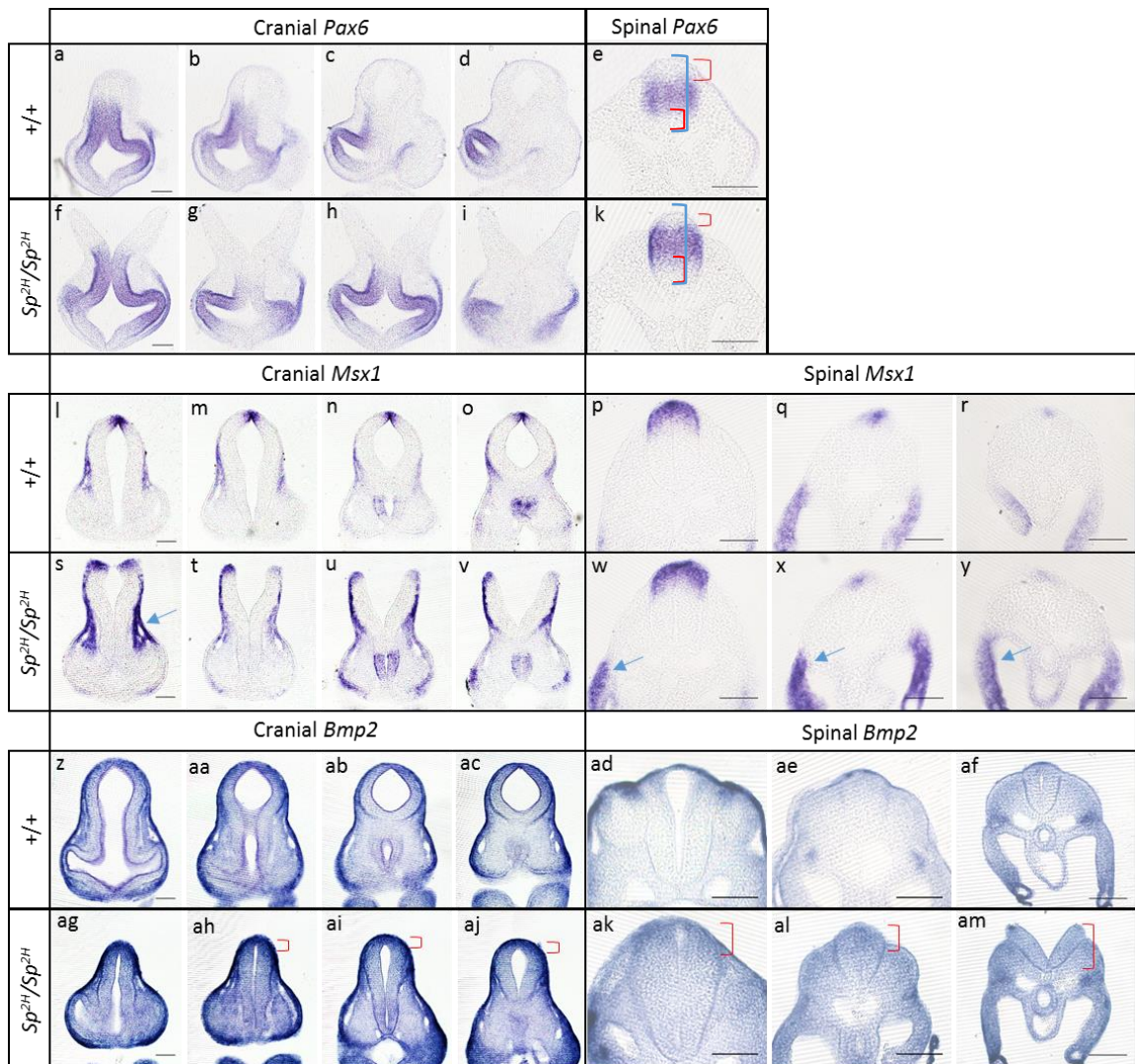


Figure 6.16. Expression of *Pax6*, *Msx1* and *Bmp2*.

Pax6 expression: coronal sections through the cranial region of *+/+* (a - d) and *Sp*^{2H}/*Sp*^{2H} (g - j) embryos. Transverse sections through the mid-spinal regions of the neural tube in *+/+* (e) and *Sp*^{2H}/*Sp*^{2H} (k) embryos. Red brackets indicate a dorsal shift in the expression domain. *Msx1* expression: coronal sections through the cranial region of *+/+* (l - o) and *Sp*^{2H}/*Sp*^{2H} (s - v) embryos. Transverse sections through the upper-spinal, mid-spinal and most caudal regions of the neural tube in *+/+* (p - r) and *Sp*^{2H}/*Sp*^{2H} (w - y) embryos. Increased mesenchymal expression indicated by blue arrows. *Bmp2* expression: coronal sections through the cranial region of *+/+* (z - ac) and *Sp*^{2H}/*Sp*^{2H} (ag - aj) embryos. Transverse sections through the hindbrain, mid-spinal and most caudal regions of the neural tube in *+/+* (ad - af) and *Sp*^{2H}/*Sp*^{2H} (ak - am) embryos. Areas of increased intensity indicated by red brackets. Two embryos for each probe per genotype assessed, except *Pax6*, where one embryo per genotype was assessed. Scale bars represent 100 μm.

6.3.2.2 Does Sonic Hedgehog pathway inhibition alter the frequency of exencephaly in Sp^{2H}/Sp^{2H} embryos?

Although loss of *Pax3* does not appear to cause any major changes to the expression of *Shh* responsive genes (*Ptch1*, *Gli1*, *Foxa2* and *Pax6*) in the cranial region, given the apparent increase in *Shh* itself, and the previous data that DAPT treatment prevented approximately 90% of exencephaly in Sp^{2H}/Sp^{2H} embryos, the effect of Shh pathway inhibition on rate of exencephaly was investigated. Partial Shh pathway inhibition (~ 60 %; see below) was accomplished using cyclopamine-KAAD (referred to as simply cyclopamine from here onwards), which is a potent synthetic, cell permeable, inhibitor of Shh signalling via inhibition of SMO activity (Taipale et al. 2000).

Litters from $Sp^{2H}/+$ matings were explanted with their yolk sacs still intact at approximately E8.75 and cultured for 30 hours with 15 nM cyclopamine, so that the embryos experienced the effects of cyclopamine after Closure 1 had occurred but before Closure 2, which then continued well past the stage when cranial closure should be complete. Cranial closure, somite stage and PNP length were assessed at the end of culture. This was considered a preliminary experiment to assess the potential for cyclopamine treatment to modulate the rate of exencephaly in Sp^{2H}/Sp^{2H} embryos and for this reason all embryos were treated.

6.3.2.2.1 Shh pathway inhibition by cyclopamine in embryo culture

A range of 5 – 50 nM cyclopamine was tested and whole embryo *Gli1* mRNA assessed by qPCR to investigate the extent of pathway inhibition. Interestingly, the results indicated that *Gli1* transcripts were reduced by approximately 60 % compared to control samples across the range of doses tested (**Figure 6. 17**). A dose of 15 nM was chosen as it was well below the toxic dose of 100 nM, but higher than the lowest dose tested.

After culture, transcription factor patterning was investigated in cyclopamine treated +/+ and Sp^{2H}/Sp^{2H} embryos by WMISH using probes for *Shh*, *Foxa2*, *Pax3*, *Pax6*, *Msx1* and *Bmp2*. DAPT treated embryos were also examined, and are shown together with control embryos which have not undergone culture and can therefore only be used to make very approximate comparisons. Whole mount embryos at the end of colour development are shown (**Figure 6. 18**), as well as coronal sections of the cranial region for each of the conditions (**Figure 6. 19**). Overall, it appears that DAPT treatment does not visibly affect patterning of the neural tube, except for *Pax6*, whose expression domain extends further dorsally and caudally in the cranial midbrain of DAPT treated embryos (**Figure 6. 18 k & m**; **Figure 6. 19 k & m**).

From the wavy neural tube phenotype seen in whole mount embryos, and more precisely in sections, cyclopamine treatment is found to deleteriously affect the morphology of the cranial neural tube. It

is interesting to note that cranial morphology is substantially more disrupted in Sp^{2H}/Sp^{2H} embryos compared to $+/+$ embryos, suggesting that loss of *Pax3* may affect cranial neuroepithelial integrity. In Sp^{2H}/Sp^{2H} embryos incubated with *Shh* and *Foxa2* probes, the floorplate can be seen to kink and protrude in the midbrain-hindbrain boundary region of whole mount embryos (orange arrowheads in **Figure 6. 18 e & j**). Both whole mount and sections suggest *Shh* (**Figure 6. 18 c – e**) and *Foxa2* (**Figure 6. 19 h – j**) expression is decreased by cyclopamine treatment, as would be expected, because floorplate expression of both genes is reliant on *Gli2* activator function (Matise et al. 1998). Cyclopamine treatment of $+/+$ embryos led to *Pax6* expression throughout the neural tube in the midbrain region, which is in keeping with decreased *Shh* expression (**Figure 6. 19 c - e**) expression in the same region (Chiang et al. 1996). In contrast, it appears that cyclopamine treatment of Sp^{2H}/Sp^{2H} embryos resulted in near elimination of *Pax6* expression in the cranial neural tube (**Figure 6. 18 o & Figure 6. 19 o**). Of interest, loss of *Pax3* in Sp^{2H}/Sp^{2H} embryos induces the misexpression of *Msx1* in the forebrain, and cyclopamine treatment was found to induce *Msx1* forebrain misexpression in $+/+$ embryos (**Figure 6. 18 s & u**; orange arrow), the extent of which is increased further in Sp^{2H}/Sp^{2H} embryos (**Figure 6. 18 u & v**; orange arrows). Another feature of cyclopamine treatment was shrinking of the *Pax3* (**Figure 6. 19 p - r**) and *Msx1* (**Figure 6. 19 s & u**) domain in the dorsal midbrain region. As these transcription factors are inhibited by *Shh*, this effect was unexpected. On the other hand, *Pax3* and *Msx1* appear to be increased in the spinal region, as would be expected when *Shh* signalling is inhibited (Chiang et al. 1996). Lastly, as mentioned, while cyclopamine treatment appeared to increase *Bmp2* in the surface ectoderm (**Figure 6. 18 y - aa**), it appeared to decrease *Bmp2* in the dorsal midbrain region (**Figure 6. 19 y - aa**).

Overall, cyclopamine treatment resulted in decreased *Foxa2* expression and the ventral expansion of *Pax6*, as expected from the literature. The substantial reduction in *Pax3* and *Msx1*, together with *Bmp2* was unexpected. This may demonstrate regional differences in transcription factor regulation along the rostrocaudal axis, and/ or involve an overall decrease in neuroepithelial tissue, which can be seen in sections of cyclopamine treated embryos (**Figure 6. 19**).

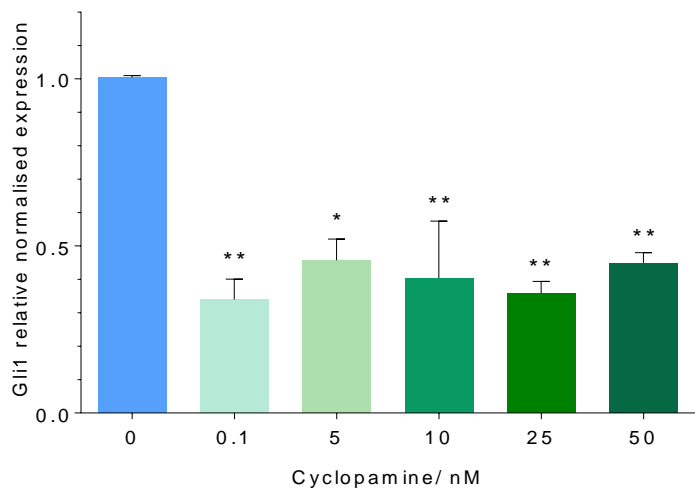


Figure 6. 17. *Gli1* mRNA expression in CD1 embryos treated with 0 – 50 nM cyclopamine

Relative expression of *Gli1* mRNA was significantly reduced in whole E9.5 embryos by 0.1 nM (0.34 ± 0.06 ; $p = 0.004$), 5 nM (0.46 ± 0.06 ; $p = 0.01$), 10 nM (0.40 ± 0.17 ; $p = 0.007$), 25 nM (0.36 ± 0.04 ; $p = 0.005$) and 50 nM (0.45 ± 0.03 ; $p = 0.01$) cyclopamine compared to control, control embryos (0 nM; 1.01 ± 0.004). Normalised to *Gapdh*. For each dose, $n = 3$.

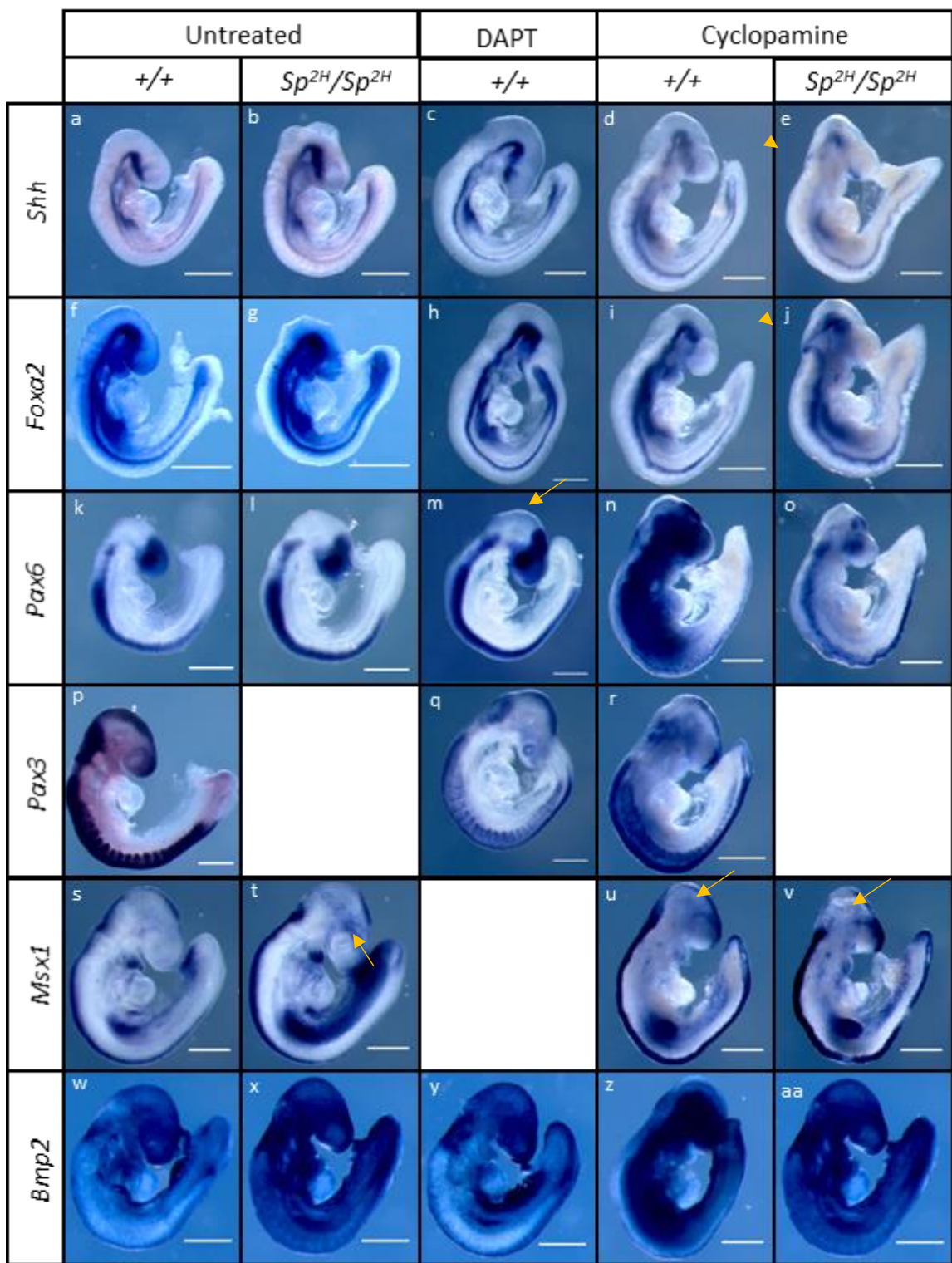


Figure 6. 18. Patterning transcription factors in DAPT and cyclopamine treated whole mount embryos

Shh (a – e), *Foxa2* (f – g), *Pax6* (k – o), *Pax3* (p – r), *Msx1* (s – v) and *Bmp2* (w – aa) expression after WMISH. Arrowheads in e and j indicate changed floorplate morphology; arrow in m indicates increased Pax6 expression; arrows u and v indicate *Msx1* misexpression. Two embryos assessed per condition and probe, except for DAPT treatment were only one embryo per probe was assessed. Scale bars represent 500 μ m.

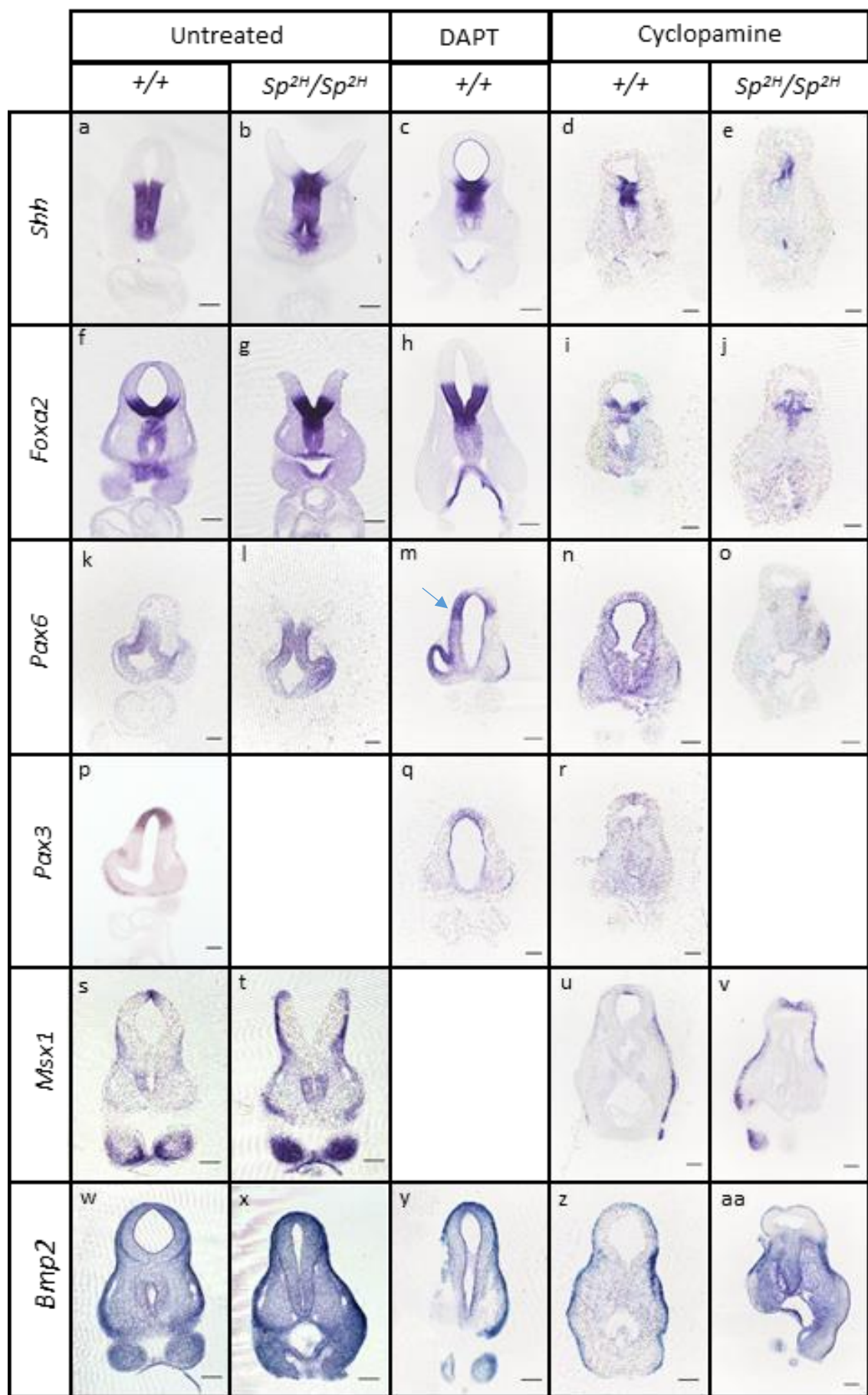


Figure 6.19. Patterning transcription factors in DAPT and cyclopamine treated sections.

Figure 6. 19. Patterning transcription factors in DAPT and cyclopamine treated sections.

Coronal section through the midbrain region of whole mount embryos shown in Figure 7.11. Blue arrow in m indicates what appears to be increased and misexpressed *Pax6* in the dorsal neural tube. Scale bars represent 100 μ m.

6.3.2.2.2 Analysis of cranial neural tube closure in Sp^{2H}/Sp^{2H} embryos

Embryos were recorded as either having failed or achieved cranial neural tube closure, after which genotyping was performed on the yolk sac. The frequency of embryos with obviously open cranial neural folds appeared lower (40%; $n = 4/0$) among cyclopamine treated embryos than among control Sp^{2H}/Sp^{2H} embryos (71%; $n = 25$ not cultured). However, more detailed examination of treated Sp^{2H}/Sp^{2H} embryos indicated that cranial neural tube closure was not complete in 4 of the 6 embryos initially thought to have achieved closure. 2 out of the 6 embryos had a phenotype where the dorsal tips of the neural tube in the midbrain region did not appear to have apposed normally (**Figure 6. 20 a & c**). After WMISH was performed and the embryos sectioned, it became clear that neural tube closure had not in fact occurred, but the ventral neural tube was elevated into the dorsal region (**Figure 6. 20 b & d**; orange arrows). This has been noted previously in *Shh* null embryos (Chiang et al. 1996). Additionally, in a further 2 mutant embryos, a region of incomplete closure of the midbrain neural tube, not much larger than 40 μ m, was detected. Therefore, the 80% of cyclopamine treated Sp^{2H}/Sp^{2H} embryos had failed to complete closure, indicating that partial inhibition of the Shh pathway does not prevent exencephaly in Sp^{2H}/Sp^{2H} embryos, at least at the dose tested.

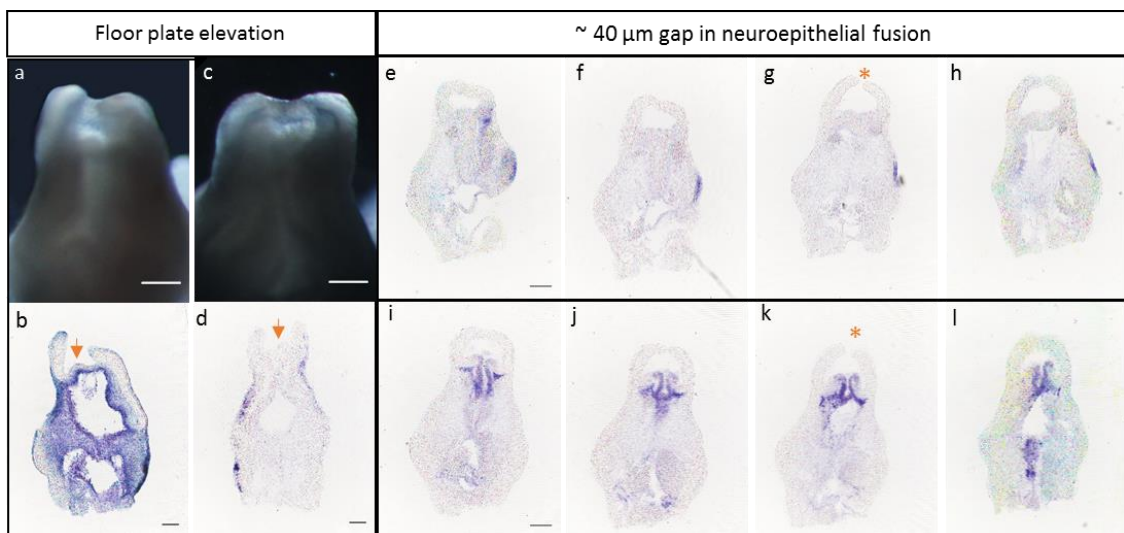


Figure 6. 20. Cranial phenotype in 4 out of 10 Sp^{2H}/Sp^{2H} embryos.

Figure 6. 20. Cranial phenotype in 4 out of 10 Sp^{2H}/Sp^{2H} embryos.

Images **a – d** demonstrate a cranial phenotype which gave the impression that closure was achieved (**a & c**) but was found to be open with a deformed and elevated floorplate (**b & d**; orange arrows). Images **e – h** and **i – l** show gaps in neuroepithelial fusion (orange asterix) which was not visible prior to sectioning. The gap is no larger than 40 μm as this is the thickness of the sections and the neuroepithelium in the adjacent sections (**f – h & j - k**) are fused. Scale bar represents 100 μm .

6.3.2.2.3 Premature closure of PNP in $+/+$ and $Sp^{2H}/+$ embryos

While examining cranial closure, it was noticed that a proportion of cyclopamine-treated embryos had completed PNP closure at somite stages ranging from 22 – 26 somite pairs, which is earlier than in control embryos or *in vivo*. This was a reproducible finding; in five out of seven culture experiments, one or two embryos had prematurely completed PNP closure. Genotyping revealed that only $+/+$ and $Sp^{2H}/+$ cyclopamine treated embryos were affected, with 71 % of $+/+$ embryos, and 16 % of $Sp^{2H}/+$ embryos, exhibiting premature PNP closure ($p < 0.0001$; **Figure 6. 21**). In comparison with data obtained from litters developing *in vivo* until explanted at E10 – 10.5, the earliest somite stage at which PNP closure was completed was 28 in the case of $+/+$, and 29 in the case of $Sp^{2H}/+$ embryos. A comparison of CR length to somite stage did not find embryos with closed PNPs to be distinguished from their littermates with open PNPs on the basis of size (**Figure 6. 22**).

The finding of premature PNP closure in $+/+$ and $Sp^{2H}/+$ cyclopamine treated embryos prompted the question of whether the PNP size of Sp^{2H}/Sp^{2H} embryos are smaller than stage matched control embryos. As all cultured litters were cyclopamine treated in this preliminary set of experiments, there is only data from control, *in vivo* developed embryos to compare with. An assessment of the CR lengths of untreated, *in vivo* developed and untreated, cultured *ct* embryos suggests that growth is not significantly delayed by culture (**Appendix; Figure A3A & B**). Therefore, a comparison of CR length and PNP size is shown for stage matched untreated, *in vivo* and cyclopamine cultured Sp^{2H}/Sp^{2H} embryos (**Figure 6. 23**). This analysis found that while cyclopamine Sp^{2H}/Sp^{2H} treated embryos had a significantly decreased mean CR length compared to untreated Sp^{2H}/Sp^{2H} embryos ($p = 0.0002$), their PNP lengths were not different in size, or may have shown some tendency towards being larger. The apparent growth retarding effect of cyclopamine was found in stage matched $+/+$ and $Sp^{2H}/+$ embryos also ($p < 0.0001$; **Figure 6. 24**). This finding is in keeping with the known mitogenic role of Shh signalling, and the decreased size of embryos genetically engineered with disruption of this pathway (Chiang et al. 1996).

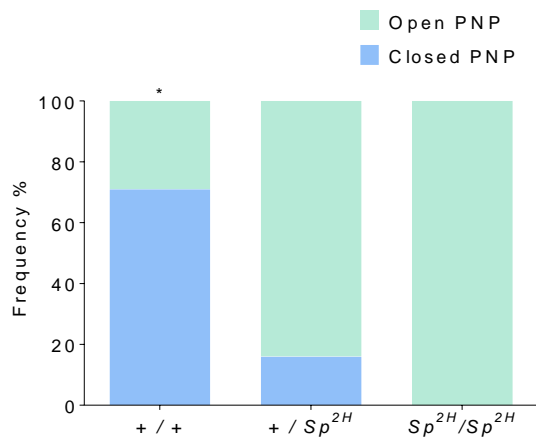


Figure 6. 21. Proportion of cyclopamine treated $+/+$, $Sp^{2H}/+$ and Sp^{2H}/Sp^{2H} embryos exhibiting premature PNP closure

71.43 % of $+/+$ (5/7), 16.00 % of $Sp^{2H}/+$ (4/25) and 0 % of Sp^{2H}/Sp^{2H} embryos exhibited closure of the PNP between 22 – 26 somite stages (* $p < 0.0001$; Chi-square test).

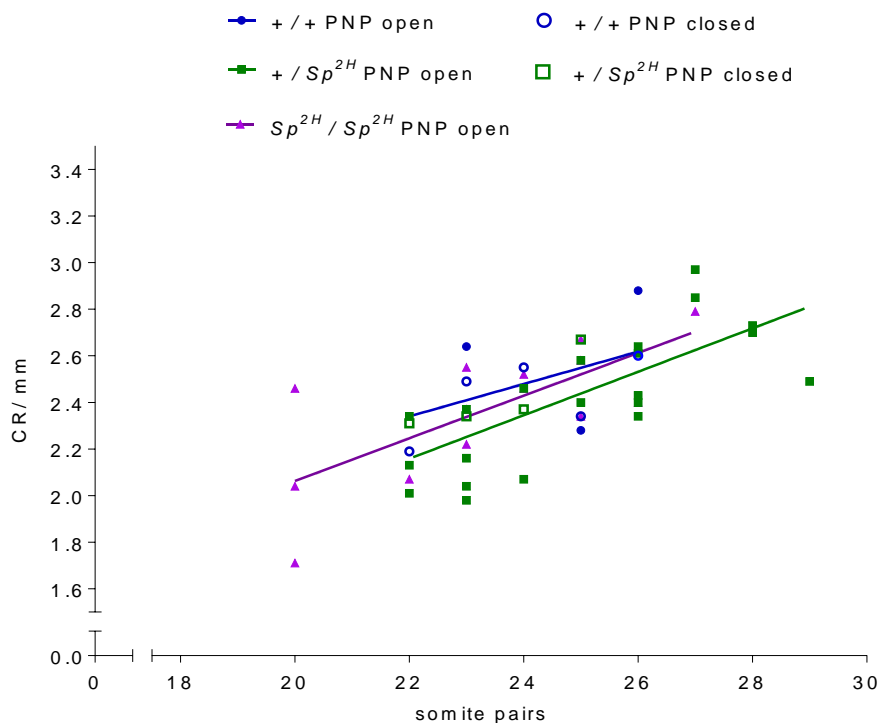
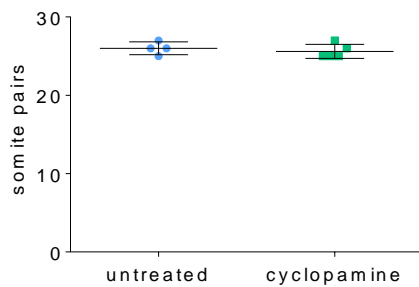


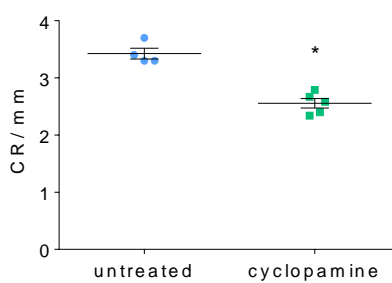
Figure 6. 22. CR length and somite stage in cyclopamine treated $+/+$, $Sp^{2H}/+$ and Sp^{2H}/Sp^{2H} embryos.

Relationship between CR length and somite pair number in $+/+$ ($r^2 = 0.22$), $Sp^{2H}/+$ ($r^2 = 0.55$) and Sp^{2H} / Sp^{2H} ($r^2 = 0.53$) embryos. Embryos with closed PNPs are distinguished by their unfilled symbols.

(A)



(B)



(C)

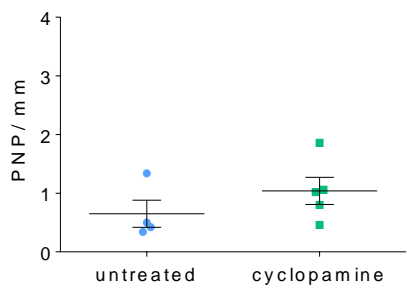


Figure 6. 23. CR and PNP lengths of untreated and treated *Sp*^{2H}/*Sp*^{2H} embryos

(A) A set of 4 *in vivo* developed, untreated *Sp*^{2H}/*Sp*^{2H} embryos (26.00 ± 0.41) and 5 cyclopamine cultured *Sp*^{2H}/*Sp*^{2H} embryos (25.60 ± 0.40) were found to be stage matched. (B) Cyclopamine cultured *Sp*^{2H}/*Sp*^{2H} embryos (2.56 ± 0.08 mm; $n = 5$) had reduced CR lengths compared to untreated *Sp*^{2H}/*Sp*^{2H} embryos (3.43 ± 0.09 mm; $n = 4$; $*p = 0.0002$; t-test). (C) There was no difference in PNP size between cyclopamine cultured *Sp*^{2H}/*Sp*^{2H} embryos (1.04 ± 0.23 mm; $n = 5$) and untreated *Sp*^{2H}/*Sp*^{2H} embryos (0.65 ± 0.23 mm; $n = 4$).

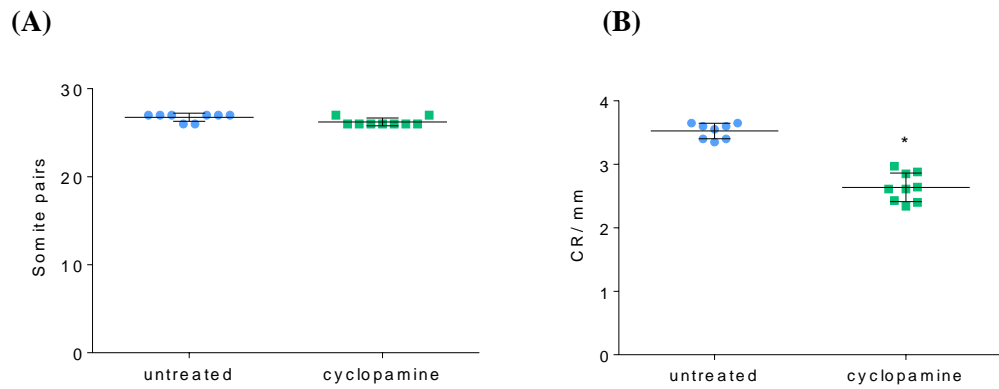


Figure 6.24. CR length of stage matchd treated $+/+$ and $Sp^{2H}/+$ embryos

(A) A group of 8 *in vivo* developed, untreated $+/+$ and $Sp^{2H}/+$ embryos (26.75 ± 0.16) and 9 cyclopamine cultured $+/+$ and $Sp^{2H}/+$ embryos (26.22 ± 0.15) were found to be stage matched. (B) Cyclopamine treated $+/+$ and $Sp^{2H}/+$ embryos (2.64 ± 0.07 mm) had reduced CR lengths compared to untreated $+/+$ and $Sp^{2H}/+$ embryos (3.53 ± 0.04 mm; $*p < 0.0001$; t-test).

6.4 Discussion

6.4.1 Folic acid supplementation and the *Splotch* mouse

Government programs for the folic acid fortification of certain grain products now exist in 87 countries (Food Fortification Initiative 2017), and this has led to a reduction in prevalence of NTDs (Eichholzer, Tonz, and Zimmermann 2006). Ensuring populations obtain the recommended daily intake of folates is undoubtedly crucial, however, the full implications of such programs on long-term population health are not clear. A study looking at the transgenerational effect of folic acid treatment in mice found that folic acid supplementation could have a deleterious effect on neural tube closure in a manner which was dependant on the genetic defect and the length of folic acid exposure (Marean et al. 2011). Additionally, excessive maternal folic acid supplementation (10 – 20 fold higher than the recommended intake for rodents) was found to be associated with embryonic delay and growth restriction (Pickell et al. 2011), and embryonic loss and heart defects (Mikael et al. 2013) in wild-type mice on a BALB/c background. These studies suggest that a better understand of how folic acid prevents NTDs, and a more nuanced approach to folic acid supplementation may be required.

The *Splotch* mouse is an established model for folic acid responsive NTDs, making it a model in which the molecular and cellular preventative effect(s) of folic acid can be better understood. However, the mechanism(s) by which loss of *Pax3* expression results in NTDs is not understood. How NTDs arise in the *Splotch* mouse is a key question in itself to better understand the requirements for neural tube closure, and is also an important question for understanding the genetic context in which folic acid can prevent NTDs.

6.4.2 Proliferation in the neural tube

The fact that folic acid can prevent a proportion of NTDs in *Splotch* may suggest an underlying proliferation defect but is certainly not proof; folic acid supplementation is able to ameliorate a variable proportion of NTDs in *Gcn5* hypomorphic mice and the *Crooked tail* (*Lrp6^{Cd}* mutant) without an underlying proliferation defect being found (Lin et al. 2008; Gray et al. 2013). However, there is evidence to suggest that loss of *Pax3* may decrease proliferation in the dorsal neural tube.

The results from this study suggest that the proportion of cells in S-phase to late G₂-phase is decreased in the dorsal midbrain region (*Pax3* expressing domain) of *Sp^{2H}/Sp^{2H}* embryos in comparison to *+/+* embryos, while the mitotic index, which is a snap-shot at the time of fixation, was unchanged. The results presented here also find that the proportion of cells in G₂-phase (non-mitotic, pHH3 positive) was increased in the dorsal forebrain and ventral regions of *Sp^{2H}/Sp^{2H}* embryos in comparison to *+/+* embryos. Overall, there is an increase in the proportion of cells in S-

phase to G₂-phase when going from the ventral to the dorsal midbrain region of +/+ embryos which is lost in *Sp*^{2H}/*Sp*^{2H} embryos, presumably as a consequence of loss of *Pax3* expression. The ventral-low, dorsal-high proliferation gradient in wild-type embryos has been demonstrated in the spinal (Megason and McMahon 2002; McShane et al. 2015) and hindbrain regions of the neural tube (Kim et al. 2007). It has not, to our knowledge, previously been described in the midbrain region.

Most significantly, folic acid supplementation increased the percentage of cells which were in S-phase during the 15-minute pulse of BrdU and then moved into G₂-phase by the time of fixation, in the dorsal midbrain of *Sp*^{2H}/*Sp*^{2H} embryos. This suggests that the transition from S-phase to G₂-phase is increased by folic acid. It is interesting to note that the percentage of mitotic or BrdU positive cells is not found to increase, suggesting that the proportion of cells in S-phase or mitosis at any given time has not increased, but the length of the cell cycle has decreased.

Overall, the results suggest that loss of *Pax3* decreases proliferation in the dorsal midbrain region of the cranial neural tube; the region which fails to close in 60 – 70 % of *Sp*^{2H}/*Sp*^{2H} embryos. While studies have found that folic acid stimulates proliferation of neural progenitors *in vitro* (Zhang et al. 2008; Ichi et al. 2010; Huan Liu et al. 2010), this study provides *in vivo* evidence to suggest that the ameliorating effects of folic acid supplementation on exencephaly in *Sp*^{2H}/*Sp*^{2H} embryos could be mediated via stimulation of the transition from S-phase to M-phase, and therefore, proliferation.

6.4.3 The Shh pathway in the *Splotch* mouse

This study investigated the possibility that signalling through the Shh pathway was increased in *Sp*^{2H}/*Sp*^{2H} embryos. Evidence supporting this hypothesis included partial rescue of exencephaly with DAPT treatment (N. Greene, person communication) and increased expression of the Shh target versican *Sp*^{2H}/*Sp*^{2H} embryos (Henderson, Ybot-Gonzalez, and Copp 1997; Fedtsova, Perris, and Turner 2003; Nagy and Goldstein 2015). Additionally, as Shh is a known mitogen (Echelard et al. 1993; Rowitch et al. 1999), the significant increase in non-mitotic pHH3 positive cells, and tendency towards increased BrdU positive cells in *Sp*^{2H}/*Sp*^{2H} compared to +/+ embryos could also be indicative of an increase in *Shh* in the ventral neural tube.

The mRNA levels of the direct, positive targets of Shh signalling, *Ptch1* and *Gli1*, were found not to vary between +/+ and *Sp*^{2H}/*Sp*^{2H} embryos, in either the anterior or posterior embryo, as measured by qPCR. Of interest, while RNA *in-situ* hybridisation in the cranial region also did not detect increased *Ptch1* or *Gli1*, but found what appears to be a slight increase in *Shh* expression itself. Together, with the finding that cyclopamine treatment does not prevent exencephaly in *Sp*^{2H}/*Sp*^{2H} embryos, these results suggest that increased Shh signalling is unlikely to be involved in the aetiology of cranial NTDs in these embryos.

There was, on the other hand, evidence that *Shh* and its targets, *Ptch1* and *Gli1*, were expressed in increased levels in the upper and caudal spinal neural tube. Whether cyclopamine treatment can prevent spina bifida in *Sp*^{2H}/*Sp*^{2H} embryos is currently an open question. Comparison of PNP lengths of stage matched *in vivo* developed, untreated and cyclopamine treated *Sp*^{2H}/*Sp*^{2H} embryos suggests not. However, as the untreated embryos were developed *in vivo*, this should be assessed using the appropriate cultured, untreated control. Additionally, due to the difference in embryo size that is likely to arise between cyclopamine treated and untreated embryos, PNP size before closure may not be suitable for comparison. The difference in PNP size between +/+ and *Sp*^{2H}/*Sp*^{2H} embryos is significant from the 10-11 somite stage (Palmer 2014), meaning that cyclopamine treatment should ideally begin just before this stage, which is the same stage that cyclopamine treatment was begun in the current experiment to assess exencephaly. In the current experiments, embryos cultured from this time point were not cultured past the stage of PNP closure (30 plus somites) as they were beginning to die. Replenishing the culture with new rat serum after 24 hours, and/or decreasing the dose of cyclopamine could be tried in order to keep the culture running longer.

The current study found that cyclopamine treatment stimulated PNP closure in +/+ and *Sp*^{2H}/+ embryos, such that closure was achieved at or before the 26 somite stage in a proportion of these embryos. *Shh* null embryos have been noted for displaying DLHPs at developmental stages earlier than +/+ embryos (Patricia Ybot-Gonzalez et al. 2002), but whether they achieve premature PNP closure is not known. Studies of *Bmp2* null embryos, which also exhibit premature, exaggerated DLHP formation also found complete closure of the spinal neural tube at the 15 somite stage (Ybot-Gonzalez et al. 2007), suggesting that premature DLHP formation could lead to premature PNP closure. It is therefore proposed that premature PNP closure observed in cyclopamine treated +/+ and *Sp*^{2H}/+ embryos is likely due to the occurrence of premature DLHP formation in response to reduced *Shh* signalling. The appearance of premature PNP closure shows a gene dosage effect in respect to *Pax3*, with a higher proportion observed in +/+, compared to *Sp*^{2H}/+ embryos, and higher in *Sp*^{2H}/+ compared to *Sp*^{2H}/*Sp*^{2H} embryos. It is possible that loss of *Pax3* interferes with DLHP formation, but it is equally possible that another process mediated by *Pax3* is required for PNP closure.

Overall, it is believed that the results do not implicate a significant role of *Shh* signalling in the cause and prevention of NTDs in *Sp*^{2H}/*Sp*^{2H} embryos. This conclusion is perhaps supported by the differences in NTDs exhibited by *Splotch* mice and mutants with *Shh* pathway over activation. While *Sp*^{2H}/*Sp*^{2H} mice display nearly fully penetrant spina bifida and 60 – 70 % display exencephaly, mutants with increased *Shh* signalling due to loss of *Gli3* (*Xt*^l; Hui & Joyner 1993), *Rab23* (Gunther et al. 1994), *Tulp3* (Ikeda et al. 2001), *Ift172* (Huangfu et al. 2003), *Kif7* (Endoh-Yamagami et al. 2009), *Fkbp38* (Shirane et al. 2008) and digenic *Prkaca*; *Prkacb* (Huang, Roelink, and McKnight 2002) present with increased rates of cranial NTDs over spinal NTDs. At the most severe end of the spectrum, *Ptch1* mutants exhibit craniorachischisis (Milenkovic et al. 1999; Goodrich et al.

1997). The exception to this is the *hitchhiker* mutant, which has hypomorphic *Tulp3* expression, and a higher frequency of spina bifida than exencephaly (Patterson et al. 2009).

6.4.3.1 Change in patterning transcription factors

The dorsoventral expression of patterning transcription factors expressed by neural progenitor cells has not been well characterised in the cranial region, while it is relatively well characterised in the upper spinal cord region. Additionally, any changes in the boundaries of patterning transcription factors, as a result of loss of *Pax3*, have not previously been investigated in the cranial or spinal neural tube. Therefore, transcription factor patterning was studied in the cranial and spinal neural tubes of $+/+$ and Sp^{2H}/Sp^{2H} embryos, as any changes may provide some indication of changes in the local signalling environment.

WMISH was used to investigate progenitor cell transcription factor (*Foxa2*, *Pax6* and *Msx1*) patterning in the cranial, intermediate spinal and caudal neural tube regions of $+/+$ and Sp^{2H}/Sp^{2H} embryos. To summarise, with the inclusion of *Shh* and *Bmp2* expression, in the cranial region Sp^{2H}/Sp^{2H} embryos were found to have increased *Shh*, *Msx1* and *Bmp2* expression, while *Foxa2* and *Pax6* appeared unchanged. In the intermediate spinal region, Sp^{2H}/Sp^{2H} embryos were found to have increased *Shh*, *Pax6*, and *Bmp2* (hindbrain expression), while *Msx1* appeared relatively unchanged. In the caudal neural tube, Sp^{2H}/Sp^{2H} embryos were found to have increased *Shh*, *Foxa2*, and *Bmp2* expression, while *Msx1* appeared reduced and *Pax6* expression was not determined. Therefore, while both *Shh* and *Bmp2* demonstrate increased expression along the entire anterior to posterior neuraxis of Sp^{2H}/Sp^{2H} embryos, the transcription factors studied show differential expression pattern changes dependant on the neuraxis, suggesting differential regulation.

The increase in *Shh* expression may be a result of loss of *Pax3* itself, which would imply a *Shh* repressive function of *Pax3*, converse to the known *Pax3* repressive function of *Shh* (Chiang et al. 1996). However, as the distance between the *Pax3* and *Shh* expression domain is quite large, it is perhaps more likely that this is an indirect effect. Which factors could be involved is currently unknown. *Foxa2* expression is induced by *Gli2* activator function in response to *Shh* from the notochord in the ventral neural tube from the midbrain, hindbrain and spinal neural tube, but not in the forebrain region (Matise et al. 1998). The finding that *Shh* but not *Foxa2* is increased in the cranial and upper spinal region, while both *Shh* and *Foxa2* are increased in the caudal region could suggest that there may be additional factors which integrate with *Gli2* activator function to control *Foxa2* expression along the anterior to posterior neuraxis.

Pax6 expression appears unchanged in the cranial region but shifts dorsally in the intermediate spinal region. *Pax6* expression in chick neural explants has been shown to be strongly induced by retinoic acid (Novitch et al. 2003), while its expression is known to be inhibited by high levels of

Shh signalling (Cooper et al. 2005; Endoh-Yamagami et al. 2009), establishing its ventral border. In the dorsal neural tube, Pax6 expression is also inhibited by high levels of BMP signalling which may define its dorsal border (Timmer, Wang, and Niswander 2002). Therefore, increased *Shh* and *Bmp2* expression may be expected to decrease the *Pax6* expression domain, with both a dorsal shift of the ventral boundary and a ventral shift of the dorsal boundary. Instead, in *Sp*^{2H}/*Sp*^{2H} embryos, the ventral and dorsal borders of *Pax6* expression were shifted dorsally, while it appeared unchanged in the cranial region. It is possible that Pax3 represses Pax6, as it does Pax7 (Borycki et al. 1999) and Dbx1 (Gard et al. 2017), which helps define the Pax6 dorsal boundary in addition to BMP signalling. It is equally possible that other, unknown factors are involved in the dorsal shift seen. The difference in *Pax6* expression found between +/+ and *Sp*^{2H}/*Sp*^{2H} embryos in the spinal region but not the cranial region could demonstrate a difference in regulation of Pax6. However, it is also possible that the lack of precisely comparable sections has interfered with the detection of any changes.

Msx1 (and *Msx2*) are known, positive, downstream targets of BMP signalling in the neural tube (Esteves et al. 2014) and *Msx2* has previously been shown to be increased in *Splotch* mutants (Kwang et al. 2002). Therefore, the observed increase in *Msx1* expression suggested that *Bmp2* may also be increased in *Sp*^{2H}/*Sp*^{2H} embryos. *Bmp2* expression was subsequently found to be increased throughout the rostro-caudal neuraxis. BMPs, in particular *Bmp2*, *Bmp4* and *Bmp7*, are expressed from the surface ectoderm before neural tube closure (Liem et al. 1995; Ybot-Gonzalez et al. 2007), while *Bmp4* is also known to be expressed from both the surface ectoderm and roofplate after closure (Liem et al. 1995). The results from this study demonstrate that *Bmp2* is also expressed from the surface ectoderm and the dorsal neural tube in the closed hindbrain region of +/+ embryos. On the other hand, *Bmp2* expression appears to cover a larger proportion of the closed dorsal neural tube in the cranial and caudal regions. In comparison to +/+ embryos, *Sp*^{2H}/*Sp*^{2H} embryos demonstrate an increased area of *Bmp2* expression in the dorsal neural tube and increased expression in the ventral region throughout the neuraxis. How loss of *Pax3* could lead to increased *Bmp2* expression is an interesting question which requires more research. As the dorsal border of *Pax3* and the ventral border of *Bmp2* expression are adjacent, it is possible that Pax3 can directly repress *Bmp2* expression. It is also possible that Pax3 induces the expression of another protein which inhibits *Bmp2* expression. A potential candidate is sFRP1, which is expressed by the surface ectoderm from E8.5 onwards, with sFRP1 null mice found to have increased surface ectoderm expression of *Bmp4* (Misra and Matise 2010).

To summarise, the mRNA expression, of all factors involved in dorsoventral neural tube patterning that were studied, were found to be increased at least at one level along the neuraxis. While the increase in *Foxa2* and *Msx1* can be attributed to the increases in *Shh* and *Bmp2* respectively, how loss of Pax3 increases *Shh* and *Bmp2* is currently not understood.

6.4.4 Increased *Bmp2* involved in aetiology of NTDs?

The finding that *Bmp2* expression is increased in *Sp^{2H}/Sp^{2H}* embryos leads to the question of whether this could be involved in the aetiology of NTDs in this model, since *Bmp2* is found to inhibit DLHP formation in the spinal neural tube (Ybot-Gonzalez et al. 2007). Additionally, mice null for the BMP inhibitor, *noggin*, exhibit exencephaly, the rate of which is dependent on genetic background (McMahon et al. 1998), and may occur due to a lack of dorsolateral bending in the cranial region (Stottmann et al. 2006).

As *noggin* is induced by *Bmp2* in the dorsal neural tube (Ybot-Gonzalez et al. 2007), it is possible that *Sp^{2H}/Sp^{2H}* embryos also express increased *noggin*, and the overall effect on BMP pathway activation remains unknown. Comparison of phospho-Smad 1,5,8 immunohistochemistry in sections from *+/+* and *Sp^{2H}/Sp^{2H}* embryos could indicate changes in pathway activation. To assess whether increased BMP signalling may be interfering with neural tube closure in *Sp^{2H}/Sp^{2H}* embryos, litters from *Sp^{2H}/+* intercrosses could be cultured with exogenously added BMP inhibitors, such as recombinant noggin protein. One important point if undertaking this experiment is that too little *Bmp2* expression also results in exencephaly (Singh et al. 2008; Castranio and Mishina 2009). Alternatively, comparing compound mutant *Sp^{2H}/Sp^{2H}*; *Bmp2^{+/−}* and *Sp^{2H}/Sp^{2H}*; *Bmp2^{+/+}* embryos may prove informative.

7 General discussion

The studies presented in this thesis have aimed to investigate: a) environmental factors and genetics which may modulate the frequency of NTDs in the folic acid-resistant *ct* mouse model, and; b) how loss of *Pax3* in the folic acid-responsive *Splotch* mouse may cause NTDs, and the effects of folic acid supplementation on cranial neuroepithelial proliferation. As the results, possible hypotheses and future perspectives have been discussed within the chapters, a summary of the findings, their possible overarching implications and relevance to human NTDs are discussed here.

7.1 Summary of key findings

This project has found:

- i. Nucleotides administered orally can prevent NTDs, as has been shown previously for intra-peritoneal administered nucleotides. A combination of nucleotides and inositol appears to prevent a greater proportion of spina bifida and exencephaly in *ct* mice compared to either nucleotide or inositol treatment alone. Treatments containing inositol were found to affect the relative distribution of folate cofactors.
- ii. Reduced expression of *Mthfd1L* in *ct* mice and *Splotch* mice, as compared to expression in C57Bl/6 wild-type mice. While *ct* mice were found to have reduced circulating formate, *Splotch* mice did not (as compared to wild-type *Gldc^{GT1}* mice on a mixed 129/Sv and C57Bl/6 background). Significantly, while NTDs in *ct* mice were prevented by formate treatment, NTDs in the *Splotch* mice were not. Formate treatment is likely to prevent NTDs by enhancing provision of one-carbon units for *de novo* nucleotide synthesis and increasing proliferation in *ct* mice.
- iii. Caffeine did not interfere with neural tube closure in wild-type, CD1 embryos. Caffeine prevented spina bifida without affecting the rate of exencephaly in *ct* mice. In *ct* mice, caffeine was found to affect the relative distribution of folate cofactors and increase the abundance of PCNA and total ERK protein. Overall, the results suggest that caffeine may increase proliferation.
- iv. *Splotch* mutants were found to have a decreased proportion of BrdU positive and (non-mitotic) pHH3 positive nuclei in the dorsal midbrain neuroepithelium, when compared to wild-type littermates. Overall, folic acid supplementation was found to normalise the proportion of BrdU and pHH3 labelled nuclei in mutant samples and increase the proportion of doubly labelled BrdU and pHH3 nuclei, suggesting stimulation of proliferation in the dorsal midbrain neuroepithelium. Additionally, increased Shh

signalling from the ventral neural tube, as a cause of NTDs in *Splotch* mutants was investigated but found to be unlikely. Increased *Bmp2* expression, which could interfere with dorsolateral bending, was found in mutant embryos.

7.2 Folate one-carbon metabolism in *curly tail* and *Splotch* mice

Both the *ct/ct* and *Sp^{2H}/Sp^{2H}* mice were found to have similarly reduced *Mthfd1L* expression compared to congenic mice (+^{ct}/+^{ct}) and wild-type mice on a C57Bl/6 background. It is possible that *Splotch* and *ct* mice have similar levels of *Mthfd1L* expression as it is part of their shared CBA background. However, experiments suggest that they are not alike in other aspects of FOCM, as summarised in **Table 7. 1**. While *Splotch* mice show deficits in *de novo* nucleotide synthesis and respond to folic acid and intra-peritoneal thymidine supplementation (Fleming and Copp 1998; Beaudin et al. 2011), they did not respond to either exogenous, oral formate or nucleotide treatment. On the other hand, *ct* mice do not show any deficit in thymidylate synthesis and do not respond to folic acid (Fleming & Copp 1998), but do respond to exogenous, oral formate (Sudiwala et al. 2016), and oral and intra-peritoneal nucleotide treatments (Leung et al. 2013). Most interestingly, while *ct* mice exhibit a lower concentration of circulating formate compared to wild-type mice on a mixed 129/Sv and C57Bl/6 background, *Splotch* mice do not.

A possible explanation for why *Splotch* mice are unresponsive to formate treatment could be that folates are limiting in some way. It may be that their function is limited rather than their absolute levels, as data from the lab indicates that total folate is similar in E10.5 *ct* and *Splotch* embryos (unpublished data). This hypothesis could be consistent with folic acid supplementation preventing NTDs in this model. It could also explain why plasma and urine formate levels are higher in *Splotch* mice compared to *ct* mice, as functional folate deficiency could be expected to mimic absolute folate deficiency and increase circulating formate concentration (Pai et al. 2015; Lamarre et al. 2012). As stated previously, supplementation of *Splotch* mice with both formate and folic acid could prove insightful, as could metabolic labelling studies in *ct*, *Splotch* and C57Bl/6 mice.

	<i>curly tail</i>	<i>Splotch</i>
<i>Mthfd1L</i> expression	Hypomorphic [^]	Hypomorphic [^]
Circulating formate levels	Low [#]	Normal [#]
Impairment in <i>de novo</i> nucleotide synthesis	None in thymidylate synthesis ¹	In both thymidylate ¹ and purine synthesis ²
Formate response	Responsive	None
Folic acid response	None ¹	Responsive ¹
Nucleotide response	Responsive to intra-peritoneal nucleotides ³ and oral nucleotides	Responsive to intra-peritoneal thymidine ¹ but not oral nucleotide

Table 7. 1. Similarities and differences in folate one-carbon metabolism between *ct* and *Splotch* mice

[^] compared to congenic wild-type (+^{ct}/+^{ct}) mice. [#] compared to *Gldc* wild-type mice (mixed 129/Sv and C57Bl/6 background). ¹ Fleming & Copp (1998). ² Beaudin et al. (2011). ³ Leung et al. (2013).

7.3 Prevention of neural tube defects in *curly tail* mice correlate with changes in abundance of folate cofactors

An interesting finding of this project had been the association between treatments leading to a decreased frequency in NTDs in *ct* mice and changes in the percentage distribution of folate cofactors, namely decreased 5-methylTHF, increased THF and the tendency towards increased formylTHF. The exception is for nucleotide treatment, which predictably had little effect on folate cofactors. A comparison of the percentage reduction in the frequency of spina bifida and the percentage change in 5-methylTHF, THF and formylTHF under each supplementation, finds that the reduction in spina bifida is most tightly correlated with the reduction in relative 5-methylTHF (**Table 7. 2**). Together with SAM and SAH measurements, this may suggest that diversion of one-carbon units away from the methionine cycle for retention in the *de novo* nucleotide synthesis pathways, leads to prevention of NTDs in *ct* mice, presumably through stimulation of *de novo* nucleotide synthesis and increased proliferation.

Change in	Treatment (% change)				
	Nucleotide + inositol	Formate	Caffeine	Inositol	Nucleotide
Spina bifida	-82	-71	-60	-53	-47
5-methylTHF	-30	-20	-23	-17	-2
THF	184	238	206	143	-1
FormylTHF	205	661	203	188	-48

Table 7. 2. Percentage change in spina bifida and folate cofactors by treatment in *ct* mice.

Negative numbers indicate a decrease in percentage while positive numbers indicate an increase in percentage.

7.4 Relevance of the *ct* and *Splotch* models to human neural tube defects

The major causes of the development of NTDs in humans, whether genetic or environmental, have not been identified to date, although cluster outbreaks in the USA have been linked to exposure to fumonisins (Missmer et al. 2006), and risk factors such as maternal diabetes and anti-epileptics have been identified (Gelineau-van Waes et al. 2005; Ornoy et al. 2015). The similarities in neural tube closure between mouse and human, which are the location and order of closure from discrete closure points along the neuraxis, and also the existence of folic acid responsive and resistant NTDs, suggest a certain conservation of the genetic and environmental factors which are required for successful neural tube closure. The mouse is therefore a tool to help understand neural tube closure, and the possible causes and prevention of NTDs in humans. However, studies to date suggest that while there is likely to be conservation between some genes, there are also likely to be species differences. Genes such as *CELSR1*, *SCRIB*, *AMT* and *GLDC* cause NTDs in mice when deleted, and suspected missense mutations in these genes are associated with human NTD cases (Lei et al. 2014, 2013; Narisawa et al. 2012; Pai et al. 2015). However, while the *MTHFR* 677C-->T mutation in humans is associated with NTDs in some human populations (van der Put et al. 1995), deletion in mice does not result in NTDs (Z. Chen et al. 2001).

Are *GRHL3* and *PAX3* function relevant to human neural tube closure? There is evidence to suggest so. Recently, a case-control study using a cohort of 233 spina bifida cases reported novel variants of *GRHL3* which are associated with spina bifida (Lemay et al. 2017). Using whole exome sequencing they identified two novel truncating variants and one missense variant which was demonstrated to cause reduced activation of target genes in a luciferase reporter assay (Lemay et al. 2015). Previously, the same group exome sequenced 43 sporadic spina bifida and anencephaly

cases and their unaffected parents. They reported one nonsense mutation in *PAX3*, predicted to result in a truncated protein, and one missense mutation in *GRHL3*, which was predicted to be damaging (Lemay et al. 2015). The *GRHL3* variant was subsequently shown to have reduced activator potential via luciferase reporter assay (Lemay et al. 2017). These studies found that protein coding mutations in *PAX3* could contribute to approximately ~ 2 % of human NTD cases in certain US populations, while coding mutations in *GRHL3* could account for ~1 %.

Mutation of *PAX3* in humans is known to cause Waardenburg syndrome types 1 and 3. Waardenburg syndrome type 1 patients manifest cranial neural crest defects, which typically include dystopia canthorum, heterochromic or hypoplastic blue irides, white forelock and congenital sensorineural deafness. Type 3 patients manifest a range of type 1 defects plus musculoskeletal abnormalities, often of the upper limb. There is now a small collection of case studies describing patients with mutations in *PAX3* and spina bifida, as well as the clinical symptoms of Waardenburg syndrome type 1 or 3 (Hol et al. 1995; Baldwin et al. 1995; Nye et al. 1998; Hart and Miriyala 2017). Hol et al. (1995) also cited seven other studies in which spina bifida was present in individuals affected by Waardenburg syndrome type 1, however mutations in *PAX3* were not screened for (de Saxe, Kromberg, and Jenkins 1984; Narod, Siegel-Bartelt, and Hoffman 1988; da-Silva 1991; Carezani-Gavin, Clarren, and Steege 1992; Begleiter and Harris 1992; Chatkupt, Chatkupt, and Johnson 1993; Moline and Sandlin 1993). Anencephaly/ exencephaly has also been reported in two cases of Waardenburg syndrome type 3, where both parents manifested Waardenburg syndrome type 1, which was confirmed as a heterozygous *PAX3* mutation in both parents of one of the cases (Mousty et al. 2015), but presumed in the other (Ayme and Philip 1995). Both patients with anencephaly/ exencephaly were presumed to carry homozygous mutations in *PAX3*. However, the appearance of an NTD with Waardenburg syndrome type 1 or 3 is considered rare; it was reported that a review of the Waardenburg Consortium database in 1999 found 6 cases of NTDs out of 617 cases of Waardenburg syndrome (Hart and Miriyala 2017), although it is not stated whether only types 1 and 3 were included. This may suggest that other predisposing factors must also be present, in addition to a mutation in *PAX3*, for human NTDs to occur. The biological consequences of each unique *PAX3* mutation could also be a factor in whether NTDs occur or not in conjunction with Waardenburg syndrome and further study is warranted.

As well as possibly being a model which is directly relevant to the aetiology of human NTDs, the *Splotch* mice are also a model for folic acid responsive NTDs. In this project, the *Splotch* mice have been used as a model in which to understand the kind of cellular defects folic acid treatment may be able to resolve and how it might be doing this. The investigations presented here are the first *in vivo* evidence to suggest that *Sp*^{2H}/*Sp*^{2H} embryos have a decreased rate of proliferation in the cranial midbrain neuroepithelium when compared with +/+ littermates, and that folic acid treatment prevents exencephaly in this model by increasing the rate of proliferation. Similarly, as well as the possibility that hypomorphic *Grhl3* expression is directly relevant to the aetiology of NTDs in

humans, the *ct* mouse is also a model of folic acid resistant NTDs. In this project, previous studies which found inositol and nucleotide treatments to prevent NTDs in the *ct* mouse have been extended, and suggest that a combination of oral nucleotide and inositol treatment is more efficacious than either treatment alone. The *ct* mouse is also a model for multifactorial NTDs, which is thought to reflect the multiple hit hypothesis concerning the majority of human NTD cases. *Lmn1b* is a genetic modifier locus in the *ct* background, with a polymorphism influencing risk of spina bifida and exencephaly (de Castro et al. 2012), while *Mthfd1L* could also affect risk of exencephaly, by itself or in conjunction with other modifier loci (Neumann et al. 1994; Letts et al. 1995). The ability of caffeine and formate treatment to prevent spina bifida may suggest that it is sufficient to address one of the underlying risk factors to make the embryo resilient to a closure defect. This project has provided a better understanding of the genetic and metabolic backgrounds of the *ct* and *Splotch* mice by investigating *Mthfd1L* expression, and formate and nucleotide treatments. As human health care moves into the era of personalised medicine, studies such as those presented here may someday assist in determining the course of preventative treatment for individual NTD cases, depending on the genetic and metabolic background of the parents.

References

Abu-Abed, S, P Dolle, D Metzger, B Beckett, P Chambon, and M Petkovich. 2001. "The Retinoic Acid-Metabolizing Enzyme, CYP26A1, Is Essential for Normal Hindbrain Patterning, Vertebral Identity, and Development of Posterior Structures." *Genes & Development* 15 (2). United States: 226–40.

Acquas, Elio, Stefania Vinci, Federico Ibba, Saturnino Spiga, Maria Antonietta De Luca, and Gaetano Di Chiara. 2010. "Role of Dopamine D(1) Receptors in Caffeine-Mediated ERK Phosphorylation in the Rat Brain." *Synapse (New York, N.Y.)* 64 (5). United States: 341–49. <https://doi.org/10.1002/syn.20732>.

Adams, R L, S Berryman, and A Thomson. 1971. "Deoxyribonucleoside Triphosphate Pools in Synchronized and Drug-Inhibited L 929 Cells." *Biochimica et Biophysica Acta* 240 (4). Netherlands: 455–62.

Akashi, M, S Akazawa, M Akazawa, R Trocino, M Hashimoto, Y Maeda, H Yamamoto, E Kawasaki, H Takino, and A Yokota. 1991. "Effects of Insulin and Myo-Inositol on Embryo Growth and Development during Early Organogenesis in Streptozocin-Induced Diabetic Rats." *Diabetes* 40 (12). United States: 1574–79.

Al-Wadei, Hussein A N, Takashi Takahashi, and Hildegard M Schuller. 2006. "Caffeine Stimulates the Proliferation of Human Lung Adenocarcinoma Cells and Small Airway Epithelial Cells via Activation of PKA, CREB and ERK1/2." *Oncology Reports* 15 (2). Greece: 431–35.

Albert, D A, and L J Gudas. 1985. "Ribonucleotide Reductase Activity and Deoxyribonucleoside Triphosphate Metabolism during the Cell Cycle of S49 Wild-Type and Mutant Mouse T-Lymphoma Cells." *The Journal of Biological Chemistry* 260 (1). United States: 679–84.

Alvarez-Medina, Roberto, Jordi Cayuso, Tadashi Okubo, Shinji Takada, and Elisa Marti. 2008. "Wnt Canonical Pathway Restricts Graded Shh/Gli Patterning Activity through the Regulation of Gli3 Expression." *Development (Cambridge, England)* 135 (2). England: 237–47. <https://doi.org/10.1242/dev.012054>.

American Pregnancy Association. n.d. "Caffeine Intake During Pregnancy." <http://americanpregnancy.org/pregnancy-health/caffeine-during-pregnancy/>.

An, Songon, Yijun Deng, John W Tomsho, Minjoung Kyoung, and Stephen J Benkovic. 2010. "Microtubule-Assisted Mechanism for Functional Metabolic Macromolecular Complex Formation." *Proceedings of the National Academy of Sciences of the United States of America* 107 (29). United States: 12872–76. <https://doi.org/10.1073/pnas.1008451107>.

An, Songon, Ravindra Kumar, Erin D Sheets, and Stephen J Benkovic. 2008. "Reversible Compartmentalization of de Novo Purine Biosynthetic Complexes in Living Cells." *Science (New York, N.Y.)* 320 (5872). United States: 103–6. <https://doi.org/10.1126/science.1152241>.

An, Songon, Minjoung Kyoung, Jasmina J Allen, Kevan M Shokat, and Stephen J Benkovic. 2010. "Dynamic Regulation of a Metabolic Multi-Enzyme Complex by Protein Kinase CK2." *The Journal of Biological Chemistry* 285 (15). United States: 11093–99. <https://doi.org/10.1074/jbc.M110.101139>.

Anderson, Donald D., Collynn F. Woeller, En Pei Chiang, Barry Shane, and Patrick J. Stover. 2012. "Serine Hydroxymethyltransferase Anchors de Novo Thymidylate Synthesis Pathway to Nuclear Lamina for DNA Synthesis." *Journal of Biological Chemistry* 287 (10): 7051–62. <https://doi.org/10.1074/jbc.M111.333120>.

Anderson, Donald D, and Patrick J Stover. 2009. "SHMT1 and SHMT2 Are Functionally Redundant in Nuclear de Novo Thymidylate Biosynthesis." *PLoS One* 4 (6). United States: e5839. <https://doi.org/10.1371/journal.pone.0005839>.

Anderson, Donald D, Collynn F Woeller, and Patrick J Stover. 2007. "Small Ubiquitin-like Modifier-1 (SUMO-1) Modification of Thymidylate Synthase and Dihydrofolate Reductase." *Clinical Chemistry and Laboratory Medicine* 45 (12). Germany: 1760–63. <https://doi.org/10.1515/CCLM.2007.355>.

Andoniadou, Cynthia Lilian, and Juan Pedro Martinez-Barbera. 2013. "Developmental Mechanisms Directing Early Anterior Forebrain Specification in Vertebrates." *Cellular and Molecular Life Sciences : CMLS* 70 (20). Switzerland: 3739–52. <https://doi.org/10.1007/s00018-013-1269-5>.

Andrews, J E, M Ebron-McCoy, R J Kavlock, and J M Rogers. 1995. "Developmental Toxicity of Formate and Formic Acid in Whole Embryo Culture: A Comparative Study with Mouse and Rat Embryos." *Teratology* 51 (4). United States: 243–51. <https://doi.org/10.1002/tera.1420510409>.

Anguera, Montserrat C, Martha S Field, Cheryll Perry, Haifa Ghandour, En-Pei Chiang, Jacob Selhub, Barry Shane, and Patrick J Stover. 2006. "Regulation of Folate-Mediated One-Carbon Metabolism by 10-Formyltetrahydrofolate Dehydrogenase." *The Journal of Biological Chemistry* 281 (27). United States: 18335–42. <https://doi.org/10.1074/jbc.M510623200>.

Arendash, Gary W, Takashi Mori, Chuanhai Cao, Małgorzata Mamcarz, Melissa Runfeldt, Alexander Dickson, Kavon Rezai-Zadeh, et al. 2009. "Caffeine Reverses Cognitive Impairment and Decreases Brain Amyloid-Beta Levels in Aged Alzheimer's Disease Mice." *Journal of Alzheimer's Disease : JAD* 17 (3). Netherlands: 661–80. <https://doi.org/10.3233/JAD-2009-1087>.

Arezzo, Franco. 1987. "Determination of Ribonucleoside Triphosphates and Deoxyribonucleoside Triphosphates in Novikoff Hepatoma Cells by High-Performance Liquid Chromatography." *Analytical Biochemistry* 160 (1): 57–64. [https://doi.org/10.1016/0003-2697\(87\)90613-0](https://doi.org/10.1016/0003-2697(87)90613-0).

Arkell, R, and R S Beddington. 1997. "BMP-7 Influences Pattern and Growth of the Developing Hindbrain of Mouse Embryos." *Development (Cambridge, England)* 124 (1). England: 1–

Arnaud, M J. 1987. "The Pharmacology of Caffeine." *Progress in Drug Research. Fortschritte Der Arzneimittelforschung. Progres Des Recherches Pharmaceutiques* 31. Switzerland: 273–313.

Atta, Callie A M, Kirsten M Fiest, Alexandra D Frolkis, Nathalie Jette, Tamara Pringsheim, Christine St Germaine-Smith, Thilinie Rajapakse, Gilaad G Kaplan, and Amy Metcalfe. 2016. "Global Birth Prevalence of Spina Bifida by Folic Acid Fortification Status: A Systematic Review and Meta-Analysis." *American Journal of Public Health* 106 (1). United States: e24-34. <https://doi.org/10.2105/AJPH.2015.302902>.

Austin, W L, M Wind, and K S Brown. 1982. "Differences in the Toxicity and Teratogenicity of Cytochalasins D and E in Various Mouse Strains." *Teratology* 25 (1). United States: 11–18. <https://doi.org/10.1002/tera.1420250103>.

Axelrod, Jeffrey D. 2009. "Progress and Challenges in Understanding Planar Cell Polarity Signaling." *Seminars in Cell & Developmental Biology* 20 (8): 964–71. <https://doi.org/http://dx.doi.org/10.1016/j.semcd.2009.08.001>.

Ayme, S, and N Philip. 1995. "Possible Homozygous Waardenburg Syndrome in a Fetus with Exencephaly." *American Journal of Medical Genetics*. United States. <https://doi.org/10.1002/ajmg.1320590227>.

Babycentre. n.d. "Caffeine during Pregnancy." <https://www.babycentre.co.uk/a3955/caffeine-and-pregnancy-whats-safe>.

Bai, C Brian, Wojtek Auerbach, Joon S Lee, Daniel Stephen, and Alexandra L Joyner. 2002. "Gli2, but Not Gli1, Is Required for Initial Shh Signaling and Ectopic Activation of the Shh Pathway." *Development (Cambridge, England)* 129: 4753–61.

Baldwin, C T, C F Hoth, R A Macina, and A Milunsky. 1995. "Mutations in PAX3 That Cause Waardenburg Syndrome Type I: Ten New Mutations and Review of the Literature." *American Journal of Medical Genetics* 58 (2). United States: 115–22. <https://doi.org/10.1002/ajmg.1320580205>.

Barbera, Juan Pedro Martinez, Tristan A Rodriguez, Nicholas D E Greene, Wolfgang J Weninger, Antonio Simeone, Andrew J Copp, Rosa S P Beddington, and Sally Dunwoodie. 2002. "Folic Acid Prevents Exencephaly in Cited2 Deficient Mice." *Human Molecular Genetics* 11 (3): 283–93. <https://doi.org/10.1093/hmg/11.3.283>.

Barlow, Christy A., Rakesh S. Laishram, and Richard A. Anderson. 2010. "Nuclear Phosphoinositides: A Signaling Enigma Wrapped in a Compartmental Conundrum." *Trends in Cell Biology* 20 (1): 25–35. <https://doi.org/10.1016/j.tcb.2009.09.009>.

Barone, J.J., and H. Roberts. 1996. "Caffeine Consumption." *Food and Chemical Toxicology* 34 (1): 119–29.

Basler, K, T Edlund, T M Jessell, and T Yamada. 1993. "Control of Cell Pattern in the Neural Tube: Regulation of Cell Differentiation by Dorsalin-1, a Novel TGF Beta Family

Member.” *Cell* 73 (4). United States: 687–702.

Baye, Lisa M, and Brian A Link. 2007. “Interkinetic Nuclear Migration and the Selection of Neurogenic Cell Divisions during Vertebrate Retinogenesis.” *The Journal of Neuroscience : The Official Journal of the Society for Neuroscience* 27 (38). United States: 10143–52. <https://doi.org/10.1523/JNEUROSCI.2754-07.2007>.

Beaudin, Anna E., Elena V. Abarinov, Olga Malysheva, Cheryll A. Perry, Marie Caudill, and Patrick J. Stover. 2012. “Dietary Folate, but Not Choline, Modifies Neural Tube Defect Risk in Shmt1 Knockout Mice.” *American Journal of Clinical Nutrition* 95 (1): 109–14. <https://doi.org/10.3945/ajcn.111.020305>.

Beaudin, Anna E., Elena V. Abarinov, Drew M. Noden, Cheryll A. Perry, Stephanie Chu, Sally P. Stabler, Robert H. Allen, and Patrick J. Stover. 2011. “Shmt1 and de Novo Thymidylate Biosynthesis Underlie Folate-Responsive Neural Tube Defects in Mice.” *American Journal of Clinical Nutrition* 93 (4): 789–98. <https://doi.org/10.3945/ajcn.110.002766>.

Bebenek, K, J D Roberts, and T A Kunkel. 1992. “The Effects of dNTP Pool Imbalances on Frameshift Fidelity during DNA Replication.” *The Journal of Biological Chemistry* 267 (6). United States: 3589–96.

Begleiter, M L, and D J Harris. 1992. “Waardenburg Syndrome and Meningocele.” *American Journal of Medical Genetics*. United States. <https://doi.org/10.1002/ajmg.1320440434>.

Beier, D. R., H. Dushkin, and T. Telle. 1995. “Haplotype Analysis of Intra-Specific Backcross Curly-Tail Mice Confirms the Localization of Ct to Chromosome 4.” *Mammalian Genome* 6 (4): 269–72. <https://doi.org/10.1007/BF00352414>.

Bello, L J. 1974. “Regulation of Thymidine Kinase Synthesis in Human Cells.” *Experimental Cell Research* 89 (2). United States: 263–74.

Ben-Sahra, Issam, Jessica J Howell, John M Asara, and Brendan D Manning. 2013. “Stimulation of de Novo Pyrimidine Synthesis by Growth Signaling through mTOR and S6K1.” *Science (New York, N.Y.)* 339 (6125). United States: 1323–28. <https://doi.org/10.1126/science.1228792>.

Ben-Sahra, Issam, Gerta Hoxhaj, Stephane J H Ricoult, John M Asara, and Brendan D Manning. 2016. “mTORC1 Induces Purine Synthesis through Control of the Mitochondrial Tetrahydrofolate Cycle.” *Science (New York, N.Y.)* 351 (6274). United States: 728–33. <https://doi.org/10.1126/science.aad0489>.

Benedum, Corey M, Mahsa M Yazdy, Allen A Mitchell, and Martha M Werler. 2013. “Risk of Spina Bifida and Maternal Cigarette, Alcohol, and Coffee Use during the First Month of Pregnancy.” *International Journal of Environmental Research and Public Health* 10 (8). Switzerland: 3263–81. <https://doi.org/10.3390/ijerph10083263>.

Bennett, G D, J An, J C Craig, L A Gefrides, J A Calvin, and R H Finnell. 1998. “Neurulation Abnormalities Secondary to Altered Gene Expression in Neural Tube Defect Susceptible Splotch Embryos.” *Teratology* 57 (1). United States: 17–29.

https://doi.org/10.1002/(SICI)1096-9926(199801)57:1<17::AID-TERA4>3.0.CO;2-4.

Bennicelli, J L, R H Edwards, and F G Barr. 1996. "Mechanism for Transcriptional Gain of Function Resulting from Chromosomal Translocation in Alveolar Rhabdomyosarcoma." *Proceedings of the National Academy of Sciences of the United States of America* 93 (11). UNITED STATES: 5455–59.

Benowitz, N L, P 3rd Jacob, H Mayan, and C Denaro. 1995. "Sympathomimetic Effects of Paraxanthine and Caffeine in Humans." *Clinical Pharmacology and Therapeutics* 58 (6). United States: 684–91. https://doi.org/10.1016/0009-9236(95)90025-X.

Berk, A J, and D A Clayton. 1973. "A Genetically Distinct Thymidine Kinase in Mammalian Mitochondria. Exclusive Labeling of Mitochondrial Deoxyribonucleic Acid." *The Journal of Biological Chemistry* 248 (8). United States: 2722–29.

Bernasconi, M, A Remppis, W J Fredericks, F J 3rd Rauscher, and B W Schafer. 1996. "Induction of Apoptosis in Rhabdomyosarcoma Cells through down-Regulation of PAX Proteins." *Proceedings of the National Academy of Sciences of the United States of America* 93 (23). UNITED STATES: 13164–69.

Berridge, M J, C P Downes, and M R Hanley. 1989. "Neural and Developmental Actions of Lithium: A Unifying Hypothesis." *Cell* 59 (3). United States: 411–19.

Berthou, F, D Ratanasavanh, D Alix, D Carlhant, C Riche, and A Guillouzo. 1988. "Caffeine and Theophylline Metabolism in Newborn and Adult Human Hepatocytes; Comparison with Adult Rat Hepatocytes." *Biochemical Pharmacology* 37 (19). England: 3691–3700.

Bezprozvanny, I, S Bezprozvannaya, and B E Ehrlich. 1994. "Caffeine-Induced Inhibition of Inositol (1, 4, 5)-Trisphosphate-Gated Calcium Channels from Cerebellum." *Molecular Biology of the Cell*.

Bjursell, Gunnar, and Peter Reichard. 1973. "Effects of Thymidine on Deoxyribonucleoside Pools and Deoxyribonucleic Acid Synthesis Chinese Hamster Ovary Cells." *The Journal of Biological Chemistry* 218 (11): 3904–9.

Blake, Judith A, and Melanie R Ziman. 2014. "Pax Genes: Regulators of Lineage Specification and Progenitor Cell Maintenance." *Development (Cambridge, England)* 141 (4). England: 737–51. https://doi.org/10.1242/dev.091785.

Blencowe, Hannah, Simon Cousens, Bernadette Modell, and Joy Lawn. 2010. "Folic Acid to Reduce Neonatal Mortality from Neural Tube Disorders." *International Journal of Epidemiology* 39 Suppl 1 (April). England: i110-21. https://doi.org/10.1093/ije/dyq028.

Blom, Henk J, Gary M Shaw, Martin den Heijer, and Richard H Finnell. 2006. "Neural Tube Defects and Folate: Case far from Closed." *Nature Reviews. Neuroscience* 7 (9): 724–31. https://doi.org/10.1038/nrn1986.

Bode, Ann M., and Zigang Dong. 2007. "The Enigmatic Effects of Caffeine in Cell Cycle and Cancer." *Cancer Letters*. https://doi.org/10.1016/j.canlet.2006.03.032.

Bollee, Guillaume, Jerome Harambat, Albert Bensman, Bertrand Knebelmann, Michel Daudon,

and Irene Ceballos-Picot. 2012. “Adenine Phosphoribosyltransferase Deficiency.” *Clinical Journal of the American Society of Nephrology : CJASN* 7 (9). United States: 1521–27. <https://doi.org/10.2215/CJN.02320312>.

Bonati, M., R. Latini, G. Tognoni, J. F. Young, and S. Garattini. 1984. “Interspecies Comparison of In Vivo Caffeine Pharmacokinetics in Man, Monkey, Rabbit, Rat and Mouse.” *Drug Metabolism Reviews* 15 (7). England: 1355–83. <https://doi.org/10.3109/03602538409029964>.

Borycki, A G, J Li, F Jin, C P Emerson, and J A Epstein. 1999. “Pax3 Functions in Cell Survival and in pax7 Regulation.” *Development (Cambridge, England)* 126 (8). ENGLAND: 1665–74.

Boyles, Abee L, Ashley V Billups, Kristen L Deak, Deborah G Siegel, Lorraine Mehltretter, Susan H Slifer, Alexander G Bassuk, et al. 2006. “Neural Tube Defects and Folate Pathway Genes: Family-Based Association Tests of Gene-Gene and Gene-Environment Interactions.” *Environmental Health Perspectives* 114 (10). United States: 1547–52.

Braasch, Katrin, Carina Villacres, and Michael Butler. 2015. “Evaluation of Quenching and Extraction Methods for Nucleotide/Nucleotide Sugar Analysis.” *Methods in Molecular Biology (Clifton, N.J.)* 1321. United States: 361–72. https://doi.org/10.1007/978-1-4939-2760-9_24.

Bray, Geraldine, and Thomas P. Brent. 1972. “Deoxyribonucleoside 5'-triphosphate Pool Fluctuations during the Mamalian Cell Cycle.” *BBA Section Nucleic Acids And Protein Synthesis* 269 (2): 184–91. [https://doi.org/10.1016/0005-2787\(72\)90425-X](https://doi.org/10.1016/0005-2787(72)90425-X).

Bree, Angelika De, W. M Monique Verschuren, Anne Lise Bjoørke-Monsen, Nathalie M J Van der Put, Sandra G. Heil, Frans J M Trijbels, and Henk J. Blom. 2003. “Effect of the Methylenetetrahydrofolate Reductase 677C→T Mutation on the Relations among Folate Intake and Plasma Folate and Homocysteine Concentrations in a General Population Sample.” *American Journal of Clinical Nutrition* 77 (3). United States: 687–93.

Brent, Robert L., Mildred S. Christian, and Robert M. Diener. 2011. “Evaluation of the Reproductive and Developmental Risks of Caffeine.” *Birth Defects Research Part B - Developmental and Reproductive Toxicology*. <https://doi.org/10.1002/bdrb.20288>.

Briscoe, James, Yu Chen, Thomas M. Jessell, and Gary Struhl. 2001. “A Hedgehog-Insensitive Form of Patched Provides Evidence for Direct Long-Range Morphogen Activity of Sonic Hedgehog in the Neural Tube.” *Molecular Cell* 7 (6): 1279–91. [https://doi.org/10.1016/S1097-2765\(01\)00271-4](https://doi.org/10.1016/S1097-2765(01)00271-4).

Briscoe, James, and Stephen Small. 2015. “Morphogen Rules: Design Principles of Gradient-Mediated Embryo Patterning.” *Development (Cambridge, England)* 142 (23). England: 3996–4009. <https://doi.org/10.1242/dev.129452>.

Briscoe, J, L Sussel, P Serup, D Hartigan-O’Connor, T M Jessell, J L Rubenstein, and J Ericson. 1999. “Homeobox Gene Nkx2.2 and Specification of Neuronal Identity by Graded Sonic

Hedgehog Signalling.” *Nature* 398 (6728). ENGLAND: 622–27. <https://doi.org/10.1038/19315>.

Brook, F A, J P Estibeiro, and A J Copp. 1994. “Female Predisposition to Cranial Neural Tube Defects Is Not because of a Difference between the Sexes in the Rate of Embryonic Growth or Development during Neurulation.” *Journal of Medical Genetics* 31 (5): 383–87. <http://www.pubmedcentral.nih.gov/articlerender.fcgi?artid=1049870&tool=pmcentrez&rendertype=abstract>.

Brosnan, J T. 1987. “The 1986 Borden Award Lecture. The Role of the Kidney in Amino Acid Metabolism and Nutrition.” *Canadian Journal of Physiology and Pharmacology* 65 (12). Canada: 2355–62.

Brosnan, Margaret E, Luke MacMillan, Jennifer R Stevens, and John T Brosnan. 2015. “Division of Labour: How Does Folate Metabolism Partition between One-Carbon Metabolism and Amino Acid Oxidation?” *The Biochemical Journal* 472 (2). England: 135–46. <https://doi.org/10.1042/BJ20150837>.

Brouns, Madeleine R, Sandra C P De Castro, Els A Terwindt-Rouwenhorst, Valentina Massa, Johan W Hekking, Caroline S Hirst, Dawn Savery, et al. 2011. “Over-Expression of Grhl2 Causes Spina Bifida in the Axial Defects Mutant Mouse.” *Human Molecular Genetics* 20 (8). England: 1536–46. <https://doi.org/10.1093/hmg/ddr031>.

Bulgakov, Oleg V, Jonathan T Eggenschwiler, Dong-Hyun Hong, Kathryn V Anderson, and Tiansen Li. 2004. “FKBP8 Is a Negative Regulator of Mouse Sonic Hedgehog Signaling in Neural Tissues.” *Development (Cambridge, England)* 131 (9): 2149–59. <https://doi.org/10.1242/dev.01122>.

Burke, R, D Nellen, M Bellotto, E Hafen, K A Senti, B J Dickson, and K Basler. 1999. “Dispatched, a Novel Sterol-Sensing Domain Protein Dedicated to the Release of Cholesterol-Modified Hedgehog from Signaling Cells.” *Cell* 99 (7). United States: 803–15.

Burren, Katie A., Dawn Savery, Valentina Massa, Robert M. Kok, John M. Scott, Henk J. Blom, Andrew J. Copp, and Nicholas D E Greene. 2008. “Gene-Environment Interactions in the Causation of Neural Tube Defects: Folate Deficiency Increases Susceptibility Conferred by Loss of Pax3 Function.” *Human Molecular Genetics* 17 (23): 3675–85. <https://doi.org/10.1093/hmg/ddn262>.

Burren, Katie A., John M. Scott, Andrew J. Copp, and N. D E Greene. 2010. “The Genetic Background of the Curly Tail Strain Confers Susceptibility to Folate-Deficiency-Induced Exencephaly.” *Birth Defects Research Part A - Clinical and Molecular Teratology* 88 (2): 76–83. <https://doi.org/10.1002/bdra.20632>.

Burren, Katie A, Kevin Mills, Andrew J Copp, and Nicholas D E Greene. 2006. “Quantitative Analysis of S-Adenosylmethionine and S-Adenosylhomocysteine in Neurulation-Stage Mouse Embryos by Liquid Chromatography Tandem Mass Spectrometry.” *Journal of Chromatography. B, Analytical Technologies in the Biomedical and Life Sciences* 844 (1).

Netherlands: 112–18. <https://doi.org/10.1016/j.jchromb.2006.07.012>.

Buters, J T, B K Tang, T Pineau, H V Gelboin, S Kimura, and F J Gonzalez. 1996. “Role of CYP1A2 in Caffeine Pharmacokinetics and Metabolism: Studies Using Mice Deficient in CYP1A2.” *Pharmacogenetics* 6 (4). England: 291–96.

Butler, M A, N P Lang, J F Young, N E Caporaso, P Vineis, R B Hayes, C H Teitel, J P Massengill, M F Lawsen, and F F Kadlubar. 1992. “Determination of CYP1A2 and NAT2 Phenotypes in Human Populations by Analysis of Caffeine Urinary Metabolites.” *Pharmacogenetics* 2 (3). England: 116–27.

Cabreiro, Filipe, Catherine Au, Kit Yi Leung, Nuria Vergara-Irigaray, Helena M. Cochemé, Tahereh Noori, David Weinkove, Eugene Schuster, Nicholas D E Greene, and David Gems. 2013. “Metformin Retards Aging in *C. Elegans* by Altering Microbial Folate and Methionine Metabolism.” *Cell* 153 (1): 228–39. <https://doi.org/10.1016/j.cell.2013.02.035>.

Candito, Mirande, Romain Rivet, Bernard Herbeth, Catherine Boisson, Rene-Charles Rudigoz, Dominique Luton, Hubert Journel, et al. 2008. “Nutritional and Genetic Determinants of Vitamin B and Homocysteine Metabolisms in Neural Tube Defects: A Multicenter Case-Control Study.” *American Journal of Medical Genetics. Part A* 146A (9). United States: 1128–33. <https://doi.org/10.1002/ajmg.a.32199>.

Carezani-Gavin, M, S K Clarren, and T Steege. 1992. “Waardenburg Syndrome Associated with Meningomyelocele.” *American Journal of Medical Genetics*. United States. <https://doi.org/10.1002/ajmg.1320420127>.

Carter, C O. 1974. “Clues to the Aetiology of Neural Tube Malformations.” *Developmental Medicine and Child Neurology* 16 (6 Suppl 32). England: 3–15.

Caspary, Tamara, and Kathryn V Anderson. 2003. “Patterning Cell Types in the Dorsal Spinal Cord: What the Mouse Mutants Say.” *Nature Reviews. Neuroscience* 4 (4). England: 289–97. <https://doi.org/10.1038/nrn1073>.

Castranio, Trisha, and Yuji Mishina. 2009. “Bmp2 Is Required for Cephalic Neural Tube Closure in the Mouse.” *Developmental Dynamics : An Official Publication of the American Association of Anatomists* 238 (1). United States: 110–22. <https://doi.org/10.1002/dvdy.21829>.

Castro, Sandra C P de. 2011. “Proteomic and Molecular Analysis of Neural Tube Defects in the Mouse Embryo,” no. February.

Castro, Sandra C P De, Kit Yi Leung, Dawn Savery, Katie Burren, Rima Rozen, Andrew J. Copp, and Nicholas D E Greene. 2010. “Neural Tube Defects Induced by Folate Deficiency in Mutant Curly Tail (Grhl3) Embryos Are Associated with Alteration in Folate One-Carbon Metabolism but Are Unlikely to Result from Diminished Methylation.” *Birth Defects Research Part A - Clinical and Molecular Teratology* 88 (8): 612–18. <https://doi.org/10.1002/bdra.20690>.

Castro, Sandra C P de, Ashraf Malhas, Kit Yi Leung, Peter Gustavsson, David J. Vaux, Andrew J.

Copp, and Nicholas D E Greene. 2012. "Lamin B1 Polymorphism Influences Morphology of the Nuclear Envelope, Cell Cycle Progression, and Risk of Neural Tube Defects in Mice." *PLoS Genetics* 8 (11). <https://doi.org/10.1371/journal.pgen.1003059>.

Cavalli, P, and A J Copp. 2002. "Inositol and Folate Resistant Neural Tube Defects." *Journal of Medical Genetics*. England.

Cavalli, Pietro, Sara Tedoldi, and Barbara Riboli. 2008. "Inositol Supplementation in Pregnancies at Risk of Apparently Folate-Resistant NTDs." *Birth Defects Research. Part A, Clinical and Molecular Teratology*. United States. <https://doi.org/10.1002/bdra.20454>.

Cavalli, Pietro, Gabriele Tonni, Enrico Grossi, and Carlo Poggiani. 2011. "Effects of Inositol Supplementation in a Cohort of Mothers at Risk of Producing an NTD Pregnancy." *Birth Defects Research. Part A, Clinical and Molecular Teratology* 91 (11). United States: 962–65. <https://doi.org/10.1002/bdra.22853>.

Cecconi, F, G Alvarez-Bolado, B I Meyer, K A Roth, and P Gruss. 1998. "Apaf1 (CED-4 Homolog) Regulates Programmed Cell Death in Mammalian Development." *Cell* 94 (6). United States: 727–37.

Chan, Chung Yu, Hong Zhao, Raymond J Pugh, Anthony M Pedley, Jarrod French, Sara A Jones, Xiaowei Zhuang, Hyder Jinnah, Tony Jun Huang, and Stephen J Benkovic. 2015. "Purinosome Formation as a Function of the Cell Cycle." *Proceedings of the National Academy of Sciences of the United States of America* 112 (5). United States: 1368–73. <https://doi.org/10.1073/pnas.1423009112>.

Chang, H, D Huylebroeck, K Verschueren, Q Guo, M M Matzuk, and A Zwijsen. 1999. "Smad5 Knockout Mice Die at Mid-Gestation due to Multiple Embryonic and Extraembryonic Defects." *Development (Cambridge, England)* 126 (8). England: 1631–42.

Chatkupt, S, S Chatkupt, and W G Johnson. 1993. "Waardenburg Syndrome and Myelomeningocele in a Family." *Journal of Medical Genetics* 30 (1). England: 83–84.

Chen, H, A Thiagalingam, H Chopra, M W Borges, J N Feder, B D Nelkin, S B Baylin, and D W Ball. 1997. "Conservation of the Drosophila Lateral Inhibition Pathway in Human Lung Cancer: A Hairy-Related Protein (HES-1) Directly Represses Achaete-Scute Homolog-1 Expression." *Proceedings of the National Academy of Sciences of the United States of America* 94 (10). United States: 5355–60.

Chen, Jiang-Fan, Patricia K Sonsalla, Felicita Pedata, Alessia Melani, Maria Rosaria Domenici, Patrizia Popoli, Jonathan Geiger, Luisa V Lopes, and Alexandre de Mendonca. 2007. "Adenosine A2A Receptors and Brain Injury: Broad Spectrum of Neuroprotection, Multifaceted Actions And 'fine Tuning' modulation." *Progress in Neurobiology* 83 (5). England: 310–31. <https://doi.org/10.1016/j.pneurobio.2007.09.002>.

Chen, W H, G M Morriss-Kay, and Andrew J Copp. 1994. "Prevention of Spinal Neural Tube Defects in the Curly Tail Mouse Mutant by a Specific Effect of Retinoic Acid." *Developmental Dynamics : An Official Publication of the American Association of*

Anatomists 199 (2): 93–102. <https://doi.org/10.1002/aja.1001990203>.

Chen, W H, G M Morriss-Kay, and Andrew J Copp. 1995. “Genesis and Prevention of Spinal Neural Tube Defects in the Curly Tail Mutant Mouse: Involvement of Retinoic Acid and Its Nuclear Receptors RAR-Beta and RAR-Gamma.” *Development (Cambridge, England)* 121 (3): 681–91.

Chen, Xiaoli, Yiping Shen, Yonghui Gao, Huizhi Zhao, Xiaoming Sheng, Jizhen Zou, Va Lip, et al. 2013. “Detection of Copy Number Variants Reveals Association of Cilia Genes with Neural Tube Defects.” *PloS One* 8 (1). United States: e54492. <https://doi.org/10.1371/journal.pone.0054492>.

Chen, Xuqi, Rebecca Watkins, Emmanuele Delot, Ramune Reliene, Robert H Schiestl, Paul S Burgoyne, and Arthur P Arnold. 2008. “Sex Difference in Neural Tube Defects in p53-Null Mice Is Caused by Differences in the Complement of X Not Y Genes.” *Developmental Neurobiology* 68 (2). United States: 265–73. <https://doi.org/10.1002/dneu.20581>.

Chen, Z F, and R R Behringer. 1995. “Twist Is Required in Head Mesenchyme for Cranial Neural Tube Morphogenesis.” *Genes & Development* 9 (6). United States: 686–99.

Chen, Z, A C Karaplis, S L Ackerman, I P Pogribny, S Melnyk, S Lussier-Cacan, M F Chen, et al. 2001. “Mice Deficient in Methylenetetrahydrofolate Reductase Exhibit Hyperhomocysteinemia and Decreased Methylation Capacity, with Neuropathology and Aortic Lipid Deposition.” *Human Molecular Genetics* 10 (5). England: 433–43.

Chiang, C, Y Litingtung, E Lee, K E Young, J L Corden, H Westphal, and P a Beachy. 1996. “Cyclopia and Defective Axial Patterning in Mice Lacking Sonic Hedgehog Gene Function.” *Nature*. <https://doi.org/10.1038/383407a0>.

Chida, Junji, Kazuhiko Yamane, Tunetomo Takei, and Hiroshi Kido. 2012. “An Efficient Extraction Method for Quantitation of Adenosine Triphosphate in Mammalian Tissues and Cells.” *Analytica Chimica Acta* 727 (May). Netherlands: 8–12. <https://doi.org/10.1016/j.aca.2012.03.022>.

Christensen, B, L Arbour, P Tran, D Leclerc, N Sabbaghian, R Platt, B M Gilfix, et al. 1999. “Genetic Polymorphisms in Methylenetetrahydrofolate Reductase and Methionine Synthase, Folate Levels in Red Blood Cells, and Risk of Neural Tube Defects.” *American Journal of Medical Genetics* 84 (2). United States: 151–57.

Christensen, K. E., L. Deng, K. Y. Leung, E. Arning, T. Bottiglieri, O. V. Malyshova, M. A. Caudill, et al. 2013. “A Novel Mouse Model for Genetic Variation in 10-Formyltetrahydrofolate Synthetase Exhibits Disturbed Purine Synthesis with Impacts on Pregnancy and Embryonic Development.” *Human Molecular Genetics* 22 (18): 3705–19. <https://doi.org/10.1093/hmg/ddt223>.

Christian, M.S., and Robert L. Brent. 2001. “Teratogen Update: Evaluation of the Reproductive and Developmental Risks of Caffeine.” *Teratology*. <https://doi.org/10.1002/tera.1047>.

Clay, HB, AK Parl, SL Mitchell, L Singh, and LN Bell. 2016. “Altering the Mitochondrial Fatty

Acid Synthesis (mtFASII) Pathway Modulates Cellular Metabolic States and Bioactive Lipid Profiles as Revealed by.” *PloS One*, no. Fig 1: 1–23. <https://doi.org/10.1371/journal.pone.0151171>.

Cockroft, D L. 1991. “Vitamin Deficiencies and Neural-Tube Defects: Human and Animal Studies.” *Human Reproduction (Oxford, England)* 6 (1): 148–57. <http://www.ncbi.nlm.nih.gov/pubmed/1874949>.

Cockroft, D L, F A Brook, and A J Copp. 1992. “Inositol Deficiency Increases the Susceptibility to Neural Tube Defects of Genetically Predisposed (Curly Tail) Mouse Embryos in Vitro.” *Teratology* 45 (2): 223–32. <https://doi.org/10.1002/tera.1420450216>.

Cogram, Patricia, Andrew Hynes, L. P E Dunlevy, N. D E Greene, and Andrew J. Copp. 2004. “Specific Isoforms of Protein Kinase C Are Essential for Prevention of Folate-Resistant Neural Tube Defects by Inositol.” *Human Molecular Genetics* 13 (1): 7–14. <https://doi.org/10.1093/hmg/ddh003>.

Cogram, Patricia, Sheila Tesh, John Tesh, Angie Wade, Geoffrey Allan, Nicholas D E Greene, and Andrew J Copp. 2002. “D-Chiro-Inositol Is More Effective than Myo-Inositol in Preventing Folate-Resistant Mouse Neural Tube Defects” 17 (9): 2451–58.

Cohen, Sabine, Mehdi Megherbi, Lars Petter Jordheim, Isabelle Lefebvre, Christian Perigaud, Charles Dumontet, and Jérôme Guitton. 2009. “Simultaneous Analysis of Eight Nucleoside Triphosphates in Cell Lines by Liquid Chromatography Coupled with Tandem Mass Spectrometry.” *Journal of Chromatography B: Analytical Technologies in the Biomedical and Life Sciences* 877 (30): 3831–40. <https://doi.org/10.1016/j.jchromb.2009.09.030>.

Conlon, F L, K M Lyons, N Takaesu, K S Barth, A Kispert, B Herrmann, and E J Robertson. 1994. “A Primary Requirement for Nodal in the Formation and Maintenance of the Primitive Streak in the Mouse.” *Development (Cambridge, England)* 120 (7). England: 1919–28.

Conway, S J, J Bundy, J Chen, E Dickman, R Rogers, and B M Will. 2000. “Decreased Neural Crest Stem Cell Expansion Is Responsible for the Conotruncal Heart Defects within the Splotch (Sp(2H))/Pax3 Mouse Mutant.” *Cardiovascular Research* 47 (2). NETHERLANDS: 314–28.

Cooke, Mariana, Andrew Magimaidas, Victoria Casado-Medrano, and Marcelo G Kazanietz. 2017. “Protein Kinase C in Cancer: The Top Five Unanswered Questions.” *Molecular Carcinogenesis*, January. United States. <https://doi.org/10.1002/mc.22617>.

Cooper, Ayanna F, Kuan Ping Yu, Martina Brueckner, Lisa L Brailey, Linda Johnson, James M McGrath, and Allen E Bale. 2005. “Cardiac and CNS Defects in a Mouse with Targeted Disruption of Suppressor of Fused.” *Development (Cambridge, England)* 132 (19). England: 4407–17. <https://doi.org/10.1242/dev.02021>.

Copp, A J. 1985. “Relationship between Timing of Posterior Neuropore Closure and Development of Spinal Neural Tube Defects in Mutant (Curly Tail) and Normal Mouse

Embryos in Culture." *Journal of Embryology and Experimental Morphology* 88 (August). England: 39–54.

Copp, A J, and F A Brook. 1989. "Does Lumbosacral Spina Bifida Arise by Failure of Neural Folding or by Defective Canalisation?" *Journal of Medical Genetics* 26 (3). England: 160–66.

Copp, a J, F a Brook, and H J Roberts. 1988. "A Cell-Type-Specific Abnormality of Cell Proliferation in Mutant (Curly Tail) Mouse Embryos Developing Spinal Neural Tube Defects." *Development (Cambridge, England)* 104: 285–95.

Copp, A J, J A Crolla, and F A Brook. 1988. "Prevention of Spinal Neural Tube Defects in the Mouse Embryo by Growth Retardation during Neurulation." *Development (Cambridge, England)* 104 (2): 297–303. <http://www.ncbi.nlm.nih.gov/pubmed/3254818>.

Copp, A J, M J Seller, and P E Polani. 1982. "Neural Tube Development in Mutant (Curly Tail) and Normal Mouse Embryos: The Timing of Posterior Neuropore Closure in Vivo and in Vitro." *J Embryol Exp Morphol* 69: 151–67.
<http://eutils.ncbi.nlm.nih.gov/entrez/eutils/elink.fcgi?dbfrom=pubmed&id=7119666&retmode=ref&cmd=prlinks%5Cnpapers3://publication/uuid/21425627-E724-472E-871B-13AEB8047713>.

Copp, Andrew J. 2005. "Neurulation in the Cranial Region--Normal and Abnormal." *Journal of Anatomy* 207 (5): 623–35. <https://doi.org/10.1111/j.1469-7580.2005.00476.x>.

Copp, Andrew J., Nicholas D. E. Greene, and Jennifer N. Murdoch. 2003. "The Genetic Basis of Mammalian Neurulation." *Nature Reviews Genetics* 4 (10): 784–93.
<https://doi.org/10.1038/nrg1181>.

Copp, Andrew J., and Nicholas D E Greene. 2013. "Neural Tube Defects-Disorders of Neurulation and Related Embryonic Processes." *Wiley Interdisciplinary Reviews: Developmental Biology* 2 (2): 213–27. <https://doi.org/10.1002/wdev.71>.

Copp, Andrew J., Philip Stanier, and Nicholas D E Greene. 2013. "Neural Tube Defects: Recent Advances, Unsolved Questions, and Controversies." *The Lancet Neurology* 12 (8). Elsevier Ltd: 799–810. [https://doi.org/10.1016/S1474-4422\(13\)70110-8](https://doi.org/10.1016/S1474-4422(13)70110-8).

Cordell, Rebecca L., Stephen J. Hill, Catharine A. Ortori, and David A. Barrett. 2008. "Quantitative Profiling of Nucleotides and Related Phosphate-Containing Metabolites in Cultured Mammalian Cells by Liquid Chromatography Tandem Electrospray Mass Spectrometry." *Journal of Chromatography B: Analytical Technologies in the Biomedical and Life Sciences* 871 (1): 115–24. <https://doi.org/10.1016/j.jchromb.2008.07.005>.

Cox, Timothy C, Timothy J Sadlon, Quenten P Schwarz, Christopher S Matthews, Phillip D Wise, Liza L Cox, Sylvia S Bottomley, and Brian K May. 2004. "The Major Splice Variant of Human 5-Aminolevulinate Synthase-2 Contributes Significantly to Erythroid Heme Biosynthesis." *The International Journal of Biochemistry & Cell Biology* 36 (2). Netherlands: 281–95.

Crider, Krista S, Owen Devine, Ling Hao, Nicole F Dowling, Song Li, Anne M Molloy, Zhu Li, Jianghui Zhu, and Robert J Berry. 2014. "Population Red Blood Cell Folate Concentrations for Prevention of Neural Tube Defects: Bayesian Model." *BMJ (Clinical Research Ed.)* 349 (July). England: g4554.

Cross, D. R., B. J. Miller, and S. J. James. 1993. "A Simplified HPLC Method for Simultaneously Quantifying Ribonucleotides and Deoxyribonucleotides in Cell Extracts or Frozen Tissues." *Cell Proliferation* 26 (4): 327–36. <https://doi.org/10.1111/j.1365-2184.1993.tb00328.x>.

Cueto, H T, A H Riis, E E Hatch, L A Wise, K J Rothman, H T Sorensen, and E M Mikkelsen. 2015. "Folic Acid Supplementation and Fecundability: A Danish Prospective Cohort Study." *European Journal of Clinical Nutrition*, no. August 2014: 1–6. <https://doi.org/10.1038/ejcn.2015.94>.

Cunningham, John T, Melissa V Moreno, Alessia Lodi, Sabrina M Ronen, and Davide Ruggero. 2014. "Protein and Nucleotide Biosynthesis Are Coupled by a Single Rate-Limiting Enzyme, PRPS2, to Drive Cancer." *Cell* 157 (5). United States: 1088–1103. <https://doi.org/10.1016/j.cell.2014.03.052>.

Cunningham, Thomas J, Sandeep Kumar, Terry P Yamaguchi, and Gregg Duester. 2015. "Wnt8a and Wnt3a Cooperate in the Axial Stem Cell Niche to Promote Mammalian Body Axis Extension." *Developmental Dynamics : An Official Publication of the American Association of Anatomists* 244 (6). United States: 797–807. <https://doi.org/10.1002/dvdy.24275>.

Czeizel, A E, and I Dudas. 1992. "Prevention of the First Occurrence of Neural-Tube Defects by Periconceptional Vitamin Supplementation." *The New England Journal of Medicine* 327 (26). United States: 1832–35. <https://doi.org/10.1056/NEJM199212243272602>.

da-Silva, E O. 1991. "Waardenburg I Syndrome: A Clinical and Genetic Study of Two Large Brazilian Kindreds, and Literature Review." *American Journal of Medical Genetics* 40 (1). United States: 65–74. <https://doi.org/10.1002/ajmg.1320400113>.

Daly, L E, P N Kirke, A Molloy, D G Weir, and J M Scott. 1995. "Folate Levels and Neural Tube Defects. Implications for Prevention." *JAMA* 274 (21). United States: 1698–1702.

Danesh, Shahab M, Alethia Villasenor, Diana Chong, Carrie Soukup, and Ondine Cleaver. 2009. "BMP and BMP Receptor Expression during Murine Organogenesis." *Gene Expression Patterns* 9 (5): 255–65. <https://doi.org/http://dx.doi.org/10.1016/j.gep.2009.04.002>.

Davidson, B P, and P P Tam. 2000. "The Node of the Mouse Embryo." *Current Biology : CB* 10 (17). England: R617-9.

Davis, Steven R, Peter W Stacpoole, Jerry Williamson, Lilia S Kick, Eoin P Quinlivan, Bonnie S Coats, Barry Shane, Lynn B Bailey, and Jesse F 3rd Gregory. 2004. "Tracer-Derived Total and Folate-Dependent Homocysteine Remethylation and Synthesis Rates in Humans Indicate That Serine Is the Main One-Carbon Donor." *American Journal of Physiology. Endocrinology and Metabolism* 286 (2). United States: E272-9. <https://doi.org/10.1152/ajpendo.00351.2003>.

Decosterd, L A, E Cottin, X Chen, F Lejeune, R O Mirimanoff, J Biollaz, and P A Coucke. 1999. "Simultaneous Determination of Deoxyribonucleoside in the Presence of Ribonucleoside Triphosphates in Human Carcinoma Cells by High-Performance Liquid Chromatography." *Analytical Biochemistry* 270 (1): 59–68. <https://doi.org/10.1006/abio.1999.4066>.

Denaro, C P, C R Brown, M Wilson, P 3rd Jacob, and N L Benowitz. 1990. "Dose-Dependency of Caffeine Metabolism with Repeated Dosing." *Clinical Pharmacology and Therapeutics* 48 (3). United States: 277–85.

Dexter, John S. 1914. "The Analysis of a Case of Continuous Variation in Drosophila by a Study of Its Linkage Relations." *The American Naturalist* 48 (576). [University of Chicago Press, American Society of Naturalists]: 712–58. <http://www.jstor.org/stable/2455888>.

Di-Gregorio, Aida, Margarida Sancho, Daniel W Stuckey, Lucy A Crompton, Jonathan Godwin, Yuji Mishina, and Tristan A Rodriguez. 2007. "BMP Signalling Inhibits Premature Neural Differentiation in the Mouse Embryo." *Development (Cambridge, England)* 134 (18). England: 3359–69. <https://doi.org/10.1242/dev.005967>.

Dietrich, Marion, Coralie J P Brown, and Gladys Block. 2005. "The Effect of Folate Fortification of Cereal-Grain Products on Blood Folate Status, Dietary Folate Intake, and Dietary Folate Sources among Adult Non-Supplement Users in the United States." *Journal of the American College of Nutrition* 24 (4). United States: 266–74.

Diez del Corral, Ruth, Dorette N Breitkreuz, and Kate G Storey. 2002. "Onset of Neuronal Differentiation Is Regulated by Paraxial Mesoderm and Requires Attenuation of FGF Signalling." *Development (Cambridge, England)* 129 (7). England: 1681–91.

Diez del Corral, Ruth, Isabel Olivera-Martinez, Anne Goriely, Emily Gale, Malcolm Maden, and Kate Storey. 2003. "Opposing FGF and Retinoid Pathways Control Ventral Neural Pattern, Neuronal Differentiation, and Segmentation during Body Axis Extension." *Neuron* 40 (1). United States: 65–79.

Diez del Corral, Ruth, and Kate G Storey. 2004. "Opposing FGF and Retinoid Pathways: A Signalling Switch That Controls Differentiation and Patterning Onset in the Extending Vertebrate Body Axis." *BioEssays : News and Reviews in Molecular, Cellular and Developmental Biology* 26 (8). United States: 857–69. <https://doi.org/10.1002/bies.20080>.

Ding, Q, J Motoyama, S Gasca, R Mo, H Sasaki, J Rossant, and C C Hui. 1998. "Diminished Sonic Hedgehog Signaling and Lack of Floor Plate Differentiation in Gli2 Mutant Mice." *Development (Cambridge, England)* 125 (14). England: 2533–43.

Douarin, N M Le. 1980. "The Ontogeny of the Neural Crest in Avian Embryo Chimaeras." *Nature* 286 (5774). England: 663–69.

Doudney, K., J. Grinham, J. Whittaker, S. A. Lynch, D. Thompson, G. E. Moore, A. J. Copp, N. D E Greene, and P. Stanier. 2009. "Evaluation of Folate Metabolism Gene Polymorphisms as Risk Factors for Open and Closed Neural Tube Defects." *American Journal of Medical Genetics, Part A* 149 (7): 1585–89. <https://doi.org/10.1002/ajmg.a.32937>.

Ducker, Gregory S, Li Chen, Raphael J Morscher, Jonathan M Ghergurovich, Mark Esposito, Xin Teng, Yibin Kang, and Joshua D Rabinowitz. 2016. “Reversal of Cytosolic One-Carbon Flux Compensates for Loss of the Mitochondrial Folate Pathway.” *Cell Metabolism* 23 (6). United States: 1140–53. <https://doi.org/10.1016/j.cmet.2016.04.016>.

Ducker, Gregory S, and Joshua D Rabinowitz. 2017. “One-Carbon Metabolism in Health and Disease.” *Cell Metabolism* 25 (1). United States: 27–42. <https://doi.org/10.1016/j.cmet.2016.08.009>.

Dumaz, Nicolas, and Richard Marais. 2005. “Integrating Signals between cAMP and the RAS/RAF/MEK/ERK Signalling Pathways. Based on the Anniversary Prize of the Gesellschaft Fur Biochemie Und Molekularbiologie Lecture Delivered on 5 July 2003 at the Special FEBS Meeting in Brussels.” *The FEBS Journal* 272 (14). England: 3491–3504. <https://doi.org/10.1111/j.1742-4658.2005.04763.x>.

Dunlevy, L. P E, Lyn S. Chitty, Katie A. Burren, Kit Doudney, Taita Stojilkovic-Mikic, Philip Stanier, Rosemary Scott, Andrew J. Copp, and N. D E Greene. 2007. “Abnormal Folate Metabolism in Foetuses Affected by Neural Tube Defects.” *Brain* 130 (4): 1043–49. <https://doi.org/10.1093/brain/awm028>.

Echelard, Y, D J Epstein, B St-Jacques, L Shen, J Mohler, J A McMahon, and A P McMahon. 1993. “Sonic Hedgehog, a Member of a Family of Putative Signaling Molecules, Is Implicated in the Regulation of CNS Polarity.” *Cell* 75 (7). United States: 1417–30.

Eggenschwiler, J T, E Espinoza, and K V Anderson. 2001. “Rab23 Is an Essential Negative Regulator of the Mouse Sonic Hedgehog Signalling Pathway.” *Nature* 412 (6843). England: 194–98. <https://doi.org/10.1038/35084089>.

Eggenschwiler, Jonathan T., Oleg V. Bulgakov, Jian Qin, Tiansen Li, and Kathryn V. Anderson. 2006. “Mouse Rab23 Regulates Hedgehog Signaling from Smoothened to Gli Proteins.” *Developmental Biology* 290 (1): 1–12. <https://doi.org/10.1016/j.ydbio.2005.09.022>.

Ehrlich, B E, E Kaftan, S Bezprozvannaya, and I Bezprozvanny. 1994. “The Pharmacology of Intracellular Ca(2+)-Release Channels.” *Trends in Pharmacological Sciences* 15 (5). England: 145–49.

Eichholzer, Monika, Otmar Tonz, and Roland Zimmermann. 2006. “Folic Acid: A Public-Health Challenge.” *Lancet (London, England)* 367 (9519). England: 1352–61. [https://doi.org/10.1016/S0140-6736\(06\)68582-6](https://doi.org/10.1016/S0140-6736(06)68582-6).

Elinson, R P, and T Holowacz. 1995. “Specifying the Dorsoanterior Axis in Frogs: 70 Years since Spemann and Mangold.” *Current Topics in Developmental Biology* 30. United States: 253–85.

Elmore, C Lee, Xuchu Wu, Daniel Leclerc, Erica D Watson, Teodoro Bottiglieri, Natalia I Krupenko, Sergey A Krupenko, et al. 2007. “Metabolic Derangement of Methionine and Folate Metabolism in Mice Deficient in Methionine Synthase Reductase.” *Molecular Genetics and Metabolism* 91 (1). United States: 85–97.

https://doi.org/10.1016/j.ymgme.2007.02.001.

Embrey, S., M.J. Seller, M. Adinolfi, and P.E. Polani. 1979. "Neural Tube Defects in Curly-Tail Mice. I. Incidence, Expression and Similarity to the Human Condition." *Proceedings of the Royal Society of London - Series B* 206: 85–94. https://doi.org/10.1098/rspb.1979.0092.

Endoh-Yamagami, Setsu, Marie Evangelista, Deanna Wilson, Xiaohui Wen, Jan-Willem Theunissen, Khanhky Phamluong, Matti Davis, et al. 2009. "The Mammalian Cos2 Homolog Kif7 Plays an Essential Role in Modulating Hh Signal Transduction during Development." *Current Biology : CB* 19 (15). England: 1320–26. https://doi.org/10.1016/j.cub.2009.06.046.

Ericson, J., P. Rashbass, A. Schedl, S. Brenner-Morton, A. Kawakami, V. Van Heyningen, T. M. Jessell, and J. Briscoe. 1997. "Pax6 Controls Progenitor Cell Identity and Neuronal Fate in Response to Graded Shh Signaling." *Cell* 90 (1): 169–80. https://doi.org/10.1016/S0092-8674(00)80323-2.

Escuin, Sarah, Bertrand Vernay, Dawn Savery, Christine B Gurniak, Walter Witke, Nicholas D E Greene, and Andrew J Copp. 2015. "Rho-Kinase-Dependent Actin Turnover and Actomyosin Disassembly Are Necessary for Mouse Spinal Neural Tube Closure." *Journal of Cell Science* 128 (14). England: 2468–81. https://doi.org/10.1242/jcs.164574.

Esteves, Francisco F, Alexander Springhorn, Erika Kague, Erika Taylor, George Pyrowolakis, Shannon Fisher, and Ethan Bier. 2014. "BMPs Regulate Msx Gene Expression in the Dorsal Neuroectoderm of Drosophila and Vertebrates by Distinct Mechanisms." *PLOS Genetics* 10 (9). Public Library of Science: e1004625. https://doi.org/10.1371/journal.pgen.1004625.

Evans, David R., and Hedeel I. Guy. 2004. "Mammalian Pyrimidine Biosynthesis: Fresh Insights into an Ancient Pathway." *Journal of Biological Chemistry* 279 (32): 33035–38. https://doi.org/10.1074/jbc.R400007200.

Fadel, R A, and T V Persaud. 1992. "Effects of Alcohol and Caffeine on Cultured Whole Rat Embryos." *Acta Anatomica* 144 (2). Switzerland: 114–19.

Fan, Jing, Jiangbin Ye, Jurre J Kamphorst, Tomer Shlomi, Craig B Thompson, and Joshua D Rabinowitz. 2014. "Quantitative Flux Analysis Reveals Folate-Dependent NADPH Production." *Nature* 510 (7504). Nature Publishing Group: 298–302. https://doi.org/10.1038/nature13236.

Fedtsova, Natalia, Roberto Perris, and Eric E Turner. 2003. "Sonic Hedgehog Regulates the Position of the Trigeminal Ganglia." *Developmental Biology* 261 (2). United States: 456–69.

Felig, P. 1975. "Amino Acid Metabolism in Man." *Annual Review of Biochemistry* 44. United States: 933–55. https://doi.org/10.1146/annurev.bi.44.070175.004441.

Fenby, Benjamin T., Vassiliki Fotaki, and John O. Mason. 2008. "Pax3 Regulates Wnt1 Expression via a Conserved Binding Site in the 5??? Proximal Promoter." *Biochimica et Biophysica Acta - Gene Regulatory Mechanisms* 1779 (2): 115–21. https://doi.org/10.1016/j.bbagr.2007.11.008.

Ferrero, J L, and A H Neims. 1983. "Metabolism of Caffeine by Mouse Liver Microsomes: GSH or Cytosol Causes a Shift in Products from 1,3,7-Trimethylurate to a Substituted Diaminouracil." *Life Sciences* 33 (12). Netherlands: 1173–78.

Field, Martha S., Elena Kamynina, Olufunmilayo C. Agunloye, Rebecca P. Liebenthal, Simon G. Lamarre, Margaret E. Brosnan, John T. Brosnan, and Patrick J. Stover. 2014. "Nuclear Enrichment of Folate Cofactors and Methylenetetrahydrofolate Dehydrogenase 1 (MTHFD1) Protect de Novo Thymidylate Biosynthesis during Folate Deficiency." *Journal of Biological Chemistry* 289 (43): 29642–50. <https://doi.org/10.1074/jbc.M114.599589>.

Field, Martha S., Doletha M E Szebenyi, and Patrick J. Stover. 2006. "Regulation of de Novo Purine Biosynthesis by Methenyltetrahydrofolate Synthetase in Neuroblastoma." *Journal of Biological Chemistry* 281 (7): 4215–21. <https://doi.org/10.1074/jbc.M510624200>.

Field, Martha S., Donald D Anderson, and Patrick J Stover. 2011. "Mthfs Is an Essential Gene in Mice and a Component of the Purinosome." *Frontiers in Genetics* 2. Switzerland: 36. <https://doi.org/10.3389/fgene.2011.00036>.

Fisone, G, A Borgkvist, and A Usiello. 2004. "Caffeine as a Psychomotor Stimulant: Mechanism of Action." *Cellular and Molecular Life Sciences : CMLS* 61 (7–8). Switzerland: 857–72. <https://doi.org/10.1007/s00018-003-3269-3>.

Fleming, A, and A. J. Copp. 1998. "Embryonic Folate Metabolism and Mouse Neural Tube Defects." *Science* 280 (June): 2107–9. <https://doi.org/10.1126/science.280.5372.2107>.

Fleming, A, and A J Copp. 2000. "A Genetic Risk Factor for Mouse Neural Tube Defects: Defining the Embryonic Basis." *Human Molecular Genetics* 9 (4). England: 575–81.

Food Fortification Initiative. 2017. "Food Fortification Initiative." 2017. http://www.ffinetwork.org/why_fortify/index.html.

Fortini, Mark E, and David Bilder. 2009. "Endocytic Regulation of Notch Signaling." *Current Opinion in Genetics & Development* 19 (4). England: 323–28. <https://doi.org/10.1016/j.gde.2009.04.005>.

Foukas, Lazaros C, Nathalie Daniele, Chariklia Ktori, Karen E Anderson, Jorgen Jensen, and Peter R Shepherd. 2002. "Direct Effects of Caffeine and Theophylline on p110 Delta and Other Phosphoinositide 3-Kinases. Differential Effects on Lipid Kinase and Protein Kinase Activities." *The Journal of Biological Chemistry* 277 (40). United States: 37124–30. <https://doi.org/10.1074/jbc.M202101200>.

Fox, I H, and W N Kelley. 1971. "Human Phosphoribosylpyrophosphate Synthetase. Distribution, Purification, and Properties." *The Journal of Biological Chemistry* 246 (18). United States: 5739–48.

Frascella, E, L Toffolatti, and A Rosolen. 1998. "Normal and Rearranged PAX3 Expression in Human Rhabdomyosarcoma." *Cancer Genetics and Cytogenetics* 102 (2). UNITED STATES: 104–9.

Fredholm, B B. 1995. "Astra Award Lecture. Adenosine, Adenosine Receptors and the Actions of

Caffeine.” *Pharmacology & Toxicology* 76 (2). Denmark: 93–101.

Fredholm, B B, M P Abbracchio, G Burnstock, J W Daly, T K Harden, K A Jacobson, P Leff, and M Williams. 1994. “Nomenclature and Classification of Purinoceptors.” *Pharmacological Reviews* 46 (2). United States: 143–56.

Fredholm, B B, K Bättig, J Holmén, a Nehlig, and E E Zvartau. 1999. “Actions of Caffeine in the Brain with Special Reference to Factors That Contribute to Its Widespread Use.” *Pharmacological Reviews* 51 (1): 83–133. [https://doi.org/0031-6997/99/5101-0083\\$03.00/0](https://doi.org/0031-6997/99/5101-0083$03.00/0).

Frej, Anna D, Grant P Otto, and Robin S B Williams. 2017. “Tipping the Scales: Lessons from Simple Model Systems on Inositol Imbalance in Neurological Disorders.” *European Journal of Cell Biology*, January. Germany. <https://doi.org/10.1016/j.ejcb.2017.01.007>.

French, Jarrod B, Sara A Jones, Huayun Deng, Anthony M Pedley, Doory Kim, Chung Yu Chan, Haibei Hu, et al. 2016. “Spatial Colocalization and Functional Link of Purinosomes with Mitochondria.” *Science (New York, N.Y.)* 351 (6274). United States: 733–37. <https://doi.org/10.1126/science.aac6054>.

French, Jarrod B, Hong Zhao, Songon An, Sherry Niessen, Yijun Deng, Benjamin F Cravatt, and Stephen J Benkovic. 2013. “Hsp70/Hsp90 Chaperone Machinery Is Involved in the Assembly of the Purinosome.” *Proceedings of the National Academy of Sciences of the United States of America* 110 (7): 2528–33. <https://doi.org/10.1073/pnas.1300173110>.

Fu, T F, J P Rife, and V Schirch. 2001. “The Role of Serine Hydroxymethyltransferase Isozymes in One-Carbon Metabolism in MCF-7 Cells as Determined by (13)C NMR.” *Archives of Biochemistry and Biophysics* 393 (1). United States: 42–50. <https://doi.org/10.1006/abbi.2001.2471>.

Fujiwara, K, K Okamura-Ikeda, and Y Motokawa. 1991. “Lipoylation of H-Protein of the Glycine Cleavage System. The Effect of Site-Directed Mutagenesis of Amino Acid Residues around the Lipoyllysine Residue on the Lipoate Attachment.” *FEBS Letters* 293 (1–2). England: 115–18.

Furman, Craig, Alisha L Sieminski, Adam V Kwiatkowski, Douglas A Rubinson, Eliza Vasile, Roderick T Bronson, Reinhard Fassler, and Frank B Gertler. 2007. “Ena/VASP Is Required for Endothelial Barrier Function in Vivo.” Comparative Study, Journal Article, Research Support, N.I.H., Extramural, Research Support, Non-U.S. Gov’t. *The Journal of Cell Biology* 179 (4). United States: 761–75. <https://doi.org/10.1083/jcb.200705002>.

Galceran, J, I Farinas, M J Depew, H Clevers, and R Grosschedl. 1999. “Wnt3a-/-like Phenotype and Limb Deficiency in Lef1(-/-)Tcf1(-/-) Mice.” *Genes & Development* 13 (6). United States: 709–17.

Gard, Chris, Gloria Gonzalez Curto, Youcef El-Mokhtar Frarma, Elodie Chollet, Nathalie Duval, Valentine Auzie, Frederic Aurade, et al. 2017. “Pax3- and Pax7-Mediated Dbx1 Regulation Orchestrates the Patterning of Intermediate Spinal Interneurons.” *Developmental Biology*, June. United States. <https://doi.org/10.1016/j.ydbio.2017.06.014>.

Garrett, Charles, and Daniel V. Santi. 1979. "A Rapid and Sensitive High Pressure Liquid Chromatography Assay for Deoxyribonucleoside Triphosphates in Cell Extracts." *Analytical Biochemistry* 99 (2): 268–73. [https://doi.org/10.1016/S0003-2697\(79\)80005-6](https://doi.org/10.1016/S0003-2697(79)80005-6).

Gelineau-van Waes, Janee, Steven Heller, Linda K Bauer, Justin Wilberding, Joyce R Maddox, Francisco Aleman, Thomas H Rosenquist, and Richard H Finnell. 2008. "Embryonic Development in the Reduced Folate Carrier Knockout Mouse Is Modulated by Maternal Folate Supplementation." *Birth Defects Research. Part A, Clinical and Molecular Teratology* 82 (7). United States: 494–507. <https://doi.org/10.1002/bdra.20453>.

Gelineau-van Waes, Janee, Mark A Rainey, Joyce R Maddox, Kenneth A Voss, Andrew J Sachs, Nicole M Gardner, Justin D Wilberding, and Ronald T Riley. 2012. "Increased Sphingoid Base-1-Phosphates and Failure of Neural Tube Closure after Exposure to Fumonisin or FTY720." *Birth Defects Research. Part A, Clinical and Molecular Teratology* 94 (10). United States: 790–803. <https://doi.org/10.1002/bdra.23074>.

Gelineau-van Waes, Janee, Lois Starr, Joyce Maddox, Francisco Aleman, Kenneth A Voss, Justin Wilberding, and Ronald T Riley. 2005. "Maternal Fumonisin Exposure and Risk for Neural Tube Defects: Mechanisms in an in Vivo Mouse Model." *Birth Defects Research. Part A, Clinical and Molecular Teratology* 73 (7). United States: 487–97. <https://doi.org/10.1002/bdra.20148>.

Gilani, S H, J J Giovinazzo, and T V Persaud. 1983. "Embryopathic Effects of Caffeine in the Chick." *Experimental Pathology* 23 (2). Germany: 79–83.

Godinho, Rosely O, Thiago Duarte, and Enio S A Pacini. 2015. "New Perspectives in Signaling Mediated by Receptors Coupled to Stimulatory G Protein: The Emerging Significance of cAMP E Ffl Ux and Extracellular cAMP-Adenosine Pathway." *Frontiers in Pharmacology* 6. Switzerland: 58. <https://doi.org/10.3389/fphar.2015.00058>.

Gofflot, Françoise, Mathew Hall, and Gillian M. Morriss-Kay. 1998. "Genetic Patterning of the Posterior Neuropore Region of Curly Tail Mouse Embryos: Deficiency of Wnt5a Expression." *International Journal of Developmental Biology* 42 (5): 637–44.

Goodrich, L V, R L Johnson, L Milenkovic, J A McMahon, and M P Scott. 1996. "Conservation of the Hedgehog/patched Signaling Pathway from Flies to Mice: Induction of a Mouse Patched Gene by Hedgehog." *Genes & Development* 10 (3). United States: 301–12.

Goodrich, L V, L Milenkovic, K M Higgins, and M P Scott. 1997. "Altered Neural Cell Fates and Medulloblastoma in Mouse Patched Mutants." *Science (New York, N.Y.)* 277 (5329). UNITED STATES: 1109–13.

Goth, Regine, and J. E. Cleaver. 1976. "Metabolism of Caffeine to Nucleic Acid Precursors in Mammalian Cells." *Mutation Research - Fundamental and Molecular Mechanisms of Mutagenesis*. [https://doi.org/10.1016/0027-5107\(76\)90025-7](https://doi.org/10.1016/0027-5107(76)90025-7).

Goulding, M D, G Chalepakis, U Deutsch, J R Erselius, and P Gruss. 1991. "Pax-3, a Novel Murine DNA Binding Protein Expressed during Early Neurogenesis." *The EMBO Journal*

10 (5). England: 1135–47.

Goulding, M D, A Lumsden, and P Gruss. 1993. “Signals from the Notochord and Floor Plate Regulate the Region-Specific Expression of Two Pax Genes in the Developing Spinal Cord.” *Development (Cambridge, England)* 117 (3). ENGLAND: 1001–16.

Gouti, Mina, Vicki Metzis, and James Briscoe. 2015. “The Route to Spinal Cord Cell Types: A Tale of Signals and Switches.” *Trends in Genetics* 31 (Box 2). Elsevier Ltd: 1–8. <https://doi.org/10.1016/j.tig.2015.03.001>.

Goveia, Jermaine, Peter Stapor, and Peter Carmeliet. 2014. “Principles of Targeting Endothelial Cell Metabolism to Treat Angiogenesis and Endothelial Cell Dysfunction in Disease.” *EMBO Molecular Medicine* 6 (9): 1–16. <https://doi.org/10.15252/emmm.201404156>.

Goyette, P, B Christensen, D S Rosenblatt, and R Rozen. 1996. “Severe and Mild Mutations in Cis for the Methylenetetrahydrofolate Reductase (MTHFR) Gene, and Description of Five Novel Mutations in MTHFR.” *American Journal of Human Genetics* 59 (6). United States: 1268–75.

Grant, D M, B K Tang, and W Kalow. 1984. “A Simple Test for Acetylator Phenotype Using Caffeine.” *British Journal of Clinical Pharmacology* 17 (4). England: 459–64.

Gray, Jason D, Stanislav Kholmanskikh, Bozena S Castaldo, Alex Hsler, Heekyung Chung, Brian Klotz, Shawn Singh, Anthony M C Brown, and M Elizabeth Ross. 2013. “LRP6 Exerts Non-Canonical Effects on Wnt Signaling during Neural Tube Closure.” *Human Molecular Genetics* 22 (21): 4267–81. <http://dx.doi.org/10.1093/hmg/ddt277>.

Greene, N D, and A J Copp. 1997. “Inositol Prevents Folate-Resistant Neural Tube Defects in the Mouse.” *Nature Medicine* 3 (1). UNITED STATES: 60–66.

Greene, Nicholas D E, and Andrew J Copp. 2009. “Development of the Vertebrate Central Nervous System: Formation of the Neural Tube.” *Prenatal Diagnosis* 29 (4). England: 303–11. <https://doi.org/10.1002/pd.2206>.

Greene, Nicholas D E, Kit-Yi Leung, Victoria Gay, Katie Burren, Kevin Mills, Lyn S Chitty, and Andrew J Copp. 2016. “Inositol for the Prevention of Neural Tube Defects: A Pilot Randomised Controlled Trial.” *The British Journal of Nutrition* 115 (6). England: 974–83. <https://doi.org/10.1017/S0007114515005322>.

Greene, Nicholas D E, Valentina Massa, and Andrew J. Copp. 2009. “Understanding the Causes and Prevention of Neural Tube Defects: Insights from the Splotch Mouse Model.” *Birth Defects Research Part A - Clinical and Molecular Teratology* 85 (4): 322–30. <https://doi.org/10.1002/bdra.20539>.

Greene, Nicholas D E, Philip Stanier, and Andrew J. Copp. 2009. “Genetics of Human Neural Tube Defects.” *Human Molecular Genetics* 18 (R2). <https://doi.org/10.1093/hmg/ddp347>.

Gregory, J F, G J Cuskelly, B Shane, J P Toth, T G Baumgartner, and P W Stacpoole. 2000. “Primed, Constant Infusion with [2H3]serine Allows in Vivo Kinetic Measurement of Serine Turnover, Homocysteine Remethylation, and Transsulfuration Processes in Human

One-Carbon Metabolism.” *The American Journal of Clinical Nutrition* 72 (6). American Society for Nutrition: 1535–41. <http://www.ncbi.nlm.nih.gov/pubmed/11101483>.

Groenen, Pascal M., Petronella G. Peer, Ron A. Wevers, Dorine W. Swinkels, Barbara Franke, Edwin C. Mariman, and Régine P. Steegers-Theunissen. 2003. “Maternal Myo-Inositol, Glucose, and Zinc Status Is Associated with the Risk of Offspring with Spina Bifida.” *American Journal of Obstetrics and Gynecology* 189 (6): 1713–19. [https://doi.org/10.1016/S0002-9378\(03\)00807-X](https://doi.org/10.1016/S0002-9378(03)00807-X).

Grüneberg, Hans. 1954. “Genetical Studies on the Skeleton of the Mouse.” *Journal of Genetics* 52 (1): 52. <https://doi.org/10.1007/BF02981490>.

Gu, L, F J Gonzalez, W Kalow, and B K Tang. 1992. “Biotransformation of Caffeine, Paraxanthine, Theobromine and Theophylline by cDNA-Expressed Human CYP1A2 and CYP2E1.” *Pharmacogenetics* 2 (2). England: 73–77.

Guan, Zhen, Jianhua Wang, Jin Guo, Fang Wang, Xiuwei Wang, Guannan Li, Qiu Xie, Xu Han, Bo Niu, and Ting Zhang. 2014. “The Maternal ITPK1 Gene Polymorphism Is Associated with Neural Tube Defects in a High-Risk Chinese Population.” *PLoS One* 9 (1). United States: e86145. <https://doi.org/10.1371/journal.pone.0086145>.

Guan, Zhen, Xiuwei Wang, Yanting Dong, Lin Xu, Zhiqiang Zhu, Jianhua Wang, Ting Zhang, and Bo Niu. 2015. “dNTP Deficiency Induced by HU via Inhibiting Ribonucleotide Reductase Affects Neural Tube Development.” *Toxicology* 328 (February). Ireland: 142–51. <https://doi.org/10.1016/j.tox.2014.12.001>.

Gunther, T, M Struwe, A Aguzzi, and K Schughart. 1994. “Open Brain, a New Mouse Mutant with Severe Neural Tube Defects, Shows Altered Gene Expression Patterns in the Developing Spinal Cord.” *Development (Cambridge, England)* 120 (11). England: 3119–30.

Gurniak, Christine B, Emerald Perlas, and Walter Witke. 2005. “The Actin Depolymerizing Factor N-Cofilin Is Essential for Neural Tube Morphogenesis and Neural Crest Cell Migration.” *Developmental Biology* 278 (1). United States: 231–41. <https://doi.org/10.1016/j.ydbio.2004.11.010>.

Gurvich, Nadia, Melissa G Berman, Ben S Wittner, Robert C Gentleman, Peter S Klein, and Jeremy B A Green. 2005. “Association of Valproate-Induced Teratogenesis with Histone Deacetylase Inhibition in Vivo.” *FASEB Journal : Official Publication of the Federation of American Societies for Experimental Biology* 19 (9). United States: 1166–68. <https://doi.org/10.1096/fj.04-3425fje>.

Gustavsson, Peter, Nicholas D E Greene, Dina Lad, Erwin Pauws, Sandra C P de Castro, Philip Stanier, and Andrew J. Copp. 2007. “Increased Expression of Grainyhead-like-3 Rescues Spina Bifida in a Folate-Resistant Mouse Model.” *Human Molecular Genetics* 16 (21): 2640–46. <https://doi.org/10.1093/hmg/ddm221>.

Guttmacher Institute. n.d. “Unintended Pregnancy in the United States.” <https://www.guttmacher.org/fact-sheet/unintended-pregnancy-united-states>.

Hale, F. 1933. "Pigs born without eyeballs." *Journal of Heredity* 24: 105–6.

———. 1935. "Relation of Vitamin A to Anophthalmos in Pigs." *American Journal of Ophthalmology* 18: 1087–93.

Hale, F. 1937. "Relation of maternal vitamin A deficiency to microphthalmia in pigs." *Texas State J.Med.* 33: 228–32.

Hammerschmidt, M, A Brook, and A P McMahon. 1997. "The World according to Hedgehog." *Trends in Genetics : TIG* 13 (1). England: 14–21.

Hansen, Jason M., Kristi M. Contreras, and Craig Harris. 2005. "Methanol, Formaldehyde, and Sodium Formate Exposure in Rat and Mouse Conceptuses: A Potential Role of the Visceral Yolk Sac in Embryotoxicity." *Birth Defects Research Part A - Clinical and Molecular Teratology* 73 (2): 72–82. <https://doi.org/10.1002/bdra.20094>.

Hanzlik, Robert P, Stephen C Fowler, and Janis T Eells. 2005. "Absorption and Elimination of Formate Following Oral Administration of Calcium Formate in Female Human Subjects." *Drug Metabolism and Disposition: The Biological Fate of Chemicals* 33 (2). United States: 282–86. <https://doi.org/10.1124/dmd.104.001289>.

Harris, Muriel J., and Diana M. Juriloff. 2007. "Mouse Mutants with Neural Tube Closure Defects and Their Role in Understanding Human Neural Tube Defects." *Birth Defects Research Part A - Clinical and Molecular Teratology* 79 (3): 187–210. <https://doi.org/10.1002/bdra.20333>.

Harris, Muriel J., and Diana M. Juriloff. 2010. "An Update to the List of Mouse Mutants with Neural Tube Closure Defects and Advances toward a Complete Genetic Perspective of Neural Tube Closure." *Birth Defects Research Part A - Clinical and Molecular Teratology* 88 (8): 653–69. <https://doi.org/10.1002/bdra.20676>.

Hart, Joseph, and Kalpana Miriyala. 2017. "Neural Tube Defects in Waardenburg Syndrome: A Case Report and Review of the Literature." *American Journal of Medical Genetics. Part A*, July. United States. <https://doi.org/10.1002/ajmg.a.38325>.

Hartwig, J H, M Thelen, A Rosen, P A Janmey, A C Nairn, and A Aderem. 1992. "MARCKS Is an Actin Filament Crosslinking Protein Regulated by Protein Kinase C and Calcium-Calmodulin." *Nature* 356 (6370). England: 618–22. <https://doi.org/10.1038/356618a0>.

Hashimoto, M, S Akazawa, M Akazawa, M Akashi, H Yamamoto, Y Maeda, Y Yamaguchi, H Yamasaki, D Tahara, and T Nakanishi. 1990. "Effects of Hyperglycaemia on Sorbitol and Myo-Inositol Contents of Cultured Embryos: Treatment with Aldose Reductase Inhibitor and Myo-Inositol Supplementation." *Diabetologia* 33 (10). Germany: 597–602.

Hashimoto, Takashi, Zhiwei He, Wei-Ya Ma, Patricia C Schmid, Ann M Bode, Chung S Yang, and Zigang Dong. 2004. "Caffeine Inhibits Cell Proliferation by G0/G1 Phase Arrest in JB6 Cells." *Cancer Research* 64 (9). United States: 3344–49.

Henderson, Deborah J., Patricia Ybot-Gonzalez, and Andrew J. Copp. 1997. "Over-Expression of the Chondroitin Sulphate Proteoglycan Versican Is Associated with Defective Neural Crest

Migration in the Pax3 Mutant Mouse (Splotch)." *Mechanisms of Development* 69 (1–2): 39–51. [https://doi.org/10.1016/S0925-4773\(97\)00151-2](https://doi.org/10.1016/S0925-4773(97)00151-2).

Hendzel, M J, Y Wei, M A Mancini, A Van Hooser, T Ranalli, B R Brinkley, D P Bazett-Jones, and C D Allis. 1997. "Mitosis-Specific Phosphorylation of Histone H3 Initiates Primarily within Pericentromeric Heterochromatin during G2 and Spreads in an Ordered Fashion Coincident with Mitotic Chromosome Condensation." *Chromosoma* 106 (6). GERMANY: 348–60.

Henrique, Domingos, Elsa Abrantes, Laure Verrier, and Kate G Storey. 2015. "Neuromesodermal Progenitors and the Making of the Spinal Cord." *Development* 142 (17): 2864 LP-2875. <http://dev.biologists.org/content/142/17/2864.abstract>.

Herbig, Katherine, En-Pei Chiang, Ling-Ru Lee, Jessica Hills, Barry Shane, and Patrick J Stover. 2002. "Cytoplasmic Serine Hydroxymethyltransferase Mediates Competition between Folate-Dependent Deoxyribonucleotide and S-Adenosylmethionine Biosyntheses." *The Journal of Biological Chemistry* 277 (41). United States: 38381–89. <https://doi.org/10.1074/jbc.M205000200>.

Hernandez-Diaz, S, M M Werler, A M Walker, and A A Mitchell. 2001. "Neural Tube Defects in Relation to Use of Folic Acid Antagonists during Pregnancy." *American Journal of Epidemiology* 153 (10). United States: 961–68.

Heseker, Helmut B, Joel B Mason, Jacob Selhub, Irwin H Rosenberg, and Paul F Jacques. 2009. "Not All Cases of Neural-Tube Defect Can Be Prevented by Increasing the Intake of Folic Acid." *The British Journal of Nutrition* 102 (2). England: 173–80. <https://doi.org/10.1017/S0007114508149200>.

Hess, Jennifer R, and Norman A Greenberg. 2012. "The Role of Nucleotides in the Immune and Gastrointestinal Systems: Potential Clinical Applications." *Nutrition in Clinical Practice : Official Publication of the American Society for Parenteral and Enteral Nutrition* 27 (2). United States: 281–94. <https://doi.org/10.1177/0884533611434933>.

Hibbard, B M. 1964. "The Role of Folic Acid in Pregnancy; with Particular Reference to Anaemia, Abruption and Abortion." *The Journal of Obstetrics and Gynaecology of the British Commonwealth* 71 (August). England: 529–42.

Hibbard, ElizabethD., and R.W. Smithells. 1965. "Folic Acid Metabolism and Human Embryopathy." *The Lancet* 285 (7398): 1254. [https://doi.org/10.1016/S0140-6736\(65\)91895-7](https://doi.org/10.1016/S0140-6736(65)91895-7).

Hildebrand, J D, and P Soriano. 1999. "Shroom, a PDZ Domain-Containing Actin-Binding Protein, Is Required for Neural Tube Morphogenesis in Mice." *Cell* 99 (5). United States: 485–97.

Hiltunen, J. Kalervo, Kaija J. Autio, Melissa S. Schonauer, V.A. Samuli Kursu, Carol L. Dieckmann, and Alexander J. Kastaniotis. 2010. "Mitochondrial Fatty Acid Synthesis and Respiration." *Biochimica et Biophysica Acta (BBA) - Bioenergetics* 1797 (6–7). Elsevier

B.V.: 1195–1202. <https://doi.org/10.1016/j.bbabi.2010.03.006>.

Ho, C Y, K V Miller, D A Savaiano, R T Crane, K A Ericson, and A J Clifford. 1979. “Absorption and Metabolism of Orally Administered Purines in Fed and Fasted Rats.” *The Journal of Nutrition* 109 (8). United States: 1377–82.

Hod, M, S Star, J Passonneau, T G Unterman, and N Freinkel. 1990. “Glucose-Induced Dysmorphogenesis in the Cultured Rat Conceptus: Prevention by Supplementation with Myo-Inositol.” *Israel Journal of Medical Sciences* 26 (10). Israel: 541–44.

Hol, F A, B C Hamel, M P Geurds, R A Mullaart, F G Barr, R A Macina, and E C Mariman. 1995. “A Frameshift Mutation in the Gene for PAX3 in a Girl with Spina Bifida and Mild Signs of Waardenburg Syndrome.” *Journal of Medical Genetics* 32 (1). England: 52–56.

Homanics, G E, N Maeda, M G Traber, H J Kayden, D B Dehart, and K K Sulik. 1995. “Exencephaly and Hydrocephaly in Mice with Targeted Modification of the Apolipoprotein B (Apob) Gene.” *Teratology* 51 (1). United States: 1–10. <https://doi.org/10.1002/tera.1420510102>.

Honarpour, N, C Du, J A Richardson, R E Hammer, X Wang, and J Herz. 2000. “Adult Apaf-1-Deficient Mice Exhibit Male Infertility.” *Developmental Biology* 218 (2). United States: 248–58. <https://doi.org/10.1006/dbio.1999.9585>.

Horder, Tim. 2001. “History of Developmental Biology.” In *eLS*. John Wiley & Sons, Ltd. <https://doi.org/10.1002/9780470015902.a0003080.pub2>.

Huang, D, Y H Zhang, and X G Chen. 2003. “Analysis of Intracellular Nucleoside Triphosphate Levels in Normal and Tumor Cell Lines by High-Performance Liquid Chromatography.” *Journal of Chromatography B-Analytical Technologies in the Biomedical and Life Sciences* 784 (1): 101–9. [https://doi.org/10.1016/S1570-0232\(02\)00780-8](https://doi.org/10.1016/S1570-0232(02)00780-8).

Huang, Yongzhao, Henk Roelink, and G Stanley McKnight. 2002. “Protein Kinase A Deficiency Causes Axially Localized Neural Tube Defects in Mice.” *The Journal of Biological Chemistry* 277 (22). United States: 19889–96. <https://doi.org/10.1074/jbc.M111412200>.

Huangfu, Danwei, Aimin Liu, Andrew S Rakeman, Noel S Murcia, Lee Niswander, and Kathryn V Anderson. 2003. “Hedgehog Signalling in the Mouse Requires Intraflagellar Transport Proteins.” *Nature* 426 (6962). England: 83–87. <https://doi.org/10.1038/nature02061>.

Hui, C C, and A L Joyner. 1993. “A Mouse Model of Greig Cephalopolysyndactyly Syndrome: The Extra-toesJ Mutation Contains an Intragenic Deletion of the Gli3 Gene.” *Nature Genetics* 3 (3). United States: 241–46. <https://doi.org/10.1038/ng0393-241>.

Hume, Joseph R., Claire E. McAllister, and Sean M. Wilson. 2009. “Caffeine Inhibits InsP3 Responses and Capacitative Calcium Entry in Canine Pulmonary Arterial Smooth Muscle Cells.” *Vascular Pharmacology*. <https://doi.org/10.1016/j.vph.2008.11.001>.

Ichi, Shunsuke, Fabricio F. Costa, Jared M. Bischof, Hiromichi Nakazaki, Yueh Wei Shen, Vanda Boshnjaku, Saurabh Sharma, et al. 2010. “Folic Acid Remodels Chromatin on Hes1 and Neurog2 Promoters during Caudal Neural Tube Development.” *Journal of Biological*

Chemistry 285 (47): 36922–32. <https://doi.org/10.1074/jbc.M110.126714>.

Ichi, Shunsuke, Hiromichi Nakazaki, Vanda Boshnjaku, Ravneet Monny Singh, Barbara Mania-Farnell, Guifa Xi, David G. McLone, Tadanori Tomita, and Chandra Shekhar K. Mayanil. 2012. “Mutant Mice Proliferate, Differentiate, and Form Synaptic Connections When Stimulated with Folic Acid.” *Stem Cells and Development* 21 (2): 321–30. <https://doi.org/10.1089/scd.2011.0100>.

Ikeda, A, S Ikeda, T Gridley, P M Nishina, and J K Naggert. 2001. “Neural Tube Defects and Neuroepithelial Cell Death in *Tulp3* Knockout Mice.” Journal Article, Research Support, Non-U.S. Gov’t, Research Support, U.S. Gov’t, P.H.S. *Human Molecular Genetics* 10 (12). England, England: 1325–34.

Ingham, Philip W, Andrew P Mcmahon, Philip W Ingham, and Andrew P Mcmahon. 2001. “Hedgehog Signaling in Animal Development : Paradigms and Principles Hedgehog Signaling in Animal Development : Paradigms and Principles.” *Genes and Development* 15 (23): 3059–87. <https://doi.org/10.1101/gad.938601>.

Ishibashi, M, S L Ang, K Shiota, S Nakanishi, R Kageyama, and F Guillemot. 1995. “Targeted Disruption of Mammalian Hairy and Enhancer of Split Homolog-1 (HES-1) Leads to up-Regulation of Neural Helix-Loop-Helix Factors, Premature Neurogenesis, and Severe Neural Tube Defects.” *Genes & Development* 9 (24). UNITED STATES: 3136–48.

Ishibashi, M, K Moriyoshi, Y Sasai, K Shiota, S Nakanishi, and R Kageyama. 1994. “Persistent Expression of Helix-Loop-Helix Factor HES-1 Prevents Mammalian Neural Differentiation in the Central Nervous System.” *The EMBO Journal* 13 (8). England: 1799–1805.

Iso, Tatsuya, Larry Kedes, and Yasuo Hamamori. 2003. “HES and HERP Families: Multiple Effectors of the Notch Signaling Pathway.” *Journal of Cellular Physiology* 194 (3). United States: 237–55. <https://doi.org/10.1002/jcp.10208>.

Jacob, John, and James Briscoe. 2003. “Gli Proteins and the Control of Spinal-Cord Patterning.” *EMBO Reports* 4 (8): 761–65. <https://doi.org/10.1038/sj.embor.embor896>.

Jacoby, Monique, James J Cox, Stephanie Gayral, Daniel J Hampshire, Mohammed Ayub, Marianne Blockmans, Eileen Pernot, et al. 2009. “INPP5E Mutations Cause Primary Cilium Signaling Defects, Ciliary Instability and Ciliopathies in Human and Mouse.” *Nature Genetics* 41 (9). United States: 1027–31. <https://doi.org/10.1038/ng.427>.

Jacombs, A, J Ryan, A Loupis, and I Pollard. 1999. “Maternal Caffeine Consumption during Pregnancy Does Not Affect Preimplantation Development but Delays Early Postimplantation Growth in Rat Embryos.” *Reproduction, Fertility, and Development* 11 (4–5). Australia: 211–18.

Jadavji, Nafisa M, Renata H Bahous, Liyuan Deng, Olga Malysheva, Marilyn Grand’maison, Barry J Bedell, Marie A Caudill, and Rima Rozen. 2014. “Mouse Model for Deficiency of Methionine Synthase Reductase Exhibits Short-Term Memory Impairment and Disturbances in Brain Choline Metabolism.” *The Biochemical Journal* 461 (2). England: 205–12.

https://doi.org/10.1042/BJ20131568.

Jessell, T M. 2000. "Neuronal Specification in the Spinal Cord: Inductive Signals and Transcriptional Codes." *Nature Reviews. Genetics* 1 (1). England: 20–29.
https://doi.org/10.1038/35049541.

Jiang, Jianxin, Yanfei Zhang, Liang Wei, Zhiyang Sun, and Zhongmin Liu. 2014. "Association between MTHFD1 G1958A Polymorphism and Neural Tube Defects Susceptibility: A Meta-Analysis." *PloS One* 9 (6). United States: e101169.
https://doi.org/10.1371/journal.pone.0101169.

Johnson, D R. 1967. "Extra-Toes: Anew Mutant Gene Causing Multiple Abnormalities in the Mouse." *Journal of Embryology and Experimental Morphology* 17 (3). England: 543–81.

Jones, Alan Wayne. 2017. "Review of Caffeine-Related Fatalities along with Postmortem Blood Concentrations in 51 Poisoning Deaths." *Journal of Analytical Toxicology*, February. England, 1–6. https://doi.org/10.1093/jat/bkx011.

Juriloff, D M, and M J Harris. 2000. "Mouse Models for Neural Tube Closure Defects." *Human Molecular Genetics* 9 (6): 993–1000. https://doi.org/10.1093/Hmg/9.6.993.

Juriloff, Diana M., and Muriel J. Harris. 2012. "Hypothesis: The Female Excess in Cranial Neural Tube Defects Reflects an Epigenetic Drag of the Inactivating X Chromosome on the Molecular Mechanisms of Neural Fold Elevation." *Birth Defects Research Part A - Clinical and Molecular Teratology* 94 (10): 849–55. https://doi.org/10.1002/bdra.23036.

Kageyama, Ryoichiro, Toshiyuki Ohtsuka, and Taeko Kobayashi. 2008. "Roles of Hes Genes in Neural Development." *Development Growth and Differentiation* 50 (SUPPL. 1): S97–S103.
https://doi.org/10.1111/j.1440-169X.2008.00993.x.

Kalter, H, and J Warkany. 1959. "Experimental Production of Congenital Malformations in Mammals by Metabolic Procedure." *Physiol. Rev.* 39 (1). United States: 69–115.

KEGG Pathway. 2016a. "Purine Metabolism (KEGG)." Kanehisa Laboratories. 2016.
http://www.genome.jp/kegg-bin/show_pathway?org_name=mmu&mapno=01100&mapscale=0.35&show_description=hide&show_module_list=

KEGG Pathway 2016b. "Pyrimidine Metabolism (KEGG)." Kanehisa Laboratories. 2016.
[http://pathcards.genecards.org/card/pyrimidine_metabolism_\(kegg\).](http://pathcards.genecards.org/card/pyrimidine_metabolism_(kegg).)

Keiper, Melanie, Matthias B Stope, Daniel Szatkowski, Anja Bohm, Karina Tysack, Frank Vom Dorp, Oliver Saur, et al. 2004. "Epac- and Ca²⁺ -Controlled Activation of Ras and Extracellular Signal-Regulated Kinases by Gs-Coupled Receptors." *The Journal of Biological Chemistry* 279 (45). United States: 46497–508.
https://doi.org/10.1074/jbc.M403604200.

Keller, Ray, David Shook, and Paul Skoglund. 2008. "The Forces That Shape Embryos: Physical Aspects of Convergent Extension by Cell Intercalation." *Physical Biology* 5 (1). England: 15007. https://doi.org/10.1088/1478-3975/5/1/015007.

Khandelwal, M, E A Reece, Y K Wu, and M Borenstein. 1998. "Dietary Myo-Inositol Therapy in Hyperglycemia-Induced Embryopathy." *Teratology* 57 (2). United States: 79–84.
[https://doi.org/10.1002/\(SICI\)1096-9926\(199802\)57:2<79::AID-TERA6>3.0.CO;2-1](https://doi.org/10.1002/(SICI)1096-9926(199802)57:2<79::AID-TERA6>3.0.CO;2-1).

Kibar, Z, K J Vogan, N Groulx, M J Justice, D A Underhill, and P Gros. 2001. "Ltap, a Mammalian Homolog of Drosophila Strabismus/Van Gogh, Is Altered in the Mouse Neural Tube Mutant Loop-Tail." *Nature Genetics* 28 (3). United States: 251–55.
<https://doi.org/10.1038/90081>.

Kibar, Zoha, Elena Torban, Jonathan R McDearmid, Annie Reynolds, Joanne Berghout, Melissa Mathieu, Irena Kirillova, et al. 2007. "Mutations in VANGL1 Associated with Neural-Tube Defects." *The New England Journal of Medicine* 356 (14). United States: 1432–37.
<https://doi.org/10.1056/NEJMoa060651>.

Kikuchi, Goro, Yutaro Motokawa, Tadashi Yoshida, and Koichi Hiraga. 2008. "Glycine Cleavage System: Reaction Mechanism, Physiological Significance, and Hyperglycinemia." *Proceedings of the Japan Academy. Series B, Physical and Biological Sciences* 84 (7). Japan: 246–63.

Killmann, Sven. 1964. "Effect of Deoxyuridine on Incorporation of Tritiated Thymidine: Difference Between Normoblasts and Megaloblasts." *Acta Medica Scandinavica* 175 (4). Sweden: 483–88. <https://doi.org/10.1111/j.0954-6820.1964.tb00597.x>.

Kim, Tae Hee, Jessica Goodman, Kathryn V. Anderson, and Lee Niswander. 2007. "Phactr4 Regulates Neural Tube and Optic Fissure Closure by Controlling PP1-, Rb-, and E2F1-Regulated Cell-Cycle Progression." *Developmental Cell* 13 (1): 87–102.
<https://doi.org/10.1016/j.devcel.2007.04.018>.

Kimura-Yoshida, Chiharu, Kyoko Mochida, Kristina Ellwanger, Christof Niehrs, and Isao Matsuo. 2015. "Fate Specification of Neural Plate Border by Canonical Wnt Signaling and Grhl3 Is Crucial for Neural Tube Closure." *EBioMedicine* 2 (6). Elsevier B.V.: 513–27.
<https://doi.org/10.1016/j.ebiom.2015.04.012>.

Kioussi, C, M K Gross, and P Gruss. 1995. "Pax3: A Paired Domain Gene as a Regulator in PNS Myelination." *Neuron* 15 (3). UNITED STATES: 553–62.

Kirke, P N, A M Molloy, L E Daly, H Burke, D G Weir, and J M Scott. 1993. "Maternal Plasma Folate and Vitamin B12 Are Independent Risk Factors for Neural Tube Defects." *The Quarterly Journal of Medicine* 86 (11). England: 703–8.

Kirke, Peadar N, James L Mills, Anne M Molloy, Lawrence C Brody, Valerie B O'Leary, Leslie Daly, Sharon Murray, et al. 2004. "Impact of the MTHFR C677T Polymorphism on Risk of Neural Tube Defects: Case-Control Study." *BMJ (Clinical Research Ed.)* 328 (7455). England: 1535–36. <https://doi.org/10.1136/bmj.38036.646030.EE>.

Kleijer, Wim J, Marianne L T van der Sterre, Victor H Garritsen, Anja Raams, and Nicolaas G J Jaspers. 2006. "Prenatal Diagnosis of the Cockayne Syndrome: Survey of 15 Years Experience." *Prenatal Diagnosis* 26 (10): 980–84. <https://doi.org/10.1002/pd>.

Kochilas, L K, J Li, F Jin, C A Buck, and J A Epstein. 1999. "p57Kip2 Expression Is Enhanced during Mid-Cardiac Murine Development and Is Restricted to Trabecular Myocardium." *Pediatric Research* 45 (5 Pt 1). UNITED STATES: 635–42. <https://doi.org/10.1203/00006450-199905010-00004>.

Kondoh, Hisato, Shinji Takada, and Tatsuya Takemoto. 2016. "Axial Level-Dependent Molecular and Cellular Mechanisms Underlying the Genesis of the Embryonic Neural Plate." *Development, Growth & Differentiation* 58 (5). Japan: 427–36. <https://doi.org/10.1111/dgd.12295>.

Kong, Jennifer H, Linlin Yang, Eric Dessaud, Katherine Chuang, Destaye M Moore, Rajat Rohatgi, James Briscoe, and Bennett G Novitch. 2015. "Notch Activity Modulates the Responsiveness of Neural Progenitors to Sonic Hedgehog Signaling." *Developmental Cell* 33 (4). United States: 373–87. <https://doi.org/10.1016/j.devcel.2015.03.005>.

Kopan, Raphael, and Maria Xenia G Ilagan. 2009. "The Canonical Notch Signaling Pathway: Unfolding the Activation Mechanism." *Cell* 137 (2). United States: 216–33. <https://doi.org/10.1016/j.cell.2009.03.045>.

Kot, Marta, and Wladyslawa A Daniel. 2008. "The Relative Contribution of Human Cytochrome P450 Isoforms to the Four Caffeine Oxidation Pathways: An in Vitro Comparative Study with cDNA-Expressed P450s Including CYP2C Isoforms." *Biochemical Pharmacology* 76 (4). England: 543–51. <https://doi.org/10.1016/j.bcp.2008.05.025>.

Kotsis, Damian H., Elizabeth M. Masko, Frederic D. Sigoillot, Roberto Di Gregorio, Hedeel I. Guy-Evans, and David R. Evans. 2007. "Protein Kinase A Phosphorylation of the Multifunctional Protein CAD Antagonizes Activation by the MAP Kinase Cascade." *Molecular and Cellular Biochemistry* 301 (1–2): 69–81. <https://doi.org/10.1007/s11010-006-9398-x>.

Kuida, K, T F Haydar, C Y Kuan, Y Gu, C Taya, H Karasuyama, M S Su, P Rakic, and R A Flavell. 1998. "Reduced Apoptosis and Cytochrome c-Mediated Caspase Activation in Mice Lacking Caspase 9." *Cell* 94 (3). United States: 325–37.

Kuida, K, T S Zheng, S Na, C Kuan, D Yang, H Karasuyama, P Rakic, and R A Flavell. 1996. "Decreased Apoptosis in the Brain and Premature Lethality in CPP32-Deficient Mice." *Nature* 384 (6607). England: 368–72. <https://doi.org/10.1038/384368a0>.

Kur, Esther, Nora Mecklenburg, Robert M Cabrera, Thomas E Willnow, and Annette Hammes. 2014. "LRP2 Mediates Folate Uptake in the Developing Neural Tube." *Journal of Cell Science* 127 (Pt 10). England: 2261–68. <https://doi.org/10.1242/jcs.140145>.

Kurki, P, M Vanderlaan, F Dolbeare, J Gray, and E M Tan. 1986. "Expression of Proliferating Cell Nuclear Antigen (PCNA)/cyclin during the Cell Cycle." *Experimental Cell Research* 166 (1). United States: 209–19.

Kwang, Stanford J, Sean M Brugger, Arthur Lazik, Amy E Merrill, Lan-Ying Wu, Yi-Hsin Liu, Mamoru Ishii, et al. 2002. "Msx2 Is an Immediate Downstream Effector of Pax3 in the

Development of the Murine Cardiac Neural Crest.” *Development (Cambridge, England)* 129 (2): 527–38. [papers3://publication/uuid/9EF077CB-7110-4526-8F67-FE5A2F582786](https://doi.org/10.1242/dev.00006).

la Pompa, J L de, A Wakeham, K M Correia, E Samper, S Brown, R J Aguilera, T Nakano, et al. 1997. “Conservation of the Notch Signalling Pathway in Mammalian Neurogenesis.” *Development (Cambridge, England)* 124 (6). England: 1139–48.

Labedzki, Andreas, Jeroen Buters, Wafaâ Jabrane, and Uwe Fuhr. 2002. “Differences in Caffeine and Paraxanthine Metabolism between Human and Murine CYP1A2.” *Biochemical Pharmacology* 63 (12): 2159–67. [https://doi.org/10.1016/S0006-2952\(02\)01019-5](https://doi.org/10.1016/S0006-2952(02)01019-5).

Lamarre, Simon G., Gregory Morrow, Luke MacMillan, Margaret E. Brosnan, and John T. Brosnan. 2013. “Formate: An Essential Metabolite, a Biomarker, or More?” *Clinical Chemistry and Laboratory Medicine* 51 (3): 571–78. <https://doi.org/10.1515/cclm-2012-0552>.

Lamarre, Simon G, Luke MacMillan, Gregory P Morrow, Edward Randell, Theerawat Pongnopparat, Margaret E Brosnan, and John T Brosnan. 2014. “An Isotope-Dilution, GC-MS Assay for Formate and Its Application to Human and Animal Metabolism.” *Amino Acids* 46 (8). Austria: 1885–91. <https://doi.org/10.1007/s00726-014-1738-7>.

Lamarre, Simon G, Anne M Molloy, Stacey N Reinke, Brian D Sykes, Margaret E Brosnan, and John T Brosnan. 2012. “Formate Can Differentiate between Hyperhomocysteinemia due to Impaired Remethylation and Impaired Transsulfuration.” *American Journal of Physiology. Endocrinology and Metabolism* 302 (1): E61–7. <https://doi.org/10.1152/ajpendo.00345.2011>.

Lamers, Yvonne, Jerry Williamson, Lesa R Gilbert, Peter W Stacpoole, and Jesse F 3rd Gregory. 2007. “Glycine Turnover and Decarboxylation Rate Quantified in Healthy Men and Women Using Primed, Constant Infusions of [1,2-(13)C2]glycine and [(2)H3]leucine.” *The Journal of Nutrition* 137 (12). United States: 2647–52.

Lamers, Yvonne, Jerry Williamson, Douglas W Theriaque, Jonathan J Shuster, Lesa R Gilbert, Christine Keeling, Peter W Stacpoole, and Jesse F 3rd Gregory. 2009. “Production of 1-Carbon Units from Glycine Is Extensive in Healthy Men and Women.” *The Journal of Nutrition* 139 (4). United States: 666–71. <https://doi.org/10.3945/jn.108.103580>.

Lammer, E J, L E Sever, and G P Jr Oakley. 1987. “Teratogen Update: Valproic Acid.” *Teratology* 35 (3). United States: 465–73. <https://doi.org/10.1002/tera.1420350319>.

Lane, Andrew N, and Teresa W-M Fan. 2015. “Regulation of Mammalian Nucleotide Metabolism and Biosynthesis.” *Nucleic Acids Research* 43 (4). England: 2466–85. <https://doi.org/10.1093/nar/gkv047>.

Lang, Deborah, Min Min Lu, Li Huang, Kurt A Engleka, Maozhen Zhang, Emily Y Chu, Shari Lipner, Arthur Skoultschi, Sarah E Millar, and Jonathan A Epstein. 2005. “Pax3 Functions at a Nodal Point in Melanocyte Stem Cell Differentiation.” *Nature* 433 (7028). England: 884–87. <https://doi.org/10.1038/nature03292>.

Laourdakis, Christian D., Emilio F. Merino, Andrew P. Neilson, and Maria B. Cassera. 2014.

“Comprehensive Quantitative Analysis of Purines and Pyrimidines in the Human Malaria Parasite Using Ion-Pairing Ultra-Performance Liquid Chromatography-Mass Spectrometry.” *Journal of Chromatography B: Analytical Technologies in the Biomedical and Life Sciences* 967. Elsevier B.V.: 127–33. <https://doi.org/10.1016/j.jchromb.2014.07.012>.

Lardelli, M, R Williams, T Mitsiadis, and U Lendahl. 1996. “Expression of the Notch 3 Intracellular Domain in Mouse Central Nervous System Progenitor Cells Is Lethal and Leads to Disturbed Neural Tube Development.” *Mechanisms of Development* 59 (2). Ireland: 177–90.

Leck, I. 1974. “Causation of Neural Tube Defects: Clues from Epidemiology.” *British Medical Bulletin* 30 (2). England: 158–63.

Lee, H, R G Nagele, and J F Pietrolungo. 1982. “Toxic and Teratologic Effects of Caffeine on Explanted Early Chick Embryos.” *Teratology* 25 (1). United States: 19–25. <https://doi.org/10.1002/tera.1420250104>.

Lee, J, K A Platt, P Censullo, and A Ruiz i Altaba. 1997. “Gli1 Is a Target of Sonic Hedgehog That Induces Ventral Neural Tube Development.” *Development (Cambridge, England)* 124 (13). England: 2537–52.

Lee, S M, P S Danielian, B Fritzsch, and A P McMahon. 1997. “Evidence That FGF8 Signalling from the Midbrain-Hindbrain Junction Regulates Growth and Polarity in the Developing Midbrain.” *Development (Cambridge, England)* 124 (5). England: 959–69.

Lei, Qiubo, Yongsu Jeong, Kamana Misra, Shike Li, Alice K. Zelman, Douglas J. Epstein, and Michael P. Matise. 2006. “Wnt Signaling Inhibitors Regulate the Transcriptional Response to Morphogenetic Shh-Gli Signaling in the Neural Tube.” *Developmental Cell* 11 (3): 325–37. <https://doi.org/10.1016/j.devcel.2006.06.013>.

Lei, Yun-Ping, Ting Zhang, Hong Li, Bai-Lin Wu, Li Jin, and Hong-Yan Wang. 2010. “VANGL2 Mutations in Human Cranial Neural-Tube Defects.” *The New England Journal of Medicine*. United States. <https://doi.org/10.1056/NEJMCo910820>.

Lei, Yunping, Huiping Zhu, Cody Duhon, Wei Yang, M Elizabeth Ross, Gary M Shaw, and Richard H Finnell. 2013. “Mutations in Planar Cell Polarity Gene SCRIB Are Associated with Spina Bifida.” *PLoS One* 8 (7). United States: e69262. <https://doi.org/10.1371/journal.pone.0069262>.

Lei, Yunping, Huiping Zhu, Wei Yang, M Elizabeth Ross, Gary M Shaw, and Richard H Finnell. 2014. “Identification of Novel CELSR1 Mutations in Spina Bifida.” *PLoS One* 9 (3). United States: e92207. <https://doi.org/10.1371/journal.pone.0092207>.

Leikola, A. 1976. “Hensen’s Node — The ‘Organizer’ of the Amniote Embryo.” *Experientia* 32 (3): 269–77. <https://doi.org/10.1007/BF01940787>.

Lelo, A, J O Miners, R Robson, and D J Birkett. 1986. “Assessment of Caffeine Exposure: Caffeine Content of Beverages, Caffeine Intake, and Plasma Concentrations of Methylxanthines.” *Clinical Pharmacology and Therapeutics* 39 (1). United States: 54–59.

Lemay, Philippe, Marie-Claude Guyot, Elizabeth Tremblay, Alexandre Dionne-Laporte, Dan Spiegelman, Edouard Henrion, Ousmane Diallo, et al. 2015. "Loss-of-Function de Novo Mutations Play an Important Role in Severe Human Neural Tube Defects." *Journal of Medical Genetics* 52 (7). England: 493–97. <https://doi.org/10.1136/jmedgenet-2015-103027>.

Lemay, Philippe, Patrizia De Marco, Alexandre Emond, Dan Spiegelman, Alexandre Dionne-Laporte, Sandra Laurent, Elisa Merello, et al. 2017. "Rare Deleterious Variants in GRHL3 Are Associated with Human Spina Bifida." *Human Mutation* 38 (6). United States: 716–24. <https://doi.org/10.1002/humu.23214>.

Leon, Jose de, Francisco J Diaz, Thea Rogers, Debra Browne, Lori Dinsmore, Omar H Ghosheh, Linda P Dwoskin, and Peter A Crooks. 2003. "A Pilot Study of Plasma Caffeine Concentrations in a US Sample of Smoker and Nonsmoker Volunteers." *Progress in Neuropsychopharmacology & Biological Psychiatry* 27 (1). England: 165–71.

Letts, V A, N J Schork, A J Copp, M Bernfield, and W N Frankel. 1995. "A Curly-Tail Modifier Locus, mct1, on Mouse Chromosome 17." *Genomics* 29 (3). United States: 719–24. <https://doi.org/10.1006/geno.1995.9946>.

Leung, K.-Y., Y.J. Pai, Q. Chen, C. Santos, E. Calvani, S. Sudiwala, D. Savery, et al. 2017. "Partitioning of One-Carbon Units in Folate and Methionine Metabolism Is Essential for Neural Tube Closure." *Cell Reports* 21 (7). <https://doi.org/10.1016/j.celrep.2017.10.072>.

Leung, Kit Yi, Sandra C P De Castro, Dawn Savery, Andrew J. Copp, and Nicholas D E Greene. 2013. "Nucleotide Precursors Prevent Folic Acid-Resistant Neural Tube Defects in the Mouse." *Brain* 136 (9): 2836–41. <https://doi.org/10.1093/brain/awt209>.

Leviton, A., and L. Cowan. 2002. "A Review of the Literature Relating Caffeine Consumption by Women to Their Risk of Reproductive Hazards." *Food and Chemical Toxicology*. [https://doi.org/10.1016/S0278-6915\(02\)00092-3](https://doi.org/10.1016/S0278-6915(02)00092-3).

Lewis, Caroline A, Seth J Parker, Brian P Fiske, Douglas McCloskey, Dan Y Gui, Courtney R Green, Natalie I Vokes, Adam M Feist, Matthew G Vander Heiden, and Christian M Metallo. 2014. "Tracing Compartmentalized NADPH Metabolism in the Cytosol and Mitochondria of Mammalian Cells." *Molecular Cell* 55 (2). United States: 253–63. <https://doi.org/10.1016/j.molcel.2014.05.008>.

Leyva, A, H Appel, and H M Pinedo. 1982. "Purine Modulation of Thymidine Activity in L1210 Leukemia Cells in Vitro." *Leukemia Research* 6 (4). England: 483–90.

Li, Deqiang, Laura Pickell, Ying Liu, and Rima Rozen. 2006. "Impact of Methylenetetrahydrofolate Reductase Deficiency and Low Dietary Folate on the Development of Neural Tube Defects in Splotch Mice." *Birth Defects Research Part A - Clinical and Molecular Teratology* 76 (1): 55–59. <https://doi.org/10.1002/bdra.20223>.

Li, J, K C Liu, F Jin, M M Lu, and J A Epstein. 1999. "Transgenic Rescue of Congenital Heart Disease and Spina Bifida in Splotch Mice." *Development (Cambridge, England)* 126 (11). ENGLAND: 2495–2503.

Li, Jun, Gongbo Li, Jian-Lin Hu, Xiao-Hong Fu, Yi-Jun Zeng, Yuan-Guo Zhou, Gang Xiong, Nan Yang, Shuang-Shuang Dai, and Feng-Tian He. 2011. "Chronic or High Dose Acute Caffeine Treatment Protects Mice against Oleic Acid-Induced Acute Lung Injury via an Adenosine A2A Receptor-Independent Mechanism." *European Journal of Pharmacology* 654 (3). Netherlands: 295–303. <https://doi.org/10.1016/j.ejphar.2010.12.040>.

Li, W, S Dai, J An, P Li, X Chen, R Xiong, P Liu, et al. 2008. "Chronic but Not Acute Treatment with Caffeine Attenuates Traumatic Brain Injury in the Mouse Cortical Impact Model." *Neuroscience* 151 (4). United States: 1198–1207. <https://doi.org/10.1016/j.neuroscience.2007.11.020>.

Li, Xiao-Di, Rong-Rong He, Yang Qin, Bun Tsoi, Yi-Fang Li, Zheng-Lai Ma, Xuesong Yang, and Hiroshi Kurihara. 2012. "Caffeine Interferes Embryonic Development through over-Stimulating Serotonergic System in Chicken Embryo." *Food and Chemical Toxicology : An International Journal Published for the British Industrial Biological Research Association* 50 (6). England: 1848–53. <https://doi.org/10.1016/j.fct.2012.03.037>.

Li, Yanli, Rufei Gao, Xueqing Liu, Xuemei Chen, Xinggui Liao, Yanqing Geng, Yubin Ding, Yingxiong Wang, and Junlin He. 2015. "Folate Deficiency Could Restrain Decidual Angiogenesis in Pregnant Mice." *Nutrients* 7 (8): 6425–45. <https://doi.org/10.3390/nu7085284>.

Liem, K F, T M Jessell, and J Briscoe. 2000. "Regulation of the Neural Patterning Activity of Sonic Hedgehog by Secreted BMP Inhibitors Expressed by Notochord and Somites." *Development* 127 (22): 4855 LP-4866. <http://dev.biologists.org/content/127/22/4855.abstract>.

Liem, K F Jr, G Tremml, and T M Jessell. 1997. "A Role for the Roof Plate and Its Resident TGFbeta-Related Proteins in Neuronal Patterning in the Dorsal Spinal Cord." *Cell* 91 (1). United States: 127–38.

Liem, K F Jr, G Tremml, H Roelink, and T M Jessell. 1995. "Dorsal Differentiation of Neural Plate Cells Induced by BMP-Mediated Signals from Epidermal Ectoderm." *Cell* 82 (6). United States: 969–79.

Lin, Wenchu, Zhijing Zhang, Geraldine Srabler, Yi Chun Chen, Maosheng Huang, Huy M Phan, and Sharon Y R Dent. 2008. "Proper Expression of the Gcn5 Histone Acetyltransferase Is Required for Neural Tube Closure in Mouse Embryos." *Developmental Dynamics : An Official Publication of the American Association of Anatomists* 237 (4). United States: 928–40. <https://doi.org/10.1002/dvdy.21479>.

Litingtung, Y, and C Chiang. 2000. "Specification of Ventral Neuron Types Is Mediated by an Antagonistic Interaction between Shh and Gli3." *Nature Neuroscience* 3 (10): 979–85. <https://doi.org/10.1038/79916>.

Liu, A, and A L Joyner. 2001. "EN and GBX2 Play Essential Roles Downstream of FGF8 in Patterning the Mouse Mid/hindbrain Region." *Development (Cambridge, England)* 128 (2).

England: 181–91.

Liu, H, G W Huang, X M Zhang, D L Ren, and X Wilson J. 2010. “Folic Acid Supplementation Stimulates Notch Signaling and Cell Proliferation in Embryonic Neural Stem Cells.” *J Clin Biochem Nutr* 47 (2): 174–80. <https://doi.org/10.3164/jcbn.10-47>.

Liu, Huan, Guo-Wei Huang, Xu-Mei Zhang, Da-Lin Ren, and John X Wilson. 2010. “Folic Acid Supplementation Stimulates Notch Signaling and Cell Proliferation in Embryonic Neural Stem Cells.” *Journal of Clinical Biochemistry and Nutrition* 47 (2). Japan: 174–80. <https://doi.org/10.3164/jcbn.10-47>.

Liu, W S, and C A Heckman. 1998. “The Sevenfold Way of PKC Regulation.” *Cellular Signalling* 10 (8). England: 529–42.

Liu, Wen-Hsin, and Long-Sen Chang. 2010. “Caffeine Induces Matrix Metalloproteinase-2 (MMP-2) and MMP-9 down-Regulation in Human Leukemia U937 Cells via Ca²⁺/ROS-Mediated Suppression of ERK/c-Fos Pathway and Activation of p38 MAPK/c-Jun Pathway.” *Journal of Cellular Physiology* 224 (3). United States: 775–85. <https://doi.org/10.1002/jcp.22180>.

Liu, Yen-Chun, Feng Li, Jesse Handler, Cheng Ran Lisa Huang, Yan Xiang, Nicola Neretti, John M Sedivy, Karen I Zeller, and Chi V Dang. 2008. “Global Regulation of Nucleotide Biosynthetic Genes by c-Myc.” *PLoS One* 3 (7). United States: e2722. <https://doi.org/10.1371/journal.pone.0002722>.

Lohnes, D, M Mark, C Mendelsohn, P Dolle, A Dierich, P Gorry, A Gansmuller, and P Chambon. 1994. “Function of the Retinoic Acid Receptors (RARs) during Development (I). Craniofacial and Skeletal Abnormalities in RAR Double Mutants.” *Development (Cambridge, England)* 120 (10). England: 2723–48.

Luo, Huijun, Xuesong Liu, Fang Wang, Qiuhua Huang, Shuhong Shen, Long Wang, Guojiang Xu, et al. 2005. “Disruption of Palladin Results in Neural Tube Closure Defects in Mice.” *Molecular and Cellular Neurosciences* 29 (4). United States: 507–15. <https://doi.org/10.1016/j.mcn.2004.12.002>.

Ma, Zheng-lai, Yang Qin, Guang Wang, Xiao-di Li, Rong-rong He, Manli Chuai, Hiroshi Kurihara, and Xuesong Yang. 2012. “Exploring the Caffeine-Induced Teratogenicity on Neurodevelopment Using Early Chick Embryo.” *PLoS One* 7 (3). United States: e34278. <https://doi.org/10.1371/journal.pone.0034278>.

MacFarlane, Amanda J, Donald D Anderson, Per Flodby, Cheryll A Perry, Robert H Allen, Sally P Stabler, and Patrick J Stover. 2011. “Nuclear Localization of de Novo Thymidylate Biosynthesis Pathway Is Required to Prevent Uracil Accumulation in DNA.” *The Journal of Biological Chemistry* 286 (51). United States: 44015–22. <https://doi.org/10.1074/jbc.M111.307629>.

MacFarlane, Amanda J, Xiaowen Liu, Cheryll A Perry, Per Flodby, Robert H Allen, Sally P Stabler, and Patrick J Stover. 2008. “Cytoplasmic Serine Hydroxymethyltransferase

Regulates the Metabolic Partitioning of Methylenetetrahydrofolate but Is Not Essential in Mice.” *The Journal of Biological Chemistry* 283 (38). United States: 25846–53. <https://doi.org/10.1074/jbc.M802671200>.

MacFarlane, Amanda J, Cheryll A Perry, Hussein H Girnary, Dacao Gao, Robert H Allen, Sally P Stabler, Barry Shane, and Patrick J Stover. 2009. “Mthfd1 Is an Essential Gene in Mice and Alters Biomarkers of Impaired One-Carbon Metabolism.” *The Journal of Biological Chemistry* 284 (3). United States: 1533–39. <https://doi.org/10.1074/jbc.M808281200>.

Macleod, K F, N Sherry, G Hannon, D Beach, T Tokino, K Kinzler, B Vogelstein, and T Jacks. 1995. “p53-Dependent and Independent Expression of p21 during Cell Growth, Differentiation, and DNA Damage.” *Genes & Development* 9 (8). UNITED STATES: 935–44.

Madeira, Maria H, Raquel Boia, Antonio F Ambrosio, and Ana R Santiago. 2017. “Having a Coffee Break: The Impact of Caffeine Consumption on Microglia-Mediated Inflammation in Neurodegenerative Diseases.” *Mediators of Inflammation* 2017. United States: 4761081. <https://doi.org/10.1155/2017/4761081>.

Maden, Malcolm. 2006. “Retinoids and Spinal Cord Development.” *Journal of Neurobiology* 66 (7). United States: 726–38. <https://doi.org/10.1002/neu.20248>.

Malinsky, J, K Koberna, D Stanek, M Masata, I Votruba, and I Raska. 2001. “The Supply of Exogenous Deoxyribonucleotides Accelerates the Speed of the Replication Fork in Early S-Phase.” *Journal of Cell Science* 114 (Pt 4). England: 747–50.

Mandel, H. G. 2002. “Update on Caffeine Consumption, Disposition and Action.” *Food and Chemical Toxicology*. [https://doi.org/10.1016/S0278-6915\(02\)00093-5](https://doi.org/10.1016/S0278-6915(02)00093-5).

Mannava, Sudha, Vladimir Grachtchouk, Linda J Wheeler, Michael Im, Dazhong Zhuang, Elena G Slavina, Christopher K Mathews, Donna S Shewach, and Mikhail A Nikiforov. 2008. “Direct Role of Nucleotide Metabolism in C-MYC-Dependent Proliferation of Melanoma Cells.” *Cell Cycle (Georgetown, Tex.)* 7 (15). United States: 2392–2400. <https://doi.org/10.4161/cc.6390>.

Mansouri, Ahmed, Patrick Pla, Lionel Larue, and Peter Gruss. 2001. “Pax3 Acts Cell Autonomously in the Neural Tube and Somites by Controlling Cell Surface Properties.” *Development* 128 (11): 1995–2005. <http://dev.biologists.org/content/128/11/1995.long>.

Marasas, Walter F O, Ronald T Riley, Katherine A Hendricks, Victoria L Stevens, Thomas W Sadler, Janee Gelineau-van Waes, Stacey A Missmer, et al. 2004. “Fumonisins Disrupt Sphingolipid Metabolism, Folate Transport, and Neural Tube Development in Embryo Culture and in Vivo: A Potential Risk Factor for Human Neural Tube Defects among Populations Consuming Fumonisin-Contaminated Maize.” *The Journal of Nutrition* 134 (4). United States: 711–16.

Marco, Patrizia De, Maria Grazia Calevo, Anna Moroni, Lorenza Arata, Elisa Merello, Richard H Finnell, Huiping Zhu, Luciano Andreussi, Armando Cama, and Valeria Capra. 2002. “Study

of MTHFR and MS Polymorphisms as Risk Factors for NTD in the Italian Population.” *Journal of Human Genetics* 47 (6). England: 319–24.

<https://doi.org/10.1007/s100380200043>.

Marco, Patrizia De, Elisa Merello, Maria Grazia Calevo, Samantha Mascelli, Daniela Pastorino, Lucia Crocetti, Pierangela De Biasio, Gianluca Piatelli, Armando Cama, and Valeria Capra. 2011. “Maternal Periconceptional Factors Affect the Risk of Spina Bifida-Affected Pregnancies: An Italian Case-Control Study.” *Child’s Nervous System : ChNS : Official Journal of the International Society for Pediatric Neurosurgery* 27 (7). Germany: 1073–81.

<https://doi.org/10.1007/s00381-010-1372-y>.

Marco, Patrizia De, Elisa Merello, Alessandro Consales, Gianluca Piatelli, Armando Cama, Zoha Kibar, and Valeria Capra. 2013. “Genetic Analysis of Disheveled 2 and Disheveled 3 in Human Neural Tube Defects.” *Journal of Molecular Neuroscience : MN* 49 (3). United States: 582–88. <https://doi.org/10.1007/s12031-012-9871-9>.

Marco, Patrizia De, Elisa Merello, Andrea Rossi, Gianluca Piatelli, Armando Cama, Zoha Kibar, and Valeria Capra. 2012. “FZD6 Is a Novel Gene for Human Neural Tube Defects.” *Human Mutation* 33 (2). United States: 384–90. <https://doi.org/10.1002/humu.21643>.

Marean, Amber, Amanda Graf, Ying Zhang, and Lee Niswander. 2011. “Folic Acid Supplementation Can Adversely Affect Murine Neural Tube Closure and Embryonic Survival.” *Human Molecular Genetics* 20 (18): 3678–83.

<https://doi.org/10.1093/hmg/ddr289>.

Marigo, V, R L Johnson, A Vortkamp, and C J Tabin. 1996. “Sonic Hedgehog Differentially Regulates Expression of GLI and GLI3 during Limb Development.” *Developmental Biology* 180 (1). United States: 273–83. <https://doi.org/10.1006/dbio.1996.0300>.

Marret, Stéphane, Pierre Gressens, Geneviève Van-Maele-Fabry, Jacques Picard, and Philippe Evrard. 1997. “Caffeine-Induced Disturbances of Early Neurogenesis in Whole Mouse Embryo Cultures.” *Brain Research*. [https://doi.org/10.1016/S0006-8993\(97\)00938-4](https://doi.org/10.1016/S0006-8993(97)00938-4).

Marti, E, D A Bumcrot, R Takada, and A P McMahon. 1995. “Requirement of 19K Form of Sonic Hedgehog for Induction of Distinct Ventral Cell Types in CNS Explants.” *Nature* 375 (6529). England: 322–25. <https://doi.org/10.1038/375322a0>.

Martinelli, David C, and Chen-Ming Fan. 2007. “Gas1 Extends the Range of Hedgehog Action by Facilitating Its Signaling.” *Genes & Development* 21 (10). United States: 1231–43.

<https://doi.org/10.1101/gad.1546307>.

Martiniova, Lucia, Martha S. Field, Julia L. Finkelstein, Cheryll A. Perry, and Patrick J. Stover. 2015. “Maternal Dietary Uridine Causes, and Deoxyuridine Prevents, Neural Tube Closure Defects in a Mouse Model of Folate-Responsive Neural Tube Defects.” *American Journal of Clinical Nutrition* 101 (4): 860–69. <https://doi.org/10.3945/ajcn.114.097279>.

Martomo, Stella A, and Christopher K Mathews. 2002. “Effects of Biological DNA Precursor Pool Asymmetry upon Accuracy of DNA Replication in Vitro.” *Mutation Research* 499 (2).

Netherlands: 197–211.

Massa, Valentina, Dawn Savery, Patricia Ybot-Gonzalez, Elisabetta Ferraro, Anthony Rongvaux, Francesco Cecconi, Richard Flavell, Nicholas D E Greene, and Andrew J Copp. 2009. “Apoptosis Is Not Required for Mammalian Neural Tube Closure.” *Proceedings of the National Academy of Sciences of the United States of America* 106 (20). United States: 8233–38. <https://doi.org/10.1073/pnas.0900333106>.

Mastick, G S, N M Davis, G L Andrew, and S S Jr Easter. 1997. “Pax-6 Functions in Boundary Formation and Axon Guidance in the Embryonic Mouse Forebrain.” *Development (Cambridge, England)* 124 (10). England: 1985–97.

Mathis, L, P M Kulesa, and S E Fraser. 2001. “FGF Receptor Signalling Is Required to Maintain Neural Progenitors during Hensen’s Node Progression.” *Nature Cell Biology* 3 (6). England: 559–66. <https://doi.org/10.1038/35078535>.

Matise, M P, D J Epstein, H L Park, K A Platt, and A L Joyner. 1998. “Gli2 Is Required for Induction of Floor Plate and Adjacent Cells, but Not Most Ventral Neurons in the Mouse Central Nervous System.” *Development (Cambridge, England)* 125 (15): 2759–70. <https://doi.org/9655799>.

Mayanil, Chandra S K, Angela Pool, Hiromichi Nakazaki, Anvesh C Reddy, Barbara Mania-Farnell, Beth Yun, David George, David G McLone, and Eric G Bremer. 2006. “Regulation of Murine TGFbeta2 by Pax3 during Early Embryonic Development.” *The Journal of Biological Chemistry* 281 (34): 24544–52. <https://doi.org/10.1074/jbc.M512449200>.

McCormick, P J, L L Danhauser, Y M Rustum, and J S Bertram. 1983. “Changes in Ribo- and Deoxyribonucleoside Triphosphate Pools within the Cell Cycle of a Synchronized Mouse Fibroblast Cell Line.” *Biochimica et Biophysica Acta* 756 (1). Netherlands: 36–40.

Mckellar, QA, and EW Scott. 1990. “The Benzimidazole Anthelmintic Agents - a Review” 13 (3): 223–47.

McMahon, A P, and A Bradley. 1990. “The Wnt-1 (Int-1) Proto-Oncogene Is Required for Development of a Large Region of the Mouse Brain.” *Cell* 62 (6). United States: 1073–85.

McMahon, Daria M, Jihong Liu, Hongmei Zhang, Myriam E Torres, and Robert G Best. 2013. “Maternal Obesity, Folate Intake, and Neural Tube Defects in Offspring.” *Birth Defects Research. Part A, Clinical and Molecular Teratology* 97 (2). United States: 115–22. <https://doi.org/10.1002/bdra.23113>.

McMahon, Jill A., Shinji Takada, Lyle B. Zimmerman, Chen Ming Fan, Richard M. Harland, and Andrew P. McMahon. 1998. “Noggin-Mediated Antagonism of BMP Signaling Is Required for Growth and Patterning of the Neural Tube and Somite.” *Genes and Development* 12 (10). United States: 1438–52. <https://doi.org/10.1101/gad.12.10.1438>.

McMartin, Kenneth, Dag Jacobsen, and Knut Erik Hovda. 2016. “Antidotes for Poisoning by Alcohols That Form Toxic Metabolites.” *British Journal of Clinical Pharmacology* 81 (3). England: 505–15. <https://doi.org/10.1111/bcp.12824>.

McShane, Suzanne G, Matteo A Mole, Dawn Savery, Nicholas D E Greene, Patrick P L Tam, and Andrew J Copp. 2015. "Cellular Basis of Neuroepithelial Bending during Mouse Spinal Neural Tube Closure." *Developmental Biology* 404 (2). United States: 113–24. <https://doi.org/10.1016/j.ydbio.2015.06.003>.

Megason, Sean G, and Andrew P McMahon. 2002. "A Mitogen Gradient of Dorsal Midline Wnts Organizes Growth in the CNS." *Development (Cambridge, England)* 129 (9): 2087–98.

Mehrmohamadi, Mahya, Xiaojing Liu, Alexander A. Shestov, and Jason W. Locasale. 2014. "Characterization of the Usage of the Serine Metabolic Network in Human Cancer." *Cell Reports* 9 (4). The Authors: 1507–19. <https://doi.org/10.1016/j.celrep.2014.10.026>.

Mellman, David L, and Richard A Anderson. 2009. "A Novel Gene Expression Pathway Regulated by Nuclear Phosphoinositides." *Advances in Enzyme Regulation* 49 (1). England: 11–28.

Memberg, S P, and A K Hall. 1995. "Dividing Neuron Precursors Express Neuron-Specific Tubulin." *Journal of Neurobiology* 27 (1). UNITED STATES: 26–43. <https://doi.org/10.1002/neu.480270104>.

Menezes, J R, and M B Luskin. 1994. "Expression of Neuron-Specific Tubulin Defines a Novel Population in the Proliferative Layers of the Developing Telencephalon." *The Journal of Neuroscience : The Official Journal of the Society for Neuroscience* 14 (9). UNITED STATES: 5399–5416.

Menzies, A Sheila, Attila Aszodi, Scott E Williams, Alexander Pfeifer, Ann M Wehman, Keow Lin Goh, Carol A Mason, Reinhard Fassler, and Frank B Gertler. 2004. "Mena and Vasodilator-Stimulated Phosphoprotein Are Required for Multiple Actin-Dependent Processes That Shape the Vertebrate Nervous System." Journal Article, Research Support, Non-U.S. Gov't, Research Support, U.S. Gov't, P.H.S. *The Journal of Neuroscience : The Official Journal of the Society for Neuroscience* 24 (37). United States: 8029–38. <https://doi.org/10.1523/JNEUROSCI.1057-04.2004>.

Meuth, M, E Aufreiter, and P Reichard. 1976. "Deoxyribonucleotide Pools in Mouse-Fibroblast Cell Lines with Altered Ribonucleotide Reductase." *European Journal of Biochemistry* 71 (1). England: 39–43.

Meuth, Mark. 1984. "The Genetic Consequences of Nucleotide Precursor Pool Imbalance in Mammalian Cells." *Mutation Research - Fundamental and Molecular Mechanisms of Mutagenesis* 126 (2): 107–12. [https://doi.org/10.1016/0027-5107\(84\)90051-4](https://doi.org/10.1016/0027-5107(84)90051-4).

Migliorini, Domenico, Eros Lazzerini Denchi, Davide Danovi, Aart Jochemsen, Manuela Capillo, Alberto Gobbi, Kristian Helin, Pier Giuseppe Pelicci, and Jean-Christophe Marine. 2002. "Mdm4 (Mdmx) Regulates p53-Induced Growth Arrest and Neuronal Cell Death during Early Embryonic Mouse Development." *Molecular and Cellular Biology* 22 (15). United States: 5527–38.

Mikael, Leonie G., Liyuan Deng, Ligi Paul, Jacob Selhub, and Rima Rozen. 2013. "Moderately

High Intake of Folic Acid Has a Negative Impact on Mouse Embryonic Development.” *Birth Defects Research Part A - Clinical and Molecular Teratology* 97 (1): 47–52.

<https://doi.org/10.1002/bdra.23092>.

Milenkovic, L, L V Goodrich, K M Higgins, and M P Scott. 1999. “Mouse patched1 Controls Body Size Determination and Limb Patterning.” *Development (Cambridge, England)* 126 (20). England: 4431–40.

Mills, J L, J M McPartlin, P N Kirke, Y J Lee, M R Conley, D G Weir, and J M Scott. 1995. “Homocysteine Metabolism in Pregnancies Complicated by Neural-Tube Defects.” *Lancet (London, England)* 345 (8943). England: 149–51.

Minguzzi, Stefano, S Duygu Selcuklu, Charles Spillane, and Anne Parle-McDermott. 2014. “An NTD-Associated Polymorphism in the 3’ UTR of MTHFD1L Can Affect Disease Risk by Altering miRNA Binding.” *Human Mutation* 35 (1). United States: 96–104.

<https://doi.org/10.1002/humu.22459>.

Misra, Kamana, and Michael P. Matise. 2010. “A Critical Role for sFRP Proteins in Maintaining Caudal Neural Tube Closure in Mice via Inhibition of BMP Signaling.” *Developmental Biology* 337 (1). Elsevier Inc.: 74–83. <https://doi.org/10.1016/j.ydbio.2009.10.015>.

Missmer, Stacey A, Lucina Suarez, Marilyn Felkner, Elaine Wang, Alfred H Jr Merrill, Kenneth J Rothman, and Katherine A Hendricks. 2006. “Exposure to Fumonisins and the Occurrence of Neural Tube Defects along the Texas-Mexico Border.” *Environmental Health Perspectives* 114 (2). United States: 237–41.

Mitchell, Laura E. 2005. “Epidemiology of Neural Tube Defects.” *American Journal of Medical Genetics. Part C, Seminars in Medical Genetics* 135C (1). United States: 88–94.

<https://doi.org/10.1002/ajmg.c.30057>.

Moldovan, George-Lucian, Boris Pfander, and Stefan Jentsch. 2007. “PCNA, the Maestro of the Replication Fork.” *Cell* 129 (4). United States: 665–79.

<https://doi.org/10.1016/j.cell.2007.05.003>.

Moline, M L, and C Sandlin. 1993. “Waardenburg Syndrome and Meningomyelocele.” *American Journal of Medical Genetics*. United States. <https://doi.org/10.1002/ajmg.1320470130>.

Molotkova, Natalia, Andrei Molotkov, I Ovidiu Sirbu, and Gregg Duester. 2005. “Requirement of Mesodermal Retinoic Acid Generated by Raldh2 for Posterior Neural Transformation.” *Mechanisms of Development* 122 (2). Ireland: 145–55.

<https://doi.org/10.1016/j.mod.2004.10.008>.

Momb, Jessica, Jordan P Lewandowski, Joshua D Bryant, Rebecca Fitch, Deborah R Surman, Steven A Vokes, and Dean R Appling. 2013. “Deletion of Mthfd1l Causes Embryonic Lethality and Neural Tube and Craniofacial Defects in Mice.” *Proceedings of the National Academy of Sciences of the United States of America* 110 (2): 549–54.

<https://doi.org/10.1073/pnas.1211199110>.

Monsoro-Burq, Anne-Helene, Estee Wang, and Richard Harland. 2005. “Msx1 and Pax3

Cooperate to Mediate FGF8 and WNT Signals during Xenopus Neural Crest Induction.” *Developmental Cell* 8 (2). United States: 167–78.

<https://doi.org/10.1016/j.devcel.2004.12.017>.

Morales, Aixa V, Sergio Espeso-Gil, Inmaculada Ocana, Francisco Nieto-Lopez, Elena Calleja, Paola Bovolenta, Mark Lewandoski, and Ruth Diez Del Corral. 2016. “FGF Signaling Enhances a Sonic Hedgehog Negative Feedback Loop at the Initiation of Spinal Cord Ventral Patterning.” *Developmental Neurobiology* 76 (9). United States: 956–71.

<https://doi.org/10.1002/dneu.22368>.

Morriss-Kay, G M. 1981. “Growth and Development of Pattern in the Cranial Neural Epithelium of Rat Embryos during Neurulation.” *Journal of Embryology and Experimental Morphology* 65 Suppl (October). England: 225–41.

Morriss-Kay, G, and F Tuckett. 1985. “The Role of Microfilaments in Cranial Neurulation in Rat Embryos: Effects of Short-Term Exposure to Cytochalasin D.” *Journal of Embryology and Experimental Morphology* 88 (August). England: 333–48.

Morriss, G M, and M Solursh. 1978. “Regional Differences in Mesenchymal Cell Morphology and Glycosaminoglycans in Early Neural-Fold Stage Rat Embryos.” *Journal of Embryology and Experimental Morphology* 46 (August). England: 37–52.

Mosley, Bridget S., Mario A. Cleves, Anna Maria Siega-Riz, Gary M. Shaw, Mark A. Canfield, D. Kim Waller, Martha M. Werler, and Charlotte A. Hobbs. 2009. “Neural Tube Defects and Maternal Folate Intake among Pregnancies Conceived after Folic Acid Fortification in the United States.” *American Journal of Epidemiology* 169 (1): 9–17.

<https://doi.org/10.1093/aje/kwn331>.

Mousty, Eve, Sarah Issa, Frederic Grosjean, Jean-Yves Col, Philippe Khau Van Kien, Marie-Josée Perez, Yuliya Petrov, et al. 2015. “A Homozygous PAX3 Mutation Leading to Severe Presentation of Waardenburg Syndrome with a Prenatal Diagnosis.” *Prenatal Diagnosis*. England. <https://doi.org/10.1002/pd.4703>.

Mun, B J, and C K Mathews. 1991. “Cell Cycle-Dependent Variations in Deoxyribonucleotide Metabolism among Chinese Hamster Cell Lines Bearing the Thy- Mutator Phenotype.” *Molecular and Cellular Biology* 11 (1): 20–26.

<http://www.ncbi.nlm.nih.gov/pubmed/1986219>.

Murciano, Antonio, Javier Zamora, Jesus Lopez-Sanchez, and Jose Maria Fraude. 2002. “Interkinetic Nuclear Movement May Provide Spatial Clues to the Regulation of Neurogenesis.” *Molecular and Cellular Neurosciences* 21 (2). United States: 285–300.

Murdoch, J N, K Doudney, C Paternotte, A J Copp, and P Stanier. 2001. “Severe Neural Tube Defects in the Loop-Tail Mouse Result from Mutation of Lpp1, a Novel Gene Involved in Floor Plate Specification.” *Human Molecular Genetics* 10 (22). England: 2593–2601.

Murdoch, Jennifer N., and Andrew J. Copp. 2010. “The Relationship between Sonic Hedgehog Signaling, Cilia, and Neural Tube Defects.” *Birth Defects Research Part A - Clinical and*

Molecular Teratology 88 (8): 633–52. <https://doi.org/10.1002/bdra.20686>.

Murko, Christina, Sabine Lagger, Marianne Steiner, Christian Seiser, Christian Schoefer, and Oliver Pusch. 2013. “Histone Deacetylase Inhibitor Trichostatin A Induces Neural Tube Defects and Promotes Neural Crest Specification in the Chicken Neural Tube.” *Differentiation; Research in Biological Diversity* 85 (1–2). England: 55–66. <https://doi.org/10.1016/j.diff.2012.12.001>.

Murone, M, A Rosenthal, and F J de Sauvage. 1999. “Sonic Hedgehog Signaling by the Patched-Smoothened Receptor Complex.” *Current Biology : CB* 9 (2). England: 76–84.

Nagai, T, J Aruga, O Minowa, T Sugimoto, Y Ohno, T Noda, and K Mikoshiba. 2000. “Zic2 Regulates the Kinetics of Neurulation.” *Proceedings of the National Academy of Sciences of the United States of America* 97 (4). United States: 1618–23.

Nagashige, M, F Ushigome, N Koyabu, K Hirata, M Kawabuchi, T Hirakawa, S Satoh, et al. 2003. “Basal Membrane Localization of MRP1 in Human Placental Trophoblast.” *Placenta* 24 (10). Netherlands: 951–58.

Nagy, Nandor, and Allan Goldstein. 2015. “Gut Epithelium-Derived Sonic Hedgehog Regulates the Extracellular Matrix During Formation of the Intestinal Nervous System.” *The FASEB Journal* 29 (1 Supplement). http://www.fasebj.org/content/29/1_Supplement/873.2.abstract.

Nakatsu, T, C Uwabe, and K Shiota. 2000. “Neural Tube Closure in Humans Initiates at Multiple Sites: Evidence from Human Embryos and Implications for the Pathogenesis of Neural Tube Defects.” *Anatomy and Embryology* 201 (6). Germany: 455–66.

Nakazaki, Hiromichi, Anvesh C. Reddy, Barbara L. Mania-Farnell, Yueh Wei Shen, Shunsuke Ichi, Christopher McCabe, David George, David G. McLone, Tadanori Tomita, and C. S K Mayanil. 2008. “Key Basic Helix-Loop-Helix Transcription Factor Genes Hes1 and Ngn2 Are Regulated by Pax3 during Mouse Embryonic Development.” *Developmental Biology* 316 (2): 510–23. <https://doi.org/10.1016/j.ydbio.2008.01.008>.

Narisawa, Ayumi, Shoko Komatsuzaki, Atsuo Kikuchi, Tetsuya Niihori, Yoko Aoki, Kazuko Fujiwara, Mitsuyo Tanemura, et al. 2012. “Mutations in Genes Encoding the Glycine Cleavage System Predispose to Neural Tube Defects in Mice and Humans.” *Human Molecular Genetics* 21 (7): 1496–1503. <https://doi.org/10.1093/hmg/ddr585>.

Narod, S A, J Siegel-Bartelt, and H J Hoffman. 1988. “Cerebellar Infarction in a Patient with Waardenburg Syndrome.” *American Journal of Medical Genetics* 31 (4). United States: 903–7. <https://doi.org/10.1002/ajmg.1320310424>.

Naviglio, Silvio, Michele Caraglia, Alberto Abbruzzese, Emilio Chiosi, Davide Di Gesto, Monica Marra, Maria Romano, et al. 2009. “Protein Kinase A as a Biological Target in Cancer Therapy.” *Expert Opinion on Therapeutic Targets* 13 (1). England: 83–92. <https://doi.org/10.1517/14728220802602349>.

Neumann, P E, W N Frankel, V A Letts, J M Coffin, A J Copp, and M Bernfield. 1994. “Multifactorial Inheritance of Neural Tube Defects: Localization of the Major Gene and

Recognition of Modifiers in Ct Mutant Mice.” *Nature Genetics* 6 (4). UNITED STATES: 357–62. <https://doi.org/10.1038/ng0494-357>.

Nguyen, Duc, and Tian Xu. 2008. “The Expanding Role of Mouse Genetics for Understanding Human Biology and Disease.” *Disease Models & Mechanisms* 1 (1). England: 56–66. <https://doi.org/10.1242/dmm.000232>.

NHS Choices. n.d. “Should I Limit Caffeine during Pregnancy?” <http://www.nhs.uk/chq/pages/limit-caffeine-during-pregnancy.aspx?categoryid=54&subcategoryid=130>.

Nicholls, P. 1976. “The Effect of Formate on Cytochrome aa3 and on Electron Transport in the Intact Respiratory Chain.” *Biochimica et Biophysica Acta* 430 (1). Netherlands: 13–29.

Niederreither, K, V Subbarayan, P Dolle, and P Chambon. 1999. “Embryonic Retinoic Acid Synthesis Is Essential for Early Mouse Post-Implantation Development.” *Nature Genetics* 21 (4). United States: 444–48. <https://doi.org/10.1038/7788>.

Nijhout, H Frederik, Michael C Reed, Shi-Ling Lam, Barry Shane, Jesse F Gregory, and Cornelia M Ulrich. 2006. “In Silico Experimentation with a Model of Hepatic Mitochondrial Folate Metabolism.” *Theoretical Biology & Medical Modelling* 3: 40. <https://doi.org/10.1186/1742-4682-3-40>.

Nishimura, H, and K Nakai. 1960. “Congenital Malformations in Offspring of Mice Treated with Caffeine.” *Proc Soc Exp Biol Med* 104 (May). United States: 140–42.

Novitch, Bennett G, Hynek Wichterle, Thomas M Jessell, and Shanthini Sockanathan. 2003. “A Requirement for Retinoic Acid-Mediated Transcriptional Activation in Ventral Neural Patterning and Motor Neuron Specification.” *Neuron* 40 (1). United States: 81–95.

Novotny, L, H Farghali, M Ryba, I Janku, and J Beranek. 1984. “Structure-Intestinal Transport and Structure-Metabolism Correlations of Some Potential Cancerostatic Pyrimidine Nucleosides in Isolated Rat Jejunum.” *Cancer Chemotherapy and Pharmacology* 13 (3). Germany: 195–99.

Nye, J S, N Balkin, H Lucas, P A Knepper, D G McLone, and J Charrow. 1998. “Myelomeningocele and Waardenburg Syndrome (Type 3) in Patients with Interstitial Deletions of 2q35 and the PAX3 Gene: Possible Digenic Inheritance of a Neural Tube Defect.” *American Journal of Medical Genetics* 75 (4). United States: 401–8.

Oka, C, T Nakano, A Wakeham, J L de la Pompa, C Mori, T Sakai, S Okazaki, et al. 1995. “Disruption of the Mouse RBP-J Kappa Gene Results in Early Embryonic Death.” *Development (Cambridge, England)* 121 (10). England: 3291–3301.

Okano, Jun-ichi, Takakazu Nagahara, Kazuya Matsumoto, and Yoshikazu Murawaki. 2008. “Caffeine Inhibits the Proliferation of Liver Cancer Cells and Activates the MEK/ERK/EGFR Signalling Pathway.” *Basic & Clinical Pharmacology & Toxicology* 102 (6). England: 543–51. <https://doi.org/10.1111/j.1742-7843.2008.00231.x>.

Okano, M, D W Bell, D A Haber, and E Li. 1999. “DNA Methyltransferases Dnmt3a and Dnmt3b

Are Essential for de Novo Methylation and Mammalian Development.” *Cell* 99 (3). United States: 247–57.

Olaopa, Michael, Hong-ming Zhou, Paige Snider, Jian Wang, Robert J Schwartz, Anne M Moon, and Simon J Conway. 2011. “Pax3 Is Essential for Normal Cardiac Neural Crest Morphogenesis but Is Not Required during Migration nor Outflow Tract Septation.” *Developmental Biology* 356 (2). United States: 308–22.
<https://doi.org/10.1016/j.ydbio.2011.05.583>.

Opdecamp, K, A Nakayama, M T Nguyen, C A Hodgkinson, W J Pavan, and H Arnheiter. 1997. “Melanocyte Development in Vivo and in Neural Crest Cell Cultures: Crucial Dependence on the Mitf Basic-Helix-Loop-Helix-Zipper Transcription Factor.” *Development (Cambridge, England)* 124 (12). ENGLAND: 2377–86.

Ornoy, Asher, E Albert Reece, Gabriela Pavlinkova, Claudia Kappen, and Richard Kermit Miller. 2015. “Effect of Maternal Diabetes on the Embryo, Fetus, and Children: Congenital Anomalies, Genetic and Epigenetic Changes and Developmental Outcomes.” *Birth Defects Research. Part C, Embryo Today : Reviews* 105 (1). United States: 53–72.
<https://doi.org/10.1002/bdrc.21090>.

Ouyang, Shengrong, Zhuo Liu, Yuanyuan Li, Feifei Ma, and Jianxin Wu. 2014. “Cystathionine Beta-Synthase 844ins68 Polymorphism Is Unrelated to Susceptibility to Neural Tube Defects.” *Gene* 535 (2). Netherlands: 119–23. <https://doi.org/10.1016/j.gene.2013.11.052>.

Ouyang, Shengrong, Zhuo Liu, Yuanyuan Li, and Jianxin Wu. 2013. “Meta-Analyses on the Association of MTR A2756G and MTRR A66G Polymorphisms with Neural Tube Defect Risks in Caucasian Children.” *The Journal of Maternal-Fetal & Neonatal Medicine : The Official Journal of the European Association of Perinatal Medicine, the Federation of Asia and Oceania Perinatal Societies, the International Society of Perinatal Obstetricians* 26 (12). England: 1166–70. <https://doi.org/10.3109/14767058.2013.777699>.

Paganelli, C.V., A. Olszowka, and A. Ar. 1974. “The Avian Egg: Surface Area, Volume and Density.” *The Condor* 76: 319–25.
<https://sora.unm.edu/sites/default/files/journals/condor/v076n03/p0319-p0325.pdf>.

Pai, Yun Jin. 2015. “The Glycine Cleavage System in Embryonic Brain Development.”

Pai, Yun Jin, Kit-Yi Leung, Dawn Savery, Tim Hutchin, Helen Prunty, Simon Heales, Margaret E. Brosnan, John T. Brosnan, Andrew J. Copp, and Nicholas D.E. Greene. 2015. “Glycine Decarboxylase Deficiency Causes Neural Tube Defects and Features of Non-Ketotic Hyperglycinemia in Mice.” *Nature Communications* 6. Nature Publishing Group: 6388.
<https://doi.org/10.1038/ncomms7388>.

Palmer, Alexandra Jayne. 2014. “Cellular and Molecular Mechanisms Underlying Pax3 -Related Neural Tube Defects,” no. July.

Pangilinan, Faith, Anne M Molloy, James L Mills, James F Troendle, Anne Parle-McDermott, Caroline Signore, Valerie B O’Leary, et al. 2012. “Evaluation of Common Genetic Variants

in 82 Candidate Genes as Risk Factors for Neural Tube Defects.” *BMC Medical Genetics* 13 (1). *BMC Medical Genetics*: 62. <https://doi.org/10.1186/1471-2350-13-62>.

Pani, Lydie, Melissa Horal, and Mary R Loeken. 2002. “Rescue of Neural Tube Defects in Pax-3-Deficient Embryos by p53 Loss of Function: Implications for Pax-3-Dependent Development and Tumorigenesis.” *Genes & Development* 16 (6). United States: 676–80. <https://doi.org/10.1101/gad.969302>.

Paolo, Gilbert Di, and Pietro De Camilli. 2006. “Phosphoinositides in Cell Regulation and Membrane Dynamics.” *Nature* 443 (7112): 651–57. <https://doi.org/10.1038/nature05185>.

Park, H L, C Bai, K A Platt, M P Matise, A Beeghly, C c Hui, M Nakashima, and A L Joyner. 2000. “Mouse Gli1 Mutants Are Viable but Have Defects in SHH Signaling in Combination with a Gli2 Mutation.” *Development (Cambridge, England)* 127 (8): 1593–1605. <https://doi.org/10.1242/dev.10725236> &id=10725236&retmode=ref&cmd=prlinks%5Cnpapers2://publication/uuid/D5FB5872-4878-4BE7-93DA-3C2DDB183F28%5Cnhttp://www.ncbi.nl.

Parker, S B, G Eichele, P Zhang, A Rawls, A T Sands, A Bradley, E N Olson, J W Harper, and S J Elledge. 1995. “p53-Independent Expression of p21Cip1 in Muscle and Other Terminally Differentiating Cells.” *Science (New York, N.Y.)* 267 (5200). UNITED STATES: 1024–27.

Parle-McDermott, Anne, Faith Pangilinan, Kirsty K. O’Brien, James L. Mills, Alan M. Magee, James Troendle, Marie Sutton, et al. 2009. “A Common Variant in MTHFD1L Is Associated with Neural Tube Defects and mRNA Splicing Efficiency.” *Human Mutation* 30 (12): 1650–56. <https://doi.org/10.1002/humu.21109>.

Parsons, D S, and M I Shaw. 1983. “Use of High Performance Liquid Chromatography to Study Absorption and Metabolism of Purines by Rat Jejunum in Vitro.” *Quarterly Journal of Experimental Physiology (Cambridge, England)* 68 (1). England: 53–67.

Patel, Harshila, Erminia Di Pietro, and Robert E. MacKenzie. 2003. “Mammalian Fibroblasts Lacking Mitochondrial NAD+-Dependent Methylenetetrahydrofolate Dehydrogenase-Cyclohydrolase Are Glycine Auxotrophs.” *Journal of Biological Chemistry* 278 (21): 19436–41. <https://doi.org/10.1074/jbc.M301718200>.

Patterson, Victoria L., Christine Damrau, Anju Paudyal, Benjamin Reeve, Daniel T. Grimes, Michelle E. Stewart, Debbie J. Williams, Pam Siggers, Andy Greenfield, and Jennifer N. Murdoch. 2009. “Mouse Hitchhiker Mutants Have Spina Bifida, Dorso-Ventral Patterning Defects and Polydactyly: Identification of Tulp3 as a Novel Negative Regulator of the Sonic Hedgehog Pathway.” *Human Molecular Genetics* 18 (10): 1719–39. <https://doi.org/10.1093/hmg/ddp075>.

Pedley, Anthony M, and Stephen J Benkovic. 2017. “A New View into the Regulation of Purine Metabolism: The Purinosome.” *Trends in Biochemical Sciences* 42 (2). England: 141–54. <https://doi.org/10.1016/j.tibs.2016.09.009>.

Pelletier, J N, and R E MacKenzie. 1995. "Binding and Interconversion of Tetrahydrofolates at a Single Site in the Bifunctional Methylenetetrahydrofolate Dehydrogenase/cyclohydrolase." *Biochemistry* 34 (39). United States: 12673–80.

Peters, Luanne L, Raymond F Robledo, Carol J Bult, Gary A Churchill, Beverly J Paigen, and Karen L Svenson. 2007. "The Mouse as a Model for Human Biology: A Resource Guide for Complex Trait Analysis." *Nature Reviews. Genetics* 8 (1). England: 58–69. <https://doi.org/10.1038/nrg2025>.

Pickell, Laura, Katharine Brown, Deqiang Li, Xiao-Ling Wang, Liyuan Deng, Qing Wu, Jacob Selhub, Li Luo, Loydie Jerome-Majewska, and Rima Rozen. 2011. "High Intake of Folic Acid Disrupts Embryonic Development in Mice." *Birth Defects Research. Part A, Clinical and Molecular Teratology* 91 (1). United States: 8–19. <https://doi.org/10.1002/bdra.20754>.

Piedrahita, J A, B Oetama, G D Bennett, J van Waes, B A Kamen, J Richardson, S W Lacey, R G Anderson, and R H Finnell. 1999. "Mice Lacking the Folic Acid-Binding Protein Folbp1 Are Defective in Early Embryonic Development." *Nature Genetics* 23 (2). United States: 228–32. <https://doi.org/10.1038/13861>.

Pierani, A, S Brenner-Morton, C Chiang, and T M Jessell. 1999. "A Sonic Hedgehog-Independent, Retinoid-Activated Pathway of Neurogenesis in the Ventral Spinal Cord." *Cell* 97 (7). United States: 903–15.

Pierfelice, Tarran, Lavinia Alberi, and Nicholas Gaiano. 2011. "Notch in the Vertebrate Nervous System: An Old Dog with New Tricks." *Neuron* 69 (5). United States: 840–55. <https://doi.org/10.1016/j.neuron.2011.02.031>.

Pierro, D Di, B Tavazzi, C F Perno, M Bartolini, E Balestra, R Caliò, B Giardina, and G Lazzarino. 1995. "An Ion-Pairing High-Performance Liquid Chromatographic Method for the Direct Simultaneous Determination of Nucleotides, Deoxynucleotides, Nicotinic Coenzymes, Oxypurines, Nucleosides, and Bases in Perchloric Acid Cell Extracts." *Analytical Biochemistry* 231 (2): 407–12. <https://doi.org/10.1006/abio.1995.0071>.

Pietro, E Di, J Sirois, M L Tremblay, and R E MacKenzie. 2002. "Mitochondrial NAD-Dependent Methylenetetrahydrofolate Dehydrogenase-Methenyltetrahydrofolate Cyclohydrolase Is Essential for Embryonic Development." *Molecular and Cellular Biology* 22 (12). United States: 4158–66.

Pike, Schuyler T., Rashmi Rajendra, Karen Artzt, and Dean R. Appling. 2010. "Mitochondrial C1-Tetrahydrofolate Synthase (MTHFD1L) Supports the Flow of Mitochondrial One-Carbon Units into the Methyl Cycle in Embryos." *Journal of Biological Chemistry* 285 (7): 4612–20. <https://doi.org/10.1074/jbc.M109.079855>.

Placzek, M, T Yamada, M Tessier-Lavigne, T Jessell, and J Dodd. 1991. "Control of Dorsoventral Pattern in Vertebrate Neural Development: Induction and Polarizing Properties of the Floor Plate." *Development (Cambridge, England)* Suppl 2: 1–19. <https://doi.org/10.1242/ds.1991.0002>.

E3860465BCC9%5Cnpapers2://publication/uuid/52B2E417-852E-4C59-A8C8-C793FA3AB369%5Cnhttp://eutils.ncbi.nlm.nih.gov/entrez/eutils/elink.fcgi?dbfrom=pubmed&id=1842349&retmode=ref&cmd=prlinks%5Cnpapers2://publicati.

Poli, Jerome, Olga Tsaponina, Laure Crabbe, Andrea Keszthelyi, Veronique Pantesco, Andrei Chabes, Armelle Lengronne, and Philippe Pasero. 2012. “dNTP Pools Determine Fork Progression and Origin Usage under Replication Stress.” *The EMBO Journal* 31 (4). England: 883–94. <https://doi.org/10.1038/emboj.2011.470>.

Pompeiano, M, A J Blaschke, R A Flavell, A Srinivasan, and J Chun. 2000. “Decreased Apoptosis in Proliferative and Postmitotic Regions of the Caspase 3-Deficient Embryonic Central Nervous System.” *The Journal of Comparative Neurology* 423 (1). United States: 1–12.

Poulson, D. F. 1940. “The Effects of Certain X-Chromosome Deficiencies on the Embryonic Development of *Drosophila Melanogaster*.” *Journal of Experimental Zoology* 83 (2). Wiley Subscription Services, Inc., A Wiley Company: 271–325. <https://doi.org/10.1002/jez.1400830207>.

Put, N M van der, R P Steegers-Theunissen, P Frosst, F J Trijbels, T K Eskes, L P van den Heuvel, E C Mariman, M den Heyer, R Rozen, and H J Blom. 1995. “Mutated Methylenetetrahydrofolate Reductase as a Risk Factor for Spina Bifida.” *Lancet (London, England)* 346 (8982). England: 1070–71.

Qi, Wenqing, Dianhua Qiao, and Jesse D Martinez. 2002. “Caffeine Induces TP53-Independent G(1)-Phase Arrest and Apoptosis in Human Lung Tumor Cells in a Dose-Dependent Manner.” *Radiation Research* 157 (2). United States: 166–74.

Qiu, Andong, Michaela Jansen, Antoinette Sakaris, Sang Hee Min, Shrikanta Chattopadhyay, Eugenia Tsai, Claudio Sandoval, Rongbao Zhao, Myles H Akbas, and I David Goldman. 2006. “Identification of an Intestinal Folate Transporter and the Molecular Basis for Hereditary Folate Malabsorption.” *Cell* 127 (5). United States: 917–28. <https://doi.org/10.1016/j.cell.2006.09.041>.

Quemeneur, Laurence, Luc-Marie Gerland, Monique Flacher, Martine Ffrench, Jean-Pierre Revillard, and Laurent Genestier. 2003. “Differential Control of Cell Cycle, Proliferation, and Survival of Primary T Lymphocytes by Purine and Pyrimidine Nucleotides.” *Journal of Immunology (Baltimore, Md. : 1950)* 170 (10). United States: 4986–95.

Radice, G L, H Rayburn, H Matsunami, K A Knudsen, M Takeichi, and R O Hynes. 1997. “Developmental Defects in Mouse Embryos Lacking N-Cadherin.” *Developmental Biology* 181 (1). United States: 64–78. <https://doi.org/10.1006/dbio.1996.8443>.

Raible, Florian, and Michael Brand. 2004. “Divide et Impera--the Midbrain-Hindbrain Boundary and Its Organizer.” *Trends in Neurosciences* 27 (12). England: 727–34. <https://doi.org/10.1016/j.tins.2004.10.003>.

Rash, B. G., and E. A. Grove. 2007. “Patterning the Dorsal Telencephalon: A Role for Sonic

Hedgehog?" *Journal of Neuroscience* 27 (43): 11595–603.
<https://doi.org/10.1523/JNEUROSCI.3204-07.2007>.

Ray, Heather J, and Lee A Niswander. 2016. "Grainyhead-like 2 Downstream Targets Act to Suppress Epithelial-to-Mesenchymal Transition during Neural Tube Closure." *Development* 143 (7): 1192 LP-1204. <http://dev.biologists.org/content/143/7/1192.abstract>.

Ray, J G, and H J Blom. 2003. "Vitamin B12 Insufficiency and the Risk of Fetal Neural Tube Defects." *QJM : Monthly Journal of the Association of Physicians* 96 (4). England: 289–95.

Ray, Joel G, Philip R Wyatt, Miles D Thompson, Marian J Vermeulen, Chris Meier, Pui-Yuen Wong, Sandra A Farrell, and David E C Cole. 2007. "Vitamin B12 and the Risk of Neural Tube Defects in a Folic-Acid-Fortified Population." *Epidemiology (Cambridge, Mass.)* 18 (3). United States: 362–66.

Reece, E A, M Khandelwal, Y K Wu, and M Borenstein. 1997. "Dietary Intake of Myo-Inositol and Neural Tube Defects in Offspring of Diabetic Rats." *American Journal of Obstetrics and Gynecology* 176 (3). United States: 536–39.

Reeves, F C, G C Burdge, W J Fredericks, F J Rauscher, and K A Lillycrop. 1999. "Induction of Antisense Pax-3 Expression Leads to the Rapid Morphological Differentiation of Neuronal Cells and an Altered Response to the Mitogenic Growth Factor bFGF." *Journal of Cell Science* 112 (Pt 2 (January)). ENGLAND: 253–61.

Reeves, F C, W J Fredericks, F J 3rd Rauscher, and K A Lillycrop. 1998. "The DNA Binding Activity of the Paired Box Transcription Factor Pax-3 Is Rapidly Downregulated during Neuronal Cell Differentiation." *FEBS Letters* 422 (1). NETHERLANDS: 118–22.

Reichard, P. 1988. "Interactions between Deoxyribonucleotide and DNA Synthesis." *Annual Review of Biochemistry* 57. United States: 349–74.
<https://doi.org/10.1146/annurev.bi.57.070188.002025>.

Rhee, S G, and K D Choi. 1992. "Regulation of Inositol Phospholipid-Specific Phospholipase C Isozymes." *The Journal of Biological Chemistry* 267 (18). United States: 12393–96.

Rhinn, M., and P. Dolle. 2012. "Retinoic Acid Signalling during Development." *Development* 139 (5). England: 843–58. <https://doi.org/10.1242/dev.065938>.

Ribes, Vanessa, Isabelle Le Roux, Muriel Rhinn, Brigitte Schuhbaur, and Pascal Dolle. 2009. "Early Mouse Caudal Development Relies on Crosstalk between Retinoic Acid, Shh and Fgf Signalling Pathways." *Development (Cambridge, England)* 136 (4). England: 665–76.
<https://doi.org/10.1242/dev.016204>.

Ribes, Vanessa, Fanny Stutzmann, Laurent Bianchetti, François Guillemot, Pascal Dollé, and Isabelle Le Roux. 2008. "Combinatorial Signalling Controls Neurogenin2 Expression at the Onset of Spinal Neurogenesis." *Developmental Biology* 321 (2): 470–81.
<https://doi.org/http://dx.doi.org/10.1016/j.ydbio.2008.06.003>.

Rifat, Yeliz, Vishwas Parekh, Tomasz Wilanowski, Nikki R Hislop, Alana Auden, Stephen B Ting, John M Cunningham, and Stephen M Jane. 2010. "Regional Neural Tube Closure

Defined by the Grainy Head-like Transcription Factors.” *Developmental Biology* 345 (2). United States: 237–45. <https://doi.org/10.1016/j.ydbio.2010.07.017>.

Robinson, Alexis, Sarah Escuin, Kit Doudney, Michel Vekemans, Roger E Stevenson, Nicholas D E Greene, Andrew J Copp, and Philip Stanier. 2012. “Mutations in the Planar Cell Polarity Genes CELSR1 and SCRIB Are Associated with the Severe Neural Tube Defect Craniorachischisis.” *Human Mutation* 33 (2). United States: 440–47. <https://doi.org/10.1002/humu.21662>.

Robitaille, Aaron M, Stefan Christen, Mitsugu Shimobayashi, Marion Cornu, Luca L Fava, Suzette Moes, Cristina Prescianotto-Baschong, Uwe Sauer, Paul Jenoe, and Michael N Hall. 2013. “Quantitative Phosphoproteomics Reveal mTORC1 Activates de Novo Pyrimidine Synthesis.” *Science (New York, N.Y.)* 339 (6125). United States: 1320–23. <https://doi.org/10.1126/science.1228771>.

Rogner, U C, D D Spyropoulos, N Le Novere, J P Changeux, and P Avner. 2000. “Control of Neurulation by the Nucleosome Assembly Protein-1-like 2.” *Nature Genetics* 25 (4). United States: 431–35. <https://doi.org/10.1038/78124>.

Rolo, Ana, Dawn Savery, Sarah Escuin, Sandra C de Castro, Hannah E J Armer, Peter M G Munro, Matteo A Mole, Nicholas D E Greene, and Andrew J Copp. 2016. “Regulation of Cell Protrusions by Small GTPases during Fusion of the Neural Folds.” *eLife* 5 (April). England: e13273. <https://doi.org/10.7554/eLife.13273>.

Rosemblit, N, M C Moschella, E Ondriasova, D E Gutstein, K Ondrias, and A R Marks. 1999. “Intracellular Calcium Release Channel Expression during Embryogenesis.” *Developmental Biology* 206 (2). United States: 163–77.

Rosenberg, L, A A Mitchell, S Shapiro, and D Slone. 1982. “Selected Birth Defects in Relation to Caffeine-Containing Beverages.” *JAMA* 247 (10). United States: 1429–32.

Rosenthal, Jorge, Jessica Casas, Douglas Taren, Clinton J Alverson, Alina Flores, and Jaime Frias. 2014. “Neural Tube Defects in Latin America and the Impact of Fortification: A Literature Review.” *Public Health Nutrition* 17 (3). England: 537–50. <https://doi.org/10.1017/S1368980013000256>.

Rowitch, D H, B S-Jacques, S M Lee, J D Flax, E Y Snyder, and A P McMahon. 1999. “Sonic Hedgehog Regulates Proliferation and Inhibits Differentiation of CNS Precursor Cells.” *The Journal of Neuroscience : The Official Journal of the Society for Neuroscience* 19 (20). United States: 8954–65.

Ruland, J, G S Duncan, A Elia, I del Barco Barrantes, L Nguyen, S Plyte, D G Millar, et al. 2001. “Bcl10 Is a Positive Regulator of Antigen Receptor-Induced Activation of NF- κ B and Neural Tube Closure.” *Cell* 104 (1). United States: 33–42.

Sadler, T W, D Greenberg, P Coughlin, and J L Lessard. 1982. “Actin Distribution Patterns in the Mouse Neural Tube during Neurulation.” *Science (New York, N.Y.)* 215 (4529). United States: 172–74.

Sah, V P, L D Attardi, G J Mulligan, B O Williams, R T Bronson, and T Jacks. 1995. "A Subset of p53-Deficient Embryos Exhibit Exencephaly." *Nature Genetics* 10 (2). United States: 175–80. <https://doi.org/10.1038/ng0695-175>.

Sahin, Bogachan, Stacey Galdi, Joseph Hendrick, Robert W Greene, Gretchen L Snyder, and James A Bibb. 2007. "Evaluation of Neuronal Phosphoproteins as Effectors of Caffeine and Mediators of Striatal Adenosine A2A Receptor Signaling." *Brain Research* 1129 (1). Netherlands: 1–14. <https://doi.org/10.1016/j.brainres.2006.10.059>.

Saito, H, M Ishibashi, H Nakano, and K Shiota. 2003. "Spatial and Temporal Expression of Folate-Binding Protein 1 (Fbp1) Is Closely Associated with Anterior Neural Tube Closure in Mice." *Dev Dyn* 226 (1): 112–17. <https://doi.org/10.1002/dvdy.10203>.

Salati, L M, C J Gross, L M Henderson, and D A Savaiano. 1984. "Absorption and Metabolism of Adenine, Adenosine-5'-monophosphate, Adenosine and Hypoxanthine by the Isolated Vascularly Perfused Rat Small Intestine." *The Journal of Nutrition* 114 (4). United States: 753–60.

Sanford, L P, I Ormsby, A C Gittenberger-de Groot, H Sariola, R Friedman, G P Boivin, E L Cardell, and T Doetschman. 1997. "TGFbeta2 Knockout Mice Have Multiple Developmental Defects That Are Non-Overlapping with Other TGFbeta Knockout Phenotypes." *Development (Cambridge, England)* 124 (13). England: 2659–70.

Sasai, Noriaki, and James Briscoe. 2012. "Primary Cilia and Graded Sonic Hedgehog Signaling." *Wiley Interdisciplinary Reviews. Developmental Biology* 1 (5). United States: 753–72. <https://doi.org/10.1002/wdev.43>.

Satoh, Kiyotoshi, Mana Kasai, Takefumi Ishidao, Kenichi Tago, Susumu Ohwada, Yoshimi Hasegawa, Takao Senda, et al. 2004. "Anteriorization of Neural Fate by Inhibitor of Beta-Catenin and T Cell Factor (ICAT), a Negative Regulator of Wnt Signaling." *Proceedings of the National Academy of Sciences of the United States of America* 101 (21). United States: 8017–21. <https://doi.org/10.1073/pnas.0401733101>.

Savaiano, D A, and A J Clifford. 1981. "Adenine, the Precursor of Nucleic Acids in Intestinal Cells Unable to Synthesize Purines de Novo." *The Journal of Nutrition* 111 (10). United States: 1816–22.

Savaiano, D A, C Y Ho, V Chu, and A J Clifford. 1980. "Metabolism of Orally and Intravenously Administered Purines in Rats." *The Journal of Nutrition* 110 (9). United States: 1793–1804.

Saxe, M de, J G Kromberg, and T Jenkins. 1984. "Waardenburg Syndrome in South Africa. Part I. An Evaluation of the Clinical Findings in 11 Families." *South African Medical Journal = Suid-Afrikaanse Tydskrif Vir Geneeskunde* 66 (7). South Africa: 256–61.

Sayed, Abdul-Rauf, David Bourne, Robert Pattinson, Jo Nixon, and Bertram Henderson. 2008. "Decline in the Prevalence of Neural Tube Defects Following Folic Acid Fortification and Its Cost-Benefit in South Africa." *Birth Defects Research. Part A, Clinical and Molecular Teratology* 82 (4). United States: 211–16. <https://doi.org/10.1002/bdra.20442>.

Schenk, Judith, Michaela Wilsch-Brauninger, Federico Calegari, and Wieland B Huttner. 2009. “Myosin II Is Required for Interkinetic Nuclear Migration of Neural Progenitors.” *Proceedings of the National Academy of Sciences of the United States of America* 106 (38). United States: 16487–92. <https://doi.org/10.1073/pnas.0908928106>.

Schmidt, M, S Evellin, P A Weernink, F von Dorp, H Rehmann, J W Lomasney, and K H Jakobs. 2001. “A New Phospholipase-C-Calcium Signalling Pathway Mediated by Cyclic AMP and a Rap GTPase.” *Nature Cell Biology* 3 (11). England: 1020–24. <https://doi.org/10.1038/ncb1101-1020>.

Schmidt, Rebecca J., Paul A. Romitti, Trudy L. Burns, Marilyn L. Browne, Charlotte M. Druschel, and Richard S. Olney. 2009. “Maternal Caffeine Consumption and Risk of Neural Tube Defects.” *Birth Defects Research Part A - Clinical and Molecular Teratology*. <https://doi.org/10.1002/bdra.20624>.

Schmidt, Rebecca J., Paul A. Romitti, Trudy L. Burns, Jeffrey C. Murray, Marilyn L. Browne, Charlotte M. Druschel, and Richard S. Olney. 2010. “Caffeine, Selected Metabolic Gene Variants, and Risk for Neural Tube Defects.” *Birth Defects Research Part A - Clinical and Molecular Teratology*. <https://doi.org/10.1002/bdra.20681>.

Schoenwolf, G C, and M V Franks. 1984. “Quantitative Analyses of Changes in Cell Shapes during Bending of the Avian Neural Plate.” *Developmental Biology* 105 (2). United States: 257–72.

Schroeter, E H, J A Kisslinger, and R Kopan. 1998. “Notch-1 Signalling Requires Ligand-Induced Proteolytic Release of Intracellular Domain.” *Nature* 393 (6683). England: 382–86. <https://doi.org/10.1038/30756>.

Schwahn, Bernd C, Maurice D Laryea, Zhoutao Chen, Stepan Melnyk, Igor Pogribny, Timothy Garrow, S Jill James, and Rima Rozen. 2004. “Betaine Rescue of an Animal Model with Methylenetetrahydrofolate Reductase Deficiency.” *The Biochemical Journal* 382 (Pt 3). England: 831–40. <https://doi.org/10.1042/BJ20040822>.

Scott, J M. 1999. “Folate and Vitamin B12.” *The Proceedings of the Nutrition Society* 58 (2). England: 441–48.

Selkoe, Dennis, and Raphael Kopan. 2003. “Notch and Presenilin: Regulated Intramembrane Proteolysis Links Development and Degeneration.” *Annual Review of Neuroscience* 26. United States: 565–97. <https://doi.org/10.1146/annurev.neuro.26.041002.131334>.

Seller, M J. 1983. “The Cause of Neural Tube Defects: Some Experiments and a Hypothesis.” *Journal of Medical Genetics* 20 (3). England: 164–68.

Seller, M J. 1994. “Vitamins, Folic Acid and the Cause and Prevention of Neural Tube Defects.” *Ciba Foundation Symposium* 181. Netherlands: 161–69.

Seller, M J, S Embury, P E Polani, and M Adinolfi. 1979. “Neural Tube Defects in Curly-Tail Mice. II. Effect of Maternal Administration of Vitamin A.” *Proceedings of the Royal Society of London. Series B, Biological Sciences* 206 (1162). England: 95–107.

Seller, M J, and K J Perkins-Cole. 1987a. "Hyperthermia and Neural Tube Defects of the Curly-Tail Mouse." *Journal of Craniofacial Genetics and Developmental Biology* 7 (4). UNITED STATES: 321–30.

Seller, M J, and K J Perkins-Cole. 1987b. "Sex Difference in Mouse Embryonic Development at Neurulation." *Journal of Reproduction and Fertility* 79 (1). England: 159–61.

Seller, M J, and K J Perkins. 1982. "Prevention of Neural Tube Defects in Curly-Tail Mice by Maternal Administration of Vitamin A." *Prenatal Diagnosis* 2 (4). ENGLAND: 297–300.

Seller, M J, and K J Perkins. 1983. "Effect of Hydroxyurea on Neural Tube Defects in the Curly-Tail Mouse." *Journal of Craniofacial Genetics and Developmental Biology* 3 (1). UNITED STATES: 11–17.

Seller, M J, and K J Perkins. 1986. "Effect of Mitomycin C on the Neural Tube Defects of the Curly-Tail Mouse." *Teratology* 33 (3). UNITED STATES: 305–9.
<https://doi.org/10.1002/tera.1420330308>.

Seller, M J, K J Perkins, and M Adinolfi. 1983. "Differential Response of Heterozygous Curly-Tail Mouse Embryos to Vitamin A Teratogenesis Depending on Maternal Genotype." *Teratology* 28 (1). United States: 123–29. <https://doi.org/10.1002/tera.1420280115>.

Shafizadeh, Tracy B, and Charles H Halsted. 2007. "Gamma-Glutamyl Hydrolase, Not Glutamate Carboxypeptidase II, Hydrolyzes Dietary Folate in Rat Small Intestine." *The Journal of Nutrition* 137 (5). United States: 1149–53.

Shangguan, Shaofang, Li Wang, Shaoyan Chang, Xiaoling Lu, Zhen Wang, Lihua Wu, Jianhua Wang, et al. 2015. "DNA Methylation Aberrations rather than Polymorphisms of FZD3 Gene Increase the Risk of Spina Bifida in a High-Risk Region for Neural Tube Defects." *Birth Defects Research. Part A, Clinical and Molecular Teratology* 103 (1). United States: 37–44. <https://doi.org/10.1002/bdra.23285>.

Shewach, Donna S. 1992. "Quantitation of Deoxyribonucleoside 5'-triphosphates By a Sequential Boronate and Anion-Exchange High-Pressure Liquid Chromatographic Procedure." *Analytical Biochemistry* 206 (1): 178–82. [https://doi.org/10.1016/S0003-2697\(05\)80030-2](https://doi.org/10.1016/S0003-2697(05)80030-2).

Shi, Ou-Yan, Hui-Yun Yang, Yong-Ming Shen, Wei Sun, Chun-You Cai, and Chun-Quan Cai. 2014. "Polymorphisms in FZD3 and FZD6 Genes and Risk of Neural Tube Defects in a Northern Han Chinese Population." *Neurological Sciences : Official Journal of the Italian Neurological Society and of the Italian Society of Clinical Neurophysiology* 35 (11). Italy: 1701–6. <https://doi.org/10.1007/s10072-014-1815-4>.

Shi, Yan, Yi Ding, Yun-Ping Lei, Xue-Yan Yang, Guo-Ming Xie, Jun Wen, Chun-Quan Cai, et al. 2012. "Identification of Novel Rare Mutations of DACT1 in Human Neural Tube Defects." *Human Mutation* 33 (10). United States: 1450–55.
<https://doi.org/10.1002/humu.22121>.

Shields, D C, P N Kirke, J L Mills, D Ramsbottom, A M Molloy, H Burke, D G Weir, J M Scott, and A S Whitehead. 1999. "The 'thermolabile' variant of Methylenetetrahydrofolate

Reductase and Neural Tube Defects: An Evaluation of Genetic Risk and the Relative Importance of the Genotypes of the Embryo and the Mother.” *American Journal of Human Genetics* 64 (4). United States: 1045–55.

Shirane, Michiko, Masaharu Ogawa, Jun Motoyama, and Keiichi I Nakayama. 2008. “Regulation of Apoptosis and Neurite Extension by FKBP38 Is Required for Neural Tube Formation in the Mouse.” *Genes to Cells : Devoted to Molecular & Cellular Mechanisms* 13 (6). England: 635–51. <https://doi.org/10.1111/j.1365-2443.2008.01194.x>.

Shum, A S, and A J Copp. 1996. “Regional Differences in Morphogenesis of the Neuroepithelium Suggest Multiple Mechanisms of Spinal Neurulation in the Mouse.” *Anatomy and Embryology* 194 (1). Germany: 65–73.

Sigoillot, Frederic D, J Andrew Berkowski, Severine M Sigoillot, Damian H Kotsis, and Hedeel I Guy. 2003. “Cell Cycle-Dependent Regulation of Pyrimidine Biosynthesis.” *The Journal of Biological Chemistry* 278 (5). United States: 3403–9. <https://doi.org/10.1074/jbc.M211078200>.

Sigoillot, Frederic D, Damian H Kotsis, Elizabeth M Masko, Monica Bame, David R Evans, and Hedeel I Guy Evans. 2007. “Protein Kinase C Modulates the up-Regulation of the Pyrimidine Biosynthetic Complex, CAD, by MAP Kinase.” *Frontiers in Bioscience : A Journal and Virtual Library* 12 (May). United States: 3892–98.

Singh, A P, T Castranio, G Scott, D Guo, M A Harris, M Ray, S E Harris, and Y Mishina. 2008. “Influences of Reduced Expression of Maternal Bone Morphogenetic Protein 2 on Mouse Embryonic Development.” *Sex Dev.* 2 (3): 134–41. <https://doi.org/10.1159/000143431>.

Skoog, L, and G Bjursell. 1974. “Nuclear and Cytoplasmic Pools of Deoxyribonucleoside Triphosphates in Chinese Hamster Ovary Cells.” *The Journal of Biological Chemistry* 249 (20). United States: 6434–38.

Slot, Andrew J, Steven V Molinski, and Susan P C Cole. 2011. “Mammalian Multidrug-Resistance Proteins (MRPs).” *Essays in Biochemistry* 50 (1). England: 179–207. <https://doi.org/10.1042/bse0500179>.

Smith, J M, S Pearson, and V Marks. 1982. “Plasma Caffeine Concentration in Outpatients.” *Lancet (London, England)*. England.

Smithells, R W, N C Nevin, M J Seller, S Sheppard, R Harris, A P Read, D W Fielding, S Walker, C J Schorah, and J Wild. 1983. “Further Experience of Vitamin Supplementation for Prevention of Neural Tube Defect Recurrences.” *Lancet (London, England)* 1 (8332). England: 1027–31.

Smithells, R W, S Sheppard, and C J Schorah. 1976. “Vitamin Deficiencies and Neural Tube Defects.” *Archives of Disease in Childhood* 51 (12): 944–50. <https://doi.org/10.1136/adc.51.12.944>.

Smithells, R W, S Sheppard, C J Schorah, M J Seller, N C Nevin, R Harris, A P Read, and D W Fielding. 1980. “Possible Prevention of Neural-Tube Defects by Periconceptional Vitamin

Supplementation.” *Lancet*. England. <http://www.ncbi.nlm.nih.gov/pubmed/6102643>.

Smithells, R W, S Sheppard, C J Schorah, M J Seller, N C Nevin, R Harris, A P Read, and D W Fielding. 1981. “Apparent Prevention of Neural Tube Defects by Periconceptional Vitamin Supplementation.” *Archives of Disease in Childhood* 56 (12). England: 911–18.

Smitherman, M, K Lee, J Swanger, R Kapur, and B E Clurman. 2000. “Characterization and Targeted Disruption of Murine Nup50, a p27(Kip1)-Interacting Component of the Nuclear Pore Complex.” *Molecular and Cellular Biology* 20 (15). United States: 5631–42.

Solloway, M J, and E J Robertson. 1999. “Early Embryonic Lethality in Bmp5;Bmp7 Double Mutant Mice Suggests Functional Redundancy within the 60A Subgroup.” *Development (Cambridge, England)* 126 (8). England: 1753–68.

Somogyi, L.P. 2010. “Caffeine Intake in the U.S. Population.” <http://www.fda.gov/downloads/AboutFDA/CentersOffices/OfficeofFoods/CFSAN/CFSANFOIAElectronicReadingRoom/UCM333191.pdf>.

Spyrou, G, and A Holmgren. 1996. “Deoxyribonucleoside Triphosphate Pools and Growth of Glutathione-Depleted 3T6 Mouse Fibroblasts.” *Biochemical and Biophysical Research Communications* 220 (1). United States: 42–46. <https://doi.org/10.1006/bbrc.1996.0353>.

St-Pierre, M V, M A Serrano, R I Macias, U Dubs, M Hoechli, U Lauper, P J Meier, and J J Marin. 2000. “Expression of Members of the Multidrug Resistance Protein Family in Human Term Placenta.” *American Journal of Physiology. Regulatory, Integrative and Comparative Physiology* 279 (4). United States: R1495–503.

Stasiulewicz, Magdalena, Shona D Gray, Ioanna Mastromina, Joana C Silva, Mia Bjorklund, Philip A Seymour, David Booth, et al. 2015. “A Conserved Role for Notch Signaling in Priming the Cellular Response to Shh through Ciliary Localisation of the Key Shh Transducer Smo.” *Development (Cambridge, England)* 142 (13). England: 2291–2303. <https://doi.org/10.1242/dev.125237>.

Stavric, B. 1988. “Methylxanthines: Toxicity to Humans. 2. Caffeine.” *Food and Chemical Toxicology : An International Journal Published for the British Industrial Biological Research Association* 26 (7). England: 645–62.

Stead, Lori M, John T Brosnan, Margaret E Brosnan, Dennis E Vance, and Rene L Jacobs. 2006. “Is It Time to Reevaluate Methyl Balance in Humans?” *The American Journal of Clinical Nutrition* 83 (1). United States: 5–10.

Steegers-Theunissen, R P, G H Boers, F J Trijbels, J D Finkelstein, H J Blom, C M Thomas, G F Borm, M G Wouters, and T K Eskes. 1994. “Maternal Hyperhomocysteinemia: A Risk Factor for Neural-Tube Defects?” *Metabolism: Clinical and Experimental* 43 (12). United States: 1475–80.

Stegmann, K, A Ziegler, E T Ngo, N Kohlschmidt, B Schroter, A Ermert, and M C Koch. 1999. “Linkage Disequilibrium of MTHFR Genotypes 677C/T-1298A/C in the German Population and Association Studies in Probands with Neural Tube defects(NTD).” *American Journal of*

Medical Genetics 87 (1). United States: 23–29.

Stern, Claudio D. 2005. “Neural Induction: Old Problem, New Findings, yet More Questions.” *Development (Cambridge, England)* 132 (9). England: 2007–21.
Development (Cambridge, England) 132 (9). England: 2007–21.
<https://doi.org/10.1242/dev.01794>.

Stern, Claudio D. 2016. “The Chick.” *Developmental Cell* 8 (1). Elsevier: 9–17.
<https://doi.org/10.1016/j.devcel.2004.11.018>.

Stork, Philip J S, and John M Schmitt. 2002. “Crosstalk between cAMP and MAP Kinase Signaling in the Regulation of Cell Proliferation.” *Trends in Cell Biology* 12 (6). England: 258–66.

Stottmann, Rolf W, Mark Berrong, Karen Matta, Murim Choi, and John Klingensmith. 2006. “The BMP Antagonist Noggin Promotes Cranial and Spinal Neurulation by Distinct Mechanisms.” *Developmental Biology* 295 (2). United States: 647–63.
<https://doi.org/10.1016/j.ydbio.2006.03.051>.

Stout, J Timothy, and C Thomas Caskey. 1985. “Hprt : Gene Structure , Expression , and Mutation.”

Straaten, H W van, H Blom, M C Peeters, A M Rousseau, K J Cole, and M J Seller. 1995. “Dietary Methionine Does Not Reduce Penetrance in Curly Tail Mice but Causes a Phenotype-Specific Decrease in Embryonic Growth.” *J Nutr* 125 (11): 2733–40.
http://www.ncbi.nlm.nih.gov/entrez/query.fcgi?cmd=Retrieve&db=PubMed&dopt=Citation&list_uids=7472652.

Straaten, H W van, and A J Copp. 2001. “Curly Tail: A 50-Year History of the Mouse Spina Bifida Model.” *Anatomy and Embryology* 203 (4). Germany: 225–37.

Straaten, H W van, J W Hekking, F Thors, E L Wiertz-Hoessels, and J Drukker. 1985. “Induction of an Additional Floor Plate in the Neural Tube.” *Acta Morphologica Neerlando-Scandinavica* 23 (2). Netherlands: 91–97.

Struhl, G, and A Adachi. 1998. “Nuclear Access and Action of Notch in Vivo.” *Cell* 93 (4). United States: 649–60.

Stumpo, D J, C B Bock, J S Tuttle, and P J Blackshear. 1995. “MARCKS Deficiency in Mice Leads to Abnormal Brain Development and Perinatal Death.” *Proceedings of the National Academy of Sciences of the United States of America* 92 (4). United States: 944–48.

Suarez, Lucina, Marilyn Felkner, and Kate Hendricks. 2004. “The Effect of Fever, Febrile Illnesses, and Heat Exposures on the Risk of Neural Tube Defects in a Texas-Mexico Border Population.” *Birth Defects Research. Part A, Clinical and Molecular Teratology* 70 (10). United States: 815–19. <https://doi.org/10.1002/bdra.20077>.

Sudiwala, Sonia, Sandra C.P. P De Castro, Kit-Yi Yi Leung, John T. Brosnan, Margaret E. Brosnan, Kevin Mills, Andrew J. Copp, and Nicholas D.E. E Greene. 2016. “Formate Supplementation Enhances Folate-Dependent Nucleotide Biosynthesis and Prevents Spina Bifida in a Mouse Model of Folic Acid-Resistant Neural Tube Defects.” *Biochimie* 126

(July). France: Elsevier B.V: 63–70. <https://doi.org/10.1016/j.biochi.2016.02.010>.

Sunden, S L, M S Renduchintala, E I Park, S D Miklasz, and T A Garrow. 1997. “Betaine-Homocysteine Methyltransferase Expression in Porcine and Human Tissues and Chromosomal Localization of the Human Gene.” *Archives of Biochemistry and Biophysics* 345 (1). United States: 171–74. <https://doi.org/10.1006/abbi.1997.0246>.

Swanson, D A, M L Liu, P J Baker, L Garrett, M Stitzel, J Wu, M Harris, R Banerjee, B Shane, and L C Brody. 2001. “Targeted Disruption of the Methionine Synthase Gene in Mice.” *Molecular and Cellular Biology* 21 (4). United States: 1058–65. <https://doi.org/10.1128/MCB.21.4.1058-1065.2001>.

Switzer, R L, and D C Sogin. 1973. “Regulation and Mechanism of Phosphoribosylpyrophosphate Synthetase. V. Inhibition by End Products and Regulation by Adenosine Diphosphate.” *The Journal of Biological Chemistry* 248 (3). United States: 1063–73.

Taipale, J, J K Chen, M K Cooper, B Wang, R K Mann, L Milenkovic, M P Scott, and P A Beachy. 2000. “Effects of Oncogenic Mutations in Smoothened and Patched Can Be Reversed by Cyclopamine.” *Nature* 406 (6799). England: 1005–9. <https://doi.org/10.1038/35023008>.

Takada, S, K L Stark, M J Shea, G Vassileva, J A McMahon, and A P McMahon. 1994. “Wnt-3a Regulates Somite and Tailbud Formation in the Mouse Embryo.” *Genes & Development* 8 (2). United States: 174–89.

Takahashi, M, and N Osumi. 2002. “Pax6 Regulates Specification of Ventral Neurone Subtypes in the Hindbrain by Establishing Progenitor Domains.” *Development* 129 (6): 1327–38. <http://www.ncbi.nlm.nih.gov/pubmed/11880342>.

Takahashi, T, R S Nowakowski, and V S Jr Caviness. 1992. “BUdR as an S-Phase Marker for Quantitative Studies of Cytokinetic Behaviour in the Murine Cerebral Ventricular Zone.” *Journal of Neurocytology* 21 (3). ENGLAND: 185–97.

Takeuchi, T, Y Yamazaki, Y Katoh-Fukui, R Tsuchiya, S Kondo, J Motoyama, and T Higashinakagawa. 1995. “Gene Trap Capture of a Novel Mouse Gene, Jumonji, Required for Neural Tube Formation.” *Genes & Development* 9 (10). United States: 1211–22.

Tam, P P, and K A Steiner. 1999. “Anterior Patterning by Synergistic Activity of the Early Gastrula Organizer and the Anterior Germ Layer Tissues of the Mouse Embryo.” *Development (Cambridge, England)* 126 (22). England: 5171–79.

The Food Fortification Initiative. 2016. “Global Progress.” Http://www.ffinetwork.org/global_progress. 2016. http://www.ffinetwork.org/global_progress.

Theiler, K., and S. Gluecksohn-Waelsch. 1956. “The Morphological Effects and the Development of the Fused Mutation in the Mouse.” *Anat.Rec.* 125 (1). United States: 83–104.

Thelander, L, and P Reichard. 1979. “Reduction of Ribonucleotides.” *Ann. Rev. Biochem.* 48: 133–58. <https://doi.org/10.1146/annurev.bi.48.070179.001025>.

Tibbetts, Anne S, and Dean R Appling. 2010. "Compartmentalization of Mammalian Folate-Mediated One-Carbon Metabolism." <https://doi.org/10.1146/annurev.nutr.012809.104810>.

Timmer, John R., Charlotte Wang, and Lee Niswander. 2002. "BMP Signaling Patterns the Dorsal and Intermediate Neural Tube via Regulation of Homeobox and Helix-Loop-Helix Transcription Factors." *Development* 129 (10): 2459–72. <http://dev.biologists.org/content/129/10/2459.long>.

Ting, Stephen B, Jacinta Caddy, Nikki Hislop, Tomasz Wilanowski, Alana Auden, Lin-Lin Zhao, Sarah Ellis, et al. 2005. "A Homolog of Drosophila Grainy Head Is Essential for Epidermal Integrity in Mice." *Science (New York, N.Y.)* 308 (5720). United States: 411–13. <https://doi.org/10.1126/science.1107511>.

Ting, Stephen B, Tomasz Wilanowski, Alana Auden, Mark Hall, Anne K Voss, Tim Thomas, Vishwas Parekh, John M Cunningham, and Stephen M Jane. 2003. "Inositol- and Folate-Resistant Neural Tube Defects in Mice Lacking the Epithelial-Specific Factor Grhl-3." *Nature Medicine* 9 (12): 1513–19. <https://doi.org/10.1038/nm961>.

Topal, Gokce, Annie Brunet, Elisabeth Millanvoye, Jean-Luc Boucher, Francine Rendu, Marie-Aude Devynck, and Monique David-Dufilho. 2004. "Homocysteine Induces Oxidative Stress by Uncoupling of NO Synthase Activity through Reduction of Tetrahydrobiopterin." *Free Radical Biology & Medicine* 36 (12). United States: 1532–41. <https://doi.org/10.1016/j.freeradbiomed.2004.03.019>.

Tozzi, Maria G., Marcella Camici, Laura Mascia, Francesco Sgarrella, and Piero L. Ipata. 2006. "Pentose Phosphates in Nucleoside Interconversion and Catabolism." *FEBS Journal* 273 (6): 1089–1101. <https://doi.org/10.1111/j.1742-4658.2006.05155.x>.

Tuson, Miquel, Mu He, and Kathryn V Anderson. 2011. "Protein Kinase A Acts at the Basal Body of the Primary Cilium to Prevent Gli2 Activation and Ventralization of the Mouse Neural Tube." *Development (Cambridge, England)* 138 (22). England: 4921–30. <https://doi.org/10.1242/dev.070805>.

Ulloa, Fausto, and Elisa Marti. 2010. "Wnt Won the War: Antagonistic Role of Wnt over Shh Controls Dorso-Ventral Patterning of the Vertebrate Neural Tube." *Developmental Dynamics : An Official Publication of the American Association of Anatomists* 239 (1). United States: 69–76. <https://doi.org/10.1002/dvdy.22058>.

Valjent, Emmanuel, Christiane Pages, Denis Herve, Jean-Antoine Girault, and Jocelyne Caboche. 2004. "Addictive and Non-Addictive Drugs Induce Distinct and Specific Patterns of ERK Activation in Mouse Brain." *The European Journal of Neuroscience* 19 (7). France: 1826–36. <https://doi.org/10.1111/j.1460-9568.2004.03278.x>.

Verrier, Florence, Songon An, Ann M Ferrie, Haiyan Sun, Minjoung Kyoung, Huayun Deng, Ye Fang, and Stephen J Benkovic. 2011. "GPCRs Regulate the Assembly of a Multienzyme Complex for Purine Biosynthesis." *Nature Chemical Biology* 7 (12). United States: 909–15. <https://doi.org/10.1038/nchembio.690>.

Viebahn, C. 2001. "Hensen's Node." *Genesis (New York, N.Y. : 2000)* 29 (2). United States: 96–103.

Voet, Donald, and Judith G. Voet. 2004. *Biochemistry*. 3rd ed. Wiley. pp.1069-1098.

Volpe, P, and T Eremenko-Volpe. 1970. "Quantitative Studies on Cell Proteins in Suspension Cultures." *European Journal of Biochemistry* 12 (1). England: 195–200.

Wachstein, M, and R Sigismondi. 1958. "5-Nucleotidase Activity and Adenosine Triphosphatase Activity in Human Serums." *American Journal of Clinical Pathology* 30 (6). England: 523–27.

Wald, N, J Sneddon, J Densem, C Frost, R Stone, and The Vitamin Study Research Group. 1991. "Prevention of Neural Tube Defects: Results of the Medical Research Council Vitamin Study." *The Lancet* 338 (8760). England: 131–37. [https://doi.org/10.1016/0140-6736\(91\)90133-A](https://doi.org/10.1016/0140-6736(91)90133-A).

Walters, R. A., R. A. Tobey, and R. L. Ratliff. 1973. "Cell-Cycle-Dependent Variations of Deoxyribonucleoside Triphosphate Pools in Chinese Hamster Cells." *BBA Section Nucleic Acids And Protein Synthesis* 319 (3): 336–47. [https://doi.org/10.1016/0005-2787\(73\)90173-1](https://doi.org/10.1016/0005-2787(73)90173-1).

Wang, B, J F Fallon, and P A Beachy. 2000. "Hedgehog-Regulated Processing of Gli3 Produces an Anterior/posterior Repressor Gradient in the Developing Vertebrate Limb." *Cell* 100 (4). United States: 423–34.

Wang, Hai Gang, Jia Li Wang, Jian Zhang, Li Xia Zhao, Guang Xi Zhai, Yu Zhu Xiang, and Ping Chang. 2012. "Reduced Folate Carrier A80G Polymorphism and Susceptibility to Neural Tube Defects: A Meta-Analysis." *Gene* 510 (2). Elsevier B.V.: 180–84. <https://doi.org/10.1016/j.gene.2012.02.020>.

Wang, He, Wenjie Guan, Wanzhi Yang, Qi Wang, Han Zhao, Feng Yang, Xiongwen Lv, and Jun Li. 2014. "Caffeine Inhibits the Activation of Hepatic Stellate Cells Induced by Acetaldehyde via Adenosine A2A Receptor Mediated by the cAMP/PKA/SRC/ERK1/2/P38 MAPK Signal Pathway." *PLoS One* 9 (3). United States: e92482. <https://doi.org/10.1371/journal.pone.0092482>.

Wang, J, A Arbuzova, G Hangyas-Mihalyne, and S McLaughlin. 2001. "The Effector Domain of Myristoylated Alanine-Rich C Kinase Substrate Binds Strongly to Phosphatidylinositol 4,5-Bisphosphate." *The Journal of Biological Chemistry* 276 (7). United States: 5012–19. <https://doi.org/10.1074/jbc.M008355200>.

Wang, Liya. 2016. "Mitochondrial Purine and Pyrimidine Metabolism and Beyond." *Nucleosides, Nucleotides & Nucleic Acids* 35 (10–12). United States: 578–94. <https://doi.org/10.1080/15257770.2015.1125001>.

Wang, Qi, Xuefei Dai, Wanzhi Yang, He Wang, Han Zhao, Feng Yang, Yan Yang, Jun Li, and Xiongwen Lv. 2015. "Caffeine Protects against Alcohol-Induced Liver Fibrosis by Dampening the cAMP/PKA/CREB Pathway in Rat Hepatic Stellate Cells." *International*

Immunopharmacology 25 (2). Netherlands: 340–52.
<https://doi.org/10.1016/j.intimp.2015.02.012>.

Wang, Richard N, Jordan Green, Zhongliang Wang, Youlin Deng, Min Qiao, Michael Peabody, Qian Zhang, et al. 2014. “Bone Morphogenetic Protein (BMP) Signaling in Development and Human Diseases.” *Genes & Diseases* 1 (1). China: 87–105.
<https://doi.org/10.1016/j.gendis.2014.07.005>.

Wang, Yanfeng, Lurong Lian, Jeffrey A Golden, Edward E Morrisey, and Charles S Abrams. 2007. “PIP5KI Gamma Is Required for Cardiovascular and Neuronal Development.” *Proceedings of the National Academy of Sciences of the United States of America* 104 (28). United States: 11748–53. <https://doi.org/10.1073/pnas.0700019104>.

Washburn, S E, M A Caudill, O Malysheva, A J MacFarlane, N A Behan, B Harnett, L MacMillan, T Pongnopparat, J T Brosnan, and M E Brosnan. 2015. “Formate Metabolism in Fetal and Neonatal Sheep.” *Am J Physiol Endocrinol Metab* 308 (10): E921–7.
<https://doi.org/10.1152/ajpendo.00046.2015>.

Wellcome Trust. n.d. “One in Six Pregnancies among Women in Britain Are Unplanned.” <https://wellcome.ac.uk/press-release/one-six-pregnancies-among-women-britain-are-unplanned>.

Werner, A. 1993. “Reversed-Phase and Ion-Pair Separations of Nucleotides, Nucleosides and Nucleobases: Analysis of Biological Samples in Health and Disease.” *Journal of Chromatography B: Biomedical Sciences and Applications* 618 (1–2): 3–14.
[https://doi.org/10.1016/0378-4347\(93\)80024-X](https://doi.org/10.1016/0378-4347(93)80024-X).

Werth, Max, Katharina Walentin, Annekatrin Aue, Jorg Schonheit, Anne Wuebken, Naomi Pode-Shakked, Larissa Vilianovitch, et al. 2010. “The Transcription Factor Grainyhead-like 2 Regulates the Molecular Composition of the Epithelial Apical Junctional Complex.” *Development (Cambridge, England)* 137 (22). England: 3835–45.
<https://doi.org/10.1242/dev.055483>.

Wiley, M J. 1980. “The Effects of Cytochalasins on the Ultrastructure of Neurulating Hamster Embryos in Vivo.” *Teratology* 22 (1). United States: 59–69.
<https://doi.org/10.1002/tera.1420220109>.

Wilkinson, J. M., and I. Pollard. 1994. “In Utero Exposure to Caffeine Causes Delayed Neural Tube Closure in Rat Embryos.” *Teratogenesis Carcinogenesis and Mutagenesis*.
<https://doi.org/10.1002/tcm.1770140502>.

Williams, Laura J, Sonja A Rasmussen, Alina Flores, Russell S Kirby, and Larry D Edmonds. 2005. “Decline in the Prevalence of Spina Bifida and Anencephaly by Race/ethnicity: 1995–2002.” *Pediatrics* 116 (3). United States: 580–86. <https://doi.org/10.1542/peds.2005-0592>.

Wilson, D W, and H C Wilson. 1962. “Studies in Vitro of the Digestion and Absorption of Purine Ribonucleotides by the Intestine.” *The Journal of Biological Chemistry* 237 (May). United States: 1643–47.

Wilson, Monita P, Christopher Hugge, Małgorzata Bielinska, Peter Nicholas, Philip W Majerus, and David B Wilson. 2009. "Neural Tube Defects in Mice with Reduced Levels of Inositol 1,3,4-Trisphosphate 5/6-Kinase." *Proceedings of the National Academy of Sciences of the United States of America* 106 (24). United States: 9831–35.
<https://doi.org/10.1073/pnas.0904172106>.

Wilson, T H, and D W Wilson. 1958. "Studies in Vitro of Digestion and Absorption of Pyrimidine Nucleotides by the Intestine." *The Journal of Biological Chemistry* 233 (6). United States: 1544–47.

Wisniewski, Jacek R, Marco Y Hein, Jurgen Cox, and Matthias Mann. 2014. "A 'proteomic Ruler' for Protein Copy Number and Concentration Estimation without Spike-in Standards." *Molecular & Cellular Proteomics : MCP* 13 (12). United States: 3497–3506.
<https://doi.org/10.1074/mcp.M113.037309>.

Włodarczyk, Bogdan J, Louisa S Tang, Aleata Triplett, Frank Aleman, and Richard H Finnell. 2006. "Spontaneous Neural Tube Defects in Splotch Mice Supplemented with Selected Micronutrients." *Toxicology and Applied Pharmacology* 213 (1). United States: 55–63.
<https://doi.org/10.1016/j.taap.2005.09.008>.

Woeller, Collynn F, Donald D Anderson, Doletha M E Szebenyi, and Patrick J Stover. 2007. "Evidence for Small Ubiquitin-like Modifier-Dependent Nuclear Import of the Thymidylate Biosynthesis Pathway." *The Journal of Biological Chemistry* 282 (24). United States: 17623–31. <https://doi.org/10.1074/jbc.M702526200>.

Wu-Zhang, Alyssa X, and Alexandra C Newton. 2013. "Protein Kinase C Pharmacology: Refining the Toolbox." *The Biochemical Journal* 452 (2). England: 195–209.
<https://doi.org/10.1042/BJ20130220>.

Wu, C L, and D W Melton. 1993. "Production of a Model for Lesch-Nyhan Syndrome in Hypoxanthine Phosphoribosyltransferase-Deficient Mice." *Nature Genetics* 3 (3): 235–40.
<https://doi.org/10.1038/ng0393-235>.

Wu, M, D F Chen, T Sasaoka, and S Tonegawa. 1996. "Neural Tube Defects and Abnormal Brain Development in F52-Deficient Mice." *Proceedings of the National Academy of Sciences of the United States of America* 93 (5). United States: 2110–15.

Xu, W, H Baribault, and E D Adamson. 1998. "Vinculin Knockout Results in Heart and Brain Defects during Embryonic Development." *Development (Cambridge, England)* 125 (2). England: 327–37.

Xu, X, C Li, K Takahashi, H C Slavkin, L Shum, and C X Deng. 1999. "Murine Fibroblast Growth Factor Receptor 1alpha Isoforms Mediate Node Regression and Are Essential for Posterior Mesoderm Development." *Developmental Biology* 208 (2). United States: 293–306. <https://doi.org/10.1006/dbio.1999.9227>.

Yadav, Upendra, Pradeep Kumar, Sushil Kumar Yadav, Om Prakash Mishra, and Vandana Rai. 2015. "Polymorphisms in Folate Metabolism Genes as Maternal Risk Factor for Neural

Tube Defects: An Updated Meta-Analysis'." *Metabolic Brain Disease* 30 (1). United States: 7–24. <https://doi.org/10.1007/s11011-014-9575-7>.

Yamaoka, T, M Kondo, S Honda, H Iwahana, M Moritani, S Ii, K Yoshimoto, and M Itakura. 1997. "Amidophosphoribosyltransferase Limits the Rate of Cell Growth-Linked de Novo Purine Biosynthesis in the Presence of Constant Capacity of Salvage Purine Biosynthesis." *The Journal of Biological Chemistry* 272 (28). United States: 17719–25.

Yang, Mei, Liping Yang, Ling Qi, Yiyang Guo, Xiaofang Lin, Yu Zhang, and Yukai Du. 2013. "Association between the Methionine Synthase A2756G Polymorphism and Neural Tube Defect Risk: A Meta-Analysis." *Gene* 520 (1). Netherlands: 7–13. <https://doi.org/10.1016/j.gene.2013.02.005>.

Yang, Yi, Jie Chen, Beiyu Wang, Chen Ding, and Hao Liu. 2015. "Association between MTHFR C677T Polymorphism and Neural Tube Defect Risks: A Comprehensive Evaluation in Three Groups of NTD Patients, Mothers, and Fathers." *Birth Defects Research. Part A, Clinical and Molecular Teratology* 103 (6). United States: 488–500. <https://doi.org/10.1002/bdra.23361>.

Yasuda, Satoru, Satoko Hasui, Masaki Kobayashi, Shirou Itagaki, Takeshi Hirano, and Ken Iseki. 2008. "The Mechanism of Carrier-Mediated Transport of Folates in BeWo Cells: The Involvement of Heme Carrier Protein 1 in Placental Folate Transport." *Bioscience, Biotechnology, and Biochemistry* 72 (2). England: 329–34.

Yasuda, Satoru, Satoko Hasui, Chiaki Yamamoto, Chihiro Yoshioka, Masaki Kobayashi, Shirou Itagaki, Takeshi Hirano, and Ken Iseki. 2008. "Placental Folate Transport during Pregnancy." *Bioscience, Biotechnology, and Biochemistry* 72 (9). England: 2277–84. <https://doi.org/10.1271/bbb.80112>.

Yazdy, Mahsa M, Sarah C Tinker, Allen A Mitchell, Laurie A Demmer, and Martha M Werler. 2012. "Maternal Tea Consumption during Early Pregnancy and the Risk of Spina Bifida." *Birth Defects Research. Part A, Clinical and Molecular Teratology* 94 (10). United States: 756–61. <https://doi.org/10.1002/bdra.23025>.

Ybot-Gonzalez, P, and A J Copp. 1999. "Bending of the Neural Plate during Mouse Spinal Neurulation Is Independent of Actin Microfilaments." *Developmental Dynamics : An Official Publication of the American Association of Anatomists* 215 (3). United States: 273–83. [https://doi.org/10.1002/\(SICI\)1097-0177\(199907\)215:3<273::AID-AJA9>3.0.CO;2-H](https://doi.org/10.1002/(SICI)1097-0177(199907)215:3<273::AID-AJA9>3.0.CO;2-H).

Ybot-Gonzalez, Patricia, Patricia Cogram, Dianne Gerrelli, and Andrew J Copp. 2002. "Sonic Hedgehog and the Molecular Regulation of Mouse Neural Tube Closure." *Development (Cambridge, England)* 129: 2507–17.

Ybot-Gonzalez, Patricia, Carles Gaston-Massuet, Gemma Girdler, John Klingensmith, Ruth Arkell, Nicholas D E Greene, and Andrew J Copp. 2007. "Neural Plate Morphogenesis during Mouse Neurulation Is Regulated by Antagonism of Bmp Signalling." *Development* 134 (17): 3203–11. <https://doi.org/10.1242/dev.008177>.

Ybot-Gonzalez, Patricia, Dawn Savery, Dianne Gerrelli, Massimo Signore, Claire E Mitchell, Clare H Faux, Nicholas D E Greene, and Andrew J Copp. 2007. "Convergent Extension, Planar-Cell-Polarity Signalling and Initiation of Mouse Neural Tube Closure." *Development (Cambridge, England)* 134 (4). England: 789–99. <https://doi.org/10.1242/dev.000380>.

Yoshida, H, Y Y Kong, R Yoshida, A J Elia, A Hakem, R Hakem, J M Penninger, and T W Mak. 1998. "Apaf1 Is Required for Mitochondrial Pathways of Apoptosis and Brain Development." *Cell* 94 (6). United States: 739–50.

Yoshikawa, Y, T Fujimori, A P McMahon, and S Takada. 1997. "Evidence That Absence of Wnt-3a Signaling Promotes Neuralization instead of Paraxial Mesoderm Development in the Mouse." *Developmental Biology* 183 (2). United States: 234–42. <https://doi.org/10.1006/dbio.1997.8502>.

Yu, Weiying, Kristen McDonnell, Makoto M Taketo, and C Brian Bai. 2008. "Wnt Signaling Determines Ventral Spinal Cord Cell Fates in a Time-Dependent Manner." *Development (Cambridge, England)* 135 (22). England: 3687–96. <https://doi.org/10.1242/dev.021899>.

Yu, Zhengquan, Kevin K. Lin, Ambica Bhandari, Joel A. Spencer, Xiaoman Xu, Ning Wang, Zhongxian Lu, et al. 2006. "The Grainyhead-like Epithelial Transactivator Get-1/Grhl3 Regulates Epidermal Terminal Differentiation and Interacts Functionally with LMO4." *Developmental Biology* 299 (1): 122–36. <https://doi.org/10.1016/j.ydbio.2006.07.015>.

Zanger, Ulrich M, Miia Turpeinen, Kathrin Klein, and Matthias Schwab. 2008. "Functional Pharmacogenetics/genomics of Human Cytochromes P450 Involved in Drug Biotransformation." *Analytical and Bioanalytical Chemistry* 392 (6). Germany: 1093–1108. <https://doi.org/10.1007/s00216-008-2291-6>.

Zeitlin, Ross, Sagar Patel, Sarah Burgess, Gary W Arendash, and Valentina Echeverria. 2011. "Caffeine Induces Beneficial Changes in PKA Signaling and JNK and ERK Activities in the Striatum and Cortex of Alzheimer's Transgenic Mice." *Brain Research* 1417 (October). Netherlands: 127–36. <https://doi.org/10.1016/j.brainres.2011.08.036>.

Zeng, L, F Fagotto, T Zhang, W Hsu, T J Vasicek, W L 3rd Perry, J J Lee, S M Tilghman, B M Gumbiner, and F Costantini. 1997. "The Mouse Fused Locus Encodes Axin, an Inhibitor of the Wnt Signaling Pathway That Regulates Embryonic Axis Formation." *Cell* 90 (1). United States: 181–92.

Zhang, Wei, Shenglan Tan, Elijah Paintsil, Ginger E. Dutschman, Elizabeth A. Gullen, Edward Chu, and Yung Chi Cheng. 2011. "Analysis of Deoxyribonucleotide Pools in Human Cancer Cell Lines Using a Liquid Chromatography Coupled with Tandem Mass Spectrometry Technique." *Biochemical Pharmacology* 82 (4). Elsevier Inc.: 411–17. <https://doi.org/10.1016/j.bcp.2011.05.009>.

Zhang, X, and P W Majerus. 1998. "Phosphatidylinositol Signalling Reactions." *Seminars in Cell & Developmental Biology* 9 (2): 153–60. <https://doi.org/10.1006/scdb.1997.0220>.

Zhang, Xiaoyan M., Miguel Ramalho-Santos, and Andrew P. McMahon. 2001. "Smoothened

Mutants Reveal Redundant Roles for Shh and Ihh Signaling Including Regulation of L/R Asymmetry by the Mouse Node.” *Cell* 105 (6): 781–92. [https://doi.org/10.1016/S0092-8674\(01\)00385-3](https://doi.org/10.1016/S0092-8674(01)00385-3).

Zhang, Xumei, Huan Liu, Gexin Cong, Zhihong Tian, Dalin Ren, John X Wilson, and Guowei Huang. 2008. “Effects of Folate on Notch Signaling and Cell Proliferation in Neural Stem Cells of Neonatal Rats in Vitro.” *Journal of Nutritional Science and Vitaminology* 54 (5): 353–56. <https://doi.org/10.3177/jnsv.54.353>.

Zhao, Q, R R Behringer, and B de Crombrugghe. 1996. “Prenatal Folic Acid Treatment Suppresses Acrania and Meroanencephaly in Mice Mutant for the Cart1 Homeobox Gene.” *Nature Genetics* 13 (3). United States: 275–83. <https://doi.org/10.1038/ng0796-275>.

Zhao, Rongbao, Ndeye Diop-Bove, Michele Visentin, and I. David Goldman. 2011. *Mechanisms of Membrane Transport of Folates into Cells and Across Epithelia. Annual Review of Nutrition*. Vol. 31. <https://doi.org/10.1146/annurev-nutr-072610-145133>.

Zhao, Rongbao, Larry H Matherly, and I David Goldman. 2009. “Membrane Transporters and Folate Homeostasis: Intestinal Absorption and Transport into Systemic Compartments and Tissues.” *Expert Reviews in Molecular Medicine* 11 (January). England: e4. <https://doi.org/10.1017/S1462399409000969>.

Zhao, Tianyu, Qini Gan, Arjun Stokes, Rhonda N T Lassiter, Yongping Wang, Jason Chan, Jane X Han, David E Pleasure, Jonathan A Epstein, and Chengji J Zhou. 2014. “ β -Catenin Regulates Pax3 and Cdx2 for Caudal Neural Tube Closure and Elongation.” *Development* 141 (1): 148–57. <https://doi.org/10.1242/dev.101550>.

Zheng, Jinyu, Xiaocheng Lu, Hao Liu, Penglai Zhao, Kai Li, and Lixin Li. 2015. “MTHFD1 Polymorphism as Maternal Risk for Neural Tube Defects: A Meta-Analysis.” *Neurological Sciences : Official Journal of the Italian Neurological Society and of the Italian Society of Clinical Neurophysiology* 36 (4). Italy: 607–16. <https://doi.org/10.1007/s10072-014-2035-7>.

Zhong, W, M M Jiang, M D Schonemann, J J Meneses, R A Pedersen, L Y Jan, and Y N Jan. 2000. “Mouse Numb Is an Essential Gene Involved in Cortical Neurogenesis.” *Proceedings of the National Academy of Sciences of the United States of America* 97 (12). UNITED STATES: 6844–49.

Zhou, X, H Sasaki, L Lowe, B L Hogan, and M R Kuehn. 1993. “Nodal Is a Novel TGF-Beta-like Gene Expressed in the Mouse Node during Gastrulation.” *Nature* 361 (6412). England: 543–47. <https://doi.org/10.1038/361543a0>.

Appendices

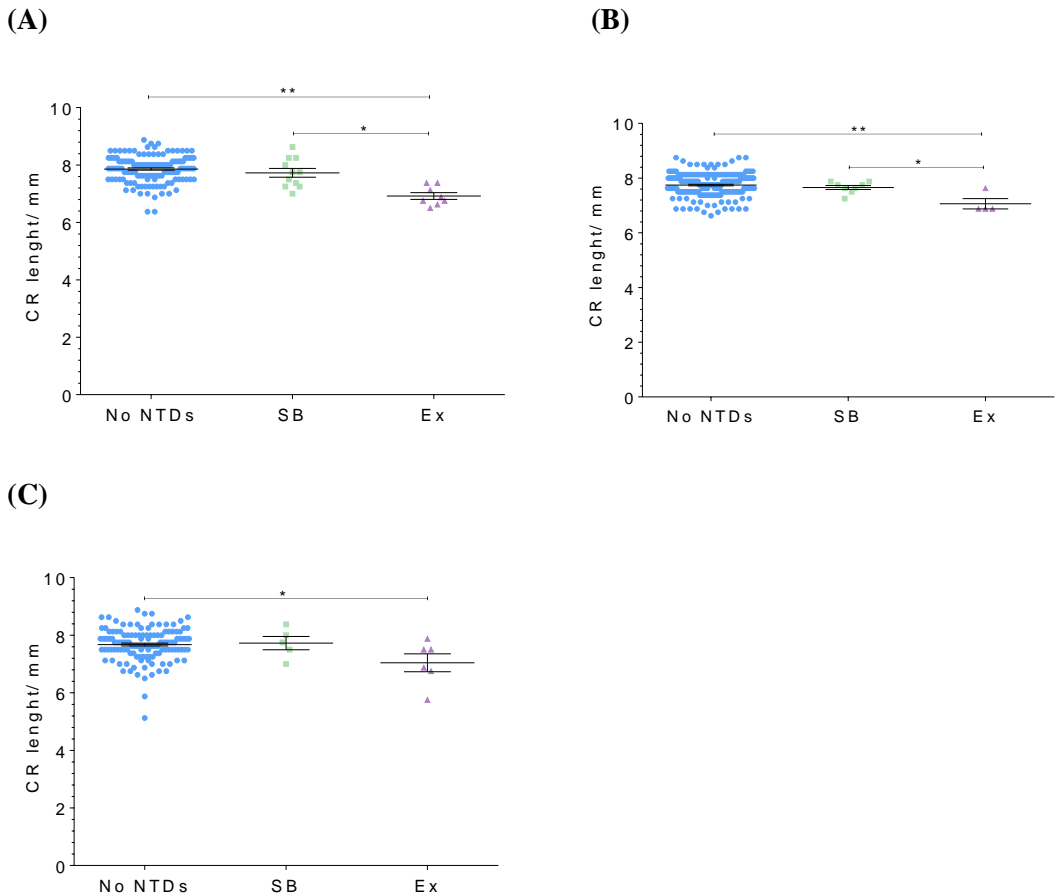
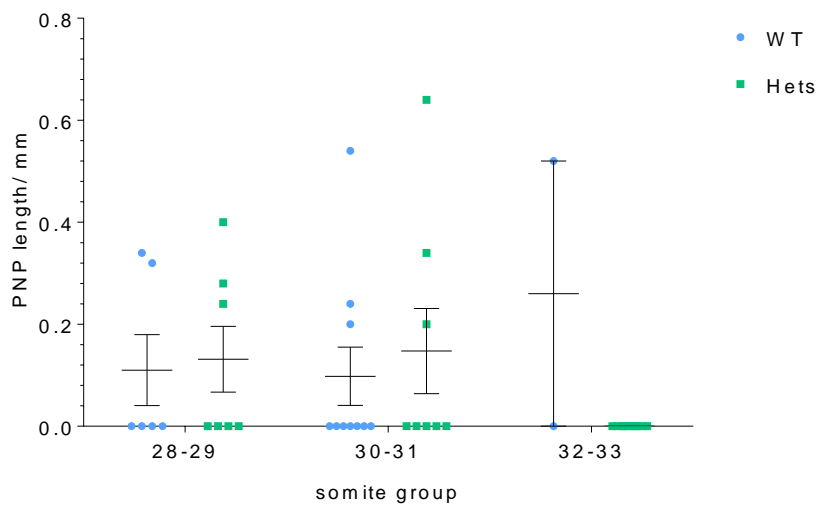


Figure A1. Comparison of CR lengths of *ct* embryos with or without NTDs on different treatments.

The CR lengths of E12.5 *ct* embryos with no NTDs, spina bifida only, or exencephaly (including embryos with exencephaly and spina bifida) which were (A) control; (B) formate treated and (C) caffeine treated.

(A) The CR lengths of exencephalic embryos (6.92 ± 0.11 ; $n = 8$) were significantly shorter than that of embryos with no NTDs (7.86 ± 0.04 ; $n = 133$; $**p < 0.0001$) and those with spina bifida only (7.73 ± 0.15 ; $n = 11$; $*p = 0.0006$). (B) The CR lengths of exencephalic embryos (7.06 ± 0.19 ; $n = 4$) were significantly shorter than that of embryos with no NTDs (7.75 ± 0.03 ; $n = 220$; $**p = 0.002$) and those with spina bifida only (7.66 ± 0.07 ; $n = 8$; $*p = 0.03$). (C) The CR lengths of exencephalic embryos (7.04 ± 0.31 ; $n = 6$) were significantly shorter than that of embryos with no NTDs (7.68 ± 0.04 ; $n = 133$; $*p = 0.02$). ANOVA followed by Holm-Sidak's multiple comparisons test for each dataset.

(A)



(B)

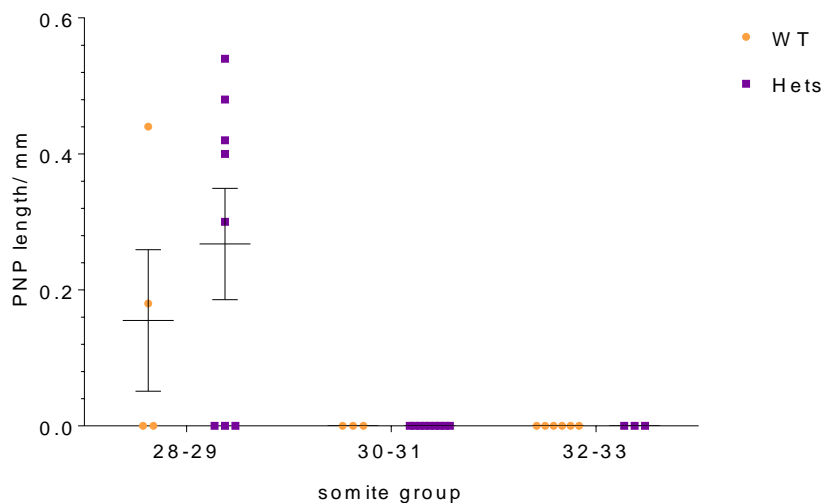
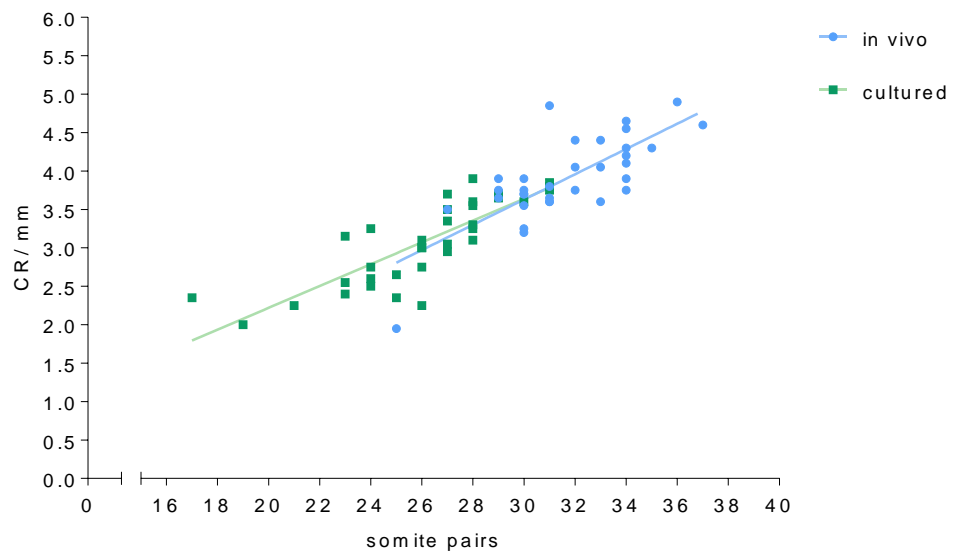


Figure A2. PNP lengths of +/+ and *Sp*^{2H}/+ embryos

The PNP lengths of either **(A)** control, or **(B)** caffeine treated, $+/+$ and $Sp^{2H}/+$ embryos are not significantly different.

(A)



(B)

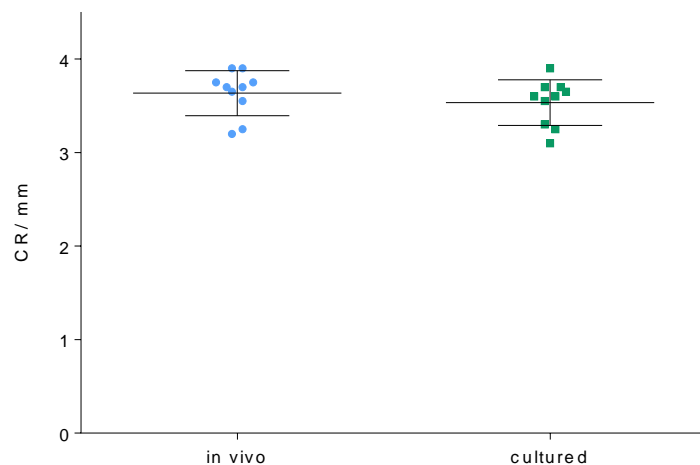


Figure A3. Comparison of CR lengths of control *ct* embryos *in vivo* and cultured.

No significant differences were found between the CR length of untreated, *in vivo* developed *ct* embryos, and untreated, cultured *ct* embryos, by (A) linear regression analysis ($r^2 = 0.57$ for *in vivo* developed embryos, and $r^2 = 0.68$ for cultured embryos), or (B), comparing CR lengths at the 28–30 somite stage ($n = 10$ for each group).

Figure A 4. Publication of the major findings of Chapter 4.

Sudiwala, S. et al., 2016. Formate supplementation enhances folate-dependent nucleotide biosynthesis and prevents spina bifida in a mouse model of folic acid-resistant neural tube defects. *Biochimie*, 126, pp.63–70. Available at: <http://dx.doi.org/10.1016/j.biochi.2016.02.010>.

(next page)



Research paper

Formate supplementation enhances folate-dependent nucleotide biosynthesis and prevents spina bifida in a mouse model of folic acid-resistant neural tube defects



Sonia Sudiwala ^a, Sandra C.P. De Castro ^a, Kit-Yi Leung ^a, John T. Brosnan ^b, Margaret E. Brosnan ^b, Kevin Mills ^c, Andrew J. Copp ^a, Nicholas D.E. Greene ^{a,*}

^a Newlife Birth Defects Research Centre and Developmental Biology & Cancer Programme, Institute of Child Health, University College London, London, WC1N 1EH, UK

^b Department of Biochemistry, Memorial University of Newfoundland, St John's, NL, A1B 3X9, Canada

^c Genetics & Genomic Medicine Programme, Institute of Child Health, University College London, London, WC1N 1EH, UK

ARTICLE INFO

Article history:

Received 3 November 2015

Accepted 19 February 2016

Available online 23 February 2016

Keywords:

Folate one-carbon metabolism

Formate

Neural tube defects

Folic acid

Grainyhead-like 3

mthfd1L

ABSTRACT

The *curly tail* mouse provides a model for neural tube defects (spina bifida and exencephaly) that are resistant to prevention by folic acid. The major *ct* gene, responsible for spina bifida, corresponds to a hypomorphic allele of *grainyhead-like 3* (*Ghrl3*) but the frequency of NTDs is strongly influenced by modifiers in the genetic background. Moreover, exencephaly in the *curly tail* strain is not prevented by reinstatement of *Ghrl3* expression. In the current study we found that expression of *Mthfd1L*, encoding a key component of mitochondrial folate one-carbon metabolism (FOCM), is significantly reduced in *ct/ct* embryos compared to a partially congenic wild-type strain. This expression change is not attributable to regulation by *Ghrl3* or the genetic background at the *Mthfd1L* locus. Mitochondrial FOCM provides one-carbon units as formate for FOCM reactions in the cytosol. We found that maternal supplementation with formate prevented NTDs in *curly tail* embryos and also resulted in increased litter size. Analysis of the folate profile of neurulation-stage embryos showed that formate supplementation resulted in an increased proportion of formyl-THF and THF but a reduction in proportion of 5-methyl THF. In contrast, THF decreased and 5-methyl THF was relatively more abundant in the liver of supplemented dams than in controls. In embryos cultured through the period of spinal neurulation, incorporation of labelled thymidine and adenine into genomic DNA was suppressed by supplemental formate, suggesting that de novo folate-dependent biosynthesis of nucleotides (thymidylate and purines) was enhanced. We hypothesise that reduced *Mthfd1L* expression may contribute to susceptibility to NTDs in the *curly tail* strain and that formate acts as a one-carbon donor to prevent NTDs.

© 2016 The Authors. Published by Elsevier B.V. This is an open access article under the CC BY license (<http://creativecommons.org/licenses/by/4.0/>).

1. Introduction

The network of reactions that comprises folate one-carbon metabolism (FOCM) supplies one carbon units for a number of downstream biosynthetic pathways including nucleotide biosynthesis and methylation reactions [1,2]. Corresponding with the crucial role of FOCM in several cellular functions, abnormal FOCM is associated with a range of diseases, including cancers, fatty liver disease, inborn errors of metabolism, autism, age-related cognitive

impairment and birth defects, particularly neural tube defects (NTDs). NTDs, including spina bifida and anencephaly, are a group of birth defects that result from incomplete formation of the neural tube which is the precursor of the brain and spinal cord in the developing embryo [3]. The causes of most NTDs in humans are not well understood owing to their complex etiology which is thought to involve multiple genetic and environmental factors [4]. Sub-optimal maternal folate status is associated with increased risk of an NTD-affected pregnancy while maternal supplementation with folic acid reduces susceptibility [5], although some NTDs are not prevented ('folic acid-resistant'). Polymorphisms and/or variants in some FOCM-related genes (e.g. *MTHFR*, *MTHFD1L*, *AMT* and *GLDC*) have been associated with NTDs [3,6], while abnormal thymidylate

* Corresponding author. Birth Defects Research Centre, UCL Institute of Child Health, 30 Guilford Street, London, WC1N 1EH, UK.

E-mail address: n.greene@ucl.ac.uk (N.D.E. Greene).

2.5. Metabolite analysis

Folate profile: Folates were quantified by ultra-pressure liquid chromatography coupled to tandem mass spectrometry (UPLC-MS/MS), as described previously [28,29]. Briefly, E10.5 embryos were resuspended in 'folate buffer' containing 20 mM ammonium acetate, 0.1% ascorbic acid, 0.1% citric acid and 100 mM dithiothreitol at pH 7 and 0.2 μ M methotrexate as internal standard. Samples were sonicated using a hand-held sonicator for 10 s at 40% amplitude and an aliquot removed for analysis of protein concentration using the Bradford assay. Protein was precipitated using 2 \times volume of acetonitrile and removed after centrifugation (12,000 \times g at 4 °C). Samples were then lyophilised and resuspended in 30 μ l 'folate buffer'. Metabolites were resolved by reversed-phase UPLC (Acquity UPLC BEH C18 column, Waters Corporation, UK) and detected using a XEVO-TQS mass spectrometer (Waters Corporation) operating in negative-ion mode using the following settings: capillary 2.5 kV, source temperature 150 °C, desolvation temperature 600 °C, cone gas flow rate 150 l h⁻¹, and desolvation gas flow rate 1200 l h⁻¹.

Formate: Blood was collected by terminal cardiac exsanguination into lithium-heparin tubes (BD Microtainer) and centrifuged for the isolation of plasma. Blood and urine samples collected from treated mice were taken after 12 days of formate treatment. Formate concentration was determined by gas-phase chromatography mass spectrometry, with urine concentration normalised to creatinine as described previously [28,30].

2.6. Nucleotide incorporation

Incorporation of ³H nucleotide precursors into genomic DNA was determined as described previously [25]. Embryos were explanted at E9.5, leaving the yolk sac and ectoplacental cone intact and cultured for 24 h in rat serum containing either [³H]-adenine (2 μ Ci/ml), [³H]-thymidine or [³H]-CTP (both 1 μ Ci/ml), with 5 mM sodium formate (formate treated) or an equivalent volume of phosphate buffered saline (Control). Genomic DNA was isolated and incorporation of ³H determined by scintillation counting as described previously [25]. DNA concentration was measured by QubitTM (Thermo Fisher Scientific).

2.7. Western blot

The cranial region of embryos at E10.5 was suspended in RIPA buffer and sonicated for 10 s using a hand-held sonicator at 40% amplitude. An aliquot was taken for protein quantitation by Bradford assay. 10 μ g of protein was run per sample on NuPAGE 4–12% Bis-Tris gel (Life technologies) and immunoblotted. Blocking was performed overnight with BSA, followed by overnight incubation at 4 °C with rabbit anti-Mthfd1L (1:1000; PA5-31360; Thermo Scientific). After incubation with secondary antibody blots were developed using ECL Prime (GE Healthcare Life Sciences). Blots were stripped and re-probed using mouse anti-Gapdh (1:20,000) and ECL Western Blotting Substrate (Promega). Densitometry was performed using Quantity One software (Bio-Rad).

2.8. Statistical analysis

Data are presented as mean \pm SEM (n), unless otherwise indicated. Statistics were conducted using GraphPad Prism (version 6.01; GraphPad Software Inc.) and SigmaStat (v3.5, Systat Software). Supplementation data were analysed using Fisher's Exact test. Means were compared using t-test or by one-way ANOVA with pairwise analysis by Holm-Sidak test as appropriate.

3. Results

3.1. Diminished expression of *Mthfd1L* in *curly tail* embryos

Curly tail embryos are sensitive to maternal folate deficiency and exhibit some FOCM alterations compared with wild-type [21]. We therefore asked whether *curly tail* embryos exhibited altered expression of genes related to FOCM by interrogating a previously reported microarray study [16], in which mRNA abundance in *ct/ct* neurulation-stage embryos was compared with a partially congenic wild-type strain (+^{ct}/+^{ct}). Among a panel of 64 genes that encode enzymes related to one-carbon metabolism [31], we noted significant alteration in expression of *Mthfd1L* (2-fold lower in *ct/ct*; $p < 0.05$). *Mthfd1L* had previously been examined in the context of neural tube closure: SNPs in *MTHFD1L* are associated with NTDs in humans [32], while loss of function of *Mthfd1L* in mice results in cranial NTDs [27]. In order to further investigate *Mthfd1L* expression in *curly tail* embryos we performed qRT-PCR. In samples derived from the caudal region of embryos at E10.5, corresponding to the tissue and stage at which spinal neurulation fails in *curly tail* embryos, *Mthfd1L* expression was approximately 50% lower in *ct/ct* embryos compared with stage-matched controls (Fig. 1A). Expression was similarly lower in the cranial region, analysed at E9.5 which is the stage when neural tube closure occurs at this axial level (Fig. 1A). We further validated this finding by western blot (Fig. 1B). Quantification of band intensity showed a significant reduction in abundance of *Mthfd1L* protein in *ct/ct* embryos compared with +^{ct}/+^{ct} (0.05 \pm 0.01 vs 0.43 \pm 0.09 arbitrary units, normalised to *Gapdh*; $p < 0.01$, t-test).

3.2. Altered *Mthfd1L* expression in *curly tail* embryos does not result from *Ghrl3* deficiency

The main genetic cause of NTDs in *curly tail* embryos is a hypomorphic allele of *Ghrl3*. We therefore tested whether *Mthfd1L* may be a direct or indirect transcriptional target of *Ghrl3* by analysing expression in *curly tail* embryos carrying a *Ghrl3*-BAC transgene [13]. Expression of *Ghrl3* was increased in *ct/ct*^{tgGhrl3}/⁰ embryos but there was no apparent effect on *Mthfd1L* expression, either in the spinal region at E10.5 or in the cranial region at E9.5 (Fig. 1A). We also analysed *Mthfd1L* expression in *Ghrl3* null embryos and found no difference from wild-type (Fig. 1C). These observations suggest that reduced *Mthfd1L* expression in *ct/ct* embryos is not a result of *Ghrl3* deficiency. We next considered the possibility that there is an effect of the *ct* genetic background on *Mthfd1L* expression.

The partially congenic +^{ct} strain, used for transcriptomic analysis, carries a region of SWR strain DNA at the *Ghrl3* locus (and is hence designated wild-type for *Ghrl3*). The remaining genetic background is predicted to be 96% identical between *ct/ct* and +^{ct}/+^{ct} embryos, with small regions of SWR DNA remaining in the +^{ct}/+^{ct} strain (as we previously found on chromosome 18 [16]). We tested the possibility that the variation in *Mthfd1L* expression between the two strains results from retention of a region of SWR DNA encompassing the *Mthfd1L* gene in the +^{ct} strain. Microsatellite markers and SNPs, flanking and within *Mthfd1L* on mouse chromosome 10, were tested for polymorphism between genomic DNA of SWR and *curly tail* strains. A synonymous coding SNP, rs47265432, was informative; this position is T in the SWR strain but C in *ct* and +^{ct}. A further intronic SNP rs218957174, typed as T in *ct* and +^{ct} but C in SWR. These data indicate that *Mthfd1L* is not in a region where the genetic background of the *ct* and +^{ct} strains differs. We also sequenced the entire coding region of *Mthfd1L* *ct/ct* and +^{ct}/+^{ct} strains and confirmed that there is no difference in sequence between the strains or variation from the reference sequence.

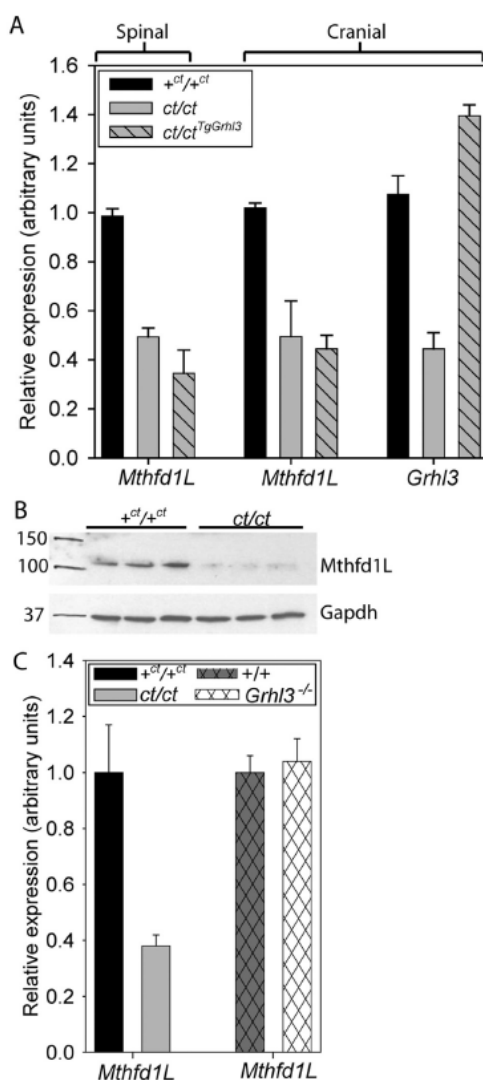


Fig. 1. Diminished expression of *Mthfd1L* in *curly tail* embryos. (A) *Mthfd1L* mRNA abundance is significantly lower in the caudal region of E10.5 (28–29 somite stage) *ct/ct* embryos ($n = 6$) and *ct/ct^{TgGrhl3}* ($n = 3$) than in stage-matched *+ct/+ct* embryos ($n = 3$; $p < 0.001$; ANOVA). The cranial region of E9.5 *ct/ct* embryos also exhibits lower abundance of *Mthfd1L* mRNA, which is not corrected in *ct/ct^{TgGrhl3}* embryos ($n = 2$ per group, $p < 0.05$). In contrast, *Grhl3* expression is diminished in the E9.5 cranial region of *ct/ct* embryos compared with *+ct/+ct* ($p < 0.001$; ANOVA), and is normalised by the presence of a *Grhl3*-containing BAC (*ct/ct^{TgGrhl3}*). (B) Immunoblots reveal a 104 kDa band corresponding to *Mthfd1L* that is less abundant in *ct/ct* samples (caudal region at E10.5) than stage-matched *+ct/+ct* samples. Immunoblot for *Gapdh* (37 kDa) is used as loading control. (C) Analysis of a second group of E10.5 *ct/ct* ($n = 5$) and *+ct/+ct* ($n = 3$) samples replicated the finding of reduced *Mthfd1L* expression in *ct/ct* ($p < 0.01$). In contrast, no difference in *Mthfd1L* expression was detected between wild-type ($n = 6$) and *Grhl3* null ($n = 7$) embryos.

3.3. Formate supplementation prevents NTDs in *curly tail* embryos

Mthfd1L is required for production of formate from 10-formyl THF in mitochondrial FOCM [1]. This is a crucial activity as formate is transferred to the cytosol where it acts as a major one-carbon donor in FOCM. The importance of mitochondrial FOCM in neural tube closure is highlighted by the occurrence of NTDs in mice carrying loss of function alleles of *Mthfd1L*, *Gldc* and *Amt* [27,28,33]. We tested whether a deficit of formate production could contribute to *curly tail* NTDs by supplementing pregnant dams with sodium formate in drinking water, as previously used in *Mthfd1L* null mice [27]. Fetuses were scored according to the presence of spina bifida, a tail flexion defect (indicative of delayed spinal neurulation) or a normal straight tail (Fig. 2). Spina bifida occurred in 10–15% of embryos in the control groups. We observed a striking dose-dependent effect on spinal NTDs, with a significant reduction in the frequency of spina bifida, which was present in only 2.9% (4/136) of offspring of dams supplemented with 30 mg/ml (Fig. 2E). The frequency of exencephaly (7.9% and 4.6% in the control groups) also appeared lower in the groups treated with 20 mg/ml or 30 mg/ml formate (2.2% and 1.5%) (Fig. 2F). Overall, exencephaly occurred at significantly lower frequency in formate-treated litters than in control litters ($p < 0.05$).

We measured crown-rump length of embryos at E11.5 to test whether formate supplementation had an effect on overall growth, but no differences were observed (Table 1). Interestingly however, the litter size among formate-supplemented dams was significantly larger than among contemporaneous control dams (Table 1).

3.4. Formate and folate analysis in supplemented dams and fetuses

Quantification of formate by GC-MS confirmed that oral supplementation in drinking water led to a significant elevation in plasma formate in both *ct* and wild-type females (Table 2). The plasma formate level appeared lower in *curly tail* mice than in wild-type, both under normal and supplemented conditions, but this was not statistically significant (Table 2). Nevertheless, we analysed formate in urine to ask whether excretion was higher in *curly tail* females, potentially accounting for lower blood formate. Instead we observed significantly lower formate concentration in urine of these mice (Table 2).

Formate produced by mitochondrial FOCM can enter cytoplasmic FOCM by acting as a one-carbon source for generation of formyl-THF from tetrahydrofolate (THF), mediated by the formyl synthetase activity of the trifunctional enzyme, *Mthfd1* (Fig. 3A). We tested whether maternal formate supplementation led to an alteration in the relative proportions of cellular folates using an LC-MS/MS method for quantification of the mono- and poly-glutamated (n1–7) forms of seven major folates [28,29]. In formate supplemented *ct/ct* embryos we noted a reduction in the relative proportion of 5-methyl-THF and an increase in the proportions of THF and formyl-THF (CHO-THF), compared with non-supplemented *ct/ct* controls (Fig. 3B). This was in striking contrast to the liver of supplemented *ct/ct* dams which showed a significant increase in relative proportion 5-methyl-THF and a decrease in THF (Fig. 3C).

3.5. Formate suppresses incorporation of exogenous nucleotides into DNA

Formyl-THF provides one-carbon units for synthesis of purines while 5,10-methylene-THF is a one-carbon donor for thymidylate (dTMP) synthesis. Alternatively, nucleotide biosynthesis can be mediated through salvage pathways that do not depend on FOCM. For example, thymidine is converted to dTMP through the action of

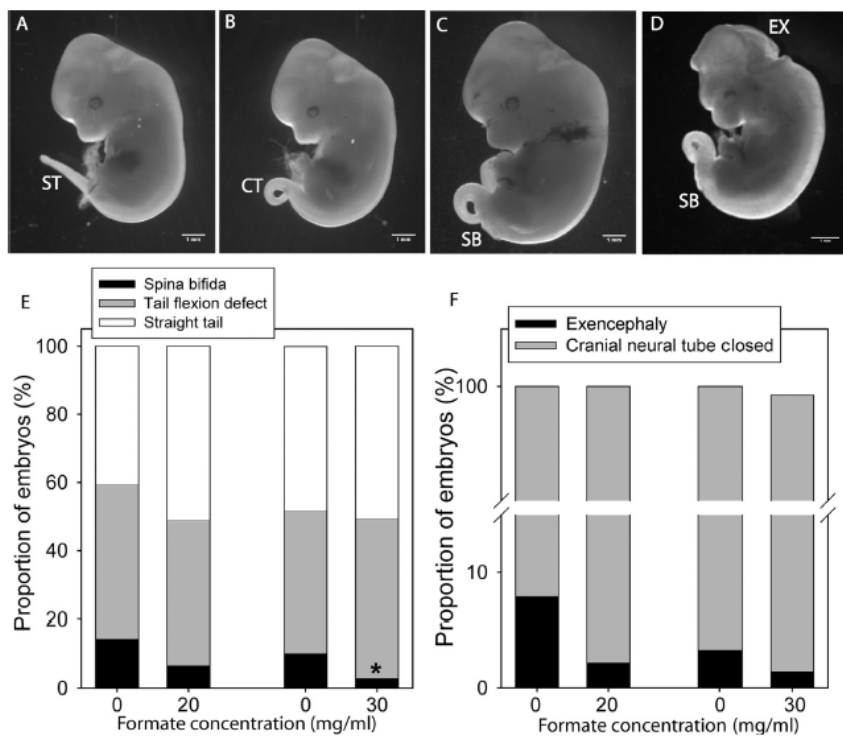


Fig. 2. Formate prevents NTDs in *curly tail* mice. Among litters at E12.5 (A–D) we observed embryos with a straight tail ('normal', ST), tail flexion defect (curly tail, CT), tail flexion defect with spina bifida (SB) and exencephaly (EX), which can occur in isolation or with a curly tail or spina bifida (scale bars represent 1 mm). (E) Among litters of dams supplemented with formate in drinking water we observed a lower frequency of spina bifida (* indicates significant difference from control group, $p < 0.05$; $n = 187$ (0 mg/ml), 90 (20 mg/ml), 91 (0 mg/ml) and 138 (30 mg/ml) embryos). (F) The frequency of exencephaly was lower among all formate-treated litters than among all controls ($p < 0.05$) although individual groups did not differ significantly ($n = 109$ (0 mg/ml), 90 (20 mg/ml), 91 (0 mg/ml) and 138 (30 mg/ml) embryos).

Table 1
Litter size and embryo size in formate-supplemented *curly tail* mice.

Formate conc.	0 mg/ml	20 mg/ml	0 mg/ml	30 mg/ml
No. Litters	15	10	13	14
Mean litter size	6.90 ± 0.50	$9.00 \pm 0.90^*$	7.00 ± 0.60	$9.57 \pm 0.40^{**}$
Mean crown-rump length (mm) (n)	7.78 ± 0.14 (25)	7.683 ± 0.04 (90)	7.88 ± 0.07 (47)	7.78 ± 0.03 (133)

Mean litter size of dams supplemented with 20 mg/ml or 30 mg/ml formate was larger than in control groups (* $p < 0.05$, ** $p < 0.01$). The crown-rump length of embryos at E12.5 did not differ among experimental groups.

Table 2
Formate concentration in plasma and urine \pm formate supplementation.

Strain	Plasma formate (μ M)		Urine formate (μ M/ μ M creatinine)	
	Controls	Formate-treated†	Control	Formate-treated††
<i>Curly tail</i> (<i>ct/ct</i>)	36.5 ± 3.6	600.3 ± 144.4	$15.5 \pm 2.8^*$	438.6 ± 199.6
Wild-type (<i>+/+</i>)	50.7 ± 5.4	1267.0 ± 564.0	47.8 ± 2.9	1884.9 ± 873.5

Formate concentration in urine of female *ct/ct* mice was significantly lower than in urine of wild-type mice (* $p < 0.001$). Among mice supplemented with 30 mg/ml formate in drinking water, the concentration of formate was significantly higher in plasma († $p < 0.01$) and in urine (†† $p < 0.05$) than in the equivalent non-supplemented controls ($n = 3$ –4 mice in each group).

thymidine kinase, while AMP is produced from adenine by the action of APRT. Supplementation of *ct/ct* mice with a combination of thymidine and adenine reduces the frequency of NTDs [25]. We tested whether formate may be utilised in nucleotide biosynthesis

by testing its effect on incorporation of exogenous thymidine or adenine in cultured *ct/ct* embryos. Among embryos cultured in the presence of formate we observed significantly lower incorporation of labelled thymidine or adenine (Fig. 4), supporting the hypothesis

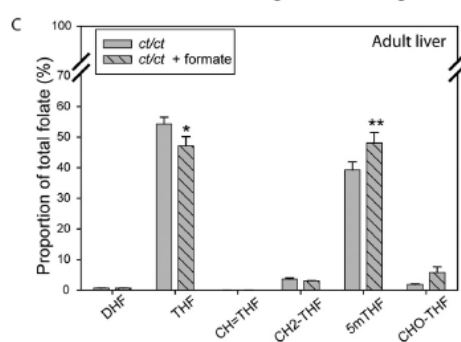
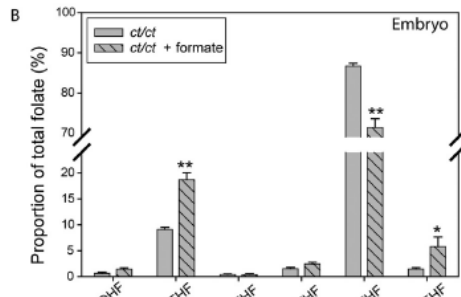
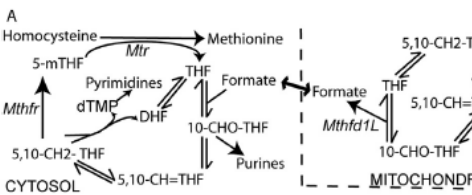


Fig. 3. Folate profile of formate-treated *curly tail* embryos and adult liver. (A) Outline diagram of key reactions in FOCM, showing folates analysed. The relative proportions of folates differ in (B) embryos ($n = 9$ embryos per group) and (C) liver ($n = 3$) of formate-treated *ct/ct* dams compared with untreated *ct/ct* dams and dams. Data represent the sum of all glutamated forms for each folate. Formate-treated embryos at E10.5 exhibit a significant increase in the relative amount of tetrahydrofolate (THF) and formyl-THF (CHO-THF) and a decrease in the proportion of 5-methyl-THF (5mTHF) ($^{*}p < 0.001$, $^{**}p < 0.0001$). In contrast, liver of treated adult mice exhibited a significant increase in proportion of 5mTHF and decrease in THF ($^{*}p < 0.05$, $^{**}p < 0.01$). The proportion of dihydrofolate (DHF), methenyl-THF (CH = THF) and methylene-THF (CH2-THF) did not significantly differ with treatment in either embryos or adult liver.

that formate suppresses the salvage pathways for thymidylate and AMP biosynthesis owing to enhanced use of the endogenous folate-dependent synthetic reactions. Although formate did not affect overall growth we considered the possibility that reduced incorporation of thymidine and adenine could result from decreased DNA synthesis rather than suppression of the salvage pathways. In a control experiment formate did not affect incorporation of labelled CTP into DNA. This finding suggests that overall DNA synthesis was not compromised and is consistent with the fact that FOCM is not required for cytidine biosynthesis.

4. Discussion

Spina bifida occurs in 10–15% of *ct/ct* embryos and can be

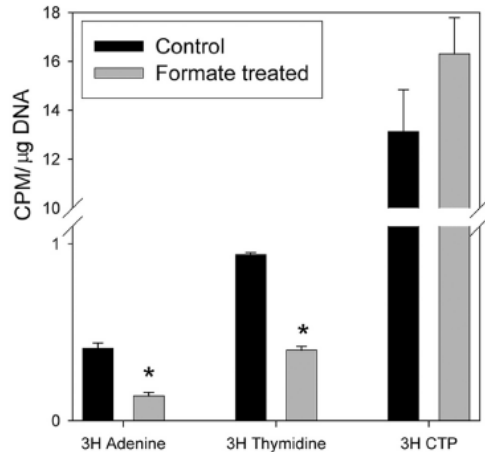


Fig. 4. Formate suppresses uptake of exogenous adenine, thymidine or CTP for 24 h from E9.5. Incorporation of [3 H]-adenine or thymidine into genomic DNA was significantly lower in the presence of additional formate ($p < 0.01$). Values are given as mean \pm SEM; $n = 4$ –6 embryos per group.

principally attributed to reduced expression of *Ghrl3*, being fully rescued by transgenic *Ghrl3* expression [13]. In the current study we also observed a significant reduction in *Mthfd1L* expression in *ct/ct* embryos at neurulation stages. Spinal NTDs have been reported in only a very small proportion of *Mthfd1L* null mice [27]. Nevertheless we cannot rule out a potential contribution of reduced *Mthfd1L* expression to spina bifida in the *ct* strain, acting to modify the *Ghrl3* effect, as we previously observed for a *Lmn1* variant (Deletion 18: 56909394) present in the *ct* genetic background. Cranial NTDs (exencephaly) also occur in *Ghrl3* null embryos, but only among 2–14% unlike the 100% penetrance of spina bifida [14,34]. In the current study we found that *Ghrl3* expression is less abundant in the cranial region of *ct/ct* embryos than wild-type and is normalised in the *ct/ct* *TgGhrl3/0* embryos. However, unlike spina bifida, cranial NTDs are not prevented in *ct/ct* *TgGhrl3/0* embryos, with exencephaly occurring among around 8% of embryos ($n = 140$), compared with 6–8% of *ct/ct* embryos (this study and [16]). These findings suggest that cranial NTDs in *ct/ct* embryos depend on genetic factors in addition to the hypomorphic *Ghrl3* allele. For example, exencephaly is reduced to 3% among a sub-strain of *ct/ct* embryos with wild-type *Lmn1* but occurs at 2.6% in a sub-strain of *+^{ct}/+^{ct}* embryos carrying the *Lmn1* Deletion 18: 56909394 variant [16]. Both the latter sub-strains exhibit diminished *Mthfd1L* expression similar to the *ct/ct* strain (data not shown). We speculate that this could contribute to cranial NTDs, as observed in *Mthfd1L* null embryos and other loss of function enzymes of mitochondrial FOCM (*Gldc* and *Amt*). In contrast, exencephaly does not occur in the *+^{ct}/+^{ct}* strain (wild-type for *Ghrl3*, *Lmn1* and *Mthfd1L* expression) unless dietary folate deficiency is imposed [21].

The protective effect of formate supplementation among *ct/ct* embryos supports the hypothesis that there may be a deficiency in supply of one-carbon units from mitochondrial FOCM, as would be predicted in *Mthfd1L* hypomorphs. In addition to reduction in NTD frequency in *Mthfd1L* null embryos [27], formate also rescues NTDs in mice with loss of function of *Gldc* (encoding glycine decarboxylase) [28], another component of mitochondrial FOCM which acts

to supply one-carbon units from glycine [1]. Analysis of folate profiles showed that the relative proportion of formyl-THF was increased in supplemented *ct/ct* embryos similar to our previous observations in wild-type or *Gldc* knockout embryos [28]. Interestingly, the proportion of 5-methyl THF declined while that of THF increased in formate-supplemented *ct/ct* embryos compared with controls. This finding may at first appear counter-intuitive. However, this alteration in folate profile was consistent with our previous observation in wild-type embryos [28], whereas formate caused an increase in proportion of 5-methyl-THF and formyl-THF and a decrease in THF in *Gldc* null embryos. In contrast to embryos, in adult liver the relative abundance of 5-methyl-THF was increased by formate treatment while THF declined in abundance. The variation in response to formate supplementation may reflect the observed difference in the baseline folate profiles in these tissues (5-methyl-THF makes up a greater proportion of total folates in the embryo than in liver), which could result from differences in metabolic requirements. In addition, the embryonic response may include secondary effects of altered maternal metabolism combined with increased formate levels.

We previously found that folate deficiency results in a significant reduction in implantations per litter and a significant increase in resorptions in the *ct* strain [21]. Although formate treatment did not affect litter size in our previous study of *Gldc* mutant mice [28], there was an apparent increase in litter size in both cohorts of formate-treated *ct* mice in the current study. This appears unlikely to result from improved survival of post-implantation embryos as there was no difference in resorption rate in control and formate-treated litters (data not shown). Moreover, supplementation was not initiated until the day of finding a copulation plug so it is unlikely that formate affected fertility *per se*. We speculate that formate supplementation may have led to more successful implantations or improved survival of pre-implantation embryos.

How does formate prevent NTDs in the *ct* model? Spinal NTDs in *ct/ct* embryos are known to result from a proliferation defect in the hindgut endoderm, which causes a growth imbalance in the caudal region of the embryo undergoing neurulation [12]. Prevention of NTDs by inositol or by a combination of nucleotides is associated with stimulation of proliferation and normalisation of this growth imbalance [25,35]. The increased abundance of formyl-THF observed in formate-treated embryos would support supply of one-carbon units for purine biosynthesis. Moreover, suppression of the salvage pathways for dTMP and AMP by exogenous formate supports the hypothesis that supplemental formate can provide one-carbon donors for FOCM-mediated biosynthesis of both purines and thymidylate. This is also consistent with the previous observation that supplementation with combinations of nucleotides (thymidine + adenine or thymidine + GMP) can reduce the frequency of NTDs in *curly tail* mice [25].

Having been found to prevent NTDs in mouse single gene mutants for enzymes of mitochondrial FOCM [27,28], this study now shows a protective effect of formate in an additional model, *curly tail*, in which NTDs have a more complex genetic basis. The fact that folic acid does not prevent NTDs in this model raises the question of whether formate, or another one-carbon donor, may have therapeutic use in human NTDs. Production of formate has been proposed as one potential mechanism underlying toxicity of excess methanol in humans and primates [36]. Moreover, formate may inhibit the respiratory chain [37]. We did not observe any deleterious effects of 5 mM sodium formate in cultured embryos, although growth retarding and embryotoxic effects of sodium formate have been reported in cultured mouse and rat embryos at concentrations higher than 20 mM [38,39]. For comparison, *in vivo* formate supplementation (30 mg/ml) of wild-type dams in the current study produced plasma formate concentrations of around

1.2 mM. Nevertheless, rodents may be less prone to formate accumulation than humans owing to a greater capacity to remove formate by oxidation [36]. Moreover, studies in sheep show higher concentrations of formate in the foetal circulation and amniotic fluid compared to maternal plasma [40]. In adult female humans, use of calcium formate at a significantly higher dosage than present in a typical supplement, led to plasma formate concentrations of around 0.5 mM and this was cleared rapidly from the circulation within 4 h [41]. This study was not however conducted during pregnancy and additional safety evaluation would be necessary before considering supplementation in pregnant women. Further studies are justified to investigate the possible value of formate supplements as part of a strategy for NTD prevention alongside folic acid.

Acknowledgements

The authors are grateful to Bogi Andersen (University of California, Irvine) for *Grl3* null mice and to Dawn Savery and Ivan Doykov for technical assistance. The project was funded by the Medical Research Council (J003794 to NG, AC), Newlife Foundation (NG, AC), Wellcome Trust (087525 to AC, NG), Great Ormond Street Hospital for Children's Charity (SS, NG) and the Peto Foundation (KM). Funding to JB and MB was provided by the Canadian Institutes for Health Research (MOP 1423231) and CIHR/RDC (JB). This study was supported by the National Institute for Health Research Biomedical Research Centre at Great Ormond Street Hospital for Children, NHS Foundation Trust and University College London.

Appendix A. Supplementary data

Supplementary data related to this article can be found at <http://dx.doi.org/10.1016/j.biochi.2016.02.010>.

References

- AS. Tibbets, D.R. Appling, Compartmentalization of Mammalian folate-mediated one-carbon metabolism, *Annu. Rev. Nutr.* 30 (2010) 57–81.
- J.W. Locasale, Serine, glycine and one-carbon units: cancer metabolism in full circle, *Nat. Rev. Cancer* 13 (8) (2013) 572–583.
- N.D. Greene, A.J. Copp, Neural tube defects, *Annu. Rev. Neurosci.* 37 (2014) 221–242.
- A.J. Copp, P. Stanier, N.D. Greene, Neural tube defects: recent advances, unsolved questions, and controversies, *Lancet Neurol.* 12 (8) (2013) 799–810.
- H.J. Blom, G.M. Shaw, M. Den Heijer, R.H. Finnell, Neural tube defects and folate: case far from closed, *Nat. Rev. Neurosci.* 7 (9) (2006) 724–731.
- P.J. Stover, Polymorphisms in 1-carbon metabolism, epigenetics and folate-related pathologies, *J. Nutr. Nutr.* 4 (5) (2011) 293–305.
- L.P.E. Dunlevy, L.S. Chitty, K. Doudney, K.A. Burren, T. Stojilkovic-Milicic, P. Stanier, et al., Abnormal folate metabolism in foetuses affected by neural tube defects, *Brain* 130 (2007) 1043–1049.
- A. Fleming, A.J. Copp, Embryonic folate metabolism and mouse neural tube defects, *Science* 280 (1998) 2107–2109.
- B.J. Wlodarczyk, L.S. Tang, A. Triplett, F. Aleman, R.H. Finnell, Spontaneous neural tube defects in splotch mice supplemented with selected micronutrients, *Toxicol. Appl. Pharmacol.* 213 (1) (2006) 55–63.
- J.P. Martinez-Barbera, T.A. Rodriguez, N.D.E. Greene, W.J. Weninger, A. Simeone, A.J. Copp, et al., Folic acid prevents exencephaly in *Cited2* deficient mice, *Hum. Mol. Genet.* 11 (2002) 283–293.
- M.J. Harris, D.M. Juriloff, Mouse mutants with neural tube closure defects and their role in understanding human neural tube defects, *Birth Defects Res. A Clin. Mol. Teratol.* 79 (3) (2007) 187–210.
- H.W.M. Van Straaten, A.J. Copp, Curly tail: a 50-year history of the mouse spina bifida model, *Anat. Embryol.* 203 (4) (2001) 225–237.
- P. Gustavsson, N.D. Greene, D. Lad, E. Pauws, S.C. de Castro, P. Stanier, et al., Increased expression of Grainyhead-like-3 rescues spina bifida in a folate-resistant mouse model, *Hum. Mol. Genet.* 16 (21) (2007) 2640–2646.
- S.B. Ting, T. Wilanowski, A. Auden, M. Hall, A.K. Voss, T. Thomas, et al., Inositol- and folate-resistant neural tube defects in mice lacking the epithelial-specific factor *Grl3*, *Nat. Med.* 9 (2003) 1513–1519.
- P.E. Neumann, W.N. Frankel, V.A. Letts, J.M. Coffin, A.J. Copp, M. Bernfield, Multifactorial inheritance of neural tube defects: Localization of the major

gene and recognition of modifiers in *ct* mutant mice, *Nat. Genet.* 6 (1994) 357–362.

[16] S.C. de Castro, A. Malhas, K.Y. Leung, P. Gustavsson, D.J. Vaux, A.J. Copp, et al., Lamin b1 polymorphism influences morphology of the nuclear envelope, cell cycle progression, and risk of neural tube defects in mice, *PLoS Genet.* 8 (11) (2012) e1003059.

[17] W.-H. Chen, G.M. Morris-Kay, A.J. Copp, Prevention of spinal neural tube defects in the curly tail mouse mutant by a specific effect of retinoic acid, *Dev. Dyn.* 199 (1994) 93–102.

[18] A.J. Copp, J.A. Crolla, F.A. Brook, Prevention of spinal neural tube defects in the mouse embryo by growth retardation during neurulation, *Development* 104 (1988) 297–303.

[19] N.D.E. Greene, A.J. Copp, Inositol prevents folate-resistant neural tube defects in the mouse, *Nat. Med.* 3 (1997) 60–66.

[20] M.J. Seller, Vitamins, folic acid and the cause and prevention of neural tube defects, in: G. Bock, J. Marsh (Eds.), *Neural Tube Defects* (Ciba Foundation Symposium 181), John Wiley & Sons, Chichester, 1994, pp. 161–173.

[21] K.A. Burren, J.M. Scott, A.J. Copp, N.D. Greene, The genetic background of the curly tail strain confers susceptibility to folate-deficiency-induced exencephaly, *Birth Defects Res. A Clin. Mol. Teratol.* 88 (2010) 76–83.

[22] J.M. Burgoon, J. Selhub, M. Nadeau, T.W. Sadler, Investigation of the effects of folate deficiency on embryonic development through the establishment of a folate deficient mouse model, *Teratology* 65 (2002) 219–227.

[23] K.A. Burren, D. Savery, V. Massa, R.M. Kok, J.M. Scott, H.J. Blom, et al., Gene-environment interactions in the causation of neural tube defects: folate deficiency increases susceptibility conferred by loss of *Pax3* function, *Hum. Mol. Genet.* 17 (2008) 3675–3685.

[24] S.C. de Castro, K.Y. Leung, D. Savery, K. Burren, R. Rozen, A.J. Copp, et al., Neural tube defects induced by folate deficiency in mutant curly tail (Grl3) embryos are associated with alteration in folate one-carbon metabolism but are unlikely to result from diminished methylation, *Birth Defects Res. A Clin. Mol. Teratol.* 88 (2010) 612–618.

[25] K.Y. Leung, S.C. De Castro, D. Savery, A.J. Copp, N.D. Greene, Nucleotide precursors prevent folate acid-resistant neural tube defects in the mouse, *Brain* 136 (Pt 9) (2013) 2836–2841.

[26] Z. Yu, K.K. Lin, A. Bhandari, J.A. Spencer, X. Xu, N. Wang, et al., The Grail-like epithelial transactivator Get-1/Grl3 regulates epidermal terminal differentiation and interacts functionally with LMO4, *Dev. Biol.* 299 (1) (2006) 122–136.

[27] J. Momb, J.P. Lewandowski, J.D. Bryant, R. Fitch, D.R. Surman, S.A. Vokes, et al., Deletion of Mthfd1l causes embryonic lethality and neural tube and craniofacial defects in mice, *Proc. Natl. Acad. Sci. U. S. A.* 110 (2013) 549–554.

[28] Y.J. Pal, K.Y. Leung, D. Savery, T. Hutchin, H. Prunty, S. Heales, et al., Glycine decarboxylase deficiency causes neural tube defects and features of non-ketotic hyperglycinemia in mice, *Nat. Commun.* 6 (2015) 6388.

[29] K.Y. Leung, S.C. De Castro, F. Cabreiro, P. Gustavsson, A.J. Copp, N.D. Greene, Folate metabolite profiling of different cell types and embryos suggests variation in folate one-carbon metabolism, including developmental changes in human embryonic brain, *Mol. Cell Biochem.* 378 (1–2) (2013) 229–236.

[30] S.G. Lamarre, L. MacMillan, G.P. Morrow, E. Randell, T. Pongnopparat, M.E. Brosnan, et al., An isotope-dilution, GC-MS assay for formate and its application to human and animal metabolism, *Amino Acids* 46 (8) (2014) 1885–1891.

[31] M. Mehrmohamadi, X. Liu, A.A. Shestov, J.W. Locasale, Characterization of the usage of the serine metabolic network in human cancer, *Cell Rep.* 9 (4) (2014) 1507–1519.

[32] A. Parle-McDermott, F. Pangilinan, K.K. O'Brien, J.L. Mills, A.M. Magee, J. Troendle, et al., A common variant in MTHFD1L is associated with neural tube defects and mRNA splicing efficiency, *Hum. Mutat.* 30 (2009) 1650–1656.

[33] A. Narisawa, S. Komatsuzaki, A. Kikuchi, T. Niihori, Y. Aoki, K. Fujiwara, et al., Mutations in genes encoding the glycine cleavage system predispose to neural tube defects in mice and humans, *Hum. Mol. Genet.* 21 (2012) 1496–1503.

[34] Z. Yu, K.K. Lin, A. Bhandari, J.A. Spencer, X. Xu, N. Wang, et al., The Grail-like epithelial transactivator Get-1/Grl3 regulates epidermal terminal differentiation and interacts functionally with LMO4, *Dev. Biol.* 299 (2006) 122–136.

[35] P. Cogram, A. Hynes, L.P.E. Dunlevy, N.D.E. Greene, A.J. Copp, Specific isoforms of protein kinase C are essential for prevention of folate-resistant neural tube defects by inositol, *Hum. Mol. Genet.* 13 (2004) 7–14.

[36] S.G. Lamarre, G. Morrow, L. MacMillan, M.E. Brosnan, J.T. Brosnan, Formate: an essential metabolite, a biomarker, or more? *Clin. Chem. Lab. Med.* 51 (3) (2013) 571–578.

[37] P. Nicholls, The effect of formate on cytochrome aa3 and on electron transport in the intact respiratory chain, *Biochim. Biophys. Acta* 430 (1) (1976) 13–29.

[38] J.E. Andrews, M. Ebron-McCoy, R.J. Kavlock, J.M. Rogers, Developmental toxicity of formate and formic acid in whole embryo culture: a comparative study with mouse and rat embryos, *Teratology* 51 (1995) 243–251.

[39] J.M. Hansen, K.M. Contreras, C. Harris, Methanol, Formaldehyde, and sodium formate exposure in rat and mouse conceptuses: a potential role of the visceral yolk sac in embryotoxicity, *Birth Defects Res. A Clin. Mol. Teratol.* 73 (2) (2005) 72–82.

[40] S.E. Washburn, M.A. Caudill, O. Malysheva, A.J. MacFarlane, N.A. Behan, B. Harnett, L. MacMillan, T. Pongnopparat, J.T. Brosnan, M.E. Brosnan, Formate metabolism in fetal and neonatal sheep, *Am. J. Physiol. Endocrinol. Metab.* 308 (10) (2015) E921–E927.

[41] R.P. Hanzlik, S.C. Fowler, J.T. Eells, Absorption and elimination of formate following oral administration of calcium formate in female human subjects, *Drug Metab. Dispos.* 33 (2) (2005) 282–286.